Anthony M. J. Bull
Jon Clasper · Peter F. Mahoney
Editors

Blast Injury Science and Engineering

A Guide for Clinicians and Researchers

Springer

Blast Injury Science and Engineering

Anthony M.J. Bull • Jon Clasper •
Peter F. Mahoney
Editors

Blast Injury Science and Engineering

A Guide for Clinicians and Researchers

Springer

Editors
Anthony M.J. Bull
Department of Bioengineering
Imperial College London
London, United Kingdom

Jon Clasper
Frimley Park Foundation Trust
Frimley
Surrey, United Kingdom

Peter F. Mahoney
The ICT Centre
Birmingham Research Park
Edgbaston, Birmingham
United Kingdom

ISBN 978-3-319-21866-3 ISBN 978-3-319-21867-0 (eBook)
DOI 10.1007/978-3-319-21867-0

Library of Congress Control Number: 2016931898

Springer Cham Heidelberg New York Dordrecht London

Printed on acid-free paper

Springer International Publishing AG Switzerland is part of Springer Science+Business Media (www.springer.com)

Contents

Contributors

Nadia Abul-Karim, BSc, MRes, PhD Department of Chemistry, University College London, London, UK

Hari Arora, MEng, PhD, DIC, ACGI Department of Bioengineering, Royal British Legion Centre for Blast Injury Studies, Imperial College London, London, UK

M. Bishop Dstl Porton Down, Salisbury, UK

John Breeze, PhD, MRCS, MFDS, MBBS, BDS Academic Department of Military Surgery and Trauma, Royal Centre for Defence Medicine, Birmingham Research Park, Birmingham, UK

Katherine A. Brown, BA, BS, PhD, DIC, FRSC, FInstP Cavendish Laboratory, Department of Physics, University of Cambridge, Cambridge, UK

Anthony M.J. Bull, PhD, CEng, FIMechE, FREng Department of Bioengineering, Royal British Legion Centre for Blast Injury Studies, Imperial College London, London, UK

Diagarajen Carpanen, PhD, BEng(Hons) Department of Bioengineering, Royal British Legion Centre for Blast Injury Studies, Imperial College London, London, UK

Debra J. Carr, CEng, FIMMM, MCSFS Impact and Armour Group, Centre for Defence Engineering, Cranfield University at the Defence Academy of the United Kingdom, Shrivenham, UK

Stephen Champion Vehicles and Weapons Group, Centre for Defence Engineering, Cranfield University at the Defence Academy of the United Kingdom, Shrivenham, UK

Jon Clasper, CBE DPhil DM FRCSEd(Orth) Department of Bioengineering, Royal British Legion Centre for Blast Injury Studies, Imperial College London, London, UK

Academic Department of Military Trauma and Surgery, Royal Centre for Defence Medicine, Birmingham, UK

Russell Delaney, MB ChB, MRCS, FRCPath South West Forensic Pathology Group Practice, Bristol, UK

Robert Dickinson, BSc, PhD Department of Surgery & Cancer, Royal British Legion Centre for Blast Injury Studies, Imperial College London, London, UK

Steven Dryden, LLB Department of Counter Terrorism Commend, Metropolitan Police Service, London, UK

Dafydd S. Edwards, BSc (Hons), MBBS, FRCS, DMCC Department of Bioengineering, Royal British Legion Centre for Blast Injury Studies, Imperial College London, London, UK

Theofano Eftaxiopoulou, PhD Department of Bioengineering, Royal British Legion Centre for Blast Injury Studies, Imperial College London, London, UK

Robert Fryer Land Battlespace Systems Department, Defence Science & Technology Laboratory, Fareham, UK

Karl Harrison, PhD, MSc Cranfield Forensic Institute, Defence Academy of the UK, Shrivenham, UK

Alan E. Hepper Dstl Porton Down, Salisbury, UK

Nicholas C.A. Hunt, BSc, MBBS, FRCPath, DipRCPath Forensic Pathology Services, Grove Technology Park, Wantage, UK

Angelo Karunaratne, MEng, PhD Department of Bioengineering, Royal British Legion Centre for Blast Injury Studies, Imperial College London, London, UK

Emrys Kirkman, PhD CBR Division, Dstl Porton Down, Salisbury, UK

Eluned A. Lewis Defence Equipment and Support, Ministry of Defence Abbey Wood, Bristol, UK

Peter F. Mahoney, CBE MBA FRCA FIMC L/RAMC Department of Military Anaesthesia and Critical Care, Royal Centre for Defence Medicine, Birmingham, UK

Department of Bioengineering, Royal British Legion Centre for Blast Injury Studies, Imperial College London, London, UK

Spyros Masouros, PhD, DIC, Dipl.Eng Department of Bioengineering, Royal British Legion Centre for Blast Injury Studies, Imperial College London, London, UK

Nicolas Newell, MEng, PhD Department of Bioengineering, Imperial College London, London, UK

Hasu D.L. Patel, MBChB, PhD, FRCS(Ed) FRCS(Plast) Department of Plastic and Reconstructive Surgery, Barts and the Royal London Hospital (Barts Health), Royal London Hospital, London, UK

Rita Campos Pires, MD Department of Surgery & Cancer, Royal British Legion Centre for Blast Injury Studies, Imperial College London, London, UK

Dan J. Pope, BEng (Hons), PhD, CEng, FICE Dstl Porton Down, Salisbury, UK

William G. Proud, BSc (Hons), PhD Department of Physics, Institute of Shock Physics and Royal British Legion Centre for Blast Injury Studies, Imperial College London, London, UK

Arul Ramasamy, MA PhD FRCS (Tr+Orth) MFSEM RAMC Department of Bioengineering, Royal British Legion Centre for Blast Injury Studies, Imperial College London, London, UK

Tobias Reichenbach, PhD, MSc Department of Bioengineering, Imperial College London, London, UK

Robert J. Russell, FRCEM, DipIMC, RCEd Academic Department of Military Emergency Medicine, Royal Centre for Defence Medicine, ICT Centre, Birmingham Research Park, Birmingham, UK

Robert A.H. Scott, FRCS (Ed), FRCOphth, DM, (RAF) Birmingham and Midland Eye Centre, Birmingham, UK

A. Sedman Dstl Porton Down, Salisbury, UK

James A.G. Singleton, MSc, MBBS, MRCS(Eng), RAMC Department of Bioengineering, Royal British Legion Centre for Blast Injury Studies, Imperial College London, London, UK

Edward J. Spurrier, BM, FRCS(Tr+Orth) Department of Bioengineering, Royal British Legion Centre for Blast Injury Studies, Imperial College London, London, UK

Nicholas T. Tarmey, FRCA, DICM, DipIMC RCS(Ed) Academic Department of Critical Care, Queen Alexandra Hospital, Portsmouth, UK

Claire Webster, MBChB MRCS RAF Department of Bioengineering, Royal British Legion Centre for Blast Injury Studies, Imperial College London, London, UK

Paul R. Wood, MB BCh, FRCA Department of Anaesthetics, Queen Elizabeth Hospital Birmingham, Birmingham, UK

Part I

Basic Science and Engineering

The Fundamentals of Blast Physics

1

William G. Proud

1.1 Overview

The basis of blast injury lies in the effects of an explosion and, by extension, in the use of explosives. There are many books on explosives that start with a historical summary of the discoveries and personalities involved before developing the theories and quantitative measure of explosive chemistry, physics and engineering. This is useful information, however, in this chapter the aim is to present the reader with a timeline of events working from the point of activation of the initiator to the arrival of the blast wave at the human body or target. On this timeline the steps will be presented in a simple, non-technical way introducing the basic concepts and placing the information within the wider context. The amount of mathematical derivation is kept to a minimum; for those who wish greater depth, a selection of references is provided to allow for further study.

1.2 The Aims of this Chapter

1. Introduce some fundamental aspects of explosives and timescales
2. Provide an outline of how mines, blast and fragmentation work
3. Describe the energy release process and the efficiency of the process
4. Describe and distinguish between waves transmitting in solids, liquids and gases
5. Describe the range of fragment sizes and velocities
6. Provide an overview of shock and blast wave propagation
7. Outline how waves expand and interact with the surrounding environment

1.3 Explosives and Blast: A Kinetic Effect

Explosives form part of a range of materials classified as '**energetic materials'**, other members of this class include propellants and pyrotechnics. The distinguishing feature of energetic materials compared to other materials is in the very fast rate of energy release. The energy release rate determines the application of the energetic material.

The basic chemical components involved are a fuel, an oxidiser and a material that allows a rapid ignition of reaction. In terms of total energy released energetic materials are not particularly distinguished from other chemical reactions, petrol and butter release more energy per molecule when oxidised than tri-nitro toluene (TNT) for

W.G. Proud, BSc (Hons), PhD
Department of Physics, Institute of Shock Physics and Royal British Legion Centre for Blast Injury Studies, Imperial College London, London, UK
e-mail: w.proud@imperial.ac.uk

A.M.J. Bull et al. (eds.), *Blast Injury Science and Engineering: A Guide for Clinicians and Researchers*,
DOI 10.1007/978-3-319-21867-0_1

example. This difference is that while petrol needs to be mixed with air and then set alight, the explosive comes with the fuel and oxidiser intimately mixed, sometimes with both fuel and oxidiser present in the same molecule. Within energetic materials the use of the chemical or composition gives information on the reaction rate.

Sound is a low magnitude stress wave, it propagates through air causing a very minor change in the density of the air and moves at a fixed velocity. An **explosion** is a term used to describe the rapid expansion of gas, it may be from the rupture of a pressure vessel, for example, a gas cylinder, the sudden vaporisation of a liquid, for example, water exposed to hot metal, or by a rapid chemical reaction as seen in an explosive. The energy associated with a blast wave causes significant compression of the air through which it passes and the blast wave travels at a velocity faster than the sound speed in air.

High Explosives, correctly called **High Order Explosives** involve materials like TNT, HMX, RDX and PETN often mixed with other chemicals which make the explosive composition more stable, easier to industrially process or fit into cavities within a munition. As these materials detonate, they release their energy due to a shock wave being produced within them. A shock wave is a high-pressure pulse which moves through the material at supersonic speed. In the case of a detonation the shock wave consists of a thin, often sub-millimetre, region where the explosive turns from a solid or liquid into a hot high-pressure gas (Fig. 1.1). The velocity of a detonation wave is of the order 8 km s^{-1} and the energy release rate is of the order of Gigawatts i.e. the same output as a large electrical plant, over the time of a few microseconds. The pressure associated with detonation waves are of many hundreds of thousands of atmospheres. The produced gases expand quickly, a rule of thumb gives the rate of product gas expansion to be ~1/4 of the detonation velocity. It is not

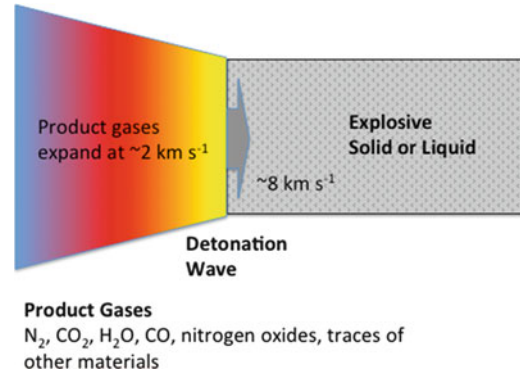

Fig. 1.1 Schematic of detonation process

surprising that such aggressive energy release is used to shatter and push materials at high velocities.

Within the class of high explosives there is a sub-division between so-called **'ideal'** and **'non-ideal'** explosives. Ideal explosives have very thin detonation-reaction zones where the reaction takes place on a sub-microsecond basis. Ideal explosives have a more pronounced shattering effect or brisance, on materials placed in contact with them, this class of materials includes TNT. Non-ideal explosives have much thicker reaction zones and give out their energy over slightly longer timescales, up to several microseconds. The most widely used explosive in the world, Ammonium Nitrate: Fuel Oil (ANFO) falls into this class. The chemical make-up of ANFO results in much lower pressures of detonation, about a quarter of the pressure seen in high explosives, producing less shattering effect. However, ANFO does generate a lot of gas, this gives the mixture a lot of 'heave'. The low detonation pressure means this mix produces cracks in rocks which are then pushed open, heaved, by the detonation gas. These materials tend to be used in the mining and quarrying industry.

Low Order Explosives are materials that give out their energy as a result of rapid burning, called deflagration. This class of materials includes much of the materials often called

gun-powders. Here the energy reaction rate is much lower, of the order of a thousandth of that seen in high explosives. The total energy output is similar to that of high explosives but the lower rate means that the pressures developed are much lower.

Both high and low explosives generally need a degree of mechanical **confinement** in order to detonate. A gramme of gun-powder on a bench will react quickly with a flash of light, a small fireball, some heat but little other effect. The same quantity placed inside a sealed metal can, where the confinement allows the hot gases to stay close to the powder, allows pressure and temperature to build-up thus accelerating the reaction until the confinement shatters and an explosion is produced.

Propellants are a wide group of materials where the reaction pressures are of the order of thousands of atmospheres and the reaction timescales are measured in milliseconds. These materials are used in rocket motors, and to drive bullets or shells. In some cases propellants, if confined or impacted at high velocity may detonate; gun-powder is an example, driving bullets if burnt inside a gun but producing explosives if confined within a metal shell. Missile motors may detonate if they overheat or if the product gas cannot vent quickly enough. As a group of materials they can present a significant fire hazard and can be used in improvised explosive systems.

Pyrotechnics are a wide range of materials including flares and obscurants. They do not produce high pressures but can generate significant heat and can be used to ignite explosives. They can be very sensitive to electrostatic discharge, but badly affected by moisture. Magnesium-Teflon-Viton (MTV) flares have been used to protect aircraft from heat-seeking missiles as they emit very strongly in the infra-red region, this can produce severe burns and cause other materials to combust due to the large energy deposited with no visible flame.

1.4 Explosive Systems: The Explosive Train

Energetic materials are extensively used in munitions, both the type of energetic material and its function cover a wide range of masses and outputs. This can be seen clearly if we consider the amount of these materials contained in a number of munitions; a small arms round often has less than 1 g of propellant to drive the bullet, while a hand grenade would contain something of the order of a few tens of grammes to shatter and throw the casing; a large anti-tank mine would contain up to 25 kg of high explosive. Given this confusing array of systems it is easiest to think of the munition in terms of the explosive train (Fig. 1.2), which indicates the pre-requisites of munition system.

A variety of stimuli can be used to put the explosive train in motion such as standing on a mine, closing an electrical switch or activating a magnetic action. These actions input energy into an initiator. The initiator contains a material that is highly sensitive, combusting with ease. The main function of the initiatory system is to produce heat or a shock wave. In anti-personnel mines a common design is based on a simple crush switch where the pressure stabs a metal pin into a small metal thimble filled with a sensitive explosive.

From the point of view of weapon system design it is useful to keep the amount of initiatory compound as low as practical, otherwise the weapon could become very sensitive to being dropped, shaken or transported. For many systems a physical space or barrier exists between the initiator and the rest of the explosive system for the purposes of safety. This barrier is removed when the system is armed either manually or using an electrical/mechanical arming system. In the case of bombs and missiles the arming sequence occurs after the weapon has been launched to provide security to the user and launch platform.

The heat is transmitted either along a delay system or directly into a booster charge.

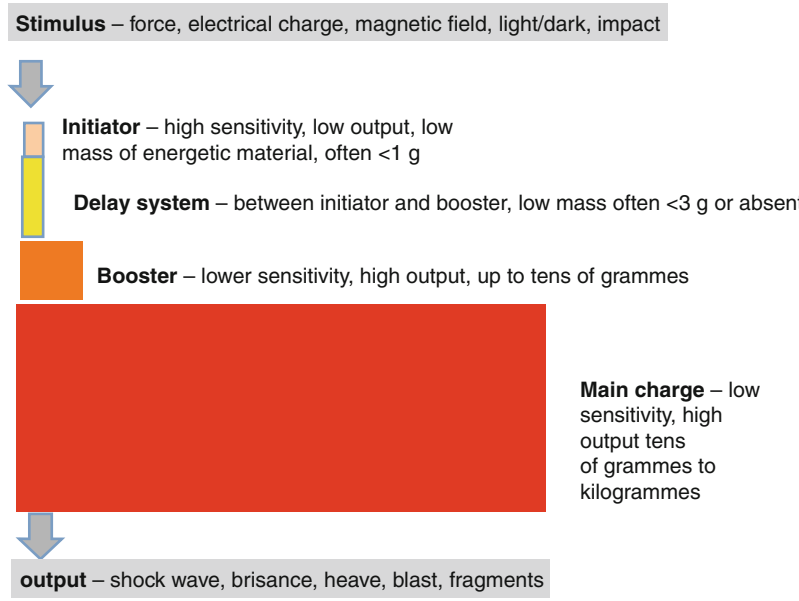

Fig. 1.2 The explosive train

The function of the delay is to burn for a known period of time allowing time for other processes to occur. These processes could be throwing a grenade or allowing a small propellant charge to 'bounce' a mine into the air. In many simple systems delays are not present.

The booster system consists of an explosive compound that is less sensitive than the initiatory compound but which will detonate due to the heat of shock wave from the initiator. The energy output of the booster is much higher than that of the detonator. The shock wave then transmits to the main charge.

The main explosive charge consists of a relatively low-sensitivity explosive composition that will detonate from the energy delivered by the booster. The mass of such main charges is extremely variable, however, the output from the main charge can be defined in terms of the outputs.

These outputs take the form of (a) shock waves transmitted into the immediate environment around the explosive, (b) the shattering of surrounding material, such as a metal case or rocks and soil, (c) the expansion of hot product gases, (d) the coupling of some of the explosive energy into the air, producing a blast wave, and (e) the aggressive acceleration of fragments, shrapnel or target vehicles and people.

1.5 Energy Levels and Energy Distribution

A rule of thumb in terms of thinking about the amount of energy output is to consider the order of magnitude of the energy and the materials involved. One gramme of propellant will produce 1 kJ of energy. Gases are about a thousand times less dense than solids and liquids. The temperature of the product gases can be easily 3000 K.

The result of this is that the 1 g of solid turns into 1 litre of gas if that gas were at room temperature, however, the gas is ten times hotter than normal atmosphere. This means that the 1 g of material turns into a gas that, if allowed to expand freely, would occupy 10 l. Alternatively it would take 10,000 atm to keep the gas from expanding. This order or magnitude calculation is for the less aggressive propellant materials.

Of the energy that is released by the energetic material the proportion that goes into different parts of processes is revealing. Again, a simple order of magnitude indicates that 20–30 % will go into the kinetic energy of the fragments, 60 % into the kinetic energy and temperature of the product gases while the remaining 10 % will be spread over a number of other effects, such as

the blast wave, fracturing of shell casings, or the motion of the ground.

1.6 Formation and Velocity of Fragments

Many munition systems have a casing, usually of metal or plastic, often with shapers to form specific fragments. Some systems have very thin casings, this is generally done to reduce the metal content of the munition, make it harder to detect. This also has the effect of increasing the blast effect as less energy is used in fragmentation and acceleration of fragments.

The initial effect of the detonation wave is to send a shock wave into the casing and produce a violent acceleration of the casing. Figure 1.3 shows the velocity profile from the outer surface of a copper cylinder subject to loading from the explosive filling. On the right hand side of this figure a schematic of the process of acceleration is shown. This diagram considers the motion of the wall of a cylinder filled with explosive, as the explosive detonates: the horizontal axis represents distance and the vertical axis time. The detonation products send a shock wave into the cylinder from the inner surface to the outer surface, this is represented by the black line with an arrow on it. A wave reflection takes place at the outer surface, sending a release wave back into the casing, towards the inner surface. This in turn is reflected from the inner surface as a shock. As this back-and-forth wave reflection process takes place each reflection represents the acceleration of the casing as it expands in a series of steps. As the casing is accelerated outwards it expands and becomes thinner. The diagram on the left also indicates the violence of this acceleration, the outer surface moves from rest to reach a velocity of 0.8 mm μs^{-1} (corresponding to 800 m s^{-1}) within 5 μs. More detailed discussion of how this can be calculated can be found in the specialised texts of the explosives engineering community, detonation symposia and shock physics literature. The total distance moved by the casing within this very narrow time window is only 0.6 mm. Thus the metal casing is subject to very violent acceleration, this causes fracture and fragmentation within the casing producing metal splinters moving at high velocity.

The study of fragments and fragmentation took a major step forward during the Second World War (1939–1945) with the scientific efforts placed in the service of militaries of industrialised nations. The two major steps are named after their main originators; Neville Mott and Ronald Gurney.

The number and size of metal fragments from a casing was addressed by the Mott fragmentation criteria. This is a statistical model based on the idea of a rapidly expanding ring of metal which contains imperfections which form the basis of fractures which eventually break the ring. As the ring breaks the stress inside the resulting fragment reduces and further fragmentation does not occur. This model was developed and populated in a semi-empirical fashion and the results of theory and experiment were then compared.

This model has been the subject of much development since the 1940s with much recent effort being given by Kipp and Grady in the USA. However, the original theory and Mott criteria are still regarded as valid and useful tools. Mathematically the fragmentation can be represented as;

$$N(m) = \frac{M_0}{2M_k^2}\, e^{-\left(\frac{m^{1/2}}{M_k}\right)} \tag{1.1}$$

N(m) is the number of fragments that are larger than mass (m), m the mass of a fragment, Mo the mass of the metal cylinder, and Mk is called the distribution factor which can be calculated from the following equation;

$$M_k = Bt^{\frac{5}{16}}d^{\frac{1}{3}}\left(1+\frac{t}{d}\right) \tag{1.2}$$

where B is a constant for the particular explosive-metal pair that is used, t is the cylinder thickness and d is the inside diameter of the cylinder.

The result of this was to produce a series of curves giving fragment size distribution. An example is shown below, in Fig. 1.4.

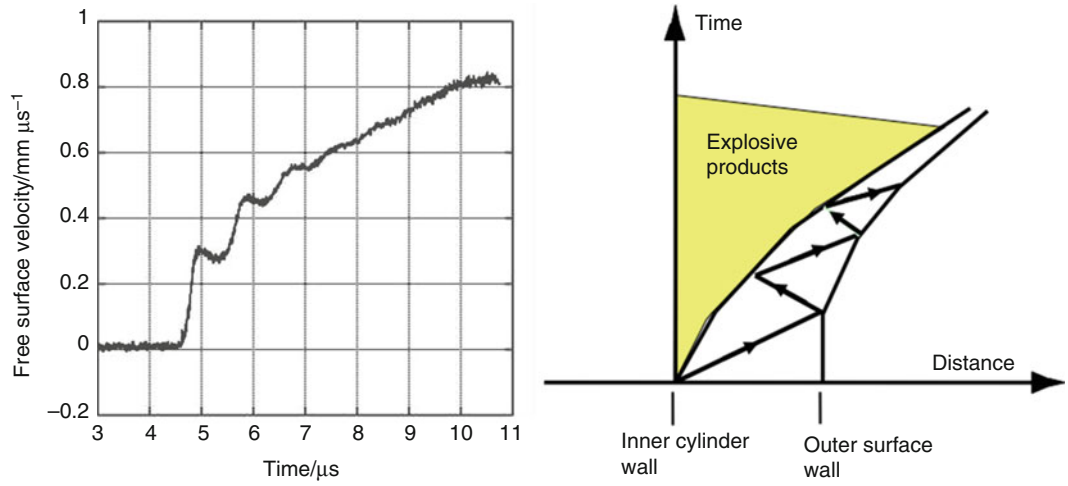

Fig. 1.3 *Left*: the velocity history of the outer surface of an explosively loaded metal cylinder. *Right*: a distance-time diagram of the wave processes taking place within the casing

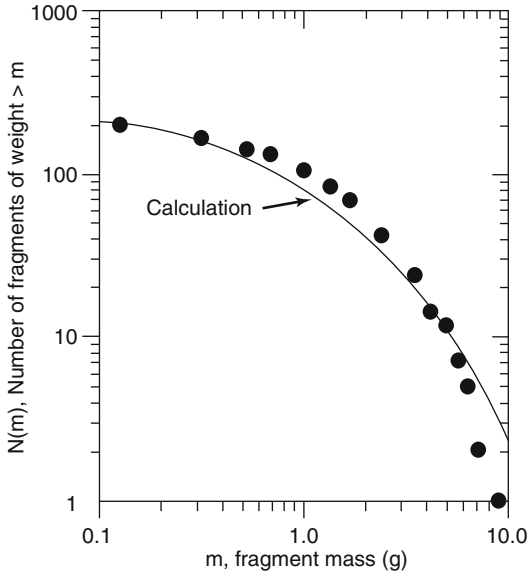

Fig. 1.4 Fragment distribution from an iron bomb (From Cooper, 1996)

The research of Gurney considered the balance of energy in the system, how much of the released energy would be captured by the metal casing and so predict the expected fragment velocity. In the derivation of the velocity the casing was assumed to remain intact. The shape of the explosive charge and the casing has a major effect; this work resulted in the production of a whole series of Gurney equations. In the equation below the expression is for the velocities achieved by explosive loading of a cylinder;

$$\frac{V}{\sqrt{2E}} = \left(\frac{M}{C} + \frac{1}{2}\right)^{-1/2} \tag{1.3}$$

C – is the mass of the explosive charge, M – The mass of the accelerated casing, and V – Velocity of accelerated flyer after explosive detonation. The term $(2E)^{1/2}$ - is the Gurney Constant for the explosive, it has the same units as velocity and is sometimes called the Gurney velocity. Each explosive has a particular value of Gurney constant and accounts for the coupling between the energy of the detonation products and the energy deposited into the metal casing.

While the two approaches may seem contradictory, one assuming fragmentation and the other an accelerated but intact material, using both approaches is useful due to the timescales of the initial acceleration and fragmentation. The energy delivery by the detonating material occurs very quickly giving the initial impulse, while fractures take time to develop and open sufficiently to allow the product gases to escape.

Overall the two approaches provide a reasonable and predictive approach to fragmentation and fragment velocity.

From this section it can be seen that explosives produce a violent acceleration producing a large number of small fragments and much fewer large fragments moving at velocities in the range from several hundred to a few thousand metres per second. These fragments can produce significant, life-threatening injury in themselves, irrespective of the blast wave associated with the explosive charge.

1.7 Shock and Stress Transmission

At this point the munition has detonated and a shock wave has passed through the casing, which is starting to move and fragment. In total time, a few tens of microseconds has passed since the main charge has started to detonate.

One effect that needs to be considered in some depth is ***the transmission of the stress waves between materials***. How does the detonation pressure transmit into the casing and then into the environment around the casing; what are the properties involved? What is the resulting velocity of material when it is subject to a stress wave?

In all cases of wave transmission it is important to consider what the type of the wave is, what the magnitude of the wave is, what are the properties of the material through which it is travelling and what is the change in materials properties across the interface.

1.7.1 Wave Type

Wave motion can be broadly defined into three classes, compression, tension and shear. Compressive waves are associated with positive stresses and pressures, tensile waves with negative stresses and pressures, while shear waves produce motion lateral to their direction of propagation. To think of the action of a lateral wave consider a pack of cards placed on a table, if you press down on the top card and move it sideways then the cards underneath will move sideways as well, each one not quite so much as the one above it, the resulting shape of the deck of cards is the result of shear. Shear waves produce the same kind of motion in materials.

The velocity at which the stress wave moves changes with stress level. For solids with strength at stress levels below that of the elastic strength, the velocity of the wave is the same as the sound speed in the material. For stress pulses that are above the strength of the material, the compression of the material results in the wave speed being higher than that in the uncompressed material, this is the definition of a shock wave.

Waves that take the stress down are called tensile waves, if the material is behaving elastically while if the material is dropping from a shock state, this is called a release fan.

There are differences between elastic waves and shock waves, the main difference being the significantly higher degree of compression and associated temperature rise associated with a shock wave. Similarly, tensile waves and release fans are different, however, for the purposes of space and clarity we will consider them to be approximately equal. There are a series of excellent texts dealing in more depth with shocks and wave propagation.

1.7.2 Magnitude of the Wave

The magnitude of the stress wave is defined in terms of its stress level. One factor that often leads to confusion in the field of stress propagation is the relationship between stress and velocity. The important thing here is to remember one of Newton's laws of motion – ***a body will continue in a state of rest or motion until acted upon by an external force*** (further description is found in Chap. 2). It is, therefore, perfectly possible to have a material or fragment moving at a high velocity under no external force and also easy to have a material under high pressure but not moving.

The basic equation to be defined is the relationship between stress, the volume through which it moves and the acceleration it produces in the material. The law to be considered here is

conservation of momentum; the product of mass multiplied by velocity.

The definition of stress (σ) is force (F) divided by the area (A) it acts over

$$\sigma = F/A \tag{1.4}$$

The mass (m) of the material that is affected by the passage of the wave is going to be the volume the stress wave has moved through multiplied by its density.

The volume (V) that the stress has swept through will be the area (A) multiplied by the velocity at which the wave moves (U_s) over the time window we are interested in (δt). The density of the material is represented by ρ.

So the mass that has been accelerated will be

$$m = V\rho \tag{1.5}$$

and from the argument above

$$V = A\ U_s\delta t \tag{1.6}$$

So the mass is

$$m = \rho\ A\ U_s\delta t \tag{1.7}$$

The final step is to consider the acceleration and the final velocity obtained. Here we use one of the fundamental equations representing the acceleration (a) produced by a force (F).

$$F = ma \tag{1.8}$$

Where the acceleration (a) is the change in velocity of the material (δu_p), sometimes this is called the particle velocity, over the time window we are considering (δt).

$$a = \delta u_p/\delta t \tag{1.9}$$

Combining these terms to relates stress to change in velocity we arrive at the equation

$$\sigma A = \rho\ A\ U_s\delta t\ \left(\delta u_p/\delta t\right) \tag{1.10}$$

Which simplifies to

$$\sigma = \rho\ U_s\delta u_p \tag{1.11}$$

This is one of the fundamental equations in shock physics, one of the so-called 'Rankine-Hugoniot' relations, where σ is stress, ρ is material density, U_s is the wave velocity, and δu_p is the change in material velocity.

The full set of these Rankine-Hugoniot relations can be found in the introductory texts by Meyers or Forbes (see Further Reading).

The fundamental property shown here is that the change in velocity produced by a stress wave is dependent on the density and the velocity of stress transmission through the material. At low stress levels the velocity at which a stress wave travels through a material is the same as the material's sound speed. At higher stresses, when a lot of force is applied as in an explosion, the velocity of the stress wave can be higher than the sound speed - a shock wave. From what we have stated earlier, a detonation wave moves through an explosive at a very high velocity, in fact a detonation wave is a shock wave that is driven and supported by the energy release of the chemical reaction.

The value of the density of the material multiplied by the wave speed is called the impedance (Z) of the material.

1.7.3 Impedance: The Property of the Material

In principle the value of impedance for low stress levels is easy to calculate, it is the product of the density multiplied by the sound speed in the material. Table 1.1 contains the density, sounds speeds and impedances of some common materials, air at 1 atm, water, iron and Perspex. All of these materials have been studied extensively and their properties are quite well known. The impedance of air changes strongly with pressure and is discussed in Sect. 1.8.1.

However, as the stress level in the wave increases then other properties such as strength and compressibility, become important. As the stress level increases so the amount of energy

Table 1.1 The density, sounds speeds and impedances of common materials

Material	Density/ kg m^{-3}	Sound speed at 1 atm pressure/m s^{-1}	Impedance/ kg m^{-2} s^{-1}
Tungsten	19,220	4030	77.4×10^6
Iron	7850	3570	28.0×10^6
Perspex	1190	2600	3.09×10^6
Water	1000	1500	1.50×10^6
Air	1.292	343	4.43×10^2

that is being deposited in the material will increase, some of this will result in increasing the kinetic energy of the material while another part of the energy will result in the material being compressed and becoming hot. The exact mathematics of this situation is complex and beyond the space available in this brief chapter, however, we can outline some simple conceptual guidelines.

The strength of a material is its ability to resist distortion; this strength will be different in compression, shear or tension (further details are included in Chap. 3). Materials with high strength tend to have high sound speeds as a result. Metals, in general have similar strengths in tension and compression, while rocks and ceramics are strong in compression but weak in tension. Granular materials have no tensile strength, but can have significant compressive strength. Given the three-dimensional jig-saw like nature of sand, the more you press down on the sand the harder it is to move it sideways (shear it).

Compressibility is the ability of a material to deform and is the inverse of strength. Highly compressible materials, foams, are often used to protect objects from impact, they do this because the energy of the impact is absorbed in locally distorting and compressing the material in the region of impact and not into globally increasing the kinetic energy of the foam. Sands, soils and granular materials absorb energy in a number of ways by grains deforming, grains fracturing and the particles moving together to fill the pores; these energy absorption mechanisms act to mitigate the shock or blast wave.

As the material compresses its density will change and its sound speed will tend to increase. At some point the amount of compression in the foam will result in the removal of the majority of the voids at which point the material will behave like a stronger, solid mass; there is a limit to energy absorption. Similarly all materials will have a yield point, where their strength is exceeded and they begin to deform and compress so there will be a change in how the energy in the stress pulse is deposited, more will go into temperature and into internal compression processes and less into velocity. In addition, time-dependent processes will also be occurring - the time for pores to collapse in foams and for particles to fracture in sands - so there will be a time dependence to the stress transmission.

The same issue of time dependence in the change of impedance, degradation of strength and interplay between kinetic energy and compressibility occur in biological materials. The impedance of the material will change through the stress pulse and so the simple equations given should always be used with caution and to produce estimates.

1.7.4 Wave Transmission Across Interfaces

When a stress wave reaches an interface it is the difference in the mechanical impedance of the materials which determines how much of the stress wave is transmitted and how much is reflected. By using conservation of momentum and the impedances of the materials the amount of the stress transmitted and that reflected can be calculated and the ***change in stress*** in the materials calculated. The result of this is given in the Eqs. (1.12) and (1.13)

$$T = 2Z_2/(Z_1 + Z_2) \tag{1.12}$$

$$R = (Z_1 - Z_2)/(Z_1 + Z_2) \tag{1.13}$$

Where T is the fraction of the stress transmitted, R is the fraction of the stress reflected, Z_1 is the impedance of the material through which the stress is originally transmitting, and Z_2 is the material on the other side of the interface. Three situations are shown in Fig. 1.5.

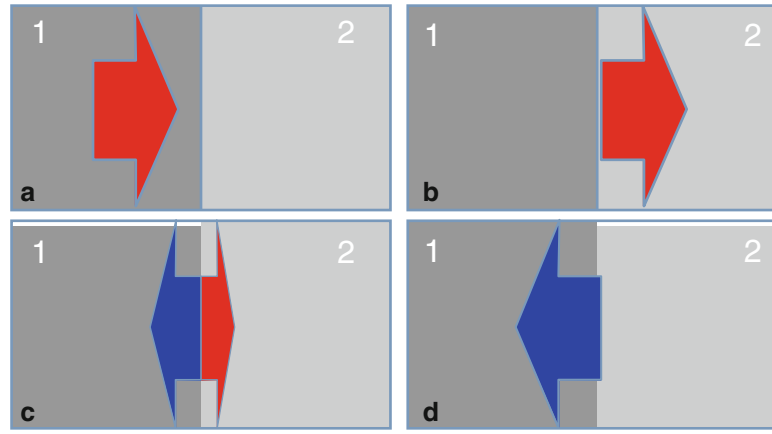

Fig. 1.5 Stress Transmission across the interface between two materials (**a**) a stress pulse approaches a boundary (**b**) If materials 1 and 2 have the same impedance the stress pulse is fully transmitted (**c**) if the materials 1 and 2 have comparable, but different, impedances the stress and energy of the pulse is partially transmitted and partially reflected (**d**) if material 2 has a very low impedance compared to material 1, virtually all of the stress pulse will be reflected back from the interface

Here it is important to remember that **stress, force and velocity are all vectors**, they have a magnitude and a direction. By convention we make an increase in velocity from left to right to be positive and right to left as negative. A wave which acts to compress a material will be regarded a positive stress and a wave which puts the material into tension or releases will be regarded as a negative change in stress.

In Fig. 1.5a a stress wave travels through material 1 of impedance Z1 towards an interface with material 2, impedance Z2.

Figure 1.5b shows what happens when the wave reaches the interface if the impedance of material 1 and 2 are the same: all the stress wave transmits through the interface. The value of the transmission coefficient is 1 and so the stress in material 2 is exactly the same as the stress level in material 1 i.e. both end up at the same stress. The amount reflected is 0 and so the stress in material 1 remains unchanged.

In Fig 1.5c the materials have impedances that are of a similar magnitude but different values: Z1 being half the value of Z2. Calculating the stress transmission and reflection coefficients gives $T = 4/3$ and $R = -1/3$. This means that that stress produced in material 2 is higher than that produced by the initial wave. This may seem odd, until it is remembered that impedance is related to density and sound speed, so material 2 in this case is denser and/or stronger than material 1; effectively material 2 slows down the motion of material 1 and the result is higher stress and less particle velocity.

While the transmitted force is still going in the positive direction it is higher by 4/3 over the initial stress in material 1. For the reflected portion there is a negative reflection coefficient and the wave is propagating in a negative direction, having a negative sign. Mathematically two negative numbers multiplied together equals a positive, so what this implies is that the amount of reflection means we have a stress change of +1/3 of the initial pressure ***adding*** to the initial pressure. The stress in material 1 increases as the denser, stronger material 2 prevents it from moving forward, effectively swapping a change in velocity for higher stress.

This reveals an important point: if surfaces remain in contact, the stress is the same in both sides of the interface. This is the basis of a technique called impedance matching used in shock physics to determine the stress and velocity of materials under the action of shock waves.

Materials with a high density and high sound speed will have a higher impedance and as a result will exert a higher pressure at a given impact velocity than a low density or low speed material. This explains why a much higher stress is produced by tungsten, a preferred material for

anti-tank weapons compared to the lower impedance iron, while Perspex will produce a much lower velocity.

In the case of Fig. 1.5(d), the impedance of material 2 is very low compared to material 1. In this case the change in the reflected stress is of value 1 and it is going in the negative direction. Following the argument above, this means it changes the stress by −1. This implies that stress change of the reflected wave cancels the stress of the original wave. In this case the stress falls to zero and the energy of the stress pulse accelerates material 1 to a higher velocity, approximately doubling the particle velocity.

1.7.5 The Solid: Air Interface

After the stress wave from the detonation has transmitted through the casing, accelerating it and ultimately shattering it, it is then transmitted through the surrounding soil and sand compressing and fracturing it. When the stress pulse arrives at the solid/air interface, from the transmission-reflection coefficient it is clear that the vast amount of the stress is reflected from the solid:air interface. This reflection is like the case in Fig. 1.5(d) discussed above, the velocity of the sand/soil particles double as the stress drops to zero. Sand/soil has a very limited tensile strength so the result of this is to throw the sand and soil from the surface as a cloud of fast-moving debris.

While the stress wave compresses the material, and ultimately results in a cloud of fast-moving debris, the product gases from the explosive devices are also pushing the soil and fragmenting the compacts formed by the stress wave. It is the expansion of the hot, product gases which results in the formation of the blast wave.

1.8 Blast Waves

The product gases have a velocity of approximately 2000 m s^{-1}, considerably higher than the sound speed in air, 330 m s^{-1}. The resulting high-pressure pulse of air is pushed outwards by the hot explosive products. In order to allow comparison between charges of different sizes and compositions, explosive engineers conducted experiments using the simplest scenario possible – a bare explosive charge in an empty, flat field. This has resulted in a large body of blast wave literature based around the classic 'Friedlander' blast wave form.

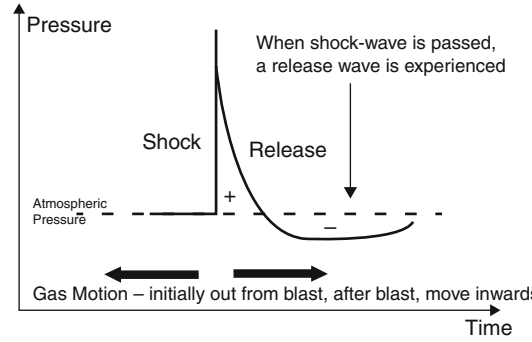

Fig. 1.6 The classic Friedlander form of a blast wave

Figure 1.6 shows the pressure time profile of this classic blast wave. After the initial rapid rise of the blast wave there is a region of positive pressure, accelerating outwards from the explosion. The speed of the gas moving behind the blast front, in the so-called 'blast wind', can be as high as 2000 km h^{-1}. This is followed by a release wave that drops the pressure below atmospheric pressure. The release occurs as both air and product gases have expanded outwards, away from the place where the explosion initiated. As a result, the explosive products have expanded and therefore performed 'work' on the surroundings and started to cool. This leaves a partial vacuum in the region of initial explosion and this lower pressure now causes air and gases to flow backwards over a longer period to equalise the pressure. The resulting push-pull movement experienced in the blast wave can be especially damaging to structures and humans.

This simple waveform was often observed in much early research into the effects of blast on humans. These studies used data either from open explosive ranges or with well controlled blast reflections from single walls or barriers. It is important to note that in a cluttered urban or vehicle environment, a casualty will experience a

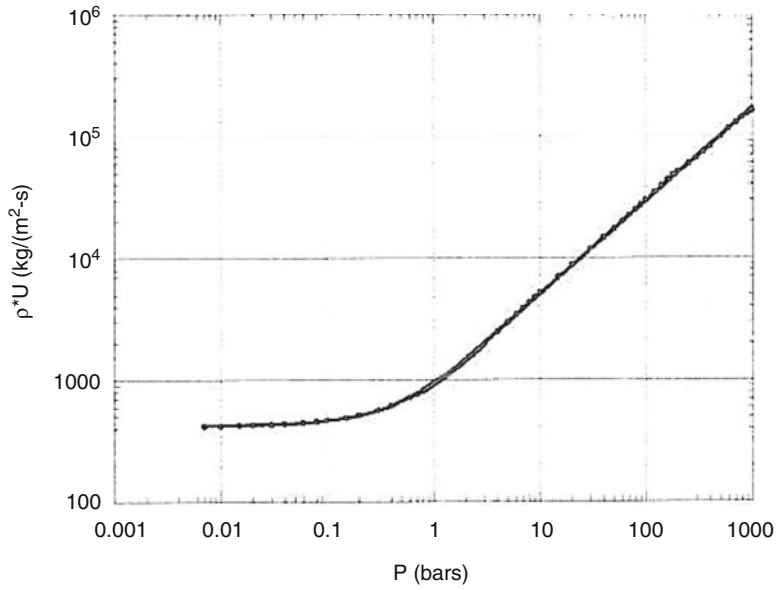

Fig. 1.7 The change in impedance of air with pressure

number of waves – those directly arising from the charge and those reflected from a wide variety of surfaces and arriving from different directions. In general the amount of reflected pressure waves can be equated to more damage and injury.

1.8.1 Change in Impedance of a Gas in a Blast Wave

In the discussion above the energy deposited in a material can manifest itself in a number of ways, it can give the material kinetic energy, for instance, and it can compress the material increasing its temperature.

In many engineering applications solids and liquid are often assumed to be incompressible. In shock wave studies this is not the case and compressions which halve the volume of the material are relatively common. However, gases are by comparison, very compressible. This means that blast waves are supersonic with respect to sound waves seen at low pressure, they also are associated with a very large change in impedance and often increase in temperature. Figure 1.7 shows the change in impedance of air with pressure. Atmospheric pressure is located at the point where the impedance increases sharply.

A major difference between shocks in solids and liquids and blasts is that blast waves from munitions tend to have durations measured in milliseconds, while shock waves in solids exist on timescales of microseconds. This 1000-fold difference in duration is why the relatively modest pressure seen in blast wave can produce more movement and damage than the much higher pressures in shock waves.

1.8.2 Reflected Waves

While the compression of the air produces a large change in impedance, it is still the case that the impedance of the compressed gas is very much lower than that of any solid or liquid. When the wave hits against a solid barrier, then a compressive pulse is transmitted and the stress in the gas also increases. Calculating the values of the reflected stress change, indicates that the stress level almost doubles.

In the case of an explosion in an enclosed space, or in the partially confined space below a vehicle there is time for multiple wave reflections, leading to complex blast wave-forms of widely differing stress histories. Within a vehicle the reflections add to the injuries seem, over and above the push-pull effect seen in the relatively simple Friedlander waveform (Fig. 1.8).

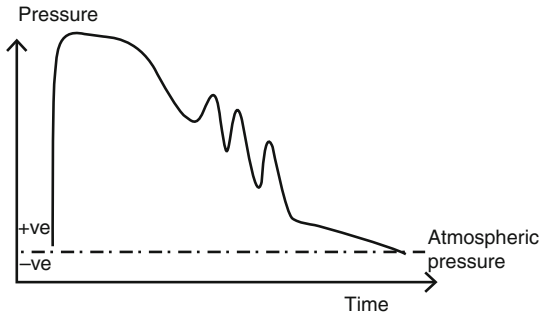

Fig. 1.8 Generic representation of a blast waveform seen inside a vehicle. The wave has many more peaks, plateau and overall variation than the relatively Friedlander waveform shown in Fig. 1.6

1.8.3 Temperature Rise

As well as the motion of the blast wave there is also an associated temperature rise. This can result in burns and combustion. Inside a vehicle the heat deposited into a material can be divided almost evenly between the heat from the intense light flash associated with the detonation or gas compression while physical contact with the hot gas deposits the other half of the energy. The timescale for this energy transfer is of the order of milliseconds.

Shock waves also result in significant heating within metals, even after the metal has been dropped back to normal stresses there may be a residual temperature increase in the fragments of over 100 °C. The timescale for this heating is on the order or microseconds.

1.9 Comparing Explosives Scenarios: Scaled Distance and TNT Equivalence

Munitions and explosive charges come in a range of sizes and vary in terms of materials. In the technical literature the term 'scaled distance' is often used to relate the effects of large explosive charges over tens of metres to those of small charges at close range. This is useful as it allows the effects of small-scale experiments to be extended to larger explosives charges.

The two terms used in virtually all scaling equations are (i) the explosive mass and (ii) the mathematical cube of the distance between the charge and the target, i.e. the increase in volume over which the energy is dispersed.

There are often other terms involved: one of the easiest to conceptualise is the distance of the charge above the ground.

If the charge is in mid-air the energy expands evenly in all directions, effectively spreading the energy through a sphere. However, if the charge is on the ground, the effects of wave reflection occur and the energy is concentrated into an expanding hemi-sphere, above the ground. Within the hemi-sphere so the energy, pressure *etc* is more or less doubled compared to that of the mid-air charge.

Another simple comparative scale between explosive types is that of 'TNT equivalence'. Historically TNT was a widely used material, which could be easily melted and cast into a variety of shapes, unlike many other explosive materials. Given its castable nature many experiment were conducted, resulting in large databases. TNT equivalence is a simple factor that allows a well-defined reference point for the broad comparison of the effects on a non-TNT explosive charge to be estimated.

1.10 The Three-Dimensional World and the Physical Basis of Blast and Fragment Injury

The real world has a complex topography and is made of a wide variety of materials many of which change their properties based on the accelerations produced in them by explosion. This somewhat mundane statement also indicates the difficulty of understanding the precise effects in terms of the materials and the three-dimensional world. However, a well-founded method is to take that complex situation and divide it into smaller, more tractable parts.

This chapter has given an overview of the basis of explosive technology and presented some of the basic processes relevant to the blast process. The importance of the detonation wave,

stress transmission, fragmentation, the ejection of sand/soil, expansion of the product gases, and flash heating have been introduced using simple first-order approximations.

The complexity of the mechanical processes and the resistance of the human body can result in injury patterns that show effects that are distant from the immediate blast or impact. However, it is increasingly possible to adopt an interdisciplinary approach that can bridge the vital mechanical-biological gap in our knowledge. Following chapters will address and expand on these issues.

Further Reading

Akhavan J. The chemistry of explosives. Cambridge: Royal Society of Chemistry; 1998.

Bailey A, Murray SG. Explosives, propellants and pyrodynamics. London: Brassey's (UK); 1989.

Batsanov AA. Effects of explosion on materials: modification and synthesis under high-pressure shock compression. New York: Springer; 1994.

Bhandari S. Engineering rock blasting operations. Rotterdam: A.A. Balkema; 1997.

Borovikov VA, Vanyagin IF. Modelling the effects of blasting on rock breakage. Rotterdam: A.A. Balkema; 1995.

Cherét R. Detonaton of condensed explosives. New York: Springer; 2011.

Cooper PW. Explosives engineering. New York: Wiley-VCH; 1996.

Forbes JW. Shock wave compression of condensed matter: a primer (shock wave and high pressure phenomena). Berlin-Heidelberg: Springer; 2013.

Fordham S. High explosives and propellants. New York: Pergamon Press; 1980.

Meyers MA. Dynamic behavior of materials. New York: John Wiley; 1994.

Biomechanics in Blast

2

Anthony M.J. Bull

2.1 Overview

Biomechanics is the study of biological systems from a mechanical perspective. In this discipline, the tools of mechanics are used in which the actions of force, motion, deformation and failure and their relationship to anatomy and functional aspects of living organisms are analysed. Traditionally biomechanics has been considered in terms of either biofluid mechanics or the biomechanics of connective tissues ("solid biomechanics"), where the former is a key branch of science and engineering that is applied to the cardiovascular and respiratory sciences and the latter is applied to orthopaedics and musculoskeletal rehabilitation. Other branches of biomechanics investigate the interactions between solids and fluids and these are applied in ocular and cellular biomechanics, or the biomechanics of the brain, for example.

These branches of biomechanics are typically associated with specific anatomical regions and physiology; for example, biofluid mechanics might focus on the effect of flow in the arteries and its relationship to cardiovascular disease, whereas connective tissue biomechanics might focus on the mechanical effect of ligaments at a joint and deal with their repair post injury.

A.M.J. Bull, PhD, CEng, FIMechE, FREng
Department of Bioengineering, Royal British Legion Centre for Blast Injury Studies, Imperial College London, London SW7 2AZ, UK
e-mail: a.bull@imperial.ac.uk

Biomechanics in blast is a key discipline in blast injury science and engineering that addresses the consequences of high forces, large deformations and extreme failure and thus relates closely to knowledge of materials science (Chap. 3) and leads onto the analysis of tissues (see Chap. 5) and, at the smaller scale, cells and molecules (see Chap. 4).

The aim of this chapter is to give the reader a basic understanding of biomechanics and its utility in the analysis of blast injuries. The specific objectives are to:

1. introduce fundamental terminology and concepts in biomechanics; and
2. describe how forces are transmitted through the human body at all loading rates, and hence provide an analytical framework to analyse forces on all relevant tissues and structures associated with blast injury.

2.2 Terminology in Biomechanics

2.2.1 Biomechanics of Motion

Kinematics is the "Biomechanics of Motion"; in other words, it is the branch of biomechanics that deals with the description of motion. It is most commonly used in the analysis of activities of daily living and sporting activities. In blast we consider the movement of the objects such as

A.M.J. Bull et al. (eds.), *Blast Injury Science and Engineering: A Guide for Clinicians and Researchers*,
DOI 10.1007/978-3-319-21867-0_2

blast fragments (secondary blast – see Chap. 6) and displacement or movement of the person due to blast and its interaction with objects such as vehicles (tertiary or solid blast – Chap. 6), where their movement is considered as *whole body* movement, or also takes into account the *relative* movement of different body parts.

Mass is how much matter an object contains. This remains constant regardless of location or gravitational conditions (for example, Earth, Mars or gravity in outer space). Weight, however, would vary under these three conditions. The importance of mass in blast biomechanics is that it represents the resistance to a change of linear motion (a speeding up or slowing down). This is important in blast when considering smaller fragments that are energised (small mass – secondary blast effects) by the blast when compared to larger items (a person or a vehicle – tertiary blast effects) that require more energy to get them moving. SI units of mass — kilogramme (kg).

A **Rigid Body** is an object that doesn't change shape. This is usually a major assumption in biomechanics, but serves to allow force analysis to be conducted (the subject of this chapter) prior to deformation analysis (the subject of subsequent chapters). Formally, a rigid body is a collection of particles that do not move with respect to each other. In a force analysis, the assumption is that however large a force may be, the rigid body does not deform. Obviously, this is an approximation in every case because all known materials deform by some amount under the action of a force. In the biomechanics of blast we tend to analyse the human body first as a series of rigid bodies (forearm, upper arm, head, trunk, shank, etc) that can move relative to each other and then secondly consider their deformation and failure.

Formulating problems in biomechanics in terms of the **Centre of Mass** (CoM) simplifies the problem to a single point. The CoM is the point on the rigid body that moves in the same way that a single particle containing all the mass of the object and is subjected to the same external forces would move. Therefore, when analysing the body, we consider this as a series of rigid bodies, each with a constant CoM. Clearly, the whole person will have a varying overall CoM when independent movement of each of the joints is taken into account and this is where rigid body biomechanics moves into the realm of dynamics.

The **Centre of Gravity** (CoG) is the point at which the weight of the body or system can be considered to act. In other words, it is the point at which the weight of the body, $W = mg$, should be applied to a rigid body or system to balance exactly the translational and rotational effects of gravitational forces acting on the components of the body or system. The CoG and the CoM are coincident when gravity is constant and are thus frequently used interchangeably. These points are important in biomechanics as they are used as reference points for calculations.

The **Moment of Inertia** is the rotational equivalent of mass in its mechanical effect; it is the resistance to a change of state (a speeding up or slowing down) during rotation. This is dependent on the mass of the object and the way the mass is distributed,

$$I = mr^2$$

where m is the mass and r is the distance of the CoM of the object from the axis of rotation.

The SI unit of moment of inertia, I is the kilogramme metre squared (kgm^2).

The moment of inertia is especially important in high loading events where the forces that are applied to the person are not applied directly through the CoM. This means that the forces produce a turning effect and thus cause the person, or body segment, to rotate. A high moment of inertia will resist that rotation. For example, a coat hanger that supports two heavy bags hooked in the middle of the hanger will have a smaller resistance to rotation than a coat hanger with the same two heavy bags hooked on either side of the hanger.

A **Torque** or **Moment** is the turning effect of a force (Fig. 2.1). This is calculated in mechanics by multiplying the magnitude of the force by its **moment arm**, or **lever arm** which is the perpen-

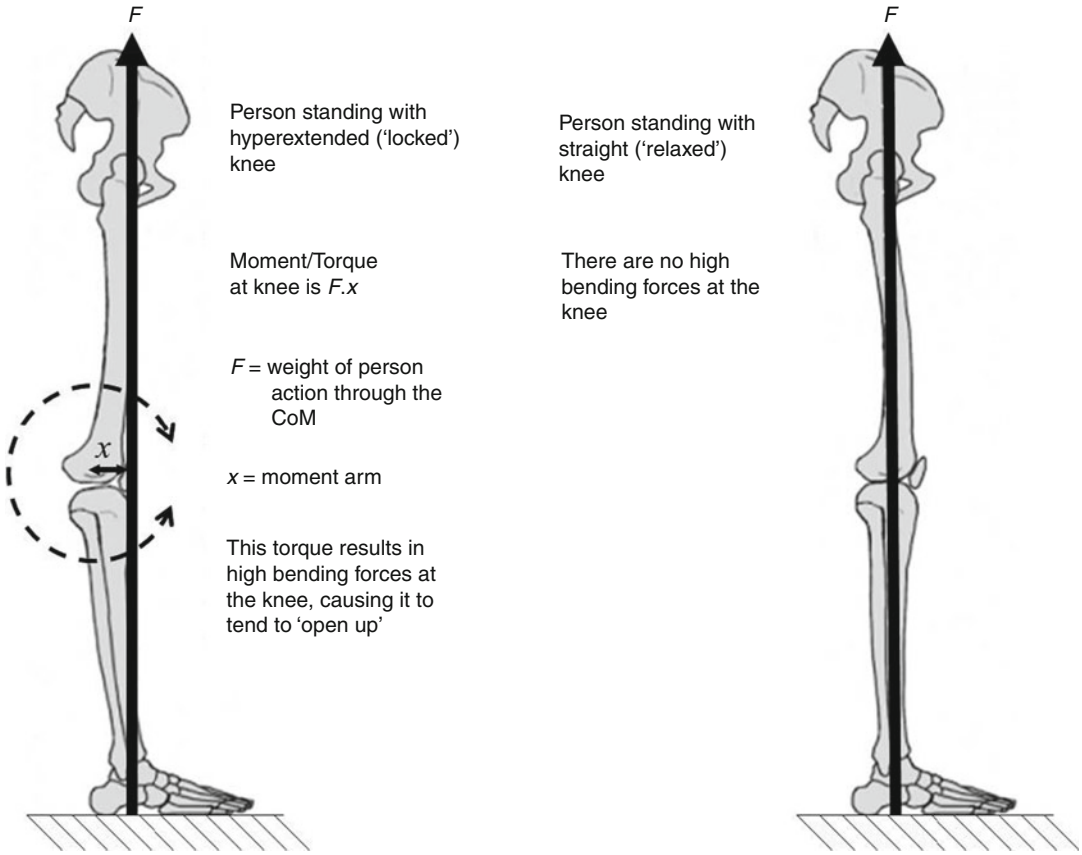

Fig. 2.1 Moment at the knee joint for different loading conditions

dicular distance from the point of application of a force to the axis of rotation. Therefore, a large force and a large moment arm will result in a large moment. As the forces in blast are extremely high, only a small moment arm will result in a large moment and thus cause angular (or rotational) acceleration of the person or body segment. In vector terms, the calculation is the vector (cross) product of force and distance. The SI unit of moment is the Newton metre (Nm).

Scalar quantities in biomechanics have magnitude only. For example, mass, length, or kinetic energy (described later) are scalar quantities and can be manipulated with conventional arithmetic.

Vector quantities in biomechanics have both direction and magnitude (Fig. 2.2). A force, for example, is always described by its magnitude and by the direction in which it is acting. Velocity is also a vector quantity because it expresses the rate of change of position in a given direction. This is experienced when going round a corner; a satellite orbiting at a constant speed (scalar) around the earth has a changing velocity (vector), because the direction of travel is moving.

This means that when performing calculations with vectors, ordinary arithmetic will give the wrong answers; therefore, vector addition and other types of vector algebra must be used.

Acceleration is the rate of change of velocity with respect to time (the first time derivative of velocity or the second time derivative of displacement). Acceleration is a vector quantity. Taking the satellite described above, the constant speed going round the earth reflects a change in velocity with respect to time and is, thus,

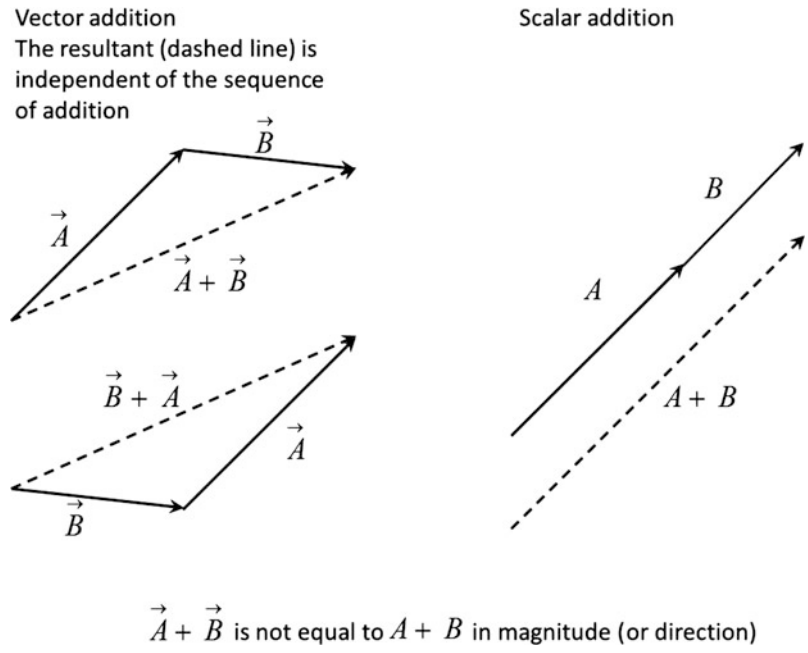

Fig. 2.2 Vector and Scalar addition

an acceleration towards the earth. An astronaut in the satellite will experience no acceleration when going in a straight line (constant speed and constant velocity), but will experience the acceleration going around the earth as a tendency to be moved away from the earth sideways. (Deceleration is simply negative acceleration and so is a term that is not normally used in biomechanics.) The SI unit of acceleration is the metre per second squared (ms^{-2} or m/s^2).

Angular Acceleration is the rate at which the angular velocity of a body changes with respect to time. The SI unit of angular acceleration is radians per second squared (radian s^{-2} or radian/s^2).

2.2.2 Forces

Force is a vector quantity that describes the action of one body on another. The action may be direct, such as the floor of a vehicle encroaching on the foot of an occupant, or it may be indirect, such as the gravitational attraction between the body and the Earth. Force can never be measured directly. It is always estimated, for example, by measuring the deflection of a spring under the action of a force. Measuring force, therefore, requires some knowledge of the deformation characteristics of materials (Chap. 3). The SI unit of force is the Newton (N).

At any one time, many forces may be acting on a body. The **Resultant Force** is the result obtained when all the forces acting are added vectorially and expressed as a single force (Fig. 2.3).

Equilibrium is when the resultant force and moment acting on a body are zero. In Fig. 2.3, if the blast force, *B*, were removed, then the forces *P*, *W* and *GRF* would be vectorially added to come to zero. Therefore, there can be equilibrium when no forces are applied to a body as well as where a combination of forces is applied to a body. This is also described in Chap. 1. Note that in blast the person, or object in proximity to the person, is rarely in equilibrium; the resultant force will be non-zero.

Weight is the force that results from the action of gravity on a mass; it acts through the CoG. Another term for this is **Gravitational Force**. When standing on weighing scales, weight is the force that the person applies on the scales

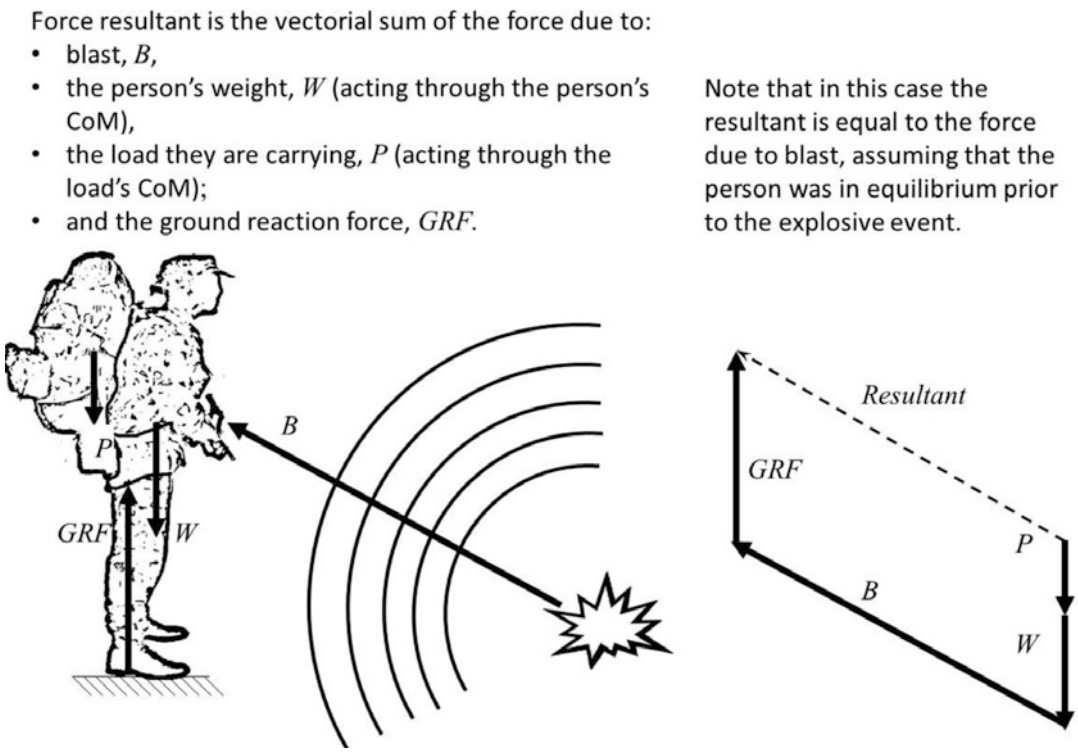

Fig. 2.3 Resultant force on a person under blast

when they are aligned perpendicular to the gravitational field, i.e. flat on the ground. This is equal and opposite to the force the scales exert on the person (Newton's third law – see section on Kinetics below).

Contact forces are the forces between objects in physical contact. The description of the force between the person and the weighing scales is a type of contact force.

Friction is a type of contact force that is often forgotten, yet can be overpowering in its effect. It is the tangential force acting between two bodies in contact that opposes motion or the tendency to motion. If the two bodies are at rest (resisting *tendency* to motion), then the frictional forces are called **static friction**. If there is motion between the two bodies, then the forces acting between the surfaces are called **kinetic friction**. Often kinetic friction is less than static friction, so when static friction is overcome, then the friction level reduces and the object accelerates. Friction is affected by many parameters, for example, the roughness of the surfaces or the presence or absence of fluid (and the type of fluid or pressured state of the fluid). Biomechanical analyses need to consider these different parameters; for example, there is friction without fluid (sometimes called *dry friction*) between your foot and the floor, and friction involving fluid (sometimes called *fluid friction*) acting within your knee joint when you move.

When fluid is not involved, the ratio of the magnitude of friction to the magnitude of the normal force is called the *coefficient of static friction* and shows the following relationship: $f = \mu P$, where f is the friction, μ the coefficient of friction, and P the magnitude of the normal force.

Taking the example in Fig. 2.3, the effect of friction at the feet has been neglected. For completeness, there will be static friction between the feet and the ground that will act to resist the movement of the feet to the left (backwards) and thus the effect of the blast force is to produce a friction force at the feet to the right that,

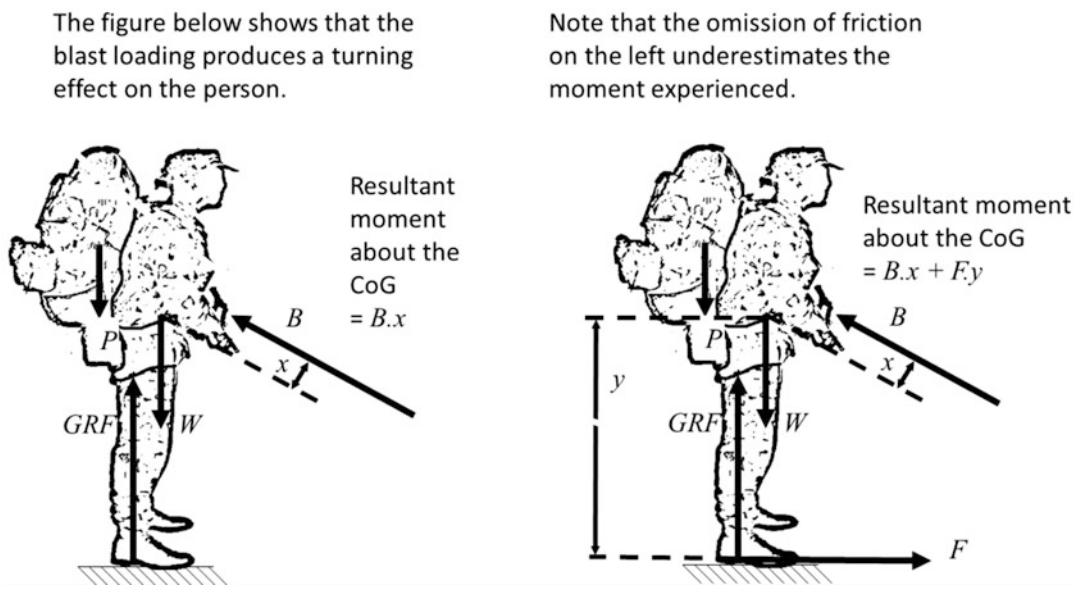

Fig. 2.4 Friction effects in blast loading. *GRF* ground reaction force, *W* weight of person and armour, *B* force due to blast, *P* weight of backpack

combined, will result in an anti-clockwise moment on the person (Fig. 2.4).

The **Joint Reaction Forces** exist between the articular surfaces of the joint, for example the forces between the surfaces of the tibia and femur at the knee joint. Joint reaction forces are the result of muscle forces, gravity, and inertial forces (usually, muscle forces are responsible for the largest part when under normal, physiological, loading; blast is a very different case – see Sect. 2.3).

Other types of contact forces are **Ground Reaction Forces** that specifically act on the body as a result of interaction with the ground. These are shown in Figs. 2.3 and 2.4. Newton's third law (see Sect. 2.2.3) implies that ground reaction forces are equal and opposite to those that the body is applying to the ground.

Pressure is the amount of force acting per unit area. Pressure is a scalar quantity. **Fluid pressure** is the pressure at some point within a fluid. There can be pressure within a fluid that is flowing in a pipe and **fluid dynamics** is used to analyse this pressure and flow. There can also be pressure due to the height of fluid. For example, a diver will experience an increase in pressure when diving to greater depth; this pressure is called **hydrostatic pressure**. The SI unit of pressure is the Newton per metre squared (Nm^{-2} or N/m^2).

Centre of Pressure (CoP) describes the centroid of the pressure distribution. It can be thought of as the point of application of the resultant force, because if all the forces across a surface were summed and their resultant taken, the CoP would coincide with the position of the resultant force acting across that surface. In the more general case, the force is applied over an area (for example, the plantar aspect of the foot or boot). In the example in Fig. 2.3, if we were to take away the blast loading, then the CoP at the boot would coincide with the line of action of the resultant force on the person, the GRF. Generally, when first conducting a rigid body analysis in blast, the CoP is considered as the point of force application. However, when deformations are being analysed, then it is important to also consider how the force is distributed. In biomechanics, the distribution of a contact force can be very important when considering conditions such as pressure sores, for example. Distribution of force is discussed in greater detail in Chap. 3.

2.2.3 Newton's Laws and Kinetics

Kinetics is the study of forces associated with motion. For example, kinematics and kinetics will be used to analyse the muscular contraction forces that are required to produce movement, or to analyse the sequence of movement for optimal performance. The key laws that form the basis of conventional mechanics are Newton's Laws.

Newton's First Law states that a body will maintain a state of rest or uniform motion unless acted on by a net force. If there is no resultant force acting on an object then that object will maintain a constant velocity. In cases where the velocity is zero, then the object is not moving ("remains at rest"). If the resultant force is not zero, then the velocity will change because of the force. Newton's First Law is often described as the Law of Inertia.

Whereas Newton's First Law describes what happens when the resultant force is zero, **Newton's Second Law** describes what happens due to a non-zero resultant force and how the velocity of the object changes. This law defines the change in force as being equal to a change in momentum per unit time. Rearranging this definition results in the formal definition of **momentum** described below. The second law also states that the change in momentum will be in the direction of the resultant force, so you see why it is important when analysing rigid bodies to be able to quantify the resultant force. Newton's Second Law is often described as the Law of Momentum. The second law is frequently stated as, "Force equals mass times acceleration"

$$F = ma$$

This is rigorously derived from the formal statement of the law regarding momentum. We won't go into that here, but the mathematics works out to allow the second law to be restated as, "The force acting on a body is equal to the mass of the body multiplied by its acceleration." Newton's Second Law is the basis for formulating the equations of motion, the formulation of the impulse momentum relationship, and, more fundamentally, defines the units of force.

Newton's Third Law is the Law of Reaction; it states that action and reaction are equal and opposite and is shown by the earlier examples, for example, someone standing on weighing scales. The force the person applies to the scales is equal and opposite to the force that the scales apply to the person.

Impulse is the effect of a force acting over a period of time. Impulse is determined mathematically by the integral of the force-time curve, the area under the force-time curve. Impulse is important in blast as the forces due to blast vary significantly with time and often act for a very short period of time. The impulse (area under the curve) due to a Friedlander curve blast (Fig. 1.6) is very different from the impulse due to blast wave reflections inside a vehicle (Fig. 1.8). Therefore impulse is a useful single measure that quantifies this difference without describing the full wave form. The SI unit of impulse is the Newton second (Ns) that reduces to kgm/s.

Linear Momentum is the product of the mass of an object and its linear velocity. Its units are the same as those for impulse (kgm/s).

Newton's second law allows us to quantify the effect of a force on the velocity of an object. If we take $F = ma$ and multiply both sides by time, t, then we end up with $Ft = mat$. Now

$a =$ the change in velocity over time $= \frac{\Delta v}{t}$, so we can rewrite our equation to be: $Ft = m\frac{\Delta v}{t}\, t$,

i.e. $Ft = m\Delta v$.

This is the **impulse-momentum relationship** and states that the change in momentum experienced by a body under the action of a force is equal to the impulse of the resultant force: Impulse = Change in Momentum. When calculating the effect of blast we seek to know how the force is changing over time and integrate that over time to calculate the impulse. This then allows us to see how the momentum of the displaced person or object changes and allows a forensic examination of the blast scenario.

Angular Momentum is the rotational equivalent of linear momentum; it is the "amount of motion" that the body possesses during rotation. Computationally, it is the product of the moment of inertia and the angular velocity:

angular momentum $L = I\omega$

Because angular momentum is a vector quantity, it can be resolved into components. It is possible to have angular momentum about one axis and none about another. Through algebraic manipulations angular momentum can be transferred from one axis to another.

A projectile (for example a bullet or blast fragment) may have both angular and linear momentum. As it travels it will have mass and linear velocity. However, it might also be spinning about its long axis (this is often desirable to reduce sideways turning of the projectile) which means that it will also have angular momentum about its long axis. In addition, the projectile may be tumbling end over end, meaning that it has angular momentum about an axis perpendicular to its long axis. These two components of angular momentum can be summed algebraically to give its total angular momentum. The SI units of angular momentum are kgm^2/s.

Work is done when a force moves an object. This is strictly defined as the integral of force with respect to distance:

$$W = \int F dx$$

If the force is constant then $W = Fd$, where d is the distance over which the force acts. Note that the definition of work is independent of time. Thus, the same amount of work is done in going up the stairs slowly or quickly. The power in these situations is not, however, the same. The SI unit of work is the Joule (J)

Power is the rate of doing work – the derivative of work as a function of time:

$$P = \frac{dW}{dt}$$

Average power is equal to the work done divided by the time during which the work is being done: $P = \frac{W}{t}$. The SI unit of power is the Watt (W)

Energy is the capacity for doing work. In any system, this capacity cannot be destroyed, but energy can be transformed from one form to another (this is a statement of the Principle of Conservation of Energy). There are many different forms of energy, for example, kinetic energy, potential energy, strain energy (all three are defined below) and heat. The units of work and energy are the same – the Joule (J) – because of the relationship of these two quantities through the work-energy principle.

Kinetic Energy is that component of the mechanical energy of a body resulting from its motion and can be split up into two constituent forms, just like acceleration (linear and rotational), forces (force and moment), and impulse (linear and angular momentum).

These are **kinetic energy of translation**: $KE_{xion} = \frac{1}{2}mv^2$ and **kinetic energy of rotation** $KE_{rot} = \frac{1}{2}I\omega^2$

Heat (or heat energy) is a form of kinetic energy in which particles within a material, substance or system transfer their kinetic energy to each other. It is always in defined in terms of the transfer of energy from one system to another, not in terms of the energy contained within systems.

Potential Energy is the energy of a body resulting from its position. Clearly the reference point for this is important and therefore potential energy is always quantified according to an arbitrary datum and can therefore assume any value depending on the choice of said reference point. Note that the change in potential energy is important in biomechanical analyses and this is independent of the choice of a reference point. Potential Energy, $PE = mgh$ where m is the mass, g is the acceleration resulting from gravity, and h is the distance above the datum.

Strain Energy is the energy stored by a system that is being deformed. The energy is released when the load that is causing the deformation is removed. Although this chapter does not go into deformation in any great amount, it is worth noting that strain energy is important in some loading conditions, for example, the energy contained within a bungee cord when fully

stretched, or the energy stored in a trampoline with someone standing on it.

The **Work—Energy Principle** states that the work done on a body is equal to the change in the energy level of the body. This principle is used widely in forensic blast analysis where the work done is visible and can be analysed through the structure or person's deformation or gross movement and thus the change in energy can be quantified. $W = \Delta KE + \Delta PE = \left(KE_f - KE_i\right) + \left(PE_f - PE_i\right)$, where f represents the final state and i the initial state.

Fluid Mechanics is the study of forces that develop when an object moves through a fluid medium. This medium can be a fluid like blood, but also very importantly in blast, this can be air (if free field blast, for example), or water (torpedo strikes, for example). In many cases of loading fluid forces have very little effect on kinetics and kinematics, yet in other cases these can be significant. For example, a shot put will not experience significant forces due to the air, yet a shuttlecock in badminton will be significantly affected by the air through which it travels.

Drag is one of the most important forces produced by a fluid. It is the resistive force acting on a body moving through the fluid. The **surface drag** depends mainly on smoothness of surface of the object moving through the fluid. Practical examples of this include shaving the body in swimming or wearing racing suits in skiing and speedskating to reduce the surface drag. **Form drag** depends mainly on the cross-sectional area of the body presented to the fluid; this is why cyclists have a crouched position rather than sitting upright when trying to go fast.

Because fluids can flow, the influence of the fluid on a body moving through it depends not only on the body's velocity but also on the velocity of the fluid. Walking headlong into a stiff wind requires more force than standing still facing the same stiff wind. Walking with the wind reduces the force required. This is amplified to an extreme level in primary blast where the fluid (air) travels at extremely high speeds.

Of course, the human body is filled with different fluids and therefore fluid mechanics effects are apparent internally as well as externally.

2.2.4 Functional Anatomy

In biomechanics, the term **functional anatomy** is used to describe the physical function of the biological structure of interest. This means that this requires knowledge of the loading on the structure, the constituent materials of the structure and their shape. In the human body the constituent materials are complex. For example, biological fluids include protoplasm, mucus, synovial fluid and blood; these are described in more detail in see Chap. 3. Solid material constituents include actin, elastin and collagen. How these combine to give material properties are described in see Chap. 3.

An example of functional anatomy is that of articular cartilage which describes the interrelationship between its shape, constituent materials, loading and motion environment, wear, deformation and pathology.

Articular Congruency is the description of how the two surfaces of a joint overlap one another. A hip joint, for example, is highly congruent in that the full surface of the spherical femoral head is in contact with the full surface of the acetabulum. This congruency allows efficient transfer of load from one articular surface to the other. The glenohumeral joint of the shoulder is incongruent in that the spherical humeral head has a very small contact area with the virtually flat glenoid. Other terms used are "conforming" and "non-conforming". (Note that there is a physiological reason for this difference in congruency; the hip joint has a smaller range of motion than the glenohumeral joint.)

2.3 Biomechanics of Force Transmission

There are multiple sources of force and deformation in the human body. Within blast, the main sources are gravity (weight), posture (deformation of tissues due to the seated/standing position), pressure (through the shock wave), and impulse (through contact with an external agent). These *external* sources result in *internal* forces, stresses and deformations.

Newtonian mechanics are used to understand these internal forces, and then fluid mechanics and stress analysis is used to understand stresses, deformation and flow. The construct used to understand these forces is a **Free Body Diagram**. In this, the region of interest is outlined and all the external forces acting on that region are identified and quantified (Fig. 2.5). Frequently such analyses are conducted where the regions of interest are in equilibrium. As described previously, in blast, the person is rarely in equilibrium and is moving and therefore a free body diagram analysis must be conducted at different time points.

2.3.1 Muscles Forces

The main purpose of a muscle is to rotate a joint against a force. This rotation is produced by a *torque*, or *moment*, therefore, the joint torque is the key mechanical parameter that muscles need to produce. Muscles attach very close to the joint centres of rotation and therefore their *lever arm* is small. Normally the external force is applied further away from the joint centre of rotation and therefore it has a large *lever arm*. Using

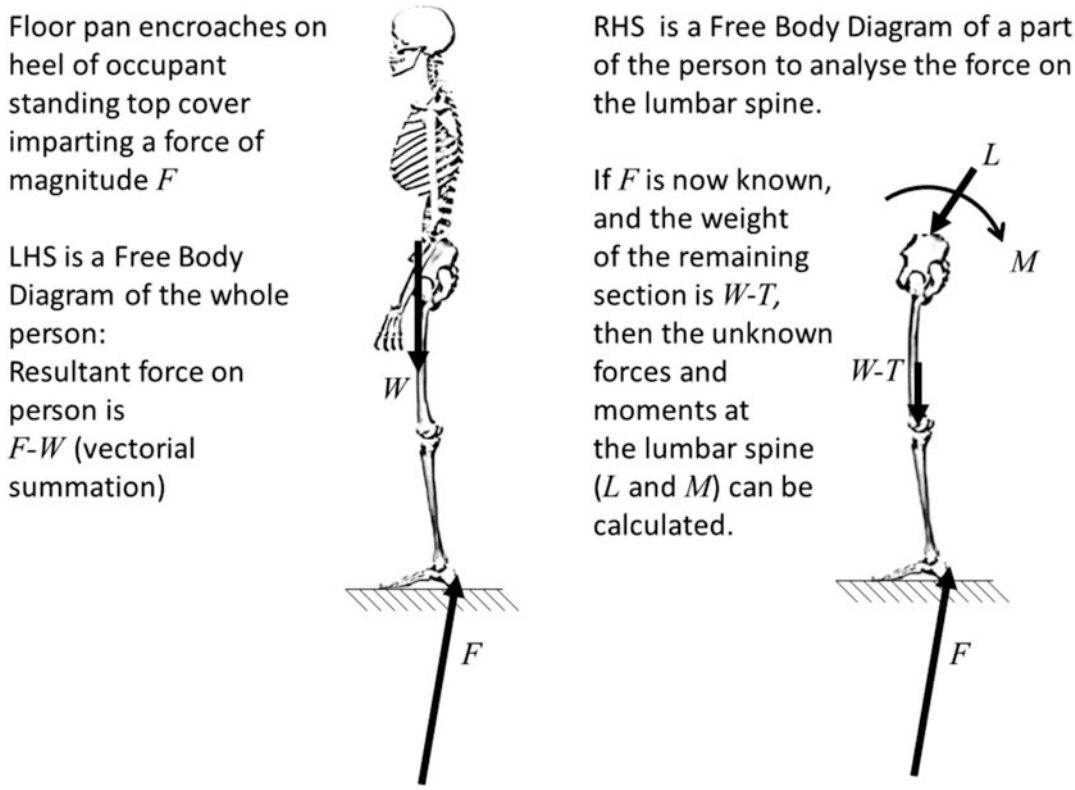

Fig. 2.5 Different free body diagrams under the same blast loading situation at time $t = 0$. These demonstrate that the appropriate choice of a free body diagram can allow internal forces to be quantified

Newtonian mechanics, we find, therefore, that forces in muscles during normal movement are orders of magnitude greater than the externally applied force.

Musculoskeletal Dynamics is the engineering tool that is used to quantify muscle forces during activities. Because very few loading scenarios can be simplified to that in Fig. 2.6 in which only one muscle force acts and an analytical solution to the problem can be found, other approaches need to be taken to quantify muscle forces in more complex situations. Musculoskeletal dynamics using biomechanics is described in this chapter and outlined in the flow chart in Fig. 2.7

Initially kinematics is used to quantify the motion of the person. The motion of each part of the person, each segment, is analysed separately. The data input for this can be video analysis or the use of optical motion tracking such as is used in the computer graphics industry. The output of this is the position, velocity and acceleration (linear and rotational) of each body segment.

This information is combined with estimated knowledge of the mass and moment of inertia of each part of the person (each "segment") as well as estimates of the external forces acting on each segment. For example, knowledge of the deformation of the floorpan of a vehicle can give an estimate of the force that such a deformation would apply to the foot segment. All of this information is brought together using inverse dynamics in which knowledge of the kinematics and forces on the body are applied to quantify the moments and forces between each body segment. These are called "intersegmental forces and moments".

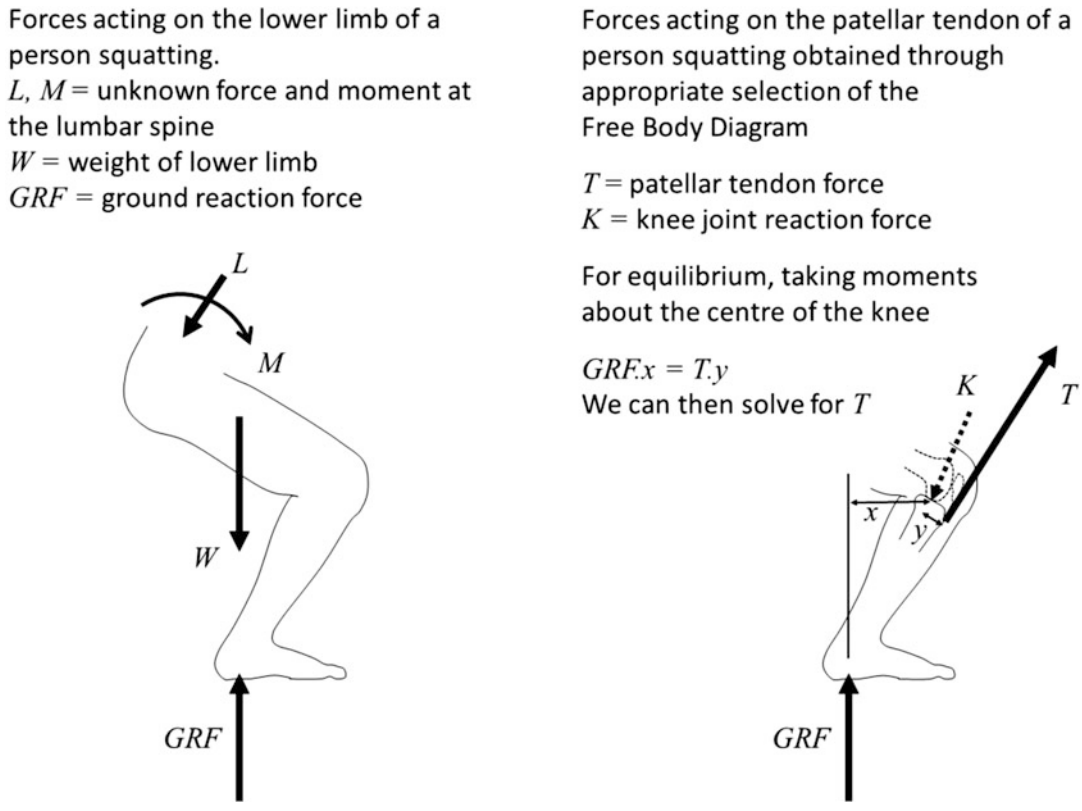

Fig. 2.6 (**a**) Forces acting on the lower limb when squatting. (**b**) Force in the patellar tendon in a simple squat. The force is much higher than the external load due to the lever arm effect ($x > y$)

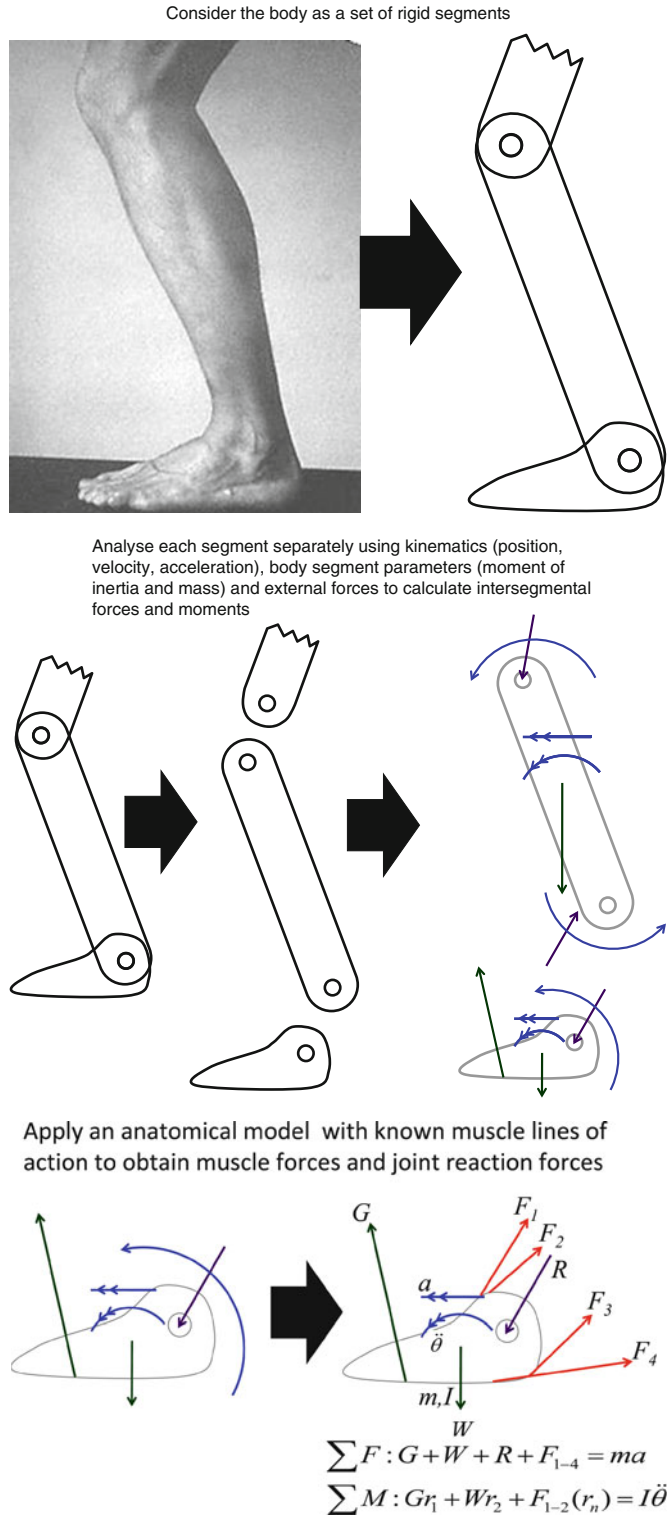

Fig. 2.7 Musculoskeletal dynamics: from motion to muscle forces. *Straight lines* with *single arrows* represent forces (GRF, weight and intersegmental forces); *single arrow curved lines* represent intersegmental moments; *double arrow lines* represent linear and angular accelerations of the body segments

Finally, the intersegmental forces and moments are combined with an anatomical model of the physiological joint (the ankle, in this case) in which the articular geometry, ligament geometry and muscle lines of action are known. The equations of motion are then solved whereby the sum of all the muscle and ligament forces gives the true joint reaction force and then the sum of all the moments due to the muscles (the product of the muscle force times its moment arm about the joint centre of rotation) gives the intersegmental moment which is known from the previous step in this technology. What is apparent is that there are many more unknowns than equations to solve the unknowns as there are many muscles crossing each joint. Numerical methods, termed "optimisation techniques", are used to solve this set of equations and the output of this is the muscle forces, ligament forces and joint reaction forces at the joints of interest [1]. There are three leading software technologies available to conduct musculoskeletal dynamics analysis (OpenSim [2]; AnyBody [www.anybodytech.com/]; Freebody [3]).

2.3.2 Forces in Joints

Once the muscle forces during a loading activity are known (as shown above), then the loading on all the other tissues of the joint can be characterised using additional free body diagrams. The example below (Fig. 2.8) shows how an understanding of the muscle forces at the knee allows quantification of the loading in the anterior cruciate ligament (based on its geometry) and the articular cartilage.

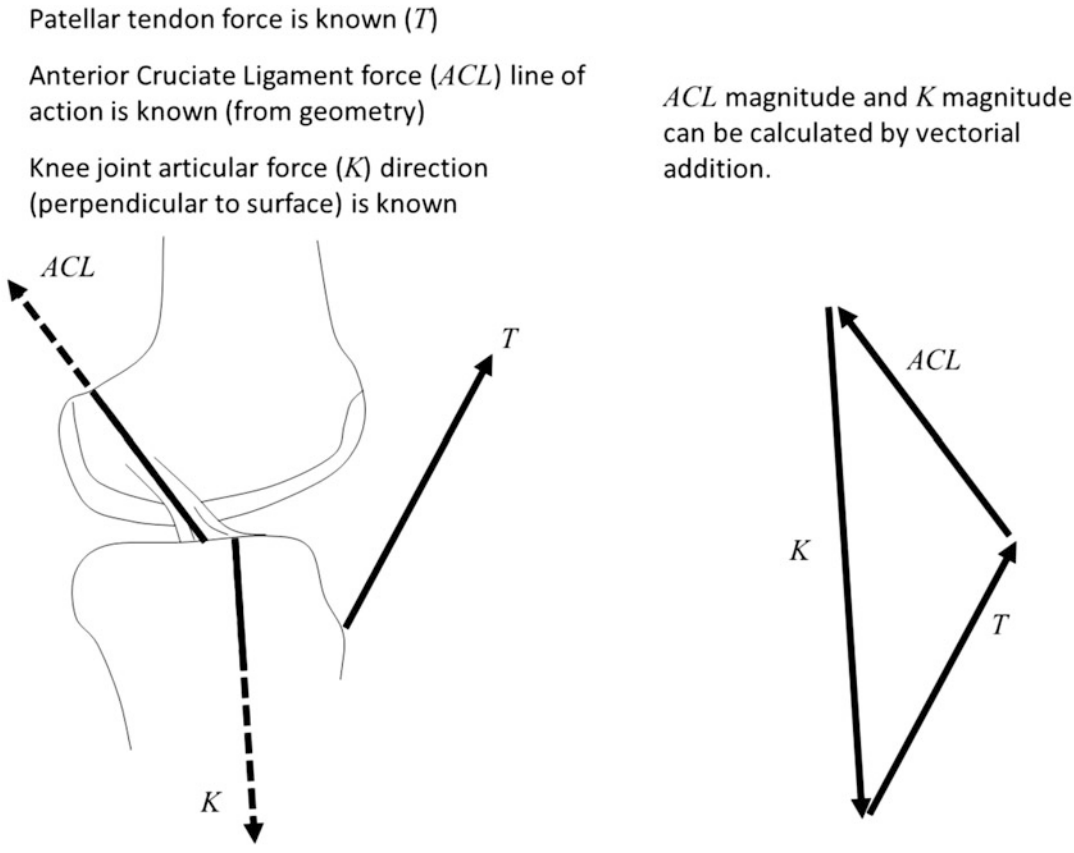

Fig. 2.8 Forces in tissues of the knee joint

The cartilage loading at the knee is then distributed over an area. A congruent joint will distribute that over the full articulating area, however, an incongruent joint will distribute that over a very small area. The analysis of how forces are distributed within a tissue or structure is called **stress analysis** and is described in Chap. 3.

What will become apparent in this simple analysis is that, because of very complex three dimensional structures, it becomes impossible at some point to analyse internal forces in the human body without some computational help. In addition, as the structures deform, so the loading on them changes due to the geometrical change. At this point computational biomechanics takes over. In computational biomechanics the same methods are used as described here, but numerical techniques are used to solve the free body diagrams for all tissues and all *parts* of tissues. At this point loading analysis and stress analysis (that accounts for deformation as well) become the same and this is the subject matter described in Chap. 17 of Part III.

2.4 Bringing It all Together: Forensic Biomechanics of Blast

The basic biomechanics described in this chapter allows for a simple analytical framework to be devised for analysing loading on the human body due to blast. Although the framework is simple, the application of this is not so straightforward due to lack of information about key aspects of the blast situation. Despite these deficiencies in data, the literature has countless examples [4] of the use of biomechanics to analyse blast loading and many of these are presented in this book. Generalising the approaches taken in the literature to a single framework is nigh on impossible and therefore the tactic taken in this book follows closely that presented in Ramasamy et al. [5] in which incident and clinical data is combined with biomechanics utilising imaging, computational models and physical models in order to understand pathophysiology of blast injuries to then devise better protection, mitigation, medical treatment and rehabilitation (Fig. 2.9).

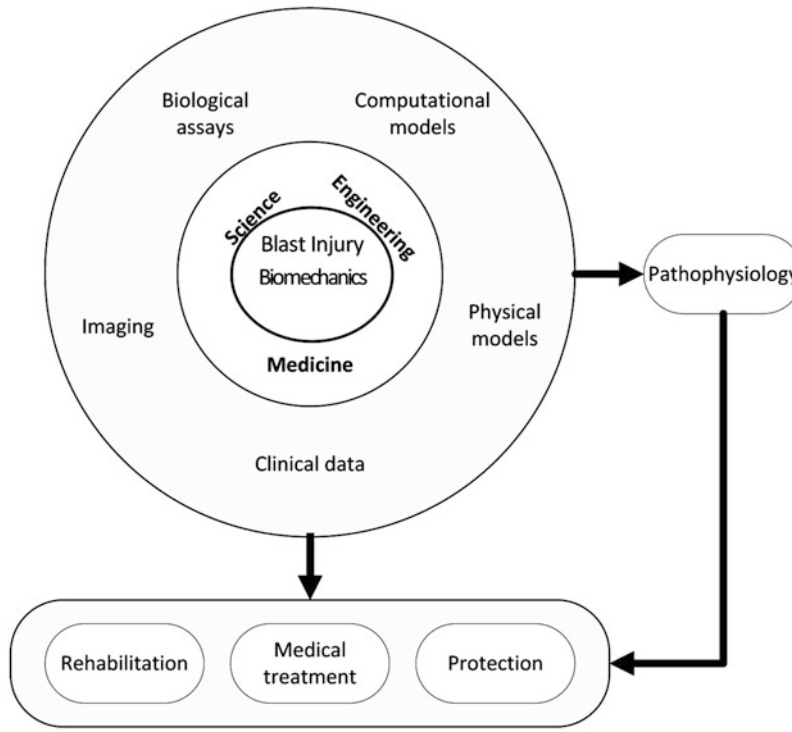

Fig. 2.9 Research approach for analysing blast injuries with biomechanics as the core discipline for much of the work

References

1. Cleather DJ, Bull AMJ. An optimization-based simultaneous approach to the determination of muscular, ligamentous, and joint contact forces provides insight into musculoligamentous interaction. Ann Biomed Eng. 2011;39:1925–34.
2. Delp SL, Loan JP, Hoy MG, Zajac FE, Topp EL, Rosen JM. An interactive graphics-based model of the lower extremity to study orthopaedic surgical procedures. IEEE Trans Biomed Eng. 1990;37:757–67.
3. Cleather DJ, Bull AMJ. The development of a segment-based musculoskeletal model of the lower limb: Introducing FreeBody. R Soc Open Sci. 2015;2: 140449.
4. Ramasamy A, Hill AM, Masouros S, Gibb I, Bull AMJ, Clasper JC. Blast-related fracture patterns: a forensic biomechanical approach. J R Soc Interface. 2011;8: 689–98.
5. Ramasamy A, Masouros SD, Newell N, Hill AM, Proud WG, Brown KA, Bull AMJ, Clasper JC. In-vehicle extremity injuries from improvised explosive devices: current and future foci. Philos Trans R Soc B. 2011;366:160–70.

Further Reading

Benham PP, Warnock FV. Mechanics of solids and structures. London: Pitman Publishing; 1973.
Benham PP, Armstrong CG, Crawford RJ. Mechanics of engineering materials. New Jersey: Prentice Hall; 1996.
Fung YC. Biomechanics. Mechanical properties of living tissues. New York: Springer; 1993.
Ozkaya N, Nordin M. Fundamentals of biomechanics. New York: Springer; 2012.
van Mow C, Huiskes R. Basic orthopaedic biomechanics and mechano-biology. Philadelphia: LWW; 2004.

Behaviour of Materials

3

Spyros Masouros and Dan J. Pope

3.1 Introduction

The aim of this chapter is to introduce the reader to the mechanical behaviour of materials. The term mechanical behaviour refers to the response of materials to load; under load the material will deform and possibly break. Various materials are considered, including biological. Engineering measures by which we quantify and model mathematically the behaviour of materials in static and dynamic conditions are presented.

3.2 Materials

Advancements in material science and engineering have been the vehicle of success in industry for solving human-centred problems and improving the quality of life. A traditional classification of types of materials is the following:

- Metals
- Non-metallic inorganic materials (for example ceramics and glass)
- Organic materials (polymers)
- Composite materials (combinations of the above)
- Biological materials (living tissue)

The first four categories comprise a selection of materials used in industry. An integral part of the design process for products, equipment and infrastructure is the selection of such materials as appropriate for the application. The study of these materials has been extensive with composite materials being the latest addition to the list in the twentieth century (Fig. 3.1). Human injury and disease and the interaction of the body with industrial materials spawned the comprehensive study of biological materials and their behaviour in the second half of the twentieth century.

3.2.1 Metals

Metals are inorganic substances that consist of a highly ordered microstructure. All metals have similar physical and material properties, exactly because of their 'metallic' microstructure. Some of these properties are summarised below:

- They are solids at room temperature (except for Hg).
- They have high density.
- They are good conductors of heat and electricity.

S. Masouros, PhD, DIC, CEng, MIMechE (✉)
Department of Bioengineering, Royal British Legion Centre for Blast Injury Studies, Imperial College London, London SW7 2AZ, UK
e-mail: s.masouros04@imperial.ac.uk

D.J. Pope, BEng (Hons), PhD, CEng, FICE
Dstl Porton Down, Salisbury SP4 0JQ, UK
e-mail: djpope@dstl.gov.uk

A.M.J. Bull et al. (eds.), *Blast Injury Science and Engineering: A Guide for Clinicians and Researchers*,
DOI 10.1007/978-3-319-21867-0_3

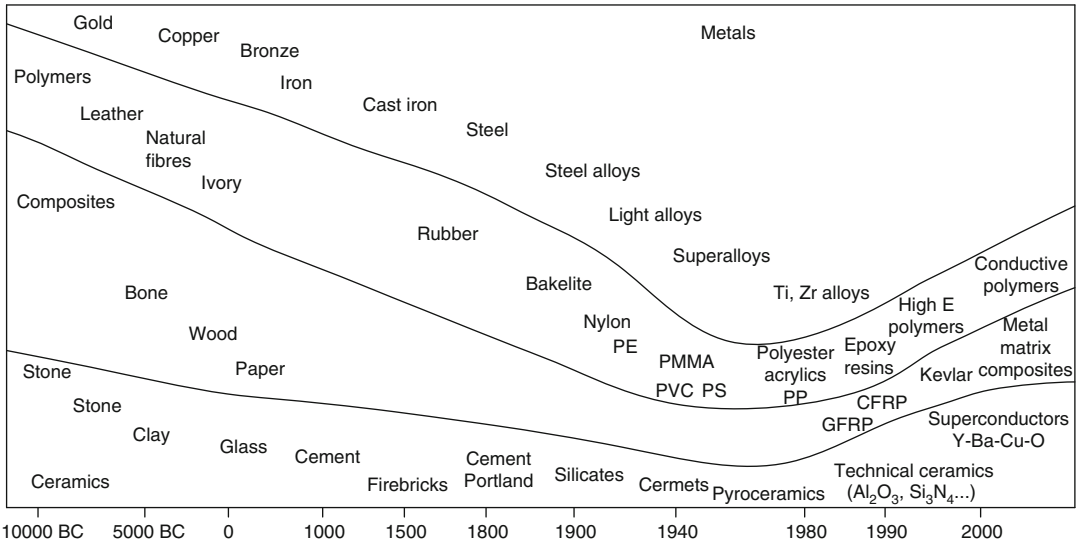

Fig. 3.1 Relative use of technical materials through the years (Adapted from Παντελής ΔΙ, 1997; *Μη μεταλλικά τεχνικά υλικά*)

- They reflect all visible wavelengths of light, and so appear white (except for Cu and Au).
- Most of them are magnetic to some degree.
- They are ductile.
- They have good machinability.

3.2.1.1 Microstructure

The metallic microstructure is formed of *crystals*. These are periodic arrangements of atoms closely positioned next to one another in a particular way to form a lattice.

The potential geometric arrangements of atoms in crystals and of crystals in the bulk metal depend primarily on the thermodynamics of the forming process as the atoms will seek the conformation with the lowest energy. Fourteen arrangements have been documented, but most metals commonly form in one, or combinations of, the following three; bcc (body-centred cubic), fcc (face-centred cubic), and hcp (hexagonal close packed). In the bcc arrangement the unit cell has atoms at each corner of a cube plus one at the centre of the cube; in the fcc arrangement the unit cell has atoms at each corner of a cube and at the centres of all cubic faces; the hcp arrangement is similar to the fcc but in a hexagonal formation rather than in a cubic.

3.2.1.2 Imperfections

The crystallic structure is never perfect; it contains imperfections that dictate some of the material's behaviour, especially in relation to plasticity, failure, corrosion, electric conductivity and alloying. These imperfections could be point, line, plane or complex (3D) defects. Point defects are of intra-atomic dimensions; they could be vacant atomic sites or extra (usually foreign) atoms positioned between atomic sites; they both result in distortion of the planes and the lattice arrangement. Line defects are also termed dislocations. They split the structure into two perfect crystals. They form during the solidification or during plastic deformation of the metal. This type of defect is also present in ceramics and polymers. The deformation mechanisms and therefore the plasticity and strength of materials are directly related to the formation of dislocations, as slip between crystal planes result when dislocations move. The greater the ability of a dislocation to move, the more ductile the material is. The density of dislocations (dislocation length per unit volume) in a metal that contains very few of them is at the order of 10^3 cm/cm^3, and when the metal is deforming plastically it could be up to 10^{12} cm/cm^3. A plane defect present in all (polycrystalline) metals is

the boundary of grains; grains (crystals) form during the solidification process and position themselves one next to the other to form a continuous, solid material. Crystallographic orientation, size and relative placement of grains all constitute some form of imperfection that reflects to the macroscopic mechanical and physical properties of the solid.

3.2.1.3 Hardening

The number and type of imperfections can be controlled in part by appropriate mechanical and heat treatments. It is usually desirable to increase the strength and toughness of a metal to make it withstand heavy loads for long times; but this is sometimes associated with reduction in ductility which is usually undesirable. The most common methods used to manipulate the imperfections (usually reduce the ability of dislocations to move)—and therefore the macroscopic mechanical properties of metals—are the following.

- Grain size reduction.
- Cold working / strain hardening.
- Solid solution strengthening and alloying.
- Precipitation hardening and ageing.
- Transformation hardening (for steels only).

3.2.1.4 Main Industrial Alloys

An alloy is a material that consists of two or more substances of which one is a metal. The most commonly used industrial alloys are ferrous alloys (steel and cast iron), copper alloys (brass and bronze), alloys of light metals such as aluminium, titanium and magnesium, superalloys such as alloys of nickel and cobalt, and alloys of zinc and of lead.

Steel

Steel is widely used today in the construction industry (in a wider sense) as it has excellent mechanical properties such as high strength and toughness. It is an alloy of iron containing carbon of less than 2.0 % by weight. Other metals may be added in the alloying process to alter as required the physical and/or mechanical properties of the end product. Mild (or carbon) steels are Fe-C alloys with no other elements for alloying. In alloyed steels carbon is no more than 1 % by weight and the most common alloying elements are Ni, Mn, Cr, Si and Mo. With regards to their use, steels can be classified as structural steels, tool steels, stainless steels and steels for electromagnetic applications. In stainless steel Cr is present at proportions of greater than 12 % by weight and it is primarily responsible for their good corrosion resistance. Tool steels are alloyed with elements that easily form carbides (such as Cr, V, W, Mo, Co, Ni, Si); these carbides do not allow the formation of large grains thus resulting in a hard alloy.

Cast Iron

Cast irons are alloys Fe-C-Si where C is at 2–4.5 % by weight and Si at 0.5–3 % by weight. These alloys are relatively cheap to make and are manufactured exclusively by casting. They are typically not as strong as any of the steels.

Copper Alloys

Copper and its alloys was the first metal used by humans. It has excellent electrical and thermal conductivity and so half of its global production is used to produce electrical goods. It is very malleable, ductile and corrosion resistive. The main alloys are brass (Cu-Zn with Zn even up to 50 % by weight) and bronze (Cu-Sn). Other Cu alloys are with Al, Sn, Ni, Zn & Ni, Be, Si.

Alloys of Light Metals

Aluminium, magnesium and titanium are light metals as their density is relatively low. The importance is that their specific strength (max stress over density) is higher compared to other metals and their alloys. They also have good resistance to corrosion.

3.2.2 Ceramics

Historically, the term ceramic meant objects made of clay and other raw materials subjected to heat; ceramics, in the form of pottery and bricks are the first man-made objects. We class

as ceramics today the inorganic, non-metallic materials that are fabricated using heat and cover a wide range of chemical compositions and physical and mechanical properties. They offer advantages compared to metals such as the relatively low density, high melting point, high modulus of elasticity, low thermal conductivity, good resistance to compression, high hardness, and wear and heat resistant behaviour. Disadvantages include low resistance to tension, shear, fatigue, buckling and impact, brittleness, high production costs for some, low resistance to crack propagation, and sensitivity of their microstructure and of pores on their physical properties and strength.

Ceramics consist of elements that form strong ionic or covalent bonds. In terms of structure, we can classify ceramics into ionic, that consist of metals and non-metal elements, and covalent, that consist of two non-metal elements.

In ionic ceramics the two elements have different electric charges resulting in attracting forces that contribute to forming the bond. The most stable microstructure is seen when the cations are closer to the anions resulting in high attracting forces that form stable crystalline shapes. The most common are the face-centred cubic shape of MgO and ZrO_2 and maximum density hexagonal shape of Al_2O_3.

In covalent ceramics every atom that belongs to a covalent bond 'shares' the electrons of the outer shell with neighbouring atoms. The resulting shape is usually cubic; either crystalline with formation of chains, 2D or 3D lattices, or amorphous.

Ceramics can be classified based on their main non-metal constituent (B, C, N, O, F and Si) into six categories; oxides (Al_2O_3, ZrO_2 UO_2), carbides (SiC, B_4C, WC, TiC), nitrides (Si_3N_4, AlN, BN), borides (ZrB_2, TiB_2), silicides ($MoSi_2$, $TiSi_2$) and fluorides (CaF_2, LiF).

Glasses are ceramics that are worthy of special mention. All commercial glasses are amorphous 3D lattices with main constituent the stable silica (SiO_2). The glass structure is a result of rapid cooling of melted oxides. The high values of viscosity and the strong bonds that form between the silicate tetrahedra do not allow for a crystallisation process to commence during solidification. Solidification of a glass occurs due to the gradual thickening of the liquid as a result of an increase of its viscosity due to the cooling. Other oxides may be added that will transform the silica lattice and so affect the properties of the final product depending on the intended use.

3.2.3 Polymers

Polymers consist of large molecules (molecules of large molecular weight), the macromolecules; hence their name (poly = many; meros = part). The building blocks of a polymer are chemical units of small molecular weight called monomers that bond to each other to form the characteristic long chains of the polymer; the monomer quantity may vary from 100 to 100,000 per chain.

A big advantage of polymers is that they can be formed relatively easily compared to other materials. Their production is of low cost, they can form into products of complex geometry, they can be transparent (and therefore substitute the more expensive glass), they have low density, and they have good mechanical properties. Disadvantages include pollution (not easily recyclable), inferior mechanical properties to other materials, especially metals, and that they don't work at high temperatures.

In terms of microstructure, the polymers can be crystalline or amorphous; this is dependent primarily on the rate of cooling of the melted polymer. When cooling is gradual, the chains have time to align to one another and form a crystalline-like structure (not to be confused with the crystallinity of metals). Conversely, in amorphous polymers the chains don't have time to align due to the rapid cooling; this structure can be loosely compared with that of liquids as it is characterised by a lack of order. Under heat the long chains of the polymers can easily slip over one another. During cooling this movement between chains reduces and the polymer transforms gradually from a liquid to an amorphous solid state. The temperature at which this transition occurs is termed the glass transition

temperature, T_g; above this temperature the polymer behaves elastically and below it the polymer is brittle and behaves similar to glass.

In terms of their physical properties there are three types of polymers; thermoplastics, thermosets and elastomers or rubbers.

3.2.3.1 Thermoplastics

They consist of primarily linear chains that soften and flow with heat due to the relaxation of the molecular bonds and so can be formed; they solidify after cooling. This process is reversible, which means that they may be reshaped by heating them up. Widely used thermoplastics include polyethylene (PE), polyvinyl chloride (PVC), polypropylene (PP), polystyrene (PS), and the polyamides (Nylon).

3.2.3.2 Thermosets

They consist of relatively short chains in 2D and 3D networks. They are usually amorphous. They are formed by a curing process of a resin with a hardening agent with or without heat; the process is irreversible. Main representatives of this family of polymers include phenolic polymers (bakelite), epoxy resins, aminoplasts (melamine or urea resins with formaldehyde), and polyesters.

3.2.3.3 Elastomers or Rubbers

These are usually linear polymers with branching chains. They can deform a lot under load and yet return back to their original dimensions when the load is removed; they are hyperelastic. Main representatives of these are synthetic and natural rubber, synthetic polyisoprene, polybutadiene, polychloroprene, and the silicones. Natural rubber vulcanises when heated with sulphur. The vulcanisation process entails the formation of cross-linking between molecules that result in reinforcing the structure of the material, making it tougher, more durable, and less sensitive to temperature changes.

3.2.4 Composites

Composite materials are those that consist of a combination of two or more of the above mentioned material types. The intention is to fabricate a material that has special properties that none of the aforementioned material types can achieve on its own. Of the constituent traditional materials in a composite, one is termed as the matrix and another as the reinforcement. Depending on the shape of the reinforcing constituent material they can be classed as fibre-reinforced composites, particulate composites and laminar composites. The strength of a composite depends on the strength of its constituents, but also on the compatibility between the two when put together.

In fibre-reinforced composites the reinforcement could be through long, continuous fibres or through short, discontinuous fibres. The strength of these composites depends on the directionality of the fibres. In unidirectional composites the fibres are orientated parallel to one another, adding strength in that particular direction to the composite. In multidirectional composites the fibres can be laid in random orientations, in a woven motif, or in layers perpendicular in orientation to one another. The intention in adding fibres to a matrix is to increase the strength of the matrix material. Therefore, the material of the fibre tends to have a high modulus of elasticity, high strength and low density. The most common materials for fibre reinforcement are glass, carbon, polymers (Nylon, PE, Kevlar), metal (boron), or other raw/ceramic materials (such as mica).

The matrix secures the reinforcement from the fibres. Under load, the stresses are transferred from the matrix to the fibres. Importantly, the matrix can interrupt the propagation of cracks that might form in the fibres whence the load is too high. The material for the matrix is usually selected to be tough, ductile, and with a high melting point, higher than the maximum intended operating temperature of the composite. The most common type of matrix is organic, either thermoplastic or, more often, thermoset, such as epoxy resins, phenolic resins, and polyester resins. At high intended operating temperatures metallic materials are necessary for the matrix. Ceramic matrices are not that common; but a special mention is due to cement. Cement is

used to form concrete (by mixing it with sand and stone) – which is a particulate composite – that can then be reinforced with steel rods; most infrastructure is at least partly built out of this composite.

Particulate composites are not that common as they don't offer the superior mechanical properties that fibre-reinforced composites do, but they are cheaper to make than fibre-reinforced composites and tend to be more wear resistant. Laminar composites can be categorised into coatings, bimetallics, multilayers and sandwich materials. The intention in coatings is mostly to improve the wear resistant properties of the surface whilst maintaining the superior material properties of the main material. The other two types have limited uses in industry.

3.2.5 Biological Materials

The constituents of the human body from the perspective of mechanical response are almost without exception a mixture of fluid and solid phases, either organic or inorganic. We will limit ourselves here to a quick overview of constituent biological materials that might be associated with blast injury; the response to some of the tissues and organs that consist of them in blast-related loading follows in Chaps. 4 and 5.

3.2.5.1 Biological Fluids

In contrast to water, most fluids in our body are non Newtonian and have a substantial elastic (solid) component. Disturbance in the material properties – primarily viscosity – of these fluids due to disease or injury may have adverse consequences on the function of tissues. Treatment, restoration or replacement of such tissues aims at recovering the unique material behaviour of their constituents in order to enable normal function.

Protoplasm

We call protoplasm (*protos* = first; *plasma* = formed object) the collection of a cell's contents that are encapsulated within the plasma membrane. It consists of the cytoplasm and various particles suspended in it. Its viscosity is several times greater than water.

Mucus

Mucus consists of glycoproteins and water. Its role is to protect epithelial cells in vital systems of the body, including the respiratory, gastrointestinal and urogenital, from infection. It does so by trapping foreign material and so its material behaviour is affected by the properties of the foreign material. The material behaviour of the mucus produced by the sex glands in both sexes – cervical mucus and semen – is appropriate for fertilisation. The properties of the cervical mucus are affected by hormones and so they vary during the menstrual cycle. The efficiency of the swimming of spermatozoa in semen and in the cervical mucus is key for enabling reproduction and so any change in the properties of either media may affect reproducing capabilities.

Synovial Fluid

Human joints undergo cyclical loading and yet can remain clinically asymptomatic for many decades. This is due to the virtually frictionless articulation provided by the articular cartilage present at the articulating surface and the lubrication from the synovial fluid. Synovial fluid is present in cavities of synovial joints. It contains hyaluronic acid and interstitial fluid. In addition to reducing friction in the joint, it acts as a shock absorber and as a medium of transportation for waste and nutrients.

3.2.5.2 Biological Solids

Actin and Elastin

Actin is a protein present in muscle and many types of cell, including leukocytes and endothelial cells. It is ~7–20 nm in diameter and its tensile strength has been measured to be approximately an impressive 2 MPa. It plays a role in many important cellular processes, including remodelling, primarily via its interactions with the cell's membrane.

Elastin is a protein present in connective tissue. It is responsible primarily for resuming the original shape of the tissue after deformation and

for storing elastic energy when loaded. It exhibits an almost perfectly linear elastic behaviour – the only biological tissue to do so.

Collagen

Collagen is a key load transferring compound for many tissues in the body. It is present in various combinations and may act beneficially in wound healing. 12 types of collagen have been identified to date. Collagen is a protein. A collagen molecule (tropocollagen) (1.5 nm in diameter) is made up of three polypeptide strands (left-handed helices) that are twisted to form a right-handed triple helix. Collagen molecules combine to make up fibrils (20–40 nm in diameter) and bundles of fibrils combine to make up fibres.

Collagen is the main structural protein in connective tissue; it combines with actin, elastin, other proteins and a ground substance (a hydrophilic gel) to form fibrils and fibres that in turn combine to form bone, cartilage, skin, muscle, ligament, blood vessels etc. The mechanical behaviour of a tissue is directly related to its microstructure and therefore the relative arrangement of fibres, cells and ground substance.

3.3 Stress Analysis

3.3.1 Introduction: General Terms

The response of materials to loading is termed mechanical behaviour. Quantifying this behaviour allows the engineer to design a product that is fit for purpose and to understand or predict what is going to happen to an existing structure under load.

When a material deforms under a small load the deformation may be elastic. In this case, when the load is removed, the material will revert to its original shape. Most of the elastic deformation will recover immediately. There may be, however, some time-dependent shape recovery; this time-dependent behaviour is called anelasticity or viscoelasticity.

A larger stress may cause permanent – often called plastic – deformation. After a material undergoes plastic deformation, it will not revert to its original shape when the load is removed. Usually, a high resistance to deformation is desirable so that a part will maintain its shape in service when loaded. On the other hand, it is desirable to have materials deform easily when forming them into useful parts or when conforming on adjacent surfaces to distribute loading.

Fracture is the breaking of a material into pieces. If fracture occurs before much plastic deformation occurs we say that the material is brittle. In contrast, if there has been extensive plastic deformation preceding fracture the material is considered ductile. Fracture usually occurs as soon as a critical amount of loading is reached; repeated application of lower loading may also cause fracture; this is called fatigue.

3.3.2 Stress and Strain Tensors

The effect of external loading on to a body can be quantified through internal reaction loads and deformation. We use the concepts of stress and strain in order to normalise for cross-sectional size and shape that allows us to quantify material rather than structural behaviour. Furthermore, the stress-strain behaviour is unique for a material; we call that the constitutive law from which we can define material properties, unique to that material.

3.3.2.1 Stress

Stress is a normalised measure of force. Consider a body subjected to a static external force, F (Fig. 3.2). For the body to be in static equilibrium, every part of the body needs to be in equilibrium. If we make a virtual cut somewhere along the length of the body through the cross-section then the remaining part should be considered to be in equilibrium. The internal reaction force at the cross-section can be considered as made up of a collection of infinitely small amounts of force dF_i acting over infinitely small areas dA_i. In order to maintain equilibrium $\Sigma dF_i = F$ whilst $\Sigma dA_i = A$. We define stress (at a point) as the internal force per unit area.

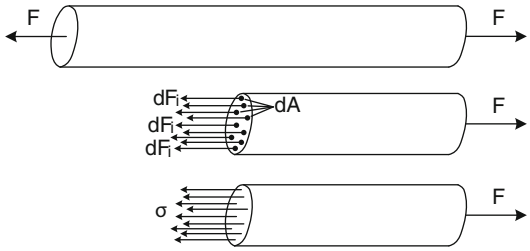

Fig. 3.2 A body with external force F acting on it with a virtual cut along its length showing a collection of infinitely small amounts of force acting over infinitely small areas the sum of which represents the stress at the cut

$$\sigma = \lim_{dA_i \to 0} \frac{dF_i}{dA_i}$$

The stress on a surface is defined as the intensity of internal distributed forces on an imaginary cut surface of the body. Stress acting perpendicular to a plane is termed direct or normal stress, whereas stress acting parallel or tangential to a plane is termed shear stress; we tend to use the symbol τ for shear stress (Fig. 3.3).

$$\text{Direct stress: } \sigma = \lim_{dA \to 0} \frac{dF_{direct}}{dA}$$

$$\text{Shear stress: } \tau = \lim_{dA \to 0} \frac{dF_{parallel}}{dA}$$

Stress is a second order tensor; this means that magnitude, direction and plane at which it acts are required to define it fully (Fig. 3.4). A vector (e.g. force), for comparison, is a first order tensor.

$$\sigma_{ij} = \lim_{dA_i \to 0} \frac{dF_j}{dA_i}$$

where i is the direction of the outward normal to the plane
and j is the direction of the internal force component.

Therefore stress can be represented by a 3×3 matrix with nine components. The diagonal elements of the matrix are the normal stresses and the rest are the shear stresses.

In order to maintain rotational equilibrium the shear forces along the sides of a material point need to be equal; this means that shear stresses on perpendicular planes need to have the same sign and magnitude; we can write $\tau_{ij} = \tau_{ji}$; we call these complementary shear stresses. Therefore the stress tensor is a 3×3 symmetric matrix and has only six independent elements. It is convenient to write the matrix as a column vector with the six independent elements.

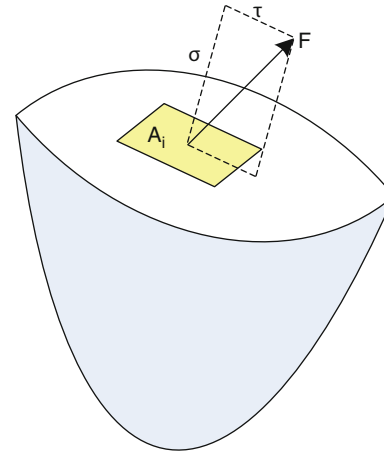

Fig. 3.3 Definitions of direct, σ and shear, τ stress on a cross section of a body in equilibrium

3.3.2.2 Strain

Strain is a normalised measure of deformation. As with stress, strain is a second order tensor and can be split in normal or direct and shear components in perpendicular and tangential directions, respectively. Let's consider an infinitesimal material plane element, dx, dy in dimensions, that displaces and deforms (Fig. 3.5). If u and v are the displacements in x and y respectively, then the deformations are $\Delta u = u + \frac{\partial u}{\partial x} dx$ and $\Delta v = v + \frac{\partial v}{\partial y} dy$. We define the direct strains in x and y as the normalised deformation along each direction; $\varepsilon_x = \frac{\partial u}{\partial x}$ and $\varepsilon_y = \frac{\partial v}{\partial y}$, respectively. We define shear strain on the plane as the change in angle; the initial right angle in Fig. 3.5 has changed by $\gamma_x + \gamma_y$, where $\gamma_x = \frac{\partial u}{\partial y}$ and $\gamma_y = \frac{\partial v}{\partial x}$. Then shear strain in the x-y plane is defined as $u + \frac{\partial u}{\partial x} dy$

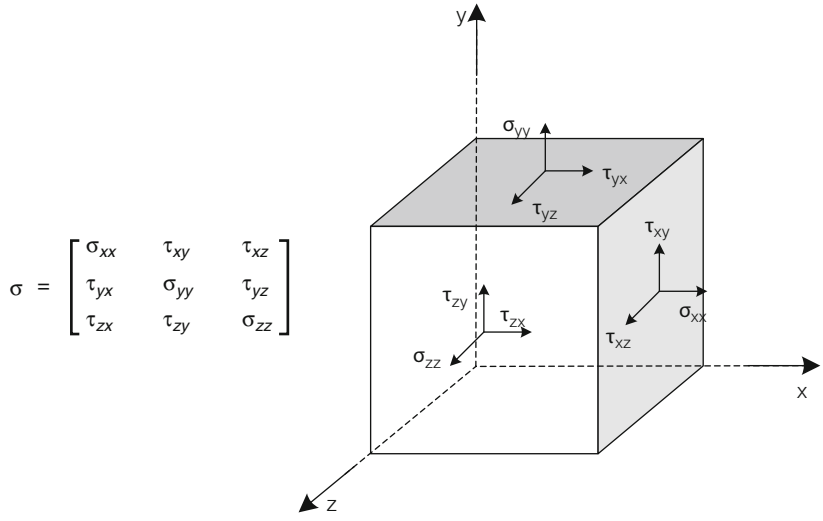

Fig. 3.4 The stress tensor. A unit cube representing a material point showing the components of stress on the 3 planes

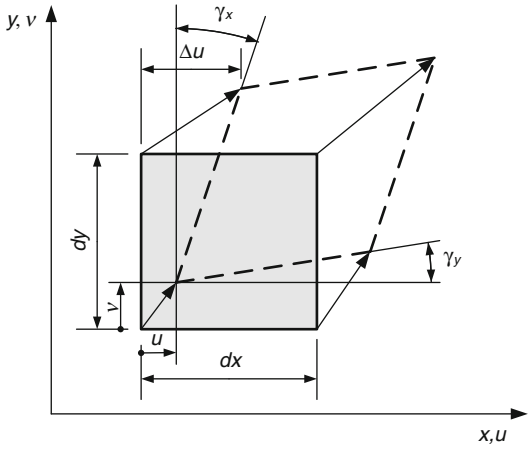

Fig. 3.5 2D strained infinitesimal element in undeformed (*solid line*) and deformed (*dashed line*) configurations

$$\varepsilon_{xy} = \varepsilon_{yx} = \frac{1}{2}(\gamma_x + \gamma_y) = \frac{1}{2}\gamma_{xy} = \frac{1}{2}\gamma_{yx} = \frac{1}{2}\left(\frac{\partial u}{\partial y} + \frac{\partial v}{\partial x}\right)$$

Using the tensorial representation of strain in three dimensions we can write

$$\varepsilon = \begin{bmatrix} \varepsilon_{xx} & \varepsilon_{xy} & \varepsilon_{xz} \\ \varepsilon_{yx} & \varepsilon_{yy} & \varepsilon_{yz} \\ \varepsilon_{zx} & \varepsilon_{zy} & \varepsilon_{zz} \end{bmatrix} = \begin{bmatrix} \varepsilon_{xx} & \frac{1}{2}\gamma_{xy} & \frac{1}{2}\gamma_{xz} \\ \frac{1}{2}\gamma_{yx} & \varepsilon_{yy} & \frac{1}{2}\gamma_{yz} \\ \frac{1}{2}\gamma_{zx} & \frac{1}{2}\gamma_{zy} & \varepsilon_{zz} \end{bmatrix}$$

Similar to the stress tensor, the strain tensor has only six independent elements.

3.3.3 Stress States

There are four basic stress states that a material could be under (Fig. 3.6). Complex loading that results in complex stress states can by analysed as a combination of these four basic states.

1. Simple tension or simple compression. In these cases the stresses are direct and uniaxial; there are no shear stresses.
2. Biaxial tension. Stresses act over two directions on every material point of the structure. A sheet being pulled equally from all directions or a closed spherical shell under gas pressure is under this stress state.

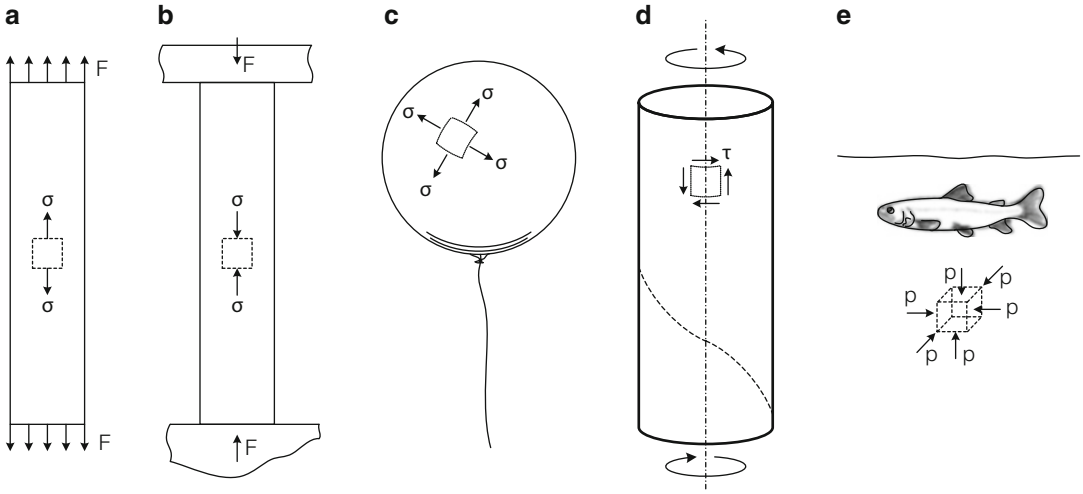

Fig. 3.6 The main stress states. (**a**) Simple tension, (**b**) simple compression, (**c**) biaxial tension, (**d**) pure shear, (**e**) hydrostatic stress/pressure

3. Hydrostatic stress. In solid mechanics we tend to use the term hydrostatic stress, σ_H instead of pressure to refer to a stress state whereby stress is equal and compressive in all directions; $\sigma_x = \sigma_y = \sigma_z = \sigma_H$. For example, an object in the sea would be under hydrostatic stress.
4. Pure shear. A stress state whereby there are no direct stresses. When we apply torsion on a rod (moment about its longitudinal axis) then the rod is in pure shear.

3.3.4 Engineering Properties of Materials

A constitutive law is a relation between physical quantities that characterise the material behaviour in full. Each material is governed by its own constitutive law. Usually this is a form of a stress-strain relationship (Fig. 3.7). For materials undergoing small deformations (infinitesimal strains), this can be written in matrix notation as $\boldsymbol{\sigma} = \mathbf{D}\boldsymbol{\varepsilon}$ whereby $\mathbf{D}$ is a 6×6 matrix containing the necessary material parameters.

The first constitutive law was developed by Hooke and is known as Hooke's law; it was developed for linearly elastic solids. Every structure has a unique, unloaded state. Elasticity is the tendency of the structure to return to that unique, unloaded state when external loads are removed. Such behaviour stems from different physical properties for each type of material. For example, in metals it is the atomic lattice that changes in shape and size when load is applied and then returns to its original state of minimum potential energy when the load is removed. In most polymers it is the polymer chains that deform under load and return to their original length when the load is removed. The energy stored and subsequently released by the structure when the load is removed is often called strain energy, U; this is the area under the stress-strain curve (which is termed strain energy density) integrated over the volume of the structure.

The stress-strain curve of linearly elastic and isotropic materials is a straight line through the origin. The slope of that line is called modulus. In a direct stress – direct strain curve the modulus is termed Young's modulus, E and $\sigma = E\varepsilon$, whereas in a shear stress – shear strain curve the modulus is termed shear modulus, G and $\tau = G\gamma$. In a linearly elastic and isotropic material two material parameters are sufficient to characterise the material fully; the $\mathbf{D}$ matrix has two independent components.

Another material constant used in linear elasticity is the Poisson's ratio, v. The Poisson's ratio

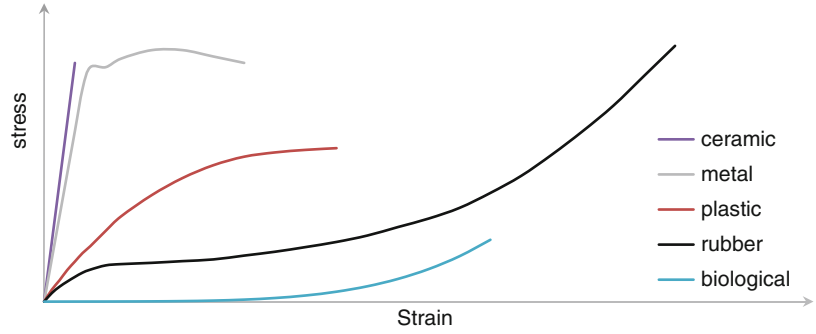

Fig. 3.7 Stress-strain curves in tension for various materials. The axes are not to scale. Note that only metals and ceramics exhibit a linearly elastic response and that response of biological tissue is very variable depending on the type of tissue/constituent

is defined as the ratio of transverse to axial strain; for example, if an isotropic material is loaded in one direction, let's say x, then there is strain in the transverse plane; $\varepsilon_y = \varepsilon_z = -\nu\varepsilon_x$. There is no Poisson's effect in shear. Due to the Poisson's effect, the strain state of a linearly elastic and isotropic material when subjected to a triaxial stress-state is the following and is termed the generalised Hooke's law.

$$\varepsilon_x = \frac{1}{E}\left[\sigma_x - \nu\left(\sigma_y + \sigma_z\right)\right] \quad \gamma_{xy} = \frac{\tau_{xy}}{G} = \frac{2(1+\nu)}{E}\tau_{xy}$$

$$\varepsilon_y = \frac{1}{E}\left[\sigma_y - \nu\left(\sigma_z + \sigma_x\right)\right] \quad \gamma_{yz} = \frac{\tau_{yz}}{G} = \frac{2(1+\nu)}{E}\tau_{yz}$$

$$\varepsilon_z = \frac{1}{E}\left[\sigma_z - \nu\left(\sigma_x + \sigma_y\right)\right] \quad \gamma_{zx} = \frac{\tau_{zx}}{G} = \frac{2(1+\nu)}{E}\tau_{zx}$$

3.4 Beyond Linear Elasticity

The most commonly used materials in the construction of useful objects have a linearly elastic and isotropic behaviour for most of their service life. There are certain materials and circumstances, however, whereby different behaviours are observed.

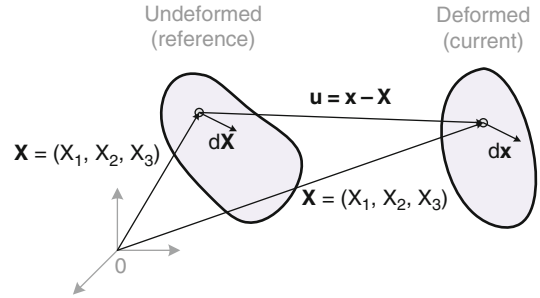

Fig. 3.8 The undeformed and deformed configurations of an object. *Uppercase letters*: reference configuration. *Lowercase letters*: current configuration. Displacement vector: $\mathbf{u} = \mathbf{x} - \mathbf{X}$

3.4.1 Finite Strain Theory (i.e. Large Deformations)

The elastic behaviour of materials that undergo finite deformations has been described using models such as hyperelastic, hypoelastic and Cauchy or Green elastic.

Let's consider mapping from an undeformed, reference configuration to a deformed, current configuration (Fig. 3.8). For a vector line element $d\mathbf{X}$ that deforms into $d\mathbf{x}$ we can write

$$dx_1 = \frac{\partial x_1}{\partial X_1}dX_1 + \frac{\partial x_1}{\partial X_2}dX_2 + \frac{\partial x_1}{\partial X_3}dX_3$$
$$dx_2 = \frac{\partial x_2}{\partial X_1}dX_1 + \frac{\partial x_2}{\partial X_2}dX_2 + \frac{\partial x_2}{\partial X_3}dX_3 \quad \text{or } d\mathbf{x} = \mathbf{F}d\mathbf{X} \text{ where } \mathbf{F} = \text{grad}\mathbf{x} = \begin{bmatrix} \frac{\partial x_1}{\partial X_1} & \frac{\partial x_1}{\partial X_2} & \frac{\partial x_1}{\partial X_3} \\ \frac{\partial x_2}{\partial X_1} & \frac{\partial x_2}{\partial X_2} & \frac{\partial x_2}{\partial X_3} \\ \frac{\partial x_3}{\partial X_1} & \frac{\partial x_3}{\partial X_2} & \frac{\partial x_3}{\partial X_3} \end{bmatrix}; \quad F_{ij} = x_{i,j}$$
$$dx_3 = \frac{\partial x_3}{\partial X_1}dX_1 + \frac{\partial x_3}{\partial X_2}dX_2 + \frac{\partial x_3}{\partial X_3}dX_3$$

and tensor [F] = **F** is the deformation gradient tensor. The determinant of the deformation gradient tensor is known as the Jacobian, J of the transformation. The deformation gradient is a measure of deformation, is not necessarily symmetric, and is invertible (i.e. $\det(\mathbf{F}) = J \neq 0$). For the deformation to be well defined (one-to-one mapping with no overlaps or gaps) the Jacobian must be positive.

The displacement vector is $\mathbf{u} = \mathbf{x} - \mathbf{X}$ and the deformation gradient can be rewritten as

$$\mathbf{F} = \text{grad}\mathbf{x} = \text{grad}(\mathbf{u} + \mathbf{X}) = \text{grad}\mathbf{u} + \text{grad}\mathbf{X} = \text{grad}\mathbf{u} + \mathbf{I}$$

For a vector line element define stretch ratio, λ

$$\lambda = \frac{L + \Delta L}{L} = \frac{l}{L} (= 1 + \varepsilon)$$

where

L is the length in the reference configuration
l is the length in the current configuration
ε is the engineering strain along the length of the element.

It can be shown that the volume change is given by the Jacobian of the deformation

$$\frac{V}{V_0} = \det[\mathbf{F}] = J$$

where

V_0 is the volume in the reference configuration
V is the volume in the current configuration

For an *isochoric* deformation (whereby the volume is preserved) $\det[\mathbf{F}] = J = 1$ and the material is termed *incompressible*.

Consider now a vector line element **Q** that deforms into **q**. We can write $\mathbf{q} = \mathbf{FQ}$. To find the change in length of the line element (and eventually the strain)

$$|\mathbf{q}|^2 = \mathbf{q}^{\mathrm{T}}\mathbf{q} = \mathbf{Q}^{\mathrm{T}}\mathbf{F}^{\mathrm{T}}\mathbf{F}\mathbf{Q}$$

$$|\mathbf{q}| = \sqrt{\mathbf{Q}^{\mathrm{T}}\mathbf{F}^{\mathrm{T}}\mathbf{F}\mathbf{Q}} = \sqrt{\mathbf{Q}^{\mathrm{T}}\mathbf{C}\mathbf{Q}}$$

where $|\mathbf{q}|$ is the length of the vector in the current configuration and **C** is the Green (or right Cauchy-Green) deformation tensor $\mathbf{C} = \mathbf{F}^{\mathrm{T}}\mathbf{F}$, which is symmetric ($\mathbf{C}^{\mathrm{T}} = \left(\mathbf{F}^{\mathrm{T}}\mathbf{F}\right)^{\mathrm{T}} = \mathbf{F}^{\mathrm{T}}\left(\mathbf{F}^{\mathrm{T}}\right)^{\mathrm{T}} = \mathbf{F}^{\mathrm{T}}\mathbf{F} = \mathbf{C}$) (Fig. 3.9).

We define the Green (or Green-Lagrange) strain tensor as $\mathbf{E} = \frac{1}{2}(\mathbf{C}\text{-}\mathbf{I}) = \frac{1}{2}(\mathbf{F}^{\mathrm{T}}\mathbf{F}\text{-}\mathbf{I})$ which is also symmetric, does not contain information on rigid rotations, its diagonal terms give length changes, and the off-diagonal terms give angle changes; i.e. similar to the infinitesimal strain tensor. The length of our vector now becomes

$$|\mathbf{q}| = \sqrt{\mathbf{Q}^{\mathrm{T}}\mathbf{C}\mathbf{Q}} = \sqrt{\mathbf{Q}^{\mathrm{T}}(2\mathbf{E} + \mathbf{I})\mathbf{Q}} = \sqrt{2\mathbf{Q}^{\mathrm{T}}\mathbf{E}\mathbf{Q} + |\mathbf{Q}|^2}$$

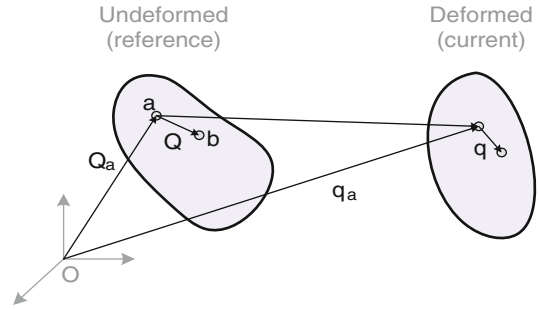

Fig. 3.9 The undeformed and deformed configurations of an object.
$\mathbf{Q} = \mathbf{Q}_b - \mathbf{Q}_a$ and $\mathbf{q} = \mathbf{q}_b - \mathbf{q}_a$

and engineering strain is

$$\frac{|\mathbf{q}|-|\mathbf{Q}|}{|\mathbf{Q}|}=\frac{\sqrt{2\mathbf{Q}^{\mathrm{T}}\mathbf{E}\mathbf{Q}+|\mathbf{Q}|^2}-|\mathbf{Q}|}{|\mathbf{Q}|}$$
$$=\sqrt{\frac{2\mathbf{Q}^{\mathrm{T}}\mathbf{E}\mathbf{Q}}{|\mathbf{Q}|^2}+1}-1$$

If we consider displacements then

$$\mathbf{E}=\frac{1}{2}\left(\mathbf{F}^{\mathrm{T}}\mathbf{F}-\mathbf{I}\right)$$
$$=\frac{1}{2}\Big((\mathrm{grad}\mathbf{u})^{\mathrm{T}}+\mathrm{grad}\mathbf{u}+(\mathrm{grad}\mathbf{u})^{\mathrm{T}}\mathrm{grad}\mathbf{u}\Big)$$

which results in

$$\mathbf{E}=\begin{bmatrix}\frac{\partial u_1}{\partial X_1}+\frac{1}{2}\left(\frac{\partial u_1}{\partial X_2}\right)^2+\frac{1}{2}\left(\frac{\partial u_2}{\partial X_2}\right)^2+\frac{1}{2}\left(\frac{\partial u_3}{\partial X_2}\right)^2 & \frac{1}{2}\left(\frac{\partial u_1}{\partial X_2}+\frac{\partial u_2}{\partial X_1}+\frac{\partial u_1}{\partial X_1}\frac{\partial u_1}{\partial X_2}+\frac{\partial u_2}{\partial X_1}\frac{\partial u_2}{\partial X_2}+\frac{\partial u_3}{\partial X_1}\frac{\partial u_3}{\partial X_2}\right) & \frac{1}{2}\left(\frac{\partial u_1}{\partial X_3}+\frac{\partial u_3}{\partial X_1}+\frac{\partial u_1}{\partial X_1}\frac{\partial u_1}{\partial X_3}+\frac{\partial u_2}{\partial X_1}\frac{\partial u_2}{\partial X_3}+\frac{\partial u_3}{\partial X_1}\frac{\partial u_3}{\partial X_3}\right)\\ \frac{1}{2}\left(\frac{\partial u_1}{\partial X_2}+\frac{\partial u_2}{\partial X_1}+\frac{\partial u_1}{\partial X_1}\frac{\partial u_1}{\partial X_2}+\frac{\partial u_2}{\partial X_1}\frac{\partial u_2}{\partial X_2}+\frac{\partial u_3}{\partial X_1}\frac{\partial u_3}{\partial X_2}\right) & \frac{\partial u_2}{\partial X_2}+\frac{1}{2}\left(\frac{\partial u_1}{\partial X_2}\right)^2+\frac{1}{2}\left(\frac{\partial u_2}{\partial X_2}\right)^2+\frac{1}{2}\left(\frac{\partial u_3}{\partial X_2}\right)^2 & \frac{1}{2}\left(\frac{\partial u_2}{\partial X_3}+\frac{\partial u_3}{\partial X_2}+\frac{\partial u_1}{\partial X_1}\frac{\partial u_1}{\partial X_3}+\frac{\partial u_2}{\partial X_1}\frac{\partial u_2}{\partial X_3}+\frac{\partial u_3}{\partial X_1}\frac{\partial u_3}{\partial X_3}\right)\\ \frac{1}{2}\left(\frac{\partial u_1}{\partial X_3}+\frac{\partial u_3}{\partial X_1}+\underbrace{\frac{\partial u_1}{\partial X_1}\frac{\partial u_1}{\partial X_3}+\frac{\partial u_2}{\partial X_1}\frac{\partial u_2}{\partial X_3}+\frac{\partial u_3}{\partial X_1}\frac{\partial u_3}{\partial X_3}}_{\text{Nonlinear terms}}\right) & \frac{1}{2}\left(\frac{\partial u_2}{\partial X_3}+\frac{\partial u_3}{\partial X_2}+\underbrace{\frac{\partial u_1}{\partial X_2}\frac{\partial u_1}{\partial X_3}+\frac{\partial u_2}{\partial X_2}\frac{\partial u_2}{\partial X_3}+\frac{\partial u_3}{\partial X_2}\frac{\partial u_3}{\partial X_3}}_{\text{Nonlinear terms}}\right) & \frac{\partial u_3}{\partial X_3}+\underbrace{\frac{1}{2}\left(\frac{\partial u_1}{\partial X_2}\right)^2+\frac{1}{2}\left(\frac{\partial u_2}{\partial X_2}\right)^2+\frac{1}{2}\left(\frac{\partial u_3}{\partial X_2}\right)^2}_{\text{Nonlinear terms}}\end{bmatrix}$$

When strains are small the second order terms can be neglected and so the Green-Lagrange strain tensor reduces to

$$\mathbf{E}=\frac{1}{2}\left(\mathbf{F}^{\mathrm{T}}\mathbf{F}-\mathbf{I}\right)=\frac{1}{2}\Big((\mathrm{grad}\mathbf{u})^{\mathrm{T}}+\mathrm{grad}\mathbf{u}\Big)$$

which is the familiar strain tensor for small strains.

$$\mathbf{E}=\begin{bmatrix}\frac{\partial u_1}{\partial X_1} & \frac{1}{2}\left(\frac{\partial u_1}{\partial X_2}+\frac{\partial u_2}{\partial X_1}\right) & \frac{1}{2}\left(\frac{\partial u_1}{\partial X_3}+\frac{\partial u_3}{\partial X_1}\right)\\ \frac{1}{2}\left(\frac{\partial u_1}{\partial X_2}+\frac{\partial u_2}{\partial X_1}\right) & \frac{\partial u_2}{\partial X_2} & \frac{1}{2}\left(\frac{\partial u_2}{\partial X_3}+\frac{\partial u_3}{\partial X_2}\right)\\ \frac{1}{2}\left(\frac{\partial u_1}{\partial X_3}+\frac{\partial u_3}{\partial X_1}\right) & \frac{1}{2}\left(\frac{\partial u_2}{\partial X_3}+\frac{\partial u_3}{\partial X_2}\right) & \frac{\partial u_3}{\partial X_3}\end{bmatrix}=\boldsymbol{\varepsilon}$$

3.4.1.1 Principal Values of Stress and Strain Tensors and Their Invariants

The stress tensor $\boldsymbol{\sigma}$ is known as the Cauchy stress tensor. It represents force over unit area in the current (deformed) configuration. There are three orthogonal planes where the shear stress is zero; the *principal planes*. The magnitude of the traction on the principal plane is the *principal stress*. The principal stresses are the eigenvalues of the stress tensor. The characteristic equation is $(\boldsymbol{\sigma} - \sigma\mathbf{I})\mathbf{n} = \mathbf{0}$ ($\mathbf{n}$ the 3 unit normals).

For nontrivial solutions

$$\det(\sigma\boldsymbol{\sigma}\mathbf{I})=0\Rightarrow\sigma^3 I_1\sigma^2+I_2\sigma I_3=0$$

where I_i are the *stress invariants* and are independent of (invariant to) the coordinate system. The roots of the cubic equation are the principal stresses σ_{I}, σ_{II}, σ_{III} ($\sigma_{\mathrm{I}} > \sigma_{\mathrm{II}} > \sigma_{\mathrm{III}}$), and the invariants can be defined as

$$I_1=\mathrm{tr}(\boldsymbol{\sigma})=\sum\sigma_{ii}=\sigma_{\mathrm{I}}+\sigma_{\mathrm{II}}+\sigma_{\mathrm{III}}$$
$$I_2=\frac{1}{2}\Big[(\mathrm{tr}(\boldsymbol{\sigma}))^2-\mathrm{tr}(\boldsymbol{\sigma}^2)\Big]=\sigma_{\mathrm{I}}\sigma_{\mathrm{II}}+\sigma_{\mathrm{II}}\sigma_{\mathrm{III}}+\sigma_{\mathrm{III}}\sigma_{\mathrm{I}}$$
$$I_3=\det(\boldsymbol{\sigma})=\sigma_{\mathrm{I}}\sigma_{\mathrm{II}}\sigma_{\mathrm{III}}$$

In fact every symmetric tensor can be expressed in a principal coordinate system in which the tensor is diagonal. For example, the Green deformation tensor, $\mathbf{C} = \mathbf{F}^{\mathrm{T}}\mathbf{F}$

$$I_1=\mathrm{tr}(\mathbf{C})=\lambda_1^2+\lambda_2^2+\lambda_3^2$$
$$I_2=\frac{1}{2}\Big[(\mathrm{tr}(\mathbf{C}))^2-\mathrm{tr}\big(\mathbf{C}^2\big)\Big]=\lambda_1^2\lambda_2^2+\lambda_2^2\lambda_3^2+\lambda_3^2\lambda_1^2$$
$$I_3=\det(\mathbf{C})=\lambda_1^2\lambda_2^2\lambda_3^2$$

In some cases of material behaviour it is convenient to split the stress into hydrostatic (change in volume) and deviatoric (change in shape) components. Then

$$\boldsymbol{\sigma}=\sigma_m\mathbf{I}+\mathbf{s}$$

where $\sigma_m = p = 1/3\Sigma\sigma_{ii} = 1/3I_1$ is the hydrostatic (or mean) stress; it is a scalar; and $\mathbf{s}$ is the deviatoric stress,

$$\mathbf{s}=\boldsymbol{\sigma}-\sigma_m\mathbf{I}$$

3.4.1.2 Hyperelastic Material Behaviour and Strain Energy Density

Materials that undergo large deformations are called *hyperelastic* (or Green-elastic) materials. Examples of such materials are rubbers (elastomers in general), and biological tissues. The constitutive law (stress-strain relationship) for hyperelastic materials is nonlinear. For example, the 1D behaviour of a collagenous tissue may be expressed as $\sigma = A(e^{B\varepsilon}\text{-}1)$, where A, B are material parameters that can be determined by fitting the mathematical model to experimental data.

We define the first Piola-Kirchhoff stress tensor, $\mathbf{P} = J\boldsymbol{\sigma}\mathbf{F}^{-\mathrm{T}}$. It is a measure of force defined in the current configuration per unit area defined in the reference configuration. This is the 'natural' tensor for large deformations because it is invariant to rotations. But the tensor is not symmetrical and so not convenient for computational manipulations. Note that for infinitesimal strains the Cauchy, $\boldsymbol{\sigma}$ and first Piola-Kirchhoff stress, $\mathbf{P}$ tensors are identical. For computational manipulations we use the second Piola-Kirchhoff stress tensor, $\mathbf{S}$ which does not have a physical interpretation but is symmetrical.

$$\mathbf{S} = \mathbf{F}^{-1}\mathbf{P} = J\mathbf{F}^{-1}\boldsymbol{\sigma}\mathbf{F}^{-\mathrm{T}} \quad \mathbf{P} = \mathbf{F}\mathbf{S} \quad \boldsymbol{\sigma} = J^{-1}\mathbf{F}\mathbf{S}\mathbf{F}^{\mathrm{T}}$$

The constitutive law for hyperelastic materials is usually expressed with a strain energy density function, W; this is the strain energy per unit volume and can be estimated as the area under the stress-strain curve. Note that the 1st P-K stress is energetically conjugate to the deformation gradient and that the 2nd P-K stress is energetically conjugate to the Green–Lagrange strain.

$$1^{\mathrm{st}}\text{ P-K stress}: \quad \mathbf{P} = \frac{\partial W(\mathbf{F})}{\partial \mathbf{F}}$$

$$\text{Cauchy stress}: \quad \boldsymbol{\sigma} = \frac{1}{J}\mathbf{P}\mathbf{F}^{\mathrm{T}} = \frac{1}{J}\frac{\partial W(\mathbf{F})}{\partial \mathbf{F}}\mathbf{F}^{\mathrm{T}} = \frac{1}{J}\mathbf{F}\left(\frac{\partial W(\mathbf{F})}{\partial \mathbf{F}}\right)^{\mathrm{T}}$$

$$2^{\mathrm{nd}}\text{ P-K stress}: \quad \mathbf{S} = \mathbf{F}^{-1}\mathbf{P} = \mathbf{F}^{-1}\frac{\partial W(\mathbf{F})}{\partial \mathbf{F}}$$

The strain energy function can be expressed in terms of invariants.

$W = W\,(I_1(\mathbf{U}), I_2(\mathbf{U}), I_3(\mathbf{U}))$ or
$W = W\,(I_1(\mathbf{C}), I_2(\mathbf{C}), I_3(\mathbf{C}))$, which is a common formulation for hyperelastic materials.

This is convenient mathematically because we only use three quantities (the invariants) rather than the nine components of the deformation gradient or the six components of the Green deformation or strain tensors. Moreover, if the behaviour is incompressible then

$$I_3(\mathbf{C}) = \det(\mathbf{C}) = \det\left(\mathbf{F}^{\mathrm{T}}\mathbf{F}\right) = \det\left(\mathbf{F}^{\mathrm{T}}\right)\det(\mathbf{F}) = \det(\mathbf{F})\det(\mathbf{F}) = J^2 = 1$$

which reduces the strain energy function to $W = W(I_1(\mathbf{C}), I_2(\mathbf{C}))$.

Invariants do not have clear physical meanings. Additional invariants can be introduced to describe anisotropic hyperelastic materials. For an isotropic and incompressible ($J = 1$) material it can be shown that the 2nd P-K stress is

$$\mathbf{S} = -p\mathbf{C}^{-1} + 2\left(\frac{\partial W}{\partial I_1} + I_1\frac{\partial W}{\partial I_2}\right)\mathbf{I} - 2\frac{\partial W}{\partial I_2}\mathbf{C}$$

where p is an unknown hydrostatic pressure. Then the Cauchy stress is

$$\boldsymbol{\sigma} = \mathbf{F}\mathbf{S}\mathbf{F}^{\mathrm{T}} = -p\mathbf{I} + 2\left(\frac{\partial W}{\partial I_1} + I_1\frac{\partial W}{\partial I_2}\right)\mathbf{F}\mathbf{F}^{\mathrm{T}} - 2\frac{\partial W}{\partial I_2}\left(\mathbf{F}\mathbf{F}^{\mathrm{T}}\right)^2$$

3.4.1.3 Mooney Rivlin Hyperelastic Models

The generalised Mooney-Rivlin models for nearly incompressible elastomeric materials express the mechanical strain energy as a sum of strain invariants

$$W = \sum_{m=1}^{N}\sum_{n=1}^{N} c_{mn}(I_1 - 3)^m(I_2 - 3)^n$$

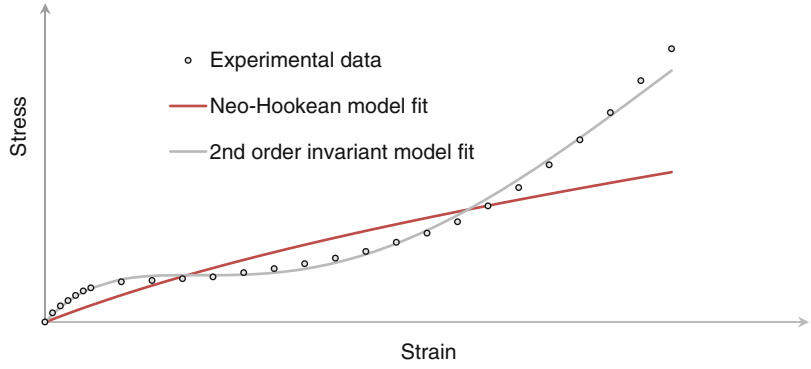

Fig. 3.10 A typical rubbery stress-strain curve with a Neo-Hookean and a second order invariant material model fit

where I_i the invariants of the Green deformation tensor, **C**
and c_{nm} material parameters.

Forms of the Mooney Rivlin function used (in order of popularity)

Neo-Hookean (appeared in ~1940)	$W = c_{10}(I_1 - 3)$
Mooney-Rivlin	$W = c_{10}(I_1 - 3) + c_{01}(I_2 - 3)$
Yeoh	$W = c_{10}(I_1 - 3) + c_{20}(I_1 - 3)^2 + c_{30}(I_1 - 3)^3$
Mooney-Rivlin 2nd order invariant	$W = c_{10}(I_1 - 3) + c_{01}(I_2 - 3) + c_{20}(I_1 - 3)^2 + c_{11}(I_1 - 3)(I_2 - 3)$

The Neo-Hookean model, for example, is a simple nonlinear model that requires only one material parameter to be defined experimentally. Tension and compression responses are different. It captures isotropic rubber well enough up to ~30 % engineering strain (Fig. 3.10).

3.4.2 Viscoelasticity

All materials have some element of time-dependent behaviour in them that can be brought out under certain loading conditions. Material behaviour which combines that of an elastic solid and a Newtonian, viscous liquid is termed viscoelastic. The resulting stress in these materials depends both on strain and on strain rate alike. Rubbers, most polymers, and biological tissues exhibit viscoelastic behaviour under normal loading conditions and temperatures. A manifestation of viscoelastic behaviour is the hysteresis loop; the loading and unloading pathways for a viscoelastic material are not the same, thus forming a loop in the stress-strain material response (Fig. 3.11). Viscoelastic materials exhibit creep and stress relaxation (Fig. 3.11). Creep is the phenomenon whereby when stress is kept constant then strain increases with time. Stress relaxation is the phenomenon whereby when strain is kept constant then the stress decreases (relaxes) with time.

3.4.2.1 Models of Viscoelastic Behaviour

Let's consider some simple models of viscoelastic response in one dimension. Although these models on their own rarely represent the behaviour of a real material, they provide insight into the separate contributions of the solid and viscous components to the overall response.

Maxwell and Kelvin-Voigt Models

The Maxwell and Kelvin-Voigt models represent the material as a combination of a spring and a damper; the spring represents the solid part and the damper represents the viscous part. In the Maxwell model these are connected in series whereas in the Kelvin-Voigt model in parallel.

$$\text{Kelvin Voigt model} \quad \sigma(t) = E\varepsilon(t) + \eta\dot{\varepsilon}(t)$$

$$\text{Maxwell model} \quad \dot{\varepsilon}(t) = \frac{\dot{\sigma}(t)}{E} + \frac{\sigma(t)}{\eta}$$

where E is the Young's modulus and η the viscosity.

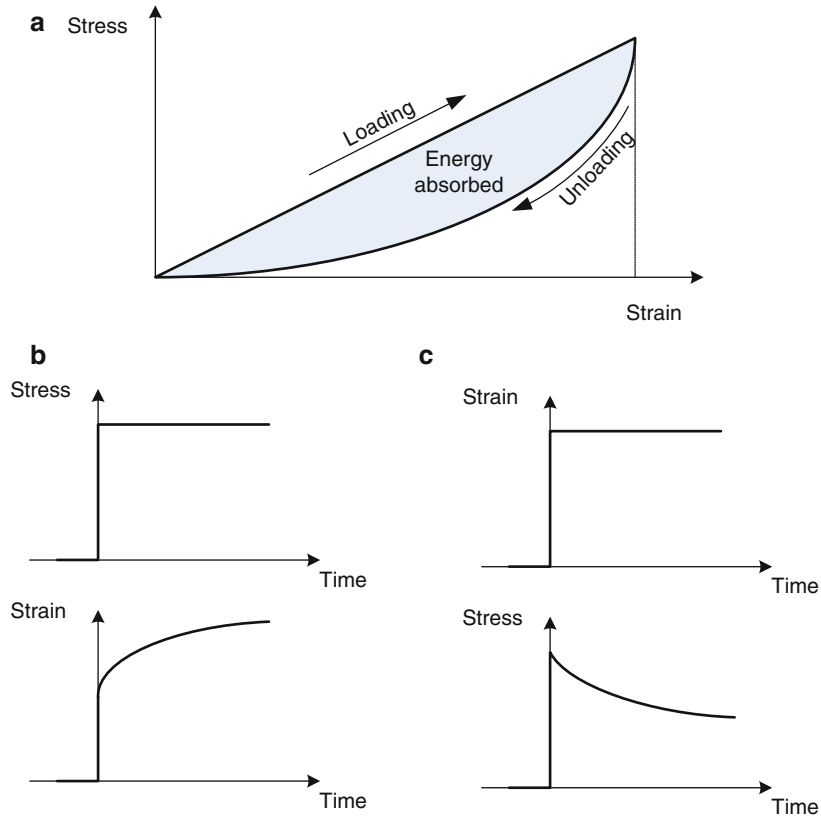

Fig. 3.11 Characteristic viscoelastic behaviours. (**a**) Hysteresis loop; the unloading path is not the same as the loading path. (**b**) Creep. When the load is held constant the strain increases with time. (**c**) Stress relaxation. When the strain is held constant then the stress required/experienced reduces with time

Quasi-Linear Viscoelastic (QLV) Model

Let's consider a three-dimensional stress state and infinitesimal strains, both functions of time in addition to space. We define a linear viscoelastic material as one whose stress relates with strain through a convolution integral.

$$\sigma(x,\tau) = \int_{-\infty}^{t} G(x, t-\tau)\frac{\partial \sigma}{\partial \varepsilon}\frac{\partial \varepsilon}{\partial \tau}(x,\tau)d\tau$$

where G is a relaxation function, $\partial\sigma/\partial\varepsilon$ represents the instantaneous elastic response, and $\partial\varepsilon/\partial\tau$ represents the strain history. This model is used widely as a first approximation to predict the behaviour of some biological tissues.

3.4.2.2 Storage and Loss Modulus

Another way of observing the behaviour of a viscoelastic material is under sinusoidal oscillations. Let's assume a simple harmonic oscillation of a material. The disturbing force F can be expressed as a complex function

$$F = F_0 e^{i\omega t} = A\sin(\omega t + \varphi) + iA\cos(\omega t + \varphi)$$

If the material is a perfectly elastic solid, then there will be no phase difference between stress and strain. If the material is a viscous fluid, then there will be a 90° phase lag of the strain response relative to that of stress. For a viscoelastic material, therefore, there is an amount of phase lag, δ ($0 < \delta < 90°$) between strain and stress responses.

$$\sigma = \sigma_0 \sin(\omega t + \delta)$$

$$\varepsilon = \varepsilon_0 \sin(\omega t)$$

where ω is the frequency of the oscillation.

The modulus, E^* (change of stress over change of strain) can be expressed as a complex number whose real part is the storage modulus and imaginary part is the loss modulus.

$$E^* = E' + iE''$$

The stored modulus is a measure of the stored energy and therefore represents the solid behaviour of the material whereas the loss modulus is a measure of lost energy that dissipates as heat and therefore represents the viscous behaviour of the material. For example, in the Kelvin-Voigt model $E^{'} = E$ (the Young's modulus) and $E^{''} = \eta\omega$.

The phase lag δ can be expressed as

$$\tan\delta = \frac{E''}{E'}$$

3.4.3 Plasticity and Failure

3.4.3.1 Plasticity

When a material experiences strain beyond some limit (usually referred to as the elastic limit) then, upon unloading, it does not return to its original shape or/and size; rather, there is residual strain. The material behaviour beyond the elastic limit and prior to failure is termed plasticity for metals as the material 'flows', i.e. offers less resistance to straining with further application of load. The term plasticity is used loosely to refer to the behaviour of all materials beyond the elastic limit. Plastic behaviour is rather complex and manifests itself in different ways for different materials.

A material that encounters large plastic deformations prior to failure is termed ductile whereas one that doesn't is termed brittle (Fig. 3.12a). Toughness is a property associated with how 'large' is the plastic region as it is a measure of the energy absorbed by the material per unit volume prior to failure; it is, therefore, a measure of resistance to failure. In most cases in construction a tough material is favourable as it guarantees the limitations of sudden, unexpected failures. Steel, for example, is a very tough material whereas concrete (as for most ceramics) is brittle.

Let's consider loading of a sample of an isotropic material with negligible viscous response in simple tension (Fig. 3.12b). The material will elongate as the load increases. Upon load release the material will follow the loading path back to zero elongation. If loaded beyond the elastic limit of the material, the sample will deform plastically and upon load release it will exhibit permanent, residual strain. The transition from elasticity to plasticity in some materials is not smooth and depends on a number of factors, mainly microstructure and loading rate. For convenience in calculations, engineers have introduced the notion of yield stress; this is a value of stress beyond which the material can be considered to behave plastically. Identification of yield stress varies among different material types; for example in metals one can observe upper and lower yield stress. However, a widely, used method to identify yield in metals and plastics is the offset rule; yield stress is the intersection between the stress-strain curve and a line parallel to the linear part of the stress-strain curve that crosses the x-axis (strain) at 0.2 %—the proof stress (Fig. 3.12c).

3.4.3.2 Failure Theories

Failure theories were firstly developed for metals and are usually expressed in terms of principal stresses as they conveniently represent the stress state of the material. All other types of material do not fail in similar ways to metals and therefore the theories described below are not necessarily valid for them.

Principal Stress Theory

Applicable mainly for brittle metallic materials and rarely used, this theory suggests that yielding will occur when either the maximum principal stress is higher than the value of yield stress in tension or the minimum principal stress is lower than the value of yield stress in compression.

Von Mises Theory of Failure and the Equivalent Von Mises Stress

The von Mises theory was originally based on the shear/distortion/deviatoric strain energy being the reason yielding will occur. A convenient measure of stress for isotropic ductile materials is the von Mises equivalent stress, which is a scalar. That's the stress against which one can compare yield when looking for failure of isotropic ductile materials. The equivalent von Mises

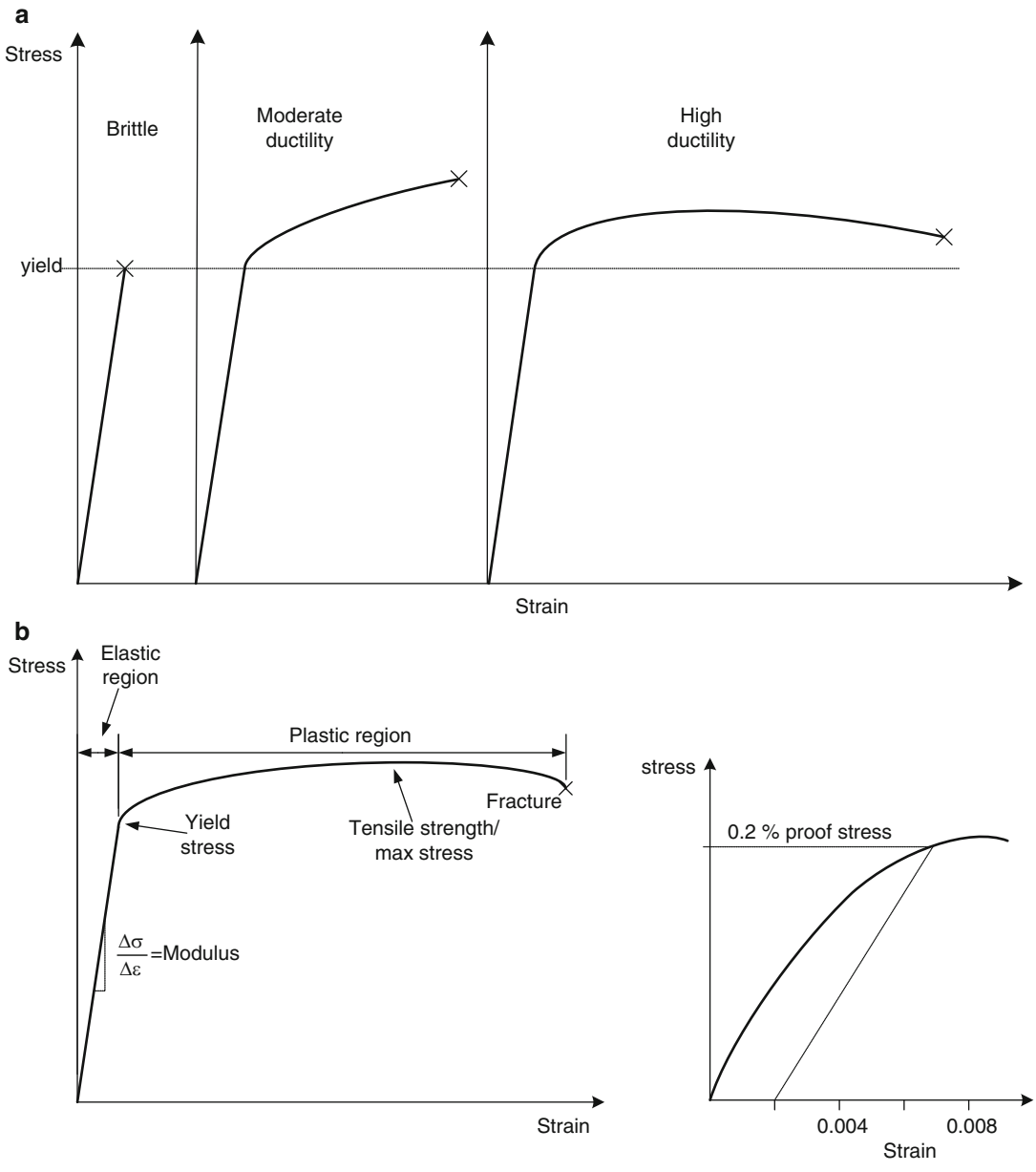

Fig. 3.12 (**a**) Stress strain curves of brittle and ductile materials. (**b**) The stress-strain curve for a metal alloy. (**c**) Definition of 0.2 % proof strength used as the yield stress for plastics and metals (Adapted from Askeland DR, 1998; *The science and engineering of materials*)

stress can be expressed through the deviatoric component of the stress tensor.

$$\sigma_{eq} = \sqrt{3I_2(\mathbf{s})} = \sqrt{\frac{3}{2}s_{ij}s_{ij}}$$

A convenient way of expressing the von Mises criterion is that yielding can occur when the root mean square of the difference between the principal stresses is equal to the yield of the material established by a simple tension test.

$$\sigma_{eq} = \sqrt{\frac{1}{3}\left((\sigma_{\mathrm{I}} - \sigma_{\mathrm{II}})^2 + (\sigma_{\mathrm{II}} - \sigma_{\mathrm{III}})^2 + (\sigma_{\mathrm{III}} - \sigma_{\mathrm{I}})^2\right)}$$
$$= \sqrt{\frac{1}{3}2\sigma_{y,t}^2}$$
$$\text{for 2D} \quad \sigma_{eq}^2 = \sigma_{\mathrm{I}}^2 + \sigma_{\mathrm{II}}^2 - \sigma_{\mathrm{I}}\sigma_{\mathrm{II}} = \sigma_{y,t}^2$$

where $\sigma_{y,t}$ the yield stress in simple tension and σ_{eq} the equivalent von Mises stress.

Tresca Failure Criterion
Originally developed by observation of metal forming, the Tresca criterion proposes that the maximum shear stress is responsible for yielding.

3.4.4 Equations of State

At conditions of high temperature and high pressure the behaviour of solids deviates substantially from what has been discussed up to now. Appropriate models of behaviour at such extreme conditions are the equations of state (EoS); these are relationships between state variables, most often describing how the density (or volumetric strain) and temperature (or internal energy) vary as a function of applied pressure.

3.4.4.1 General Form of EoS

In circumstances where deformations are small and the behaviour is independent of temperature, then a simple bulk modulus, K, can be used to relate hydrostatic stress (or pressure), p with volume changes; $\sigma_H = -K\varepsilon_v$ where ε_v is the volumetric strain as it represents the volume change over the original volume; $\varepsilon_v = \varepsilon_x + \varepsilon_y + \varepsilon_z = \frac{\Delta V}{V}$.

For harsh loading environments where linear elasticity fails, mathematical expressions have been developed to express the EoS for different materials. Depending on type of material these nonlinear behaviours may take the form of shock wave generation, crushing of pores, or compaction of a granular material, to name but a few. Such behaviours may be fitted conveniently to a polynomial (power series) EoS in line with the principles established by Mie & Gruneisen,

$$p = a_0 + a_1\varepsilon_v + a_2\varepsilon_v^2 + a_3\varepsilon_v^3 + \left(b_1 + b_2\varepsilon_v + b_3\varepsilon_v^2\right)E$$

where a third order polynomial with constants a_i is used to reflect how the pressure varies with the volumetric change in the material, and a second order polynomial with constants b_i is used to account for the influence of temperature change, inherent in the internal energy per unit volume, E of the material. Note that use of the second term alone in this relationship is equivalent to the bulk modulus expression used above. Although discussion so far has been limited to materials under compression, similar general expressions can be developed for materials undergoing expansion.

3.4.4.2 Shock Loading

Under loading conditions such as high velocity impact or contact detonation of explosives, the pressures experienced by the material are far greater in magnitude than its strength; this results in a hydrodynamic behaviour – similar to a fluid that has negligible shear strength – and the generation of a shock. For convenience, in line with the typical measurements made during testing – such as plate impact – deformation can be expressed as a relationship between the velocity of the shock in the material, u_s, and the particle velocity in the material, u_p; for example in quadratic form

$$u_S = c_0 + s_1 u_P + s_2 u_P^2$$

where c_0 is the bulk speed of sound in the material and s_i are parameters obtained by fitting the experimental data. This relationship is usually termed a Rankine-Hugoniot, which has been discussed in more detail in Sect. 3.1. Such relationship can be exploited to attain the full Mie-Gruneisen EoS.

3.4.4.3 Compaction and Unloading

With granular materials or materials exhibiting significant porosity it is often convenient to define their nonlinear behaviour using a

compaction EoS, based on experimental observation, which simply expresses the pressure as a function of volumetric strain in a piecewise fashion. Upon loading, these materials can undergo irreversible deformation (as a consequence of particle rearrangement or pore collapse, for example) and so relationships for unloading have to be determined. A simple way to do this is to define a series of unloading bulk moduli, also a function of volumetric strain, which are "stiffer" (steeper) than the loading path for the material at this deformation point.

3.5 Dynamic Loading

All loading in nature is inherently dynamic, as the loading itself or the behaviour of the structure due to the loading change with time. In some cases time can be neglected in the analysis of a structure without loss of accuracy; we call this a static analysis. There are loading scenarios whereby time cannot be neglected. These include impact, shock, and repeated/oscillatory loading.

Impact can be defined as the collision of two objects/masses with initial relative velocity. The term shock is used to describe any loading applied suddenly to a structure. These types of loading are associated with short durations, typically sub-second.

Depending on the application and the amount of detail required in the analysis, impact and shock are studied either by considering the bodies involved as rigid or as deformable. When the bodies are considered rigid then a system of differential equations can be formulated that describes the coupled motion of the objects as a function of the disturbance/loading. This system is usually solved computationally. When the bodies are considered deformable, then the behaviour of the materials from which the objects are made is taken into account. This system is also solved computationally, employing advanced computational methods such as the finite element method. These computational techniques are described in more detail in Chap. 9.

3.5.1 Vibrations

Vibrations occur when a mechanical system oscillates about an equilibrium point. When the oscillations are forced, then the dynamic behaviour may be expressed by

$$m\ddot{x} + c\dot{x} + kx = F(t)$$

whereas if the vibrations are free, the behaviour may be expressed by

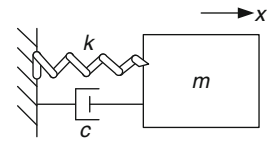

$$m\ddot{x} + c\dot{x} + kx = 0$$

where x is the displacement, m is the mass, c is the damping and k is the stiffness of the system represented by simple elements in the figure; $F(t)$ is the external force applied to the system.

When the oscillation is natural, i.e. free and undamped ($m\ddot{x} + kx = 0$) with no loss of energy due to resistance to motion, then, by solving the second order ordinary differential equation, the displacement of the system is $x(t) = A\cos(\omega t + \varphi)$, where A is the amplitude of the oscillation and ω is the natural frequency of the system, $\omega = \sqrt{\frac{k}{m}}$. This frequency is important because when the loading environment has a frequency close to the natural frequency of the system it stimulates, then the amplitude of oscillation maximises and may cause structural failure.

Solving for the displacement (and its derivatives) of forced and free damped vibrations can be done analytically. The resulting behaviour largely depends on the level of damping; one can plot a measure of the amplitude against a measure of the frequency (ratio of forced over natural) in order to quantify the frequency response of the system.

In a multiple degree-of-freedom problem, where the system consists of multiple masses,

then the system's behaviour can be expressed by a system of differential equations.

$$\mathbf{M}\ddot{\boldsymbol{x}} + \mathbf{C}\dot{\boldsymbol{x}} + \mathbf{k}\boldsymbol{x} = \mathbf{F}(t)$$

where the bold suggests matrix or vector notation.

It is often useful to extract the natural response of the system (using matrix algebra or the finite element method), which can be done by extracting the eigenvalues of the system; these are in essence the natural frequencies of the system. Of those, usually only the first few are important for practical applications. In order to solve for displacements and deformations (and therefore strains) for a system/structure that behaves dynamically (not limited to vibrations), then the system of differential equations above may be solved computationally usually using the finite element method (Chap. 17, Sect. 17.3).

3.5.2 Elastodynamics: The Wave Equation

Transmission of stress waves through a solid is important when impact and shock loading is expected. For an elastic bar that is loaded axially suddenly, and assuming that plane cross sections remain plane, then the displacement u, along the axis of the bar x, will cause strain of $\varepsilon_x = \frac{\partial u}{\partial x}$ and thus axial stress of $\sigma_x = E\varepsilon = E\frac{\partial u}{\partial x}$, where E is the Young's modulus of the bar. If we apply Newton's law of motion ($F = ma$) on an infinitesimal section of the bar dx, the change in axial force through it should be equal to its mass ($\rho A dx$) times acceleration.

$$Ad\sigma = \rho A dx \frac{\partial^2 u}{\partial t^2}$$

$$A\frac{\partial \sigma}{\partial x}dx = \rho A dx \frac{\partial^2 u}{\partial t^2}$$

$$A\frac{\partial \sigma}{\partial x}dx = \rho A dx \frac{\partial^2 u}{\partial t^2}$$

$$AE\frac{\partial^2 u}{\partial x^2}dx = \rho A dx \frac{\partial^2 u}{\partial t^2}$$

Therefore the wave equation is the following second order partial differential equation

$$\frac{\partial^2 u}{\partial t^2} = c^2 \frac{\partial^2 u}{\partial x^2}$$

where $c = \sqrt{\frac{E}{\rho}}$ is the speed of sound through the bar.

Solution of the differential equation results in a displacement $u = f(x - ct) + g(x + ct)$; functions f and g are arbitrary; the g function represents a wave travelling in the opposite direction to the applied load. Solving for the particle velocity, v we get $v = \frac{\partial u}{\partial t} = \pm c\frac{\partial u}{\partial x}$ and using the stress-strain relationship yields $\sigma_x = \pm\frac{E}{c}v = \pm\rho c v$. There is more discussion on the importance of this relationship in Chap. 1, Sect. 1.5.2.

3.5.3 Design for Strength and Endurance: Fatigue Strength

3.5.3.1 Design of Parts and Structures

Designing parts and structures to serve a specific purpose is an important part of the engineering profession. The designer needs to take into account multiple factors in order to meet the specification and produce something that is fit for purpose. From a stress analysis point of view, the main considerations usually are strength and endurance. No one can guarantee absolutely that a design/part will not fail; there is always a finite probability of failure. One way of addressing this is regular inspection of critical areas of a part. Another way is to provide redundant load paths in case a primary load path fails. No matter what though, the engineer needs to ensure s/he has done their utmost to ensure reliability of the design and predict lifespan in advance. In order to deal with variations and uncertainty, and to guarantee maximum safety we utilise a safety factor. The safety factor value comes from experience and intention. The safety factor should be defined based on the application, common/previous practice and

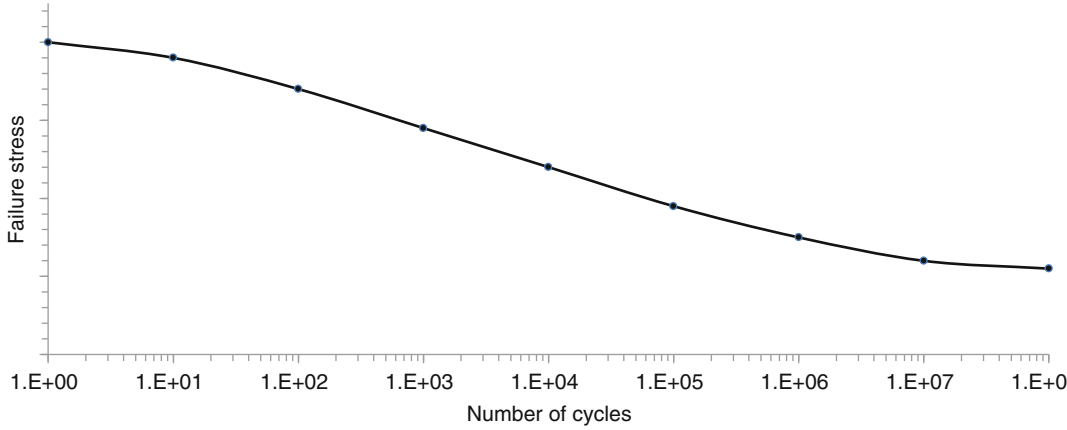

Fig. 3.13 A typical S-N curve for a metal. The *x*-axis represents the number of cycles to failure. One can look up fatigue life by finding how many cycles are required for failure for the mean operating stress that is expected due the estimated loading environment

lessons learned. A common process in ensuring safety from a strength perspective is more-or-less (depending on application) the following.

- Choose the safety factor.
- Estimate maximum loading in operation (this is no easy task usually).
- Conduct static (and dynamic, if appropriate) stress analysis.
  - Hand calculations (for simple features and loadings and for most machine elements and connections).
  - Computational calculations (finite element analysis) of parts or assemblies.
- Estimate fatigue life.
- Other (e.g. wear, corrosion resistance).

Dynamic stress analysis is conducted far less in the industry than static stress analysis as dynamics are associated with uncertainties in estimating the loading and in complexities (including man-hours) with the calculations. Even for estimating strength in dynamic events the tendency is to calculate an equivalent static loading scenario with an appropriate safety factor. If the structure is going to be subject to impact or blast, however, a dynamic analysis is usually necessary and is almost exclusively conducted computationally.

3.5.3.2 Fatigue

Fatigue is associated with repeated application of loading for long periods of time. It is the most common culprit for failure of metal components in structures, and therefore needs to be considered in the design process. Such failures tend to initiate from design features (including connections) that result in stress concentrations. It is a process that starts with the movement of dislocations that in turn form short cracks that propagate with continuous loading (cumulative damage).

Estimating the fatigue life of a component is based primarily on past experience and lots of testing, as the process of fatigue itself is fairly stochastic. Multiple experiments with coupons have made available fatigue (*S-N* or Wöhler) curves for various materials and geometries (for example sheet versus bar) (Fig. 3.13). The loading to produce the curve is oscillatory with specific amplitude about a mean stress. Most metals have an endurance limit, which is the mean stress below which fatigue failure would never occur.

A simple way to estimate fatigue life is the following.

- Calculate expected maximum or equivalent stress. This will depend on the application and available experimental data. The expected loading is usually not periodical,

but stochastic. One, therefore, usually needs to estimate an average stress level and its variation (alternating stress).

- Consider a fatigue level factor, K_f (e.g. ultimate tensile strength for most metals, then $K_f = 0.667$).
- Consider stress concentration, K_t based on the design of your component and available fatigue curves.
- Calculate the effective stress (i.e. reduced for K_f and K_t).
- Look up life on an appropriate fatigue curve.

Suggested Further Reading

Askeland DR. The science and engineering of materials. Stamford: Cengage Learning; 2010.

Benham PP, Warnock FV. Mechanics of solids and structures. London: Pitman; 1973.

Callister WD. Materials science and engineering. New York: Wiley; 2010.

Fung YC, Tong P. Classical and computational solid mechanics. London: Springer; 1993.

Shigley JE, Mitchell LD. Mechanical engineering design. New York: McGraw Hill Higher Education; 2003.

Blast Loading of Cells

4

Katherine A. Brown

Blast affects the body at physiological, cellular, sub-cellular and molecular levels. As with any trauma-related injury, a large number of cellular responses are initiated at both the injury site (local), and throughout the body (systemic). A myriad of biochemical pathways are involved and sometimes a "dis"-regulated interplay between pro- and anti-inflammatory responses occurs [1], which can considerably influence wound repair and patient recovery. Identification of the key cellular responses to and pathways affected by blast injury will be an important step towards developing improved patient therapies. Increasing interest in post-traumatic effects of blast wave exposure, such as traumatic brain injury (TBI) [2, 3] and heterotopic ossification (HO) [4, 5], has led to more research into how cells respond to strain rates at the moderate to high level. This chapter will provide a brief introduction to the cellular responses induced by blast. Also, this chapter will present examples of the types of experimental platforms developed to study cells under blast-type conditions. Finally, future directions for this research will be discussed in the context of improving the fundamental understanding of blast damage at a cellular level and improving the treatment of non-lethal blast injuries.

K.A. Brown, BA, BS, PhD, DIC, FRSC, FInstP
Cavendish Laboratory, Department of Physics, University of Cambridge, Cambridge, UK
e-mail: kb518@cam.ac.uk

4.1 Cellular Responses

Blast injuries result in damage to humans at all length scales, from skeleton, organs, and tissues to cells and sub-cellular components (see Chap. 6, Sect. 6.2). In general, cellular responses to blast-like forces depend on the magnitude of stress, the rate of application, and on the intrinsic mechanical properties of the cells [6, 7]. Intrinsic mechanical properties can differ between different cell lines and culture conditions. In a blast scenario the assumption is that the high magnitudes of the pressure wave result in severe cellular damage that contribute to a range of morbidities and sometimes fatality. In this case the entire body will experience the effects of the blast, and the level of the resulting trauma is determined, in general, by the magnitude (>0.1 MPa) and duration of the resulting pressure wave (10–1000 ms) [8, 9]. Other factors that together determine the level of trauma include distance from the blast, the amount of compression experienced by the body, and the amount of accompanying differential acceleration, which causes rupture of soft and hard tissue structures [reviewed in Ref. 10].

There is a paradoxical relationship about the interaction of pressure waves with cells. Specifically, depending on the pressure, duration, and site of application, a pressure wave can either cause injury or have a therapeutic effect. In biomedical literature, the term "shock wave" is

A.M.J. Bull et al. (eds.), *Blast Injury Science and Engineering: A Guide for Clinicians and Researchers*,
DOI 10.1007/978-3-319-21867-0_4

generally used to describe pressure waves generated with high peak-stress that propagate at speeds higher than the velocity of sound [11]. Interestingly, shock waves have found wide use in applications such as treatment of musculoskeletal disorders and wound healing [12, 13], lithotripsy (disintegration of urinary tract or gallstones) [14], cancer therapies [15] and drug delivery [16]. The therapeutic use of shock waves for treating soft tissue disorders is known as extracorporeal shock wave treatment (ESWT). Typically ESWT involves the delivery of highly-focused short-duration shock waves, generated externally, over a 2–8 mm region of tissue with magnitudes of 35–120 MPa and 1–3 s^{-1} durations [12, 14]. Shock waves used in this way have been shown to be facilitative for inducing or normalising biological responses to support tissue repair and regeneration [13].

The mechanisms of action that explain how pressure waves induce biological responses that either promote healing or cause injury are not well understood. Therapeutic shock waves have been shown to release cytokines and chemokines that can enhance tissue perfusion and angiogenesis, both essential for the wound healing cascade. ESWT also affects intracellular signalling events that involve integrins, calcium channels, phospholipase C, and mitogen-activated protein kinases (MAPKs), as well as NO production, growth factor stimulation, extracellular matrix metabolism, and apoptosis [see Ref. 13 for a comprehensive review]. More recently, it has been shown that shock waves trigger the release of cellular adenosine triphosphate (ATP), causing activation of Erk1/2 signalling pathway [17]. These biological responses are generally viewed as favourable for enabling soft tissue wound healing by promoting appropriate levels of inflammation, neo-vascularisation and tissue repair mechanisms [13]. In comparison, "damaging" biological responses of tissues and cells have also been observed in studies using ESWT (spanning more than 20 years), as well as for blast injury. Vascular and nerve tissue damage are among the known complications. ESWT can also alter the homeostasis of cellular calcium, resulting in cell and tissue damage, and cause bone fractures with accompanying damage to periosteal soft tissue and to the bone marrow cavity [reviewed in Ref. 13]. ESWT has also been shown to produce aseptic necrosis and damage of osteocytes in rat bone marrow [18]. Recent studies of equine mesenchymal stem cells show that increasing the intensity of the shock wave results in increased levels of apoptosis, correlated with reorganisation of the cytoskeletal f-actin fibres and inhibition of actin dynamics [19]. Shock waves can also be used for membrane permeabilisation, and both *in-vivo* and *in-vitro* experiments suggest cavitation is the primary mechanism of action [12]. Cellular destruction and reduced viability, due to lysis and other mechanisms, has also been observed in suspended and immobilised cell cultures that have been subjected to ESWT [20, 21]. Steinbach et al. [22] identified energy densities thresholds for different cell components, organelles and membranes, using laser scanning microscopy following specific fluorescence staining. Table 4.1 summarises the results of the study, which indicates that the plasma membrane is the cell component most sensitive to ESWT.

Table 4.1 Threshold sensitivities of cellular components to high energy shock waves

Cellular component	Damage threshold mJ mm^{-2}	Identification method
Plasma membrane	0.12	Permeability to propidium iodide
Cytoskeleton	0.21	Morphological changes in vimentin structure observed using FITC-labelled anti-vimentin antibody
Mitochondria	0.33	Morphological changes observed in mitochondrial membranes using 3,3′- dihexyloxacarbocyanine
Nucleus	0.55	Morphological changes observed in nucleoli and nuclear membranes using 2-[4-(Dimethylamino)styryl]-1-methylpyridinium iodide

Adapted from Steinbach et al. [22]

Similar biological responses have been described using data obtained from either clinical studies or laboratory models of blast injury. These effects include but are not limited to loss of cell viability, profound inflammatory responses (cytokines and chemokines), changes in signalling and phosphorylation pathways, changes in membrane permeability, induction of oxidative stress, protein nitration, degradation of the cytoskeleton, changes in neurotransmitters, disruption of cation homeostasis, and changes in mitochondrial integrity [e.g. Refs. 4, 6, 13, and references elsewhere in this text]. Examples of how some of these blast-related biological responses have been observed from studies of cells will be described in the discussion of experimental platforms in the following section.

4.2 Experimental Platforms

A considerable body of literature, dating back more than 25 years, describes the effects of pressure waves on cells. However, there have been few studies aimed at understanding the biochemical, structural and biomechanical responses of cells under pressures and/or strain rates approaching blast injury conditions. With the increased interest in traumatic brain injury (TBI), more such studies involving neural cell types have been published recently. This section will provide examples of more recently described experimental platforms for applying blast-like pressure waves to cell samples.

4.2.1 Compression Systems

Compression is used to simulate blast injury conditions in simplified biological systems as a means to understand the effects of high strains rates on cell integrity and function. Compression studies have been undertaken with cells in suspension [23, 24], cells adhered to coverslips [24, 25], and cells encapsulated in alginate [26].

Pressure bar systems have been adapted to enable the delivery of controlled pressure pulses to cells in suspension or adhered to a surface. These systems are based on Hopkinson pressure bars, developed by Bertram Hopkinson in 1914 to measure the pressure produced by explosives [27]. In 1949, these bars were used by Kolsky to characterise the dynamic response of materials in compression at high strain rates [28]. Kolsky's innovation was to place a sample between two bars – creating the Split Hopkinson Pressure Bar (SHPB) experimental platform. A number of modifications to traditional SHPB systems have been made to enable the material properties of biological tissues to be studied under compression. These modifications have involved the bar materials, gauges, pulse shapes and sample thickness [Ref. 29 and references therein]. More recently modifications in sample loading devices, described below, have allowed researchers to study cells in culture.

A compressive SHPB system is shown in Fig. 4.1. It is composed of a pressure chamber and four bars (a projectile, an input bar, an output bar, and a momentum trap) supported by metal blocks. In order to achieve dynamic equilibrium during the early stages of an SHPB experiment, and to enhance the output signal, the bars are made from low-impedance materials [24]. In order to measure the pulses generated on the bars following the impact of the striker bar, strain gauges are applied on the surface of the input and output bars. The positions of the strain gauges are chosen so that incident and reflected pulses do not overlap. The signals are recorded with high-speed digital oscilloscopes. Traditional one-dimensional SHPB stress wave analysis uses the measured incident, transmitted and reflected bars' strain to calculate the strain rate, strain and stress developed in the sample during the experiments.

Figure 4.2 shows the configuration of a SHPB system mounted with a biocompatible confinement chamber for applying pressure pulses to cell cultures is suspension. The chamber permits recovery of samples for further cellular and molecular analyses [23]. This system was used to study the effects of high strain rates on mesenchymal stem cells culture suspensions. Recovered material could be analysed using three different assays, for cell survival, viability and damage, respectively. Data obtained indicated

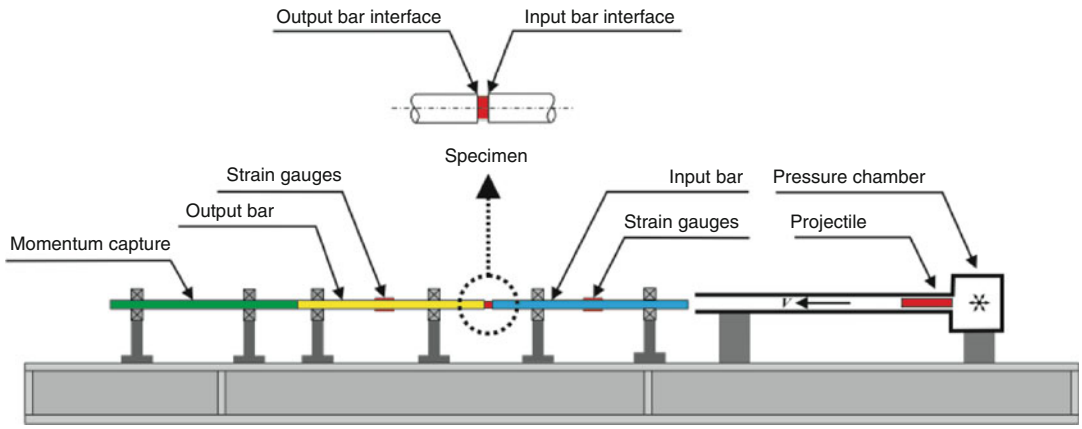

Fig. 4.1 Schematic diagram of a typical Split-Hopkinson Bar Pressure (SHPB) system for compression studies. A mass (shown as a *Projectile*) is fired from a *Pressure chamber* (shown *right*). Its trajectory is aligned using a guide, to enable it to accelerate into an *Input Bar*. The stress wave generated propagates along the *Input Bar* and interacts with the *Specimen*, which is sandwiched between the *Input* and *Output Bars*. Reflected and transmitted waves are generated and measured by *Strain gauges*. A *Momentum capture* trap may be included in this system to ensure that the sample is only impacted once. The magnitude and shape of the waves generated can be used to calculate the stress and strain in a sample as a function of time (Figure prepared by David Sory, Imperial College London, UK)

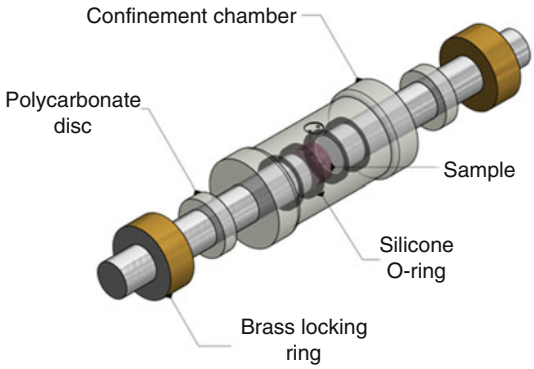

Fig. 4.2 Schematic diagram of an SHPB system mounted with a confinement chamber for studying cells in compression (Adapted from Bo et al. [23]). The polycarbonate Confinement Chamber is placed on to the input and output bars of the SHPB system. The chamber is secured in place using *Polycarbonate* Discs and *Brass Locking Rings*. Biocompatible *Silicone O-rings* are used to seal the chamber and prevent leakage of the *Sample*. Disposable syringes are used to introduce and remove samples from the chamber, through small bore holes located at the chamber's centre (Figure prepared by Benjamin Butler, University of Cambridge, UK)

that the level of damage in these cell cultures increases with the peak pressures generated in the confinement chamber [24].

SHPB systems can also be adapted for use with adherent cell cultures grown on glass coverslips. In the configuration shown in Fig. 4.2, the SHPB was further modified with the addition of two titanium (TI6Al4V) 60-mm long bars. A glass coverslip or plastic inserts [for use with three-dimensional (3D) cell culture] can be secured and immersed in culture media within the biocompatible chamber [24]. Alternatively, Nienabor et al. [25] used a slightly different loading device, in which coverslips were placed in a cell pressurisation chamber sandwiched between two aluminium alloy bars. That system generates a single-pulse type impulsive pressurisation. The design also enables the user to control both the magnitude and the duration of the impulsive overpressure applied. Using SH-SY5Y neuronal cells, they observed significant neurite and axonal loss at 2 MPa pressure as compared to controls.

An alternative approach to study cells in a 3D culture under short-load uniaxial compression was described by Yan et al. [26]. A cell-printing system was used to prepare 3D tissue cultures of rat adrenal medulla endothelial cells encapsulated in an alginate matrix. Samples (9 mm, height × 4 mm, radius), were placed on a 4442 Instron materials testing machine and compressive strains of 1, 5 and 10 % were applied. Samples were then recovered and assessed for cell survival and injury using optical microscopy assays. Their data showed that

at 1 % strain cell viability was 23 % and decreased with increasing compressive strain. In addition, this study also used a 3D multi-scale modelling approach, applying numerical models at macro-, multi-cellular and single cell levels, as shown in Fig. 4.3. The 3D multi-scale finite element model was capable of simulating realistic mechanical loads studied in this experiment. This platform methodology thus provides an effective means to quantify the stresses and strains at the cell's micro-environment when it is within engineered tissue scaffolds. This platform also has the potential to provide insights into cellular responses modulated by the application of high strains rates.

4.2.2 Pressure Systems

Recreating *in-vitro* the transient pressures a cell experiences during an actual blast is challenging. The two pressure-based experimental platforms most widely used for this type of application are the barochamber and, more recently, the shock tube. Both of these platforms have been adapted for studying *in-vitro* cell culture samples.

A schematic of a barochamber is shown in Fig. 4.4. This example from Vandevord et al. [30] consists of a five-piece aluminium chamber. The chamber contains a pedestal in the centre for housing cell cultures. A transient pressure wave is created using a metal ball that strikes a piston in a water-filled driving cylinder. The pressure time-history of the resulting "damped" pulse sequence is recorded by pressure transducers located within the chamber. The first pulse is of a high amplitude and short duration and the sum of all the integrated positive components of the pulse sequence is the time integral of the pressure, referred to as the 'positive impulse'. In Vandevord et al. [30] this system was used to examine the effects of short duration overpressures on adherent cultures of rat astrocytes. In this setup, Petrie dishes containing cell culture were filled with culture media, covered with Parafilm so that no air bubbles are present, and placed on the pedestal. The wave front of pressure pulse was then made to pass over the cells with a long duration peak pressure of approximately 270 kPA and an average positive impulse (total integrated positive pressure) of approximately 3 kPa.s. The cell cultures were then retrieved and analysed using molecular and cell-

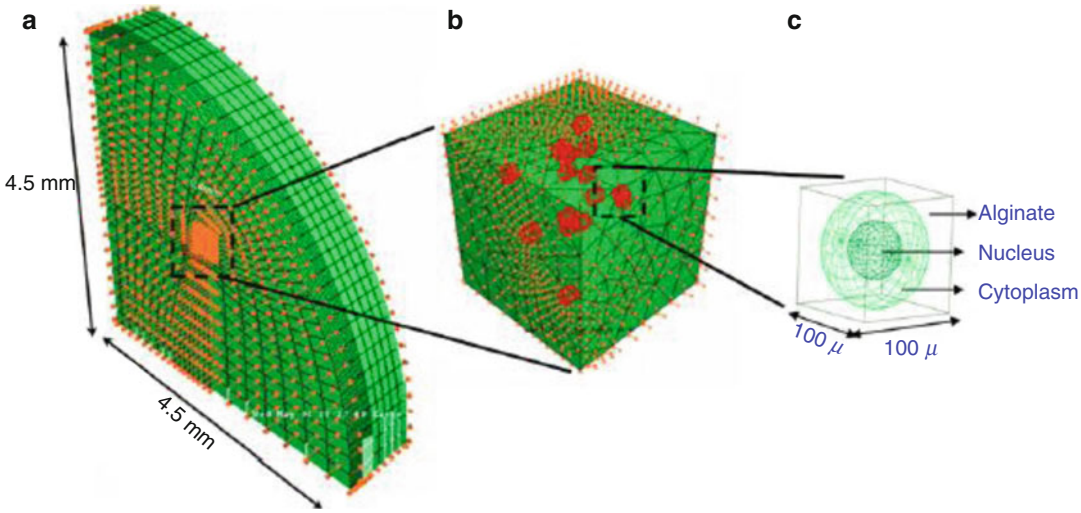

Fig. 4.3 Schematic images of three-dimensional finite element numerical models used to simulate compression of cell-encapsulated alginate constructs (Reprinted from Yan et al. [26] with permission of Elsevier). The numerical models shown here were developed to simulate the compression tests at (**a**) the macro-level, representing the printed alginate/endothelial cell constructs, (**b**) the meso-level representing the multi-cellular organization with the tissue construct, and (**c**) the micro-level, representing a single cell

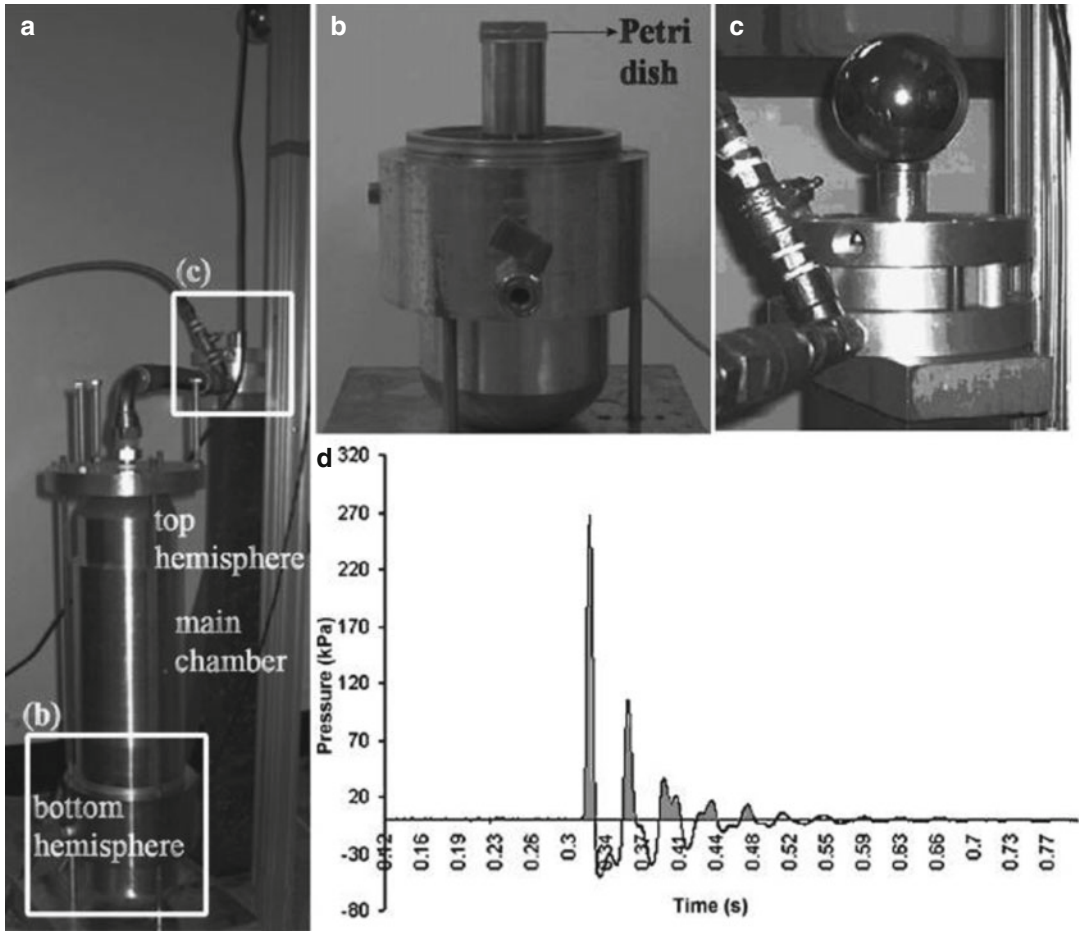

Fig. 4.4 Images depicting the assembly and output of a barochamber, designed to study how short duration overpressures affect cells (Reprinted from Vandevord et al. [30], with the permission of Elsevier). (**a**) A five-piece aluminium barochamber including the driving cylinder shown on the right-hand side of the image. (**b**) Inner components of the bottom hemisphere of the barochamber, showing Petrie dish mounting. (**c**) Inner components of the driving chamber showing the metal ball dropping on the rod, which drive the piston to create a shock wave. (**d**) Pressure-time history of a pressure wave generated by the barochamber (Figure prepared by Benjamin Butler, University of Cambridge, UK)

based assays. In this study, cells cultures were allowed to grow over a 3-day period and effects were assessed every 24 h. The resulting data demonstrated elevated levels of reactivity, elevated levels of survival gene expression, but also decreased expression of apoptotic genes after 2 days post-exposure to the pressure wave. Examples of cell-types studied using barochamber-generated overpressures include microglia, which showed mild activation [31], and dorsal root ganglion cells, which showed extensive injury, including cytoskeletal and plasma membrane abnormalities [32]. More recently, shock tubes, typically used to study hard condensed matter, have been adapted for use with cell cultures. Shock tubes can be arranged either vertically, as shown in Fig. 4.5, or horizontally, as in Fig. 4.6. In either configuration, compressed gas (e.g., helium or air) is used to pressurise the driver section that then delivers the shock wave. Peak pressures and profiles depend on the design and material used in a burst diaphragm. In the system shown in Fig. 4.5 [7], a compressed helium source is connected to an adjustable driver section, which

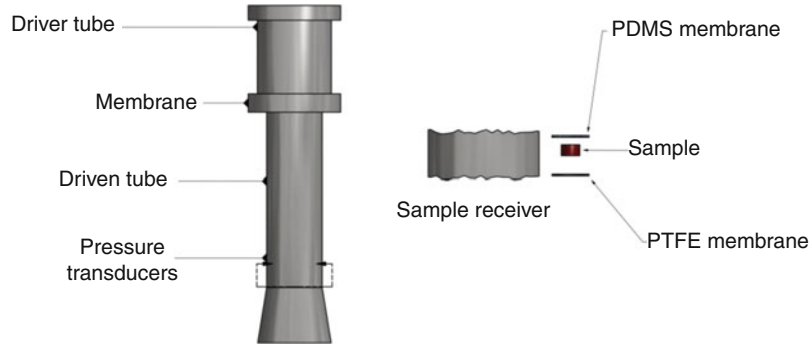

Fig. 4.5 Vertically-oriented shock tube with a fluid-filled sample receiver (Adapted from Effgen et al. [7]). The schematic diagram shows an example of an experimental shock tube configuration used to study the effects of blast overpressure on tissues culture, submerged in a fluid-filled reservoir designed to simulate the environment of the surrounding brain. Compressed helium is used to generate blast overpressures along the *Driver Tube*. Burst pressures can be modified by varying the thickness and composition of the polyethylene terephthalate membranes in the *Diaphragm*. Pressure-time histories are recorded using *Pressure Transducers*. In this study, the *Sample Receiver* is a fluid-filled chamber containing the tissue culture *Sample*, which is sandwiched between a polydimethylsiloxane (*PDMS*) and polytetrafluoroethylene (*PTFE*) *Membranes* (Figure prepared by Benjamin Butler, University of Cambridge, UK)

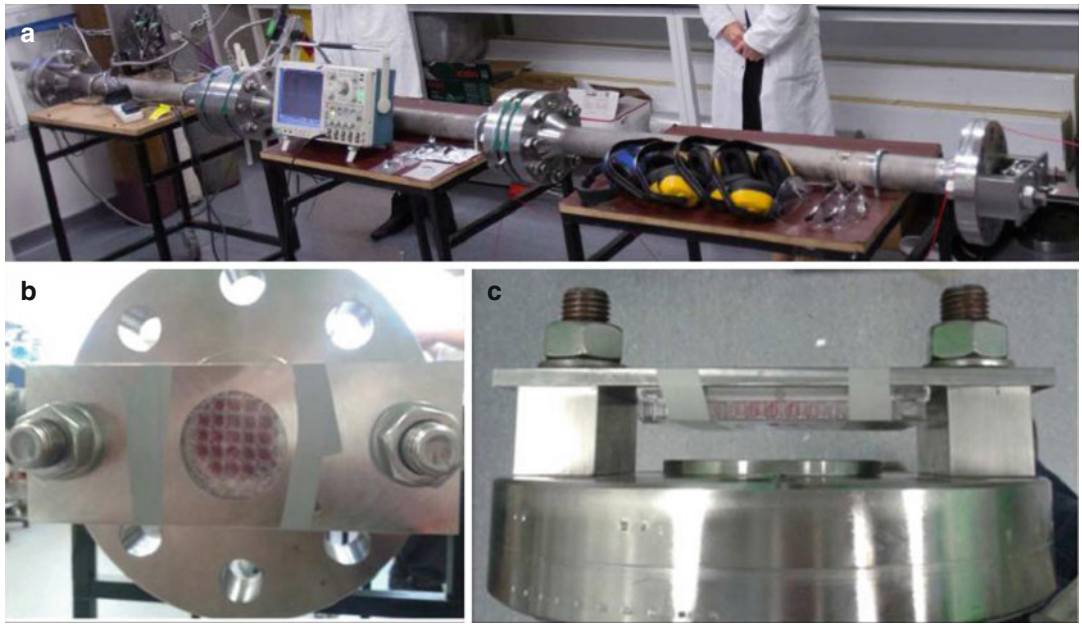

Fig. 4.6 Horizontally-oriented shock tube at the Centre for Blast Studies at Imperial College, configured for applying blast overpressures to cells in tissue culture wells. (**a**) A double-diaphragm shock tube. A fluid-filled 24-well cell culture plate attached to the end of the tube is shown from the side (**b**) and from the top (**c**). Pressure transducers record the pressure-time profiles of pressure pulses in the shock tube. Samples can be oriented with sealed wells facing towards or away from the end of the shock tube (Figure prepared by Chiara Bo, Imperial College London, UK)

is aligned vertically over the water-filled section where the sample is placed. This section is called a "sample receiver." In-air transducers are located at the exit of the shock tube. Pressure profiles are recorded by transducers, three of which are located at the end of the shock tube (in air) and two more submerged near the sample. For cell cultures, plates are sealed in sterile bags containing culture

medium, being sure to exclude bubbles. This system was used to study the effects of blast exposure on adherent primary mouse endothelial cell cultures. These cells were exposed to peak incident overpressures of approximately 581 kPA with a duration of 1 ms and an in-air impulse of 222 kPa.ms were used. Under these conditions levels of cell death were relatively insignificant and the primary effect reported was the disruption of tight junction integrity in these cultures.

Figure 4.6a shows an example of a shock tube in a horizontal orientation, configured for use with tissue cultures. A tissue culture plate is secured on a custom-made stainless steel support mounted at the end of the shock tube, which is open to air (Fig. 4.6b, c). Each well of the tissue culture plate is filled with liquid medium and the entire plate is sealed with a non-permeable tape (Corning). A custom made polycarbonate sensor mount is attached with epoxy resin to the rear surface of the tissue culture plate, in which a hole is drilled to allow insertion of the pressure sensor (Dytran Instruments – 2300C4). In these experiments, adherent mesenchmyal stem cell monolayer cultures were exposed to a peak incident overpressure of about 400 kPa with a duration of 10 ms. In this example cell viability was reduced compared to controls and plate orientation on the shock tube was also shown to affect the level of cell survival [24]. A similar study, carried out using adherent cell cultures of rat or human neural cells, and using a horizontal shock tube showed that plate orientation was also an important parameter in this type of experimental setup [33]. These studies were carried out using peak pressures of about 145 kPa. Post-exposure analysis of cell cultures showed decreased intracellular adenosine triphosphate levels, increased amounts of reactive oxygen species and loss of cell viability after a single blast exposure. Interestingly, administering two or three blast exposures 24 h after the initial blast caused less cell damage than the initial blast. This result led the authors to speculate about the possibility that cellular factors produced or released after the initial blast provided some additional protection to surviving cells, but no candidate factors were identified in this study.

4.2.3 Laser-Based Systems

Systems that use laser-induced shock or stress waves to study effects on biological materials were first described nearly 20 years ago [12], particularly for applications related to ESWT. More recently, laser-based systems have been used to study adherent cell cultures, primarily as model systems in experiments investigating trauma and injury. One of the better-characterised systems is flyer-plate model, shown in Fig. 4.7 [34]. In this experimental setup a Nd-Yt-Al- -garnet (Nd-YAG) laser is used to generate a pulse directed toward a fused silica window coated with a thick layer of copper. Expansion of the hot copper vapour, created by the laser pulse, accelerates the remaining superficial layer of metal—the flyer-plate—away from the surface. In this configuration an individual vial from a 24-well polystyrene cell culture plate is located over the copper layer to enable it to interact with a shock wave generated by this system. A glass coverslip with an adherent cell culture on its surface is placed "face-up" in the vial and fluid added. Pressure profiles are recorded using a transducer shown submerged in the fluid of the tissue culture vial, directly above the glass coverslip containing the adhered cells. Using this system human endothelial cells were exposed to shock waves with peak amplitudes of about 23 MPa. Cells were assayed used a variety of optical microscopy methods, which showed extensive evidence of cell damage, including the formation of stress fibres, expression of inflammatory biomarkers, and impaired regeneration [35]. A similar setup was used to study the biological responses of a rat and a mouse macrophage cell line as models of high energy trauma. In this study, only mouse macrophages showed significant level of cellular responses, when assayed using a variety of molecular and biochemical assays. The key result was that macrophages exhibited an inflammatory response, which did not involve the production of NO or iNOS. The information about the mechanism responsible for these effects remains unknown.

Alternative platforms have used irradiation of an adsorber material, rather than expansion of copper vapour, to generate a pressure pulse. In

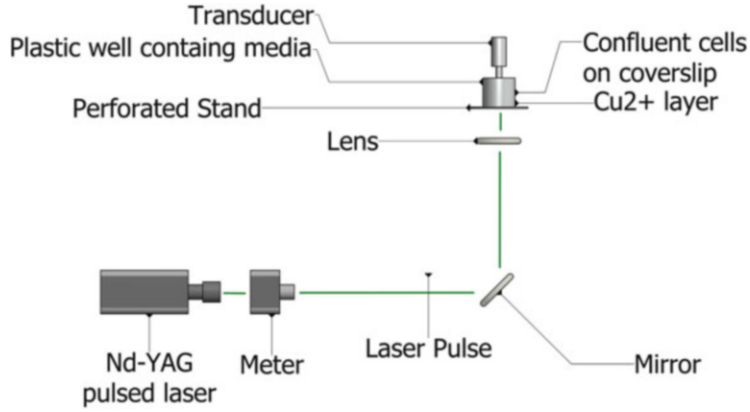

Fig. 4.7 The flyer-plate model for application of shock waves to cell cultures with or without surface cavitation (Adapted from Sondén et al. [34]). A *Laser Pulse*, generated with a *Nd-YAG* (neodymium:yttrium-aluminium-garnet) pulsed laser and monitored by an energy *Meter*, is reflected with a *Mirror* and focused with a *Lens* towards a *Perforated Stand* at the base of the sample stage. In this example, hot copper vapour accelerates the "flyer plate" (the outermost Cu^{2+} *layer*) towards the *Plastic well containing media*, where the sample, *Confluent cells on a coverslip*, is located. The well can be partially filled with media, generating surface cavitation, or fully filled with no bubbles to eliminate cavitation effects. Pressure-time profiles are measured using a polyvinylidene difluoride pressure *Transducer* (Figure prepared by Benjamin Butler, University of Cambridge, UK)

a recent report by Schmidt et al. [36], this type of system was used to study cell destruction of adherent neural cell (glioblastoma) cultures. In this particular setup, a thick black varnish was used as the absorber and pressure profiles were measured using a needle hydrophone that could be submerged into the liquid of tissue plate wells containing the cultures. Cell survival was studied after exposure to peak pressures between 60 and 90 MPa with a duration of 6 ns. Under the experimental conditions used, the threshold for cell death of these cultures was shown to be 80 MPa. Interestingly, this system also used photon Doppler velocimetry (PDV) to obtain velocity profiles of the cell culture vessel at the passage of the pressure waves. These profiles were subsequently used in numerical pressure wave simulations to characterise pressure conditions on the cellular length scale. A similar setup was previously used by Hu et al. [37] to study cell adhesion of neural cells cultured on a Si substrate. Although no pressure profiles were reported, the data obtained were used in a finite element simulation of cell detachment [38]. The model derived suggested that the cells behaved like a soft elastic solid during the detachment process due to the large difference between their characteristic response time and the ultrashort (ns) duration of the applied stress wave.

4.2.4 Mechanical Deformation Systems

Many different experimental platforms have been designed for the purpose of applying mechanical deformation forces to cells. Some of these platforms have modelled blast injury by stretching, shearing or lacerating cells [reviewed in Ref. 6]. As an introduction to these types of models, four contemporary examples are described below.

Figure 4.8 shows the experimental setup for a microfluidic flow chamber designed to create defined shear stresses using an ultra-fast pressure servo [39]. Cells are cultured directly in the chamber, which can be placed on an inverted microscope to enable imaging using, for example,

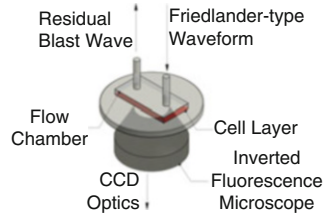

Fig. 4.8 Schematic diagram of a microfluidic chamber and pressure servo used for applying blast waves to cell cultures (Adapted from Maneshi et al. [39]). Cells, shown, were subjected to blast waves in fluid, generated using an ultra-fast piezo-driven Pressure Servo (ALA Scientific Instruments, NY). A classic *Frielander-type waveform* was applied to a *Cell Layer* that was cultured in a microfluidic *Flow chamber*. An *Inverted Fluorescent Microscope*, equipped with a *CCD Optics*, was used to follow real-time fluctuations in cellular calcium ion levels as a function of blast-like overpressures (Figure prepared by Benjamin Butler, University of Cambridge, UK)

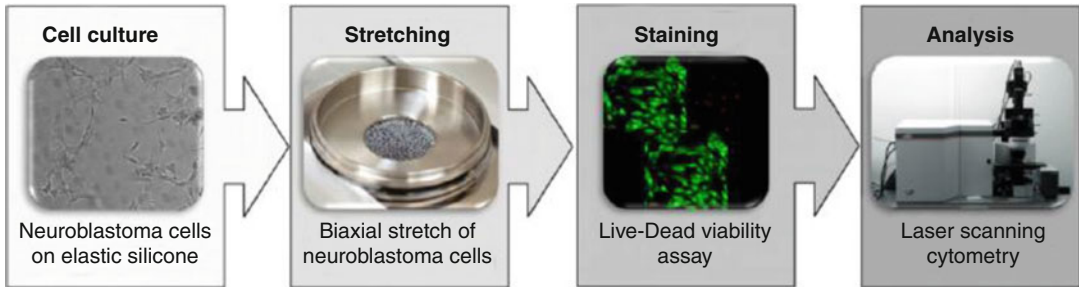

Fig. 4.9 Workflow for an *in vitro* cell model of blast-induced traumatic brain injury (Reprinted from Skotak et al. [40], with the permission of Elsevier). In this model, *Neuroblastoma cells* are initially cultured on an *elastic silicone* substrate and then subjected to *biaxial stretching*, at strain rates as high as 50 s^{-1}, using a modified Cultured Axonal Injury device. Cell viability is then assessed using a *Live-Dead* fluorescent dye-based *assay* that labels cells based upon the integrity of their membranes. Finally, *Laser Scanning Cytometry* of the sample is used in conjunction with the Live-Dead assay to provide a visual readout to enable classification of cells as live, dead or injured

fluorescent probes. Pressure pulses of known waveform (e.g., a Friedlander curve to mimic blast waves) with a time resolution on the order of ~1 ms can be applied to the cells using the servo. The flow velocity is obtained experimentally by tracking fluorescent microbeads. This system was used to study how blast-like shear forces affect intracellular calcium responses in cultured astrocytes. To mimic shear forces considered representative of blast conditions, the authors applied pulses of different magnitudes but with a constant pulse width of 10 ms. Calcium levels in each cell sample studied were monitored by optical microscopy using a fluorescent dye assay. The data revealed that mechanical shear stress induced significant increases in intracellular calcium levels, though the mechanisms and/or biochemical pathways involved are not yet known.

In blast and other traumatic injuries, it is generally assumed that mechanical damage of cells arises from stretching, compression, torsion or shear (or a combination of these factors). Stretch-induced damage, in particular, has been an attractive area of study for TBI, leading to the development of a number of experimental platforms for studying how cells respond to uniaxial, biaxial and equibiaxial strains [6, 40]. Figure 4.9 shows a workflow chart for a relatively recent model used to study neuronal cell stretching as a TBI model over a wide range of strain and strain rates [40]. In that study, a Cultured Axonal Injury (CAI) device [41, 42] was modified to enable high strain and strain rates to be applied to the whole neuronal body of cells cultured on an elastic silicone substrate. Pulses of 15 ms were delivered using a compressed air system. These experiments were

carried out over a range of strains (0–140 %) and strain rates (15–68 s^{-1}). Pressure sensor data and high-speed video were used here to obtain the strain history of each experiment. Cells can be recovered in this system. In this case recovered cells were assayed for viability using optical and flow cytometry methods. Analysis of these data indicated the presence of a dose dependence in which increased amounts of strain resulted in increased cell death, though the mechanisms involved are not yet fully defined [40]. In a different study, high-velocity stretching was also used to simulate the mechanical forces of a blast pulse on the vasculature, using engineered arterial lamellae as a model for TBI cerebral vasospasm [43]. The arterial tissue mimics were cultured on an elastomer membrane, which was then stretched at high-velocity to create acute injury. Strain history was recorded using high-speed video. The effects of strain on these tissue mimics were studied using a number of molecular and biochemical assays. The assays revealed changes in calcium dynamics within an hour of injury and also alterations in the expression of proteins. These changes in protein expression were indicative of vascular remodelling that is likely related to cerebral vasospasm that is observed in TBI patients.

As a final example in this section, atomic force microscopy (AFM) has been adapted to characterise strain-dependent dynamic behaviour of single neurons *in-vitro* as a means to improve understanding of cellular responses that occur in TBI. AFM is a state-of-the art technique typically using for imaging and studying material properties of all types of matter at the nanoscale. In biological applications it can be used to study cells, subcellular structures and even macromolecules over a large range of forces, load levels and length scales [44]. In the example here [44], AFM "compression" tests were performed on individual cortical neurons using microsphere-modified cantilevers. These experiments used Load–unload cyclic sequences spanning three orders of magnitude of displacement rates, 10, 1, and 0.1 μm s^{-1}. The key findings of this study were that cell responses exhibit hysteretic features, strong non-linearities, and substantial time/rate dependencies. The authors also created a constitutive model, using a 3D finite element framework, for quantifying the mechanical behaviour of cortical neurons. They validated this model using their experimental data. In a subsequent study, this data was used to calibrate a more complex continuum model aimed at describing neuronal cell responses under blast loading [45]. In that study the authors created separate constitutive models of different subcellular structures and subjected these models to blast loading within a complete fluid-structure interaction computational framework. The authors observed that their models appear to simulate some of the deformations of intracellular structures predicted to occur under blast loading. Modelling studies such as these provide a means for generating hypothesis-driven questions about cell damage mechanisms.

4.3 Future Research

The recent interest in cellular level blast models of injury, particularly in the area of TBI, has stimulated the development of contemporary experimental platforms for studying biological and biomechanical responses to simulated blast loading conditions. This emerging field of study is clearly benefitting from new technological advances in materials and biological research. The studies above also highlight some of the current weaknesses that need to be addressed in future studies. For example, there is an increased recognition that experimental conditions used in these systems need to re-create blast type conditions, but there is little consensus about what those conditions should be. Studies use a variety of literature to guide the choice of pressures, strain rates, etc. Values in the literature, however, also vary widely. Bass and colleagues have re-analysed data for whole body lethality of both short and long duration blast [8, 9], providing at least a more recent critical analysis of blast conditions. Perhaps even more importantly, these papers emphasise the need to provide sufficient data about peak pressures, durations, profiles and impulse, which is sadly often missing in many published studies. When detailed data is not provided it is often extremely difficult to conduct realistic comparisons of data between laboratories, even when similar or

identical cell lines are used in studies. Without doubt, future studies need to focus on defining biologically relevant blast conditions and attempt to more critically interpret this data, whenever possible, against other studies in the field.

With regard to biological responses, it is clear that the majority of the current studies have focused on cell viability and/or establishing thresholds for cell death. Unlike the experimental platforms being developed, which in many cases use state-of-the-art technology to deliver blast-like conditions, the biological analysis carried out is fairly basic. As a result, the bulk of cellular responses reported are phenotypic (an experimentally observable change) and there is the lack of knowledge about underlying mechanisms. This gap in knowledge could be addressed by implementing systems biology approaches, which would apply modern genomic, proteomic, and bioinformatic technologies and tools [for examples see Refs. 46–49]. Such tools have the potential to identify molecular species and candidate biochemical pathways responsible for cellular responses to blast loading conditions. Modelling efforts are also emerging, mainly for understanding cell mechanics related to loading. Aligning modelling efforts at all scales with clinically relevant molecular and biochemical data would also contribute to understanding cellular responses in higher order structures (e.g., tissues, organs, bone) in which cells are embedded.

In summary, most cell-based blast models are at an early stage of development. Combining contemporary platforms for delivering pressure pulses with modern molecular systems biology approaches holds promise for identifying molecular species, biochemical pathways and networks that contribute to the aetiology of blast injuries. Fundamental knowledge about blast-related cellular responses will be essential for the development of new medical approaches to improve patient outcomes such as: the identification of biomarkers for improved diagnosis; promotion of appropriate control of inflammatory pathways for rapid recovery and reduced complications; therapeutic-directed control of stem cell differentiation for regenerative processes; and enhancement of drug delivery and drug performance. Furthermore, given the complex and sometimes unusual nature of the post-traumatic complications (e.g., HO and TBI), blast injury will undoubtedly benefit from personalised medicine approaches that use molecular or cellular assays of patient samples to help guide the selection of optimal therapies. Again, for such an approach to be successful it is critical to identify what assays should be used or developed. Information derived from cell-based blast models, put in the context of the physiological responses of a patient, therefore holds great promise for improving the medical management of the post-traumatic effects of blast injury.

References

1. Cobb JP, O'Keefe GE. Injury research in the genomic era. Lancet. 2004;363(9426):2076–83.
2. Bass CR, Panzer MB, Rafaels KA, Wood G, Shridharani J, Capehart B. Brain injuries from blast. Ann Biomed Eng. 2012;40(1):185–202.
3. Rosenfeld JV, McFarlane AC, Bragge P, Armonda RA, Grimes JB, Ling GS. Blast-related traumatic brain injury. Lancet Neurol. 2013;9:882–93.
4. Alfieri KA, Forsberg JA, Potter BK. Blast injuries and heterotopic ossification. Bone Joint Res. 2012;1 (8):192–7.
5. Edwards DS, Clasper JC. Heterotopic ossification: a systematic review. J R Army Med Corps. 2014;161 (4):315–21. pii: jramc-2014-000277.
6. Chen YC, Smith DH, Meaney DF. In-vitro approaches for studying blast-induced traumatic brain injury. J Neurotrauma. 2009;26(6):861–76.
7. Effgen GB, Hue CD, Vogel 3rd E, Panzer MB, Meaney DF, Bass CR, Morrison 3rd B. A Multiscale approach to blast neurotrauma modeling: part II: methodology for inducing blast injury to in vitro models. Front Neurol. 2012;3:23.
8. Bass CR, Rafaels KA, Salzar RS. Pulmonary injury risk assessment for short-duration blasts. J Trauma. 2008;65(3):604–15.
9. Rafaels KA, Bass CR, Panzer MB, Salzar RS. Pulmonary injury risk assessment for long-duration blasts: a meta-analysis. J Trauma. 2010;69(2):368–74.
10. Proud WG. The physical basis of explosion and blast injury processes. J R Army Med Corps. 2013;159 Suppl 1:i4–9.
11. Doukas AG, Flotte TJ. Physical characteristics and biological effects of laser-induced stress waves. Ultrasound Med Biol. 1996;22(2):151–64.
12. Speed CA. Extracorporeal shock-wave therapy in the management of chronic soft-tissue conditions. J Bone Joint Surg Br. 2004;86(2):165–71.
13. McClain PD, Lange JN, Assimos DG. Optimizing shock wave lithotripsy: a comprehensive review. Rev Urol. 2013;15(2):49–60.

14. Mittermayr R, Antonic V, Hartinger J, Kaufmann H, Redl H, Téot L, Stojadinovic A, Schaden W. Extracorporeal shock wave therapy (ESWT) for wound healing: technology, mechanisms, and clinical efficacy. Wound Repair Regen. 2012;20(4):456–65.
15. Assmus B, Walter DH, Seeger FH, Leistner DM, Steiner J, Ziegler I, Lutz A, Khaled W, Klotsche J, Tonn T, Dimmeler S, Zeiher AM. Effect of shock wave-facilitated intracoronary cell therapy on LVEF in patients with chronic heart failure: the CELLWAVE randomized clinical trial. JAMA. 2013;309(15):1622–31.
16. Steinhauser MO, Schmidt M. Destruction of cancer cells by laser-induced shock waves: recent developments in experimental treatments and multiscale computer simulations. Soft Matter. 2014;10(27):4778–88.
17. Weihs AM, Fuchs C, Teuschl AH, Hartinger J, Slezak P, Mittermayr R, Redl H, Junger WG, Sitte HH, Rünzler D. Shock wave treatment enhances cell proliferation and improves wound healing by ATP release-coupled extracellular signal-regulated kinase (ERK) activation. J Biol Chem. 2014;289(39):27090–104.
18. Wang FS, Yang KD, Chen RF, Wang CJ, Sheen-Chen SM. Extracorporeal shock wave promotes growth and differentiation of bone-marrow stromal cells towards osteoprogenitors associated with induction of TGF-beta1. J Bone Joint Surg Br. 2002;84(3):457–61.
19. Raabe O, Shell K, Goessl A, Crispens C, Delhasse Y, Eva A, Scheiner-Bobis G, Wenisch S, Arnhold S. Effect of extracorporeal shock wave on proliferation and differentiation of equine adipose tissue-derived mesenchymal stem cells in vitro. Am J Stem Cells. 2013;2(1):62–73.
20. Delius M. Medical applications and bioeffects of extracorporeal shock waves. Shock Waves. 1994;4:55–72.
21. Brummer F, Brauner T, Hulser DF, Wieland W. The combined effects of high-energy shock waves and cytostatic drugs or cytokines on human bladder cancer cells. World J Urol. 1990;8:224–32.
22. Steinbach P, Hofstadter F, Nicolai H, Rossler W, Wieland W. Cytoplasmic molecular delivery with shock waves: importance of impulse. Ultrasound Med Biol. 1992;18:691–9.
23. Bo C, Balzer J, Brown KS, Walley SM, Proud WG. Eur Phys J Appl Phys. 2011;55:31201.
24. Bo C, Williams A, Rankin S, Proud WG, Brown KA. Development of a chamber to investigate high-intensity compression waves upon live cell cultures. Phys Conf Ser. 2014;500:102001.
25. Nienaber M, Lee JS, Feng R, Lim JY. Impulsive Pressurization of Neuronal Cells for Traumatic Brain Injury Study. J Vis Exp. 2011;(56):2723.
26. Yan KC, Nair K, Sun W. Three dimensional multi-scale modelling and analysis of cell damage in cell-encapsulated alginate constructs. J Biomech. 2010;43 (6):1031–8.
27. Hopkinson B. A Method of Measuring the Pressure Produced in the Detonation of High Explosives or by the Impact of Bullets. Phil Trans R Soc A. 1914;213:437–56.
28. Kolsky H. An investigation of the mechanical properties of materials at very high rates of loading. Proc Phys Soc B. 1949;62:676–700.
29. Trexler MM, Lennon AM, Wickwire AC, Harrigan TP, Luong QT, Graham JL, Maisano AJ, Roberts JC, Merkle AC. Verification and implementation of a modified split Hopkinson pressure bar technique for characterizing biological tissue and soft biosimulant materials under dynamic shear loading. J Mech Behav Biomed Mater. 2011;4:1920–8.
30. Vandevord PJ, Leung LY, Hardy W, Mason M, Yang KH, King AI. Up-regulation of reactivity and survival genes in astrocytes after exposure to short duration overpressure. Neurosci Lett. 2008;434(3):247–52.
31. Kane MJ, Angoa-Pérez M, Francescutti DM, Sykes CE, Briggs DI, Leung LY, VandeVord PJ, Kuhn DM. Altered gene expression in cultured microglia in response to simulated blast overpressure: possible role of pulse duration. Neurosci Lett. 2012;522(1):47–51.
32. Suneson A, Hansson HA, Lycke E, Seeman T. Pressure wave injuries to rat dorsal root ganglion cells in culture caused by high-energy missiles. J Trauma. 1989;9:10–18.
33. Arun P, Spadaro J, John J, Gharavi RB, Bentley TB, Nambiar MP. Studies on blast traumatic brain injury using in-vitro model with shock tube. Neuroreport. 2011;22(8):379–84.
34. Sondén A, Johansson AS, Palmblad J, Kjellström BT. Proinflammatory reaction and cytoskeletal alterations in endothelial cells after shock wave exposure. J Investig Med. 2006;54(5):262–71.
35. Günther M, Plantman S, Gahm C, Sondén A, Risling M, Mathiesen T. Shock wave trauma leads to inflammatory response and morphological activation in macrophage cell lines, but does not induce iNOS or NO synthesis. Acta Neurochir (Wien). 2014;156 (12):2365–78.
36. Schmidt M, Kahlert U, Wessolleck J, Maciaczyk D, Merkt B, Maciaczyk J, Osterholz J, Nikkhah G, Steinhauser MO. Characterization of a setup to test the impact of high-amplitude pressure waves on living cells. Sci Rep. 2014;4:3849.
37. Hu L, Zhang X, Miller P. Ozkan M, Ozkan C, Wang J. Cell adhesion measurement by laser-induced stress waves. J Appl Phys. 2006;100:084701–5.
38. Miller P, Hu L, Wang J. Finite element simulation of cell-substrate decohesion by laser-induced stress waves. J Mech Behav Biomed Mater. 2010;3 (3):268–77.
39. Maneshi MM, Sachs F, Hua SZ. A Threshold Shear Force for Calcium Influx in an Astrocyte Model of Traumatic Brain Injury. J Neurotrauma. 2014;32 (13):1020–9.

40. Skotak M, Wang F, Alai A, Holmberg A, Harris S, Switzer RC, Chandra N. Rat injury model under controlled field-relevant primary blast conditions: acute response to a wide range of peak overpressures. J Neurotrauma. 2013;30(13):1147–60.
41. Smith DH, Wolf JA, Meaney DF. A new strategy to produce sustained growth of central nervous system axons: continuous mechanical tension. Tissue Eng. 2001;7(2):131–9.
42. Geddes-Klein DM, Serbest G, Mesfin MN, Cohen AS, Meaney DF. Pharmacologically induced calcium oscillations protect neurons from increases in cytosolic calcium after trauma. J Neurochem. 2006;97(2):462–74.
43. Alford PW, Dabiri BE, Goss JA, Hemphill MA, Brigham MD, Parker KK. Blast-induced phenotypic switching in cerebral vasospasm. Proc Natl Acad Sci U S A. 2011;108(31):12705–10.
44. Bernick KB, Prevost TP, Suresh S, Socrate S. Biomechanics of single cortical neurons. Acta Biomaterialia. 2011;7(3):1210–9.
45. Jérusalem A, Dao M. Continuum modeling of a neuronal cell under blast loading. Acta Biomater. 2012;8(9):3360–71.
46. Vodovotz Y, An G, Androulakis IP. A Systems Engineering Perspective on Homeostasis and Disease. Front Bioeng Biotechnol. 2013;1:6.
47. Vodovotz Y, Constantine G, Faeder J, Mi Q, Rubin J, Bartels J, Sarkar J, Squires Jr RH, Okonkwo DO, Gerlach J, Zamora R, Luckhart S, Ermentrout B, An G. Translational systems approaches to the biology of inflammation and healing. Immunopharmacol Immunotoxicol. 2010;32(2):181–95.
48. Zhou J-Y, et al. Trauma-associated human neutrophil alterations revealed by comparative proteomics profiling. Proteomics Clin Appl. 2013;(7–8):571–83.
49. Kamnaksh A, Kwon SK, Kovesdi E, Ahmed F, Barry ES, Grunberg NE, Long J, Agoston D. Neurobehavioral, cellular, and molecular consequences of single and multiple mild blast exposure. Electrophoresis. 2012;33(24):3680–92.

Biological Tissue Response

5

Angelo Karunaratne

5.1 Blast Loading Effects on Biological Tissues

Loading rates applied to tissues can vary enormously, from that seen during normal walking, where strain rates are estimated to be in the range of 0.001 s^{-1}, rising to 0.1 s^{-1} during downhill running [1]. The strain rates experienced by biological tissues during blast can be orders of magnitude higher, with an associated increase in the damage sustained. Biological tissues have been – and still are – studied mostly at relatively low loading rates that are not representative of loading rates in trauma or falls, for example. There have been few attempts to examine the load transfer to internal biological tissues due to external trauma. Also, little is known about biological tissue response across the strain rates from quasi static to extremely fast strain rates. Some previous work has shown that increasing the strain rate affected the mechanical properties of hard and soft tissues [2]. It is also important to note that mechanical properties of these tissues also are dependent on the strain rates to which they are subjected (i.e. increased stiffness and reduced toughness in bone tissue with increasing strain rates). The exact mechanism for these alterations in mechanical properties and the behaviour at different strain rates has not been explained previously due to the lack of equipment to test extreme loading rates at different hierarchical levels for biological tissues. This chapter will provide an overview of the current state of knowledge of the biological tissue response across strain rates ranging from quasi static to blast conditions, and to address these issues, whenever possible in the context of the hierarchical nature of bone, cartilage, ligaments, tendons, respiratory tissues and brain tissue. With rates of survivorship from the recent conflicts rising, devastating injuries to the extremities are becoming more frequent, with associated cost and societal implications. Knowledge of the behaviour of biological tissues at different strain rates including specifically ultra-high strain rate may help to understand load transfer mechanisms during different injury scenarios [3] and guide strategies for the management of blast in order to reduce the devastating sequelae seen.

5.2 Bone

Bone is a hierarchical biological composite [4]. It is one of the three main classes of mineralised tissue found in vertebrates with the other two being cartilage and enamel [5]. Bone is also an organ that forms the skeleton of the human body. Bone exhibits a hierarchical structure which is

A. Karunaratne, MEng, PhD
Department of Bioengineering, Royal British Legion Centre for Blast Injury Studies, Imperial College London, London SW7 2AZ, UK
e-mail: a.karunaratne@imperial.ac.uk

A.M.J. Bull et al. (eds.), *Blast Injury Science and Engineering: A Guide for Clinicians and Researchers*,
DOI 10.1007/978-3-319-21867-0_5

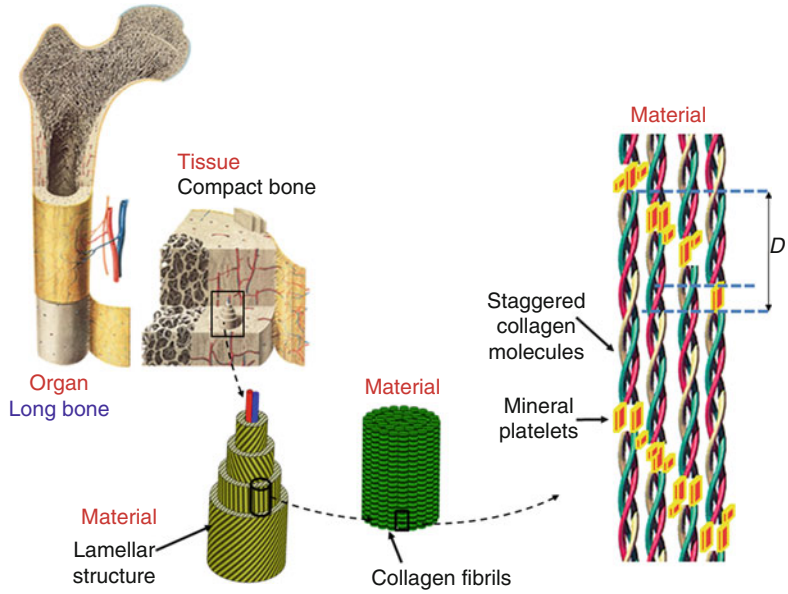

Fig. 5.1 Bone as a hierarchical structure

optimised for its mechanical performance [6]. Compositionally, it is made up of three major components: 65 % mineral, 25 % organic materials and 10 % water [7, 8]. The mineral platelets are carbonate-substituted hydroxyapatite (dahllite [4]) embedded in an organic extracellular matrix, while type I collagen is the main component of the organic phase [7]. Bone can be resolved into several levels of organisation from the molecular to the macroscopic level. While various authors have proposed slightly different classifications of this hierarchical structure (Fig. 5.1), all start with molecular level components at the smallest level and end with the different types of (macroscopic) whole bones [4, 9]. Each level of structural hierarchy plays an important role in the mechanical properties of bone. Considerable structural and mechanical experiments have been carried out to understand the structure-function relationship of bone at the macro- and microscale [6, 10], and more recently, at the nano- and molecular scale [11, 12].

Macromechanical experiments have shown that bone has a higher compressive strength compared to tensile strength. When bones are subjected to bending forces, they experience a higher strain at the tensile zones, and the maximum stress occurs in the compressive region [13]. Under tensile loading bone exhibits a greater amount of inelastic strain (~2 %) compared to when under compressive loading (~0.5 %) [13, 14]. Furthermore, bone is an anisotropic tissue, both macroscopically and microscopically (considering the oriented lamellae, fibrils and fibril bundles). The stiffness of the lamellae along the fibril direction is 23 GPa, while in contrast, stiffness in directions transverse to the fibrils is slightly less, 16.5 GPa [15]. At the microscale, trabecular bone exhibits a lower elastic modulus compared to interstitial bone of the diaphysis of cortical bone (1 vs. 20 GPa) [16].

The mechanical properties presented above were measured at quasi static strain rates. There have been few attempts to determine the behaviour of the bone tissue at extremely fast strain rates [1, 2, 17, 18] using uniaxial compression and tensile testing experiments. In those studies it was found that increasing strain rate produced an increase in the modulus of elasticity (0.001/s – 19GPa and 1500/s – 42 GPa) and ultimate strength (0.001/s 176 MPa and 1500/s – 365 MPa) and a reduction in strain to failure (0.001/s – 1.9 % and 1500/s – 0.9 %) and an increased brittleness. Critical strain rates were identified between 0.1/s – 1/s, where a

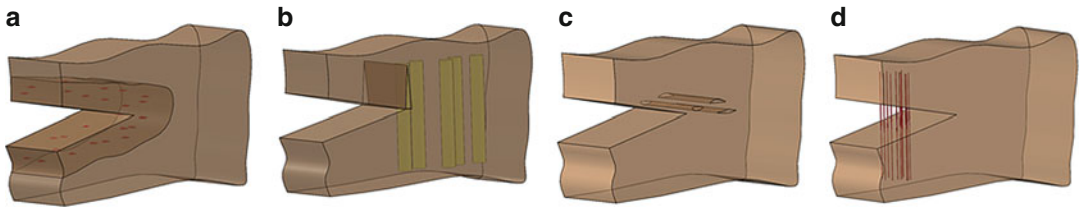

Fig. 5.2 (**a**) Microcracks, (**b**) Crack deflection along the secondary osteonal boundary, (**c**) Uncracked ligament bridging, (**d**) Crack bridging by collagen fibres

slight increment in strain rates produced a significant increment in energy absorption capacity. As a consequence, at low strain rates bone fracture occurred; at high rates the bone exhibited vertical splintering with multiple fragments produced. These relationships were found to hold for both trabecular and cortical bone, as these material properties are proportional to the apparent density of the bone (hydrated tissue weight over bulk volume); compressive modulus is approximately proportional to the cube of the density, and compressive ultimate strength is proportional to the square of the density. In the context of the material properties of bone at various strain rates, there is a relatively simple linear relationship between strain rate and elastic characteristics, with more complicated fracture mechanisms. At low strain rates, toughening mechanisms such as crack deflection, uncracked ligament bridging and microcracking (Fig. 5.2) operate, which act to inhibit further crack propagation. The crack path will, for example, be deflected at weak interfaces like cement lines around the osteons at the microscopic level. In contrast, at high strain rates splintering and fragmentation of the specimens was observed; this may be due to accumulation of multiple small cracks. Bone toughness diminishes with increasing strain rates as cracks penetrate through the osteons instead of deflecting at the cement lines.

The precise explanation for the positive correlation between modulus of elasticity with strain rate and the origin of bony fracture is not fully understood, particularly during physiologically relevant loading conditions (falls) and higher loading rates that are observed in traumatic injuries. While macro level mechanical tests alone provide valuable information on the bulk mechanical properties, they do not explain the functional role of individual components (i.e. mineral and organic) in hierarchically structured materials (lamellar, osteons and fibrillar level) like bone tissue.

Synchrotron small angle X-ray diffraction experiments demonstrates stiffening of the mineralised collagen fibrils and reduction of fibril to tissue ratio at dynamic strain rates associates with changes in the organic matrix of the bone. This mechanism could make the bone stiffer and more predisposed to catastrophic fracture simply by overloading the mineral phase. Since the collagen fibrils are surrounded by extrafibrillar matrix, a possible mechanism could be that at higher strain rates critical interfacial shear strength between fibrils and matrix is exceeded rapidly. When this occurs, due to frictional loss, the matrix flows past the fibrils and hence there is reduced fibrillar strain.

5.3 Ligament and Tendon

Both ligaments and tendons are soft collagenous tissues that have similar hierarchical structure. Tendons function to transfer forces to bones from muscles as efficiently as possible, with minimal energy loss. Ligament tissues attach bone to bone and maintain the skeletal frame in a stable condition. Therefore, ligaments and tendons play a vital role in musculoskeletal biomechanics. Collagen type I is the most abundant structural protein in tendons and ligaments, which determines the mechanical integrity of connective tissues.

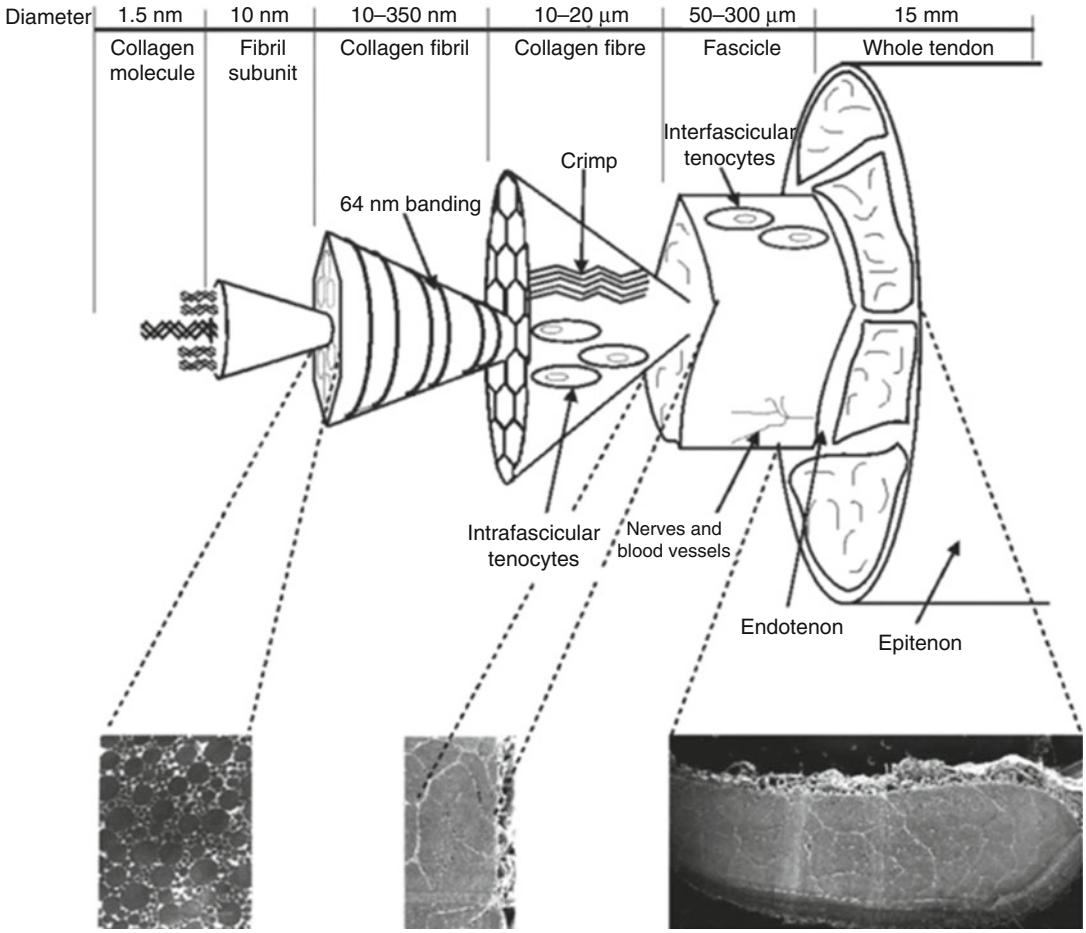

Fig. 5.3 Representation of hierarchical structure of a flexor tendon (Thorpe et al. [21] with permission from Wiley)

At each hierarchical level type I collagen is interspersed with non-collagenous matrix. The collagen to non-collagenous matrix ratio is slightly less in ligaments compared to tendons [9]. Not all the elements of the structural hierarchy of ligaments and tendons and their mechanical function are fully understood. At the angstrom scale tropocollagen molecules, tightly bound by cross links make collagen fibrils with 65–67 axial periodicity which in turn make mesoscopic fascicles with a crimping pattern and finally these aggregate to form the tendon [19]. Tendon and ligament extension at different loading rates is enabled by mechanisms occurring simultaneously at the above mentioned length scales, encompassing tropocollagen molecule extension, as well as sliding between collagen fibrils and fibres, probably controlled by the interspersed proteoglycan matrix [20] (Fig. 5.3).

The linear viscoelasticity (see Chap. 3, Sect. 3.4.2) of tendons and ligaments is very important for optimising tissue stiffness for absorbing and returning energy associated with transmission of tensile stresses across joints of the human body under different loading regimes. Tendons act as an effective biological spring providing some damping to the loading response due to their high resilience. A wide range of joint movements is possible due to the ability of tendons and ligaments to resist tensile forces only. The high affinity of non-collagenous proteins with water contributes through mechanisms such as fluid flow, friction and fibre sliding to the viscoelastic properties of tendons and ligament tissue.

The stress strain curve of tendons and ligaments usually exhibits three distinct regions, namely the toe region, the heel region and the linear region which can be correlated with deformation at different structural levels. These distinct regions are most prominent only in quasi static loading rates. With increasing strain rates a reduction in the size of the toe and heel regions have been observed. A very small load is adequate to elongate the tendon in the toe region, as microscopic uncrimping occurs in the initial part of the stress strain curve. Subsequently, stiffness of the tissue increases rapidly due to the entropic activity of collagen fibrils, where sequential straightening of disordered molecular kinks in the gap of the collagen fibrils occurs. When all the molecular kinks are removed, elongation of the collagen triple helices and the cross links between helices will initiate stretching which corresponds to the linear part of the stress strain curve. The characterisation of these deformation mechanisms during quasi static strain rates have received considerable attention. In-situ synchrotron experiments on human collateral ligaments demonstrates that at the relatively higher strain rates (0.01/s) collagen fibrils started to stretch without toe or heel regions, which implies that the collagen fibrils debond from the highly viscous matrix and fibrillar sliding occurs leading to macroscopic failure (Fig. 5.4). Tendon and ligament tissue elastic properties such as the elastic modulus and ultimate tensile stress were found to be sensitive to strain rates up to a limit of approximately 1/s. Tensile modulus and failure stress increased by 315 % (288 $\pm$ 834 MPa to 906 $\pm$ 195 MPa) and 194 % (40 $\pm$ 11 MPa to 77 $\pm$ 15 MPa) respectively from 0.01/s (quasi static) to 130/s (traumatic) strain rates. However, this increase occurred almost entirely over the lower strain rates (0.001, 0.01 and 0.94/s). This increase of tissue modulus with strain rates (up to 1/s) is most probably due to the stiffening of collagen fibrils and matrix with increasing strain rates [22]. The reasons for the strain rate sensitivity limit of ligament and tendons is still an open question which requires further investigation.

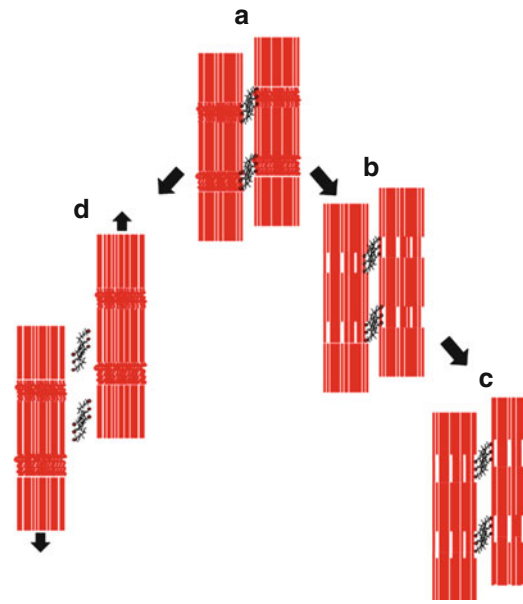

Fig. 5.4 (**a**) Unloaded state. (**b**) Toe region – removed kinks in the gap regions of collagen fibrils. (**c**) *Linear region* – tropocollagen molecules starts to glide each other. (**d**) Debonded stiff matrix from collagen fibrils

5.4 Articular Cartilage

Cartilage can be characterised as a three dimensional collagen network or fibril reinforced composite material which consist of proteoglycans, interstitial fluid and cartilage cells (chondrocytes). Cartilage tissue located between articulating joints provides an almost frictionless surface for the movement of the joint. Synovial fluid plays a major role in this by lubricating the joint space. Compared to tissues such as bone and muscle, articular cartilage has a low level of metabolic activity possibly due to the lack of blood vessels, lymphatic vessels and nerves. Chondrocytes are responsible for synthesis and organising of collagen, proteoglycans and non-collagenous proteins into a highly ordered structure. The structure and mechanical properties of the matrix and cell function vary with the depth from the articular surface. It is possible to identify four different layers from articular surface to the subchondral bone depending on the cell morphology and the organisation of the matrix [23]. These zones – the superficial zone, the transitional zone, the radial

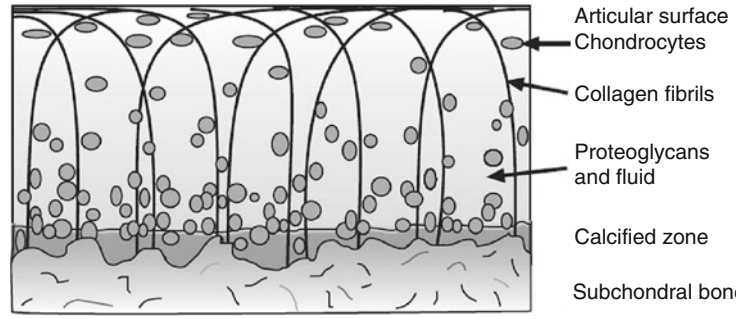

Fig. 5.5 Schematic of the four zones of cartilage tissue

zone and the calcified cartilage zone – are shown schematically in Fig. 5.5.

The relative size and appearance of these zones varies among species and within joints of the same species. Recent studies have shown that regional variations in water, proteoglycan and collagen concentrations, collagen network orientation and cell metabolic activity in different zones plays a vital role in function [24]. The joint surface is covered with an acellular transparent sheet of collagen fibrils arranged parallel to the surface with few proteoglycans. Underneath this thin layer, ellipsoidal–shaped chondrocytes are organised along collagen fibrils so that their major axis is parallel to the joint surface. The densely packed collagen fibrils in the superficial zone affect the movement of molecules in and out of cartilage. Disruption or deterioration of the superficial zone triggers an inflammatory response by releasing the cartilage molecules to the synovial fluid. At the transitional zone spheroidal shaped cells synthesise larger diameter collagen fibrils. The collagen fibrils in the middle zone arrange themselves perpendicular to the joint surface. These collagen fibrils penetrate into the boundary (tidemark) between calcified and uncalcified cartilage (middle zone) [25]. A thin zone that separates subchondral bone and the middle zone is known as the calcified cartilage layer. Chondrocytes in this layer surrounded by the calcified cartilage show a low level of metabolic activity compared to the cells in the other zones.

The inhomogeneous collagen network affects the mechanical integrity by effectively resisting the tissue deformation in the direction of the fibrils. The heterogeneity of fibrillar orientation results in inhomogeneous strains under loading, resulting in a depth-dependent tensile stiffness of cartilage [26]. Articular cartilage is subjected to numerous ranges of static, quasi static and dynamic mechanical loads. Peak dynamic stress and compressive deformation strain on cartilage is approximately 15–20 MPa and 1–3 % respectively under normal physiologically relevant loading activities such as walking and stair climbing. The equilibrium compressive, shear and tensile moduli of adult cartilage are approximately 0.5–2.5 MPa, 0.25 MPa and 10–50 MPa respectively during quasi static loading rates. The compositional and structural integrity of the collagen network and negatively charged glycosaminoglycan constituents of aggrecan molecules contribute to the ability of cartilage to withstand compressive, tensile and shear loads. The static compressive stiffness of articular cartilage is greatly (more than 50 %) associated with the electrostatic repulsion and the swelling pressure exerted by proteoglycans. The viscoelastic nature of the cartilage tissue has been determined by stress relaxation and creep testing. During compressive loading, the collagen network and fluid exerts reaction forces and the tissue resists the fluid flow leading to low permeability in the tissue. Due to the depth dependent composition and structure as discussed above, anisotropic and nonlinear properties are observed across cartilage tissue. The parameters of aggregate modulus, elastic modulus and Poisson's ratio increase, while permeability decreases with depth,

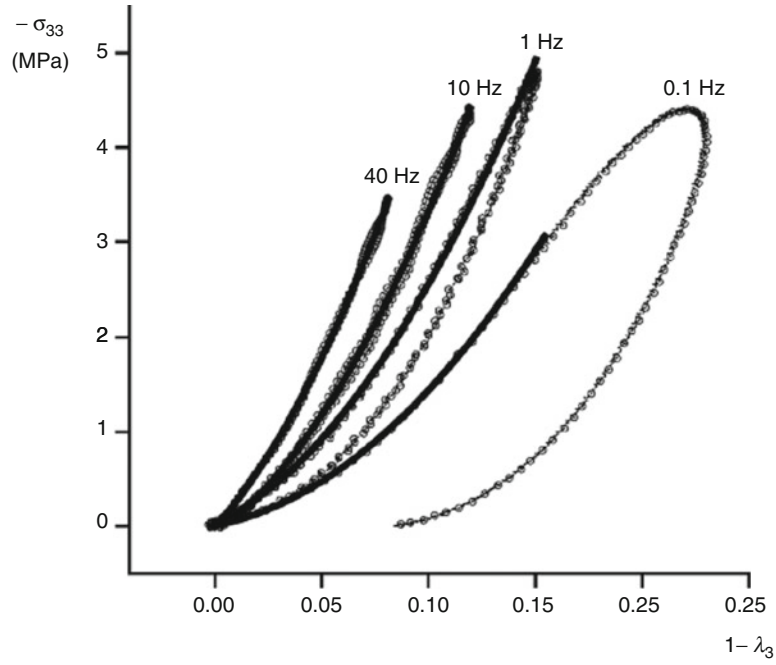

Fig. 5.6 Stress–strain response for a typical cartilage specimen, at various loading frequencies, and corresponding polynomial curve fits (Park et al. [28] with permission from Elsevier)

reflecting variability in collagen fibre orientation and composition with depth [27].

Due to the viscoelastic or poroelastic fibre composite nature of the articular cartilage, its mechanical properties also depend on the rate of loading. As is similar to other connective tissues, most of the mechanical investigation has previously been performed at slow strain rates. There are few studies which have specifically looked at cartilage tissue behaviour under traumatic loading rates [29]. The loading rate and strain rate across the knee joint during walking have been estimated to be about 20 kN/s and 5/s respectively [30]. In order to simulate the behaviour of cartilage during an automobile accident, strain rates of 1000/s have been proposed [31]. Compression experiments were conducted on isolated cartilage specimens, for these matrix stiffness (2.5–20 MPa) increased progressively from quasi static (5×10^{-5}/s) to medium strain rates (5×10^{-3}/s). During high and impact strain rates (1000/s), stiffness (25 MPa) is almost insensitive to large increases in the strain rates. The non-linear increment of cartilage modulus with strain rates gives the tissue an ability to attenuate the peak force experienced by the underlying subchondral bone and distribute the impact load over a longer period [32]. This has been confirmed by others, who performed cyclic loading using frequencies that represent physiologically relevant activities to traumatic impact loading (10–40 Hz) which occurs over durations of 5–50 ms [28]. Over the range of physiological loading frequencies (0.1–10 Hz), dynamic modulus increases up to a factor of 2 due to the viscoelastic behaviour of the cartilage tissue (Fig. 5.6). These experimental studies further confirm that at traumatic strain rates or frequencies (above 1000/s or 40 Hz), the dynamic modulus of cartilage is insensitive to strain rate. At loading rates representative of light to moderate physical activities, the cartilage behaviour is dominated by fluid flow dependent and independent viscoelasticity [33]. In contrast, at high loading rates the cartilage matrix behaves effectively as an elastic solid and no further increase in dynamic modulus is to be expected as there is no contribution from fluid flow [28, 34]. During impact loading rates, modulus mismatch between cartilage and subchondral bone is not as great as is

observed at quasi static strain rates, when there is a difference of two orders of magnitude. Therefore under traumatic and blast loading conditions, severe impact produces damage in the bone rather than in the cartilage in diarthrodial joints [34].

5.5 Brain Tissue

The most complex organ in the vertebrate's body is the brain. The largest part of the human brain is the cerebrum, which contains approximately 20 billion neurons. Neurons pass signals to other neurons, muscles and glands using their slender projections called axons. The myelinated axons are organised into densely packed regions which makes white matter regions in the brain. The brain sections appear in matter that is darker than white matter called grey matter which consists of neuron cell bodies, neurophils, glial cells and capillaries [35]. The cerebral cortex is folded in a way to increase the surface area in order to fit into the volume available. The cortex is divided into four lobes namely the frontal lobe, parietal lobe, temporal lobe and occipital lobe. MRI studies have shown that the frontal area is the most common region of injury following mild to moderate traumatic brain injury. The brainstem is located underneath the cerebrum and resembles a stalk on which the cerebrum is attached. The structure that attaches to the bottom of the brain beneath the cerebrum and behind the brainstem is the cerebellum. Traumatic injuries to the cerebellum may cause disorders in fine movement and posture.

The brain is the most vulnerable organ in the human body that is often involved in life-threatening injuries. Over 3.3 million casualties and a cost over 180 billion euros was incurred in Europe in 2001 due to brain injuries caused by transport crashes [36]. The leading causes of traumatic brain injuries for the general public involve impacts from falls, transport accidents and physical assaults. In combat regions, improvised explosive devices, rocket-propelled grenades, and landmines have become the main cause of brain injuries for active military personnel and civilians [37]. Brain damage can be classified as primary and secondary according to the associated pathways to the neuronal damage after a brain injury. The mechanism of brain injury is due predominantly to direct impact of the brain against the inner contour of the skull and forces exerted on the brain due to acceleration, deceleration and rotation inside the cranium. Brain damage that occurs within days of the immediate impacts can be classified as secondary brain injuries. Among these different types of traumatic brain injuries, diffuse axonal injury is one of the most common blast induced injuries that leads to devastating effects for the affected person. Biomechanical investigation of diffuse white matter damage has shown some associating factors that link brain material response and white matter injury. Due to these escalating traumatic brain injuries, the brain has become the emphasis of studies designed to investigate its structure function relationships and sensitivity to different loading rates. These studies are important to understand the potential causes of brain injuries, to develop protective measures and to achieve more accurate safety assessments [38].

Furthermore, computational modelling is often used to simulate traumatic brain injuries to gain insight into the brain injury mechanisms. The accuracy of these model predictions will depend on the bio fidelity of the material properties. In the literature mechanical testing of brain tissue has been conducted using cyclic shear, compression, oscillatory, creep, and stress relaxation testing. A linear viscoelastic model (a four parameter Maxwell-Kelvin model; see Chap. 3, Sect. 3.4.2) has been proposed as a first estimation for the mechanical behaviour of human brain tissue. However, the creep compliance modulus changes by varying the stress level and it shows that the material behaviour is not completely linearly viscoelastic (stress-strain increases linearly with strain rate). For example, the instantaneous elastic response of the brain tissue increased by 28 % when the creep stress level increased by 50 %; the instantaneous strains were 20–40 % [39]. Shear experiments performed on human brain specimens (midbrain, corona radiate) using a linear motor to apply

displacement on one surface of the cylindrical specimens at different rates, from quasi-static to 1201/s found significantly different viscous constants when fitting the Kelvin-Voigt model to data at the different strain rates. This indicates that the linear viscoelastic model with fixed constants cannot represent the brain tissue shear response over a range of strain rates [40]. Due to inhomogeneity and anisotropy, it is important to define material properties for different regions separately. Shear tests at large strains (up to 50 %) on porcine and human brain tissue have shown that mechanical behaviour of grey and white matter is relatively different. Samples were excised from corpus callosum, corona radiate and thalamus (grey matter) and material constants were obtained by fitting data with a modified first-order Ogden hyperelastic model (see Chap. 3, Sect. 3.4.1) for all strains to isochoric (constant volume) data (at a certain time) obtained from confined stress relaxation tests (max strain rate 8.33/s, hold time 60 s). Grey matter showed isotropic behaviour, corona radiate showed slight anisotropic behaviour and corpus callosum showed significant anisotropy. The average stiffness of the corpus callosum was smaller than the average stiffness of the other two regions [41].

In order to predict brain injuries under blast loading conditions biofidelic human brain finite element models are required. The following data have been used:

Mixed white and grey matter were investigated using compression (unconfined), tensile and stress relaxation tests at strain rates of 30, 60, 90/s.

Experimental results from these studies showed that hyperelastic models are not adequate in explaining the stiffening response of brain tissue with increasing strain rates. For completeness, the results show that at 30 % strain, the compressive nominal stresses were 8.83 ± 1.94, 12.8 ± 3.10 and 16.0 ± 1.41 kPa [42] and tensile stresses were 3.1 ± 0.49 kPa, 4.3 ± 0.86 kPa, 6.5 ± 0.76 kPa [43] for strain rates of 30, 60 and 90/s, respectively.

Hyperviscoelastic behaviour of brain tissue has been investigated by stress relaxation experiments. These compression, tension and relaxation experiments combined with numerical analysis showed that One-term Fung, Gent and Ogden strain energy function models (see Chap. 3, Sect. 3.4.1) are capable of determining the behaviour of brain tissues during dynamic compression events [42, 43]. The mechanical properties were determined at high strain rates such as 1000–3000/s that are associated with blast loading incidents, including penetrating gunshot injuries to the head and open skull blast brain injuries. In order to develop finite element models to study brain injury mechanisms during traumatic brain injury, cases among armed forces due to blast, high strain rate (100, 500 and 800/s) shear experiments have been performed. It was observed that brain shear moduli are not sensitive to strain rates indicating that at these rates the viscoelastic response of brain tissue has reached a plateau. In contrast to this, tissue failure stress at 100/s was significantly lower than at the higher rates [44].

5.6 Respiratory Tissue

Blast injuries to the respiratory system and other gas containing structures (gastrointestinal tract and ears) are mainly caused by the force generated by the blast wave impacting the human body surface without obvious external injury to the chest. These types of injuries may be a significant cause of death or morbidity in survivors at the time of explosion. Due to the dynamic interaction of the blast wave with the chest wall, pressure differentials generated between tissue surfaces of different densities leads to tearing, haemorrhage, pulmonary contusion and oedema with direct alveolar and surrounding vascular injury [45]. These respiratory tissue injuries caused by primary blasts are collectively known as blast lung. Several injury mechanisms have been proposed to explain the soft tissue damage, including, pressurised waves disrupting the air liquid interface, violent contraction and expansion of air filled structures (i.e. alveoli) and alterations in pressure at different body surfaces leading to shear and stress waves dispersed

Table 5.1 Porcine airway segments and their Young's modulus [50]

Airway segment	Young's modulus (MPa)		
Tracheal	1.78 ± 0.51		
Bronchial	Generation 1: 1.35 ± 0.17	Generation 2: 0.41 ± 0.09	Generation 3: 0.35 ± 0.10
Tracheal cartilage	1.74 ± 0.85		
Bronchial cartilage	Generation 1: 1.44 ± 0.25	Generation 2: 0.44 ± 0.05	Generation 3: 0.16 ± 0.03
Tracheal mucosa	0.14 ± 0.02		
Bronchial mucosa	Generation 1: 0.041 ± 8e-3	Generation 2: 0.031 ± 1.7e-3	Generation 3: 0.042 ± e-7

through neighbouring tissue [46]. Adult respiratory distress syndrome and injuries to upper airway tissues (for example, the trachea) are delayed life threatening risks among survivors from an initial blast. These conditions could lead to a development of airway oedema and blast lung 6–12 h after the blast exposure. In order to improve mitigation strategies and develop novel therapeutic interventions for the wounded, a comprehensive understanding of the response of respiratory tissues to different loading rates is required.

Material properties of human and animal respiratory tissues have been studied in the past 2 decades for various applications including reference values for ultrasound and MRI electrography and scientific understanding of respiratory ventilation mechanisms [47–49]. Advances in ultrasound technology have been used to measure the bulk modulus and stress-strain relationships of tracheal segments that are isolated in a spontaneously breathing newborn lamb. The stiffness measurements of tracheal smooth muscle cytoskeletal tissues show a positive correlation between indentation rate and elastic storage modulus and dissipation modulus. However, these observations were not present when muscle cells were stimulated to contract. The methodology used in this study was capable of investigating the dynamic mechanical properties and viscous behaviour and kinetic response of tracheal tissue during physiological and injurious conditions [49]. In order to understand mechanical properties of the airways (trachea and the first three generations of bronchial airway walls, cartilages, and mucosa) of the respiratory system, pig air way tissue has been used as this has many similarities to human airways. The measured Young's modulus of different parts of pig airway tissues are tabulated above (Table 5.1) [50].

The Young's modulus of each airway segment is found to decrease with each generation. The modulus of airway cartilage is greater than the other segments of the airways in every generation. As these load deformations measurements were obtained under a constant rate of 0.1 Hz, these Young's modulus values represent quasi static strain rates. Minimisation of damage from primary blasts to the respiratory tissue and for the design of effective interventions at the chest level (for example, protective vests) requires a quantitative model of the human lung tissue to blast loading. The dynamic bulk and shear response of human lung, heart, liver and stomach tissues have been measured under dynamic confined compression and dynamic simple shear using the modified Kolsky bar experimental method (see Chap. 4, Sect. 4.2.1) at strain rates of 200–7700/s [51]. A linear relationship was observed between the pressure and the volumetric strain in lung tissue under dynamic compression testing. The bulk modulus (given by a linear fit) for lung tissues was 0.15 GPa which was the most compliant compared to other tissues. The shear stress versus shear strain curves for these soft tissues exhibit an initial toe region, followed by a rapid increase in shear stress. Tangent shear moduli of lung tissue during applied strain rates of 400–2300/s was determined by calculating the slope of the final quasilinear stage of the stress-strain curves. Shear modulus for lung tissue increased by 440 % (10–54 KPa) with increasing strain rates (400/s to 2300/s). However, lung tissue was most compliant compared to heart, liver and stomach tissues that were tested with the same experimental protocol [51]. Information from high strain rate experiments on respiratory tissue can be used to develop simulations of lung tissue to elucidate how they respond to the primary blast wave that leads to blast lung

conditions. A split Hopkinson bar system has been used on freshly harvested swine trachea tissue to investigate material properties during dynamic loading rates. Once the sample reached equilibrium in the split-Hopkinson bar, (see Chap. 4, Sect. 4.2.1) the calculated modulus was 10.6 ± 0.6 MPa for the strain rate of 6000/s. Optical imaging of damaged trachea samples indicated loss of the outermost layer of cells (cilia), whereas fresh control samples showed healthy cilia layers similar to live trachea. These micrographs further showed that an underlying collagen-rich hyaline cartilage layer was still intact; this may be due to the stiffening effects from structural changes of collagen fibrils [52]. High strain rate loading combined with high resolution tissue imaging will be required in order to obtain detailed information on blast induced structural alterations in connective tissues.

5.7 Skin Tissue

Human skin is a complex, biological material comprised of three layers including an outmost epidermis and dermis and the deeper subcutaneous tissue (hypodermis). In mammalian skins the dermis is 20 times thicker than the epidermis and made out of gel like ground substance with elastin and collagen (60–80 %) fibres embedded within it. The structure and density of collagen fibres governs the constitutive behaviour of skin tissue [53]. The collagen fibres in human skin have a preferred orientation due to pre-tension, whereas the collagen orientation in other mammalian skin has an orthotropic structure. Skin functions as a protective barrier for underlying structures and also regulates body temperature and permits the sensations of touch, heat and cold.

Blast injury frequently involves damage to the skin, with skin loss, or even deep skin tissue injuries such as burns or scars. These deep skin tissue injuries require prolonged treatments often leading to poor outcomes including infections [54]. The understanding of skin tissue behaviour at blast strain rates is not adequate to develop realistic model systems of fresh skin response to blast injuries. In this context there are limited number of attempts to examine the response of skin tissue at quasi static to extremely fast strain rates [55, 56].

Human skin has a stiffness of 0.3–1.0 MPa at low strains. For strains above 0.6 skin undergoes strain hardening and has an increasing tangent modulus (20–70 MPa) [57]. The bending stiffness of the collagen fibres and the viscous shear between fibres dominates the constitutive response at low engineering strains (0.3). In contrast to this, at high engineering strains (0.5) the constitutive response is dominated by the tensile elastic response of the collagen fibres [58]. It should be noted that human skin material properties have not yet been investigated for fast strain rates such as those seen in blast.

Some studies on mammalian skin properties at higher strain rates have been conducted. For example, the ultimate tensile strength of rat skin increased 50–100 % with increased strain rates (0.3–60/s). Porcine skin under compression loading also shows strain hardening with a six- to fivefold increase in compressive modulus over strain rates from 10^{-3}/s to 10^{3}/s [59]. Histological studies show that most of the damage accumulates across the entire thickness of the dermis during low strain rates and therefore, skin tissue response at low strain rates can be explained by the van der Waals' formulation of viscoelasticity. In contrast, at high strain rates the damage is not uniform. For example, voids have been observed within the dermis at these rates which is most likely due to the disruption of extracellular matrix [59]. These results were confirmed by the porcine study presented above [54] in which porcine skin is shown to stiffen and strengthen with increasing strain rate. This response allows a simple one term Ogden strain energy density function (Chap. 3, Sect. 3.4.1) to characterise porcine skin compressive and tensile stress verses strain behaviour at slow and fast strain rates [54].

5.8 Summary

This chapter has shown that the properties of tissues vary significantly along many dimensions: loading rate, direction (anisotropy), and

Table 5.2 Material properties for biological tissues at high loading rates. Data obtained from literature

Tissue	Strain rate	Loading mode	Modulus	Ultimate strength	Strain to failure	Nominal stress	Reference
Cortical bone	0.001/s	Compression	19 GPa	176 MPa	1.9 %		[2]
Cortical bone	1500/s	Compression	42 GPa	365 MPa	0.9 %		
Cortical bone	0.001/s	Tension	22 MPa	140 MPa			[17]
Cortical bone	500/s	Tension	40 MPa	275 MPa			[60]
Ligaments	0.01/s	Tension	40 MPa	388 MPa	17 %		[61]
Ligaments	130/s	Tension	77 MPa	906 MPa	9.5 %		
Cartilage	0.005/s	Compression	2.5 MPa				[29]
Cartilage	1000/s	Compression	25 MPa				
Brain	30/s	Compression				8.83 KPa	[42]
Brain	60/s	Compression				12.8 KPa	
Brain	90/s	Compression				16.0 KPa	
Brain	30/s	Tension				3.17 KPa	[43]
Brain	60/s	Tension				4.37 KPa	
Brain	90/s	Tension				6.57 KPa	
Lung	400/s	Shear	10 KPa				[51]
Lung	2300/s	Shear	54 KPa				
Trachea	6000/s	Compression	10.6 MPa				[52, 53]
Skin	<0.01/s	Compression	0.3–1 MPa				

location (inhomogeneity). Despite a large body of tissue property data in the literature, little is known about the behaviour of biological tissues under blast loading rates. The data known are summarised in the Table 5.2 above.

References

1. Hansen U, Zioupos P, Simpson R, Currey JD, Hynd D. The effect of strain rate on the mechanical properties of human cortical bone. J Biomech Eng. 2008;130(1):011011.
2. McElhaney JH. Dynamic response of bone and muscle tissue. J Appl Physiol. 1966;21(4):1231–6.
3. Cobb JP, O'Keefe GE. Injury research in the genomic era. Lancet. 2004;363(9426):2076–83.
4. Weiner S, Wagner HD. The material bone: structure mechanical function relations. Annu Rev Mater Sci. 1998;28:271–98.
5. Hall B. Bones and cartilage: developmental skeletal biology. San Diego/London: Academic Press; 2005.
6. Currey JD, editor. Bones: structure and mechanics. Princeton: Princeton University Press; 2002.
7. Currey JD. Role of collagen and other organics in the mechanical properties of bone. Osteoporos Int. 2003;14:29–36.
8. Currey JD, Zioupos P, Davies P, Casino A. Mechanical properties of nacre and highly mineralized bone. Proc Biol Sci. 2001;268(1462):107–11.
9. Fratzl P, Gupta HS, Paschalis EP, Roschger P. Structure and mechanical quality of the collagen-mineral nano-composite in bone. J Mater Chem. 2004;14(14):2115–23.
10. Reilly DT, Burstein AH. The elastic and ultimate properties of compact bone tissue. J Biomech. 1975;8(6):393–405.
11. Karunaratne A, Terrill NJ, Gupta HS. Chapter nineteen – synchrotron X-ray nanomechanical imaging of mineralized fiber composites. In: James JDY, editor. Methods in enzymology, vol. 532. Academic Press; 2013. p. 415–73.
12. Zimmermann EA, Gludovatz B, Schaible E, Busse B, Ritchie RO. Fracture resistance of human cortical bone across multiple length-scales at physiological strain rates. Biomaterials. 2014;35(21):5472–81.
13. Mercer C, He MY, Wang R, Evans AG. Mechanisms governing the inelastic deformation of cortical bone and application to trabecular bone. Acta Biomater. 2006;2(1):59–68.
14. Currey JD. The mechanical properties of bone. Clin Orthop Relat Res. 1970;73:209–31.
15. Turner CH, Rho J, Takano Y, Tsui TY, Pharr GM. The elastic properties of trabecular and cortical bone tissues are similar: results from two microscopic measurement techniques. J Biomech. 1999;32(4):437–41.

16. Chatterjee S, Blunn G. Biomaterial behaviour. In: Ramachandran M, editor. Basic orthopaedic sciences: the Stanmore guide. London: Hodder Arnold; 2007.
17. Currey JD. The effects of strain rate, reconstruction and mineral content on some mechanical properties of bovine bone. J Biomech. 1975;8(1):81–6.
18. Wright TM, Hayes WC. Tensile testing of bone over a wide range of strain rates: effects of strain rate, microstructure and density. Med Biol Eng. 1976;14(6): 671–80.
19. Gupta HS, Seto J, Krauss S, Boesecke P, Screen HR. In situ multi-level analysis of viscoelastic deformation mechanisms in tendon collagen. J Struct Biol. 2010; 169(2):183–91.
20. Thorpe CT, Birch HL, Clegg PD, Screen HR. The role of the non-collagenous matrix in tendon function. Int J Exp Pathol. 2013;94(4):248–59.
21. Thorpe CT, Clegg PD, Birch HL. A review of tendon injury: why is the equine superficial digital flexor tendon most at risk? Equine Vet J. 2010;42(2): 174–80.
22. Bonner TJ, Newell N, Karunaratne A, Pullen AD, Amis AA, Bull AMJ, Masouros SD. Strain-rate sensitivity of the lateral collateral ligament of the knee. J Mech Behav Biomed Mater. 2015;41:261–70.
23. Buckwalter JA, Mankin HJ, Grodzinsky AJ. Articular cartilage and osteoarthritis. Instr Course Lect. 2005; 54:465.
24. Buckwalter J, Rosenberg L, Hunziker E. Articular cartilage: composition, structure, response to injury, and methods of facilitating repair. In: Ewing J, editor. Articular cartilage and knee joint function: basic science and arthroscopy. New York: Raven Press ltd; 1990. p. 19–56.
25. Grogan SP, et al. Zone-specific gene expression patterns in articular cartilage. Arthritis Rheum. 2013; 65(2):418–28.
26. Julkunen P, et al. Maturation of collagen fibril network structure in tibial and femoral cartilage of rabbits. Osteoarthritis Cartilage. 2010;18(3):406–15.
27. Boschetti F, Pennati G, Gervaso F, Peretti GM, Dubini G. Biomechanical properties of human articular cartilage under compressive loads. Biorheology. 2004;41(3):159–66.
28. Park S, Hung CT, Ateshian GA. Mechanical response of bovine articular cartilage under dynamic unconfined compression loading at physiological stress levels. Osteoarthritis Cartilage. 2004;12(1):65–73.
29. Oloyede A, Flachsmann R, Broom ND. The dramatic influence of loading velocity on the compressive response of articular cartilage. Connect Tissue Res. 1992;27(4):211–24.
30. Bergmann G, et al. Hip contact forces and gait patterns from routine activities. J Biomech. 2001; 34(7):859–71.
31. Repo R, Finlay J. Survival of articular cartilage after controlled impact. J Bone Joint Surg Am. 1977;59: 1068–76.
32. Julkunen P, Jurvelin J, Isaksson H. Contribution of tissue composition and structure to mechanical response of articular cartilage under different loading geometries and strain rates. Biomech Model Mechanobiol. 2010; 9(2):237–45.
33. Mak AF. The apparent viscoelastic behavior of articular cartilage—the contributions from the intrinsic matrix viscoelasticity and interstitial fluid flows. J Biomech Eng. 1986;108(2):123–30.
34. Burgin L, Aspden R. Impact testing to determine the mechanical properties of articular cartilage in isolation and on bone. J Mater Sci Mater Med. 2008; 19(2):703–11.
35. Gefen A, Margulies SS. Are in vivo and in situ brain tissues mechanically similar? J Biomech. 2004;37(9): 1339–52.
36. Hrapko M, Van Dommelen J, Peters G, Wismans J. Characterisation of the mechanical behaviour of brain tissue in compression and shear. Biorheology. 2008;45(6):663–76.
37. Grujicic M, et al. A study of the blast-induced brain white-matter damage and the associated diffuse axonal injury. Multidiscip Model Mater Struct. 2012; 8(2):213–45.
38. Park E, Bell JD, Baker AJ. Traumatic brain injury: can the consequences be stopped? Can Med Assoc J. 2008;178(9):1163–70.
39. Galford JE, McElhaney JH. A viscoelastic study of scalp, brain, and dura. J Biomech. 1970;3(2):211–21.
40. Donnelly B, Medige J. Shear properties of human brain tissue. J Biomech Eng. 1997; 119(4):423–32.
41. Prange MT, Margulies SS. Regional, directional, and age-dependent properties of the brain undergoing large deformation. J Biomech Eng. 2002;124(2): 244–52.
42. Rashid B, Destrade M, Gilchrist MD. Mechanical characterization of brain tissue in compression at dynamic strain rates. J Mech Behav Biomed Mater. 2012;10:23–38.
43. Rashid B, Destrade M, Gilchrist MD. Mechanical characterization of brain tissue in tension at dynamic strain rates. J Mech Behav Biomed Mater. 2014;33: 43–54.
44. Shafieian M, Bao J, Darvish K. Mechanical properties of brain tissue in strain rates of blast injury. Bioengineering Conference (NEBEC) IEEE 37th Annual Northeast, Rensselaer Polytechnic Institute (RPI) in Troy, NY; 2011. p. 1–2.
45. Phillips YY. Primary blast injuries. Ann Emerg Med. 1986;15(12):1446–50.
46. Mellor SG. The relationship of blast loading to death and injury from explosion. World J Surg. 1992;16(5): 893–8.
47. Noble P, Sharma A, McFawn P, Mitchell H. Elastic properties of the bronchial mucosa: epithelial unfolding and stretch in response to airway inflation. J Appl Physiol. 2005;99(6):2061–6.

48. Lambert RK, Baile EM, Moreno R, Bert J, Pare PD. A method for estimating the young's modulus of complete tracheal cartilage rings. J Appl Physiol (1985). 1991;70:1152–9.
49. Miller TL, Altman AR, Tsuda T, Shaffer TH. An ultrasound imaging method for in vivo tracheal bulk and young's moduli of elasticity. J Biomech. 2007; 40(7):1615–21.
50. Jau-Yi W, Mesquida P, Tak L. Young's modulus measurement of pig trachea and bronchial airways. Engineering in Medicine and Biology Society (EMBC) annual international conference of the IEEE Boston Marriott Copley Place Hotel, Boston; 2011. p. 2089–92.
51. Saraf H, Ramesh KT, Lennon AM, Merkle AC, Roberts JC. Mechanical properties of soft human tissues under dynamic loading. J Biomech. 2007;40(9):1960–7.
52. Butler BJ, et al. Mechanical and histological characterization of trachea tissue subjected to blast-type pressures. J Phys: Conference Series. 2014;500(18): 182007.
53. Reihsner R, Balogh B, Menzel EJ. Two-dimensional elastic properties of human skin in terms of an incremental model at the in vivo configuration. Med Eng Phys. 1995;17(4):304–13.
54. Shergold OA, Fleck NA, Radford D. The uniaxial stress versus strain response of pig skin and silicone rubber at low and high strain rates. Int J Impact Eng. 2006;32(9):1384–402.
55. Haut RC. The effects of orientation and location on the strength of dorsal rat skin in high and low speed tensile failure experiments. J Biomech Eng. 1989; 111(2):136–40.
56. Dombi GW, Haut RC, Sullivan WG. Correlation of high-speed tensile strength with collagen content in control and lathyritic rat skin. J Surg Res. 1993;54(1): 21–8.
57. Jansen LH, Rottier PB. Some mechanical properties of human abdominal skin measured on excised strips: a study of their dependence on age and how they are influenced by the presence of striae. Dermatologica. 1958;117(2):65–83.
58. Cohen RE, Hooley CJ, McCrum NG. Viscoelastic creep of collagenous tissue. J Biomech. 1976;9(4): 175–84.
59. Butler BJ, et al. Composite nature of fresh skin revealed during compression. Bioinspired, Biomimetic and Nanobiomaterials. 2015;4:133–9.
60. Reilly DT, Burstein AH, Frankel VH. The elastic modulus for bone. J Biomech. 1974;7(3):271–5.
61. Bonner TJ, et al. Strain-rate sensitivity of the lateral collateral ligament of the knee. J Mech Behav Biomed Mater. 2015;41:261–70.

Part II

Weapon Effects and the Human

Blast Injury Mechanism

6

Dafydd S. Edwards and Jon Clasper

6.1 Principles of Explosive Devices

6.1.1 Definition

An explosion is defined as a rapid increase in volume and pressure associated with a sudden release of energy [1]. It has a force with a direction of travel perpendicular to the surface of the explosive and the speed of reaction itself dictates the property of the resulting pressure wave. An explosive is defined as a chemical material which inherently contains enough potential energy that when initiated, and the energy is released, the transfer of that energy to the local environment causes an increase in pressure. The subsequent volume, a function of the increase in pressure, travelling away from the centre of the explosion must be larger than the original material [2].

6.1.2 Classification

Explosives are classified by the speed at which the blast front expands and travels away from the centre of explosion following detonation. High explosive (HE) describes the process whereby the initial detonation creates a shock wave which compresses the explosive with the subsequent release of heat. This enables propagation of the explosion via chemical decomposition of the explosive material which travels through the material at speeds greater than the speed of sound. In contrast with low explosives (LE), decomposition occurs at subsonic speeds, is usually propagated by heat alone, and is referred to as deflagration.

6.1.3 Physics

6.1.3.1 Detonation/Deflagration

As detailed earlier an explosive has within itself energy in the form of molecular bonds. If the bonds are broken then energy is released; this is usually initiated by a detonator. A detonator is an explosive itself which is used to initiate another explosive to release its energy. A detonator causes a supersonic exothermic blast front that travels through the material. 2,4,6-trinitrotoluene, or TNT, is commonly used as an example where the detonation front travels at between 2000 and 9000 m/s through the material. This is an example of an HE and results in a supersonic exothermic rapidly expanding pressure wave [1].

Deflagration is the process by which an explosive material is triggered to release its energy by a front travelling at subsonic speeds. Typically

D.S. Edwards, BSc (Hons), MBBS, FRCS, DMCC (✉) • J. Clasper, CBE, DPhil, DM, FRCSEd (Orth)
Department of Bioengineering, Royal British Legion Centre for Blast Injury Studies, Imperial College London, SW7 2AZ London, UK
e-mail: taffedwards@mac.com; jonclasper@aol.co.uk

A.M.J. Bull et al. (eds.), *Blast Injury Science and Engineering: A Guide for Clinicians and Researchers*,
DOI 10.1007/978-3-319-21867-0_6

this is at speeds of less than 100 m/s and does not produce a pressure, or overpressure, wave of significance. An example can be as simple as a flame igniting coal.

6.1.3.2 Propagation

The blast front created by the detonator travels thought the explosive material and in doing so compresses it. As the explosive is compressed it generates heat and, together with the heat generated by the detonator, the explosion temperature continues to rise. As a consequence it can be said that the reaction rate is proportional to the material's temperature and the relationship is exponential. This is compared to heat lost to the environment which is linear. As the exponential curve continues, heat production dominates therefore accelerating the reaction rate creating a "runaway process" where the reaction and release of energy is almost instantaneous providing that the explosive material contains an adequate source of oxygen within its molecular structure. Temperatures and pressures associated with the blast front in a high explosive are in the order of 7000 °C and 20 GPa (approx. 200,000 atm).

6.1.3.3 Pressure and Friedlander Wave

The detonation, propagation and rapid release of energy from the explosive results in a blast wave. A blast wave is defined by its pressure and direction of travel, or flow, which in a simple free field explosion is perpendicular to the surface of the explosive. A simple free field explosion is one where the field of explosion and blast wave do not come into contact with any interference. In addition a blast wind is generated due to large pressure gradients travelling at speed and subsequent mass movement of air. The blast wave has a leading front, which is composed of compressed gas, and a peak (static) overpressure, and travels at supersonic speed. It is followed by a blast wind, which travels at subsonic speeds as a mass movement of air, and an increase in pressure referred to as the dynamic overpressure. This relationship and the form the blast wave assumes in a simple free field explosion, and the wave characteristics are described by Friedlander (Fig. 6.1) [3].

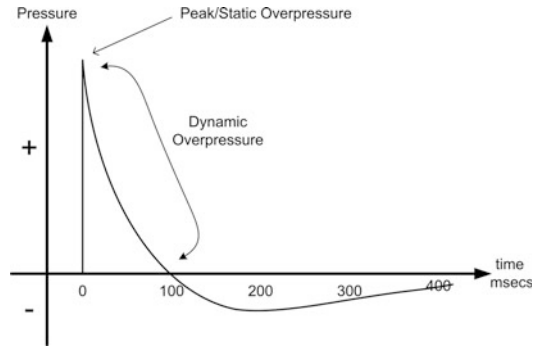

Fig. 6.1 Friedlander Wave form in a simple free field explosion

6.1.3.4 Mach Stem

A simple free field explosion rarely occurs. Interaction with structures changes the wave form, and resulting pressures. A basic model is that of reflection of the wave from an explosion above the ground on a surface parallel to the wave front (Fig. 6.2). Once reflected, the reflected wave front travels faster than the incident wave and draws level to it and due to constructive interference the pressure at this point is at least twice the pressure of the incident wave. However, in explosions, unlike sound waves, the angle of reflection does not equal the angle of the incident. As the blast front develops, and subsequently the angle of incidence increases and exceeds 40°, the incident wave not only reflects but deflects. The deflected portion of the wave spurts along the surface and travels parallel to the reflected surface. This results in the formation of a triple point (the meeting point of the reflected wave, incident wave and deflected or Mach stem) with a Mach stem that increases in size in accordance with the angle of the triple point formation (Fig. 6.3). As previously stated the Mach stem travels parallel to the surface and creates peak pressures several times greater than that seen in the incident front [1]. The interaction of these properties in different environments is discussed later in this chapter.

6.1.3.5 Injury Mechanism

When considering the mechanism of injury of blast weapons it is convenient to consider the order of events during an explosion with

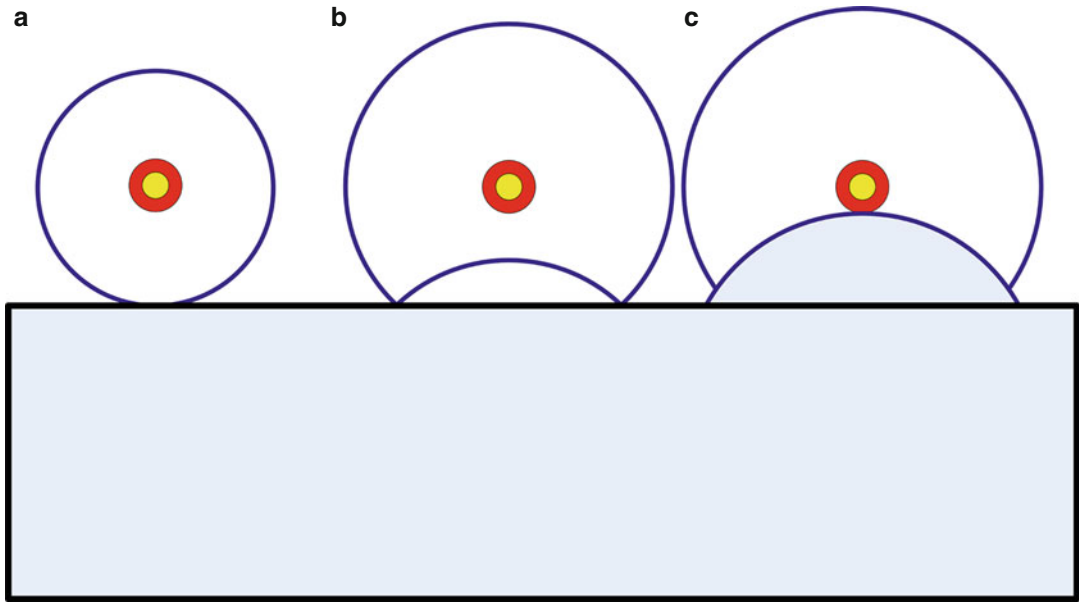

Fig. 6.2 Blast front reflection and Mach Stem effect (**a**) Pre-reflection, (**b**) simple reflection, (**c**) reflected front catches up with primary front

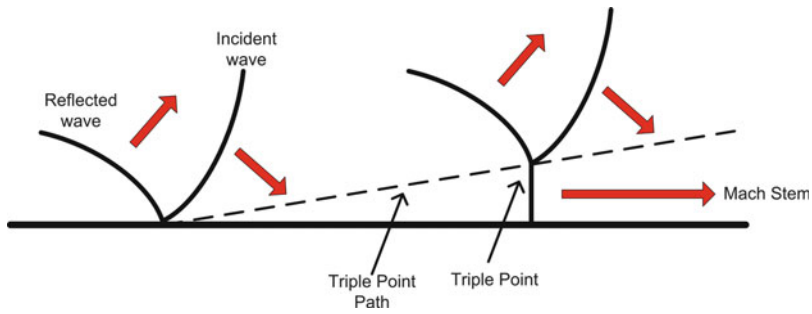

Fig. 6.3 Mach stem formation

HE. During detonation the high intensity exothermic reaction assists further initiation of the explosive material. Cullis reported that in 1 kg of TNT the energy available to be released at detonation is 4 MJ which is the equivalent to 400,000 kW (400 power stations) emitting their energy in 10 μs [1]. Temperatures can reach 7000 °C. Incineration at the centre or severe burns in the local environment are likely.

From initiation to propagation the blast wave front is established: a high-pressure zone attaining pressures of 20 GPa (200,000 atm). The body is composed of air, liquid and solids. These are occasionally found in distinct separate compartments, such as the inner ear, blood, and solid organs respectively, but these are mostly in overlapping states between the three mediums. The dynamic overpressure front causes damage to air containing compartments such as the ears, lungs and gastro-intestinal tract [4]. The large pressure gradient between the blast front and these compartments characteristically causes tympanic membrane rupture, alveolar damage and bowel mucosal surface injury respectively.

6.2 Blast Injury Mechanisms

Traditionally the injurious effects from explosions have been divided into primary to

quinary mechanisms, with the initial descriptions credited to Zuckerman during the Second World War [5]; a more detailed description was subsequently produced by the US Department of Defense in 2008. Whilst the classification is considered by many as the definitive one, it has limitations, particularly as the initial work related to free field blast explosions in the open environment. It was acknowledged in the early literature that different environments will result in different injury patterns, but this seems less well appreciated in recent literature. This will be discussed in greater detail following a description of the traditional classification.

6.2.1 Primary Blast Injury

A primary blast injury results from the blast overpressure which can result in direct transmission of the wave through the tissue, as well as compression and acceleration; differential acceleration can occur at the interface of tissues of different densities and impedance. This can result in compression, shearing forces and spallation. In addition it has been suggested that a more subtle biochemical injury mechanism can occur; given the complex nature of the body it is likely that there are multiple injury mechanisms, which almost certainly create and increase the effects of one another.

Previously it was believed that only the gas containing structures, the lungs, ears and the hollow abdominal organs were affected; however it is now appreciated that the blast overpressure also affects the brain, solid abdominal organs, the musculoskeletal tissues as well as other tissues. The exact extent and mechanism of injury is still not fully understood.

Blast-related lung injury is probably the most important effect of the blast overpressure in air. From a pathophysiological basis, alveoli septal rupture occurs with pulmonary haemorrhage and oedema, resulting in impaired gas exchange and hypoxia which may be fatal. Pneumothoraces and evolving pulmonary contusions further exacerbate the effects. The exact cause of the lung damage is not fully understood and the microscopic and metabolic effects have also not been described in detail. Lung injury is further complicated in survivors, particularly the critically ill, as resuscitation, transfusion and ventilation strategies will also complicate the clinical picture.

In addition, it is believed that significant air emboli can occur, leading to cardiac and central nervous system effects; this may be the mechanism of the fatalities with no external signs of injury (see below). It has been proposed that emboli result from the re-expansion of compressed gases in the lungs, which can access the circulation via the damaged microvasculature.

Blast bowel and tympanic membrane rupture are influenced by the environment, blast bowel being more common when the victim is in water, particularly when half-submerged such as when wearing a life vest. The impulse travels faster and further in the almost incompressible water compared to air, presumably resulting in relative protection to the chest which is above water. The concept that different injuries occur from transmission of the blast wave through the different states of matter, gas, liquid and solid was recognised soon after the original classification [6]. Solid blast will be considered in more detail below.

Although tympanic membrane is considered a primary blast injury, it seems to be related to the position of the head, and may also be related to any head protection that is being worn. It is associated with head injury rather than other primary blast injuries; tympanic membrane rupture has been shown to be unrelated to significant lung problems, the most serious consequence of the blast overpressure [7].

It has also been reported that the blast overpressure can affect the skeletal system resulting in fracture of long bones, and this was thought to be the initial event with traumatic amputations following explosions. Stress concentration at the diaphyseal/metaphyseal junction and a shattering effect has been proposed as a possible mechanism [8–11]. However, this is incompletely understood and, as will be described later, there is likely to be a flail element as well as a solid blast element, re-enforcing the concept that the

specific environment is at least as important as the proposed blast mechanism.

The majority of survivors of blast have sustained secondary or tertiary injuries and, in general, there are few survivors with significant primary blast injuries, as casualties with the necessary blast loading will have usually been killed immediately from a combination of all effects. This is as a direct result of the fact that the energy carried by the blast wave rapidly diminishes as the energy is subjected to the inverse cube rule.

$$E \propto \frac{1}{r^3} \quad \text{(where E is energy and r is distance from the explosion)}$$

However, this also appears to be related to the environment, with a higher incidence of primary blast injuries in confined spaces. Leibovici et al. [12, 13] reported that all confined space casualties who died in hospital succumbed to respiratory failure secondary to blast injuries, and Katz et al. [14] noted a higher than expected incidence of primary blast injuries following a bus explosion when all the windows were closed.

6.2.2 Secondary Blast Injury

Secondary effects are due to fragments accelerated by the blast wind; these might be from the device itself (confusingly referred to as primary fragments by some authors, despite being a secondary effect), or other environmental objects such as stones or soil, particularly when the explosive device is buried. These objects are sometimes referred to as secondary fragments. Shrapnel is a specific rather than a collective term, and refers to a fragment containing artillery, designed as an anti-personnel device to increase its injurious effects. It is the fragments that are the most lethal mechanism following explosions, with a greater radius of effect than that of the blast overpressure. This is as a consequence of the fact that, unlike the blast wave, the energy of a fragment is subjected to the inverse square rule of dissipation.

$$E \propto \frac{1}{r^2} \quad \text{(where E is energy and r is distance from the explosion)}$$

6.2.3 Tertiary Blast Injury

Tertiary effects relate to the displacement of the body, or the displacement of solid objects which come in contact with the body, by the blast wind and are often similar to the effects of civilian blunt trauma, although usually at greater injury levels. Head injuries are common (and may be fatal), as are fractures. Crush injuries and injuries from buildings collapsing are also included in this group.

Recently the concept of 'solid blast' has been re-described, having been ignored in the literature since the Second World War [15]. As this is related to transmission through a solid structure such as a vehicle floor or a ship's hull from an underwater blast, it cannot be adequately classified using a free-field blast classification; however it results in injury patterns predominately to the musculo-skeletal system, similar to those seen from the tertiary effects of blast. In addition, flailing can also cause injury, either from relative restraint or protection of one part of the body compared to another, usually a limb. It appears that it can also result from solid blast. At its most extreme it seems to result in traumatic amputation of the limb, again illustrating the need to consider the specific situation when considering blast injury mechanisms.

The concept of behind armour blunt trauma (BABT) is well placed in the tertiary blast injury category. BABT is defined as a non-penetrating injury due the deformation of body armour that lies in close proximity to the body, such as a helmet or Kevlar© chest plate, and the injury mechanism similar to that of the "solid blast" in that the armour transfers energy to the body [16]. Whilst the injurious mechanism is that of the tertiary category, the energy can arise due to the primary or secondary effects of the blast. (See Chap. 24).

6.2.4 Quaternary Blast Effects

Quaternary effects are essentially a miscellaneous group of injuries not specifically associated with one of the other groups. The category was added after the original classification. Burns, inhalation injuries and other toxic effects would also be included in this category. The extent and distribution of burns has been reported to fall into two distinct patterns with one group sustaining burns to the exposed areas of the hands and face, often relatively superficial flash burns from the initial detonation [17]. The second group have more extensive, deeper burns from fires that break out after the explosion; in this group the clothing offers much less protection.

More recently it has been proposed that quinary effects of blast should be included. These are effects from specific non-explosion related effects such as radiation, bacteria or viral infections. They have been referred to as 'dirty bombs' [18]. This has been a concern with suicide bombers who may deliberately infect themselves with the hope that the infection will be transmitted from biological fragments. This is considered in more detail later.

6.2.5 Cause of Death After Explosions

Human casualty research suffers from the inability to control the environment, and lack of specific injury details, particularly fatality data. In many papers the most common causes of death were head injury, both blunt and penetrating, and haemorrhage usually from penetrating fragment injury. With the use of Computerised Tomography in Post-Mortem (CTPM) analysis, further evidence will be produced which may also help understand the phenomenon of victims who died without any external evidence of injury; this is said to be one of the initial stimuli to blast research in the early twentieth century [4].

CTPM findings have been reported from British fatalities from Afghanistan [19]. These reported different patterns of injuries when comparing service personnel who were on foot to those within a vehicle, again emphasising the need to consider the environment. Those on foot were most likely to die from haemorrhage commonly associated with severe lower limb injuries, whilst those in vehicles were more likely to die of head injuries, possibly from a tertiary mechanism. It is worth repeating that this may just be relevant to a specific scenario, that of a buried improvised explosive device, and the effects of the soil on modifying the injury mechanism have to be considered. In particular, the victims may have been protected from the blast overpressure, and most of these weapons were not designed to injure by fragments. As will be described in the next section the patterns of injuries in survivors suggest that a solid blast element may be responsible, a mechanism not usually considered in the classical description of blast injuries.

6.3 Weapons

Broadly speaking explosive weapon systems are manufactured to produce their effect by two distinct mechanisms – blast or fragmentation [20]. However, the mechanisms of injury are not mutually exclusive. Casualties can be injured by the blast or fragmentation or both. Weapon systems can be further classified according to the manufacturer and the target to which they are directed (Table 6.1). It is conventionally thought that they exert their effect through the release of energy and subsequent physical injuries, however, in this chapter we will discuss the physical effects and special circumstances, such as in suicide bombings where psychological elements come into play.

6.3.1 Blast Weapons

Conventionally the use of the blast wave as a primary means of causing injury to a casualty is rare. The exceptions are those of the unburied anti-personnel mine (see Sect. 6.2.4), and the fuel-air explosive (FAE). The energy that can

Table 6.1 Weapon systems classification

Weapon system	Manufacture	Conventional
		Improvised
	Mechanism of injury	Blast
		Fragmentation
	Target	Anti-personnel
		Anti-vehicular

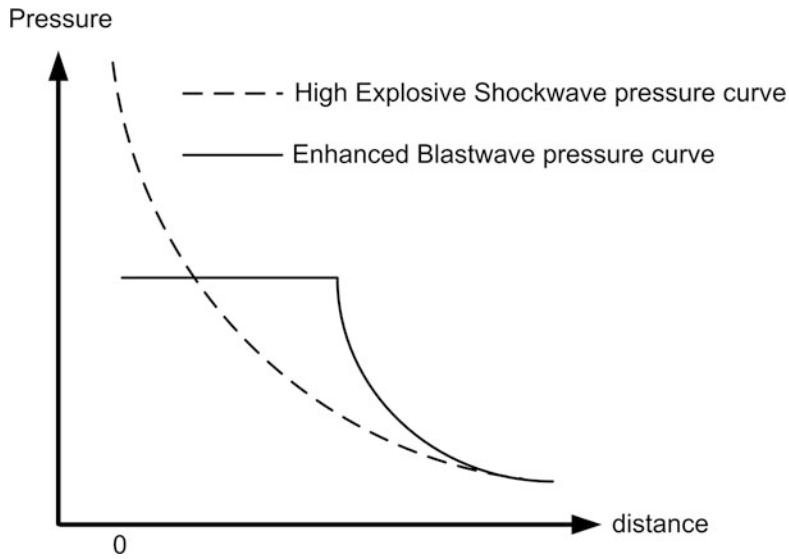

Fig. 6.4 High explosive and enhanced blast wave pressure graphs

be transferred from a blast wave to a subject rapidly decreases the further away the subject is from the centre of the detonation, according to the inverse cube law, and is affected by environmental factors such as buildings. The exception is the FAE which utilises a double detonation sequence to ignite the fuel explosive which has been dispersed and vaporised in a large volume of air by the first explosion. A casualty caught in either the FAE area or the centre of a traditional munition is likely to be subject to lethal levels of blast and/or blast fragmentation respectively. As a consequence, physiological effects of the blast front, for example primary blast lung, are not relevant in the casualty cohort that these munitions create.

Two scenarios are now considered where the blast peak and overpressure related injuries need to be considered: the emerging family of Enhanced Blast Weapons (EBW) and the Improvised Explosive Device (IED – see Sect. 6.3.7). The ability of EBWs to produce a sustained uniform dynamic overpressure results in a shock wave front carrying further and with more energy, since the energy a shock wave possesses is a function of the area under the curve of a pressure-distance graph [20]. The change in the wave characteristics enables it to behave differently to a simple static-dynamic wave. Due to its sustained pressure, the EBW blast wave is able to expand into buildings, spaces and around corners by diffraction (Fig. 6.4).

Due to the combined effect of the initial explosion, sustained pressure front and the increased distance it is able to apply to its effect, in addition to the increased fragmentation, thermal and environmental interaction, and

Table 6.2 Blast pressure effects on personnel

Pressure (atmosphere)	Injury
0.34	Tympanic membrane injury
1	50 % chance tympanic rupture
5.44	50 % chance lung injury
9.14–12.66	50 % chance of death
14.06–17.58	Death

subsequently translates into increased casualties from a single explosion when compared to a conventional HE munition. This may be by direct targeting of personnel or as collateral damage when EBW is used in an anti-material role.

Injuries sustained due to blast overpressure are well documented in the literature. Work in the 1970s details the pressures at which the hierarchy of injury is likely to be sustained (Table 6.2) [18, 21]. Focussing on air containing compartments, the most common injury seen in blast weapons is that of tympanic membrane injury, from simple contusions through to rupture.

6.3.2 Fragmentation Weapons

Weapons whose primary purpose is to cause damage due to fragmentation generally share a design that has a high casing to explosive ratio, the casing being the source of fragmentation. Whilst the lethality zone is greater than that of a conventional blast weapon, the probability of death relies upon a direct strike to vital organs. The most common type of injury seen in this scenario is that of extremity penetration. The coverage of an area by fragmentation is almost a random event and, due to the diverging effect of their trajectories and an increase in volume of the lethal zone, the further a fragment carries, the probability of coverage decreases with distance.

The mechanism of delivery of the fragment to the target is by the utilisation of the blast wave from the detonation of the HE. The quantity of HE is determined by the intended target, mass of fragmentation and size of the munition.

The sources of fragmentation are multiple (Fig. 6.5). The simplest and most well-known form of fragmentation device is the hand grenade. The word is thought to be derived from its comparison to the Pomegranate fruit from the French and Spanish languages. However, the use of grenade type devises extends back to the Byzantine period where "Greek fire" was contained in ceramic jars. In contemporaneous times it is William Mills, and the bomb that shares his name, that is credited with the modern well known design of the "pineapple" hand grenade. Its obvious limitation is that of accuracy and range of the thrower. Modern rifles now frequently allow the modular extension of an Underslung Grenade Launcher (UGL). This is often laser guided increasing its accuracy, and a range of up to 1000 m more than compensates for its lack of lethality. With respect to artillery munitions, the fragmentation may be derived from the casing, formally called fragmentation, or by pre-formed fragments, or shrapnel within the casing. Improvised shrapnel is seen in IED and suicide scenarios where everyday objects, such as ball bearings, nuts and bolts, are utilised.

Finally, objects in the environment near the field of detonation may themselves become part of the fragmentation load. This can be intentional or unintentional. Masonry, rubble or building material may be considered in a similar manner to formal fragments, however, agricultural material, sewage or soil, which again may contaminate the injured person intentionally or unintentionally must carry special consideration during the medical management of the casualty. The possibility of biological implantation either from agriculture, other injured persons or the suicide bomber must be established from the scene.

In the modern battle field, fragmentation injuries predominate.

6.3.3 Blast and Fragmentation effects

In reality, blast and fragmentation mechanisms are not mutually exclusive of each other. The degree and ratio to which an individual is subjected to either modality is proportional to the distance they are from the centre of

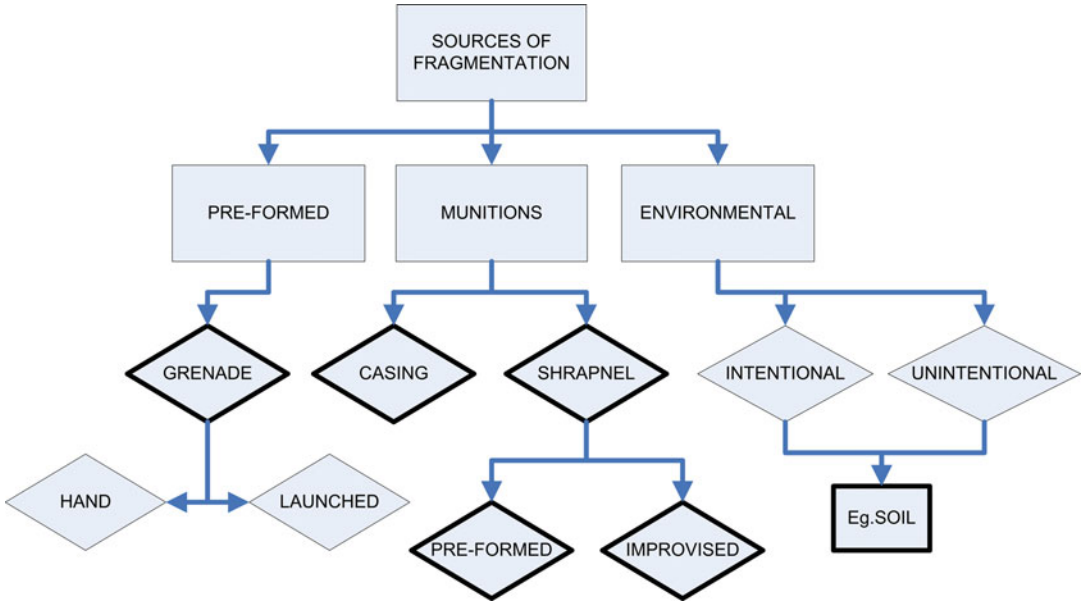

Fig. 6.5 Sources of fragmentation

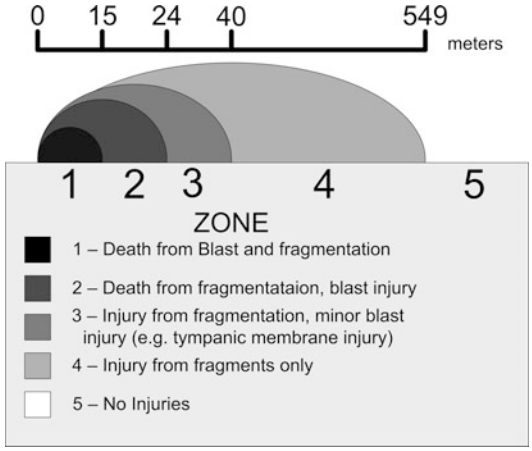

Fig. 6.6 Zones of injury from blast and fragmentation munitions

detonation (Fig. 6.6) [18]. As previously stated, it is fragmentation injury that usually predominates as casualties subjected to significantly high-pressure wave fronts to cause blast related injury experience un-survivable levels of trauma. Signs of blast injury itself may not become apparent for 48 h. Therefore, other blast related injuries noted should alert the clinician to intensive observations of the effects of hidden primary blast injury. The British and American experience in recent conflicts in Iraq and Afghanistan is that over one-third of casualties demonstrated blast injuries [22].

In the use of blast weapons the simple interaction of the blast front and subsequent fragments is not the complete picture. Section D covers classification and different mechanisms of injury seen in these weapons.

6.3.4 Mines

In contemporary history the principle use of mines has been as a potent defensive force multiplier [22]: protecting the military assets and/or boundaries with the added advantage of freeing valuable personnel. Blast land mines exploit the simple physical properties of blast weapons, that of supersonic detonation of a HE explosive. However, it is the unique interaction with the local environment that leads to specific mechanism of injury or vehicle disablement [23]. Three distinct processes determine and quantify the degree of kinetic energy transfer that occurs once detonated [22]:

Interaction with soil – Following total consumption of the explosive by the detonation wave heat is transferred to the adjacent soil whilst the wave front passes in the surrounding of the explosive. The heated soil is subsequently compressed creating a "cap". On interaction of the compression soil with the air-soil interface two processes occur. Either the compressed cap is reflected back towards the explosive, fracturing the soil cap as it does so, or the wave is transmitted into air but with relatively little kinetic energy.

Gas expansion – All HE explosives produce large quantities of expanding gas which expands at supersonic speeds. The high pressure gas expansion escapes the detonating area by travelling through the fracture lines caused by the compression soil cap. In direct correlation with the Venturi effect the gas pressure decreases as it seeks out the fracture lines but as it does so its velocity increases. The velocity reaches supersonic speeds. Together with the escaping jets of compressed gas and the ejected soil plug due to gas expansion the combined effect of transfer of energy is enough to cause vehicle floor deformation or significant injury to personnel.

Soil ejecta – Soil disturbance occurs with the initial radial compression wave but as detailed before often poses little threat to individuals or vehicles. Towards the end of gas expansion, shear forces at the boundary area of the explosion crater cause the upward mass movement of the soil. Together with the detonation gases this may cause the vertical displacement or movement of a vehicle or individual.

6.3.5 Anti-personnel Devices or Mines

Despite the Ottowa Convention (Prohibition of the Use, Stockpiling, Production and Transfer of Anti-personnel Mines) in 1997 Anti-Personnel (AP) mines continue to create significant casualties every year [24]. The International Campaign to Ban Landmines states that in 2010, 4000 people were injured or killed due to legacy mines. The problem is compounded by groups who do not subscribe to the above convention (e.g. USA, Russia, China, Pakistan and India) and the presence of large numbers of legacy mine fields un-cleared, or un-marked.

The same Convention defines an AP mine as

> a mine designed to be exploded by the presence, proximity, or contact of a person and that will incapacitate, injure or kill. . .

In general, they are designed to maim or injure, thereby causing not only devastating injury to the casualty but also damaging the logistical supply chain due to the mechanism required to treat and evacuate an injured soldier [25]. AP mines are classified into Blast or Fragmentation types which denotes the primary mechanism of injury, but in reality a significant overlap exists.

Blast AP mines exploit the use of small amounts of HE and the subsequent formation of a blast front. They are often triggered by short-trip wire or direct pressure and, as a consequence, the intended casualty is rarely more than a foot from the centre of detonation. Upon detonation, a shock front is delivered directly upwards through the soil and into the lower limb. Longitudinal stress is applied through the foot and tibia and related soft tissues and traumatic-amputations ensue. This is compounded by the secondary effects of the mine by the carriage of soil and casing and the dynamic overpressure after the font. The injury patterns are relatively reproducible and have been classified into three distinct groups by the International Committee of the Red Cross (Table 6.3).

Typically blast mines are no more than 15 cm in diameter and often consist of plastic, rather than metal, casing and often contain no more than 20–40 g of high explosive [25]. The advantage of plastic is that it allows the mine to be light-weight for ease of transportation of large numbers, and the added benefit of not being detected by metal detectors.

Fragmentation AP mines deliver their effect primarily through the release of preformed fragments or the fragmentation load consists

Table 6.3 International committee of the red cross classification of anti-personnel mine injuries (Coupland and Korver 1991)

Type 1	Injuries from standing on a mine	Traumatic-amputations or devastating soft-tissue injuries
Type 2	Injuries from a mine triggered in the vicinity	Randomly located fragmentation type injuries
Type 3	Injuries sustained from handling a mine	Sever upper limb and facial injuries

intentionally of the metal casing of the mine. Three types of fragmentation mine exist – the Stake, Bounding and Directional (or Claymore) mines. In its simplest form the fragmentation mine consists of an HE explosive impregnated with preformed fragments held off the ground on a stake. The Bounding mine launches itself from underground to a pre-determined height, usually chest high, where it is then detonated. The Directional or Claymore mine delivers its munition in a pre-determined direction and is also staked into the ground. These mines are often larger than blast mines and made of ferrous metal casing making them easier to detect using conventional mine or metal detectors. Their trigger mechanism more often than not consists of a trip wire configuration to allow the casualty or casualties to enter an optimal "killing zone". Their mechanism of injury predominantly falls in the ICRC Type 2 injury category.

6.3.6 Anti-vehicle Devices

Anti-vehicle mines (AV) were primarily manufactured in response to tanks. Initially manufactured purely as large AP mines, subsequent modifications have made them vehicle or tank specific. In comparison to AP mines, AV mines are often in excess of 5 kg in weight, including casing and detonator, with HE charges of typically 3.5–7 kg [22]. The logistic demand of carrying and placing large numbers of landmines is greater than that of AV mines. The triggering mechanism is traditionally set at 100 kg to ensure target specific detonation and so therefore not waste mine strikes on smaller targets.

Whilst modern shaped AV mines are able to penetrate vehicles this is a departure from the normal mechanism of targeting the track or wheels of vehicles which are seen as their weak points. The gas expansion phase of mine detonation is enough to cause damage to vehicle chasses or tank tracks to immobilise the vehicle in question. The floor pan may deform but rarely penetrate the vehicle sufficiently to cause bodily harm. However, it is the shape of the underbelly of the vehicle that dictates further energy transfer to the vehicle during the "soil ejecta" phase. A flat underbelly surface will create high concentration fields of the soil ejecta and detonation products whereas a "V" shaped underbelly, designed to mitigate this effect, will allow the detonation products to flow in a linear pattern horizontal to the vehicle surface and not produce increased field pressure concentration [22].

Weapons development in response to manufacturing changes to the underbelly of vehicles to mitigate against mine blast is to produce shaped charges that penetrate vehicles. In its simplest form, the shaped charge utilises the Munroe effect to focus the energy generated during an explosive detonation by shaping the explosive surface. At the end of the nineteenth century Charles Munroe noticed that a raised or indented shape on an explosive surface created similar shaped patterns on a metal plate in the blast wave path; the changes in the explosive surface caused a much localised concentration to the pressure front. In 1910 Egon Neuman extended these experiments and noted that a conical defect in the explosive resulted in penetration of a metal surface by the focused blast front. The creation of an Explosively Formed Penetrator (EFP) is now formally exploited in the manufacturing of specific vehicle/tank penetrating land mines (Fig. 6.7) where the intended vehicle is immobilised and where the occupants are subjected to the effects of the blast wave, its thermal characteristics and fragmentation from the mine, vehicle structure and internal components. These result in damage

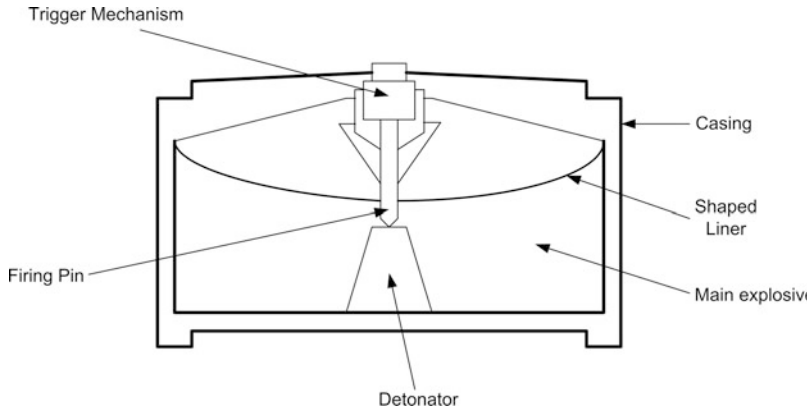

Fig. 6.7 Cross-section of a typical anti-vehicle landmine

and injuries now classified as Behind Armour Effect/Damage (BAE/BAD). This Munroe effect has also been exploited by terrorists with devastating success in the formation of Improvised Explosive Devices (IEDs) targeted against ground troops (see Sect. 6.3.7).

6.3.7 Improvised Explosive Devices

The Improvised Explosive Device (IED) has become the explosive weapon of choice of terrorist organisations worldwide. The term IED has almost become synonymous with the conflicts in Iraq and Afghanistan due to the large number of casualties as a direct result of their use. Their design has been to ultimately not only cause devastating injuries but their magnitude is such that it will also overwhelm logistical elements of the force to which they are directed. Whilst the road-side bomb has been used effectively, an IED is any device that uses modified conventional, or unconventional, munitions to exert their effect. They have been used to great effect in the form of pipe bombs, car bombs (Vehicle Bourne – VBIED), letter bombs and indeed suicide bombs (see later in Chapter, Sect. 6.5). According to the United States Department of Defence the definition of IED is any "*devices placed or fabricated in an improvised manner incorporating destructive, lethal, noxious, pyrotechnic or incendiary chemicals, designed to destroy, disfigure, distract or harass and often incorporate military stores.*"

Broadly speaking IEDs can be classified into 3 groups – (1) Conventional explosive formed from munitions, (2) Explosive-Formed Projectiles (EFP), and (3) Suicide or vehicle delivered devices. In reality an IED may fall into any or all of the above groups. Their construction has 5 core components – an activator or switch, an initiator or detonator, a container, the explosive and a power source. In an IED devised against a vehicle or armour the explosive charge or munitions are commonly shaped to form an EFP. Further modifications of an IED may be to incorporate fragmentation into the explosive or body to enhance its lethality or the opportunistic use of environmental factors such as stationary vehicles, soil and buildings to enhance its effect.

Increased awareness and improvements in detection equipment has led to novel techniques in explosive delivery. The use of animals as carriers was noted during the insurgency after the second Iraq war, whilst some terrorist organisations have resorted to extortion of local communities and farmers to conceal IEDs [26]. The security services of the United States of America and the United Kingdom revealed the acquisition of intelligence suggesting the emergence of surgically implanted explosives and the containment of explosives within the heel of a shoe. Equally as ingenious is the trigger mechanism that individuals manufacturing IEDs have

developed. In its simplest form, an IED is detonated via a command-wire that relies on visual line of sight targeting by the initiator. Further advanced, but proved less in control of targeting, is the mine-type or victim-operated IED. With telecommunications equipment now readily available on the high street and open market, infra-red, radio and cellular phone triggers are now common place. The distinct advantages of these devices being that the perpetrator can be many miles away from the device, if not on different continents.

6.4 Environmental Factors

The majority of the research into blast effects and injuries dates from during and after the Second World War, particularly in relation to the effects of nuclear weapons, hence the focus on free-field blast. However as bombs have always been a favoured weapon of terrorists, it is this aspect rather than conventional warfare that has provided injury data. This experience has led to the understanding that the fatality rate, and the pattern of injury is related to the environment in which the explosion occurs. In terms of air blast (as opposed to liquid or solid blast) these can be considered as:

explosions in the open air;
explosions associated with structural (building) collapse; and
explosions in confined spaces.

Arnold et al. [15] reviewed the outcome of 29 incidents that collectively produced 8364 casualties and 903 immediate deaths. They analysed the relative mortality for the three types of bombing and noted that this differed depending on the environment. One in four victims died in bombings involving structural collapse, one in twelve in confined space explosions and one in twenty-five in open air bombings.

Freidlander's classical work describes the changes seen in pressure when dealing with a single, free field detonation of an explosive (see Chap. 1). The increase in pressure seen on the blast front leading edge in explosions is referred to as the Blast Overpressure (BOP). However, further work summarised by Cullis [1] clearly details the complex interaction of physical properties of the blast wave with the environment, particularly the effects of reflection and refraction. The reality is rarely simple. Explosions usually come under the influence of objects, walls, buildings and water resulting in complex wave forms and varying modalities of energy transfer.

6.4.1 Open

In a free field or open environment, the blast front, BOP and subsequent pressure changes follow a well-defined and predictable pressure-time curve. Air as a gas is compressible and so the BOP consists of a narrow leading edge. As defined by Friedlander, there exists a positive overpressure followed by a negative phase; negative in relation to both the peak pressure and eventually atmospheric pressure. In reality the wave form is superimposed with peaks and troughs of smaller amplitude caused by artefact, vibration or reflections from minor surfaces or the ground. The mean wave form, however, remains simple. A bystander will experience an initial sudden increase in acceleration of local air with a large increase in pressure and a rise in temperature. This is then followed by a blast wind travelling in the same direction as the blast front. This quickly decays and is followed by a blast wind of reduced magnitude travelling in the opposite direction to the initial front.

Fragments are by far the most common cause of injury in the open environment. Blast lung and other conditions associated with primary blast injury do occur in survivors, but are much less common than in confined space explosions.

Fractures can occur from both the fragments and the casualty been thrown by the blast wind.

6.4.2 Semi-confined and Enclosed Spaces

This generates an environment where large pressures are created for extended periods of time allowing for further energy transfer to a casualty, increasing the lethality of an explosion (Fig. 6.8). This has been demonstrated in literature emerging from suicide bus bombings in Israel and the Underground Train bombing in London in 2005.

Casualties caught in enclosed blast explosions are subjected to the peak BOP and also the sustained peak pressures. As a consequence of this, fatality rates are increased. Individuals experiencing these primary blast injury effects are less likely to survive.

Bus and train bombings can be considered as a separate 'ultra-confined' space based on injury profile, with particular reference to primary blast injuries.

Kosashvili et al. [33] in a review of 12 separate incidents from Israel noted that explosions that occurred in buses had the highest mortality rates (21.2 %) both as a result of crowding and reflection of the blast in the confined space. Similar findings were reported from the Madrid train bombings, with Turégano-Fuentes et al. [17, 27] noting that more deaths occurred in the 2 trains that had their doors closed, compared with the 2 that had their doors open in the station.

When compared to the other 2 environments, Primary Blast Injuries such as blast lung are far more common in confined space explosions. Burns are also far more common, and fractures and head injuries are also more common than the other 2 groups. This is likely to be due to the close proximity to the blast, causing flash burns, and throwing the casualty against the sides of the structure. The energy involved in throwing the casualty can cause severe head injuries, as well as fractures. There is also a higher rate of abdominal injury to the liver and spleen which may cause bleeding into the abdomen, and, if severe, could result in a casualty bleeding to death internally. However, this is still less common than penetrating injuries from fragments and much less common than blast lung.

As a result of these different injury patterns, a casualty who survives the initial explosion and appears responsive but dies soon afterwards, is more likely to be in an enclosed space environment than the other 2 environments. A casualty who is initially conscious and talking, is more likely to have died of blast injuries to the lung, or bleed to death internally, as casualties with severe head injuries are usually deeply unconscious from the time of the explosion.

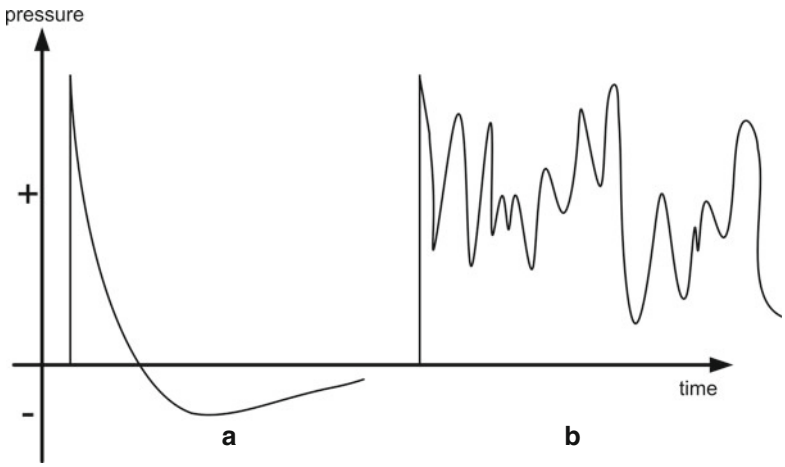

Fig. 6.8 Pressure wave form of a simple open/free-field Friedlander type explosion (**a**) and an enclosed blast (**b**)

6.4.3 Buried

In comparison to land mines, the total energy transfer to the target from buried explosives is dependent on (1) the explosive's interaction with soil, (2) the permitted gas expansion and finally (3) the soil ejecta. The gas expansion occurs in the first 5–10 ms after detonation whilst the ejection of soil occurs shortly after and lasts 50–100 ms.

6.4.4 Solid

The medium, or material, through which a blast wave travels also contributes to its characteristics, wave form and magnitude. Solid media, including liquids, are, when compared to air, relatively non-compressible. As a consequence they are good propagators of blast waves and also increase the duration of positive pressure generated.

In the case of hollow structures or vehicles, such as ships and armoured personnel carriers the rapid propagation and increased speed of the blast wave results in displacement or deformation of the vessel. As in buried land mines, it is the point at which the blast wave crosses the interface between solid and air that dictates energy transfer and the injury or damage ensued.

6.4.5 Deck Slap

An increased IED threat during the Iraq and Afghanistan conflicts resulted in the change of tactics by coalition forces. Troops patrolling on foot were replaced by patrols in vehicles. Strategies developed to avoid or mitigate death or serious injury succeeded but a new cohort of lower limb casualties was borne. These injuries have subsequently been named the "modern deck-slap" injury.

First described in World War 2, the deck-slap injuries comprise fractures to the foot and lower limb in response to a rapidly accelerating floor, or deck, of a vehicle or ship. In the instance of the original deck-slap injuries cases were described when ships were targeted by sea-mines. It was noted that the "*deck rose suddenly beneath the feet of those injured, and the force transmitted upward through the skeleton produced a series of injuries including fractures of the Os Calcis, tibia and knee*" [28]. These injuries are created by the direct transfer of energy from the blast wave through the ship via solid blast mechanism where the victims are not subjected to primary blast effects. It was hypothesised by Barr et al. [28] that ancient wooden ships would better protect its crew from sea-mines than modern steel hulled vessels.

An almost identical pattern of injuries has been noted in passengers of military vehicles following IED under-vehicle explosions [15]. Of note is that this casualty cohort experienced multiple segment injury to their limbs of a severity that resulted in nearly half requiring amputation. The field of injury mitigation in the "deck-slap" scenario is an area of significant research in the military and civilian environment.

6.5 Suicide Bombings

Suicide bombings have significantly increased in number in the last 50 years. Their history dates back 2000 years to Roman occupied Judaea and the establishment of the Sicarii ("daggers") Jewish sect. The following millennia saw the rise of the Muslim Hashashin Group, which lends itself to the contemporary term "assassin".

Whilst the vast majority of contemporary attacks have been seen in the middle East and Asian subcontinent, notable incidents in the developed world, e.g. London, New York, Madrid and Oklahoma, have raised its profile in the eyes of emergency services globally. The attraction of suicide bombing by terrorist organisations is multifactorial. The combination of low cost, high lethality and pinpoint target accuracy are devastating. Bloom showed that suicide attacks cause 6 times more fatalities, 12 times more casualty figures and eight times more media coverage [29]. The effects of a suicide bomb extend further than the physical

injuries caused by the index event but also the on-going psychological impact on those that witness the incident and the local community and population.

The simplest and most effective method of delivery of an explosive is that of the individual suicide bomber. The first 10 years of this millennium witnessed the devastating effect of the individual suicide bombers using an explosive belt in Israel [30]. The clear advantage of this method of deployment is that the bomber himself or herself may choose the optimal temporal and geographical environment to detonate the explosive to cause maximum damage. Other modes particularly used by the IRA in London, although not suicide, is the use of the car bomb; the advantage being to deploy large quantities of explosives whilst the clear disadvantage being a static delivery method of the parked vehicle or final access to a target. The 11th September 2001 saw the use of multiple aircrafts in a combined attack in New York, Washington and Pennsylvania resulting in 2986 deaths. The advantage of this type of attack to the terrorist organisation involved the large quantity of casualties, logistical consumption of the emergency services and obvious media coverage. However, this form of attack requires large-scale planning, many individuals party to the plans (19 attackers used in the hijacking of 4 airplanes) and significant funding requirements. The mechanism of injury differs between these three modes. The former two primarily resulted in a blast injury mechanism, and possible secondary additional environment factors such as building collapse, whilst the aeroplane method causes death by crash landing, such as in Pennsylvania or as seen in New York, deliberate crashing into high-rise buildings causing building collapse.

The effectiveness of suicide bombing depends on mode of delivery, accuracy, concentration of target population and volume of explosive used. A sample of 89 % (135) human suicide attacks in Israel between 2000 and 2005 resulted in a mean of 3.7 fatalities and a mean of 24.2 injured personnel [30]. Benmelch and Berrebi continue to explore the specifics of human capital of suicide bombers and their subsequent effectiveness [31]. Statistically significant results demonstrate a suicide bomber with an increased age, increased level of education and the detonation in a city environment results in higher fatality and casualty figures.

As previously discussed in this chapter, 3 environmental scenarios exist that dictate blast and injury profiles. These are the open, semi-confined and confined environments. The difference between open and closed explosion fatality rates appears significant. It is expected that twice as many deaths occur in a confined explosion compared to an open-air explosion, such as a road checkpoint or an open-air market [13]. This correlates with the fact that in an enclosed confined environment an increased number of primary blast injuries are seen in both the surviving and fatally wounded. These include pulmonary blast effects, pneumothorax, blast lung syndrome and tympanic membrane rupture. Results from experiments emerging as a consequence of the London bombings in 2005 demonstrate that in a closed environment a single Freidlander waveform is abolished. Multiple peaks and a sustained waveform result in a quasistatic pressure (QSP) development. This results in a propagated increase in the primary blast field area and subsequently increased number of primary blast injuries [32].

However, the injury profiles of surviving casualties between groups seem comparable. Of those injured, 30–50 % require admission to hospital, 5–10 % on to intensive care units. A third of those admitted require surgical intervention with over half of those being orthopaedic procedures, including extremity wound debridement, fracture fixation and amputations.

Detonation inside a bus is a favourable environment for a suicide bomber. Whilst it represents a semi-confined environment, and therefore fatalities figures fall between that of open and confined, the victims are static and in a predictable density [33].

As mentioned earlier the impact of suicide bombings extend beyond that of those injured during the incidents. Psychological evaluation of a cross-sectional group of the population of New York and London after their respective suicide bombings revealed that approximately 30 % had significantly increased stress levels 1–2 weeks

after the incident after the respective incidents despite no direct exposure [33]. Dissemination of information regarding terrorist attacks by the media has been shown to increase stress levels in a population via an indirect means.

A scenario which is particular to suicide bombing, is that of biological implantation. Whilst biologically implantation amongst casualties from non-suicide explosions is possible, deliberate self-contraction of blood-borne viruses such as hepatitis B, hepatitis C and HIV, poses additional medical concerns. Biological implantation can be in the form of bony and soft tissue contamination and also the contamination of metal from the environment, or indeed fragmentation from the explosive, contaminated by the perpetrator's tissue or blood [34]. Environmental contaminants resulting in infection should be considered after an explosion within a market or agricultural environment. This has been demonstrated by high rates of candidaemia seen in casualties from marketplace suicide bombings [35]. The literature suggests routine prophylactic treatment with intravenous antibiotics, anti-tetanus and vaccinations against hepatitis B [36].

In addition to the casualties, the protection of first responders to the scene handling potentially infected material must also be considered and personal protection equipment and prophylactic immunisation should be considered in that cohort of medical caregivers.

6.6 Summary

- An explosion is defined as a rapid increase in volume and pressure associated with a sudden release of energy.
- An explosive is defined as a chemical material which inherently contains enough potential energy. When initiated, the transfer of energy to the local environment causes an increase in pressure.
- High explosive (HE) describes the process whereby the initial detonation creates a shock wave which enables propagation of the explosion via chemical decomposition which travels through the material at speeds greater than the speed of sound.
- The detonation, propagation and rapid release of energy from the explosive results in a blast wave.
- At detonation a 1 kg of TNT releases 4 MJ of energy which is the equivalent to 400,000 kW (400 power stations) emitting their energy in 10 μs. Temperatures can reach 7000 °C. A high-pressure zone attaining pressures of 20 GPa (200,000 atm) is possible.
- A primary blast injury results from the blast overpressure which can result in direct transmission of the wave through the tissue and subsequent transfer of energy.
- Secondary blast injuries are due to fragments accelerated by the blast wind.
- Tertiary effects relate to the displacement of the body, or the displacement of solid objects which come in contact with the body, by the blast wind.
- Broadly speaking explosive weapon systems are manufactured to produce their effect by two distinct mechanisms – blast or fragmentation.
- In reality, blast and fragmentation mechanisms are not mutually exclusive of each other.
- IEDs can be classified into three groups – (1) Conventional explosive formed from munitions, (2) Explosive-Formed Projectiles (EFP), and (3) Suicide or vehicle delivered devices.
- Suicide bombings have significantly increased in number in the last 50 years.
- Suicide attacks cause 6 times more fatalities, 12 times more casualty figures and eight times more media coverage.

References

1. Cullis IG. Blast waves and how they interact with structures. J R Army Med Corps. 2001;147(1):16–26.
2. Covey DC, Born CT. Blast injuries: mechanics and wounding patterns. J Surg Orthop Adv. 2010;19(1):8–12.

3. Friedlander FG. The diffraction of sound pulses. I. Diffraction by a semi-infinite plane. Proc R Soc Lond A Math Phys Sci. 1946;186(1006):322–44.
4. Mayorga MA. The pathology of primary blast overpressure injury. Toxicology. 1997;121(1):17–28.
5. Zuckerman S. Discussion on the problem of blast injuries. Proc R Soc Med. 1941;34:171–88.
6. Draeger RH, Barr JS, Sager WW. Blast injury. J Am Med Assoc. 1946;132(13):762–7.
7. Harrison CD, Bebarta VS, Grant GA. Tympanic membrane perforation after combat blast exposure in Iraq: a poor biomarker of primary blast injury. J Trauma. 2009;67(1):210–1.
8. Hull JB. Traumatic amputation by explosive blast: pattern of injury in survivors. Br J Surg. 1992;79 (12):1303–6.
9. Hull JB. Blast: injury patterns and their recording. J Visual Commun Med. 1992;15(3):121–7.
10. Hull JB. Pattern and mechanism of traumatic amputation by explosive blast. J Trauma. 1996;40 (3S):198S–205S.
11. Hull JB, Bowyer GW, Cooper GJ, Crane J. Pattern of injury in those dying from traumatic amputation caused by bomb blast. Br J Surg. 1994;81(8):1132–5.
12. Leibovici D, Gofrit ON, Shapira SC. Eardrum perforation in explosion survivors: is it a marker of pulmonary blast injury? Ann Emerg Med. 1999;34(2):168–72.
13. Leibovici D, Gofrit ON, Stein M, Shapira SC, Noga Y, Heruti RJ, et al. Blast injuries: bus versus open-air bombings – a comparative study of injuries in survivors of open-air versus confined-space explosions. J Trauma. 1996;41(6):1030–5.
14. Katz E, Ofek B, Adler J, Abramowitz HB, Krausz MM. Primary blast injury after a bomb explosion in a civilian bus. Ann Surg. 1989;209(4):484–8.
15. Ramasamy A, Hill AM, Phillip R, Gibb I, Bull AMJ, Clasper JC. The modern "deck-slap" injury—calcaneal blast fractures from vehicle explosions. J Trauma. 2011;71(6):1694–8. 10.097/TA.0b013e318227a999.
16. Cannon L. Behind armour blunt trauma-an emerging problem. J R Army Med Corps. 2001;147(1):87–96.
17. Turégano-Fuentes F, Caba-Doussoux P, Jover-Navalón J, Martín-Pérez E, Fernández-Luengas D, Díez-Valladares L, et al. Injury patterns from major urban terrorist bombings in trains: the Madrid experience. World J Surg. 2008;32(6):1168–75.
18. Champion HR, Holcomb JB, Young LA. Injuries from explosions: physics, biophysics, pathology, and required research focus. J Trauma. 2009;66 (5):1468–77.
19. Singleton JAG, Gibb IE, Bull AMJ, Mahoney PF, Clasper JC. Primary blast lung injury prevalence and fatal injuries from explosions: insights from postmortem computed tomographic analysis of 121 improvised explosive device fatalities. J Trauma Acute Care Surg. 2013;75(2):S269–S74. doi:10.1097/TA.0b013e318299d93e.
20. Dearden P. New blast weapons. J R Army Med Corps. 2001;147(1):80–6.
21. Owen-Smith M. Bomb blast injuries: in an explosive situation. Nurs Mirror. 1979;149(13):35–9.
22. Ramasamy A, Hill AM, Hepper AE, Bull AM, Clasper JC. Blast mines: physics, injury mechanisms and vehicle protection. J R Army Med Corps. 2009;155(4):258–64.
23. Galbraith K. Combat casualties in the first decade of the 21st century-new and emerging weapon systems. J R Army Med Corps. 2001;147(1):7–15.
24. Coupland RM, Korver A. Injuries from antipersonnel mines: the experience of the International Committee of the Red Cross. BMJ. 1991;303(6816):1509–12.
25. Trimble K, Clasper J. Anti-personnel mine injury; mechanism and medical management. J R Army Med Corps. 2001;147(1):73–9.
26. Global Counter IED. Markets & technologies forecast – 2008–2012. Washington, DC: Homeland Secuirity Research; 2007.
27. Turégano-Fuentes F, Caba-Doussoux P, Jover-Navalón JM, Martín-Pérez E, Fernández-Luengas D, Díez-Valladares L, et al. Injury patterns from major urban terroriest bombings in trains: the Madrid experience. World J Surg. 2008;32(6):1168–75.
28. Keating C. Wounds in naval action. In: Bailey H, editor. Surgery of modern warfare. Edinburgh: E&S Livingstone; 1944.
29. Bloom M. Dying to kill: the allure of suicide terror. New York: Columbia University Press; 2005.
30. Mekel M, Bumenfeld A, Feigenberg Z, Ben-Dov D, Kafka M, Barzel O, et al. Terrorist suicide bombings: lessons learned in Metropolitan Haifa from September 2000 to January 2006. Am J Disaster Med. 2009;4 (4):233–48.
31. Benmelech E, Berrebi C. Human capital and the productivity of suicide bombers. J Econ Perspect. 2007;21(3):223–38.
32. Hepper AE, Pope DJ, Bishop M, Kirkman E, Sedman A, Russell R, et al. Modelling the blast environment and relating this to clinical injury: experience from the 7/7 inquest. J R Army Med Corps. 2014;160 (2):171–4.
33. Kosashvili Y, Loebenberg MI, Lin G, Peleg K, Zvi F, Kluger Y, et al. Medical consequences of suicide bombing mass casualty incidents: the impact of explosion setting on injury patterns. Injury. 2009;40 (7):698–702.
34. Eshkol Z, Katz K. Injuries from biologic material of suicide bombers. Injury. 2005;36(2):271–4.
35. Wolf DG, Polacheck I, Block C, Sprung CL, Muggia-Sullam M, Wolf YG, et al. High rate of candidemia in patients sustaining injuries in a bomb blast at a marketplace: a possible environmental source. Clin Infect Dis. 2000;31(3):712–6.
36. Wong JM, Marsh D, Abu-Sitta G, Lau S, Mann HA, Nawabi DH, et al. Biological foreign body implantation in victims of the London July 7th suicide bombings. J Trauma. 2006;60(2):402–4.

Part III

Principles of Investigating and Modelling Blast and Blast Mitigation

The Examination of Post-blast Scenes

7

Karl Harrison and Nadia Abdul-Karim

Bomb scene, or blast scene examination has traditionally formed a component of the general training and awareness undertaken by Crime Scene Investigators (CSIs).[1] While the environments of operation (potentially widely dispersed fields of disrupted or detonated debris), nature of the examination (the prospect of large numbers of casualties) and the surrounding investigative concerns of a high-profile investigation with wide-ranging political ramifications all conspire to distance the post-blast scene from the general experience of most CSIs, the application of their core technical disciplines remains as important throughout the scene examination as with more routine examinations. Indeed, the requirement to provide exhaustive photographic and locational documentation is even greater, given the chaotic nature of such scenes and the importance of reconstructing the distribution of debris at a later date for the courtroom, for understanding the relative position of affected individuals, or for modelling the nature and placement of the charge. As a consequence, it is crucial to understand the 'standard' model of training and approach to scenes adopted by CSIs in order to understand how adaptations to post-blast scenes might be managed.

Crime Scene Investigators working for UK police forces are now almost entirely a body of civilian specialists operating in a niche role. The shift away from warranted police officers began as early as the late 1960s in some police forces, but this small number greatly expanded following the publication of the recommendations of the Touche Ross Report in 1987 [1]. A further expansion of civilian specialists followed as a consequence of the growing importance of DNA evidence, as the required level of technical knowledge increased beyond the general forensic awareness of most warrant-holding police officers. By contrast, Bomb Scene Managers (BSMs) who to some extent supersede the role of the Crime Scene Manager on the post-blast scene are much more likely to be warranted police officers who do not engage in the core CSI training outlined below, but rather gain their training and experience through specialised roles within Counter-Terrorism posts.

In what was the National Police Improvement Agency (NPIA), and is now the College of Policing (CoP) model, CSI training is designed

[1] Crime Scene Examiner (CSE), Crime Scene Investigator (CSI) and Scenes of Crime Officer (SoCO) are different titles for the same role used in different police forces in England and Wales, referred to in this piece as CSIs.

K. Harrison, PhD, MSc (✉)
Cranfield Forensic Institute, Defence Academy of the UK, Shrivenham, UK
e-mail: k.harrison@cranfield.ac.uk

N. Abdul-Karim, BSc, MRes, PhD
Department of Chemistry, University College London, London, UK
e-mail: nadia.abdul-karim.10@ucl.ac.uk

A.M.J. Bull et al. (eds.), *Blast Injury Science and Engineering: A Guide for Clinicians and Researchers*,
DOI 10.1007/978-3-319-21867-0_7

to continue over an extended period, beginning with a two stage initial course, in which each stage consists of a phase of pre course learning, a formal residential training course and the subsequent completion of a Professional Development Portfolio [2]. Following this initial training, CSIs would complete 2 years of work before reattending Harperly Hall to complete a two-week Development Course. Beyond this, further specialist training is delivered within specific courses (i.e., fire investigation, crime scene management), and continuing CSI development is underpinned by the provision of Refresher Courses, designed to be attended by operational CSIs every 5 years. Scenes of Crime (SoC) training is competency based, with a framework of skills demonstrated in class and their successful use being evidenced on return to operational duty in force. These competencies are coordinated through the National Occupational Standards (NOSs) via Skills for Justice [3], and their successful implementation within the workplace forms the basis of a CSI's annual Performance Development Review with their line manager.

As a consequence of this centralised structure, which has been challenged in recent years by the issue of lessening training budgets, a generally standardised approach to major scenes can be expected, implemented by the Crime Scene Manager (CSM) or Bomb Scene Manager (BSM) depending on the nature of the scene.

The confirmation of suspected scenes of major crime, in which post-blast scenes might be considered, will initially be the responsibility of uniformed police response teams, who in relation to this role are referred to as the first officers attending (FOA). The role of the FOA entails not only the confirmation of the suspected major offence but also the initial identification of obvious foci of forensic attention (the presence of a body or weapon, for example), the administering of emergency first aid, the identification of obvious risks to health and safety and the recording of details relating to witnesses still present at the scene. The fulfilment of these duties should ideally be completed in a non-invasive manner that does not jeopardise the forensic potential offered by the scene,[2] but clearly in relation to any wide-ranging disruption such as the aftermath of a blast, this would be an impossible task, and initial disturbance of elements of the scene is an inescapable fact. Any intervention an FOA is forced to undertake in the commission of their duties (such as forcing a door to reach the body of a victim thought to still be alive) should be recorded in detail and that record be made available to the incident room at the earliest opportunity. In the example of a blast scene of magnitude, this is likely to comprise the actions of numerous first responders including police, ambulance and fire and rescue assets, and the recording synthesis and reconstruction of the timings and position of their initial actions is an important and time-consuming duty for investigating officers.

Initial attendance at the major scene and ongoing examination would generally be completed by CSIs. Any CSIs deployed to a major scene would be managed directly by a CSM or BSM who has a responsibility to ensure that a forensic strategy is complied with, and that findings from the crime scene are communicated back to the Incident Room (See Fig. 7.1). Whilst the CSM is deployed to the scene with CSIs, the Crime Scene Coordinator[3] has overall responsibility for deploying staff to scenes[4], coordinates the examination strategies of numerous CSMs and ensures integration between the forensic strategy and the overall investigation directed by the Senior Investigating Officer (SIO).

[2] The preservation of life is recognised as the one FOA responsibility that takes precedence over scene preservation.

[3] It is routine for a major crime to feature more than one crime scene. A murder might entail the examination of a body deposition site, a separate kill site, a victim, numerous suspects and their associated addresses and vehicles. Whilst only the more complex of these scenes might require a CSM, best practice dictates that separate staff should be used for separate but linked scenes wherever possible.

[4] The role of CSC might be filled by any suitably trained individual within the Scientific Support Department, from Senior CSI to Head of Scenes of Crime, depending on the size of the police force, the complexity of the forensic investigation and the wider public impact of the offence.

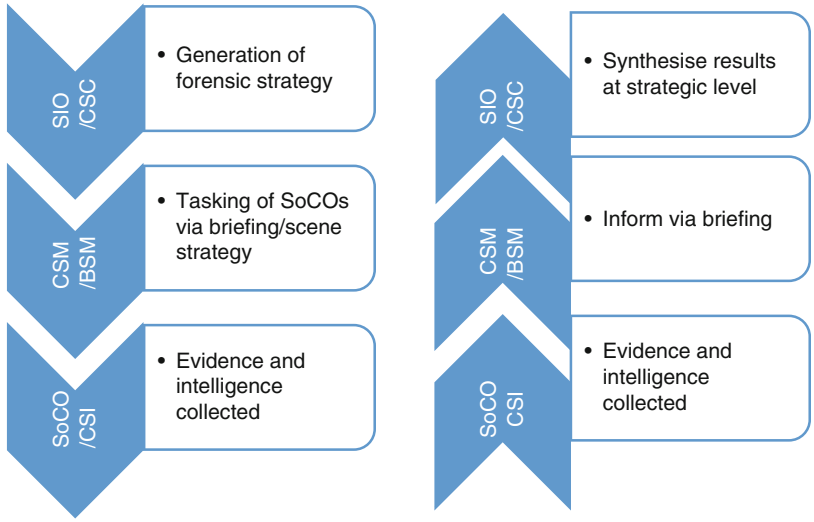

Fig. 7.1 Flows of information and tasking at a major crime scene

Because of the close relationship between the SIO and CSC, there is an expectation that crime scene coordination should be managed from the Incident Room. As such there is generally no requirement for CSCs to deploy to crime scenes, as this would compromise their pivotal management role.

Whilst the methods of scene examination can be adapted depending on the requirements of the investigation, the general commanding concept is that of unrepeatability; a crime scene can be revisited, but it can be examined in its entirety only once, hence there is a duty on the CSM or CSI to ensure the capture of optimum forensic evidence from the scene. The notion of 'optimum' rather than 'maximum' is crucial; any one scene examined in its entirety to the smallest degree might contain hundreds of items suitable for some form of recovery or analysis, which in turn might generate thousands, if not tens of thousands of fragments of forensic data (trace evidence, fingerprints, partial DNA profiles for instance). Consequently whilst it is important that a forensic examination maintains a degree of independence from the investigation, it must remain driven by an investigative strategy if it is to retain any form a focus that can bring meaning to the results of forensic examination. The gathering of data at the scene informed by initial briefings should result in the passage of that data back up the chain of strategic command to the CSC, who is best placed to interpret meaning behind the findings of a number of different scenes.

The concept of unrepeatability of examination and the requirement to optimise evidence gathering puts great emphasis on the sequence of examination. Generally speaking, whatever techniques of examination are required at a scene, they are undertaken in a sequence that begins with the least invasive and ends with the most disturbing or potentially destructive.

All major scenes are likely to see some adaptations from the general approach that form part of the written forensic strategy; such adaptations might be required by limitations of access to a scene (i.e., a body lying in a doorway to an otherwise inaccessible room), or environmental variations (i.e., impending rain forcing the prioritisation of the examination of the exterior of a property. Blast scenes are more likely than other major scenes to see the need to adapt an otherwise standard approach; initial scene and safety assessments must include a consideration of potential threats such as the presence of secondary devices and CBRN materials, or the risks associated with extensive structural damage to buildings – all of which can cause considerable delay to the forensic examination commencing.

Whilst perimeters need to be established for all crime scenes, control of access through extensive double cordons is frequently required for post-blast scenes together with large numbers of scene guards, and these might be located within highly populated urban areas with people's residences located within the cordoned area. The inner cordon encompasses the explosion area and has a radius of approximately one and a half times the distance from the explosion seat or centre to the furthest identifiable piece of evidence; only the BSM and their team can enter the inner cordoned area until the examination and evidence retrieval is complete. The outer cordon marks a perimeter which ensures public safety whilst preventing those who are not associated with the investigation from observing the examinations too closely, overhearing conversations pertinent to it or disturbing the scene; it also provides a safe working area within which members of the police and other emergency services can operate [4].

The dispersal of debris over a wide area will lead to complexes of material preserving multiple instances of forensic opportunities that would require the imposing of a sequence. Explosives officers from the 11th Ordnance Disposal Regiment (EOD) are often present to assist the BSM by providing invaluable advice regarding the cordoning and scene safety.

Just as 'standard' major scenes require the identification of a range of key scenes,[5] post-blast examination has similar specific challenges. The identification of the focus of the blast is crucial for both the sampling of material that might retain chemical traces of the explosive used [5, 6], but also to facilitate a reconstruction of material that might relate directly to the placement of a device. In terms of reconstructing events around the blast, the Bomb Scene Manager must consider a strategy of examination that seeks to identify material traces that assist in building a picture of events that extends prior to the placement of a device, the complex of activity around the blast itself, and the events that follow a blast which might disturb, subvert or modify conclusions built up around the nature of the event. The construction of a detailed map of initial evidential finds, surrounding vehicles, buildings and locations of bodies in relation to the central blast area can aid in the development of such a strategy.

Activities and events that predate the blast event itself are likely to include relatively simple considerations, such as the position and fabrics of fixings within the blast scene and a reconstruction of associated building layouts. Such 'backdrops' are essential for tying in events with recovered CCTV and recorded witness statements. In this manner, forensic traces might be utilised in order to confirm the intelligence offered by such sources.

The events immediately surrounding the blast are likely to include the placement of vehicles and moveable items around the scene, and the movement of people directly affected. The patterning of fatalities and types of injuries associated with these individuals are likely to assist in understanding the placement, size and nature of the blast, in addition to the dispersal of any associated debris. Additionally, the search of debris directly associated with the centre of the blast may reveal components of the device (timers, switches and batteries) that both assist with understanding the nature of operation (and hence potentially providing intelligence regarding the technical capability of the maker of the device), as well as providing forensic opportunities related directly to the identification of the makers or placers of a device.

The activities that follow a blast are almost certain to include the action of first responders discussed above, and the associated evacuation of casualties or the movement of walking wounded. The disturbance of debris associated with their activities might result in the contamination of items later found to be of forensic importance.

One of the key challenges that faces the BSM is that nature of identifying exhibits that might prove to be of significance, forensic or otherwise, amongst a vast quantity of scattered and

[5] In a standard murder investigation, the range of scenes to be identified might include a body deposition site, an attack site, offenders' and victims' home addresses and vehicles used as transport.

disordered debris. The standard means by which this is dealt with is by the zoning of the scene, and the grouping of debris collected by zone, to enable the rapid clearance of material, while still being able to trace an item back to a generalised location. Whilst zoning depends on the scene geography and the extent of debris field, this long-standing technique can now be supplemented with three-dimensional scanning techniques that assist in the reconstruction of scenes and the more specific location of items within zones. Liaison with the Forensic Explosives Laboratory, and if deemed necessary then the attendance of the scientists themselves at the scene, can also benefit the decision making process regarding evidence location, retrieval or best practice.

The identification of potential evidence items requires a teamwork approach and is initiated with a walk through of the scene, during which time, as is the case for other crime scenes, evidence marking, photography and recording are constant tasks. Each evidence item is collected into an appropriate sterile container (e.g., metal cans, glass containers, or paper, nylon or Tyvek bags) upon which details including a description of the item, its location, the date, time and name of the individual collecting it are recorded in order to originate the chain of custody. During post-blast investigation, upon 'clearing' a zone, all debris and loose material is then swept and either sieved at the scene or placed into bags or containers for further examination in the laboratory; the purpose of collecting such material being to single out component pieces of the device; a combination of coarse and fine mesh sieving can reveal very small components such as metal fragments of a device, detonator caps or wires [7].

The meticulous examination of the bomb centre or seat area is usually one of the most painstaking tasks, requiring swabbing of the area for trace explosive residues, measurement of crater dimensions, the removal of loose debris (which is treated as a single evidence exhibit), and further excavation of the crater with the use of digging tools in order to locate any embedded components of the device.

In addition to searches of the ground and the crater region, if one is obviously present, the examination of any secondary craters in the vicinity (formed by the penetration of a nearby structure, such as a wall or ceiling, by blast forces or fragments of the explosive device) can also be forensically lucrative. Furthermore, items in the vicinity of the central explosion area which are positioned perpendicular to the ground – such as signposts, the walls of buildings or nearby car doors if outside; or furniture or walls if indoors – may harbour pertinent forensic evidence (e.g., trace explosive residues) whether they exhibit signs of blast damage or not. Fragmented remains of a device and explosive residues can also become embedded within skin and tissue; intended and unintended victims of the incident are therefore also sources of evidence. The BSM must ensure that if casualties are involved, then investigating personnel are dispatched to hospitals to recover any evidence either with emergency room staff or pathologists.

There is an implicit challenge for the Bomb Scene Manager and investigating police in the recognition of important intelligence gathered from blast scenes. This recognition touches on the conflation that persists between concepts of forensic intelligence and evidence, and the tendency to regard only certain specific forensic evidence types as being suitable providers of intelligence (most specifically PACE DNA samples; [8]). By contrast, the experience of the security services and military over many years of gathering weapons intelligence from Improvised Explosive Devices (IEDs) is that devices and their placement locations represent rich loci of potential intelligence. Whereas some complex enquiries that might be led in some part by forensic intelligence in its broadest sense can be hamstrung by a syndrome of tunnel vision that directly equates the term 'intelligence' with biometric identification (an equation shared somewhat by military application of forensic exploitation), blast scene examination tends to benefit from a wider consideration of the value of associated intelligence.

Alongside the role of developing and delivering strategies to conduct a full methodological

forensic examination, it is the responsibility of the BSM to ensure the welfare and safety of the forensic team. All must be suitably equipped with the appropriate materials to do their job effectively, be supplied with sufficient food, drink and breaks during lengthy investigations and the required personal protective equipment, which during a post-blast investigation can include hard-hats to protect from falling debris (particularly glass when challenged with scenes in a built up city) and face masks to protect from noxious gases and dust which may be present in confined areas. It is also up to the BSM to consider the use of devices such as tents or screens which can be used to guard the examinations from prevailing weather conditions or to provide some privacy to the investigators, as well as to determine if and when it may be necessary to halt the investigations due to poor lighting for example (the use of flood lights can cause evidence to remain 'hidden in shadows' and it may not best to work through nights – this is often a judgement call which is made by the BSM).

One role of particular importance for the BSM is to maintain consultation and liaison with relevant parties throughout the investigation. If there are disruptions to the investigation, zone clearance can take many days, and throughout this time it is the duty of the BSM to regularly update the SIO as well as facilitate contact with the media in order to ensure the community and other interested agencies remain suitably informed about progress. The estimated length scale of the investigation and extent of damage needs to be communicated to the appropriate officers in order to keep the local community appropriately informed as well as to consider potential modes of further disruption – for example to that of public transport (such as the closure of nearby train stations), in which case the BSM would need to liaise directly with the British Transport Police. It is after all the one of the main objectives of the BSM – to facilitate recovery of evidence and return the scene to the public domain as soon as possible. Further to co-investigative personnel, the media must also be consulted and updated; the BSM has to manage the media, and work together with them in order to deliver public appeals and allow them to access vantage points from which they can record or photograph the scene.

As with any major crime scene, no bomb scene is the same as another, each varying substantially in size and impact. The roles, responsibilities and considerations outlined above are relevant to all scenes but investigative tactics in particular will vary depending on the unique set of challenges each post–blast scene presents to the personnel who attends, be they FAOs, BSMs, SIOs, emergency services or the forensic investigators. Moreover, that summarised above is predominantly applicable to civilian scenarios which are only time-gated by the pressure of closure of urban areas; for example, post-blast investigation in military contexts varies not only in the limited time allowed for the investigations but the potential lack of resources available as well as the demanding environment which needs to be worked in. In such circumstances, it is the vital basics of safety first and 'get what you can' which may have to make do.

Specialist systems of operation, and skillsets of specialist personnel, assist in distinguishing bomb and blast scenes from other major incidents. Despite this, the fundamental reliance on the core skills of scene examination are clearly present throughout the investigation process and the mindset of those involved. Combining incident and clinical data is crucial to forensic biomechanics in order to understand the pathophysiology of injuries.

References

1. Tilley N, Ford A. Forensic science and crime investigation. London: Home Officer Police Research Group; 1996.
2. NPIA. Forensic training [online]; 2011. www.npia.police.uk/en/5235.htm. Accessed 15 May 2011.
3. Skills for Justice. 2011 [online]. www.skillsforjustice.com. Accessed 15 May 2011.
4. Technical Working Group for Bombing Scene Investigation. A guide for explosion and bombing scene investigation: research report. US Department of Justice; 2000.
5. Abdul-Karim N, Morgan R, Binions R, Temple T, Harrison K. The spatial distribution of post-blast

RDX residue: Forensic implications. J Forensic Sci. 2013;58(2):365–71.
6. Abdul-Karim N, Blackman CS, Gill PP, Wingstedt EM, Reif BAP. Post-blast explosive residue – a review of formation and dispersion theories and experimental research. RSC Adv. 2014;4(97):54354–71.
7. Thurman JT. Practical bomb scene investigation. Boca Raton: CRC Press, Taylor and Francis Group; 2006.
8. Ribaux O, Gorid A, Walsh SJ, Margot P, Mizrahi S, Clivaz V. Forensic intelligence and crime analysis. Law Prob Risk. 2003;2(1):47.

Clinical Forensic Investigation of the 2005 London Suicide Bombings

8

Hasu D.L. Patel and Steven Dryden

8.1 Introduction

In the civilian environment in the United Kingdom the forensic investigation of a suicide bombing is carried out by a dedicated counter terrorism team with a view to determining identity of victims and participants, clarifying the cause of death and collecting evidence to support the coroner's enquiry and any potential criminal prosecutions.

It is carried out with the aim of collecting and preserving all relevant data on the explosive device and securing and recording the recovery of exhibits which will assist with the identification process and broader investigation (see Chap. 7).

It is recognised that a more detailed forensic capture is required to accurately reconstruct the events in detail and to elicit information to understand mechanisms of injury seen following a blast event (see Chap. 2). For the latter to take place it requires a diverse group of experts to work in close collaboration to ensure accuracy and coherence of the police evidential capture and then subject it to extensive analysis and application to understand these dynamic and variable events.

Suicide bombings significantly challenge the emergency response and healthcare systems. The emergency service rescue and recovery teams working alongside medical teams play a key role in the immediate aftermath of an explosive blast and these teams require an understanding of the complexities of blast injuries, how they present and how they are managed from the scene to trauma centre and onwards.

On July 7th 2005 four suicide bombers detonated improvised high explosive devices in a coordinated attack on three underground trains and a double decker bus in Central London. The Metropolitan Police response to the 7/7 bombings was codenamed "Operation Theseus" and was by far the largest terrorism related investigation ever undertaken in the United Kingdom.

The victims were treated at various London hospitals; more than half were treated at the Royal London Hospital, a busy Major Trauma Centre in East London.

A total of 775 people at the four extended scenes reported injuries out of whom 24 were critically injured and there were 52 fatalities. It was the largest mass casualty on the UK mainland since the Second World War.

The Resilience Mortuary, a temporary, portable self-contained structure, was set up to receive

H.D.L. Patel, MBChB, PhD, FRCS(Ed), FRCS(Plast) (✉)
Department of Plastic and Reconstructive Surgery, Barts and the Royal London Hospital (Barts Health), Royal London Hospital, London, UK
e-mail: Hasu.patel@bartshealth.nhs.uk

S. Dryden, LLB
Department of Counter Terrorism Commend, Metropolitan Police Service, London, UK
e-mail: stevedryden@talk21.com

A.M.J. Bull et al. (eds.), *Blast Injury Science and Engineering: A Guide for Clinicians and Researchers*,
DOI 10.1007/978-3-319-21867-0_8

the bodies of the fatalities, body parts from the scenes and hospitals and personal possessions of those present. A team of pathologists and mortuary staff assisted by police forensic teams carried out postmortem examination and appropriate investigations.

The damage to the human body sustained from these types of bombings presents with unique patterns of injuries not seen in other forms of trauma. These characteristic injury patterns are well documented in the literature [1, 2], (see Chap. 6, Sect. 6.2.1) however each bombing incident is highly variable in terms of scene location, crowd density, explosive characteristics and the surrounding environment. As a result there is a variation in the morbidity and mortality observed with each incident.

In the aftermath of the London 7/7 suicide bombings the authors carried out a forensic investigation of the bombings at each of the scenes using a multiagency approach. The aim was to analyse the injury patterns and mechanisms with respect to the position and orientation of the victims on the carriages and the bus in relation to the bombers and the devices. The data captured was primarily injury to, and disruption of, the bodies of victims present but also included damage to the vehicles and the surrounding environment, fragments, residue and constituent parts of the bombing devices and forensic and hospital data. The detailed reconstruction of these dynamic events contribute to understanding the blast injuries and follows a similar approach to that espoused in Chap. 2.

Injuries caused by explosive devices depends on the types of explosives used, the addition of primary fragments, chemical, biological, radiological or nuclear (CRBN) agents, the position and orientation of the device, and the environment and proximity of the victims relative to the device and surrounding structures.

We present collated data from the four affected blast scenes which include position of the victims and bombers, mechanism and patterns of injury and the influence of crowd density and surrounding structures on morbidity and mortality.

The unique patterns of injuries sustained include penetrating injuries from human projectiles in the form of human bone fragments, traumatic limb amputations, tympanic membrane rupture and burn injuries. We describe techniques used to identify victims' positions prior to the explosion, describe severity of injury in terms of injury severity scores (ISS) and assess post-blast body and body part distribution. This approach may be useful in future emergency planning and resource allocation in any country subject to terrorist bombing attacks on civilian and military populations.

The collection of these datasets can also have future application in the validation of computerised human injury predictor tools [3] (see Chap. 9, Sect. iii-1.2.2).

8.2 Methodology

This study was carried out by a multi-agency team including scientists from the UK Defence Science and Technology Laboratory (Dstl), Porton Down. The information was gathered from a combination of police witness statements, hospital records and forensic data. The latter included scene and post-mortem photography, laser scanning and digital imaging which were all utilised to capture injuries sustained, post blast positioning, body part distribution and damage to the trains, tunnels and the bus.

Body parts found inside and outside the carriages and those recovered from survivors were subject to DNA and forensic analysis as part of the reconciliation process (the consolidation of data and final identification) and their positions were plotted onto maps of the involved carriages and the area within the tunnels where material had exited the car. This exercise allowed an understanding of the blast energy on particular individuals as all body parts with a 2D surface area greater than 4 cm^2 were identified back to source.

The injury severity score (ISS) was calculated for all survivors and victims. ISS is an anatomical scoring system that provides an overall score for patients with multiple injuries. Each injury is assigned an Abbreviated Injury Scale score (see Chap. 20) and is allocated to one of six anatomical body regions: head, neck and spine,

thorax, abdomen and upper and lower extremities. These injuries were further sub-divided according to the standard blast injury classification system and specific anatomical injuries further analysed. It became evident that the position, orientation and proximity of the survivors relative to the devices, the crowd density, the surrounding structures and positioning of other people determined the injuries and survivability. The tunnels in which the bombs were detonated also had a bearing on the complexity of the blast wave and hence the severity of the injuries.

The collated data was utilised in a Dstl study to validate the human injury predictor tool (HIP), a computer model which is utilised to predict type and severity of injuries in diverse blast scenarios [3]. This is described in detail in Chap. 9, Sect. iii.

The position, distance from the device and orientation of each of the victims on the carriages whether seated or standing was determined using detailed analysis of their injuries, information from police witness statements and forensic data.

The positional analysis of the bombers was carried out by a forensic anthropologist using radiographic and photographic survey of the disrupted body parts. This examination helped reconstruct their positions relative to the devices. The injuries sustained by the bombers were modelled in relation to their position at the point of detonation.

Plotting the individual positions required numerous models and alterations to accurately identify their locations and orientation. These models included computer generated imaging (CGI) and hydrocode modelling techniques of each scenario. Hydrocode modelling is a computational tool employed to recreate the blast wave based on the data from the post blast positional and body part analysis (see Chap. 17, Sect. 4.2). The position of the bombers and the environment at time of detonation determined the direction of the blast wave and also its complex characteristics.

8.2.1 Stages of Positional Analysis

The methodology for positional analysis was performed in several stages, using all the available information and plotted as accurately as possible onto scene maps [4].

8.2.1.1 Stage 1

Stage 1 was a positional analysis based on witness statements collated by the Metropolitan Police.

Every person in the bomb carriage or the bus, or who had sustained any injury or was in close proximity to the bomb carriage were subject to interview by the Metropolitan Police Anti Terrorist Branch enquiry team and gave a detailed account of their movements on the day, position at time of detonation, positions of others they could describe or identify and details of their evacuation. Any injuries and subsequent treatment were logged and, where required, medical notes were obtained to ensure accuracy of personal testimony.

It was found that these accounts could not be relied upon as people are not particularly spatially aware on public transport, they do not particularly know which carriage they enter or which seat or standing position they occupy and this is then coupled with the shock and trauma of being involved in an explosion. There were many instances of personal testimonies contradicting others as to positions of themselves and other people.

8.2.1.2 Stage 2

Stage 2 was an examination of injuries sustained in survivors treated and was based on clinical data.

The survivability and injury patterns in victims were largely dependent on their position in the involved carriage and the unique injury patterns sustained.

8.2.1.3 Stage 3

Stage 3 was positional analysis based on witness statement, ISS, digital images of victims with the injuries and damage to the structures.

A combination of environmental factors in the immediate vicinity of the blast, the victims' and bombers' positions and analysis of specific patterns of damage and injury from digital imagery were used to contextualise the positional data. This enabled the authors to study the physical

aspects of the blast wave, how this was affected by intervening objects and victims, the structural components of the carriage and the resultant structural distortions and damage, particularly regarding reflection and venting of blast wave through windows, doors and on the bus through the roof.

The victims' positions were also determined using digital images of the survivors and fatalities and how the blast energy interacted with them relative to other factors. These images were enlarged and positioned on a makeshift carriage. The nature of injuries was dependant on the proximity to the device, the position of the bomber and any shielding or energy reflection that took place.

8.2.1.4 Stage 4

Stage 4 was a positional analysis of the bombing device and its composition and a positional analysis of the bombers.

The positional analysis of the bombers was carried out following reconstruction of completely disrupted body parts by a forensic anthropologist using radiographic and photographic survey of the remains. The fragments identified were matched to the DNA profile of the bombers and reconciled with their main body parts.

This examination helped reconstruct the remains of the four bombers and identify the injuries they sustained. The main objective was to investigate the circumstances surrounding the detonation of the explosive device and position of the bombers relative to the devices.

The pre blast positions of the bombers were modelled in relation to the point of detonation which then helped to determine the blast wave characteristics in the computer models. The inference from the patterns of injury was that the bombs were floor based.

8.2.1.5 Stage 5

Stage 5 was an analysis of the final positions combining all the above parameters.

The victims were plotted into their final positions using the following:

(i) Injury Severity Score,
(ii) analysis of actual injuries sustained,
(iii) distance from the device,
(iv) position of the bombers,
(v) nature of the complex blast waves,
(vi) interaction with confined train environment,
(vii) damage to carriages,
(viii) damage to tunnels, and
(ix) body and body part mapping.

Forensic analysis of the residual parts of the explosive devices used suggest a similar construction and content at all four scenes and it is believed that they were all manufactured and assembled simultaneously.

The bombing device was reconstructed by the Metropolitan Police and was estimated to be 1–1.5 kg TNT equivalent. It was composed of black pepper and hydrogen peroxide and did not have any primary fragments, in the form of nails or bolts.

The devices were contained in rucksacks and consisted of 6.25 l standard plastic food containers which held the explosive mixture and detonator. This was activated by completing an electrical circuit to the detonator via wires through the lid to a 9 V battery snap connector which was accessed by opening the top of the rucksack. A light bulb with the glass breached, exposing the filament sat within the detonator. Bringing the snap connector terminals in contact with a 9 V battery's terminals was sufficient to complete the circuit. The explosive fuel was ground black pepper and hydrogen peroxide mix.

The detonator was a cardboard tube containing approximately 8–12 g of HMTD (Hexamethylenetriperoxidediamine, N $(CH_2\text{-O-O-}CH_2)3N$). This high order explosive is extremely volatile, sensitive to friction, light, metal and exposure to heat. The heat from the exposed filament of the light bulb in close proximity to the HMTD was sufficient to fire the detonator.

8.3 Results

The detonation of an explosive device results in the release of energy causing a sudden rise in pressure above atmospheric resulting, in the

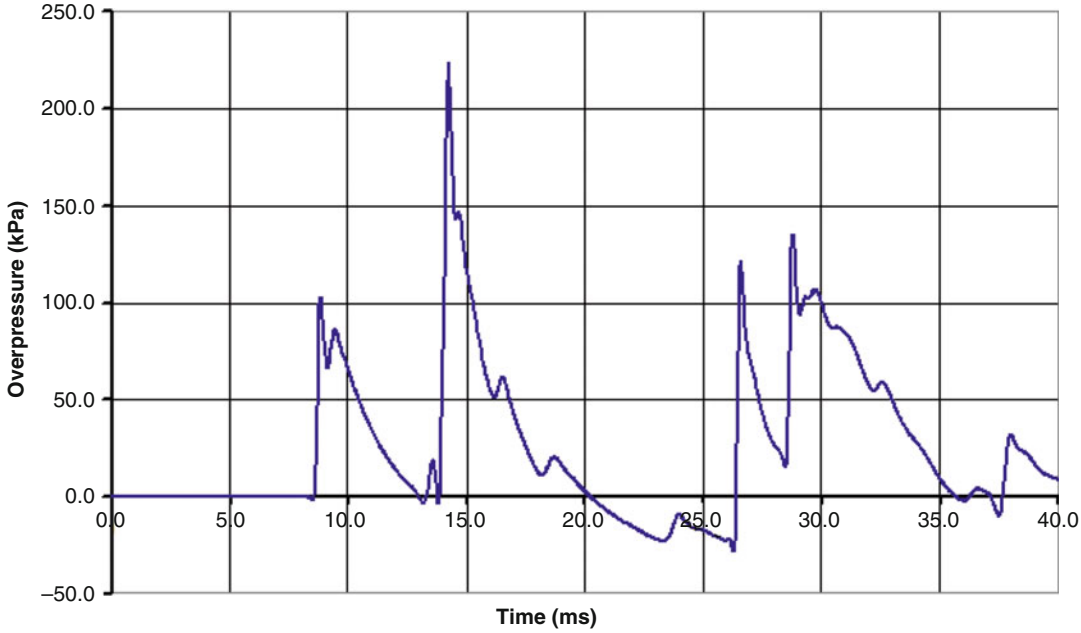

Fig. 8.1 The resultant (complex) waveform of a blast in an enclosed space due to reflection from solid structures

open field, in an idealised blast overpressure wave form [5]. In an enclosed space, this results in a complex blast wave form (see Chap. 1, Sect. 1.6) as a result of reflection from solid structures (Fig. 8.1).

This complex blast wave reflects throughout the enclosed space and results in damage to the carriages and the bus; its complexity and duration are very much dependent on the surrounding structures and the crowd density. On the carriage at Aldgate which was in a double tunnel, some of the blast energy dissipated through the roof of the carriage where it was blown outward. The damage to the carriage at King's Cross was different. The train was in a single tight tunnel which did not allow the blast wave to dissipate but was significantly confined and this was a major contributing factor in the different injury patterns that were encountered at this scene.

The crowd density was also a significant factor as crowds absorb blast waves. On the carriage at Aldgate and Edgware Road there were two people per square metre spread out sitting and standing throughout the carriages but at King's Cross there were five people per square metre most standing tightly packed around the bomber, which had implications on the figures for mortality and morbidity.

The positions and orientation of the victims on the involved carriages and on the bus and their relative distance in metres from the bombing device was determined. The Injury Severity Score (ISS) determined casualty triage status and was designated T1–T4:

T1 (ISS of 18-49),
T2 (ISS of 10-17),
T3 (ISS of 1-9), and
T4 (ISS of 50-74).

The types of injuries sustained by the survivors and fatalities were documented in terms of the anatomical regions involved.

8.3.1 Mortality in the Involved Carriages and the Bus at Each Scene

At Aldgate there were 43 people on the carriage and 8 fatalities, at Edgware Road 37 with

7 fatalities. At Kings Cross there were 82 people within the blast affected area with 27 fatalities and on the bus there were 75 present with 14 fatalities.

8.3.2 Results of Positional Analysis at All Scenes

Figure 8.2 shows a comprehensive positional analysis of all four bombing scenes. It depicts the uninjured (grey), injured (green) and severely injured (yellow) survivors and the deceased (red) and their ISS score.

8.3.3 Triage

The triage designations used were the universal indicators of combined injury severity score calculated for each victim at each scene. The majority of victims in the involved carriages were in the T3 (ISS 1-9) category and thus the walking wounded. There were 24 people triaged as T1

Fig. 8.2 (continued)

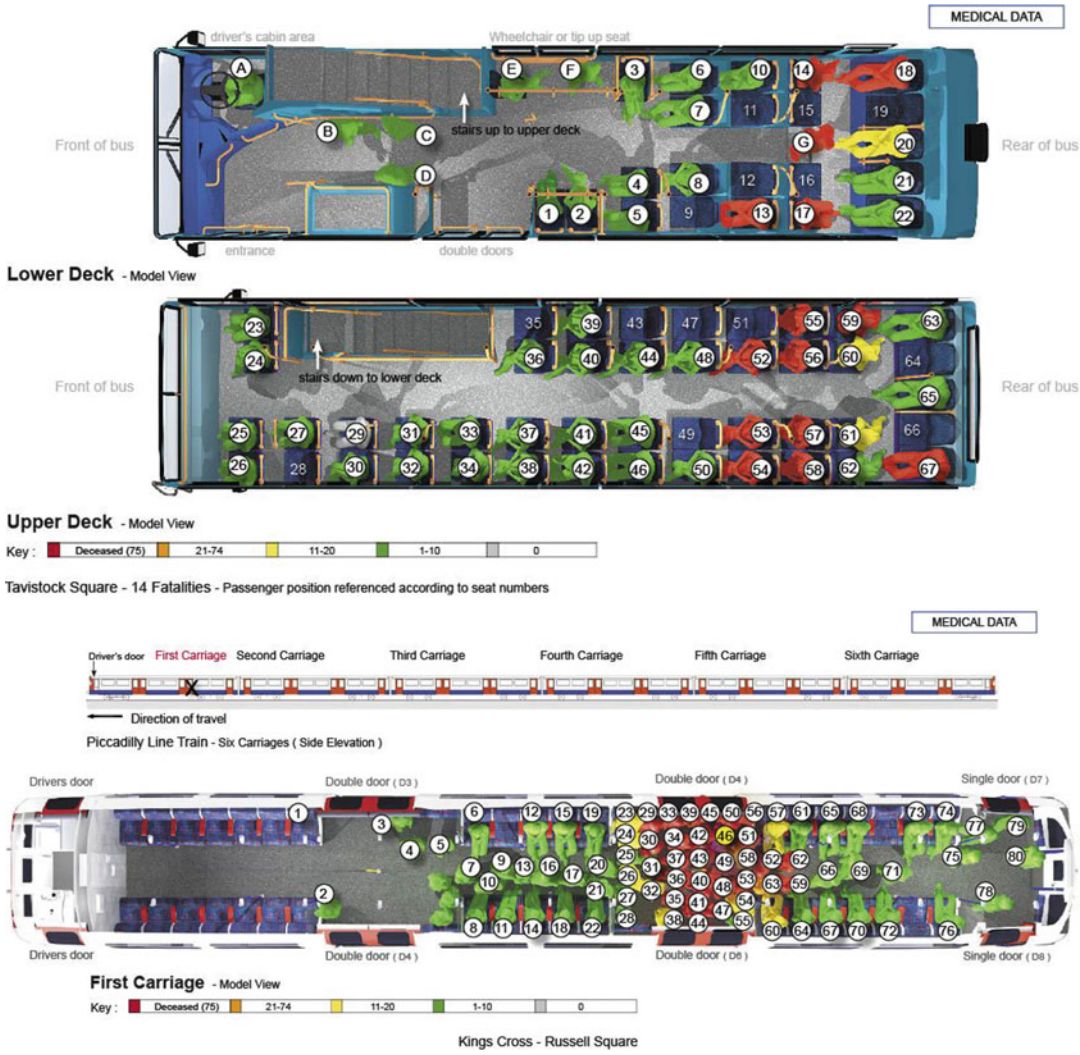

Fig. 8.2 Position of victims on the carriages and the bus

and T2 and of these 3 died in hospital. The critical mortality was 12.5 %. In total, 56 people including the four bombers died. The injury severity score for the three patients who died in hospital was 41, 25 and 50.

8.3.4 Patterns of Injuries Sustained

The injuries sustained by victims were analysed for those on the involved carriages and on the bus only. There were a total of 148 people who sustained injuries and of these; the majority (125 people) were the walking wounded (Table 8.1).

Figure 8.3 shows the most frequent types of anatomical body parts injured. There is significant overlap among the groups as many of the patients had more than one injury. The most frequent injury was tympanic membrane perforations, with traumatic amputations of the lower limb. Wound debridement was the most common operative procedure.

Table 8.1 Frequency of most common injuries

	Overall injured					
	Aldgate east	Edgware road	King's cross St	Carriages Total	Bus	Critically injured
Head injuries						
Fractured skull (brain exposed)						1
Fractured maxilla/mandible	1	1		**2**	**2**	1
Disrupted brain tissue	3			**3**		3
Intracranial bleeds	1			**1**		2
Descalping/Laceration	11	10	14	**35**	**14**	11
Tympanic membrane rupture	12	15	17	**44**	**21**	11
Deep thermal burns	2	6	2	**10**		1
Eviscerated eye		1		**1**		1
Foreign body-eye	3		2	**5**	**1**	3
Orbital injury	2		1	**3**	**1**	4
Bruising	1			**1**		
Neck & Spine						
Excessive mobility/fractured spine			2	**2**	**2**	3
Paravertebral haematoma	2			**2**		1
Deep thermal burns	1			**1**		
Foreign body-neck		2		**2**		
Laceration		1		**1**	**2**	
Thorax						
Excessive Bruising					**1**	1
Penetrating foreign body		2	1	**3**		
Lacerations	2	1	1	**4**	**1**	1
Haemothorax/pneumothorax	2	1	1	**4**		8
Lung contusions	3	3		**6**		5
Fractured/Disrupted ribs	1	1	2	**4**	**1**	5
Deep Thermal burns		1		**1**		
Inhalation injury	4	1	1	**6**		4
Abdomen						
Penetrating foreign body	1			**1**		
Laceration	1			**1**		
Thermal burns						1
Splenic Rupture		2		**2**		
Renal injury					**1**	
Upper extremities						
Fractured upper/forearm		1		**1**		3
Disruption at shoulder/ elbow/wrist					**1**	
Hand injury	6	2	6	**14**	**7**	7
Penetrating human foreign body			1	**1**		1
Penetrating metallic/ glass foreign body		3	1	**4**	**1**	
Traumatic amputation	1			**1**	**1**	1
Laceration	3	2	2	**7**	**7**	2
Degloving					**2**	
Deep thermal burn	3	6	4	**13**		2

(continued)

Table 8.1 (continued)

Lower extremities						
Fractured Tibia/Fibular/Femur		2	2	**4**	**1**	4
Foot injury	2	2	2	**6**	**1**	3
Disrupted/Fractured Pelvis			1	**1**		
Penetrating human foreign bodies	1	1		**2**		
Penetrating metallic foreign body	1	2	2	**5**	**3**	4
Traumatic amputation	3	3	4	**10**	**1**	10
Lacerations	7	4	6	**17**	**23**	5
Degloving	1	1		**2**	**2**	1
Deep thermal burns	4	1	3	**8**		5
External						
Peppering					**1**	
Bruising		1	2	**3**	**13**	
Total victims	40	30	41	**111**		**22**

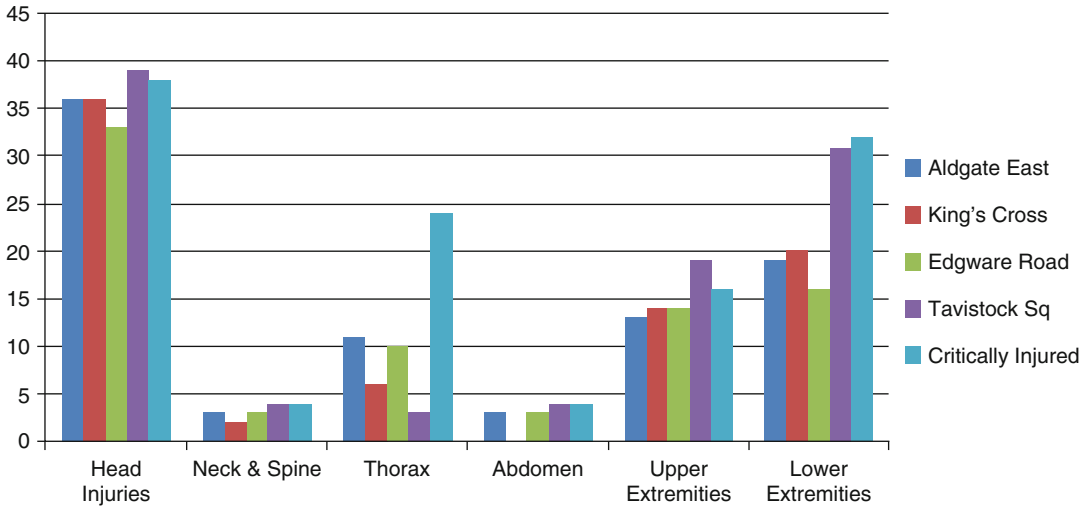

Fig. 8.3 Frequency of most common injuries at all sites

8.3.5 Results of Positional Analysis of the Bombers

At Aldgate and Edgware Road the bombers detonated their devices by hand whilst bending over the rucksacks. Their bodies were severely disrupted with body parts spread throughout the two scenes. At Kings Cross due to the dense crowds it was not possible to ascertain this position. It is likely the bomber squatted down keeping his torso vertical with his head slightly forward and above the open rucksack, with his knees either over the top or either side of the device. This position explains the injuries sustained; all four limbs were severely disrupted as was the front of the head but the torso was substantially intact. At Tavistock Square it is believed that the bomber had his device at his

feet or on his lap at time of detonation and this resulted in severe disruption to the bomber's body.

8.3.6 Aldgate

Results showed a 48 % prevalence of tympanic membrane rupture in survivors up to 8 m away from the blast. Fragmentation and burns were seen in those up to 6 m away, whilst abdominal injuries were seen in those up to 3 m away and traumatic amputations in those 1.9 m from the device. We are unable to comment on blast lung as documentation in the records was very poor and it was often described as inhalational injury.

8.3.7 Edgware Road

The types of injuries sustained at this blast site were similar to those seen at Aldgate. This was most likely due to similar surrounding characteristics and crowd density. Up to a 10 m radius, most survivors had tympanic membrane rupture and injuries from secondary fragments. Radiant burns occurred up to 8 m from the device and full thickness burns were seen in those who were within the fireball. Traumatic amputation and abdominal injuries occurred within a 2 m radius from the device.

8.3.8 King's Cross

At King's Cross, injuries occurred over a much shorter distance (5 m). This was due to increased crowd density at this scene, with those closest to the device absorbing most of the blast wave. Most fatalities occurred within a 1 m radius due to an engulfing fireball resulting in thermal burns at temperature up to 2000 °C as well as from other primary blast injuries. Traumatic amputation occurred within a 1.7 m radius as the blast wave from the floor based device swept through a sea of legs.

8.3.9 Tavistock Square

The types of injuries sustained were complicated by the dynamic collapse of the upper deck onto passengers on the lower deck. As a result there were two clear injury groups at that scene, those who sustained injuries as a direct result of the blast on the upper deck where the device was detonated and those on the lower deck who suffered predominantly crush injuries, previously defined as tertiary blast (see Chap. 6). Tympanic membrane rupture occurred up to 7.6 m from the device. Serious head injuries occurred up to a distance of 3 m, but these were mostly probably as a result of crush injuries on the lower deck, and on the upper deck as a direct result of being subjected to the blast energy.

8.3.10 Traumatic Limb Amputations in Survivors and Fatalities

Eleven survivors and 36 fatalities sustained lower limb amputations, and 14 fatalities sustained upper limb amputation and with only one person surviving an upper limb amputation.

8.3.11 Patterns of Burn Injury in Survivors and Fatalities

Twenty-one survivors sustained burn injuries; the victims were within 2–8 m from the device with injury severity scores of 1–35. The burns were less than 20 % total body surface area and were radiant burns, superficial to partial dermal and healed within days. The fatalities who sustained burns were those within the fireball and were between 20 and 80 % total body surface area (Fig. 8.4). The burns at Kings Cross scene occurred within a distance of 1 m and those at Aldgate and Edgware Road were within 3.6 m and 3.8 m respectively.

Fig. 8.4 Percentage of burn distribution in fatalities

Percentage Burns (%)	Aldgate	Edgware	Kings Cross	Tavistock Square
<20%	3	2	2	13
21–40%	2	1	2	0
41–60%	2	2	2	1
61–80%	0	0	2	0
>80%	0	2	18	1

8.4 Discussion

Terrorist bombings are a constant threat worldwide and the injuries they cause present with unique triage, diagnostic and management challenges. These incidents occur indiscriminately and many factors contribute to the types of injuries seen. The environment of the bombing scene is an important determining factor in the mortality and severity of injuries [6]. The enclosed surroundings of the London underground system and the semi enclosed London double decker bus and their structural components contributed to injury patterns. These environmental factors contributed further to the complexity of the blast wave resulting in unique injury patterns and hence specific mechanism for types of injuries seen and previously only studied experimentally [7]. Injury mechanisms and their classification are important in understanding survivability and in the future mitigation against them.

Mass casualty events, by definition, will overwhelm the emergency medical response system and the resultant accompanying chaos is not an optimum environment for non-pre-planned recording of accurate data. Data capture in any terrorist incident is key to accurate prospective analysis of injuries, triage and injury mechanism. The explosions in the tavern in the Town public house and in the Mulberry Bush public house in Birmingham 21/11/1974 were studied with respect to position of each person within the two bars at the time of explosion and hence to severity of the injuries sustained. The positional analysis of the victims together with the severity of the injuries sustained were crucial to understanding survivability [8].

The 7/7 forensic investigation enabled us to accurately piece together the events of the London bombings retrospectively. The positional analysis of victims and their ISS was the key to determining triage, injury patterns and mechanisms.

The biological response to a shock wave resulting from an improvised high explosive is dependent on peak over pressure and its duration. Bowen et al. [9] carried out studies on the predicted survival curves for a 70 kg man when the long axis of the body is perpendicular to the direction of propagation of the blast wave. Many factors influence morbidity and mortality suffered by victims. This includes the orientation and the position of the victim relative to a reflecting surface which will significantly affect susceptibility to the incident pressure wave.

The overpressure we calculated in the enclosed train carriages in the underground system following an explosive was a complex pressure wave due to the confinement of the blast wave and its multiple reflections off the ceiling,

other people, glazing, windows and doors. Its intensity is dependent on the volume of the underground space, the degree of venting through doors and windows (different in a single bore tunnel as compared to a double cut and cover tunnel). Additionally, the degradation of the overpressure is inversely related to the cube of the time from detonation and thus the distance from source - the proximity to the device - determines the traumatic amputations and body disruptions.

The majority of severe injuries such as traumatic amputations and severe burns occurred in the enclosed environment as opposed to the semi enclosed environment of the bus. In both the bus and the carriages the incidence of penetrating injuries was similar revealing that this was a feature of an explosive event which was determined by proximity rather than environmental design.

The crowd density on the train carriages also had a significant implication on the types of injuries sustained. The crowd density on the carriage at Aldgate and Edgware Road was similar (2 people/sq. metre) and injuries occurred at a greater distance as the blast was able to dissipate further. The crowd density on the carriage King's Cross was 5 people/sq. metre and the bomber had placed himself in midst of them. These crowds absorbed the blast and this resulted in increased mortality and greater numbers of traumatic amputation in the vicinity of the floor-based device. The crowd density and the position of the bomber explains why four times as many people died at this scene compared to Aldgate and Edgware Road.

The staged methodology for positional and injury analysis from these incidents may contribute to the development of a standard technique where the captured data may convey information about the nature and severity of injuries with the hope that treatment and outcome can be improved and maximised. The information sharing with the various institutes made a significant contribution to this process. The additional use of computer modelling techniques validated the positional methodology. The triage data and allocation of injury severity scores was a retrospective analysis exercise for the 7/7 events but a dynamic triage and injury severity exercise, utilising the lessons from this study, needs to be applied at the time to any such future events so as not to overwhelm major trauma centres with the walking wounded. Victims in the T1 & T2 category require careful allocation to major trauma centres unburdened by those less injured who can be dispersed to other local facilities.

The main findings of this study in relation to patterns of injuries include tympanic membrane rupture, traumatic limb amputations and human projectile injuries in the survivors. Limb amputations and burn injuries were studied both in the survivors and the fatalities. The patterns of injuries have implications in relation to their management in mass casualty events.

Tympanic membrane rupture (TMR) traditionally has been thought to be biomarker of other blast injuries such as underlying pulmonary or gastrointestinal primary blast injuries. Recent research has shown that the prevalence of TMR far outweighs the prevalence of other primary blast injuries [10, 11]. The suggestion has been that patients with isolated TMR can be briefly monitored and safely discharged. Our study of the survivors in the train carriages showed a high prevalence of TMR evenly spread among survivors across a range of distances from the blast. This is contrasted to the cluster of survivors with other primary blast injuries near the detonation. The nature of blasts in an enclosed environment would have contributed to this distribution with multiple reflections of blast pressure wave. TMR is a useful biomarker of potential primary blast injuries in the open field as it helps to identify patients with these underlying injuries requiring immediate management. In the enclosed environment of a tube carriage it is likely that some patients presenting with TMR will have no other injuries as a result of the blast. Concealed primary blast injury is extremely rare. The traditional categorisation of blast injuries is by their pathophysiology, but this does not help to determine the potential severity of the injury, the triage or the management strategy. All

survivors of blast injury require thorough assessment and monitoring to determine specific injuries [12].

Suicide bomb blasts cause high velocity human fragmentation projectiles as well as a spray of blood products creating a risk of blood borne pathogens such as HIV, Hepatitis B and C. It is known that some suicide bombers deliberately infect themselves to increase the risk of injuries [13]. We identified 11 cases of victims exposed to penetrating injuries from foreign human bony projectiles, and we now have a protocol for the management of these injuries [14].

Traumatic lower limb amputations as a result of explosive blast has previously been synonymous with fatal injuries. The literature suggests that in an open field only 1–2 % of those injured would survive, however, our findings from the enclosed environment are that 24.5 % of those who suffered traumatic amputations survived. In the unique enclosed environment of the underground systems the channelling and reflections of blast overpressure can cause none-fatal amputations of the lower limbs. The pressures required to cause upper limb amputation are the same magnitude as those required to cause near fatal lung injuries. The majority of the victims with upper limb amputations died: there was only one survivor [15].

Radiant burns were prevalent in the survivors and occurred out with the fire ball and affected those areas not covered with clothing such as the face, hands, and lower legs. These burns healed within days. Fire ball burns resulting in full thickness burns occurred in fatalities and the most severe cases were seen at Kings Cross where the fatalities were closely packed around the bomber. These victims also had other primary blast injuries and the injuries were not survivable [16].

This study has also enabled the validation and development of the Human Injury Predictor model (Chap. 9, Sect. iii-1.2.1) to assist in the target hardening of the structural design of populated spaces susceptible to terrorist attack. This, in turn, has developed the strategic and tactical planning for any possible future events.

In conclusion, the study carried out in the aftermath of 7/7/05 London bombings has contributed towards understanding numerous individual facets of blast injury mechanics. The application of this new understanding can equip emergency service responders and medical teams to more accurately assess survivability of victims with multiple injuries and thus influence prioritisation of immediate treatment, evacuation and hospital care.

References

1. Kluger Y, Peleg K, Daniel-Aharonson L, et al. The special injury pattern in terrorist bombings. J Am Coll Surg. 2004;199(6):875–9.
2. Hirshberg A. Multiple casualty incidents: lessons from the front line. Ann Surg. 2004;239(3):322–4.
3. Pope DJ. The development of quick-running prediction tool for the assessment of human injury owing to terrorist attack within crowded metropolitan environments. Philos Trans R Soc Lond B Biol Sci. 2011;366:127–43.
4. Dryden S, Patel HDL. London 7/7 terrorist bombings: from bomb factory to Human Injury Predictor – a multi-agency approach to blast analysis. Explos Eng. 2013:15–20.
5. Horrocks CL. Blast injuries. Biophysics, pathophysiology and management principles. J R Army Med Corps. 2001;147:28–40.
6. Leibovici D, Gofrit O, Stein M, et al. Blast injuries open-air bombings – a comparative study of injuries in survivors of open-air versus confined space explosions. J Trauma. 1996;41:1030–5.
7. Hull JB, Bowyer GW, Johansen KH. Patterns of injury in those dying from traumatic amputation caused by bomb blast. Br J Surg. 1994;8:1132–5.
8. Cooper GJ, Maynard RL, Cross NL, et al. Causalities from terrorist bombings. J Trauma. 1983;23 (11):955–67.
9. Bowen IG, Fletcher, ER, Richmond, DR. Estimate of man's tolerance to the direct effects of air blast. Technical Progress Report, DASA-2113, Washington, DC. Defence Atomic Support Agency, Department of Defense, October 1968.
10. Leibovici D, Gofrit ON, Shapira SC. Eardrum perforation in explosive survivors: is it a marker of pulmonary blast injury? Ann Emerg Med. 1999;34:168–72.
11. Harrison CD, Bebarta VS, Grant GA. Tympanic membrane perforation after combat blast exposure in Iraq: a poor biomarker of primary blast injury. J Trauma. 2009;67:210–1.
12. Radford PD, Patel HDL, Hamilton N, et al. Tympanic Membrane rupture in the survivors of the 07/07/2005

London Bombings. Submitted for publication in Otolaryngology – Head and Neck Surgery.
13. Braverman I, Wrexler D, Oren M. A novel mode of infection with hepatitis B: penetrating bone fragment due to the explosion of a suicide bomber. Isr Med Assos J. 2002;4:528–9.
14. Patel HDL, Dryden S, Gupta A, Ang SC. Pattern and Mechanism of traumatic limb amputations after explosive blasts: experience from the 07/07/05 bombings. J Trauma Acute Care Surg. 2012;73 (3):784.
15. Patel HDL, Dryden S, Gupta AK, et al. Human body projectiles implantation in victims of suicide bombings and implications for health and emergency care providers – 07/07 experience. Ann R Coll Surg Engl. 2012 Jul; 94(5):313–317.
16. Patel HDL, Chukwu-Lobelu R. Burn injury in mass casualty and their classification. In Prepation 2016.

Modelling the Blast Environment and Relating this to Clinical Injury: Experience from the 7/7 Inquest

9

Alan E. Hepper, Dan J. Pope, M. Bishop, Emrys Kirkman, A. Sedman, Robert J. Russell, Peter F. Mahoney, and Jon Clasper

9.1 Introduction

On 2nd August 2010, the United Kingdom Surgeon General was instructed by Her Majesty's Assistant Deputy Coroner for Inner West London (Rt Hon Lady Justice Hallett DBE) to provide Expert Witness Reports relating to the terrorist events of 7 July 2005 on the London Public Transport Network (see Chap. 8, Sect. ii). These Reports were required to review the evidence that had been gathered during the investigations into the events surrounding the bombings. Her Majesty's Coroner asked a series of specific questions relating to the survivability and preventability (with respect to the medical interventions and care) of the deaths of many of the victims, and these had to be answered on an individual basis with a review of all of the relevant information. It was appreciated that the most appropriate and current experience of dealing with personnel injured in this type of event came from the UK Ministry of Defence Surgeon General's Department who are experienced in dealing with combat-related injuries; particularly in the context of the current operations. This was also assisted by the fact that the UK Military Medical community already had a proven technique for the regular review of operational mortality and medical response [1, 2].

There had also been concerns about the nature of the events, criticism about the initial response, and one review in particular was highly critical of the communication systems of the emergency services which led to delays in understanding what was happening during the first few hours of the events of 7 July 2005 [3]. Survivors had also raised concern at the response of the emergency services [4].

A.E. Hepper (✉) • D.J. Pope, BEng (Hons), PhD, CEng, FICE • M. Bishop • E. Kirkman, PhD • A. Sedman
Dstl Porton Down, Salisbury SP4 0JQ, UK
e-mail: AEHEPPER@mail.dstl.gov.uk; djpope@dstl.gov.uk; ekirkman@dstl.gov.uk

R.J. Russell, FRCEM, DipIMC, RCEd
Academic Department of Military Emergency Medicine, Royal Center for Defence Medicine, ICT Centre, Birmingham Research Park, Birmingham, UK
e-mail: robrussell@doctors.org.uk

P.F. Mahoney, CBE, MBA, FRCA, FIMC, L/RAMC
Department of Military Anaesthesia and Critical Care, Royal Centre for Defence Medicine, Birmingham, UK

Department of Bioengineering, Royal British Legion Centre for Blast Injury Studies, Imperial College London, London SW7 2AZ, UK
e-mail: Peterfmahoney@aol.com

J. Clasper, CBE, DPhil, DM, FRCSEd (Orth)
Academic Department of Military Trauma and Surgery, Royal Centre for Defence Medicine, Birmingham, UK

Department of Bioengineering, Royal British Legion Centre for Blast Injury Studies, Imperial College London, London SW7 2AZ, UK
e-mail: jonclasper@aol.co.uk

A.M.J. Bull et al. (eds.), *Blast Injury Science and Engineering: A Guide for Clinicians and Researchers*,
DOI 10.1007/978-3-319-21867-0_9

9.2 Approach

In order to answer all of the questions posed by Her Majesty's Coroner, a multi-disciplinary team was essential. This would take expertise from the Royal Centre for Defence Medicine (RCDM) and Defence Science and Technology Laboratory (Dstl).

Her Majesty's Coroner was particularly concerned with the victims who were not killed immediately by the explosions, but died prior to reaching hospital. Of interest was what happened to them: what attention and/or treatment they received, whether there were any failings in the way that they were treated, the circumstances of their eventual death, and whether any failings in the emergency response contributed to or were causative of their death.

The decision was made at an early stage that a single report covering all personnel would be inappropriate and unique reports for each of the people in question would be written. There were two reasons for this:

- The victims were all individuals and should be regarded on an individual basis.
- The reports may be released to the families of the deceased and the reports would need to be redacted to ensure what was released was only relevant to their relative. There was a risk that such redaction would leave the feeling that some vital information had been removed, and this would simply amplify any conspiracy theory or any feeling that the Government (or in particular, the Ministry of Defence or Ministry of Justice) wanted to hide something of relevance.

This increased the workload substantially, resulting in multiple unique reports.

9.2.1 Work Strands

The broad ranging and complex nature of these questions required a substantial investment of time to address these questions. A three phase approach was adopted as the only practical way to answer the questions within the challenging timescale (3 months start to delivery). These three phases were conducted in series; however, any hypotheses, assumptions or conclusions from either of the analysis phases were not allowed to affect or influence the other, in order to keep all options open.

The first phase required an engineering expert in blast effects on structures and injury modelling to review photographs of the damaged carriages and bus to give a view on the likely physical effects on people close to the explosions. This was coupled with a review of the forensic evidence relating to the explosions. This provided one strand of opinion on the nature of the injuries (the blast effects and injury mechanism) that was used in the final comparison.

The second phase was a clinical review of the evidence by military clinicians to assess blast injury in the casualties. This used techniques developed both in the deployed environment and at regular morbidity and mortality reviews over a number of years [1, 2] to review mechanisms of blast injury and likely cause of death. This method has shown significant benefit in demonstrating the survivability and preventability of the deaths of personnel and to provide a robust evidence base to guide the changes in medical care and response to the critically injured patient. This was coupled with a review of the nature of injuries from other terrorist incidents to provide a baseline comparison of injury mechanisms, as well as a review in the progression of pre-hospital care to advise the Court of changes in treatment strategies that may assist in survival rates.

In the third phase, the blast environment was modelled by the structural dynamics experts [5] to assess likely blast loading on victims. This loading information was then assessed by physiology experts with access to data from experimental studies that provided a correlation of precisely measured blast data with injury, focusing principally on blast lung [6] since this is one of the most difficult aspects to evaluate from post-mortem reports. Simple modelling was also undertaken in isolation of the complex structural dynamics modelling to provide simple

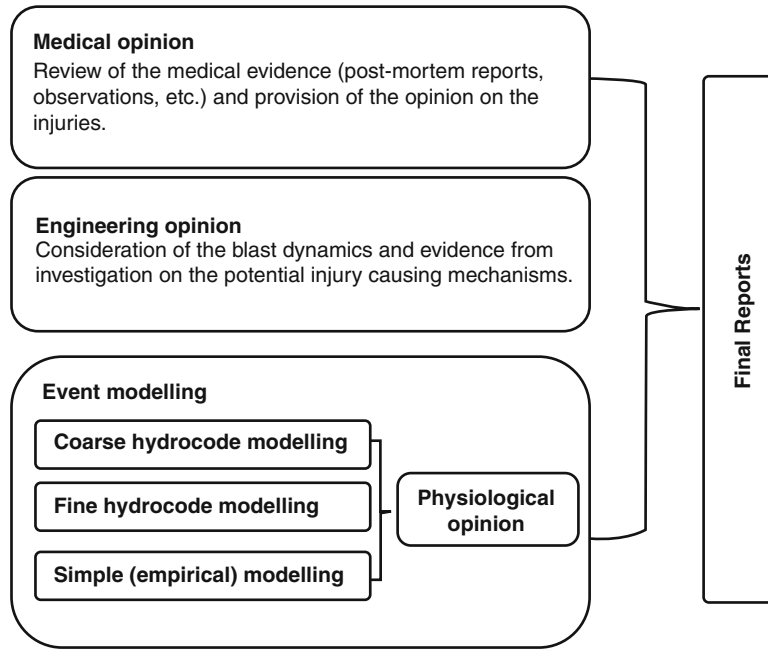

Fig. 9.1 Relationship of three phase work strands

predictions of the risk of blast lung and other injury mechanisms.

The relationship of these phases is shown in Fig. 9.1.

The outputs from these three phases were combined into a joint report and a single opinion on the nature of the injuries and the survivability of personnel as described in the transcripts from the Inquest [7–9]. Each report was formatted to provide a main section written by the principal author and summarising the work that was undertaken.

9.2.2 Model Design and Risk Reduction

Substantial risks were inherent in the mathematical models of the blast environment because of the model complexity and the degree of uncertainty (exact charge size, exact charge dynamics, exact charge location, location and orientation of victims, etc.). As a result, three different levels of model were run for each of the events in the trains:

- A coarse hydrocode model (see Chap. 17, Sect. 4.2) was used to:
  - Study the mechanisms of blast load development and provide broad levels of peak overpressure and specific impulse.
  - Establish 'zones of blast wave intensity'.
  - Determine the extent to which the fireball extended within the carriage during the event.
- A fine hydrocode model to quantify the probable pressure time history loading sustained by occupants within each carriage. This model also produced images and videos of the effects of the blast that showed the blast propagation (see Fig. 9.2). These images were useful for the team, the Court and families to understand the nature of the blast environment.
- A simple (uniform blast wave model) to give an empirical relationship of blast pressure from idealised explosives and compare the results to simple estimates of lethality from blast lung.

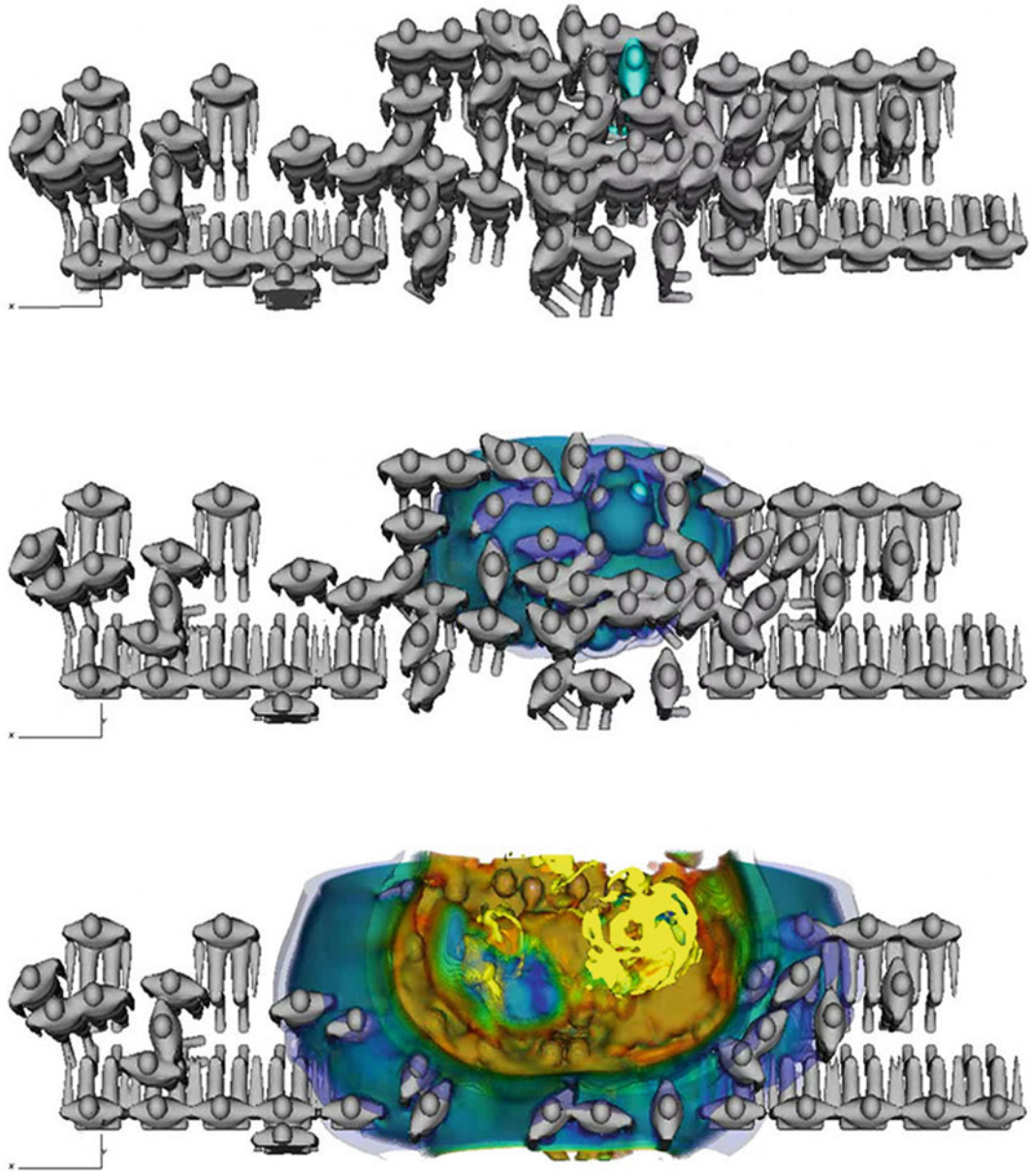

Fig. 9.2 Sample blast propagation from fine hydrocode model

9.2.3 Resources

The team had access to a combination of scene photographs, post mortem photographs, external post mortem reports and witness statements (see Chap. 8, Sect. ii) to form an opinion of the internal and external injuries received by the victims and for how long they showed signs of life after the bombing (if at all).

The team looked particularly at witness statements to understand if the victims were noted to be breathing and have a pulse after the bombing, whether or not they were conscious and the likely time course over which they died from their injuries.

Information provided by the court to support this activity was stored on encrypted memory drives, secured at Dstl Porton Down and at

RCDM Birmingham, where they could be examined in a secure environment.

The scene reports included seating plans for the underground carriages and the bus indicating positions of individuals pre- and post-explosion (where this information was known) and during recovery of the deceased.

As some deceased and live casualties had to be moved at some of the bombing locations after the attacks to allow access to other casualties, the position of a victim post-explosion does not always indicate where that person was prior to the explosion or if that position was the location where they died. This meant that the team needed to use a number of methods to try and work out how close a victim was to the seat of the explosion and from this offer a view on likely internal injuries, as well as providing a review of relevant related information to inform a final opinion on the probable nature of injuries.

9.2.4 Challenges: Quality of Information

Usually when conducting such a review the clinicians and scientists looking at the information would have a complete list of the victim's injuries derived from a combination of a full post-mortem examination plus X-ray imaging. This in turn would be used to calculate mathematical trauma and injury scores which help in assessing whether or not a particular combination of injuries would or would not be expected to be survivable. On this occasion the information from internal post-mortem examination was not available and the X-ray imaging information was limited to fluoroscopy. The fluoroscopic examination was used to identify some fractures and foreign materials present in the victims' bodies.

The team, therefore, relied upon a number of sources of information and scientific methods to come to a considered opinion for each of the victims; however, in an ideal world, more structured observations, measurements and opinions would have been available for the team to consider.

The amount of information missing from a simple external post-mortem was a significant challenge in this work. If anything can be stressed from this work, the importance of a detailed post-mortem examination must be one element.

9.3 Conclusion

We believe that this detailed understanding of the nature of injury from blast and fragmentation threats, and the modelling and understanding of the physical interaction of combat related threats can only come from a multi-disciplinary grouping such as the group formed to address the events of 7 July 2005 and the applicability of this form of analysis should be considered in the event of other terrorist events.

Acknowledgements The original version of this material was first published by the Research and Technology Organisation, North Atlantic Treaty Organisation (RTO/NATO) in meeting proceedings RTO-MP-HFM-207 'A survey of blast injury across the full landscape of military science' held in Halifax, Canada, 3–5 October 2011.
A shortened version was published, with permission, in the Journal of the Royal Army Medical Corps as Hepper AE et al., J R Army Med Corps 2014;160: 171–174.
This chapter reproduces the J R Army Med Corps material, with permission

References

1. Russell RJ, Hodgetts TJ, McLeod J, Starkey K, Mahoney P, Harrison K, Bell E. The role of trauma scoring in developing trauma clinical governance in the Defence Medical Services. Philos Trans R Soc Lond B Biol Sci. 2011;366:171–91.
2. Hodgetts TJ, Davies S, Midwinter M, Russell R, Smith J, Clasper J, Tai N, Lewis E, Ollerton J, Massetti P, Moorhouse I, Hunt N, Hepper A. Operational mortality of UK service personnel in Iraq and Afghanistan: a one year analysis 2006–7. JRAMC. 2007;153(4):252–54.
3. London Assembly. Report of the 7 July Review Committee, June 2006. http://legacy.london.gov.uk/assembly/reports/7july/report.pdf. ISBN 1 85261 878 7.

4. Alexandra Topping. The Guardian. http://www.guardian.co.uk/uk/2011/may/06/london-bombings-victims-relatives-call-for-overhaul. Accessed 6 May 2011.
5. Pope DJ. The development of a quick-running prediction tool for the assessment of human injury owing to terrorist attack within crowded metropolitan environments. Philos Trans R Soc Lond B Biol Sci. 2011;366:127–43.
6. Kirkman E, Watts S, Cooper G. Blast injury research models. Philos Trans R Soc Lond B Biol Sci. 2011;366:144–59.
7. http://7julyinquests.independent.gov.uk/hearing_transcripts/31012011am.htm.
8. http://7julyinquests.independent.gov.uk/hearing_transcripts/31012011pm.htm.
9. http://7julyinquests.independent.gov.uk/hearing_transcripts/01022011am.htm.

The Mortality Review Panel: A Report on the Deaths on Operations of UK Service Personnel 2002–2013

10

Robert J. Russell, Nicholas C.A. Hunt, and Russell Delaney

10.1 Introduction

Healthcare Governance is a central function within the Defence Medical Services (DMS) [1–4]. Assuring optimal performance of the DMS operational trauma system is an important contribution to the moral effect for troops, families and the public. In the assessment of the performance of any trauma system, a review of adverse outcomes is essential [4, 5].

The UK Joint Theatre Trauma Registry (JTTR), maintained by the Academic Department of Military Emergency Medicine (ADMEM) at the Royal Centre for Defence (RCDM) and Defence Statistics (Health) is a prospective trauma database that collects information on all casualties admitted to UK deployed military hospitals as the result of a trauma call or who are evacuated back to the "Role 4" base hospital at Queen Elizabeth Hospital, Birmingham as a result of trauma. As a result, JTTR holds data on all UK military deaths as a result of operations and exercises abroad. Details are collected from clinical notes, post mortem reports and incident reports and a member of ADMEM attends all military post mortems to prevent the loss of potentially important medical intelligence [6, 7] and provide appropriate feedback to the theatre of operations as soon as possible via the Defence Professor. This clinical presence also ensures that the military and medical contexts can be clarified to the pathologists and other experts present to monitor personal and vehicle protective equipment effectiveness.

Box 10.1: Members of the Military Mortality Review Panel

Defence Professor, Anaesthetics and Critical Care
Defence Professor, Surgery
Defence Professor, Orthopaedics and Trauma
Home Office Pathologists
Senior Scientist, Dstl Porton Down
Senior Consultant Critical Care, Queen Elizabeth Hospital Birmingham
OC Nursing, RCDM, Queen Elizabeth Hospital Birmingham
Representative from Inspector General DMS

R.J. Russell, FRCEM, DipIMC, RCEd (✉)
Academic Department of Military Emergency Medicine, Royal Centre for Defence Medicine, ICT Centre, Birmingham Research Park, Birmingham, UK
e-mail: robrussell@doctors.org.uk

N.C.A. Hunt, BSc, MBBS, FRCPath, DipRCPath
Forensic Pathology Services, Grove Technology Park, Wantage OX12 9FA, UK
e-mail: nickhunt@forensicpathologyservices.co.uk

R. Delaney, MB, ChB, MRCS, FRCPath
South West Forensic Pathology Group Practice, Bristol, UK
e-mail: rjdelaney@me.com

A.M.J. Bull et al. (eds.), *Blast Injury Science and Engineering: A Guide for Clinicians and Researchers*,
DOI 10.1007/978-3-319-21867-0_10

In addition to the initial evaluation, the Military Mortality Peer Review Panel meets 2–3 times a year to provide senior multidisciplinary review of deaths in the intervening periods. The panel first met in late 2006 and reported in 2008 on 12 months from 01 Apr 2006 [8] and is currently convened and chaired by the Defence Professor Emergency Medicine. Members are shown in Box 10.1. This chapter describes the patterns of UK Service deaths and results from the panel meetings.

10.2 Methods

A search was conducted of JTTR for all UK military deaths held from Jan 2002 to Nov 2013 and the judgement made by the Mortality Peer Review panel. The panel reviews each case using a description of the mechanism of injury, evacuation timelines, injuries sustained and procedures undergone at each location. A summary including trauma scoring results is given for each case and the clinical notes, post-mortem reports and incident details are also available.

Salvage-ability is determined first in each case using the definitions in Box 10.2. If a case is rated as non-survivable (S4) then further analysis is not recorded. If there are lessons identified, these are fed along the relevant channels. In all other cases, discussion as to the factors affecting survival takes place. These factors are grouped into 3 categories—Tactical, Equipment and Clinical, and a brief description of each factor and its impact is recorded if appropriate. This latter process replaced a further rating, which was given as to preventability until 2010 as it allowed more detail to be recorded and similar cases grouped together if necessary.

Box 10.2: Definitions of Salvage-Ability

Salvage-ability: "If these injuries had occurred 5 mins from a Major Trauma Centre what is the likelihood that surgical intervention would be attempted for given injuries and the predicted influence on survival":

S1: *Salvage-able*: intervention would likely have influenced survival (probability of survival >95 %)

S2: Potentially salvage-able: intervention would have been attempted and may have influenced survival (probability of *survival* 5–95 %).

S3: Possibly salvage-able: intervention would have been attempted but with a high probability of mortality (probability of *death* >95 %).

S4: Non-salvage-able: intervention would not have led to survival.

For cases reported in this paper prior to the start of the review panel process in 2006, an initial sifting process of all deaths from 2002 was undertaken by the Defence Professor EM. Cases that were clearly S4 (e.g., decapitation, whole body disruption) were recorded on JTTR as such, and only those in which salvage was thought possible or where there was doubt as to the grading were brought to the panel.

10.3 Results

JTTR holds records of 621 cases dating from 2002. The Army accounted for 500 (80.5 %), Royal Marines 70 (11.3 %), Royal Air Force 43 (6.9 %), and Royal Navy 8 (1.3 %). 611 (98.4 %) were male Service personnel with 10 (1.6 %) female. The age range was 18–51 with a mean of 26.7 years. The definitions and distributions of casualty categories are shown in Fig. 10.1 and Box 10.3. The ratio of Killed:Died overall was 6.48:1, but if Hostile Action only is included the ratio is 6.28:1.

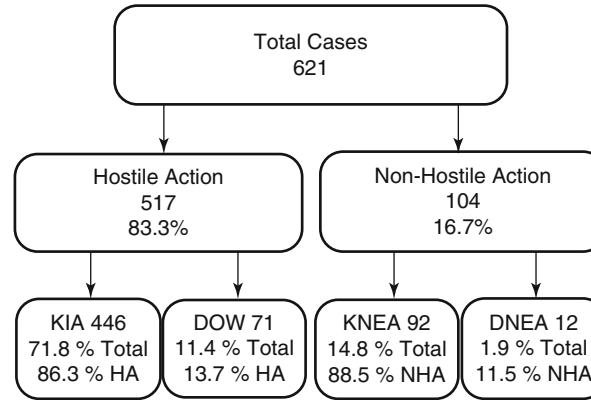

Fig. 10.1 Casualty category distributions

Table 10.1 Cases by year, theatre, operation and roulement

Operation/Roulement		Operation/Roulement	
TELIC 1	32	HERRICK 3	3
TELIC 2	15	HERRICK 4	34
TELIC 3	7	HERRICK 5	13
TELIC 4	11	HERRICK 6	29
TELIC 5	17	HERRICK 7	11
TELIC 6	10	HERRICK 8	27
TELIC 7	12	HERRICK 9	32
TELIC 8	12	HERRICK 10	70
TELIC 9	28	HERRICK 11	60
TELIC 10	24	HERRICK 12	60
TELIC 11	3	HERRICK 13	21
TELIC 12	0	HERRICK 14	19
TELIC 13	3	HERRICK 15	26
		HERRICK 16	23
Total	174	HERRICK 17	8
		HERRICK 18	3
Other	6	HERRICK 19 to Nov	2
		Total	441

Box 10.3: Casualty Category Definitions

KIA: personnel killed instantly or dying before reaching a UK or a coalition ally medical treatment facility as a result of hostile action.

DOW: personnel who die as a result of injuries inflicted by hostile action after reaching a UK or coalition ally medical treatment facility.

KNEA: personnel killed instantly or before reaching a UK or a coalition ally medical treatment facility as a result of non-hostile activity.

DNEA: personnel who die as a result of injuries caused by non-hostile activity after reaching a UK or coalition ally medical treatment facility.

Cases are shown by year, theatre of operation in Table 10.1 and by Operation and roulement in Table 10.2. The mechanisms of injury for the 620 cases for which it been determined at the

Table 10.2 Injury distribution by body region and AIS

Body region	No. region highest score	No with injury in region	Max no. injuries recorded (range)	Av. no. injuries	No. with max. AIS 6 (fatal)	No. with max AIS 5 (critical)	No. with max AIS 4 (severe)	No. with max AIS 3 (serious)	No. With max AIS 2 (moderate)	No. with max AIS 1 (minor)
Head	249	321	18	3.32	220	44	19	0	2	4
Face	2	208	8	1.94	0	18	14	10	86	80
Neck	43	155	7	2.03	22	58	18	3	37	6
Spine	18	179	11	1.98	47	21	13	14	85	0
Thorax	99	273	19	3.78	108	58	91	62	22	7
Abdomen	39	342	15	3.97	14	76	86	45	47	11
Upper extremity	3	242	12	2.13	0	3	54	63	101	21
Pelvis and legs	53	348	12	3.55	0	139	56	51	14	12
External	27	75	5	1.22	37	1	1	3	3	30

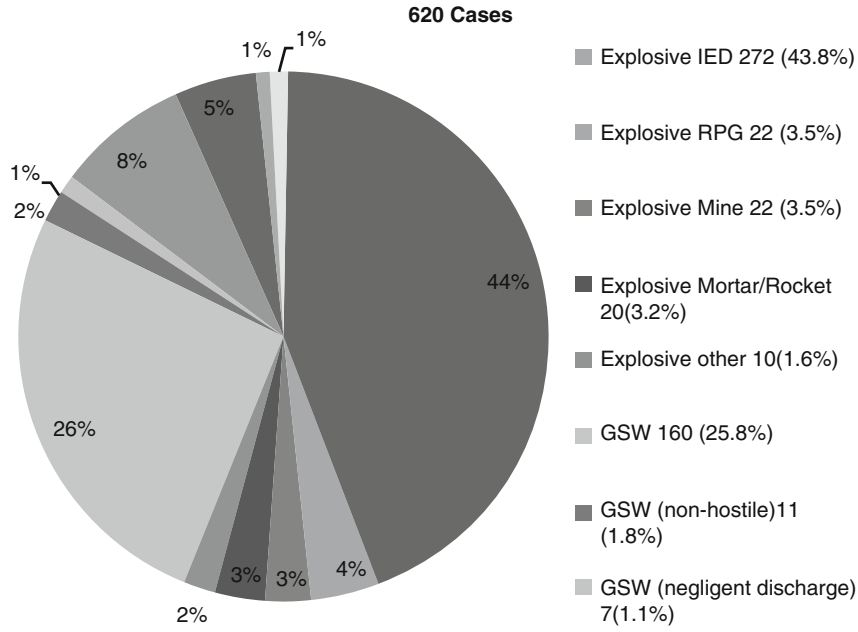

Fig. 10.2 Mechanism of injury

time of writing are demonstrated in Fig. 10.2. Explosive mechanisms produced 345 (55.65 %) and penetrating 178 (28.71 %).

10.3.1 Injury Scoring

The lowest Injury Severity Score (ISS) [9] was 4, the highest the maximum, 75. The median was also 75 with an inter-quartile range of 57–75. Twenty-one did not have a recorded score. Three cases were below an ISS of 15, 164 were in the range 16–59 and 454 had a score of 60–75, which has been defined as "un-survivable trauma". The New Injury Severity Score (NISS) [10] showed similar results but the inter-quartile range was 75–75.

The Triage Revised Injury Severity Score (TRISS) [11] and A Severity Characterisation of Trauma (ASCOT) [12] values could be calculated for 559. Missing physiological data accounted for the other 62 cases not having recorded values. For TRISS, 8 had a Ps >50 %; this being the cut off between "expected" and "unexpected deaths". ASCOT uses a calculated <50 % percentage chance of death (Pd) as a similar cut off and there were 16 in this category.

The total number of injuries recorded ranged from 1 to 57 with an average of 10.56 per casualty. The Abbreviated Injury Scale (AIS) [13] body regions injured per casualty ranged between 1 and 9 (all) with the mean number of regions injured being 3.34 and the median 3 (inter-quartile range 2–5). The distribution is shown in Fig. 10.3. Further data on the distribution of injuries to body regions is shown in Table 10.2.

10.3.2 Salvage-Ability

Six hundred seventeen cases have a recorded Salvage-ability judgement by the Peer Review Panel. Two cases were outstanding and 2 cases do not have enough information on injuries and medical treatment to form a considered opinion. Both these cases occurred outside the usual UK DMS medical chain. Table 10.3 shows the judgements by year.

One of the 3 "definitely salvage-able" casualties died as tactical issues prevented

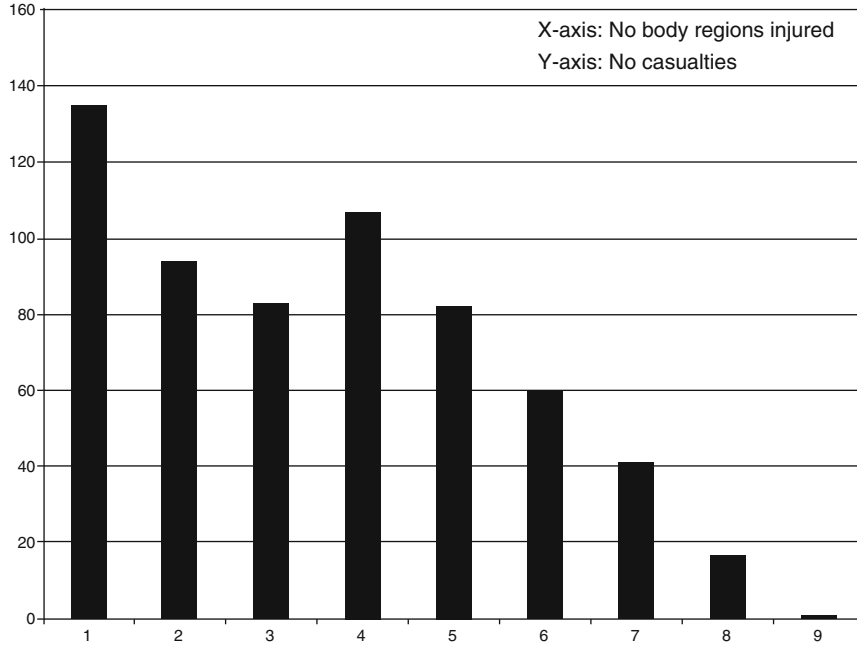

Fig. 10.3 Distribution of number of AIS body regions injured

Table 10.3 Results of mortality peer review panel

Year of fatality	S1 definite	S2 potential (>5 %, <95 %)	S3 possible (<5 %)	S4 (not salvage-able)	Outstanding/not rated	Total
2002	–	–	–	3	–	3
2003	1	–	–	47	–	48
2004	–	1	–	22	–	23
2005	–	–	–	24	–	24
2006	–	1	1	66	1	69
2007	1	2	6	80	–	89
2008	–	3	3	49	–	55
2009	1	4	14	90	–	109
2010	–	2	6	96	–	104
2011	–	–	2	43	1	46
2012	–	–	3	39	–	42
2013 (to Nov)	–	–	–	7	2	9
Total	3 (0.5 %)	13 (2.1 %)	35 (5.6 %)	556 (91.1 %)	4 (0.6 %)	621

medical aid reaching him. In both the other cases, treatment issues were thought to play a part (poor application of tourniquets, failure to call a trauma team, possible over-administration of opiates and poor handling of massive transfusion and hypothermia). The factors affecting the S2 cases were tactical in 9, military equipment in 1 and treatment in 4 (tourniquet application, incorrect drain site and development of complications). In 1 S3 case, a single aspect of treatment (tourniquet application) could have been improved but it would be unlikely to have produced a different outcome. Twenty-four cases were affected by tactical considerations and in the remaining

10 it was considered that everything possible had been done and that whilst survival was possible, it would be extremely unlikely in even the best circumstances (percentage chance of survival <5 %).

10.4 Discussion

The Peer Review Panel is an important part of providing assurance to the Chain of Command that the DMS Trauma system is functioning optimally and that Healthcare Governance of the system is in place in that continuous adjustments and improvements are made. As well as immediate feedback to theatre following a post mortem, comments are passed to clinicians through the Deployed Medical Director (DMD) and at the weekly Joint Theatre Clinical Conference. Feedback can also be passed from the DMD to the Medical Regiment and thus to the Combat Medical Technicians, who dealt with the casualty at the point of wounding. This also allows everyone involved in a casualty's care the opportunity to raise questions and receive answers about what happened. Where there has been deviation from standardised procedures, explanations are sought that may result in identification of a training gap and appropriate measures taken.

Further benefits derived from the in-depth review of military operational mortality have been the increased linkages between clinical personnel and those working for other Defence agencies. The review has been used to determine emerging injury and treatment patterns, to determine potential areas of clinical research and to inform the on-going development of personal and vehicular protective systems and equipment.

There is a potential overlap in the definitions of KIA and DOW that is duplicated for KNEA and DNEA. Depending on circumstances, a casualty that arrives at hospital in cardiac arrest may receive blood and undergo surgery before resuscitation attempts are ceased and death pronounced. The convention that has been applied in these cases is that if there have been any signs of life at any time after arrival at the hospital then DOW is used, otherwise KIA is the designation. There are 32 cases that received blood in ED and/or theatre but as they did not regain a cardiac output at any stage, are still classified as KIA. In one case 9 units of packed red blood cells and 5 units of fresh frozen plasma were given. This case and 28 others were S4 when reviewed. The 2 S2 and 5 S3 cases all had prolonged evacuation periods as a result of tactical issues. The S4 cases potentially represent failure to recognise futility. In the resource-rich environment of Bastion Role 3 this may not have further ramifications if there are no other casualties requiring immediate treatment. However, as the Armed Forces move to contingency operations, resources will be much more limited. Whilst the final decision to stop resuscitative efforts should always rest with the clinicians at the trolley-side, a further study of these cases will be undertaken to determine if lessons can be drawn and if there is any potential for "rules of thumb" to be developed.

Comparison with the experience of American Forces described by Eastridge et al. [5] is interesting but no firm conclusions can be drawn as there has been no cross-review or communication on this subject between the reviewers and parameters may have differed. The KIA:DOW ratios of HA casualties between KIA and DOW are very similar (UK 6.28 v.US 6.87) but the UK review panel rated 93.5 % (416 cases) of HA casualties non-salvage-able compared with the US figure of 75.7 % rated non-survivable. There are many potential explanations for this difference not least a different application of the cut-off between KIA and DOW as described above. The KIA:DOW ratio has in the past been suggested as a measurement of trauma system performance but "inevitable" deaths surviving to reach hospital before dying make it a poorer tool than identifying unexpected outcomes [8].

The results of this work point to the overwhelming severity and nature of military trauma described in other studies [14, 15] especially given the proportion of injuries caused by IEDs. Data from the Vietnam War and previous modern conflicts showed a preponderance of single life-threatening injuries [16]. In the battlefield environment, any AIS score 4 or greater is potentially fatal [17]. In this study, 371 cases had AIS

4+ injuries to more than one body region, the highest being 6 regions, and 80 had AIS 6 injuries to 2 or more regions (highest 4). Of those killed by an AIS 4+ injury to a single body region, the head (72 cases) and thorax (46) were most often involved.

A further finding is the necessity to apply a clinical dimension to the review process as well as using the different trauma scoring methods, especially when considering individual cases. As was observed when analysing survivors over 18 months between 2006 and 2008 [4], there is not necessarily agreement between the methods themselves or between them and experienced clinical opinion. 17 cases were identified by ASCOT and/or TRISS as "expected survivors" (1 TRISS only, 8 ASCOT and 8 by both). Of these, clinical review graded 10 as S4, 3 S3, 1 S2 and 2 S1. 3 further cases had an ISS of <15 thus not reaching the threshold for "major trauma". All 3 were expected deaths on TRISS and ASCOT due to their physiological status on arrival at hospital and peer review award 1 to S2, S3 and S4. In all three, tactical aspects caused a delayed evacuation.

The members of the review panel have not been identical throughout the period of this study due in particular to deployments. This is a source of weakness but it is also a potential strength as it has meant that all the military members of the panel have had recent operational experience. Regardless, the membership has been relatively stable with the personnel listed in acknowledgements attending over two thirds of meetings and three of whom have attended all but one or two. Judgements have, as a result, been consistent to the standard of the best practice available at the time of that particular meeting. However, over time the parameters within which those judgements have been made have been shifting on a regular basis as advances in trauma treatment in the DMS developed. An injury pattern illustrating this is multiple amputations following an IED strike. This has been the signature injury pattern of OPERATION HERRICK and, when first seen in the meetings, survival was thought to be unlikely. As the DMS experience has developed along with training, equipment and techniques, good outcomes have been achieved on a regular basis and scrutiny of cases reaching the mortality meeting is intense.

A further study of the DOW cases dying at the UK Role 4 is in progress to determine if there are any specific lessons to be learned from this sub-group. A similar project is also ongoing into "unexpected survivors" over a longer period than described previously [4]. Whilst tactical issues were the most common factor identified in the cases graded S1-3 and each case has been examined individually, a more in-depth study of the group is required as a whole to identify if there are any key learning points that may inform clinical practice or force protection.

10.5 Conclusions

Mortality Peer Review has identified that 91.1 % of UK military operational deaths since 2002 were the result of un-survivable trauma. For casualties categorised as KIA, this figure is 93.5 %. Whilst trauma scoring systems are useful tools, clinical peer review is an essential part of the robust Healthcare Governance process that is in place to identify potential lessons and give feedback.

Acknowledgements 1. The following have been regular members of the peer review panel: Surg Capt M Midwinter; Col J Clasper, Col P Mahoney, Col R Russell, Mr A Hepper, Dr R Delaney, Dr N Hunt, Dr P Wood.
2. The staff of the Joint Theatre Trauma Registry, ADMEM attended post mortems, collected data on casualties and co-ordinated review panel meetings.
3. This material was originally published as Russell R, et al. J R Army Med Corps 2014: 160:150–154 and is reproduced here with some amendments with permission.

References

1. Hodgetts TJ, Davies S, Russell RJ, et al. Benchmarking the UK military deployed trauma system. J R Army Med Corps. 2007;153:237–8.
2. Smith J, Hodgetts TJ, Mahoney PF, et al. Trauma Governance in the UK Defence Medical Services. J R Army Med Corps. 2007;153:239–42.

3. Healthcare Commission. Defence Medical Services: a review of the clinical governance of the Defence Medical Services in the UK and overseas. London; 2009.
4. Russell RJ, Hodgetts TJ, McLeod J, et al. The role of trauma scoring in developing trauma clinical governance in the Defence Medical Services. Philos Trans R Soc Lond B Biol Sci. 2011;366:171.
5. Eastridge BJ, Mabry RL, Seguin P, et al. Death on the battlefield (2001–2011): implications for the future of combat casualty care. J Trauma Acute Care Surg. 2012;73:S431–7.
6. Marx WH, Simon HM, Jumbelic M, et al. Severity of Injury is underestimated in the Absence of Autopsy Verification. J Trauma. 2004;57:46–50.
7. Sharma BR, Gupta M, Harish D, et al. Missed diagnoses in trauma patient vis-à-vis significance of autopsy. Injury. 2005;36:976–83.
8. Hodgetts TJ, Davies S, Midwinter M, et al. Operational mortality of UK service personnel in Iraq and Afghanistan: a one year analysis 2006–7. J R Army Med Corps. 2007;153:252–4.
9. Baker SP, O'Neill B, Haddon W, et al. The injury severity score: a method of describing patients with multiple injuries and evaluating emergency care. J Trauma. 1974;14:187–1966.
10. Osler T, Baker S, Long W. A modification of the Injury Severity Score that both improves accuracy and simplifies scoring. J Trauma. 1997;43:922–6.
11. Boyd CR, Tolson MA, Copes WS. Evaluating trauma care: the TRISS method. J Trauma. 1987;27:370–8.
12. Champion HR, Copes WS, Sacco WJ, et al. A new characterisation of injury severity. J Trauma. 1990;30:539–46.
13. Association for the Advancement of Automotive Medicine. Abbreviated Injury Scale 2005. Barrington; 2005.
14. Singleton JAG, Gibb IE, Hunt NCA, et al. Identifying future 'unexpected' survivors: a retrospective cohort study of fatal injury patterns in victims of improvised explosive devices. BMJ Open. Published Online First: 1 Aug 2013. doi:10.1136/bmjopen-2013-003130.
15. Ramasamy A, Harrisson SE, Clasper JC, et al. Injuries from roadside improvised explosive devices. J Trauma. 2008;65:910–4.
16. Bellamy RF. The causes of death in conventional land warfare: implications for combat casualty care research. Mil Med. 1984;149:55–62.
17. Champion HR, Holcomb JB, Lawnick MM, et al. Improved characterization of combat injury. J Trauma. 2010;68:1139–50.

Physical Models: Tissue Simulants

11

John Breeze and Debra J. Carr

11.1 Introduction

The most common manner of reproducing the effects of energised fragments penetrating human tissues is to use a physical model as a tissue simulant. Such physical models encompass simulants including animal based simulants such as gelatine, animal physical models, and in more limited circumstances, post mortem human subjects (PMHS). No physical model can currently accurately reproduce all of the complex projectile and tissue variables that occur within live human tissues. Therefore, individual models attempt to accurately reproduce a limited number of variables, with data produced from different types of model often being used synergistically to generate the bigger picture. For example, a freshly killed animal surrogate may closely resemble the tissue properties of a live human but may not be able to reproduce the complex anatomy if that is required.

J. Breeze, PhD, MRCS, MFDS, MBBS, BDS (✉)
Academic Department of Military Surgery and Trauma, Royal Centre for Defence Medicine, Birmingham Research Park, Birmingham B15 2SQ, UK
e-mail: johno.breeze@me.com

D.J. Carr, CEng, FIMMM, MCSFS
Impact and Armour Group, Centre for Defence Engineering, Cranfield University at the Defence Academy of the United Kingdom, Shrivenham SN6 8LA, UK
e-mail: d.j.carr@cranfield.ac.uk

The main limitations to physical models are the time and cost involved in their manufacture, preparation, experimental testing requirements and subsequent interpretation. A simple numerical injury model in comparison could be run from a computer single handed, although the objective information that they produce varies in the time that it takes to be calculated. However, the information to populate these numerical models in the first place necessitates testing of physical models and therefore for the time being there is likely to be a need for their use.

11.2 Projectile Effects

Energy loss along a wound track is not uniform. Variations may be due either to behaviour of the projectile, or changes in the structure of the tissues as the projectile traverses the subject. There are a number of projectile specific effects that all physical simulants are able to reproduce in the context of terminal ballistics:

(a) ***Shape and size***: those projectiles with a greater presenting surface area will result in more energy deposition assuming mass and velocity are equal sooner after impact.
(b) ***Yaw***: a full metal- jacketed rifle bullet will produce a cylindrical cavity until it begins to yaw. At this time, the bullet's cross-sectional area will become larger, and the

A.M.J. Bull et al. (eds.), *Blast Injury Science and Engineering: A Guide for Clinicians and Researchers*,
DOI 10.1007/978-3-319-21867-0_11

drag force will be increased. The result is an increase in kinetic energy dissipation and thus an increase in the diameter of the temporary cavity. In addition to the increase in size of the temporary cavity, there will also be an increase in the amount of tissue damaged as the bullet is presenting a larger impacting surface area.

(c) ***Fragmentation***: projectile fragmentation can amplify the effects of the temporary cavity increasing the severity of a wound.

(d) ***Deformation***: in contrast to full metal-jacketed military bullets, with hunting ammunition, the bullet begins to expand shortly after entering the body, with a resultant rapid loss of kinetic energy. Thus, a large temporary cavity is formed almost immediately on entering the body. This is augmented by shredding of the lead core and jacket.

The main difference between physical models is the ability to visualise these differences and their reproducibility. For example, gelatine is translucent and homogenous whereas animal tissue is opaque and, even in isolated tissues such as muscle, still has tissue planes. For this reason projectile effects are most commonly compared using an artificial simulant such as gelatine in combination with high speed video.

11.3 Tissue Effects

Energised fragments can cause injury to living tissues through three potential mechanisms. The first mechanism is the crushing and cutting effect of the presented surface of the projectile, which is responsible for the production of a Permanent Wound Cavity (PWC); this immediate impact area is often referred to as the 'neck'. In the second mechanism the further passage of the projectile leads to radial acceleration of the tissue, which will expand, contract and oscillate after the projectile has passed through. The maximum extent of this pulsating temporary cavity produced in tissues occurs several milliseconds after the projectile has passed through that section of tissue and spreads out, potentially asymmetrically due to weaknesses in the tissue planes or projectile tumbling. The third mechanism is the pressure wave, occasionally also named the 'shock' or 'sonic' wave, which has been demonstrated experimentally in distant parts of the body. Strongly expressed opinion as to the potential wounding effects of the pressure wave continues to occur, but a recent review of the wound ballistics literature could not find objective evidence that this mechanism causes significant injury that either currently warrants, or enables, modelling [1].

For the purposes of modelling, the damage to tissue that ideally requires quantification is the Permanent Wound Tract (PWT). However as will become evident in the following sections it

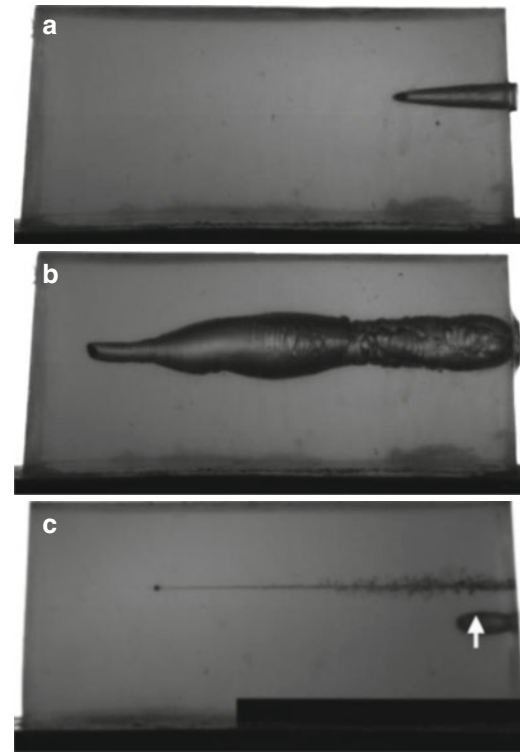

Fig. 11.1 High-speed video stills of a 20 % gelatine block being penetrated by a 5 mm spherical fragment simulating projectile (**a**), demonstrating temporary cavity (**b**) and permanent cavity (**c**). *Arrow* marks the position of temperature probe (Images courtesy of Dr Alexander Mabbott)

is currently not possible to objectively quantify the size of the PWT. Therefore it is necessary to ascertain its constituent components or causative mechanisms, namely the permanent cavity and temporary cavity, as indirect markers of the size of the PWT (Fig. 11.1).

11.3.1 Permanent Wound Tract

This is the clinical result of the crushing and cutting effect of a projectile in all tissues, in conjunction with the rapid radial displacement of the temporary cavity. It comprises a central PWC, together with a zone of irreversible tissue damage lateral to the PWC that heals by scarring [2, 3] (Fig. 11.2). Macroscopic damage can be reversible or irreversible, with the area immediately adjacent to the PWC generally having irreversible changes (referred to as the Contusion Zone [4] or Zone of Massive Quakes [5]) and the outer layer (Concussion Zone) having reversible changes. Clinically however, such discrete zones are rarely found and do not form in regular circles around the projectile path. Damage is usually patchy and not necessarily correlated to distance from the path of the projectile, reflecting that the clinical effect is dependent on both tissue type and architecture. Macroscopic damage will heal completely in some tissue types but this effect is likely to be rare, especially in complicated military wounds and in the presence of infection and contamination. Although irreversible macroscopic tissue damage in muscle may lead to scarring, in many cases there will be little residual clinical effect should the area of scarring be small or other muscles may compensate. As only macroscopic tissue damage has been demonstrated to be potentially irreversible, a clearer term would be to call this zone of damage lateral to the PWC the zone of Irreversible Macroscopic Tissue Damage (IMTD).

11.3.2 Damage Produced Specifically by the Temporary Cavity

The temporary cavity results in a transient, rapid strain of tissues that may, depending on the mechanical characteristics of the tissue, produce injury. Dense homogenous tissues, particularly if enclosed by a connective capsule or casing such as the liver or brain, suffer the greatest injury from the temporary cavity. Conversely elastic tissues with a high strain to failure such as lungs and large arteries resist its effects. This stretching effect is responsible for a small portion of the PWC as well as some macroscopic damage lateral to that. Skin is damaged by both the direct crushing effect of the projectile as well as the rapid radial tissue displacement produced by the temporary cavity, demonstrated by the stellate exit wounds in tumbling projectiles that can be greater than the largest dimensions of the projectile. Indirect bone fractures can occur at a distance from the projectile path [6] due to temporary cavity formation [6–10], although clinically their occurrence is rare. Indirect vertebral fractures are particular important as they may damage the adjacent spinal cord directly or through the production of secondary fragments [11].

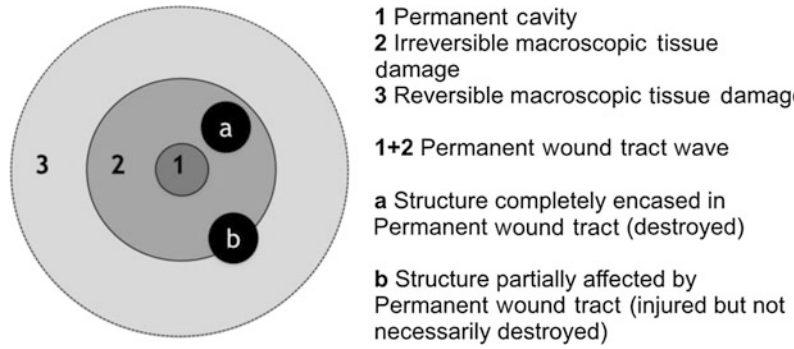

Fig. 11.2 Diagrammatic representation of the results of these mechanisms of potential tissue damage. Clinically damage is patchy and rarely forms in such distinct layers

Although the temporary cavity has been found to result in microscopic tissue damage to isolated arteries, muscles and large nerves lateral to the PWT, the largest systematic review of its kind to look into these effects could find no experimental evidence to demonstrate that these changes translated to permanent damage [1]. For example, microscopic changes to all of the layers in the arterial wall have been demonstrated in blood vessels up to 50 mm from the most lateral aspect of macroscopic tissue damage [12]. Although it has been suggested that this microscopic arterial damage has warranted debridement of macroscopically normal sections of the artery lateral to the PWT, it is generally agreed that there is no correlation between microscopic arterial damage and long-term morbidity [1, 13, 14]. Damage to peripheral nerves and spinal cord damage from missiles that do not touch them directly is potentially due to microscopic damage to small blood vessels supplying large nerves [6]. Although temporarily impaired neuronal conduction due to microscopic axonal damage has been experimentally demonstrated up to 18 mm from the PWC [15], or 3 mm from the most lateral point of macroscopically damaged tissue [15], there is no evidence that this causes long term morbidity.

11.4 Tissue Simulants

These are materials that attempt to reproduce the physical properties of animal or human tissues in terms of both projectile and tissue effects. In general, manufactured simulants such as gelatine are able to reproduce projectile effects better than tissue effects, and currently each individual tissue type requires representation by one or more of these simulants. In contrast, although animal models may represent tissue effects more closely to that of a human, the lack of reproducibility in results necessitates testing of isolated tissue types as well as manufactured simulants such as gelatine (Table 11.1).

Table 11.1 Most common physical simulants used in current terminal ballistics experiments comparing their individual advantages and disadvantages

Simulant	Advantage	Disadvantage
Ballistic gelatine	Elasticity resembles muscle Translucent enabling high speed photography Cheap One use	Temporary cavity collapses so difficult to measure Shorter storage time and requires refrigeration
Ballistic soap	Temporary cavity remains after firing so can be measured Long shelf life Easy to handle Can be recycled	Opaque Requires factory production Expensive
PermaGel™	Can be recycled Easy to handle Long shelf life Transparent enabling high speed photography Cheap	Equivalence to 10 % gelatin as marketed questioned Number of times it can be melted and reformed without changing material properties unproven
Animal	Tissue properties likely to be close to human, especially if tested immediately post mortem Anatomical relationships of structures to one closer to humans in some body areas than others e.g. thigh (similar) versus neck (dissimilar)	Effect of time and storage post mortem on tissue properties unknown Ethical issues if live testing
Post mortem human subject	Anatomical relationships of structures to one another correct Material properties likely to be similar to live human for certain anatomical structures e.g. bones and skin	Effect of time and storage post mortem on tissue properties unknown Ethical issues Availability

11.4.1 Ballistic Gelatine

Ballistic grade gelatine remains the most commonly utilised ballistic testing medium and has the greatest evidence base behind it. It is comprised of a complex mixture of proteins generally derived from collagen found in the bones of pigs. A process of hydrolysis enables it to be dissolved in hot water and it sets to a gel on cooling. The mechanical properties of gelatine are very susceptible both to the temperature that it is stored at, as well as the temperature of the water used in its production. Therefore, it is of great importance to describe the exact method used when writing up the results of any experimentation. Attempts at standardisation in terms of preparation have been made but the exact method is often institution specific.

The strength of the gel used is quantified using the bloom test, with commonly used values for ballistic gelatine being around 250 bloom [16]. There are various international standards regarding gelatine preparation that pertain to the ratio of water to gelatine and the temperature that it is mixed at. Again it is therefore essential that this is described in great detail in the methodology. The most commonly used concentrations are 10 and 20 %, with forensic and US sources generally favouring the former, and many UK authors the latter. To improve conformity among the testing of individual blocks immediately prior to use, each block should be calibrated. This usually involves firing a 4.5 mm steel sphere at a specified velocity range and producing depth of penetration within another range. Depth of penetration is usually measured using a steel rod, remembering to add the length (or diameter if spherical) of the projectile as DoP is usually to its presenting face (Fig. 11.3).

Ballistic gelatine closely simulates the density and viscosity of human and animal muscle tissue. Both 10 and 20 % concentrations of gelatine have been stated as being comparable to goat and pig muscle in terms of depth of penetration for both bullets and fragments [17, 18]. It is also generally agreed that the dimensions of the temporary cavity produced by projectiles traversing ballistic gelatine is representative of that produced in homogenous animal muscle [9]. However the same close relationship between the permanent cavity produced in gelatine compared to muscle is less clear, primarily due to their differing elasticity [19, 20]. Fackler, probably the most enduringly respected opinion on the subject, specifically stated that the permanent cavity volume in simulants should not be used to estimate that in animals [21], although he did agree with other authors [4] that their shapes are representative of one another (Table 11.2).

Fig. 11.3 Measuring depth of penetration of 5 mm spherical fragment simulating projectiles fired at a range of velocities into a block of ballistic gelatine

11.5 Other Physical Simulants

Although gelatine continues to be the mainstay of ballistic testing, in a small number of institutions the use of hard solids such as clay, soap and paraffin continues. The plasticity of these testing materials means that the resultant maximum temporary cavity produced does not appreciably collapse and remains permanently displayed in the medium [1, 22] (Fig. 11.4). The most common of these materials is ballistic soap, which is based on glycerine mixed with a combination of fatty acids. It is complex to produce and due to variations in its constituents, it is very difficult to standardise. Although soap can be stored for a considerable period of time, some

Table 11.2 The varying ability of different physical models to reproduce the projectile and tissue effects of penetration

Variable		Simulant		
		Manufactured	Animal	PMHS
Projectile	Yaw	Y	Y	Y
	Deformation	Y	Y	Y
	Fragmentation	Y	Y	Y
Tissue	Depth of penetration	Y	Y	U
	Anatomical relationships	N	N	Y
	Material properties	N	Y	U
	Permanent cavity	N	Y	U
	Temporary cavity	Y	Y	U
	Permanent wound tract	N	Y	N

Y yes, *N* no, *U* unknown

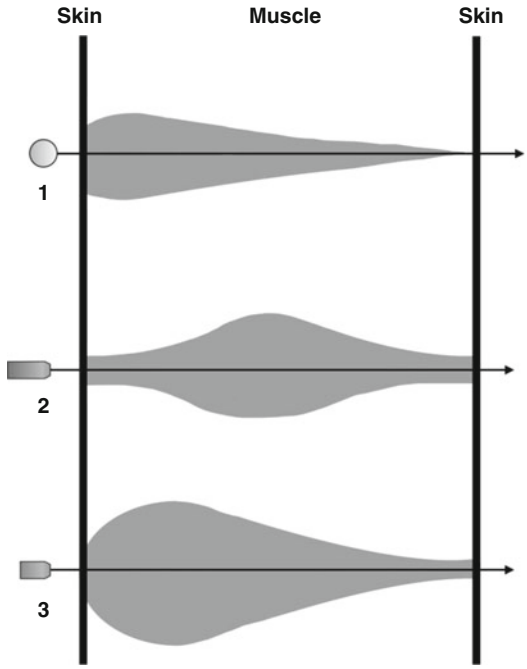

Fig. 11.4 Stylised appearances of comparison of different shapes of temporary cavitation produced in blocks of ballistic soap: (1) stainless steel spherical FSP, (2) stainless steel cylindrical FSP tumbling within tissue, (3) copper FSP deforming on impact

of its constituents do change, such that it has been suggested that 6 months is the maximum time at which measurements taken from it can be reproduced [23]. The primary disadvantage of soap is that it is opaque and measurements of temporary cavity size need to be made by either sectioning the block or for a large constant cavity, it can be filled with water. There is also some evidence to suggest these materials provide a greater resistance to projectile penetration and that soft materials such as gelatine and are more likely to fragment.

The desire to produce a soft ballistic medium analogous in properties has led to the development of many synthetic substitutes. Currently the most commonly used of these is PermaGel™, which is stated by the manufacturer to be analogous to 10 % ballistic gelatine (Fig. 11.5). PermaGel™ remains solid at room temperature, does not need temperature conditioning, is reusable by melting it down and reshaping it (up to approximately 10 times according to the manufacturer). It also has superior clarity, is not affected by water and is not subject to bacteria growth. However results from ballistic testing using spherical projectiles suggested that it behaves in a similar manner to 10 % gelatine at velocities around 400 m/s but not at slower or faster velocities [24]. When tested with high velocity rifle bullets, PG is not a suitable replacement for gelatin; burning of the PermaGel™ occurs and no appreciable permanent tract us formed.

11.6 Animal Physical Models

No animal can reproduce the complex anatomy of a human being, and testing generally involves measuring depth of penetration in small groups of tissue types such as skin and muscle alone

Fig. 11.5 A block of PermaGel™ being used to simulate the penetration of 5 mm spheres: note the physical similarity to gelatin

[17, 18]. Animal testing is also beset with significant difficulties, including expense, a lack of reproducibility (so called 'biological variation') and understandable ethical considerations. It should be recognised that experimental testing of the effects of the temporary cavity generally used isolated tissues and that it is the method of attachment of these structures to their surroundings that may result in damage from this mechanism, such as tearing the attachment of an artery at a fixed point (for example its entry into a bony foramen). The temporary cavity clearly has varying injurious effects dependent on tissue type and architecture and we would therefore encourage the term temporary tissue cavity (TTC) instead of temporary wound cavity to differentiate the effect of this mechanism in tissues rather than simulants, and that the cavity itself does not necessarily wound.

In terms of material properties, animal tissue is the closest surrogate to that of human, and significant effort is being made in instructions worldwide to derive material models at high strain rates to inform finite element models. However, limited evidence exists as to how fresh that tissue must be to be truly representative. Animals would need to be slaughtered with testing starting as soon after death as possible, to ensure that the material properties of the tissues through which the projectile passes are as close to that of a live subject as possible. There is no evidence describing the effect on projectile penetration as tissues age after death; however it is likely that the process of rigor mortis, which increases the rigidity of muscle tissues in humans 3–5 hours post death, would in some manner affect its material properties. The time to initiation and effect of rigor mortis on muscle is also believed to vary by breed and anatomical location, as well as the presence of stress pre-mortem and refrigeration post mortem. It will therefore be of great importance to clearly document variables such as breed, storage conditions and times between death and firing commencing. The elements within the model will be populated with the material models that are identified to be specific for each tissue type, and the actual results can be compared to that predicted by the model.

As stated previously, the PWT represents a demarcation between a zone of irreversible and reversible tissue damage. Demarcating between that viable and non-viable tissue however remains a subjective clinical decision [20, 25]. Clinical criteria have been well validated in their accuracy and include colour, consistency, contractility and capillary bleeding [2, 26]. For this reason it has been suggested that the mass of surgically debrided tissue (mSDT) is a better metric of the PWT [4, 26]. This concept of mSDT remains the metric more closely aligned with the true definition of the PWT and enables distinctions between tissues other than homogenous muscle to be made. Also, utilising experienced trauma surgeons to differentiate between non-viable and viable tissue is analogous to the method that would be undertaken on injured soldiers in an operating theatre. However, the limited existing experimental data for mSDT produced by bullets fired into porcine tissue demonstrates poor correlation to variables such as impact velocity or energy absorption, demonstrating again the difficulties in testing whole animal specimens. Computed Tomography (CT) is an emerging technology in the field of wound ballistics and has been used to measure the dimensions of the permanent cavity in both gelatin [27] and porcine tissue [17] (Fig. 11.6). However currently, only limited experiments have attempted to utilise this method such that there is insufficient data to

Fig. 11.6 Coronal section of a computed tomography scan following ballistic experimentation using a chisel nosed fragment simulating projectile fired into porcine tissue

compare it to cavity sizes produced in simulants. CT however is excellent at demonstrating bone impact or projectile fragmentation, both of which may result in false values for depth of penetration or energy absorption. Dead animal tissue also cannot determine the true demarcation between vital and non-vital tissue, but histological analysis of sections of the wound tract is a potential alternative and is currently being investigated.

11.7 Post Mortem Human Subjects

Post Mortem Human Subjects (PMHS) have been used intermittently in the past for the purposes of projectile penetration testing, but most of the evidence pertains to skin or bones. These tissues have always been utilised in isolation, with skin being separated from muscle or bone set in a manufactured simulant such as gelatin. The use of whole fresh, frozen or refrigerated Post Mortem Human Subjects (PMHS) has potentially huge advantages over animal models in specific cases, as the relationships between anatomical structures will clearly be representative of live humans in most cases. However, little objective evidence exists as to the effect of decomposition, refrigeration and freezing on tissue material properties, especially to ballistic impacts, such that currently this method cannot be used alone. Significant research is currently being undertaken to demonstrate how tissue changes post mortem in both PMHS and animal models affect material properties, as well as tissue effects to projectile penetration.

References

1. Breeze J, Sedman AJ, James GR, et al. Determining the wounding effects of ballistic projectiles to inform future injury models: a systematic review. J R Army Med Corps. 2013;160(4):273–8. doi:10.1136/jramc-2013-000099.
2. Berlin RH, Gelin LE, Janzon B, et al. Local effects of assault rifle bullets in live tissues. Acta Chir Scand Suppl. 1976;459:1–76.
3. Orlowski T, Piecuch T, Domaniecki J, et al. Mechanisms of development of shot wounds caused by missiles of different initial velocity. Acta Chir Scand Suppl. 1982;508:123–7.
4. Wang ZG, Tang CG, Chen XY, et al. Early pathomorphologic characteristics of the wound track caused by fragments. J Trauma. 1988;28(1 Suppl):S89–95.
5. Korac Z, Crnica S, Bozo N. Histologic analysis of pig muscle tissue after wounding with a high-velocity projectile-preliminary report. Acta Clin Croat. 2006; 45:3–7.
6. Cooper GJ, Ryan JM. Interaction of penetrating missiles with tissues: some common misapprehensions and implications for wound management. Br J Surg. 1990;77(6):606–10.
7. Kieser DC, Carr DJ, Leclair SC, Horsfall I, Theis JC, Swain MV, Kieser JA. Gunshot induced indirect femoral fracture: mechanism of injury and fracture morphology. J R Army Med Corps. 2013;159:294–9.
8. Black AN, Burns BD, Zuckerman S. An experimental study of the wounding mechanism of high-velocity missiles. Br Med J. 1941;2(4224):872–4.
9. Li M, Ma YY, Fu RX, et al. The characteristics of the pressure waves generated in the soft target by impact and its contribution to indirect bone fractures. J Trauma. 1988;28(1):S104–9.
10. Dougherty PJ, Sherman D, Dau N, et al. Ballistic fractures: indirect fractures to bone. J Trauma. 2011; 71(5):1381–4.
11. Amato JJ, Syracuse D, Seaver Jr PR, et al. Bone as a secondary missile: an experimental study in the fragmenting of bone by high-velocity missiles. J Trauma. 1989;29:609–12.
12. Lai X, Liu Y, Chen L. The effect of indirect injury to peripheral nerves on wound healing after firearm wounds. J Trauma. 1996;40(3 Suppl):S56–9.
13. Amato JJ, Rich NM, Billy LJ, et al. High-velocity arterial injury: a study of the mechanism of injury. J Trauma. 1971;11(5):412–6.

14. Rich NM, Manion WC, Hughes CW. Surgical and pathological evaluation of vascular injuries in Vietnam. J Trauma. 1969;9(4):279–91.
15. Oehmichen M, Meissner C, König HG. Brain injury after gunshot wounding: morphometric analysis of cell destruction caused by temporary cavitation. J Neurotrauma. 2000;17(2):155–62.
16. Jussila J. Measurement of kinetic energy dissipation with gelatine fissure formation with special reference to gelatine validation. Forensic Sci Int. 2005;150(1): 53–62.
17. Breeze J, Hunt NC, Gibb I, et al. Experimental penetration of fragment simulating projectiles into porcine tissues compared with simulants. J Foren Legal Med. 2013;20:296–9.
18. Breeze J, James GR, Hepper AE. Perforation of fragment simulating projectiles into goat skin and muscle. J R Army Med Corps. 2013;159:84–9.
19. Harvey EN. The mechanism of wounding by high velocity missiles. Proc Am Philos Soc. 1948;92(4): 294–304.
20. Harvey EN, Korr IM. Secondary damage in wounding due to pressure changes accompanying the passage of high velocity missiles. Surgery. 1947;21(2):218–39.
21. Fackler ML, Bellamy RF, Malinowski JA. A reconsideration of the wounding mechanism of very high velocity projectiles- importance of projectile shape. J Trauma. 1988;28(1 Suppl):S63–7.
22. Janzon B. Edge size and temperature effect in soft soap block simulant targets used for wound ballistic studies. Acta Chir Scand Suppl. 1982;508: 105–22.
23. Kneubuehl B, Coupland R, Rothschild MA, Thali MJ, editors. Wound ballistics: basics and applications. 1st ed. Berlin: Springer Science & Business Media; 2011. ISBN 9783642203565.
24. Mabbott A, Carr DJ, Champion S, Malbon C, Tichler C. Comparison of 10% gelatine, 20% gelatine and Perma-GelTM for ballistic testing. In: Proceedings of International Symposium on Ballistics, 22–26 April, Freiberg, 2013.
25. Hopkinson DA, Watts JC. Studies in experimental missile injuries of skeletal muscle. Proc R Soc Med. 1963;56:461–8.
26. Berlin RH, Janzon B, Rybeck B, et al. Local effects of assault rifle bullets in live tissues. Part II. Further studies in live tissues and relations to some simulant media. Acta Chir Scand Suppl. 1977;477:5–48.
27. Korac Z, Kelenc D, Hancevic J, et al. The application of computed tomography in the analysis of permanent cavity: a new method in terminal ballistics. Acta Clin Croat. 2002;41:205–9.

Physical Models: Organ Models for Primary Blast

12

Hari Arora and Theofano Eftaxiopoulou

12.1 Introduction

With primary blast, when a shock wave strikes, some of the energy is reflected and some absorbed by the body. As tissue within the body possesses both elastic and viscous properties (as well as some organs being multi-phasic in nature), their reactions to blast loading is complicated and difficult to predict. Different parts of the body, specifically organs, react differently to impulsive loading. This is due to a combination of their unique structure, which responds in a certain way to a mechanical stimulus, as well as the unique stress-strain state experienced in that part of the body, due to a given blast wave profile and the support conditions of that organ. This can lead to local injury development within a given organ resulting in consequences to the system as a whole (e.g. inflammation) or with interwoven and superposed damage mechanisms. Multiple injury sites generate increased burden on the system leading to added complications in their treatment. Although *in-vivo* blast models continue to dominate the existing literature, these models tend to analyse whole body responses and sometimes fail to identify physical injury at the tissue level. Isolated organ experiments, termed *ex-vivo* models, maintain the architecture and functionality of the tissue for a short period of time and constitute a close representation of the *in-vivo* state [1]. This section focusses on the work assessing primary blast evaluation of the body at an organ level.

12.2 Blast Induced Neurotrauma

Traumatic brain injury (TBI) is a leading cause of mortality and disability in injured service personnel. Blast induced TBI (also referred to as blast induced neurotrauma, BINT) is a specific area of research focusing on how the impulsive nature of a primary blast changes both the physical status of the brain as well as any neural functionality. Duckworth et al. [2] give an overview of the differences between the three common types of battlefield TBI from closed-head (brain impacting against the skull wall – tertiary blast effect), penetration injuries (secondary blast effect) and finally explosive blast TBI (primary blast effect).

Blast induced TBI has been hypothesised to occur via a thoracic pressurisation as well as trans-cranially [3]. An extensive summary of TBI models in use has been collated by Sundaramurthy et al. [4], who then extended the studies to explore the effect of positioning of test samples within and in front of a shock tube. The

H. Arora, MEng, PhD, DIC, ACGI (✉) •
T. Eftaxiopoulou, PhD
Department of Bioengineering, Royal British Legion Centre for Blast Injury Studies, Imperial College London, London SW7 2AZ, UK
e-mail: hari.arora04@imperial.ac.uk; Theofano.eftaxiopoulou06@imperial.ac.uk

A.M.J. Bull et al. (eds.), *Blast Injury Science and Engineering: A Guide for Clinicians and Researchers*,
DOI 10.1007/978-3-319-21867-0_12

optimal position of the head for ensuring primary blast induced neurotrauma was found to be within the shock tube with the dominant mode of stress wave transmission determined numerically to be through the cranium. Chavko et al. [5] reinforced this via direct measurement of intracranial pressures during blast loading. The intensity of the pressure wave seemed relatively undisturbed by the skull, with decay variations arising in the pressurisation due to orientation. Further numerical work by Panzer et al. [6] on a brain and head model showed the dependence of pressure arising within the brain on the peak pressure of the blast wave, whilst the largest brain tissue strains were shown to be controlled by the shock wave duration, or impulse.

Advanced methods such as diffusion tensor imaging (DTI) have revealed the extent of mild blast-induced TBI with scans on extracted brains in rats after they were subject to transverse cranial loading in a shock tube [7] and pigs subjected to blast from free-field explosives [8]. This method has previously been exploited *in-vivo* in other areas of TBI and brain degradation assessment [9, 10] as well as *ex-vivo* in human brain. Therefore, there is the capacity to use the current state-of-the-art imaging methods such as DTI to map in detail the injury profile (damage pathways) in blast TBI whether *in-vivo* or *ex-vivo*. This is in addition to traditional imaging modalities that would highlight only structural disruption such as normal MRI.

In addition, high-speed photography based methods can be used to capture experimentally shock wave profiles and their interaction with the body. Sarntinoranont et al. [11] used living tissue slices from rat brain, attached them to a ballistic gelatin substrate and subjected them to high strain rate loads of 1584 ± 63.3 psi, using a polymer split Hopkinson pressure bar (PSHPB) (see Chap. 4 Sect. 4.2.1). Simultaneously, they used real time high speed imaging and noted cavitation due to a trailing under-pressure wave. Neuronal injury was quantified at 4 and 6 h. post blast. Ouyang et al. [12] and Connell et al. [1] exposed isolated sections of guinea pig spinal cord white matter to a shock-wave produced from a small scale explosive event (Fig. 12.1).

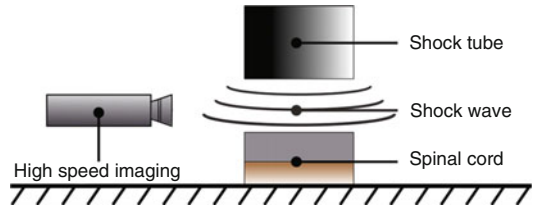

Fig. 12.1 Schematic of *ex-vivo* spinal cord experimental set-up [6]

The latter study explored dose response with regard to input shock pressures and functional and anatomical deficits. Direct exposure to the blast wave compressed nervous tissue at a rate of 60 m/s and led to significant functional deficits [1]. Results also showed that an inverse relationship exists between the magnitude of the shockwave overpressure and the degree of functional deficits [1]. Damage to the spinal cord was marked by increased axonal permeability suggesting that compression from the shockwave results in acute membrane disruption [1].

Work such as these complement the studies ongoing *in-vivo* (see Chap. 13, Sect. iii), which forms the majority of active research in the area, to isolate injury mechanisms worth pursuing.

12.3 Lung

Shocks interact more intensely with larger surface areas of the body, therefore regions such as the thorax and abdomen can be more susceptible to a larger reaction from primary blast. Moreover, these delicate internal membranes are not equipped to sustain significant forces and can lead to internal rupture and bleeding.

Respiratory mechanics has often involved *ex-vivo* perfused lung samples varying in size from rodents to humans. Extracted lungs are often degassed and filled/washed with saline before experimentation in order to effectively eliminate surface tension effects. This helps to maintain the lung in a condition similar to that in which it would be expected to occur *in-vivo* – although the mechanics are naturally disrupted by extraction [13]. In terms of models for blast, specifically, there are little or no models in the

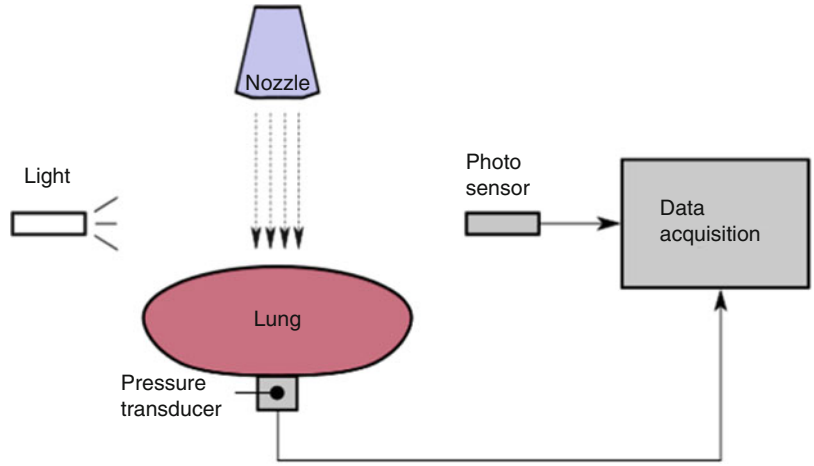

Fig. 12.2 Water jet system for simulating shock waves on lung tissue

literature at the organ level, much like the other organs of the body. Fung et al. [13] did explore the effect of transpulmonary pressure on the wave speed through different animal lungs. A water jet was used to generate the characteristic incident pressure-time profiles observed in blast. Measurements were taken on the front and rear surface of the lungs as shown in Fig. 12.2. Since the square of the wave speed is proportional to modulus and inversely proportional to density, transpulmonary pressure had a significant effect on wave speed (as it controls the stiffness of the lung). The influence of having a perfused lung was also highlighted as this significantly affects the density of tissue. Methods for blast lung injury evaluation (beyond *in-vivo models*) currently concentrate on isolated tissues being exposed to shock waves such as in Butler et al. and Curry et al. [14, 15] to complement clinical observations and *in-vivo* models currently in general use.

12.4 Abdominal Organs

With regard to primary blast interaction with soft organs, lung and brain are usually the first clinical priorities to be described. However, gas-containing sections of the gastrointestinal tract are also vulnerable to the primary blast effect. Observed injury mechanisms include immediate bowel perforation, haemorrhage, mesenteric shear injuries, solid organ lacerations and testicular rupture (see Chap. 6, Sect. 2.1). The majority of studies into this area are clinical observations and commonly reported in combination with other injuries. Some isolated studies using isolated perfused kidneys, researching treatment for kidney stones, have been extended to look at the effects of shock waves on kidney integrity in various animal kidneys such as pig [16] as well as human [17]. Köhrmann et al. [18] were able to evaluate vessel lesions by micro-angiography to determine the size and number of damage sites formed in the different areas of the organ subjected to focused ultrasound waves. The variation in the different patterns of lesions observed helped to characterise the pathway of the shock wave. Light microscopy revealed dose-dependent necrosis of tubular cells up to macro-scale parenchymal level defects [18]. This platform can be scaled up to explore higher intensity shocks in addition to the multiple doses of low level shocks, relevant to ultrasonic treatments.

12.5 Ocular Trauma

Tissue damage from primary blast injury can be an important cause of trauma to the ocular system (see Chap. 29) which can result in severe vision loss and injuries to the peri-orbital area [19]. Ocular injury occurs in up to 28 % of blast survivors. The most common injuries include corneal abrasions and foreign bodies, eyelid

lacerations, open globe injuries and intraocular foreign bodies [19].

Glickman et al. [20] subjected *ex-vivo* porcine eyes to blasts produced by a shock tube and demonstrated that this approach could be used to detect trauma-induced biomarkers. Similarly, Sherwood et al. [21] also subjected porcine eyes to a range of primary blast energy levels and showed that, whilst the same damage was observed in the control eyes, the incidence and severity of it in the exposed eyes increased with impulse and peak pressure [21]. Moreover, these data also suggested that primary blast alone can produce clinically relevant ocular damage in a postmortem model. These models are relatively new and require further validation, however, they could become useful in determining direct effects of primary blast on ocular trauma.

12.6 Summary

The bulk of current research on primary blast effects lies at the two extremes of cellular models and *in-vivo* models. Organ level research *in-vitro* or *ex-vivo* is predominantly being covered as preliminary experiments to *in-vivo* work (or might simply be unreported). Neurotrauma research is fairly advanced, including research on whole explanted brains, brain sections and spinal cord tissue. Soft organ research, such as for lungs and the abdominal organs is less advanced mainly due to the complexities involved in extraction and perfusion, although other, niche, areas such as ocular models are now beginning to be developed with demonstrable utility in blast research.

This whole area, with the modern advanced techniques for preserving tissues and organs in a viable manner, and our understanding from organ transplant research, will certainly lead to the possibility of more sophisticated models being developed in the future for blast injury. Several models from other areas of physiological research have and can be extended towards blast injury research. These need to address key concerns, including, maintaining the extracted tissues over appropriate long time periods [11] and ensuring appropriate perfusion and physiologically relevant support conditions during a given experiment, as raised by Fung et al. [13] amongst others. *Ex-vivo* models however, can assist researchers in gaining a better understanding of the key components of blast injury by mitigating any confounding factors associated with *in-vivo* models [1], including significant control of additional variables. Current work in conjunction with the rise of computational methods to help govern the nature of appropriate loading as well as understanding stress wave transmission can help to extend the understanding of blast injury development.

References

1. Connell S, Gao J, Chen J, Shi R. Novel model to investigate blast injury in the central nervous system. J Neurotrauma. 2011;28:1229–36.
2. Duckworth JL, Grimes J, Ling GSF. Pathophysiology of battlefield associated traumatic brain injury. Pathophysiology. 2013;20:23–30.
3. Courtney A, Courtney M. A thoracic mechanism of mild traumatic brain injury due to blast pressure waves. Med Hypotheses. 2009;72(1):76–83.
4. Sundaramurthy A, Alai A, Ganpule S, Holmberg A, Plougonven E, Chandra N. Blast-induced biomechanical loading of the rat: an experimental and anatomically accurate computational blast injury model. J Neurotrauma. 2012;29:2352–64.
5. Chavko M, Koller A, Prusaczyk K, McCarron M. Measurement of blast wave by a miniature fiber optic pressure transducer in the rat brain. J Neurosci Methods. 2007;159(2):277–81.
6. Panzer MB, Myers BS, Capehart BP, Bass CR. Development of a finite element model for blast brain injury and the effects of CSF cavitation. Ann Biomed Eng. 2012;40(7):1530–44.
7. Kamnaksh A, Budde MD, Kovesdi E, Long JB, Frank JA, Agoston DV. Diffusion tensor imaging reveals acute subcortical changes after mild blast-induced traumatic brain injury. Sci Rep. 2014;4:4809.
8. Kwok HT, Baxter D, DeFelice J, Hellyer P, Kirkman E, Watts S, Midwinter N, Gentleman S, Sharp DJ. The neuropathology of blast traumatic brain injury in a porcine polytrauma model. Brain Inj. 2014;28(5–6):517–878.
9. Sharp DJ, Beckmann CF, Greenwood R, Kinnunen KM, Bonnelle V, De Boissezon X, Patel MC, Leech R. Default mode network functional and structural connectivity after traumatic brain injury. Brain. 2011;134:2233–47.

10. Leech R, Sharp DL. The role of the posterior cingulate cortex in cognition and disease. Brain. 2014;137: 12–32.
11. Sarntinoranont M, Lee SJ, Hong Y, King MA, Subhash G, Kwon J, Moore DF. High-strain-rate brain injury model using submerged acute rat brain tissue slices. J Neurotrauma. 2012;29(2):418–29.
12. Ouyang H, Galle B, Li J, Nauman E, Shi R. Biomechanics of spinal cord injury: a multimodal investigation using ex vivo guinea Pig spinal cord white matter. J Neurotrauma. 2008;25(1):19–29.
13. Fung YC, Yen MR, Zeng YJ. Characterization and modelling of thoraco-abdominal response to blast waves, vol 3, Lung dynamics and mechanical properties determination. Final Report to WRAIR under Contract DAMD17-82-C-2062; 1985.
14. Butler BJ, Bo C, Tucker AW, Jardine AP, Proud WG, Williams A, Brown KA. Mechanical and histological characterisation of trachea tissue subjected to blast-type Pressures. J Phys Conf Ser. 2014;500(18): 182007.
15. Curry RJ. The Blast Impact and Survivability Research Unit (BISRU), University of Cape Town, 4th international conference on impact loading of lightweight structures (ICILLS), 12–16 January 2014, Cape Town, South Africa.
16. Shao Y, Connors BA, Evan AP, Willis LR, Lifshitz DA, Lingeman JE. Morphological changes induced in the pig kidney by extracorporeal shock wave lithotripsy: nephron injury. Anat Rec A Discov Mol Cell Evol Biol. 2003;275A:979–89.
17. Brewer SL, Atala AA, Ackerman DM, Steinbeck GS. Shock wave lithotripsy damage in human cadaver kidneys. J Endourol. 1988;2(4):333–40.
18. Köhrmann KU, Back W, Bensemann J, Florian J, Weber A, Kahmann F, Rassweiler J, Alken P. The isolateci perfused kidney of the pig: new model to evaluate shock wave-induced lesions. J Endourol. 1994;8(2):105–10.
19. Morley MG, Nguyen JK, Heier JS, Shingleton BJ, Pasternak JF, Bower KS. Blast eye injuries: a review for first responders. Disaster Med Public Health Prep. 2010;4(2):154–60.
20. Glickman RD, Stidger D, Lund BJ, Bach S, Kelley A, Gray W, Sponsel WE, Reilly MA. Identification of trauma-related biomarkers following blast injuries to the eye. Invest Ophthalmol Vis Sci. 2014;55(13):4469.
21. Sherwood D, Sponsel WE, Lund BJ, Gray W, Watson R, Groth SL, Thoe K, Glickman RD, Reilly MA. Anatomical manifestations of primary blast ocular trauma observed in a postmortem porcine model. Inves Ophthalmol Vis Sci. 2014;55(2):1124–32.

In-Vivo Models of Blast Injury

13

Theofano Eftaxiopoulou

13.1 Introduction

Over the years, several *in-vivo* injury models have been developed to study the effects of blast injuries to experimental animals, in order to identify the injury mechanisms involved in the pathobiology of blast injury. This review provides an overview of the most commonly used blast injury models and the local and systemic changes induced in a wide range of tissues following blast.

13.2 Injury Models of Blast

13.2.1 Shock Tube

The Shock tube is a device able to generate pressure waves of varying intensity and duration. Because of its ability to produce repeatable blast waveforms that resemble the shock waves seen in free field blasts (Friedlander curve) as described in Chap. 1, it is by far the most common experimental design employed in studies involving *in-vivo* models, in order to study the effects of primary blast waves [1–6]. A shock tube is usually comprised of two chambers separated by one, two or multiple diaphragms. Compressed gas (air or helium) is loaded into the first chamber (often referred to as the overpressure chamber or the driver section), causing the diaphragm to deform plastically and fail [1, 2, 7]. This sudden rupture of the diaphragm releases the pressure into the low-pressure section forming a shock wave that travels along the tube [1]. Recently, more complex shock tubes have been designed, capable of reproducing complex shockwave signatures [8]. By a careful change of the volume and the pressure on the driver section, the output pulse of the system can be changed to vary from the ideal 'Friedlander' curve to a flat, long-duration pressure pulse corresponding to that seen inside vehicles subjected to an external blast (Fig. 13.1).

Animals in *in-vivo* studies are placed either within the main section [2, 4, 6, 10] or across the outlet of the shock tube [3, 5, 11]. In both set ups animals can be in either a supine or prone position [2] facing away, towards or on the side of the pressure wave. However, in all cases the animals are fixed in custom made holders or platforms, that prevent any potential movement of their bodies during blast, in order to minimise any tertiary blast effects [12].

13.2.2 Blast Tubes

A blast tube is a device that produces shock waves with a short duration of the primary peak [8]. Blast tubes were originally designed to study how

T. Eftaxiopoulou, PhD
Department of Bioengineering, Royal British Legion Centre for Blast Injury Studies, Imperial College London, London, UK
e-mail: a.bull@imperial.ac.uk

A.M.J. Bull et al. (eds.), *Blast Injury Science and Engineering: A Guide for Clinicians and Researchers*,
DOI 10.1007/978-3-319-21867-0_13

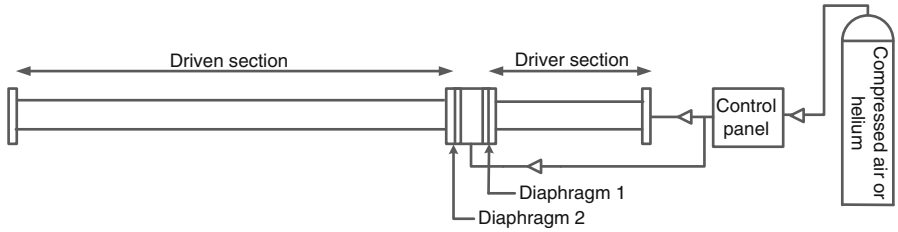

Fig. 13.1 Simplified schematic of a shock tube. Different designs exist in the literature. The length of the driver section can vary significantly, with values ranging from 0.76 m [3] to 1.22 m [1] reported in the literature. The two sections can be separated from each other by either one [2], two [1] or multiple diaphragms [9]. The driven section has also been seen to vary in length from 2.45 m [1] to 6.225 m [9]. In addition, a shock tube can have either a circular cross section (varying from 5.9 cm [1] to 30.5 cm [3] in diameter) or a square cross section (of 23 × 23 cm for instance [9])

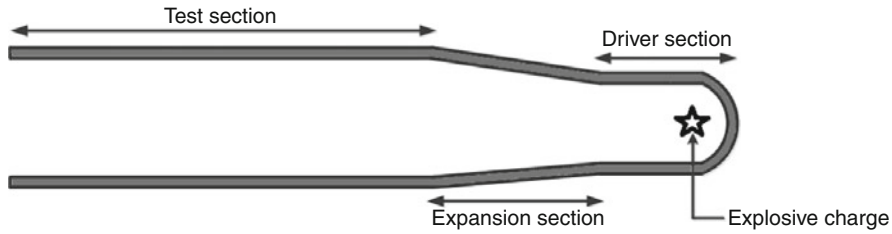

Fig. 13.2 Simplified schematic of a blast tube. Usually 1–2 g of pentaerythritol tetranitrate (PETN) explosive are used [16]. Saljo et al. and Risling et al. used a 1.54 m long blast tube with a 40 cm diameter [16, 17]. Bauman et al. used a much larger blast tube. The dimensions of the driven section were 2.44 m in length and 60.96 cm in diameter. The expansion section was about 3.05 m in length whilst the test section was 15.24 m long and 180.34 cm in diameter [15]

construction parts withstand shock waves of varying intensities [8]. However, during the 1950s these were modified by Clemedson and Jonsson to investigate vascular, respiratory and nervous effects of blast waves in rabbits [8, 13, 14].

A blast tube commonly comprises three chambers. The first chamber consists of a heavy-walled driver chamber in which explosives are placed [15]. The middle segment is called the expansion section and is connected to the third chamber called the test section where the animal is placed. An increase in the charge has been found to lead to a proportional increase in the peak pressure, but to have a small effect in the duration of the wave [8]. Similar to the shock tube, animals need to be restrained inside the blast tube to minimise any secondary or tertiary blast effects. Even though, blast tubes can produce repeatable and controlled waves, the smoke and gas emissions from the detonation of the explosives can lead to the development of quaternary blast effects, thus limiting their use in *in-vivo* studies [8] (Fig. 13.2).

13.2.3 Open/Free Field Blasts

In open/free field blast tests, shock waves are generated using explosives in an open field or concrete pad [18]. Very few studies have used chemical explosives to recreate battlefield injuries in a controlled environment to study their effects on animals. Most of these experiments were carried out primarily to determine thresholds for mortality and severity of injury [8]. More recently, Cheng et al. used an electric detonator with the equivalent of 400 mg TNT to develop a rat model to simulate blast injuries that occur in the battlefield [19] whilst, Rubovitch et al. used 500 g TNT, elevated 1 m above

ground, to replicate a low-level blast trauma using a murine model [20]. Open field blasts allow for more realistic experiments and for the investigation of the poly-traumatic nature of blast injuries, however, outdoor conditions in combination with the large number of animals needed are often too expensive. This, in addition to some lack of control variables, renders their use limited [8]. Similarly to the blast tubes, smoke/gas emissions from the explosives can cause quaternary blast effects (see Chap. 6, Sect. 6.2.4) whilst, isolating the blast effects into a particular organ/tissue is challenging.

13.2.4 Cranium Only Blast Injury Apparatus (COBIA)

The Cranium Only Blast Injury Apparatus (COBIA) was employed by Kuehn et al. in order to isolate the effect of direct cranial blast injury (dcBI) from the indirect blast injury to the brain mediated by thoracic transmission of the blast wave which can affect all the previous *in-vivo* models [21]. The experimental set up delivers blast overpressures generated by detonating cartridges of smokeless powder [21]. The peak pressure from the blast wave can reach up to 1000 kPa and the pressure traces show a large brief transient overpressure, followed by smaller slower transient under and overpressures, fully damped within 2 s [21]. This model could potentially be useful in isolating direct from indirect effects of blast. However, at this stage further validation is required to ensure that the pressure waves produced are related to the ones seen by conventional blast waves.

13.2.5 Laser-Induced Stress Waves (LISWs)

Laser-induced stress waves (LISWs) can be generated through the irradiation of a laser target with a laser source [22]. With respect to blast, LISWs have been used to investigate traumatic brain injury and pulmonary blast injury in rodent models. In both models the experimental animal is anaesthetised and fixed on a plate whilst, the region of interest is positioned in the focal area of a LISW and exposed to the stress waves which are described in detail in Chap. 1. In order to match the peak pressures seen in blast conditions, Hatano et al. and Satoh et al. used a natural black rubber disk covered and bonded with a transparent polyethylene terephthalate (PET) sheet as their laser target to generate waves with peak overpressures up to 604 MPa [23, 24] .

Laser-induced stress waveforms are dominated by a positive stress component that lasts for about 1 microsecond (μs) [22]. This duration is significantly shorter than that of a blast wave from a conventional weapon, which usually ranges between 2 and 6 millisecond (ms) [25]. Even though LISWs can reproduce some characteristics of shock waves and isolate effectively blast effects onto a particular tissue/organ, further investigation is needed to compare injuries induced by LISWs to the ones induced by conventional blast waves [23].

13.2.6 Secondary Blast Injury Models

Many explosive devices contain metallic and other fragments that along with the disintegrated munition casing can cause penetrating wounds [26]. Penetrating injuries can result either from fragments that are part of the device (primary fragments) or from the explosion (secondary fragments) [26] as previously discussed in Chap. 6. Few studies have addressed high-speed penetrating objects that produce shockwaves such as missiles and cause injury in large animal models for example in primates [27], sheep [28], pigs [29], cats [30] and dogs [31]. More recently, Plantman et al. (2009) recreated a penetrating traumatic brain injury to a rat model in the laboratory, using a modified air rifle that initially accelerated lead pellets that then impact a small probe that penetrated the surface of the brain with a speed ranging between 1 and 100 m/s [32]. Animals used in this work need to be

anaesthetised and fixed in a frame so as to avoid any acceleration injuries [16].

13.2.7 Tertiary Blast Injury Models

Proctor et al. used a rat model to investigate the effect of blast-induced acceleration on the brains of laboratory animals, in the absence of exposure to blast waves and of secondary impacts. In this model anaesthetised animals are secured to a metal platform and wrapped in a thick cotton "blanket" to minimise secondary movement. This platform is then accelerated vertically at either 20 or 50 G. What causes the acceleration is the detonation of pentaerythritol tetranitrate (PETN) placed in the water precisely under the centre of the plate [33]. This is the only study so far to have developed an underbody blast induced hyper-acceleration trauma model on the brains of laboratory animals [33]. However, to this point only two maximal G forces have been used, much lower than the survivable G forces experienced by service personnel within vehicles [33].

Another model developed to look at the effects of acceleration – deceleration due to blast, has been described by Risling et al. (2011). In this model the skull of an anaesthetised rat is tightly secured to a bar. An air rifle is used to accelerate a striker that is then used to impact the bar causing the head to rotate rearward [16]. By changing the air pressure in the rifle acceleration ranging between 0.3 and 2.1 Mrad/s^2 can be achieved. Following impact, the acceleration phase lasts 0.4 ms and then the head rotates at a constant speed and finally decelerates.

13.2.8 Underwater Blast Models

When an explosive is detonated under water, it produces a large volume of gaseous by-products in the form of an underwater bubble. The denser water spalls into the less dense air, causing fragmentation [34]. Underwater explosions are generally characterised by a much higher shock speed and a greater range of various effects than air blasts with primary blast injury and mortality rate being greater when the blast is under water [35]. However, Philips and Richmond submerged dogs in water and exposed them to underwater blast showing that the animals experienced internal injuries pathologically identical to that of air blast [36]. In the majority of these models, anaesthetised animals are submerged in water and exposed to under water blast [17, 36, 37]. One different approach, is the blast-amputation model developed by Tannous et al., whereby the animals were not submerged in water but secured on an aluminium platform with a hole, elevated above the surface a water-filled steel tank. Under water detonation of PETN led a column of water to rise at a maximum speed of 534 m/s through the hole in the platform [38].

13.3 *In-Vivo* Models

13.3.1 Traumatic Brain Injury

Blast waves generated by conventional and improvised explosive devices (IEDs) cause traumatic brain injury (TBI) in military personnel and civilians. Blast TBI is generally characterised by a primary injury that occurs at the time of exposure due to the immediate mechanical disruption of brain tissue followed by a secondary injury that develops hours to months after the initial trauma. Traumatic brain injury specific to blast is classified into three types:

- mild, whereby loss of consciousness for less than 1 h and posttraumatic amnesia for less than 24 h are noted,
- moderate, whereby loss of consciousness is less than 24 h and posttraumatic amnesia lasts anywhere up to 7 days, and
- severe, where patients exhibit loss of consciousness for time periods longer than 24 h and amnesia persistent for longer than 7 days [39, 40].

In-vivo animal models have been used to simulate blast conditions in an attempt to identify the mechanisms of TBI in a controlled environment

and to develop injury thresholds and therapeutic interventions. Primary blast-induced brain injury in rodents classified as mild usually shows no signs of structural damage at gross pathological examination [2], however, several authors have reported signs of limited neuronal/axonal injury in the cortex, corpus callosum, and periventricular areas [41–43]. Cernak et al. found that a single, mild blast in exposed mice induced glial activation, whilst Goldstein et al. showed that their histopathology 2 weeks after the blast event was similar to chronic traumatic encephalopathy (CTE), exhibiting signs of phosphorylated tauopathy, myelinated axonopathy, microvasculopathy, chronic neuroinflammation, and neuro-degeneration [2, 4].

Behavioural and functional changes associated with mild blast TBI (bTBI) often include weight loss, motor deficits, memory decline and impaired spatial learning [2, 15, 17, 41]. Cernak et al. (2011) showed that even though most of these symptoms were normalised 1 month after the exposure, some behaviour characteristics remained changed. Goldstein et al. showed that immobilisation of the head during the blast prevented associated learning and memory deficits [4], suggesting that head acceleration and subsequent deceleration may be critical factors in the development of bTBI [4, 44].

Fewer studies have focused on the effects of moderate and severe blasts on *in-vivo* models. Cernak et al. (2011) showed that moderate levels of blasts caused memory deficits and increased stress/anxiety in mice, whilst Svetlov et al. (2009) showed that head acceleration and deformation after severe blast trauma to the head of rats, was accompanied by typical focal and massive intracranial hematomas and brain swelling [5]. Changes on β-amyloid (Aβ) peptide that have been reported to occur rapidly after acute TBI in humans, as early as 2 h after a severe TBI [45, 46], have been seen to decrease acutely following injury in rodent models [47]. In addition, some authors have reported levels of the amyloid precursor protein (APP) to be increased following blast exposure [21, 47] whilst others [7, 42, 48], noted no APP accumulation in axons of rats exposed to over pressure waves ranging from 130 to 260 kPa. *In-vivo* animal models of primary blast-induced brain injury (bTBI) will be reviewed further in Chap. 14, Sect. 14.4, focusing on the effects of repetitive blast-induced TBI and acceleration – deceleration injury on animal models.

A large number of models also exist that describe the effect of penetrating traumatic injury, although very few of them are clinically relevant to blast conditions. Most notably, Plantman et al. (2009) recreated a penetrating traumatic brain injury to a rat model that caused tissue destruction such as white matter degeneration, haemorrhage, oedema, and gliosis accompanied by impairment of reference memory function. Long et al. (2009) [3] compared neuro-pathological changes evoked by blast to those described following controlled cortical contusion or fluid percussion injuries [49, 50] finding significant differences between the models and showing that exposure to airblast elicits fibre degeneration without being associated with obvious cell loss or injury. Similarly, Singleton et al. found that fluid percussion injury caused traumatic axotomy which also did not result in neuronal cell death [51, 52].

In summary, the existing literature on the pathobiology of blast-induced TBI presented is contradictory [12] and only partially imitates real life conditions. These variations in the models reported are often due to the broad range of experimental animals and blast injury models being used [12]. The shape and size of different brain structures can also influence the response under blast loading. Another severe limitation in developing animal models of TBI is that the classification of human blast TBI is based on the behavioural symptoms of injury [39]. Animal welfare regulations require that animals are anaesthetised when subjected to procedures that can potentially cause stress or pain thus, rendering diagnosis a challenging task [12]. Finally, the position and orientation of the experimental animal within the injury model and the presence or absence of noise stressors also play a crucial role in the biomechanical loading on the animal, the

type of injury that it sustains as well as the severity [12].

13.3.2 Blast Lung

Exposure to blast overpressures has been found to result in contusion or barotrauma-like injury mainly to air-filled organs such as lungs [53]. Indeed, exposure to blast pressure waves can result in cardiovascular and respiratory impairment because of the disruption of the alveolar septa and pulmonary capillaries, resulting in acute pulmonary haemorrhage [6]. *In-vivo* studies of blast TBI have identified that significant damage is observed in the lungs regardless of the body position of the experimental animal [2, 3, 54, 55]. In fact it has been suggested that there is an indirect thoracic mechanism of mild traumatic brain injury due to blast pressure waves [35, 54, 56, 57]. In addition, it has also been suggested that blast injury to the lower extremities may lead to systemic inflammatory changes affecting the limbs in addition to distal sites such as the lungs [58, 59].

Delius et al. implanted pressure probes into dogs to determine the conditions leading to lung damage. They found that shock wave pressures over 10 MPa caused bleeding [60] and attributed this to vessel rupture. Chavko et al. (2006) placed anaesthetised rats into a shock tube and exposed them to blast waves of a mean peak overpressure of 140 kPa. Characteristic landmarks of lung contusion such as intra-alveolar and subpleural haemorrhage, massive infiltration of neutrophils, and activation of macrophages in the lung parenchyma were noted [6, 24, 61]. More interestingly, administration of the antioxidant NACA prior to blast was seen to facilitate lung recovery from inflammatory damage [6]. Skotak et al. defined a lower peak overpressure of 100 kPa as the threshold for 'blast lung' injury that is characterised by pulmonary haemorrhage, vascular damage, direct alveolar injury, and oedema [10, 62]. In addition, extensive release of cytokines IL-1, IL-6, MCP-1, and MIP-2 have been observed in the Bronchoalveolar Lavage (BAL) fluid and blood plasma [63].

Rafaels et al. and Bass et al. developed curves for the assessment of the risk of fatality from primary pulmonary injury for long-duration (>10 ms positive overpressure phase) and short-duration blast waves respectively. They outlined the differences in the injury mechanisms from the two types of blast stating that for long durations the injury risk had little dependence on the duration parameter [64, 65].

Chai et al. investigated lung injury induced by a combined burn–blast trauma. They showed that rats with burn-blast combined injury had more severe lung injuries and abnormal coagulation and fibrinolytic function than those induced by either a blast or a burn only injury [66, 67]. Elsayed et al. (1997) investigated the effects of multiple low level shock waves (62 ± 2 kPa) in the lungs of rats and showed that repeating blasts did not significantly add to the effect of the first one [68].

13.3.3 Heterotopic Ossification

It has often been hypothesised that Heterotopic Ossification (HO) is caused by a combination of systemic and wound specific responses to trauma [69]. Whilst, there are several *in-vivo* models that reproduce HO in a laboratory environment, [70–72] the majority of these models use injections of bone morphogenetic proteins BMPs to induce HO, thus not replicating the conditions under which HO is formed in blast injuries. Nevertheless, through these studies a significant correlation between injury to the peripheral nervous system (PNS) and HO formation has been made attributed to the decreased expression of substance P (SP) and calcitonin gene-related peptide (CGRP) [69, 70]. Tannous et al. used a blast-amputation model to produce HO in rat residual limbs. Heterotopic bone was then radiographically classified as periosteal growth (Type A) or noncontiguous growth (Type B) in the rats. Whilst this is a very promising technique, relevant to blast scenarios,

limitations such as the high mortality rates and the variations in the blast overpressure delivered to the animals still need to be addressed [38, 69].

More recently, Polfer et al. established a rat HO model consisting of full body blast exposure, controlled femur fracture, crush injury and transfemoral amputation through the zone of injury [73]. In detail, they divided rats into three groups: animals exposed to a full body blast overpressure (120 ± 7 kPa), animals that sustained only a crush injury and femoral fracture followed by amputation through the zone of injury and animals exposed all insults. HO developed in all the rats in the third group and in about 65 % of the animals in the second group. Exposure to blast waves was seen to increase the prevalence of HO in this model [73] and the genes that regulate this early chondrogenic and osteogenic signalling and bone development (COL1a1, RUNX-2, OCN, PHEX, and POU5F1) were found to be induced early during the tissue reparative/healing phase [74]. This model simulates quite closely a combat-related extremity injury and can be used to further investigate the effects of different blast pressures and durations and provide an insight into the cellular and molecular pathways that lead to HO development [73, 74].

13.3.4 Hearing Loss

Blast overpressure can produce injury to the ears resulting in rupture of the tympanic membrane, dislocation or fracture of the ossicular chain, and damage to the sensory structures on the basilar membrane [75]. Animal studies have demonstrated that trauma to the auditory system induces hyperactivity in the inferior colliculus which may occur immediately after noise exposure and last for up to 3 months following exposure or cochlear ablation [76]. Mao et al. (2012) exposed rats to a single 10 ms blast at 14 psi and with a sound pressure level of 194 dB. Blast exposure induced early onset of tinnitus and central hearing impairment due to significant damage to certain auditory brain regions, in particular the inferior colliculus and medial geniculate body [77]. Absence of microstructural changes in the corpus callosum, led the authors to suggest that primary blast mainly exerts effects through the auditory pathways [77].

Kurioka et al. used LISW generated overpressures up to 400 MPa, applied to the cochlea of rats through bone conduction that revealed that the presence of an inner ear dysfunction is proportional to the peak overpressure [78]. In addition, severe oxidative damage accompanied by a lower survival rate of hair cells and spiral ganglion neurons were observed in the inner ear. Newman et al. also reported extensive loss of cochlear hair cells and a reduced cochlear outer hair cell function of rats exposed to three low level blast waves (of a 50.4 kPa peak pressure and a sound pressure level of 188 dB) separated by approximately 5 min using a blast tube [79].

Wu et al. used a D-86 spark pulse generator that caused deafness to rats when exposed to a 172 dB sound pressure level for 30 times with 2 s intervals and 0.5 ms pulse width [80]. The study then showed that adenovirus-mediated human β-nerve growth factor has a protective effect on rat cochlear spiral ganglion cells after blast exposure.

13.3.5 Skeletal Blast Trauma & Nerve Injuries

Blast injuries as a result of conventional and improvised explosive devices (IEDs) account for 75 % of modern war injuries. Over 70 % of these injuries involve the limb [81] (see Chap. 21, Sect. 21.1). However, very few animal models have been developed to look at the effects of blast injuries to the skeletal and peripheral nervous system. Christensen et al. exposed cadaveric pigs to semi-controlled free field blast events of varying explosive type charge size, and distance, including some cases with shrapnel. They found extensive skeletal trauma and amputation of the limbs and cranium. Usually, long bone shafts were the most severely fracture, whilst transverse and oblique fractures were commonly noted in the head, neck, and

shaft of numerous ribs. What is of interest is that specimens exposed to blasts that included shrapnel displayed even greater fracture severity, with extreme bone fragmentation of the long bones [82]. This study showed that primary and secondary blast mechanisms can produce traumatic amputations and skeletal fractures, although it is fairly limited in scope. One of its limitations is the fact that only small blast distances and open-air settings were studied. Data from blasts occurring in a confined space would add significant information to this work.

An interesting poly-traumatised model was developed by Claes et al. to investigate the effect of a thoracic trauma and an additional soft-tissue trauma on fracture healing in a rat tibia model. The tibial fracture was created using a 3-point bending guillotine device and a drop tower was used to create additional soft tissue-trauma. Finally, the thoracic trauma was induced by a single blast wave centered on the thorax with a modified blast wave generator. Results confirmed that fracture healing was increasingly impaired with increasing severity of trauma, especially when a soft tissue trauma was applied in addition to the thoracic trauma [83]. The authors explained this effect reporting that in the poly-traumatised animals there was reduced callus formation in comparison to animals with isolated fractures. Although only the thoracic trauma was created using a primary blast set up, such models could be further improved and become very useful in understanding the nature of human polytrauma from blast injuries.

Contrary to central nervous injury that has been extensively studied in blast conditions, peripheral nerve injury has not been addressed despite the significant burden of peripheral nerve damage seen following exposure to blast [84]. Suneson and Seeman used a high-energy missile that impacted to the left thigh of a large animal creating a short lasting shockwave. This shockwave caused immediate contralateral sciatic nerve dysfunction, as revealed by the decreased number of microtubules and the Schwann cells exhibiting signs of damage and swelling, despite demonstrating no haemorrhage or major tissue deformation [85]. In addition, similar changes were noticed in the phrenic nerves as well as in unmyelinated axons in both sciatic and phrenic nerves.

13.4 Summary

Based on the work presented in this chapter it can be seen that *in-vivo* models are widely used to study several aspects of the blast injuries, especially blast traumatic brain injury and blast lung. However, one fundamental question that arises is how can we compare the existing models, the findings from which are often contradictory? When looking into the effects of primary blast for instance, there is significant variability among researchers in the peak overpressures and the duration of the waves used. The majority of the existing models are often vague about the characteristics of the shockwaves produced, in some cases reporting only the peak overpressure and thus limiting comparability between studies [2]. Furthermore, there is also significant variability in the position and orientation of the experimental animal during blast which has an important role in the biomechanical loading on the animal, the injury sustained and its severity [4, 12].

Another significant limitation is associated with the species of the experimental animals used in these studies. Existing large animal models require large scale settings and are often too expensive, thus their use is limited. Large animal models also can have difference ethical considerations associated with their use. More often rodent models, rats and mice in particular, are used. However, even in these cases it has been argued that different strains may exhibit different inflammatory responses to blast [86]. In addition, researchers have also suggested that the rodent's lissencephalic cortex makes them inappropriate for modelling changes in cognition and behaviour after bTBI [12].

A second key question is how do we validate these *in-vivo* models? Due to differences in properties, size and mass between humans and animals, scaling has been proposed and used in several studies. Panzer et al. (2014) recently reviewed a number of different approaches to scaling the dose and response of animal models

to humans. In the majority of the existing scaling techniques the animal's blast duration is scaled to the equivalent human duration while the amplitude of the overpressure remains unchanged [87]. During IED explosion shockwaves with peak pressures from 50 to 1000 kPa and 2–6 ms duration have been measured, whereas most of the experimental models involve blast waves with durations between 4 and 8 ms [2, 4, 17] and some with durations longer than 10 ms [25]. Without considering scaling, the shock wave characteristics of most of the animal models developed are comparable to what has been reported during actual blast conditions. However, when scaling is considered, then these scaled durations are much longer than the ones reported during real blast events [25]. Researchers still debate as to whether scaling methods should be used and if so which are appropriate. To this end more data from real blast events are needed. Finally, the majority of *in-vivo* models tend to replicate only single factors involved in pathology of specific tissue/organs, simplifying the clinical problem. Despite these limitations, animal models have contributed substantially in the interpretation of some of the key injury mechanisms involved in blast injuries. However, more complex models are needed to gain a better understanding of the highly heterogeneous nature of blast injuries.

References

1. Nguyen TTN, Wilgeroth JM, Proud WG. Controlling blast wave generation in a shock tube for biological applications. In: 18th APS-SCCM and 24th AIRAPT, Seattle/Washington, DC.
2. Cernak I, et al. The pathobiology of blast injuries and blast-induced neurotrauma as identified using a new experimental model of injury in mice. Neurobiol Dis. 2011;41(2):538–51.
3. Long JB, et al. Blast overpressure in rats: recreating a battlefield injury in the laboratory. J Neurotrauma. 2009;26(6):827–40.
4. Goldstein LE, et al. Chronic traumatic encephalopathy in blast-exposed military veterans and a blast neurotrauma mouse model. Sci Transl Med. 2012;4:134ra60.
5. Svetlov S, et al. Morphological and biochemical signatures of brain injury following head-directed controlled blast overpressure impact. J Neurotrauma. 2009;26(8):A75.
6. Chavko M, Prusaczyk WK, McCarron RM. Lung injury and recovery after exposure to blast overpressure. J Trauma. 2006;61(4):933–42.
7. Risling M, et al. Experimental studies on mechanisms of blast induced brain injuries. J Neurotrauma. 2009;26(8):A74.
8. Risling M, Davidsson J. Experimental animal models for studies on the mechanisms of blast-induced neurotrauma. Front Neurol. 2012;3(30).
9. Chandra N, et al. Evolution of blast wave profiles in simulated air blasts: experiment and computational modeling. Shock Waves. 2012;22(5):403–15.
10. Skotak M, et al. Rat injury model under controlled field-relevant primary blast conditions: acute response to a wide range of peak overpressures 7. J Neurotrauma. 2013;30(13):1147–60.
11. Mohan K, et al. Retinal ganglion cell damage in an experimental rodent model of blast-mediated traumatic brain injury. Invest Ophthalmol Vis Sci. 2013;54(5):3440–50.
12. Cernak I. Animal models of head trauma. NeuroRx J Am Soc Exp Neurother. 2005;2(3):410–22.
13. Clemedson CJ, Jonsson A. Effects of frequency content in complex air shock-waves on lung injuries in rabbits. Aviat Space Environ Med. 1976;47(11):1143–52.
14. Clemedson CJ. Shock wave transmission to the central nervous system. Acta Physiol Scand. 1956;37(2–3):204–14.
15. Bauman RA, et al. An introductory characterization of a combat-casualty-care relevant swine model of closed head injury resulting from exposure to explosive blast. J Neurotrauma. 2009;26(6):841–60.
16. Risling M, et al. Mechanisms of blast induced brain injuries, experimental studies in rats. Neuroimage. 2011;54:S89–97.
17. Saljo A, et al. Mechanisms and pathophysiology of the low-level blast brain injury in animal models. Neuroimage. 2011;54:S83–8.
18. Bass CR, et al. Brain injuries from blast. Ann Biomed Eng. 2012;40(1):185–202.
19. Cheng JM, et al. Development of a rat model for studying blast-induced traumatic brain injury. J Neurol Sci. 2010;294(1–2):23–8.
20. Rubovitch V, et al. A mouse model of blast-induced mild traumatic brain injury. Exp Neurol. 2011;232(2):280–9.
21. Kuehn R, et al. Rodent model of direct cranial blast injury. J Neurotrauma. 2011;28(10):2155–69.
22. Ogura M, et al. In vivo targeted gene transfer in skin by the use of laser-induced stress waves. Lasers Surg Med. 2004;34(3):242–8.
23. Hatano B, et al. Traumatic brain injury caused by laser-induced shock wave in rats: a novel laboratory model for studying blast-induced traumatic brain injury. Proc SPIE. 2011;7897:78971V.
24. Satoh Y, et al. Pulmonary blast injury in mice: a novel model for studying blast injury in the laboratory using

laser-induced stress waves. Lasers Surg Med. 2010;42 (4):313–8.
25. Panzer MB, Wood GW, Bass CR. Scaling in neurotrauma: how do we apply animal experiments to people? Exp Neurol. 2014;261:120–6.
26. DePalma RG, et al. Current concepts: blast injuries. N Engl J Med. 2005;352(13):1335–42.
27. Crockard HA, et al. An experimental cerebral missile injury model in primates. J Neurosurg. 1977;46:776–83.
28. Finnie JW. Pathology of experimental traumatic craniocerebral missile injury. J Comp Pathol. 1993;108: 93–101.
29. Suneson A, Hansson HA, Seeman T. Peripheral high-energy missile hits cause pressure changes and damage to the nervous-system – experimental studies on pigs. J Trauma. 1987;27(7):782–9.
30. Carey ME, et al. Experimental missile wound to the brain. J Neurosurg. 1989;71(5):754–64.
31. Tan YH, et al. A gross and microscopic study of cerebral injuries accompanying maxillofacial high-velocity projectile wounding in dogs. J Oral Maxillofac Surg. 1998;56(3):345–8.
32. Plantman S, Davidsson J, Risling M. Characterization of a novel model for penetrating brain injury. J Neurotrauma. 2009;26(8):A86.
33. Proctor JL, et al. Rat model of brain injury caused by under-vehicle blast-induced hyperacceleration. J Trauma Acute Care Surg. 2014;77:S83–7.
34. Elder GA, et al. Blast-induced mild traumatic brain injury. Psychiatr Clin North Am. 2010;33(4):757–81.
35. Courtney MW, Courtney AC. Working toward exposure thresholds for blast-induced traumatic brain injury: thoracic and acceleration mechanisms. Neuroimage. 2011;54:S55–61.
36. Phillips YY, Richmond DR. Primary blast injury and basic research: a brief history. In: Textbook of military medicine, Part I, Conventional warfare: ballistic, blast and burn injuries. Washington, DC: Office of the Surgeon General of the US Army; 1990.
37. Andersen P, Loken S. Lung damage and lethality by underwater detonations. Acta Physiol Scand. 1968;72 (1–2):6–14.
38. Tannous O, et al. Heterotopic ossification after extremity blast amputation in a Sprague–Dawley rat animal model. J Orthop Trauma. 2011;25(8):506–10.
39. de Lanerolle NC, et al. Characteristics of an explosive blast-induced brain injury in an experimental model. J Neuropathol Exp Neurol. 2011;70(11):1046–57.
40. Warden D. Military TBI during the Iraq and Afghanistan wars. J Head Trauma Rehabil. 2006;21 (5):398–402.
41. Park E, et al. Electrophysiological white matter dysfunction and association with neurobehavioral deficits following low-level primary blast trauma. Neurobiol Dis. 2013;52:150–9.
42. Pun PBL, et al. Low level primary blast injury in rodent brain. Front Neurol. 2011;2:1–15.
43. Park E, et al. A model of low-level primary blast brain trauma results in cytoskeletal proteolysis and chronic functional impairment in the absence of lung barotrauma. J Neurotrauma. 2011;28(3): 343–57.
44. Gao W, et al. Association between reduced expression of hippocampal glucocorticoid receptors and cognitive dysfunction in a rat model of traumatic brain injury due to lateral head acceleration. Neurosci Lett. 2013;533:50–4.
45. Ikonomovic MD, et al. Alzheimer's pathology in human temporal cortex surgically excised after severe brain injury. Exp Neurol. 2004;190(1):192–203.
46. DeKosky ST, et al. Association of increased cortical soluble A beta(42) levels with diffuse plaques after severe brain injury in humans. Arch Neurol. 2007;64 (4):541–4.
47. De Gasperi R, et al. Acute blast injury reduces brain abeta in two rodent species. Front Neurol. 2012;3 (177):1–17.
48. Garman RH, et al. Blast exposure in rats with body shielding is characterized primarily by diffuse axonal injury. J Neurotrauma. 2011;28(6):947–59.
49. Lighthall JW. Controlled cortical impact: a new experimental brain injury model. J Neurotrauma. 1988;5(1):1–15.
50. Hall KD, Lifshitz J. Diffuse traumatic brain injury initially attenuates and later expands activation of the rat somatosensory whisker circuit concomitant with neuroplastic responses. Brain Res. 2010;1323: 161–73.
51. Singleton RH, et al. Traumatically induced axotomy adjacent to the soma does not result in acute neuronal death. J Neurosci. 2002;22(3):791–802.
52. Singleton RH, Povlishock JT. Diffuse brain injury-mediated neuronal somatic plasmalemmal wounding: a study of the effects of membrane disruption on neuronal reaction and fate. J Neurotrauma. 2003;20 (10):1125.
53. Chavko M, Prusaczyk WK, McCarron RM. Protection against blast-induced mortality in rats by hemin. J Trauma. 2008;65(5):1140–5.
54. Koliatsos VE, et al. A mouse model of blast injury to brain: initial pathological, neuropathological, and behavioral characterization. J Neuropathol Exp Neurol. 2011;70(5):399–416.
55. Rafaels K, et al. Brain injury from primary blast. Brain Inj. 2012;26(4–5):745–6.
56. Cernak I, et al. Involvement of the central nervous system in the general response to pulmonary blast injury. J Trauma. 1996;40(3):S100–4.
57. Bhattacharjee Y. Neuroscience – shell shock revisited: solving the puzzle of blast trauma. Science. 2008;319(5862):406–8.
58. Ning JL, et al. Lung injury following lower extremity blast trauma in rats. J Trauma Acute Care Surg. 2012;73(6):1537–44.

59. Ning JL, et al. Transient regional hypothermia applied to a traumatic limb attenuates distant lung injury following blast limb trauma. Crit Care Med. 2014;42(1): E68–78.
60. Delius M, et al. Biological effects of shock-waves – lung hemorrhage by shock-waves in dogs – pressure-dependence. Ultrasound Med Biol. 1987;13(2): 61–7.
61. Seitz DH, et al. Pulmonary contusion induces alveolar type 2 epithelial cell apoptosis: role of alveolar macrophages and neutrophils. Shock. 2008;30 (5):537–44.
62. Sasser SM, et al. Blast lung injury. Prehosp Emerg Care. 2006;10(2):165–72.
63. Gorbunov NV, et al. Pro-inflammatory alterations and status of blood plasma iron in a model of blast-induced lung trauma. Int J Immunopathol Pharmacol. 2005;18(3):547–56.
64. Rafaels KA, et al. Pulmonary injury risk assessment for long-duration blasts: a meta-analysis. J Trauma. 2010;69(2):368–74.
65. Bass CR, Rafaels KA, Salzar RS. Pulmonary injury risk assessment for short-duration blasts. J Trauma. 2008;65(3):604–15.
66. Chai JK, et al. Role of neutrophil elastase in lung injury induced by burn-blast combined injury in rats. Burns. 2013;39(4):745–53.
67. Chai JK, et al. A novel model of burn-blast combined injury and its phasic changes of blood coagulation in rats. Shock. 2013;40(4):297–302.
68. Elsayed NM. Toxicology of blast over-pressure. Toxicology. 1997;121(1):1–15.
69. Alfieri KA, Forsberg JA, Potter BK. Blast injuries and heterotopic ossification. Bone Joint Res. 2012;1 (8):174–9.
70. Salisbury E, et al. Sensory nerve induced inflammation contributes to heterotopic ossification. J Cell Biochem. 2011;112(10):2748–58.
71. Apel PJ, et al. Effect of selective sensory denervation on fracture-healing an experimental study of rats. J Bone Joint Surg Am. 2009;91A(12): 2886–95.
72. Yano H, et al. Substance-P-induced augmentation of cutaneous vascular-permeability and granulocyte infiltration in mice is mast-cell dependent. J Clin Invest. 1989;84(4):1276–86.
73. Polfer EM, et al. The development of a rat model to investigate the formation of blast-related post-traumatic heterotopic ossification. Bone Joint J. 2015;97-B (4):572–6.
74. Qureshi AT, et al. Early characterization of blast-related heterotopic ossification in a rat model. Clin Orthop Relat Res. 2015;473(9):2831–9.
75. Patterson JH, Hamernik RP. Blast overpressure induced structural and functional changes in the auditory system. Toxicology. 1997;121(1):29–40.
76. Luo H, et al. Blast-induced tinnitus and spontaneous firing changes in the rat dorsal cochlear nucleus. J Neurosci Res. 2014;92(11):1466–77.
77. Mao JC, et al. Blast-induced tinnitus and hearing loss in rats: behavioral and imaging assays. J Neurotrauma. 2012;29(2):430–44.
78. Kurioka T, et al. Characteristics of laser-induced shock wave injury to the inner ear of rats. J Biomed Opt. 2014;19(12):125001.
79. Newman AJ, et al. Low-cost blast wave generator for studies of hearing loss and brain injury: blast wave effects in closed spaces. J Neurosci Methods. 2015;242:82–92.
80. Wu JA, et al. Study of protective effect on rat cochlear spiral ganglion after blast exposure by adenovirus-mediated human beta-nerve growth factor gene. Am J Otolaryngol. 2011;32(1):8–12.
81. Birch R, et al. Nerve injuries sustained during warfare part II: outcomes. J Bone Joint Surg Br. 2012;94B (4):529–35.
82. Christensen AM, et al. Primary and secondary skeletal blast trauma. J Forensic Sci. 2012;57(1):6–11.
83. Claes L, et al. The effect of both a thoracic trauma and a soft-tissue trauma on fracture healing in a rat model. Acta Orthop. 2011;82(2):223–7.
84. Birch R, et al. Nerve injuries sustained during warfare part I – epidemiology. J Bone Joint Surg Br. 2012;94B (4):523–8.
85. Suneson A, Seeman T. Pressure wave injuries to the nervous-system caused by high-energy missile extremity impact.1. Local and distant effects on the peripheral nervous-system – a light and electron-microscopic study on pigs. J Trauma. 1990;30(3):281–94.
86. Bellander BM, et al. Genetic regulation of microglia activation, complement expression, and neurodegeneration in a rat model of traumatic brain injury. Exp Brain Res. 2010;205(1):103–14.
87. Panzer MB, Bass CRD. Human results from animal models: scaling laws for blast neurotrauma. J Neurotrauma. 2012;29(10):A151.

Modelling Blast Brain Injury

14

Rita Campos-Pires and Robert Dickinson

The consequences of blast traumatic brain injury (blast-TBI) in humans are largely determined by the characteristics of the trauma insult and, within certain limits, the individual responses to the lesions inflicted [1]. In blast-TBI the mechanisms of brain vulnerability to the detonation of an explosive device are not entirely understood. They most likely result from a combination of the different physical aspects of the blast phenomenon, specifically extreme pressure oscillations (blast-overpressure wave – primary blast), projectile penetrating fragments (secondary blast) and acceleration-deceleration forces (tertiary blast), creating a spectrum of brain injury that ranges from mild to severe blast-TBI [2]. The pathophysiology of penetrating and inertially-driven blast-TBI has been extensively investigated for many years. However, the brain damage caused by blast-overpressure (primary blast) is much less understood and is unique to this type of TBI [3]. Indeed, there continues to be debate about how the pressure wave is transmitted and reflected through the brain and how it causes cellular damage [4]. No single model can mimic the clinical and mechanical complexity resulting from a real life blast-TBI [3]. The different models, non-biological (*in-silico* or surrogate physical) and biological (*ex-vivo, in-vitro* or *in-vivo*), tend to complement each other.

R. Campos-Pires, MD (✉) • R. Dickinson, BSc, PhD (✉)
Department of Surgery & Cancer, Royal British Legion Centre for Blast Injury Studies, Imperial College London, London, UK
e-mail: r.santos-e-sousa12@imperial.ac.uk; r.dickinson@imperial.ac.uk

14.1 *In-Silico* Models

Computer simulation represents a valuable link between laboratory experiments and the study of human cases (see Chap. 17). These models may provide a better understanding of the damaging mechanisms resulting from the blast wave and may reduce the number of trial-and-error tests involving laboratory animals [4, 5]. A comprehensive computational model of blast TBI should be multidisciplinary and should be validated by data from animal tests [5, 6].

14.2 *Ex-Vivo* Models

Human cadaveric models (see Chap. 11) have been used to determine the anatomical response to blast-TBI [7]. However, the biomechanical properties may be altered *post mortem* and the models lack the post-injury physiological response [7]. Through the understanding of the biomechanics of the forces that act upon the human head, these models provide valuable information for the development of protective equipment and helmets [8].

A.M.J. Bull et al. (eds.), *Blast Injury Science and Engineering: A Guide for Clinicians and Researchers*,
DOI 10.1007/978-3-319-21867-0_14

14.3 *In-Vitro* Models

In-vitro models offer several advantages in the study of blast-TBI, allowing for a carefully controlled experimental environment, both in terms of cellular characteristics and regarding physiologic conditions, such as temperature, pH and nutrient concentrations, which reduce experimental variation and result in greater reproducibility. The time scale for the completion of *in-vitro* studies is usually shorter than for *in-vivo* experimental protocols, making them less expensive than more complex models. The *in-vitro* models also permit a precise control and characterisation of the injury biomechanics. Arun and colleagues have described an *in-vitro* model using human neuroblastoma cells exposed to a pressure wave from a compressed air-driven shock tube [9]. They showed a transient increase in the permeability of neuronal nuclear and plasma membranes. The authors suggest that the blast exposure disturbs the integrity of the cell membrane and hypothesised that this may underlie the development of acute tissue damage seen in blast-TBI victims. Simple cellular models lack the heterogeneity of cell types and synaptic connectivity found in the intact brain. The *in-vitro* organotypic brain-slice culture technique represents an intermediate model between the single cell and the whole organ. A thin slice of brain tissue can be kept alive *in-vitro* for many days or even months, preserves the different cell types (e.g. neurons and glia) and maintains synaptic connectivity mirroring that in the intact brain [10]. Organotypic hippocampal slice culture models have been used to investigate mechanisms of injury in other types of brain injury including blunt-traumatic brain injury and ischemic brain injury [11, 12]. Effgen and colleagues have recently demonstrated that a shock wave from a compressed air shock tube induces cell dysfunction and death in hippocampal organotypic slice cultures [13, 14]. Nevertheless, in spite of the aforementioned advantages, *in-vitro* models are relatively simple biologic systems of cells or tissue that do not fully mirror the *in-vivo* situation. Cultures are typically obtained from young animals whose cells may not be fully differentiated, and may exhibit a different phenotype from the mature tissue. Moreover, the artificial controlled environment is not the same as the cells experience *in-vivo* and this can affect their morphology and function. Therefore, novel *in-vitro* findings must be validated and confirmed by *in-vivo* tests in whole animals. Thus, while *in-vitro* models are a powerful tool for mechanistic analysis and a convenient, cost-effective method of screening, they cannot completely replace animal studies.

14.4 *In-Vivo* Animal Models

Animal models (see Chap. 13) are the gold standard translational research method for blast-TBI, allowing hypothesis testing in the controlled laboratory environment [15, 16]. Despite the usefulness of human clinicopathological analysis in providing evidence of correlative association, the use of animal models is the most important tool in investigating causal mechanisms of disease [16]. An animal model's value and relevance are directly proportional to its adequacy in recapitulating the histopathological features and/or neurological deficits of the corresponding human disorder [16]. Irrespective of the research questions to be addressed, a clinically relevant blast-TBI model should fulfil the following criteria [17]:

1. the injurious mechanical component of the blast should be clearly identified and replicated in a controlled, reproducible, and quantifiable manner;
2. the inflicted injury should be reproducible, quantifiable, and mimic components of human blast-TBI;
3. the injury outcome should be chosen based on morphological or histological and/or behavioural parameters; and

4. the mechanical properties of the injurious pressure wave should predict the outcome severity.

A considerable number of animal models have been used in blast-TBI research. In the following paragraphs, critical aspects of blast-TBI models will be described based on the available literature.

14.4.1 Animal Species

Blast-TBI models have used many different species of animals, from mice, rats and rabbits to ferrets and pigs [7]. Rodents, mainly rats, remain the most commonly used animals for modelling human blast-TBI [17]. The relatively small size and lower cost of rodents permits repetitive measurements of relevant experimental parameters that require relatively large numbers of animals. Rat models allow better monitoring and control of physiological parameters (e.g. blood pressure, blood gases). Mice offer the additional possibility of conducting tests where genetic manipulation is possible. Due to ethical, technical and/or financial limitations, blast-TBI studies are less feasible in phylogenetically higher species [17]. However, rodents have a lissencephalic cortex, i.e. they lack the gyri and sulci found in the human brain; it has been suggested that this characteristic makes rodents less than ideal for modelling complex injury-induced changes in functional outcomes and is a factor that most likely affects the brain's mechanical response to a pressure transient and an acceleration impulse [18]. Pigs and non-human primates have brains more similar to humans. However the cost of larger animal models and, in the case of non-human primates, ethical issues and availability, limit their use [19]. The choice of a species also affects scaling considerations, namely the selection of the pressure wave parameters. Skull size and geometry (including the anatomy of the orbits and sinuses), skull biomechanical properties and histologic characteristics of bone affect how external forces act upon the brain [4].

14.4.2 Generation of Overpressure Waves

14.4.2.1 Free-Field Explosives

In free-field blast testing, blast waves are generated using high explosives in an open field (Fig. 14.1a). Experiments with explosives in the open field have been used to determine thresholds of mortality and injuries in air-filled organs, such as the lungs. These experiments provided fundamental data on blast magnitude-response curves (the Bowen curves) [6, 20, 21]. Free-field explosive tests allow realistic experiments in large animals that are more similar in size to humans, closely replicating real-world blast conditions [6]. There are, nonetheless, some significant drawbacks. Large adjacent structures such as buildings or vehicles can reflect the pressure wave, potentially exposing the specimen to a complex blast waveform, often more damaging than the initial waveform. The explosives produce by-products (e.g. heat, noxious gases, fragments), which summed to the overpressure damage may cause complex blast injuries due to the possibility of penetrating and burn injuries for example [7]. To summarise, this setup offers less experimental control over the physical characteristics of the blast (when compared to a shock tube, see below), making it more difficult to quantify the overpressure transient and represents an expensive and time consuming protocol [7, 19].

14.4.2.2 Blast Tubes

During the 1950s blast tubes were often used to study materials' responses to high pressures. The blast tube (see Chap. 13) was modified for studies with rodents in the 1990s [6]. A small explosive charge is detonated in a conical or parabolic driver section, and the blast wave is allowed to propagate down the driven section (Fig. 14.1b). By-products of the explosion, such as smoke and gases, may contribute to quaternary blast effects [6]. Also, the handling and storage of explosives in the laboratory environment demands strict safety considerations. For these reasons, shock tubes are typically preferred over blast tubes for blast-TBI testing in the laboratory setting [7].

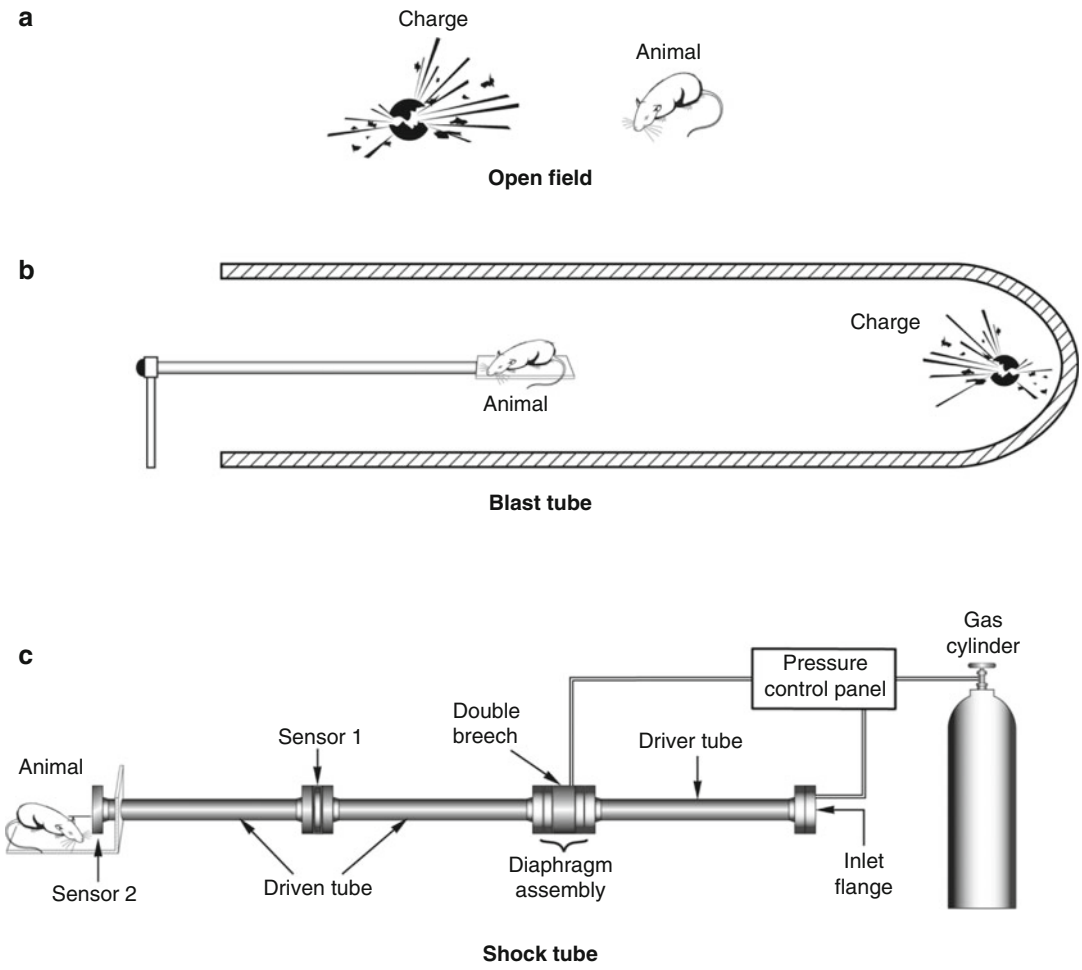

Fig. 14.1 Different methods of generating blast overpressure waves in *in-vivo* models of blast injury. (**a**) Open field experiments using an explosive charge outside of a laboratory. (**b**) In a laboratory setting a blast tube can be used with an explosive charge. (**c**) In the laboratory, a gas-driven shock-tube results in a more reproducible and controlled shock wave

14.4.2.3 Shock Tubes

Most published blast studies have used shock tubes to investigate the effect of blast-TBI using animal models [4]. A shock tube (see Chap. 13) is a long tube with constant cross-section (Fig. 14.1c). The device is divided into two chambers separated by a membrane or diaphragm: the driver section of high-pressure gas and the driven or main section of low pressure gas (atmospheric pressure). Compressed gas (typically air, helium or nitrogen) is loaded into the driver section. The diaphragm either ruptures spontaneously, or rupture may be triggered electronically (in so called "double breach" configuration), at a given pressure dependent on diaphragm thickness and material. Upon rupture of the diaphragm, the discontinuous pressure differential between the driver section and the driven section creates a shock wave that propagates along the driven section towards the test specimen [6, 7]. With an open-end configuration the animal or specimen can be placed either inside or outside the tube. Testing inside the tube ensures that the shock wave is planar, but the diameter of the

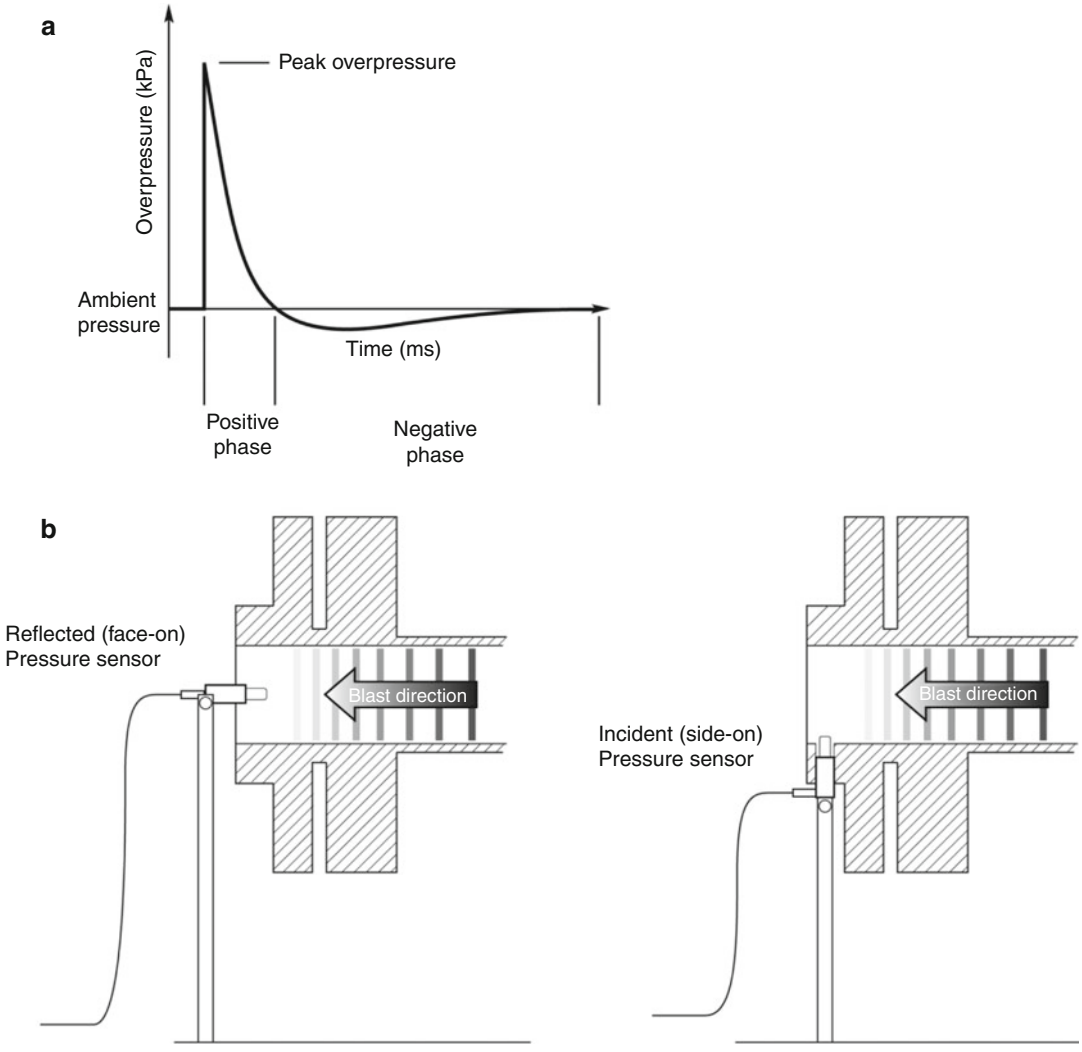

Fig. 14.2 (**a**) Schematic of a typical Friedlander waveform produced in a shock-tube experiment. (**b**) The magnitude of the peak-overpressure for a given shock wave depends on the orientation of the pressure sensor relative to the shock wave, with face-on configuration giving a higher value than a side-on configuration

shock tube must be large enough for the specimen. Outside the tube, the specimen should be placed as close to the tube as possible, to ensure the shock wave is planar [7]. Shock tubes can be designed to reproduce any characteristic of an ideal blast wave in terms of magnitude of peak overpressure, duration of positive-phase, impulse and shape of the pulse [6, 7].

The shock tube has several advantages over the use of high explosives. Shock tubes allow blast overpressure effects to be studied in isolation. Shock tubes can produce a variety of repeatable pressure transients that closely resemble free-field blast waves, in a controlled laboratory environment (Fig. 14.2a). Furthermore, shock tube testing is more economical and safe compared to either free-field blast or blast tube testing. However, shock tubes can only reproduce certain aspects of real-life explosions; while they replicate the ideal pressure wave, they cannot

model the non-ideal complex blast wave and they are unable to reproduce other real blast effects such as thermal injury [7, 19].

14.4.3 Critical Aspects

14.4.3.1 Anaesthesia and Analgesia

Most authors anaesthetise their animals before and during the pressure wave exposure (an exception is Ahlers and colleagues [22]). Different methods of anaesthesia have been used, the majority allowing the animals to be under spontaneous ventilation during the procedure. Inhalation general anaesthetics, such as isoflurane, are often used due to their advantages of providing effective anaesthesia with rapid onset and rapid recovery at the end of the protocol [23, 24]. These drugs may be supplemented with an opioid-based analgesia (for example, buprenorphine). Another common choice is the administration of intraperitoneal drugs, as the combination of ketamine and xylazine [24, 25]. This method requires less equipment than an inhalational anaesthesia technique, has the advantage of providing concurrent analgesia (ketamine) but it is less versatile in terms of anaesthetic induction and recovery times. Anaesthetics are usually potent respiratory and cardiovascular depressants, so the researchers using them need to be familiar with their side-effects. Some particular anaesthetic side-effects should also be considered carefully according to the goal of the experimental protocol. For example, some drugs, such as medetomidine, induce profound hypothermia [26], while others, such as ketamine, may modify neurological impairment [27], which are aspects that should be taken into account in blast-TBI studies of neuroprotection.

14.4.3.2 Pressure Wave Characteristics

The characteristics of the pressure wave are determined by the device used and in the case of a shock tube, by the thickness, material and number of the diaphragm(s) used. Animals have been exposed to blast waves as low as 36 kPa [15] or as high as 500 kPa [28], but typically are exposed to blast waves with peak overpressures between 150 and 340 kPa [17]. The overpressure wave is sustained for varying durations of time, typically from 2 to 10 ms [28, 29]. The magnitude of the peak overpressure and wave duration used should be based on the severity of the injury being modelled (mild, moderate or severe blast-TBI) and should take into account the hypothesis being tested [15]. An important consideration is that the reported characteristics of a given overpressure wave depend on the orientation of the pressure sensor relative to the wave (Fig. 14.2b). For example, the face-on peak-overpressure reading of a shock wave will be higher than a side-on reading for the same wave [7].

14.4.3.3 Animal Head Orientation Relative to the Direction of the Pressure Wave

The amplitude and duration of the pressure wave to which the animal brain is exposed depends on the orientation of the animal relative to the pressure device [15]. Different orientations of experimental animals relative to the direction of the pressure wave have been reported. The most common are the frontal or head-on orientation in which the animal faces the source of the pressure wave and the transverse or side-on orientation in which the body of the animal is perpendicular to the source of the pressure wave (Fig. 14.3). The frontal orientation results in greater overpressure exposure than does the side-on orientation [25]. However, Ahlers and colleagues reported different functional outcomes based on orientation in the shock tube, including greater impairment in gross motor function for rats in the side-on position [22].

14.4.3.4 Head Mobile *Versus* Head Restrained

Several recent studies have highlighted the value of investigating how the presence or absence of head motion affects histopathologic injury patterns and neurobehavioural deficits. Goldstein and colleagues [30] reported learning and memory deficits in mice with unrestrained heads exposed to a blast wave. Notably, restrained head movement resulted in the

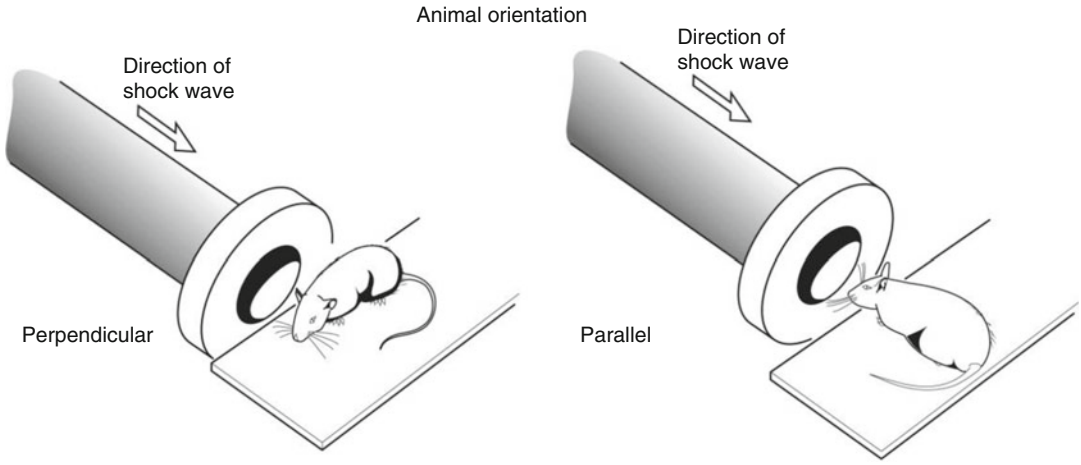

Fig. 14.3 The orientation of the animal relative to the shock-tube is a key variable in the experimental setup. Shown are perpendicular (or side-on) (**a**) and parallel (or head-on) (**b**) configurations

disappearance of functional deficits, implicating blast-induced acceleration–deceleration of the head ("bobblehead effect") as the main pathogenic mechanism by which the blast exposure induces brain injury [30]. Gullotti and colleagues [29] have shown that minimising head acceleration led to an increase in survival rate and an decrease in the duration of loss of righting reflex following blast. However, increase in duration of loss of righting reflex was achieved by significantly increasing the peak blast overpressure [29]. When planning the experimental design of a blast-TBI study and interpreting its results the head mobility is a very important feature of the protocol that must be considered according to the intended goals of the study.

14.4.3.5 Head Only Blast Exposure (Thorax Protection) *Versus* Whole Body Blast Exposure (No Thorax Protection)

Some investigators use chest protection on their animals arguing that the use of appropriate shielding isolates the effects of blast injury to the brain from injury to the body, particularly the lung. Different materials have been used, such as Kevlar fabric [23], plastic tubes [28] or metal cylinders [29, 31]. A considerable number of blast-TBI investigators do not use chest protection [24, 32, 33]. Long and colleagues reported that rats wearing protective vests when exposed to 126 or 147 kPa overpressure were more likely to survive 24 h after the procedure compared with rats not wearing vests [23]. Some investigators have examined the use of protective shields on animals placed inside the shock tube and found that their use does not significantly reduce the effects of the pressure wave [15, 25].

14.4.3.6 Single Blast *Versus* Repeated Blasts

Most of the experimental blast-TBI studies published so far have used protocols consistent with single blast exposure. However, multiple blast exposures are common in the war zones even in subjects not known to have suffered a TBI [19]. Repetitive blast exposure in military service personnel has been associated with long term neuropathology and psychiatric disturbances, including cognitive impairment similar to what is seen in athletes with repetitive concussive injury [34, 35]. These findings suggest that repeated blast overpressure waves, blast secondary or tertiary mechanisms excluded, have a synergistic effect causing cumulative brain damage, as shown by Calabrese and colleagues [36].

14.4.3.7 Outcomes

Outcomes relevant in animal models include physiological, pathological and behavioural

parameters [19]. Animal models of blast-TBI will be more useful from a translational perspective if the experimental emphasis focuses on reproduction of clinically relevant endpoints, accelerating the development of new preventive, diagnostics, treatment and rehabilitative strategies for blast-TBI victims [16]. Blood-brain barrier disruption, brain oedema and vasospasm, neuronal degeneration, axonal injury, glial cell activation, chronic neuroinflammation and subsequent cognitive deficits, including memory impairment and anxiety-related behaviours have been shown both after human and experimental blast-TBI [16, 17, 37, 38]. An additional aspect that is usually overlooked by many investigators studying TBI models is the measurement of physiological variables before and after blast-TBI, including arterial blood oxygen and carbon dioxide partial pressures, pH, heart rate, blood pressure, and core body temperature. These variables are extremely important in determining pathophysiological responses to injury and therapy, both for acute outcomes and long-term outcomes [39].

Although overlapping clinical features of blast TBI models and related findings in humans suggest common pathobiology, the underlying pathophysiological mechanisms and interactions are poorly understood. Furthermore, the temporal course of the acute and chronic stages following blast-TBI injury is largely unknown [16]. One aspect of particular note is that blast-TBI patients often present with cognitive and anxiety-related symptoms similar to those resulting from post-traumatic stress disorder (PTSD). In these blast-TBI patients it can be difficult to disentangle symptoms resulting from the physical blast and those related to being in the stressful environment of combat or civilian blast situation. In a controlled laboratory environment where the animal is anaesthetised it should be possible to study isolated blast-TBI with minimal confounding PTSD pathophysiology. Together these aspects emphasise the importance and clinical relevance of developing reproducible validated animal models that can be used to understand the mechanisms of brain injury following exposure to blast.

14.5 Conclusion

A broad range of experimental animals and models are being used in blast-TBI research. Early models focused mainly on biomechanical aspects of brain injury, while more recent ones are targeted towards improving the understanding of the damaging injury processes initiated by blast-TBI [17]. However, translational research in this area has been fraught by a number of methodological issues. The shock tube devices (or alternative methods) and blast injury conditions, as well as specimen or animal mounting, degree of head restraint and location relative to the driven section can vary significantly between different laboratories. Blast waves are characterised by several parameters including the peak overpressure, duration and impulse. Different shock tubes may produce pressure waves with differing characteristics leading to different biological effects. Many studies do not report the full pressure wave data, or report only peak overpressures, but not duration or impulses. Some laboratories that do report pressures omit key setup information, such as the pressure sensor orientation. This makes interpretation and comparison between studies extremely difficult. Blast TBI is particularly challenging due to scarce exposure data from actual operational/clinical situations [18]. Reliable *in-vivo* blast-TBI experimental studies, complemented by *in-silico* and *in-vitro* models, led by multidisciplinary teams, are of great importance not only in the identification of the complex mechanisms leading to short and long-term functional deficits, but also in guiding novel approaches to diagnosis and treatment modalities.

References

1. Maas AIR, Stocchetti N, Bullock R. Moderate and severe traumatic brain injury in adults. Lancet Neurol. 2008;7:728–41.
2. Hicks RR, Fertig SJ, Desrocher RE, Koroshetz WJ, Pancrazio JJ. Neurological effects of blast injury. J Trauma. 2010;68:1257–63.

3. Chen YC, Smith DH, Meaney DF. In-vitro approaches for studying blast-induced traumatic brain injury. J Neurotrauma. 2009;26:861–76.
4. Nakagawa A, Manley GT, Gean AD, Ohtani K, Armonda R, Tsukamoto A, Yamamoto H, Takayama K, Tominaga T. Mechanisms of primary blast-induced traumatic brain injury: insights from shock-wave research. J Neurotrauma. 2011;28: 1101–19.
5. Gupta RK, Przekwas A. Mathematical models of blast-induced TBI: current status, challenges, and prospects. Front Neurol. 2013;4:59.
6. Risling M, Davidsson J. Experimental animal models for studies on the mechanisms of blast-induced neurotrauma. Front Neurol. 2012;3:30.
7. Bass CR, Panzer MB, Rafaels KA, Wood G, Shridharani J, Capehart B. Brain injuries from blast. Ann Biomed Eng. 2012;40:185–202.
8. Yoganandan N, Stemper BD, Pintar FA, Maiman DJ. Use of postmortem human subjects to describe injury responses and tolerances. Clin Anat. 2011;24: 282–93.
9. Arun P, Spadaro J, John J, Gharavi RB, Bentley TB, Nambiar MP. Studies on blast traumatic brain injury using in-vitro model with shock tube. Neuroreport. 2011;22:379–84.
10. Bahr BA. Long-term hippocampal slices: a model system for investigating synaptic mechanisms and pathologic processes. J Neurosci Res. 1995;42: 294–305.
11. Banks P, Franks NP, Dickinson R. Competitive inhibition at the glycine site of the N-methyl-D-aspartate receptor mediates xenon neuroprotection against hypoxia-ischemia. Anesthesiology. 2010; 112:614–22.
12. Harris K, Armstrong SP, Campos-Pires R, Kiru L, Franks NP, Dickinson R. Neuroprotection against traumatic brain injury by xenon, but Not argon, is mediated by inhibition at the N-methyl-D-aspartate receptor glycine site. Anesthesiology. 2013;119 (5):1137–48.
13. Effgen GB, Hue CD, Vogel 3rd E, Panzer MB, Meaney DF, Bass CR, Morrison 3rd B. A multiscale approach to blast neurotrauma modeling: part II: methodology for inducing blast injury to in vitro models. Front Neurol. 2012;3:23.
14. Effgen GB, Vogel 3rd EW, Lynch KA, Lobel A, Hue CD, Meaney DF, Bass CR, Morrison 3rd B. Isolated primary blast alters neuronal function with minimal cell death in organotypic hippocampal slice cultures. J Neurotrauma. 2014;31:1202–10.
15. Yarnell AM, Shaughness MC, Barry ES, Ahlers ST, McCarron RM, Grunberg NE. Blast traumatic brain injury in the rat using a blast overpressure model. Curr Protoc Neurosci/editorial board, Jacqueline N Crawley [et al]. (2013) Chapter 9:Unit 9 41.
16. Goldstein LE, McKee AC, Stanton PK. Considerations for animal models of blast-related traumatic brain injury and chronic traumatic encephalopathy. Alzheimers Res Ther. 2014;6:64.
17. Cernak I. Animal models of head trauma. NeuroRx. 2005;2:410–22.
18. Cernak I. Blast-induced neurotrauma models and their requirements. Front Neurol. 2014;5:128.
19. Elder GA, Stone JR, Ahlers ST. Effects of low-level blast exposure on the nervous system: is there really a controversy? Front Neurol. 2014;5:269.
20. Bowen IG, Fletcher ER, Richmond DR. Estimate of man's tolerance to the direct effetcs of air blast. DASA-2133 Lovelace for Medical Education and Reaserch, NM; 1968. p. 1–44.
21. White CS, Bowen IG, Richmond DR. Biological tolerance to air blast and related biomedical criteria. CEX Rep Civ Eff Exerc. 1965;CEX-65.3:1–239.
22. Ahlers ST, Vasserman-Stokes E, Shaughness MC, Hall AA, Shear DA, Chavko M, McCarron RM, Stone JR. Assessment of the effects of acute and repeated exposure to blast overpressure in rodents: toward a greater understanding of blast and the potential ramifications for injury in humans exposed to blast. Front Neurol. 2012;3:32.
23. Long JB, Bentley TL, Wessner KA, Cerone C, Sweeney S, Bauman RA. Blast overpressure in rats: recreating a battlefield injury in the laboratory. J Neurotrauma. 2009;26:827–40.
24. Sosa MA, De Gasperi R, Paulino AJ, Pricop PE, Shaughness MC, Maudlin-Jeronimo E, Hall AA, Janssen WG, Yuk FJ, Dorr NP, Dickstein DL, McCarron RM, Chavko M, Hof PR, Ahlers ST, Elder GA. Blast overpressure induces shear-related injuries in the brain of rats exposed to a mild traumatic brain injury. Acta Neuropathol Commun. 2013;1:51.
25. Chavko M, Watanabe T, Adeeb S, Lankasky J, Ahlers ST, McCarron RM. Relationship between orientation to a blast and pressure wave propagation inside the rat brain. J Neurosci Methods. 2011;195:61–6.
26. Sinclair MD. A review of the physiological effects of alpha2-agonists related to the clinical use of medetomidine in small animal practice. Can Vet J. 2003;44:885–97.
27. Wang C, Liu F, Patterson TA, Paule MG, Slikker Jr W. Preclinical assessment of ketamine. CNS Neurosci Ther. 2013;19:448–53.
28. Turner RC, Naser ZJ, Logsdon AF, DiPasquale KH, Jackson GJ, Robson MJ, Gettens RT, Matsumoto RR, Huber JD, Rosen CL. Modeling clinically relevant blast parameters based on scaling principles produces functional & histological deficits in rats. Exp Neurol. 2013;248:520–9.
29. Gullotti DM, Beamer M, Panzer MB, Chen YC, Patel TP, Yu A, Jaumard N, Winkelstein B, Bass CR, Morrison B, Meaney DF. Significant head accelerations can influence immediate neurological impairments in a murine model of blast-induced traumatic brain injury. J Biomech Eng. 2014;136:091004.

30. Goldstein LE, Fisher AM, Tagge CA, Zhang XL, Velisek L, Sullivan JA, Upreti C, Kracht JM, Ericsson M, Wojnarowicz MW, Goletiani CJ, Maglakelidze GM, Casey N, Moncaster JA, Minaeva O, Moir RD, Nowinski CJ, Stern RA, Cantu RC, Geiling J, Blusztajn JK, Wolozin BL, Ikezu T, Stein TD, Budson AE, Kowall NW, Chargin D, Sharon A, Saman S, Hall GF, Moss WC, Cleveland RO, Tanzi RE, Stanton PK, McKee AC. Chronic traumatic encephalopathy in blast-exposed military veterans and a blast neurotrauma mouse model. Sci Transl Med. 2012;4:134ra60.
31. Budde MD, Shah A, McCrea M, Cullinan WE, Pintar FA, Stemper BD. Primary blast traumatic brain injury in the rat: relating diffusion tensor imaging and behavior. Front Neurol. 2013;4:154.
32. Readnower RD, Chavko M, Adeeb S, Conroy MD, Pauly JR, McCarron RM, Sullivan PG. Increase in blood–brain barrier permeability, oxidative stress, and activated microglia in a rat model of blast-induced traumatic brain injury. J Neurosci Res. 2010;88:3530–9.
33. Elder GA, Dorr NP, De Gasperi R, Gama Sosa MA, Shaughness MC, Maudlin-Jeronimo E, Hall AA, McCarron RM, Ahlers ST. Blast exposure induces post-traumatic stress disorder-related traits in a rat model of mild traumatic brain injury. J Neurotrauma. 2012;29:2564–75.
34. McKee AC, Cantu RC, Nowinski CJ, Hedley-Whyte ET, Gavett BE, Budson AE, Santini VE, Lee HS, Kubilus CA, Stern RA. Chronic traumatic encephalopathy in athletes: progressive tauopathy after repetitive head injury. J Neuropathol Exp Neurol. 2009;68:709–35.
35. Peskind ER, Petrie EC, Cross DJ, Pagulayan K, McCraw K, Hoff D, Hart K, Yu CE, Raskind MA, Cook DG, Minoshima S. Cerebrocerebellar hypometabolism associated with repetitive blast exposure mild traumatic brain injury in 12 Iraq war Veterans with persistent post-concussive symptoms. Neuroimage. 2011;54 Suppl 1:S76–82.
36. Calabrese E, Du F, Garman RH, Johnson GA, Riccio C, Tong LC, Long JB. Diffusion tensor imaging reveals white matter injury in a rat model of repetitive blast-induced traumatic brain injury. J Neurotrauma. 2014;31:938–50.
37. Kovacs SK, Leonessa F, Ling GS. Blast TBI models, neuropathology, and implications for seizure risk. Front Neurol. 2014;5:47.
38. Kamnaksh A, Kovesdi E, Kwon SK, Wingo D, Ahmed F, Grunberg NE, Long J, Agoston DV. Factors affecting blast traumatic brain injury. J Neurotrauma. 2011;28:2145–53.
39. Xiong Y, Mahmood A, Chopp M. Animal models of traumatic brain injury. Nat Rev Neurosci. 2013;14:128–42.

Military Wound Ballistics Case Study: Development of a Skull/Brain Model

15

Debra J. Carr and Stephen Champion

15.1 Introduction

Penetration of the cranium typically results in secondary projectile formation (bone and primary projectile fragments); the formation of a temporary cavity and resulting increase in internal pressure which is enhanced by the confined space of the cranium and the stiff bones of the skull [1]. This enhanced internal pressure can result in fractures of the base of the cranium, because it is not as strong as other parts of the skull [1]. Radial fractures are typical at the impact point, but concentric fractures can also occur connecting the radial cracks due to flexing of the skull. This through-thickness failure is commonly referred to as cratering [2–4]. Bullet wipe is reported on the scalp in forensic case studies e.g. [2–4]. The fact that bullet wipe can be identified to specific bullets is of interest forensically when investigating attempted murder or murder incidents in civilian and military scenarios [5].

In combat, head wounds are recognised as accounting for substantial mortality and morbidity; the head accounts for 9 % of the human body, 20 % of penetrating combat injuries and its wounding accounts for 50 % of combat deaths [6]. The major cause of injury during warfare is from fragments and therefore, military helmets are designed to protect from fragments; when they are perforated it is most commonly by high kinetic energy projectiles e.g. high-velocity rifle bullets or fragments due to blast (secondary blast) [7–10].

While a number of models for bullet/fragment-head impact recreations have been proposed, these are not anatomically correct e.g. [3, 4, 11]. The models include a polyurethane sphere filled with 10 % gelatine conditioned at 4 °C [3], a cylinder composed of a plastic/ wood/ polymer outer filled with gelatine [4] and polymeric spheres containing 10 % gelatine [11]. These models reportedly compared well to actual gunshot injuries or secondary blast injuries; however, it would not be possible to mount a helmet on them.

Literature describing ballistic rate impacts on human skulls with or without a simulated brain is sparse [2, 12, 13]. In 1970, Miller reported on the penetration of skulls by steel cubes and spheres,

This section draws heavily on a published paper and is reproduced with permission by Springer: Carr DJ, Lindstrom A, Jareborg A, Champion S, Waddell JN, Miller D, Teagle M, Horsfall I, Kieser J. Development of a skull/brain model for military wound ballistics studies. *Int J Leg Med*. 2014. doi:10.1007/s00414-014-1073-2 (License number: 3563580567511, 7 Feb 2015).

D.J. Carr, CEng, FIMMM, MCSFS (✉)
Impact and Armour Group, Centre for Defence Engineering, Cranfield University at the Defence Academy of the United Kingdom, Shrivenham SN6 8LA, UK
e-mail: d.j.carr@cranfield.ac.uk

S. Champion
Vehicles and Weapons Group, Centre for Defence Engineering, Cranfield University at the Defence Academy of the United Kingdom, Shrivenham SN6 8LA, UK

A.M.J. Bull et al. (eds.), *Blast Injury Science and Engineering: A Guide for Clinicians and Researchers*,
DOI 10.1007/978-3-319-21867-0_15

Table 15.1 Summary of Watkins' work [13]

Specimen	Test details	Outcome
	1.045 g ball bearing Impact location side of head	
n = 3	~370 m/s	Penetrated skull (n = 1 perforated skull, 72 J deposited)
n = 3	~750 m/s	Perforated skull, 250 J deposited, "significant damage"
n = 3	~1000 m/s	Perforated skull, 440 J deposited, "severe damage"
n = 1	7.62 mm ball (no further details)	Perforated skull, 351 J deposited, damage in between 750 and 1000 m/s ball bearings

Table 15.2 Pertinent examples from the literature of penetrating injury to the head

Reference	Scenario	Outcome
Fenton et al. [2]		
Case 1	303 (no further details) Contact shot mouth	Extensive fractures to the facial and frontal bones Occipital remained whole but removed from the remaining skull Fractures to the base 36 relatively large bone pieces (observation from the images provided)
Case 2	303 (no further details) Contact shot mouth	Similar to case 1 except occipital fractured into multiple pieces
Betz et al. [14] 4 cases	243 Winchester and 7.62 mm (no further details) Contact shots temporal, mouth, sub-mental region	Completely perforated and fractured skull Ejected brain as a result of the vault exploding (Krönlein shot)

this government report is not accessible in the open literature. However, some of Miller's data are mentioned in another report which describes a model for projectiles impacting skulls [12]. The fact that dried skulls and fresh skull caps performed differently, and the need to consider the additional contribution of hair and the scalp in live human impacts with respect to these projectiles were noted [12]. Some early work that is easily accessible was published by Watkins et al. [13]. Watkins used dried Asiatic[1] skulls filled with 20 % gelatine and covered with two layers of chamois covered in gelatine (no details of the chamois were provided and presumably the gelatine used was 20 % by mass). Watkins' work included a series of nine impacts; the majority of this work involved ball bearings at velocities up to ~1000 m/s, but Watkins did note one head was tested with a 7.62 mm ball round (no further details given) at 750 m/s (Table 15.1).

Reports on penetrating ballistic head injuries in the forensic literature are dominated by case studies of suicides; the penetrating ammunition usually being .22 rimfire or shotgun. There are some exceptions that report outcomes of interest to the current work [2, 14] (Table 15.2). Analysis of skull fracture patterns resulting from self-inflicted gunshot injury identified key patterns of injury including the formation of linear fractures and fragmentation with reference to the anatomical structures of the skull [2]. A further interesting study that includes a high-velocity rifle impact considers the reconstruction of the head after injury and does not discuss skull fractures [15].

The aim of this work summarised here was to develop an anatomically correct skull and brain model for use in military wound ballistic studies incorporating helmets.

[1] Watkins' terminology.

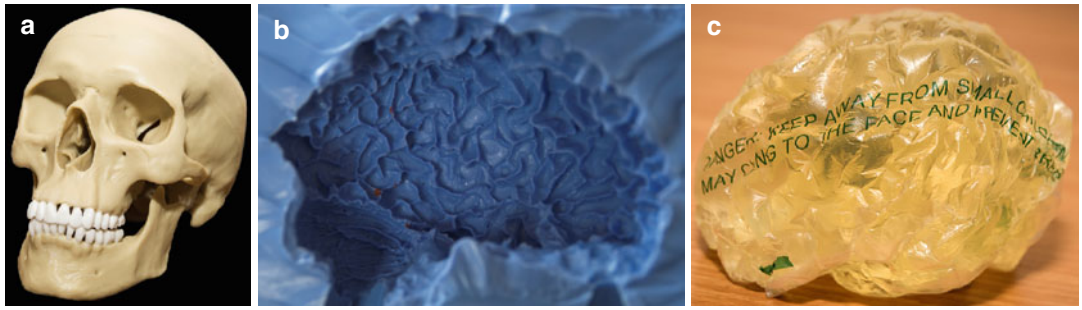

Fig. 15.1 Model elements. (**a**) Skull. (**b**) One half of brain mould. (**c**) Cast brain

15.2 Materials and Methods

Anatomically correct polyurethane skulls were manufactured from rapid prototype data obtained by 3D mapping of both the internal and external surfaces of a human skull (Fig. 15.1a). The polyurethane used to manufacture the skulls had a hardness of 85 Shore D, a tensile strength of 70 MPa and an impact strength of 10 kJ/m^2. Tensile strength of bone from human skulls has been reported to be 225 MPa. However, these properties are reported for quasi-static rates; as testing conducted on the polymeric skulls was at ballistic strain rates, the difference in these mechanical properties is not critical, although further work should explore these differences at the appropriate loading rates.

A two-part silicone mould made from a human brain was used to cast 10 % (by mass) gelatine brains (Fig. 15.1b); 10 % gelatine was chosen as the density was similar to reported values for human brain tissue [16]. A thin polymeric bag was inserted into the brain mould and gelatine poured in, the gelatine was allowed to set for 24 h and then conditioned at 4 °C for 24 h [17, 18]. The polymeric bag was softened by the warm gelatine and thus excellent definition of the mould surface was achieved; additionally, the polymeric bag acted as a representation of the meninges (Fig. 15.1c).

Models were shot using 7.62 × 39 mm M43 ball (Chinese, mild steel core, Factory 71 made in 1984) ammunition at a range of 10 m from a No. 3 Enfield proof mount fitted with an AK-47 barrel (Table 15.3). Projectile velocity was tracked using a Weibel Doppler, and impacts filmed using a Phantom V12 high-speed video; projectiles were soft-captured after model perforation using a PermaGel^{TM} block.

Fractured skull pieces were collected and weighed post ballistic testing. Skull pieces showing signs of bullet wipe and bullets soft-captured after skull perforation were subjected to further analysis. The presence and distribution of inorganic residues was confirmed by using scanning electron microscopy coupled with energy-dispersive x-ray spectroscopy (SEM EDS).

15.3 Results and Discussion

Mean projectile impact velocity was 675 m/s (s.d. = 6 m/s). All skulls were perforated as intended. Bullet impact wounds demonstrated cratering damage with radial cracks. Inorganic residues representative of bullet wipe were found at impact sites. Results are presented in Table 15.3 and a typical impact sequence is presented in Fig. 15.2.

Without a 'brain' (skulls 1 and 2), minimal damage to the skull occurred due to the lack of development of a temporary cavity when a projectile passes through the brain and the associated increase in pressure in the cranial vault which leads to multiple fractures of the skull [1]. Damage was confined to the impact and exit sites and associated radial cracking. Models comprising of a skull and brain (skulls 3–6) fragmented into multiple pieces of diverse

Table 15.3 Test details and results

Specimen	Details of test	Results
1	*Skull with no brain, skull not glued, mass = 551 g* Shot 1: impact velocity = 665 m/s, anterior to posterior along the sagital plane, impact location frontal bone Shot 2: impact velocity = 674 m/s, left to right along the coronal plane, impact location parietal bone	Skull remained whole Skull remained whole
2	*Skull with no brain, skull not glued, mass 551 g* Shot 1: impact velocity = 682 m/s, anterior to posterior along the sagital plane, impact location frontal bone Shot 2: impact velocity = 677 m/s, left to right along the coronal plane, impact location parietal bone	Skull remained whole Skull remained whole
3	*Skull completely filled with gelatine, skull glued (bag inserted through the foramen magnum, filled with gelatine), mass = 1277 g* Shot 1: impact velocity = 682 m/s, anterior to posterior along the sagital plane, impact location frontal bone	Fragmented into 22 pieces Facial bones and the majority of the inferior (excluding the occipital) Remaining 21 fragments varied in mass from 0.13 to 84.76 g (mean = 9.46 g, s.d. = 18.54 g)
4	*Skull completely filled with gelatine, skull glued (bag inserted through the foramen magnum, filled with gelatine), mass 1753 g* Shot 1: impact velocity = 666 m/s, left to right along the coronal plane, impact location parietal bone	Fragmented into 20 pieces Facial bones, inferior including the occipital Parietal/occipital (108.99 g) 18 smaller fragments varied in mass from 0.13 to 27.72 g (mean = 7.00 g, s.d. = 6.83 g)
5	*Skull plus moulded brain, skull not glued, mass = 1132 g* Shot 1: impact velocity = 675 m/s, anterior to posterior along the sagital plane, impact location frontal bone	Fragmented into 7 pieces Facial bones and the majority of the inferior including the occipital Frontal/temporal/parietal (90.14 g) Temporal/parietal (60.72 g) 4 small fragments varying in mass from 0.38 to 15.35 g (mean = 7.12 g, s.d. = 6.25 g)
6	*Skull plus moulded brain, skull glued, turned upside down filled with water, mass = 1684 g* Shot 1: impact velocity = 675 m/s, anterior to posterior along the sagital plane, impact location frontal bone	Fragmented into 30 pieces The facial bones, inferior excluding most of the occipital Occipital (56.71 g) Temporal/parietal (45.84 g) 27 smaller fragments varying in mass from 0.14 to 27.06 g (mean = 4.49 g, s.d. = 7.29 g)

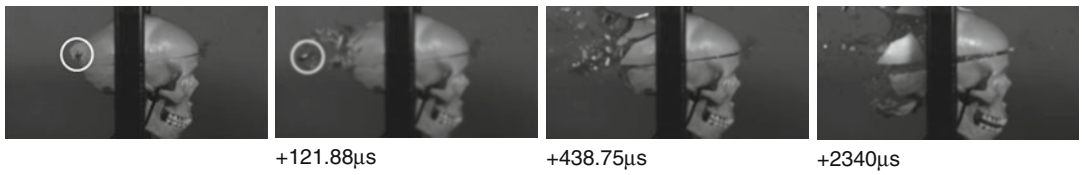

Fig. 15.2 Typical impact sequence (skull 3)

size and shape. These models were reconstructed and compared to data in the forensic anthropology literature. Probably, the most useful comparisons can be found among the case studies reported by Fenton et al. [2] and Betz et al. [14], although the types of ammunition used were reportedly different to that in the current paper. Of particular interest were the complete perforation of the skull, the relatively large pieces of fractured bone, the bilateral fractures

occurring adjacent to buttresses, the fractures to the inferior and posterior of the skull and the ejected brains. All of these features were observed in the skull and brain models developed in the current paper. Thus, the presence of a 'brain' resulted in different fracture patterns (compared to shooting a skull only) that related well to previously proposed models and to data reported in the literature of actual incidents. As the skulls used in the current work were anatomically correct, the various thicknesses of the polymer varied at different points in the skull mimicking a human skull. Post-testing analysis identified that fractures occurred at weaker areas dictated by actual anatomical features. In particular, fractures were influenced by the various buttresses within the skull, as reported in case studies of actual events, e.g. [2]. The amount of gelatine used in the skull to represent the brain affected the severity of the fracture patterns. Use of an anatomically correct brain (skull 5) resulted in the least severe result; although the skull was extensively fractured, the cranial base remained intact. Completely filling the cranial cavity with either gelatine or a gelatine brain and water combination resulted to similar fracture patterns (skulls 3, 4, 6), which were both more severe than with the gelatine brain alone. In particular, it was noticeable that a fully filled cranial cavity resulted in fractures to the inferior and a more catastrophic result.

15.4 Conclusions

An anatomically correct model for studying military wound ballistic and secondary blast events to the human skull and brain has been developed. The advantage of using an anatomically correct skull model in combination with a gelatine brain has been demonstrated by the fracture patterns obtained which compare favourably to the limited reports of actual high velocity rifle wounds to the head. Comparisons with complex secondary blast fragments has not been conducted. Impact and exit wounds were as expected; evidence of cratering and radial cracking was observed. Bullet-wipe was observed at the impact sites. Completely filling the cranial cavity with either gelatine or a gelatine brain and water combination resulted in similar fracture patterns.

Acknowledgments This work was internally funded by The Impact and Armour Group at Cranfield University.

References

1. Karger B. Penetrating gunshots to the head and lack of immediate incapacitation I. Wound ballistics and mechanisms of incapacitation. Int J Leg Med. 1995; 108:53–61.
2. Fenton TW, Stefan VH, Wood LA, Sauer NJ. Symmetrical fracturing of the skull from midline contact gunshot wounds: reconstruction of individual death histories from skeletonized human remains. J Forensic Sci. 2005;50:1–12.
3. Thali MJ, Kneubuehl BP, Zollinger U, Dirnhofer R. The skin–skull-brain model: a new instrument for the study of gunshot effects. Forensic Sci Int. 2002;125:178–89.
4. Lieske K, Janssen W, Kulle K-J. Intensive gunshot residues at the exit wound: and examination using a head model. Int J Leg Med. 1991;104:235–8.
5. Kieser DC, Carr DJ, Girvan L, Leclair SCJ, Horsfall I, Theis J-C, Swain MVJAK. Identifying the source of bullet wipe—a randomised blind trial. Int J Leg Med. 2013. doi:10.1007/s00414-0130874-z.
6. Carey ME. Learning from traditional combat mortality and morbidity data used in the evaluation of combat medical care. Mil Med. 1987;152:6–13.
7. Breeze J, Gibbons AJ, Shieff C, Banfield G, Bryant DG, Midwinter MJ. Combat-related craniofacial and cervical injuries: a 5-year review from the British military. J Trauma. 2011;71:108–13.
8. Spalding TJW, Stewart MPM, Tulloch DN, Stephens KM. Penetrating missile injuries in the Gulf war 1991. Br J Surg. 1991;78:1102–4.
9. Eskridge SL, Macera CA, Galarneau MR, Holbrrok TL, Woodruff SI, MacGregor AJ, Morton D, Sahaffer RA. Injuries from combat explosions in Iraq: injury type, location, and severity. Injury. 2012;43:1678–82.
10. Lewis EA. Between Iraq and a hard plate: recent developments in UK military personal armour. In: IPAC, editor. Personal armour systems symposium 2006 (PASS2006). Leeds: The Royal Armouries, 18–22 Sep 2006.
11. Schyma C, Greschus S, Urbach H, Madea B. Combined radiocolour contrast in the examination of ballistic head models. Int J Leg Med. 2012;126:607–13.
12. Sturdivan LM, Bexon R. A mathematical model of the probability of perforation of the human skull by a

ballistic projectile. Aberdeen Proving Ground: Chemical Systems Laboratory; 1981.
13. Watkins FP, Pearce BP, Stainer MC. Physical effects of the penetration of head simulants by steel spheres. J Trauma. 1988;28(1 Supplement):S40–54.
14. Betz P, Steiefel D, Hausmann R, Eisenmenger W. Fractures at the base of the skull in gunshots to the head. Forensic Sci Int. 1997;86:155–61.
15. Hejna P, Safr M, Zatopkova L. Reconstruction of devastating head injuries: a useful method in forensic pathology. Int J Leg Med. 2011;125:587–90.
16. Barber TW, Brockway JA, Higgins LS. The density of tissues in and about the head. Acta Neurol Scand. 1970;46(1):85–92.
17. Jussila J. Preparing ballistic gelatine – review and proposal for a standard method. Forensic Sci Int. 2004;141:91–8.
18. Mabbott A, Carr DJ, Champion S, Malbon C, Tichler, C. Comparison of 10 % gelatine, 20 % gelatine and Perma-Gel for ballistic testing. In: International Symposium on Ballistics, Freiberg, 22–26 April 2013.

Surrogates of Human Injury

16

Diagarajen Carpanen, Spyros Masouros, and Nicolas Newell

16.1 Introduction

In this chapter we will explore surrogates that are being used to help in our understanding of the pathophysiology of human injury and of predicting injury risk when exposed to a set loading environment. We will mainly focus on anthropomorphic test devices (ATDs), usually known as dummies. Dummies are physical human surrogates that have been designed to evaluate occupant protection in response to collision. Even though ATDs are classified according to size, age, sex and impact direction, injury assessment in automotive and blast applications is mostly conducted using the adult midsize dummy.

ATDs are designed to be biofidelic meaning that they aim to represent the geometry, mass, mass distribution, kinematics, and kinetics of the human body for a given application. This does not, typically, mean that they are fidelic in terms of failure, or biological response. They are instrumented with transducers to measure the accelerations, deformations and loads of various body parts. These measurements are then used to determine the risk of injury. The goal of a vehicle or mitigation system design is for the ATD's response for all test conditions at regions of interest to be below a certain value that corresponds to a certain risk of injury [1].

Standardised ATDs and equivalent injury thresholds for blast-related loading only exist for assessing the protective efficacy of light armoured vehicles. There is a limited amount of surrogates for investigating the effects of primary blast; these include the Facial and Ocular Countermeasure Safety (FOCUS) head. The external geometry of the FOCUS head-form is designed to replicate a 50^{th} percentile male soldier across the three branches of the US military (Army, Navy, and Air Force). The FOCUS head-form is capable of measuring forces imposed onto facial structures using internal load cells. Other surrogates for assessing primary blast effects exist within the boundaries of national authorities, but none of these has been standardised. For the remaining chapter only ATDs that feature in international standards will be presented.

16.2 Surrogates of Human Injury

The surrogates that are commonly used to understand human injury are human cadavers, human volunteers, animals, animal cadavers, anthropometric test devices (ATDs), and computational models [2].

D. Carpanen, PhD, BEng(Hons) • S. Masouros, PhD, DIC, CEng, MIMechE (✉) • N. Newell, MEng, PhD
Department of Bioengineering, Royal British Legion Centre for Blast Injury Studies, Imperial College London, London SW7 2AZ, UK
e-mail: d.carpanen@imperial.ac.uk; s.masouros04@imperial.ac.uk; n.newell09@imperial.ac.uk

A.M.J. Bull et al. (eds.), *Blast Injury Science and Engineering: A Guide for Clinicians and Researchers*,
DOI 10.1007/978-3-319-21867-0_16

Human cadavers, or post-mortem human subjects (PMHS), have been instrumental in the development of injury countermeasures in the areas of occupational safety, transportation, and the military. Indeed, injury risk curves (discussed in Sect. 16.5) are mostly based on data from human cadaveric experiments. An advantage of cadavers relative to animal and physical surrogates is the exact representation of anatomical structures. However, the ability to produce comparable response and injury is dependent on the geometry and tissue properties of the surrogate. In addition, the availability of specimens that meet selection criteria appropriate for biomechanical studies is diminished significantly when the cadavers are screened for pre-existing pathologies, age, gender and anthropometric requirements.

Human volunteers are an obvious experimental model for studying the response of living humans. Although investigations of human response can be performed either through epidemiological studies of people involved in actual crashes or through laboratory studies of human volunteers, both of these approaches have severe practical limitations. Human volunteer experiments in the laboratory have the obvious shortcoming that testing must be performed at sub injurious levels of exposure.

Given the sub injury threshold limitations on human volunteer testing, animals provide the only viable surrogate to study the pathophysiological response to impact or blast injury. In addition, testing of living and dead animals can provide insight into controlling for differences between living humans and cadavers when used to develop response and injury targets. Although injury tolerance of virtually every body region has been studied using an animal model, differences in anatomy and physiology complicate the interpretation of animal data.

ATDs must exhibit both internal biofidelity (i.e., comparable deformations, accelerations, and articulations of the body regions) and external biofidelity (i.e., similar response when interacting with the surrounding environment) to replicate human behaviour for similar loading conditions. The main design objective is to be robust and repeatable. ATDs do not assess failure directly. Instead, they require the use of injury criteria to interpret the injury risk using recorded kinematic and kinetic parameters. These injury criteria are generally expressed as probability curves instead of absolute thresholds, since the likelihood of being injured varies by individual and is dependent on factors such as age, gender and physiological condition. The injury criteria have been derived traditionally from experiments with cadaveric human or animal tissue, although computational models may be used in the future (Sect. 16.5). The requirement for this link between probability curves and injury is, of necessity, an extrapolation from the source data that produced the original injury curves, as the injury curves will have been obtained from a single set of experiments and will not replicate exactly the test being conducted using ATDs. This extrapolation could be ameliorated by having frangible ATDs. However, this is costly and entails other complications.

Computational models allow the analysis of intrinsic and extrinsic factors experienced by humans under load that are too complex or impossible to test and measure in a laboratory context. In addition, with ever increasing computing power it is possible to create ever more sophisticated models of the human body and simulate a wide spectrum of conditions. One disadvantage of computational models is that they are deterministic, although modern techniques allow a probabalistic approach to also be taken using these. Probabilistic analyses present several challenges, including significant computational time due to the many trials required, but they may have the potential to represent the anatomical variability of humans and the variability in loading and boundary conditions.

Engineers are striving to characterise the response and injury using a combination of these surrogates to develop effective countermeasures. Although the use of each surrogate has strengths and weaknesses, the combined knowledge gained from experimenting with these surrogates has led to a dramatic improvement of protective systems and hence reduction in lives lost due to road vehicle accidents. Similar approaches are being applied to mitigate injury due to explosions

(IED/mine detonation). The next sections of this chapter will concentrate on ATDs that are mainly used to assess occupants' protection in tertiary blast.

16.3 A Brief History of ATDs

There are various types of ATD, each designed to be biofidelic under a specific type of impact mainly for automotive crash research. For example, the Hybrid III 50th percentile male dummy is commonly used to evaluate automotive restraint systems in frontal crash testing. It was designed to mimic human responses for forehead impacts, neck bending, distributed sternal impacts, and knee impacts. The Hybrid III midsize male dummy has been improved since 1976 to enhance biofidelity at the hip and ankle joints. The THOR (Test device for Human Occupancy Restraint) is another dummy used for frontal crash testing. Compared to the Hybrid III, the distinguished features of THOR are its two-segment thoracic spine, a human-like rib cage, and more human-like neck and ankle structures.

The SID (Side Impact Dummy), developed in 1979, is based on the predecessor of the Hybrid III (the Hybrid II) without arms and shoulder structures. It was designed mainly to measure injury risk to the head, chest, and pelvis when the body is impacted from the side. The SID-HIII is the SID dummy with its Hybrid II head and neck having been replaced with the Hybrid III head and neck. This improved the biofidelity of its head and neck response. The EUROSID1 is the European side impact dummy developed in 1986 and finalised in 1989. The BioSID (Biofidelic Side Impact Test Dummy) was designed to the International Organization for Standardization (ISO) impact response biofidelity guidelines for the head, neck, shoulder, thorax, abdomen, and pelvis in 1989.

16.4 ATDs in Blast

In comparison to the automotive crash research area, there is no specific ATD designed to assess injury associated with mine/IED detonation. North Atlantic Treaty Organisation (NATO) task groups (HFM-090/TG25 and HFM148/RTG) have suggested the use of the most relevant existing surrogates with appropriate injury criteria when assessing blast injury. These were consulted to inform the NATO standard that encompasses vehicle assessment under blast loading; STANAG-4569 [3].

As current ATDs have been designed to be biofidelic in automotive impact conditions, their validity in predicting injury risk under blast conditions is uncertain (see Chap. 22, Sect. 22.3.2). In addition, these ATDs are direction specific. Selection of the appropriate ATDs by the NATO groups was based on the location of the IED with respect to the vehicle occupant, independently from the seating orientation in the vehicle. The standard Hybrid III dummy was chosen for scenarios where the IED is located underneath, in front or at the rear of the ATD. The EuroSID-2re dummy (ES-2re) was chosen for the scenario where the IED is located laterally with respect to the ATD. This point highlights how an ATD has to be 'tuned' for a specific threat or insult and its response cannot be easily extrapolated to a wide range of threats.

Specifically for injury assessment of the leg, the Military Lower Extremity (MIL-Lx) dummy was designed in 2009 with the objective of being biofidelic under a set loading condition that might occur in an explosion under a military vehicle. It now features in the STANAG 4569 standard as an additional option to the original Hybrid III leg, albeit with a different injury criterion.

The next sections of this chapter elaborate on the ATDs used in the vehicle IED/mine qualification tests.

16.4.1 The Hybrid III ATD

The Hybrid III (H3) 50th percentile male ATD was developed for automotive frontal crash tests. It represents the average male of the USA population between 1970 and 1980 and has the following characteristics:

- Stature (standing position): 1.72 m;
- Weight: 78 kg;
- Erect sitting height: 884 mm.

These figures may not represent accurately the current USA population any longer or, indeed, the global population. For example, the northern European population is significantly taller than the H3 50th percentile male ATD [4, 5]; the size difference between the used 50th percentile H3 and the real user population is especially important for the head clearance and thus the risk of head/neck injury due to head contact. The use of the existing 95th percentile H3 does not solve this problem as the difference of this version of the dummy with the user population is large. Therefore, the HFM-148 task group recommended that attention should be paid to the head clearance and to quantify the space required for free vertical head motion without contact. This information can be used to advise the desired head clearance for the required tallest population for the tested vehicle.

The H3 ATD can be instrumented with transducers to measure accelerations, forces, moments, and displacements in several body parts. It can withstand a range of loading conditions and is re-useable.

The total body mass of the 50th percentile H3 ATD is still close to the mass of the current population when looking at a mixture of male/female 50th percentile population. The use of personal protective equipment (PPE) can increase the human body weight significantly and thus might have an influence on the response observed. There is, however, no standardised method yet to take the body mass issue into account.

The standard H3 50th percentile ATD comes with a non-instrumented tibia. This means that there are no sensors on the tibial component. For IED/mine vehicle qualification tests both legs (including tibia, ankle and foot) have to be replaced by instrumented ones. In addition, it has a curved spine in its standard version in order to represent the seating posture of a driver in a car. The spine can be replaced by a Hybrid II straight spine to simulate standing and lying postures. The HFM-148 task group has suggested the use of the standard version of the Hybrid III (curved spine) for the most realistic seating posture in the majority of the current seats in military vehicles. It is known that the spine configuration has an influence to the load transfer into the upper body. However, this is deemed to have little influence on the pelvis acceleration, which is used as input for the lumbar-spine injury risk assessment. More investigations need to be carried out to analyse the response of the two available spines (straight/curved) for future development of the spine injury criterion. For standing or lying positions the same measurement method could be used to assess injury risk, but it is not known whether the injury criteria and risk curves are still valid for these conditions.

16.4.2 The EuroSID-2RE ATD (ES-2re)

The EuroSID-2RE (ES-2re) ATD is a side impact dummy developed in the European automotive community to expand the capabilities for the crash safety protection measures. The ES-2re 50th percentile male ATD represents the average adult male, but without lower arms. It has the following anthropomorphic characteristics:

- Weight: 72 kg;
- Erect sitting height: 909 mm;
- Shoulder width: 470 mm;
- Pelvis lap width: 366 mm

Like for the 50th percentile H3 ATD, there are differences in the anthropomorphic data compared to the current population. The same comments as the H3 with regards to the size of the ATD hold for the ES-2re. The most salient point, however, is the difference in shoulder width, because this determines the free space to the side wall. The narrower the free space is, the harder the impact to the shoulder will be in some loading situations. This means that when the shoulder force in the 50th percentile ES-2re shows low risk of shoulder injuries ($<$10 %), the risk for a real occupant with wider shoulders might be higher. Accurate measurements of side

wall intrusion during side blast could help to formulate ATD requirements.

The head of the ES-2re is the same as the H3 head, albeit the neck has a different design in order to mimic the kinematic behaviour of the human under lateral loads. There is an upper neck load cell with which loads through the neck can be measured. Compressive force can be measured on both shoulders.

The thorax of the ES-2re incorporates a rear rib extension bracket on the impact side of each rib that, together with a rear rib extension guide, provides more realistic interaction with vehicle seatbacks. The deflection caused by lateral impact is measured in each rib. In the abdomen the lateral force at three positions is measured and summed to get the total force for the injury risk assessment. In the pelvis the lateral force is measured at the pubic symphysis.

The standard ES-2re ATD comes with non-instrumented tibiae. For IED/mine vehicle qualification tests, both of its legs (including tibia, ankle and foot) have to be replaced by instrumented ones.

16.4.3 MIL-Lx

The Military Lower Extremity (MIL-Lx) was designed with the objective to be biofidelic under a set loading condition that might occur in an explosion under a military vehicle (Fig. 16.1). The design of the leg is based on both the original H3 leg as well as the THOR-

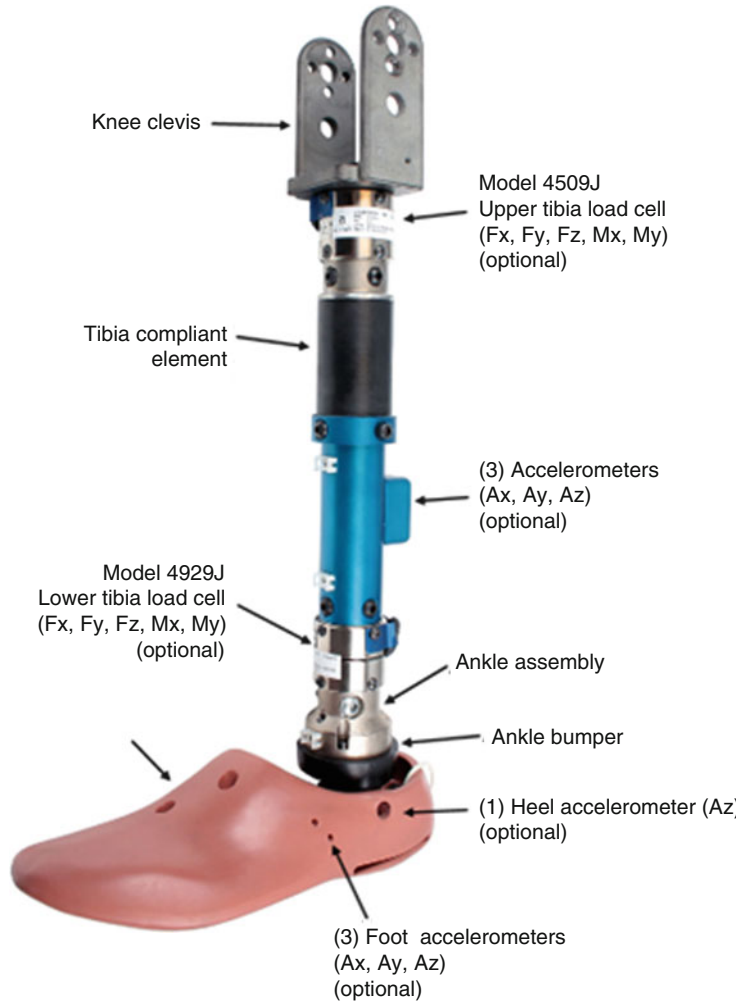

Fig. 16.1 The military lower extremity (MIL-Lx) (Source: Humanetic Innovative Solutions)

Lx leg and optimised for measurements of the vertical force through the tibia.

The said biofidelity of the MIL-Lx was achieved using an intensive lower limb injury assessment study at Wayne State University (WSU). The loading regime for under-vehicle explosions was used as input for PMHS testing. The same set-up was used to develop and tune the MIL-Lx by aiming for a good correlation in the load-time (impulse) response at approximately 50 % injury risk.

The biofidelic tuning of the MIL-Lx was achieved primarily by the use of a rubbery, compliant element in the tibial shaft. The axial load measured at the upper tibia load cell (located above the compliant element) is the one that correlates to the load measured on the PMHS study at Wayne State University and therefore is the one to be used for the prediction of risk of leg injuries. This is in contrast to the H3 leg where the measurement used for injury assessment is the axial load measured at the lower tibia load cell.

The Hybrid III, EuroSID-2re and MIL-Lx are commonly referred to as multi-use surrogates. They are designed to be used for multiple impacts at loading conditions beyond those normally intended for testing evaluations. As discussed above in Sect. 16.2, ATDs lack frangibility by intention of design and therefore do not assess failure directly.

16.4.4 Frangible Single-Use Surrogates

Frangible single-use surrogate lower limbs have been designed specifically to assess the effects of solid blast. Frangible surrogates may consist of anatomically correct synthetic bones and soft tissues to mimic closely the human anatomy. Examples of these include the Complex Lower Leg (CLL) and the Frangible Surrogate Leg (FSL) [7–9]. Developed in Canada, the CLL was claimed to show realistic injury patterns and biofidelic response under footplate velocities of 3.4–8.5 m/s [7]. More recently experiments conducted at Wayne State University have shown that the CLL failed at lower loads in comparison to cadavers [5]. The FSL has been compared with human cadaveric data in a landmine experimental setup; the findings showed good correlation with respect to gross bony damage, but low biofidelity in soft tissue and cancellous bone response [8]. The FSL has not been validated for under-vehicle blast research. More research needs to be carried out before single-use surrogates can be implemented in test standards.

16.5 Injury Risk Assessment

Physical injury occurs when loading to the human body causes damage to anatomical structures and/or alteration in normal function. The mechanism involved to cause such damage/alteration is then called an injury mechanism.

An injury criterion is defined as a physical parameter or a function of several physical parameters which correlates well with the injury severity of the body area under consideration for a specific loading condition. Parameters that can be measured when testing may include the linear acceleration experienced by a body part, the global forces or moments acting on the body or the deflection of a structure.

Injury risk curves are used to define the probability of exceeding the severity of a set injury. Examples of risk curves are shown in Fig. 16.2. The vertical axis shows the injury risk as a function of an injury criterion (horizontal axis). These are usually produced from series of PMHS, animal, or human volunteer experiments under appropriate loading/boundary conditions, noting that these conditions are never perfectly replicated in an ATD test, because ATDs test new mitigation strategies, vehicles, etc. Sometimes, anthropomorphic factors such as age and

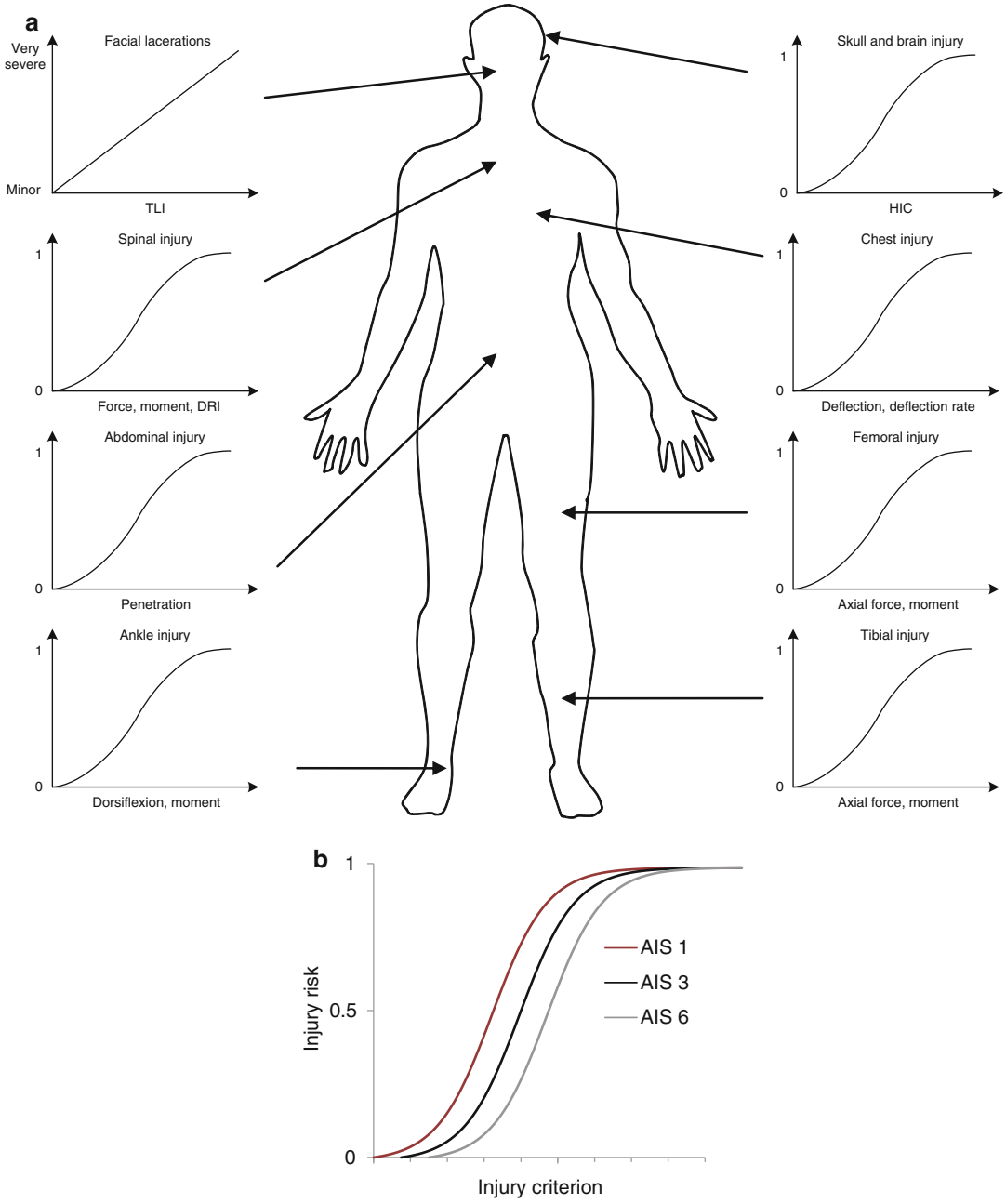

Fig. 16.2 Examples of injury risk curves suggested for (**a**) different body parts and (**b**) different injury severities (Adapted from NATO HFM-148/RTG [5])

Table 16.1 The abbreviate injury scale [5, 6]

AIS code	Injury description	Examples of blast related injuries
1	Minor	Eardrum rupture, Great toe fracture, Cerebral concussion without loss of consciousness
2	Moderate	Fractures of foot and lower leg (e.g. tibia, calcaneus, talus fracture, fibula, patella)
		Cerebral concussion with loss of consciousness <1 h
		Skull fracture
3	Serious	Open or closed femur fracture
		Cerebral concussion with loss of consciousness 1–6 h
4	Severe	Traumatic amputation of upper leg (at/above knee at/below hip)
		Cerebral concussion with loss of consciousness >6–24 h (traumatic coma)
5	Critical	Fracture at/below 4th cervical vertebra with paralysis of torso and legs, or arms and legs
		Cerebral concussion with loss of consciousness >24 h (traumatic coma)
6	Untreatable	Fracture at/above third cervical vertebra with paralysis of torso and limbs
		Crush injury cerebrum
9	Unknown	Died of head injury without further substantiation of injuries or no autopsy confirmation of specific injuries

gender are included in the risk curves. The data set on which the risk curves have been developed, however, is usually unable to account for such factors. Depending on the shape of the risk curve, a small difference for tolerance level could result in large differences in injury risk. Tolerance level or injury criterion level is defined as the threshold of the injury criterion corresponding to a specific risk to sustain a specific injury severity (range).

The injury severity can be defined using an injury scale which is defined as the numerical classification of severity of an injury and can be related to injury type and body part affected. The Abbreviated Injury Scale (AIS) (see Chap. 20, Sect. 20.3) was developed in the 1970s to score the severity of injuries in victims of road traffic accidents on a scale of 1–6, based on the likelihood of the event to cause a fatal injury (Table 16.1); higher AIS levels indicate an increased threat to life. The numerical values do not indicate relative magnitudes, in other words an AIS 2 level is not twice as severe as an AIS 1 level injury. The AIS has since undergone several iterations in order to improve the clinical relevance of scores for certain injury mechanisms, including injuries caused by penetration of fragments and military injury patterns [6]. The NATO HFM-090 task group suggests the use of the 10 % probability of an AIS 2 or greater (AIS 2+) injury to establish the acceptable injury threshold for the different body regions of interest; this is included in the standard STANAG 4569 for light armoured vehicle assessment. Accepting a 10 % risk of AIS 2+ implies a lower risk (less than 10 %) of higher severity (AIS 3+) injuries and a higher risk (more than 10 %) of AIS 1+ injuries. Higher injury severity levels or other injury severity scales with refined discriminating capacities are used if the available AIS2+ information is lacking or if AIS 2 injuries are considered not to be acceptable. Table 16.2 gives an overview of the injury criteria and corresponding ATD that should be used for the different body parts recommended by the NATO HFM-148 task group.

Table 16.2 Injury assessment reference values and corresponding ATD to be used in order to assess injury risk for the different body parts according to NATO

Body region	Injury criteria	Metric	Pass/fail level	ATD
Head	Head injury criterion	HIC15	250	H3 or ES-2re + MIL-Lx
Neck	Axial compression force	Fz−	4.0 kN @ 0 ms/1.1 kN >30 ms	ES-2re + MIL-Lx
	Axial tension force	Fz +	3.3 kN @ 0 ms/2.8 kN @35 ms/ 1.1 kN >60 ms	
	Shear force	Fx±/Fy±	3.1 kN @ 0 ms/1.5 kN @25–35 ms/1.1 kN >45 ms	
	Bending moment (flexion)	Moc_y +	190 Nm	
	Bending moment (extension)	Moc_y−	96 Nm	
Neck	Axial tension force	Fz +	1.8 kN	ES-2re + MIL-Lx
Shoulder	Compression force	Fy	1.4 kN	ES-2re + MIL-Lx
Thorax (ribs) (upper/middle/lower)	Rib deflection criterion	$RDC_{lateral}$	28 mm	ES-2re + MIL-Lx
Thorax	Thoracic compression criterion	$TCC_{frontal}$	30 mm	H3 + MIL-Lx
Thorax	Viscous criterion	$VC_{frontal}$	0.70 m/s	H3 + MIL-Lx
Thorax	Viscous criterion	$VC_{lateral}$	0.58 m/s	ES-2re + MIL-Lx
Abdomen (front/middle/rear)	Abdominal peak force	F_{total}	1.8 kN	ES-2re + MIL-Lx
Spine	Dynamic response index	DRI_z	17.7	H3 or ES-2re + MIL-Lx
Pelvis	Maximum pubic force	Fy	2.6 kN	ES-2re + MIL-Lx
Upper legs	Axial compression force	Fz−	6.9 kN	H3 or ES-2re + MIL-Lx
Lower legs	Axial compression force	Fz−	2.6 kN	H3 or ES-2re + MIL-Lx
Internal organs/lungs	Chest wall velocity predictor	CWVP	3.6 m/s	H3 or ES-2re + MIL-Lx

Adapted from NATO HFM-148/RTG [5]

16.6 Summary

Human surrogates have been utilised throughout the years to aid in the understanding and prediction of injury under impact in order to improve protective systems and inform mitigation strategies. Commercial ATDs used in standardised test procedures in blast have been designed for the automotive industry, and therefore their response in blast is not optimally representing the human body. Cadaveric tests are used to derive injury risk curves in blast-related loadings; these are ever more utilised currently to improve our understanding of current ATDs and to develop new ATDs or parts thereof that are biofidelic in blast-related loadings for use in evaluation of military vehicle design and mitigation strategies.

References

1. Yoganadan N, Nahum AM, Melvin JW. Accidental injury. New York: Springer; 2015.
2. Crandall JR, Bose D, Forman J, Untaroiu CD, Arregui-Dalmases C, Shaw CG, Kerrigan JR. Human surrogates for injury biomechanics research. Clin Anat. 2011;24: 362–71.

3. North Atlantic Treaty Organisation AEP-55 STANAG 4569. Protection levels for occupants of logistics and light armored vehicles. 2010.
4. North Atlantic Treaty Organisation HFM 090. Test methodology for protection of vehicle occupants against anti-vehicular landmine and/or IED effects. 2007.
5. North Atlantic Treaty Organisation HFM-148/RTG. Test methodology for protection of vehicle occupants against anti-vehicular landmine and/or IED effects. 2011.
6. Gennarelli TA, Wodzin E, editors. Association for the advancement of automotive medicine. Barrington: AIS; 2005.
7. Manseau J, Keown M. Development of an assessment methodology for lower leg injuries resulting from nti-vehicular blast landmines. IUTAM proceedings on impact biomechanics: from fundamental insights to applications, Doratecht; 2005. p. 41–9.
8. Berron DM, Coley GG, Fall RW. Assessment of lower leg injury from land mine blast-phase 1. Defence Research and Development Canada. 2006.
9. Cronin D, Salisbury C, Worswick MJ, Pick RJ, Williams KV, Bourget D. Appropriate material selection for surrogate leg models subjected to blast loading. In: Fundamental issues and applications of shock-wave and high strain rate phenomena. Amsterdam: Elsevier; 2001. p. 201–8.

Further Reading

Committee on Medical Aspects of Automotive Safety. Rating the severity of tissue damage: I. The abbreviated scale. JAMA. 1971;215:277–80.

Committee on Medical Aspects of Automotive Safety. Rating the severity of tissue damage: II. The comprehensive scale. JAMA. 1972;220:717–20.

Ramasamy A, Masouros SD, Newell N, Hill AM, Proud WG, Brown KA, Bull MJ, Clasper JC. In-vehicle extremity injuries from improvised explosive devices: current and future foci. Philos Trans R Soc B. 2011;366:160–70.

Schmitt K, Niederer P, Cronin DS, Muser MH, Walz F. Trauma biomechanics. Springerpverlag Berlin Heidelberg: Springer; 2014.

Yoganadan N, Stemper BD, Pintar FA, Maiman DJ. Use of postmortem human subjects to describe injury responses and tolerances. Clin Anat. 2011;24:282–93.

Computational Methods in Continuum Mechanics

17

Dan J. Pope and Spyros Masouros

17.1 Introduction

A continuum is a mathematical representation of a real material such as a solid, liquid or gas. By examining such media we disregard the molecular structure of matter and assume the material is continuous. Continuum mechanics is concerned with the behaviour of such materials and is based on fundamental physical laws.

The mathematical description of a continuum mechanics problem is often not amenable to a closed-form analytical solution and a numerical procedure is often required to obtain a solution. With the advent of computational techniques, computational continuum mechanics has become an increasingly powerful tool to obtain solutions to continuum mechanics problems. A wide range of numerical procedures have been developed, including the Finite Element (FE), Finite Volume (FV), Boundary Integral and Finite Difference methods. The FE method has been the most widely used for the analysis of solid mechanics problems, while the FV method is the most popular method for the analysis of fluid mechanics problems. Algorithms that combine the two methods have also been developed recently in order to address problems where deformable solids interact with fluids.

The numerical methods used to solve the problem involve the transformation of the mathematical model into a system of algebraic equations. In order to achieve this, the equations have to be discretised in time and space. In doing this, a number of approximations are made; the continuum is replaced by a 'finite' set of computational points (or nodes), areas or volumes (or elements) (Fig. 17.1); the notions of nodes and elements are discussed in more detail later in the text. The constitutive laws, which describe the material behaviour, are simplified and continuous functions representing the exact solution to the mathematical model are generally approximated by polynomials of a finite order. The resulting set of algebraic equations is then solved either by direct or approximate, iterative methods. Finally, post-processing facilities are required in order to interpret the resulting numerical solutions and present them in a graphical way, for example, stress contours.

The FE method is a computer based, approximate method to solve engineering problems. The robust mathematical framework means that the method is now being employed to solve problems for static and dynamic stress analysis in solid mechanics (including biomechanics), thermal and thermal/structural coupled analysis,

D.J. Pope, BEng (Hons), PhD, CEng, FICE
Dstl Porton Down, Salisbury SP4 0JQ, UK
e-mail: djpope@dstl.gov.uk

S. Masouros, PhD, DIC, CEng, MIMechE (✉)
Department of Bioengineering, Royal British Legion Centre for Blast Injury Studies, Imperial College London, London SW7 2AZ, UK
e-mail: s.masouros04@imperial.ac.uk

A.M.J. Bull et al. (eds.), *Blast Injury Science and Engineering: A Guide for Clinicians and Researchers*,
DOI 10.1007/978-3-319-21867-0_17

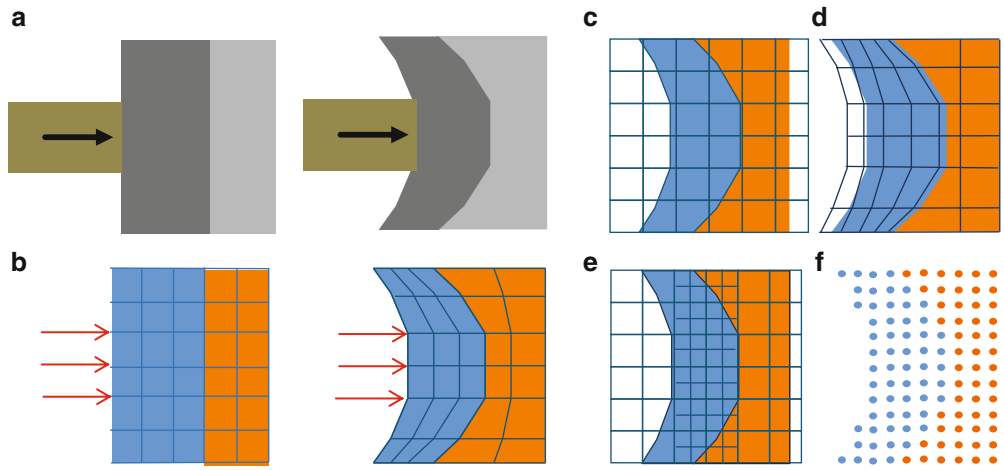

Fig. 17.1 Various meshing techniques. Each finite element is represented diagrammatically by a rectangle. (**a**) Schematic showing impact of a bar on a bi-material structure. (**b**) Lagrangian. (**c**) Eulerian (generic mesh from which (**d**) and (**e**) stem). (**d**) Adaptive Eulerian. (**e**) Arbitrary Lagrange-Euler (ALE). (**f**) Smooth Particle Hydrodynamics (SPH)

electromagnetic analysis, and other multi-physics problems including some fluid mechanics problems. It is one area of Computer Aided Engineering (CAE); others are Computational Fluid Dynamics (CFD), Multi-Body Modelling (MBD) and Optimisation.

In this chapter we will explore the mathematical implementation of finite element analysis for structural static and dynamic problems in solid mechanics.

17.2 Material, Spatial and Other Descriptions

The essence of the FE method revolves around the spatial discretisation of the region of interest. This representation may be defined in different ways, depending on the problem at hand. As an example, consider a typical pre- and post- impact scenario as shown in Fig. 17.1a.

17.2.1 Lagrangian Representation

When quantities are phrased in terms of their initial position, x, the description is known as Lagrangian and the position itself is tracked with time (Fig. 17.1b). When the motion or deformation is described using the current configuration this is known as the updated Lagrangian description (Fig. 3.9). The Lagrangian and updated Lagrangian descriptions are also referred to jointly as a material description as a material particle is followed in time.

17.2.2 Eulerian Representation

An alternative formulation is the Eulerian method. It is commonly used in fluid mechanics or when solid material deformations would be large enough to cause unfavourable element distortions or mesh entanglement within a Lagrangian framework. (The approach has some similarities with the updated Lagrangian approach and in some solid mechanics textbooks updated Lagrangian is referred to as Eulerian.) The Eulerian formulation describes the motion at a given spatial point of different particles which occupy that point at different times. Thus we examine a fixed region of space that does not change throughout the simulation (the 'control volume'), as opposed to following a changing configuration, and particles pass through this fixed region (Fig. 17.1c). The position vector x is then used to denote the point in space

which can be occupied by different particles at different instants of time.

Using an Eulerian mesh typically requires the definition of more elements than when using a Lagrangian approach to model substantively the same problem. Additional nodes are required to track the constituent materials as they move away from their initial position and, for this reason, a rough idea of the expected response is also useful to the analyst. Perhaps one of the main disadvantages when using an Eulerian framework is the inherent difficulty in keeping track of the 'local axis' associated with materials that exhibit general anisotropy or fracture in a 'directional' manner.

17.2.3 Other Forms of Spatial Integration

Additional schemes have been developed that attempt to hybridise the virtues of the Lagrangian and Eulerian approaches such as the Arbitrary Lagrange Euler (ALE) method (Fig. 17.1d). Within this framework material can flow between elements whilst the mesh also concurrently deforms. The manner in which this occurs can be dictated by imposing particular arbitrarily-defined constraints on the global and local elemental behaviour within the mesh. The method can, for example, be exploited when attempting to temporarily achieve finer resolution in a particular part of a mesh which contains highly transient or localised behaviour, such as the development and subsequent expansion of a blast wave. The mesh may contract appropriately (Fig. 17.1e) providing potentially greater accuracy, when resolving the thin high pressure zone that constitutes the front of the wave. Once the wave has passed through this part of the model, and less transient behaviour ensues, the mesh automatically coarsens again. Adaptive Mesh Refinement (AMR) schemes have also been developed that are based on a similar principle of providing finer resolution where required; an Euler-based example of this is shown in Fig. 17.1e. In this case, although all elements within the mesh maintain a rectilinear shape, during the simulation, temporary local subdivision occurs where greater resolution is desired.

Within aggressive, dynamic loading regimes, failure, fracturing and subsequent fragment production is a common occurrence but, in addition to providing adequate material models, representing these phenomena spatially can also be a significant challenge. Whilst a Lagrangian scheme can be tailored to deal with relatively complex, directional material behaviour, problems with element distortion or mesh entanglement can limit its use when simulating structures undergoing large deformation. In other situations a particular stress or strain state should lead to material facture and hence a way to allow portions of material to 'detach' within the solution framework has to be found. One expedient way of dealing this within a Lagrangian system is to allow unstable or highly distorted elements to be so deleted or 'eroded' from the simulation. The criterion for erosion can be based, for example, on a particular stress or strain state within the element, or a combination of both. Erosion can also be enforced if element distortions lead to a very small controlling time step. Although effective in many situations, the use of different erosion criteria can lead to very different model outputs and it must be remembered that the process largely violates physical laws, for example, mass from eroded elements is either ignored or somehow distributed amongst their surrounding elements.

Alternative schemes, such as particle-based approaches, have been developed to cope partly with the issues discussed above. One example is the Smooth Particle Hydrodynamics (SPH) method (Fig. 17.1f). Here, the solution space is populated with particles, rather than elements. A 'kernel' is defined that effectively determines the radius of influence that each particle has on its neighbouring particles. As with the classic Lagrangian method, this provides the interdependence within the model to allow quantities such as stress to be transferred from one zone to another. In contrast to the Lagrangian approach, however, if the distance between particles exceeds the radius of influence at any point, they can simply detach from one another.

17.3 Implicit Finite Element Analysis

The FE method was developed for stress analysis of large objects with complex geometry. Practically, it stems from the structural analysis of large frames with the advent of computers (1930–50) by implementing the direct stiffness method that employs matrix algebra; it was pioneered by the aeronautics industry in the 50s by taking the idea of the 'discretised' frame consisting of individual trusses and applying it to any solid by splitting it into finite regions. Mathematically, the method was documented in the late 60s and is based on the Galerkin numerical methods.

Epigrammatically in order to run a finite element analysis of a part or an assembly using commercial FE software one needs to carry out the following steps;

- acquire the geometry of the part(s) (usually from CAD);
- mesh it (split it into small regions, the finite elements);
- assign material properties;
- define initial and boundary conditions (including loading);
- run the simulation (solve/stress recovery); and
- interpret the results.

The objective of the finite element code is to calculate the field in question (the displacement field in the structural case) using functions defined over the whole structure and, secondly, satisfy the boundary conditions. The objective in a structural FE analysis is to calculate the displacement field $\mathbf{u}(\boldsymbol{x})$ over the structure and from that the strain, and therefore – through the constitutive laws – stress. Hence, the FE method converts the problem of identifying a field over the whole body – of an infinite number of degrees of freedom (DOFs) – to a surrogate problem of identifying the field over a finite number of DOFs.

We will develop the formulation here for a static FE analysis of a linearly elastic material and small strains, and generalise later in the text.

17.3.1 Meshing

The essence of the finite element method is the division of the body in discrete regions, the finite elements. The finite elements are of ordinary shapes (depending on the dimension of the simulation) such as lines, triangles, rectangles, cubes, tetrahedra, etc., and are connected with one another at the corners of each edge with *nodes*. A set number of DOFs is associated with every node. Elements and nodes are collectively termed the finite element *mesh*.

17.3.2 Shape Functions

The shape (or basis) functions are interpolation functions - unique to each element type - that relate the displacement across the element $\mathbf{u}(\boldsymbol{x})$ to that at its nodes, $\mathbf{U}$, where $\mathbf{U}$ is a vector of dimension equal to the DOFs of the element, and

$$\mathbf{u}(\boldsymbol{x}) = \begin{Bmatrix} u(x,y,z) \\ v(x,y,z) \\ w(x,y,z) \end{Bmatrix}$$

The interpolation functions are polynomials, usually linear or quadratic. The number of finite elements in which the body is divided and the degree of the polynomial of the interpolation functions are directly related to the accuracy of the solution.

Let's consider a one-dimensional truss element (Fig. 17.2). A truss is a structural member that can only resist tension and compression, i.e. axial loading; it cannot take bending moments. Using the general form of a polynomial to represent the interpolation function the displacement at a point x along the length of the element is;

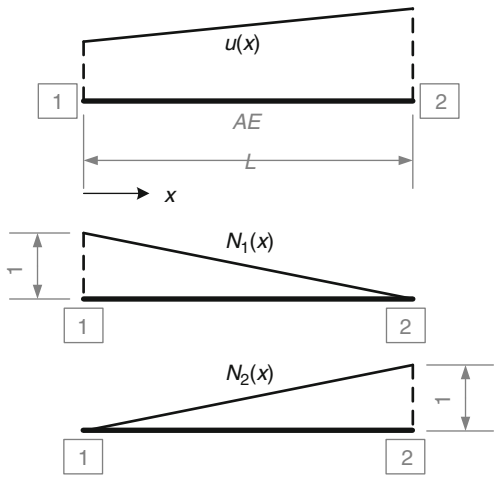

Fig. 17.2 A line element with 2 nodes of length L, cross sectional area A, and Young's modulus E

$$u(x) = a_1 + a_2 x + a_3 x^2 + \ldots + a_{m-1} x^m + \ldots$$

$$u(x) = \begin{bmatrix} 1 & x & x^2 & \cdots & x^m & \cdots \end{bmatrix} \begin{Bmatrix} a_1 \\ a_2 \\ \vdots \\ a_m \\ \vdots \end{Bmatrix}$$

$$u(x) = \mathbf{M}(x)\mathbf{a}$$

The terms a_i are constants, depend on the element type, and are associated with the displacements (but could also be associated with their derivatives, for example in bending; a type of loading that results in curving the structure). Their total number is equal to the total number of nodes, NNODES. At node N_i, $i = 1, 2, \ldots,$ NNODES of the element the displacement will be

$$u_{N_i}(x_i) = U_i = \mathbf{M}(x_i)$$

where x_i are the coordinates of node i. Applying this to all the nodes we get

$$\mathbf{U} = \mathbf{A}\mathbf{a}$$

Combining we get

$$u(x) = \mathbf{M}(x)\mathbf{a} = \mathbf{M}(x)\mathbf{A}^{-1}\mathbf{U}$$
$$u(x) = \mathbf{N}(x)\mathbf{U}$$

We call the matrix $\mathbf{N}$ the *shape function* of the element.

For example, let's consider the simplest possible interpolation

$$u(x) = a_1 + a_2 x = \begin{bmatrix} 1 & x \end{bmatrix} \begin{Bmatrix} a_1 \\ a_2 \end{Bmatrix}$$
$$u(x) = \mathbf{M}(x)\mathbf{a}$$

Apply this to the displacements at the two nodes

$$\begin{Bmatrix} U_1 \\ U_2 \end{Bmatrix} = \begin{bmatrix} 1 & 0 \\ 1 & L \end{bmatrix} \begin{Bmatrix} a_1 \\ a_2 \end{Bmatrix}$$
$$\mathbf{U} = \mathbf{A}\mathbf{a}$$

Solve and substitute

$$u(x) = \left(1 - \frac{x}{L}\right) U_1 + \frac{x}{L} U_2$$
$$u(x) = \begin{bmatrix} 1 - \frac{x}{L} & \frac{x}{L} \end{bmatrix} \begin{Bmatrix} U_1 \\ U_2 \end{Bmatrix}$$
$$= \begin{bmatrix} N_1(x) & N_2(x) \end{bmatrix} \begin{Bmatrix} U_1 \\ U_2 \end{Bmatrix}$$
$$u(x) = \mathbf{N}(x)\mathbf{U}$$

There is a computationally more elegant way to represent shape functions, which is what commercial FE codes actually utilise; that is the 'parent' element on the dimensionless s-space. No matter what the shape of the element is, the FE code would always calculate at the simple, unit, parent element and map the result to the actual element (Fig. 17.3).The parent line element lies between $s = -1$ (node 1) and $s = 1$ (node 2).

17.3.3 Strains and Stresses; Constitutive Laws (See Chap. 3 for More Details)

Strain in each finite element is related to the displacement field:

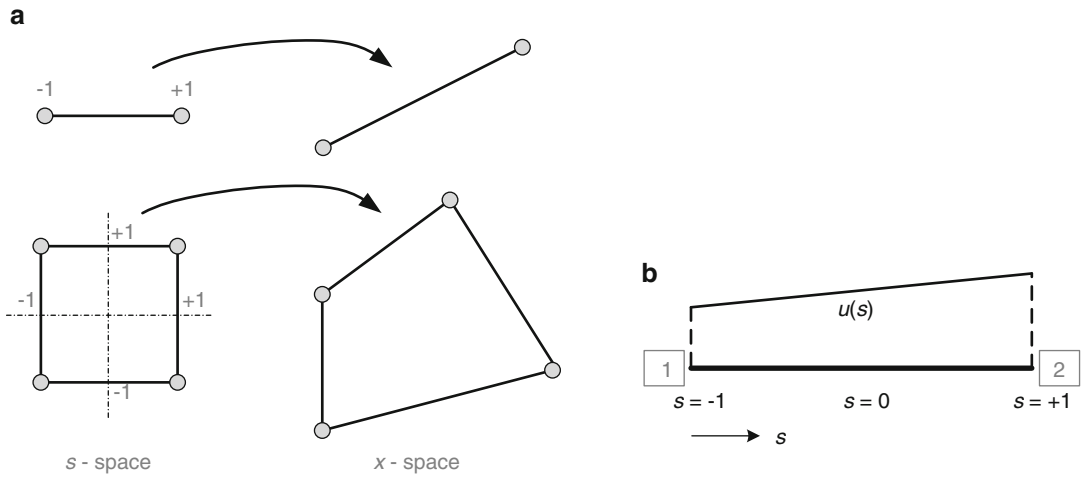

Fig. 17.3 (**a**) Schematic showing mapping from the *s*-space to the *x*-space for a line and a square parent element. (**b**) The parent line element in the dimensionless *s*-space

$$\begin{Bmatrix} \varepsilon_x \\ \varepsilon_y \\ \varepsilon_z \\ \gamma_{xy} \\ \gamma_{yz} \\ \gamma_{zx} \end{Bmatrix} = \begin{bmatrix} \frac{\partial}{\partial x} & 0 & 0 \\ 0 & \frac{\partial}{\partial y} & 0 \\ 0 & 0 & \frac{\partial}{\partial z} \\ \frac{\partial}{\partial y} & \frac{\partial}{\partial x} & 0 \\ 0 & \frac{\partial}{\partial z} & \frac{\partial}{\partial y} \\ \frac{\partial}{\partial z} & 0 & \frac{\partial}{\partial x} \end{bmatrix} \begin{Bmatrix} u(x,y,z) \\ v(x,y,z) \\ w(x,y,z) \end{Bmatrix}$$

$$\boldsymbol{\varepsilon} = L\mathbf{u}$$

$$\boldsymbol{\varepsilon} = L(\mathbf{NU}) = L(\mathbf{N})\mathbf{U} = \mathbf{BU}$$

where L is a differential operator.

Stress is related to strain through the constitutive law.

$$\boldsymbol{\sigma} = \mathbf{D}\boldsymbol{\varepsilon} = \mathbf{DBU}$$

17.3.4 Formulation

Consider a finite element of volume V^e with boundary S^e as part of the mesh. The following forces will be contributing to the overall external loading of that element:

- traction forces (normal stresses), $\mathbf{p} = \boldsymbol{\sigma}\widehat{\mathbf{n}} = \{p_x, p_y, p_z\}$ due to neighbouring elements;
- global, body forces, $\mathbf{b} = \{b_x, b_y, b_z\}$; and
- concentrated nodal forces, $\mathbf{P} = \{P_x, P_y, P_z\}$.

Then the work done by external forces (force times displacement) on the element, Ψ^e, is

$$\Psi^e = \int_{V^e} \{\mathbf{u}^e\}^{\mathrm{T}} \mathbf{b}^e dV^e + \int_{S^e} \{\mathbf{u}^e\}^{\mathrm{T}} \mathbf{p}^e dS^e + \{\mathbf{u}^e\}^{\mathrm{T}} \mathbf{P}^e$$

$$\Psi^e = \{\mathbf{U}^e\}^{\mathrm{T}} \mathbf{F}_b^e + \{\mathbf{U}^e\}^{\mathrm{T}} \mathbf{F}_p^e + \{\mathbf{U}^e\}^{\mathrm{T}} \mathbf{F}_P^e$$

$$\Psi^e = \{\mathbf{U}^e\}^{\mathrm{T}} \mathbf{F}^e$$

where

$\mathbf{F}^e$ the element force vector $\quad \mathbf{F}^e = \mathbf{F}_b^e + \mathbf{F}_p^e + \mathbf{F}_P^e$

$\mathbf{F}_b^e$ the body force vector $\quad \mathbf{F}_b^e = \int_{V^e} \{\mathbf{N}^e\}^{\mathrm{T}} \mathbf{b}^e dV^e$

$\mathbf{F}_p^e$ the surface traction vector $\quad \mathbf{F}_p^e = \int_{V^e} \{\mathbf{N}^e\}^{\mathrm{T}} \mathbf{p}^e dV^e$

$\mathbf{F}_P^e$ the nodal force vector $\quad \mathbf{F}_P^e = \mathbf{P}^e$

$\mathbf{F}^e$ the element force vector $\quad \mathbf{F}^e = \mathbf{F}_b^e + \mathbf{F}_p^e + \mathbf{F}_P^e$

Using the stress and strain relationships with the dispalcement as derived above we can evaluate the strain energy (internal/stored) of the element, W^e

$$\left.\begin{aligned} W^e &= \int_{V^e} \{\boldsymbol{\varepsilon}^e\}^{\mathrm{T}} \boldsymbol{\sigma}^e dV^e \\ \boldsymbol{\sigma}^e &= \mathbf{D}^e \boldsymbol{\varepsilon}^e \\ \boldsymbol{\varepsilon}^e &= \mathbf{B}^e \mathbf{U}^e \end{aligned}\right\} \Rightarrow W^e$$

$$= \{\mathbf{U}^e\}^{\mathrm{T}} \left(\int_{V^e} \{\mathbf{B}^e\}^{\mathrm{T}} \mathbf{D}^e \mathbf{B}^e dV^e \right)$$

$$\mathbf{U}^e = \{\mathbf{U}^e\}^{\mathrm{T}} \mathbf{k}^e \mathbf{U}^e$$

where $\mathbf{k}^e = \int_{V^e} \{\mathbf{B}^e\}^{\mathrm{T}} \mathbf{D}^e \mathbf{B}^e dV^e$ is the stiffness matrix of the element.

The principle of virtual work may be applied in the FE context. Virtual work is the 'weak' formulation of the balance of linear momentum and states that if a system of forces acts on a body that is in static equilibrium and the body is given any virtual displacement then the net work done by the forces is zero and so the virtual work is equal to zero. *Virtual work* is the work done by real loads on a solid body when virtual displacements are applied. *Virtual displacement* is an imaginary, small, arbitrary displacement that must be geometrically possible. An important note is that stresses do not change due to the virtual change in displacement, but forces do work due to the virtual change in displacement. In essence, the principle of virtual work suggests that in order for a deformable body to be in equilibrium then the work done by external forces when a virtual displacement is applied is equal to the virtual strain energy; that is the energy stored within the material due to it deforming under load (Fig. 17.4).

In the context of FE, virtual displacement and virtual strain may be associated with virtual nodal displacements using the shape functions and the matrix **B**.

$$\delta\mathbf{U}^e = \mathbf{N}\delta\mathbf{u}^e$$
$$\delta\boldsymbol{\varepsilon}^e = \mathbf{B}\delta\mathbf{U}^e$$

When we apply a virtual displacement $\delta\mathbf{u}$ to the element we were considering above, then the virtual external and internal energies, $\delta\Psi^e$ and δW^e, respectively, would be

$$\delta\Psi^e = \{\delta\mathbf{U}^e\}^{\mathrm{T}} \mathbf{F}^e$$
$$\delta W^e = \{\delta\mathbf{U}^e\}^{\mathrm{T}} \mathbf{k}^e \mathbf{U}^e$$

and by applying the principle of virtual work the total work done should be equal to zero.

$$\delta\Psi^e - \delta W^e = 0$$
$$\{\delta\mathbf{U}^e\}^{\mathrm{T}} (\mathbf{F}^e - \mathbf{k}^e \mathbf{U}^e) = 0$$
$$\mathbf{F}^e - \mathbf{k}^e \mathbf{U}^e = 0$$

17.3.4.1 Assemble

In order to account for all elements in the mesh, NEL,

$$\sum_{e=1}^{\mathrm{NEL}} (\mathbf{F}^e - \mathbf{k}^e \mathbf{U}^e) = 0$$
$$\mathbf{K}\mathbf{U} = \mathbf{F}$$

where **K** is the global stiffness matrix
F the global force matrix, and
U the global displacement vector.

Some remarks about the stiffness matrix.

- The matrix is symmetric ($K_{ij} = K_{ji}$)

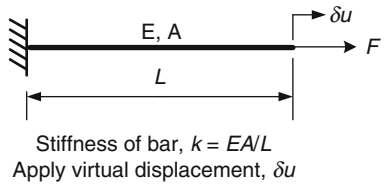

External virtual work done, $\delta We = F\delta u$
Internal virtual work done, $\delta Wi = ku\delta u$
Total virtual work done, $\delta W = \delta We - \delta Wi$
Principle of virtual work states that $\delta W = 0$
Therefore $\delta We - \delta Wi = 0$
and so $F = ku$

Fig. 17.4 A simple example of the principle of virtual work using a bar in tension. Try calculating the internal virtual work done by calculating the internal strain energy (integral of stress times virtual strain ($\sigma\delta\varepsilon$) over the volume) instead of just using the 'spring' reaction force ku

- The coefficients of the matrix K_{ij} are the force F_i required to achieve a unit displacement U_j and zero other displacements.
- The sum of the coefficients in each column is zero as each column represents global forces/loads that are in equilibrium.
- The matrix is singular (i.e. det$\mathbf{K} = 0$); since the sum of the coefficients in each column is zero, the lines are linearly dependent. This means that one cannot inverse the matrix (and so cannot solve for nodal displacements, $\mathbf{U}$) unless one includes appropriate boundary conditions.

17.3.4.2 Solve

In order to solve for the unknown nodal displacements an appropriate numerical method needs to be implemented that can calculate the inverse of the stiffness matrix.

$$\mathbf{U} = \mathbf{K}^{-1}\mathbf{F}$$

Several numerical techniques may be used to solve this problem (Gauss elimination, Cholesky decomposition, etc). The size of the system stiffness matrix will depend on the number of degrees of freedom present in the system.

17.3.5 Evaluation of the Stiffness Matrix; Numerical Quadrature

The stiffness matrix for each element is an integral over the element's volume. In order to carry out the integration numerically FE codes use Gaussian quadrature. Consider the one dimensional integral

$$I = \int_{-1}^{1} f(s)ds$$

This integral can be approximated by a sum

$$I = \int_{-1}^{1} f(s)ds \approx \sum_{n=1}^{\mathrm{NQ}} w_n f(\xi_n)$$

Table 17.1 Gaussian quadrature

Order of quadrature, NQ	Position of Gauss points, ξ	Weight assigned to each Gauss point, w
1	0	2
2	$-\frac{1}{\sqrt{3}}$ $\frac{1}{\sqrt{3}}$	1 1
3	$-\frac{6}{\sqrt{10}}$ 0 $\frac{6}{\sqrt{10}}$	$\frac{5}{9}$ $\frac{8}{9}$ $\frac{5}{9}$

Coordinates of Gauss points and weight assigned to each of them for up to third order quadrature

where ξ_n the position of the Gauss points;
w_n the 'weight' assigned to each Gauss point;
NQ the order of the quadrature; for a linear quadrate NQ = 1; for a quadratic quadrature NQ = 2 and so on.

If we have NQ quadrature points then we can integrate exactly a polynomial of order 2NQ-1; e.g. with 1 Gauss point we can integrate a linear function exactly (polynomial of order 1 has two parameters: $p(x) = a_0 + a_1 x$). Coordinates and weights of Gauss points that correspond to a particular order of integration can be evaluated easily by integrating simple expressions with known results (see Table 17.1).

If we consider a double integral, then it will be approximated by a double sum

$$\begin{aligned} I &= \int_{-1}^{1}\int_{-1}^{1} f(s_1, s_2)ds_1 ds_2 \\ &= \sum_{m=1}^{\mathrm{NQ}}\sum_{n=1}^{\mathrm{NQ}} w_m w_n f(\xi_m, \xi_n) \end{aligned}$$

and if we consider a triple integral, then it will be approximated by a triple sum.

One can apply Gaussian quadrature in order to integrate the element matrix over the element's volume. For example, if we assume 2D space, that the material properties do not depend on position, and that parent element and actual element coincide, then

$$\begin{aligned} \mathbf{k} &= \int_V \mathbf{B}^{\mathrm{T}}\mathbf{D}\mathbf{B}dV \\ &= \sum_{m=1}^{\mathrm{NQ}}\sum_{n=1}^{\mathrm{NQ}} w_m w_n \mathbf{B}^{\mathrm{T}}(\xi_m, \xi_n)\mathbf{D}\mathbf{B}(\xi_m, \xi_n) \end{aligned}$$

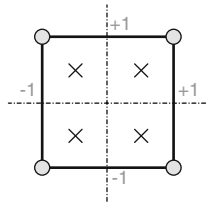

Fig. 17.5 A 2D quadrilateral parent element with four Gauss points that are required for full integration of the stiffness matrix over the element volume; the coordinates in x and y of the points are from the second row (NQ = 2) in Table 17.1

which means use of four Gauss points, marked with × in Fig. 17.5.

17.3.5.1 Mapping of Elements from the *s*- to the *x*-Space: The Jacobian

It is convenient numerically to calculate matrix **B** always at the parent element. Therefore, in the calculation of the stiffness matrix the parent element needs to be mapped to the actual element (Fig. 17.6). If we consider integration of a function $f(x)$ in one dimension, then

$$\int_x f(x)dx = \int_x f(x)\frac{dx}{ds}ds = \int_x f(x)J(s)ds$$

where $\frac{dx}{ds}$ is known as the Jacobian, J of the mapping.

Mapping insofar as elements are concerned happens through the shape functions (Fig. 17.6).

$$\mathbf{x}_i(s) = \sum_{n=1}^{\mathrm{NEL}} \mathbf{N}^e(s)\mathbf{X}_i^e$$

where $\mathbf{x}_i$ the coordinates of a point on the mapped element

and $\mathbf{X}_i$ the coordinates of the nodes of the mapped element.

Elements that use the same shape functions to map the nodal coordinates and the nodal displacements are known as isoparametric elements. The vast majority of elements do so.

In 2D, the Jacobian of the mapping, J is the determinant of the Jacobian matrix

$$J = \det\left(\frac{\partial x_i}{\partial s_j}\right) = \det\left(\frac{\partial}{\partial s_j}\left(\sum_{n=1}^{\mathrm{NEL}} \mathbf{N}^e(s)\mathbf{X}_i^e\right)\right)$$

In 2D

$$\frac{\partial x_i}{\partial s_j} = \begin{bmatrix} \frac{\partial x_1}{\partial s_1} & \frac{\partial x_1}{\partial s_2} \\ \frac{\partial x_2}{\partial s_1} & \frac{\partial x_2}{\partial s_2} \end{bmatrix}.$$

This can be easily generalised to 3D.

Then the element stiffness matrix of the actual element, for example a quadrilateral element (Fig. 17.6), can be evaluated as

$$\mathbf{k} = \int_V \mathbf{B}^{\mathrm{T}}\mathbf{D}\mathbf{B}dV = \sum_{m=1}^{\mathrm{NQ}}\sum_{n=1}^{\mathrm{NQ}} w_m w_n \mathbf{B}^{\mathrm{T}}(\xi_m,\xi_n)\mathbf{D}\mathbf{B}(\xi_m,\xi_n)J(\xi_m,\xi_n)$$

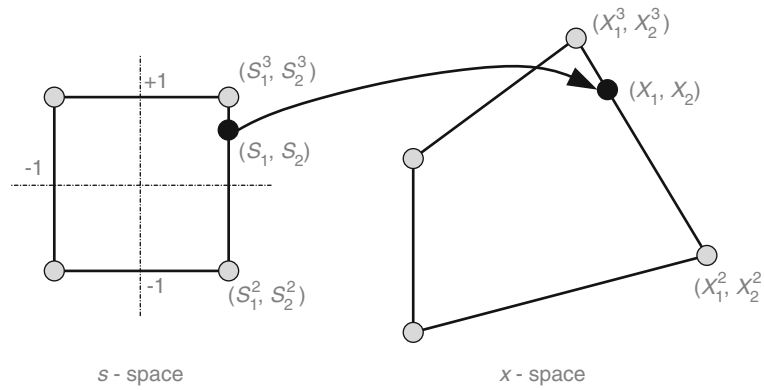

Fig. 17.6 A 2D quadrilateral parent element (s-space) is being mapped onto the actual element in the x-space

17.3.6 Recover Strain and Stress

As the **B** matrix is evaluated at the Gauss points, it is straightforward to evaluate strain and then stress – using the constitutive law – also at the Gauss points. Then strain and stress output may be extrapolated to the nodes or averaged over the element to give a single value for each element. The single value of stress/strain per element is a source of numerical error. Therefore one needs to carry out a mesh sensitivity study (discussed in detail in the last section of this chapter) and refine the mesh appropriately in order to eliminate unacceptably large variations of stress and strain between adjacent elements.

17.3.7 Overview of the Linear Static FE Method

Epigrammatically, these are the steps taken to run a linear static FE analysis. Steps 4–8 are carried out by the FE code whereas 1–3 and 9 by the analyst.

1. Set up finite element mesh and define element type;

$$\mathbf{u} = \mathbf{N}\mathbf{U}$$

2. Assign material properties;
3. Apply boundary (including loading) conditions;
4. Set up element matrices and assemble global stiffness matrix;

$$\mathbf{k}^e = \int_{V^e} \{\mathbf{B}^e\}^{\mathrm{T}} \mathbf{D}^e \mathbf{B}^e dV^e \text{ and}$$

$$\mathbf{K} = \sum_{e=1}^{\mathrm{NEL}} \mathbf{k}^e;$$

5. Set up force matrix

$$\mathbf{F} = \sum_{e=1}^{\mathrm{NEL}} \mathbf{F}^e$$

6. Apply displacement boundary conditions and therefore eliminate known DoFs from the system of equations;
7. Invert stiffness matrix and solve for displacements;

$$\mathbf{U} = \mathbf{K}^{-1}\mathbf{F}$$

8. Recover strain and stress;

$$\boldsymbol{\varepsilon} = \mathbf{B}\mathbf{U} \quad \text{and} \quad \boldsymbol{\sigma} = \mathbf{D}\boldsymbol{\varepsilon}$$

9. Carry out post-processing.

17.3.8 Nonlinear Finite Element Formulation

As discussed earlier, the above formulation is valid for linear analysis, linear geometry (small displacements and rotations) and linear material response. The formulation that accounts for nonlinear responses is similar, but the stiffness matrix and the external force will be a function of the displacement and therefore an iterative numerical schema (such as the Newton–Raphson) needs to be implemented.

$$\mathbf{K}(\mathbf{U})\mathbf{U} = \mathbf{F}(\mathbf{U})$$

As most nonlinear problems - and definitely those with nonlinear material models - are associated with large deformations, finite strain theory is implemented (see Chap. 3, Sect. 3.4.1). This means that the stress and strain values that are evaluated at recovery are either the second Piola-Kirchhoff stress with Green-Lagrange strain (when using a total Lagrange schema) or Cauchy stress with logarithmic strain (when using an updated Lagrange schema).

17.3.8.1 Dynamic FEA: Modal and Transient Analysis

If we consider dynamic effects, the equation to be solved in FE will be of the form

$$\mathbf{M}\ddot{\mathbf{U}} + \mathbf{C}\dot{\mathbf{U}} + \mathbf{K}\mathbf{U} = \mathbf{F}$$

where **M** is the FE mass matrix, **C** the damping matrix, $\ddot{\mathbf{U}}$ the nodal accelerations and $\dot{\mathbf{U}}$ the nodal velocities (see also Sect. 3.5.1).

$$\mathbf{M} = \int_V \mathbf{N}^{\mathrm{T}} \rho \mathbf{N} dV$$

To carry out a *modal analysis* of a structure, one needs to solve the undamped free vibration problem (see also Sect. 3.5.1)

$$\mathbf{M}\ddot{\mathbf{U}} + \mathbf{K}\mathbf{U} = 0$$

from which natural frequencies and the corresponding (modal) shapes of the structural system can be evaluated.

17.4 Explicit FEA for Dynamic Systems

17.4.1 The Single Degree of Freedom System (SDOF)

Perhaps the simplest form of numerical analysis of a dynamic system would be the solution of a single degree of freedom (SDOF) system via an explicit, time-stepping analysis. Consider a spring-mass system, as discussed in Sect. 3.5.1 (Fig. 17.7a). The equation of the (undamped) motion is

$$m\ddot{y} + ky = F(x, t, \ldots)$$

This equation can be used to represent a simple structural element, such as a beam, that is loaded by a force per unit length, p. For each of the terms of the equation, at every point during transient response, the energies associated with the SDOF must be equal to those in the real system. A real system has spatially-varying properties (in this case in the x direction) whilst the properties within a SDOF act at a single point. As a consequence, simple integration techniques must be used to 'transform' the 'distributed' mass and loading into 'effective' quantities as follows:

$$m_e = \frac{m}{L} \int_0^L \phi(x)^2 dx$$

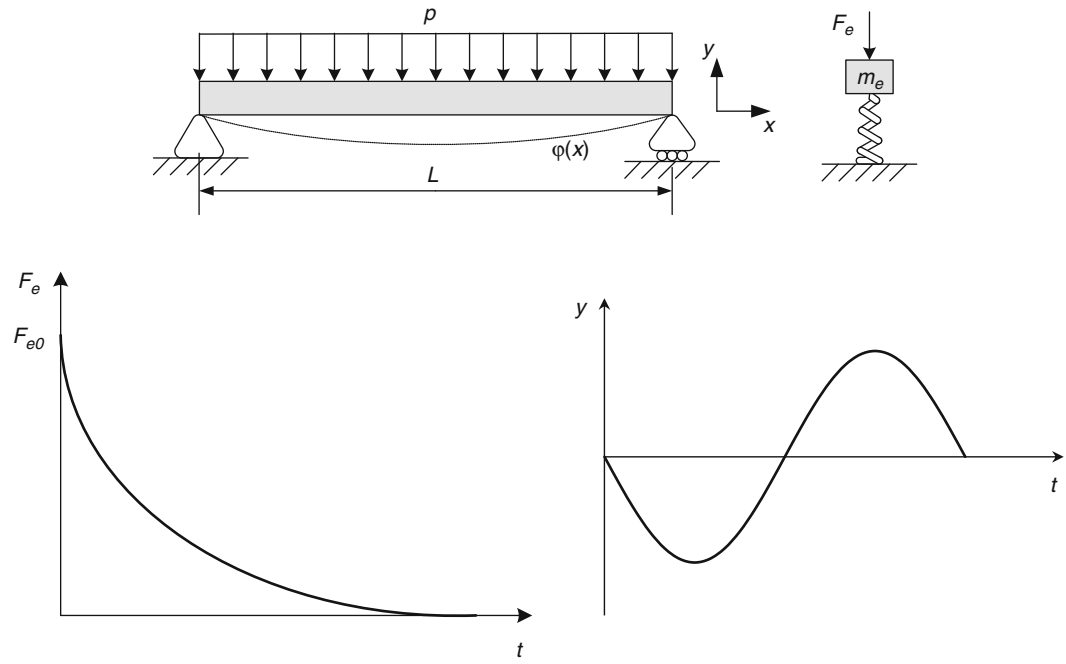

Fig. 17.7 (**a**) Simply supported beam under a distributed load and its SDOF equivalent representation. (**b**) Exponentially decaying blast loading. (c) Harmonic solution to the resulting ordinary differential equation (ODE)

$$F_e = p\int_0^L \phi(x)dx$$

φ is a dimensionless 'shape function' and in this case describes the spatial deflection of the beam as a function of x. The deformed shape will depend on the support conditions of the beam as well as the loading distribution upon it and its material characteristics. For example, the simply-supported, elastic beam exposed to a uniform spatial loading, as shown in Fig. 17.7a would produce the following shape function:

$$\phi(x) = \frac{16}{5L^4}\left(L^3x - 2Lx^3 + x^4\right)$$

17.4.1.1 Closed Form Solution

For scenarios in which strong approximations or idealisations are acceptable, the functions representing the individual terms in the ordinary differential equation above can be contrived to allow solution in a closed-form manner. For such cases it must also be assumed that the shape function remains constant throughout the entire motion of the structure. For example, the equation of motion of a purely elastically deforming, simply-supported beam (of effective stiffness, k) exposed to an idealised blast wave, exponentially-decaying as a function of T (Fig. 17.7b), is

$$m_e\ddot{y} + k_e y = F_{e0}e^{-(t/T)}$$

This ordinary differential equation (ODE) can be solved in a closed-form manner to yield a harmonic displacement response (Fig. 17.7c)

$$y(t) = y_{stat}A\left(\frac{\sin(\omega t)}{\omega T} - \cos(\omega t) + Be^{-\left(\frac{\omega t}{\omega T}\right)}\right)$$

where y_{stat} is the deflection that the structure would attain if the load were applied statically and A is given by

$$A = \frac{(\omega T)^2}{1 + (\omega T)^2}$$

with $\omega = \sqrt{\frac{k_e}{m_e}}$ being the Natural frequency of the system.

Whilst solution in this case is extremely quick its scope of usage is highly limited. Where a structure possesses a complex geometry, is exposed to a highly variable temporal loading, exhibits non-linear material behaviour or experiences a change in mode during its transient deformation, a purely mathematical solution is not possible and a numerical approach must be implemented.

17.4.1.2 Numerical Solution with Explicit Time-Stepping: The Linear Acceleration Method

The linear acceleration method represents one of the most simple and effective ways of attaining a solution for an equation of motion that cannot be solved analytically. Its application within a SDOF framework is shown in the flow diagram in Fig. 17.8a. Instead of providing a continuous solution, here the response of the system, similar to that shown in Fig. 17.7b for example, is predicted over a series of discrete time-steps with linear changes in acceleration being assumed between them (Fig. 17.8b). By utilising the Simpson's rule, the velocity at a given instant, t_i can be estimated as

$$\dot{y}_i = \dot{y}_{i-1} + \frac{\Delta t}{2}\left(\ddot{y}_i + \ddot{y}_{i-1}\right)$$

whilst displacement at the next time step can be estimated as

$$y_{i+1} = y_i + \dot{y}_i\Delta t + \frac{(\Delta t)^2}{6}\left(2\ddot{y}_i + \ddot{y}_{i+1}\right)$$

For an equation of motion of the type described above the acceleration at any given instant of time and as such at, t_{i+1}, can be expressed by

$$\ddot{y}_{i+1} = \frac{F_e(t_{i+1}) - k_e y_{i+1}}{m_e}$$

and this expression can be substituted into the one above and rearranged to yield

$$y_{i+1} = \frac{y_i + \dot{y}_i\Delta t + \frac{(\Delta t)^2}{3}\ddot{y}_i + \frac{(\Delta t)^2}{6}\frac{F_e(t_{i+1})}{m_e}}{1 + \frac{(\Delta t)^2}{6}\frac{k_e}{m_e}}$$

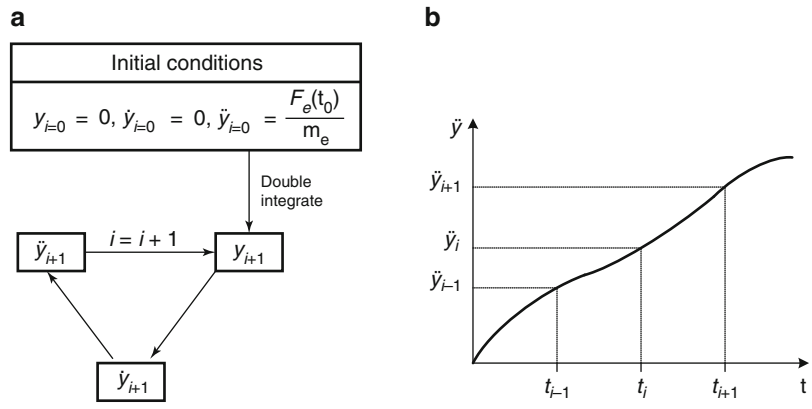

Fig. 17.8 Linear acceleration method when applied within a SDOF framework. (**a**) Calculation framework. (**b**) Temporal integration technique

In order to instigate the calculation process initial conditions must be assumed such as velocity ($\dot{y}_0$) and displacement (y_0). In this case the force term in the equation of motion can be exclusively equated to the inertial term to yield an initial acceleration as follows

$$\ddot{y}_0 = \frac{F_e(t_0)}{m_e}$$

This can then be substituted into the equation directly above it to determine the displacement for the next time step and the output, in turn, substituted into the velocity equation to establish the velocity for the next time step.

As equilibrium must only be satisfied at an instant in time, non-linear functions can be readily accommodated for all terms of the equation of motion but the time-step must be small enough to avoid instability and inaccuracy.

17.4.2 Explicit FE and Hydrocode Techniques

In cases where levels of spatial variation (in terms of geometry, loading distribution and material characteristics) are too great to be represented via the coarse, 'lumping' approach as described above, explicit FE and Hydrocode (HC) techniques can be applied. These are often used to tackle dynamic problems where, at times, the strength of the loaded material is substantially lower than the pressures exerted during the simulation. There is a requirement, therefore, for information on material behaviour at extreme regimes; this is provided by equations of state (EoS) (see Sect. 3.4.4). The EoS and the constitutive relationship of a material usually are termed collectively as a material model.

Despite the relative spatial complexity, the transient deformations within the model can be predicted using a similar explicit, time-stepping scheme to that described above for a SDOF. In terms of the spatial treatment, when operating within a Lagrangian numerical framework, the application of the external load (during the initial time-step) causes deformation of the nodes which bound the elements in immediate proximity to the loading. Deformation, displacements and rotations in this scheme are calculated in a similar manner to what was discussed in the previous section, whereby the stiffness matrix is evaluated at every time step. In contrast to an implicit (Newton–Raphson-type) iterative, dynamic scheme, an explicit method does not require equilibrium between the internal structural forces and the externally applied loads to be satisfied at each time step.

For the stability to be maintained during the calculation, a 'disturbance' originating in one particular element must not travel beyond its immediate neighbours. The time step can be determined based on the Courant criterion for the element.

$$\Delta t = \frac{l_{min}}{2c}$$

where l_{min} is the minimum element length dimension
and c the factored wave speed (a factor of two is applied here).

When loading rates produce velocities that exceed the material wave speeds then it is these which may dictate the time step. The mesh (or series of interacting meshes) that constitute a numerical model may contain elements of different type and size; for numerical calculations using an explicit temporal solution scheme it is the minimum element dimension within the whole model that often dictates the absolute calculation time-step size. Generally speaking, smaller elements (higher mesh resolution) produce results of greater accuracy but care must be taken when developing a model that appropriate element sizes are used to avoid prohibitively long calculation times.

When considering the general stress state affecting a material under load, it is convenient in numerical analysis to separate the stresses that cause deviatoric response, (change in deformation shape or 'shearing behaviour' but no volume change) from those that result in hydrostatic response (volume change but no change in shape) (see Sect. 3.4.1). When generating a solution it is worth considering that the strength-related behaviour (including aspects of failure and damage) are usually controlled by the deviatoric response whilst volumetric changes, pressure dependency and temperature (internal energy) changes are dictated by the hydrostatic response.

The time-step dependence of explicit methods can lead to long run times compared to equivalent implicit approaches but the lack of dependency on convergence often allows the representation of more complex material interactions (such as those associated with component contact). In scenarios involving highly transient phenomena, explicit methods can also better facilitate the coupling of two different numerical schemes. For example, Fluid Structural Interaction (FSI) can be readily implemented to couple a Lagrangian structural mesh to an Eulerian mesh which contains a fluid. The approach is often used when modelling the effect of a blast loading on a structural entity. As discussed in Sect. 17.2, the Eulerian scheme is better suited to tracking the rapidly expanding blast wave whilst the Lagrangian scheme is often better suited to tracking complex material responses when excessive deformations are not involved. An example of explicit FSI is described in Sect. 17.6.3 for analysis of human response to fragment penetration. In relation to the discussion on stability earlier in this section, the consideration of interactions between different materials or different schemes can result in yet further time-step factoring.

17.5 Verification, Validation and Sensitivity Studies in FEA

A computational model is an approximation of a physical phenomenon, as such it is inherently inaccurate to some extent. It is important, therefore, to ascertain the utility, credibility, predictive ability, and interpretation of each computational model.

17.5.1 Verification

Verification of a computational model according to the American Society of Mechanical Engineers (ASME) is "the process of determining that a computational model accurately represents the underlying mathematical model and its solution."

Verification is associated with the writing of the mathematical code itself. A verified code will have been tested against benchmark problems for which analytical solutions exist; this means that the underlying physics, numerical discretisation, solution algorithms and convergence criteria of the code are correctly implemented. This process

has been conducted for all commercially available FEA software.

What an FE code cannot guarantee is the so called 'calculation verification' since it is associated with the user. Calculation verification in FEA is usually conducted by assessing the adequacy of the discretisation in space and time. Usually FE model predictions are 'stiffer' compared to analytical solutions and so a mesh refinement will make the model more 'compliant'. At the same time, if the problem is dynamic, the time step has to be decreased to account for the smaller element sizes as per the discussion in Sect. 17.4.2 above. Refinement is a process of diminished returns, as there exists a level of discretisation beyond which the change in the resulting values of variable(s) the modeller is interested in (such as stress and strain) is adequately small. Refinement comes with computational cost, therefore the modeller needs to decide how much discretisation is 'enough' and communicate it appropriately. Terms such as mesh convergence or mesh validation are used to refer to verification of the spatial discretisation in FEA. Verification of a model does not guarantee adequate predictive ability of a physical phenomenon, but only consistency in prediction. If the model is used with substantially different loading or boundary conditions to those that the verification process was carried out initially, then a consequent mesh verification study might be necessary. Experience and good engineering judgement are critical in this process.

17.5.2 Validation

A model can be considered validated when its predictions fall within an acceptable range of the corresponding experimental results. The range over which an FE model has been validated depends on the case and should be communicated appropriately. It is not uncommon and usually good practice to design validation experiments that are well controlled and test specific predictive abilities of the FE model; the intention is not to carry out the complex experiment that the FE model is trying to simulate (else what do you need to model for?), but to build confidence in the predictions of the FE model at specific key locations for specific variables (e.g. strain). After all, an FE model is usually developed in order to explore parameters and behaviours that are impossible or very expensive to quantify experimentally. It may be that model predictions are not similar to the corresponding experimental data in which case the model cannot be deemed fit for its intended use; a reassessment of FE model parameters and assumptions is therefore then essential.

17.5.3 Sensitivity

Sensitivity studies involve altering key FE model input parameters over a sensible/expected/physiological range in order to assess the dependency of key outputs (e.g. strain) to them. It is common for a number of input parameters to be associated with uncertainty. It is important to assess the dependency of the prediction on especially uncertain input data; this in essence forms part of the validation process as it will dictate the range (of input/loading parameters) over which the model is valid. Sensitivity studies may be conducted using statistical (e.g. Monte Carlo or Taguchi methods) or one-at-a-time approaches depending on the application.

17.6 Examples of Numerical Modelling in Blast Injury

17.6.1 Axelsson Model for Blast Loading of the Chest Wall

Axelsson and Yelverton [1] used a single degree of freedom system to represent the response of the human chest wall exposed to blast loading (Fig. 17.9). The thorax is represented as a dynamic system with an effective stiffness, K and damping, C that aggregate the response to the insult of skeletal tissue, soft tissue, liquid (e.g. blood), and gas in the lung. The applied

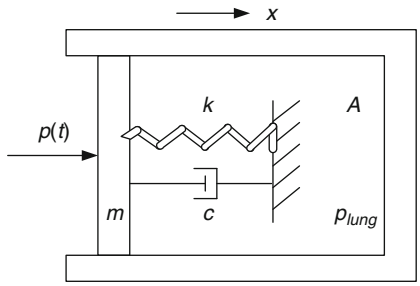

Fig. 17.9 SDOF representation of a thorax exposed to blast loading (representing the human lungs)

force is derived from the difference between the transient blast pressure and the lung pressure.

$$m\ddot{x} + c\dot{x} + kx = A\left(p(t) - p_{lung}(t)\right)$$

where p_{lung} is the pressure within the lung, A is the effective lung area.

Solving this differential equation numerically using the numerical calculation cycle described above (Fig. 17.8) allows one to examine the response caused by relatively complex blast signals (e.g. multi-reflection loading resulting from internal explosions).

17.6.2 Projectile Flight and Penetration

Penetrating fragmentation resulting from the detonation of cased, military munitions or an improvised explosive device can be a significant source of human injury (secondary blast injury). Once the driving forces from the explosion have ceased to act upon it, a fragment may travel for a period within the surrounding air environment before penetrating a human at a given proximity from the explosive source. In order to assess the likelihood and severity of injury the trajectory and velocity profiles of the fragments need to be calculated (Fig. 17.10). For a fragment of mass m the inertial force acting on it in the horizontal direction is balanced by retardation forces such as drag (which is a function of velocity squared), friction (which is a function of velocity), and stiffness and strength of the propagation medium. Balance in the vertical direction is similar with the addition of gravity.

$$-m\frac{d\boldsymbol{u}}{dt} = \boldsymbol{A}\left(u^2\right) + \boldsymbol{B}(u) + \boldsymbol{C}$$

Fig. 17.11 shows a practical, numerical implementation of the method within the Human Injury Prediction (HIP) software; a fast running tool developed by the Centre for the Protection of National Infrastructure (CPNI) to predict blast and fragmentation injury risk due to explosive events in crowded public spaces. Here, the trajectories of multiple fragments, produced by Person Borne Improvised Explosive Device (PBIED), are being tracked within an environment containing a crowd of people, each represented by a cylinder with broadly human-like material properties. The approach allows the depth of penetration within the humans to be predicted, or indeed determines whether the fragments are sufficiently penetrative to pass through the human with a residual velocity and then affect others standing further away within the crowd. When undertaking such analysis, the use of a temporal integration scheme with a fixed time step, such as within the standard linear acceleration method explained above, may be inefficient as velocity changes in the fragment trajectory during transit in the air are much more gradual than those when the fragment is penetrating the humans. The HIP software makes use of a more advanced, Runge–Kutta schema – an iterative method developed for solving numerically a system of ordinary differential equations - with a variable time step size dictated by the characteristics of the penetration medium.

17.6.3 Fragment Penetration to the Neck

Upon detonation blast weapons often produce high velocity fragmentation from their casing or from other material in close proximity to the

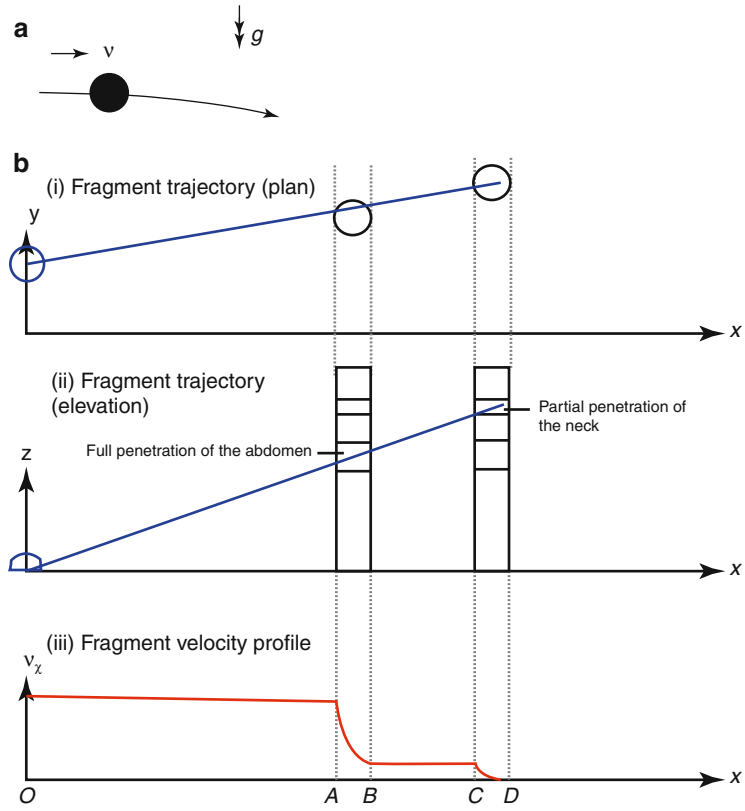

Fig. 17.10 Use of ordinary differential equations to represent projectile flight and the process of penetration into the human body. Trajectory and velocity profiles of the fragment (Adapted from [2])

Fig. 17.11 Use of numerical fragment flight algorithms within the HIP code to represent the effect of protective barriers within (**a**) a tiered, stadium-type environment and (**b**) a crowded space during an explosive attack

charge. Penetration of such fragments into the human body can result in serious or fatal injury (secondary blast injury). The model shown in Fig. 17.12 simulates the penetration of a cylindrical fragment through a human neck. Within this Euler-based framework the components of the neck (i.e. bones, veins, nerves and arteries as well as skin and muscle) are spatially generated by 'filling' the pertinent elements of the mesh with the appropriate material. In this case either elastic, viscoelastic or inviscid fluid material models have been used in accordance with the behaviour of the component being simulated. The fragment is modelled as a rigid Lagrangian

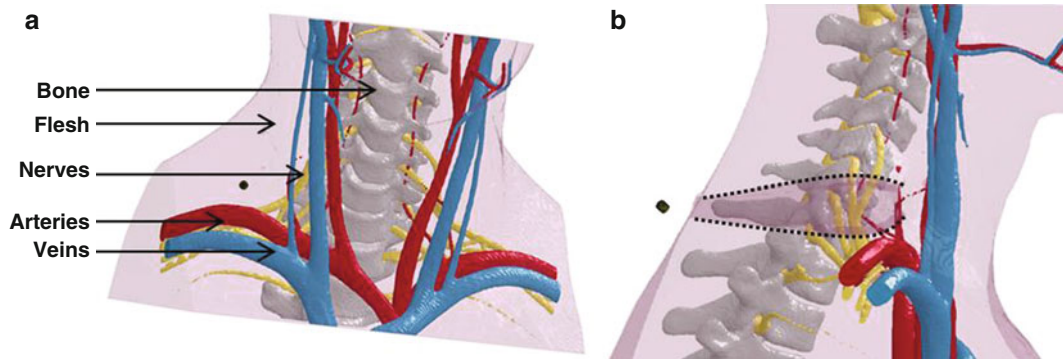

Fig. 17.12 Simulation of fragment penetration in the human neck

entity and fluid–structure interaction has been assigned to couple the projectile at it penetrates the neck.

17.6.4 The Lower Extremity in Tertiary Blast

Leg injury within military vehicles due to floor-plate ingress during a mine-loading event has been common in recent conflicts. In the example shown in Fig. 17.13 a Lagrangian model of the human leg has been developed using a variety of element types. The bone components of the leg have been represented using a combination of shell and solid elements whilst solid elements have been used to represent the surrounding soft tissue. Contact logic is assigned between the bone and its surrounding soft tissue that could potentially interact during the deformation process. Ligaments and tendons are modelled as a collection of one-dimensional, discrete elements that join the bone components together at the appropriate anatomical locations. To secure the leg in space a 'joint-type' boundary condition is enforced at the hip; This effectively allows the leg to translate upward and rotate about a prescribed axis (crudely representing the hip joint). As further boundary conditions, point masses have been applied to nodes around the joint to account for the weight of the rest of the human. All material models in this preliminary simulation are linearly elastic. The simulation is of a laboratory experiment using a traumatic injury simulator [3] (see Chap. 22, Sect. 22.3.2). The foot is located against a steel plate, formed of shell elements, which represents the floor of the military vehicle and contact

Fig. 17.13 Lower limb FE model that simulates injury due to floor-plate ingress during a mine-loading event

interaction is defined between the sole of the foot and the plate. The leg is relaxed under gravity until equilibrium is established. Then the dynamic phase of the simulation is initiated by assigning a velocity time history to the plate which is representative of that produced by mine loading.

References

1. Axelsson H, Yelverton JT. Chest wall velocity as a predictor of non-auditory blast injury in a complex blast wave environment. J Trauma Inj Infect Crit Care. 1996;40(3S):31S–7S.
2. Pope DJ. The development of a quick-running prediction tool for the assessment of human injury owing to terrorist attack within crowded metropolitan environments. Philos Trans R Soc B. 2011;366:127–43.
3. Masouros SD, Newell N, Ramasamy A, Bonner TJ, West ATJ, Hill AM, Clasper JC, Bull AMJ. Design of a traumatic injury simulator for assessing lower limb response to high loading rates. Ann Biomed Eng. 2013;41(9):1957–67.

Suggested Further Reading

Anderson AE, Ellis BJ, Weiss JA. Verification, validation and sensitivity studies in computational biomechanics. Comput Methods Biomech Biomed Engin. 2007;10(3):171–84.
ASME V&V 10–2006. Guide for verification and validation in computational solid mechanics. New York: American Society of Mechanical Engineers; 2006.
Biggs JM. Introduction to structural dynamics. New York: McGraw Hill Higher Education; 1964.
Hallquist JO. LS-Dyna keyword user's manual, version 970. California: Livermore Software Technology Corporation; 2003.
MSC. Marc User's manual, vol. A: theory and user information. Santa Ana: MSC Software Corporation; 2005.
Ottosen NS, Ristinmaa M. The mechanics of constitutive modelling. Massachusetts: Burlington/Elsevier Science; 2005.
Shigley JE, Mitchell LD. Mechanical engineering design. London: McGraw Hill Higher Education; 2003.
Zienkiewicz OC, Taylor RL, Zhu JZ. The finite element method. 7th ed. Oxford: Butterworth-Heinemeann/Elsevier; 2013.
Zukas J. Introduction to hydrocodes. Oxford: Elsevier Science; 2004.

Energised Fragments, Bullets and Fragment Simulating Projectiles

18

John Breeze and Debra J. Carr

18.1 Introduction

The pattern of injuries sustained by soldiers is determined by the types of wounding agent, the tissues they penetrate and any methods of preventing that initial injury. In current conflicts the burden of injuries directly sustained from conflict far outweighs that sustained outside of battle or secondary to disease, in direct contrast to almost every conflict ever experienced in history prior to the twenty-first century. Throughout the history of warfare, penetrating injury has been the most common cause of death on the battlefield, with only a small proportion (4 %) of battle injuries from blunt trauma. Blunt trauma is commonly caused from the force of the explosive blast wave throwing the soldier against an object (the tertiary blast effect) [1]. Blunt injury due to interpersonal assault or road traffic accidents is responsible for most non battle injuries, with patterns reflective of that seen in civilian wounds. The term 'ballistic wounds' is loosely used in both popular culture as well as medicine to describe any injury due to firearm. In terms of potential wounding mechanisms produced in a military environment, ballistic injuries can be broadly divided into those from bullets and those from energised fragment producing munitions and devices [2–11] (Table 18.1). These injuries can be termed "secondary blast injuries", following on the definitions in Chap. 6.

18.2 Bullets

In the military context, a bullet is a projectile propelled by a firearm that in itself does not normally contain explosives but damages the intended target through penetration. Most military bullet wounds are from high velocity rifles, usually resulting in significant energy transfer and tissue cavitation. Low velocity bullet wounds are rare on the current battlefield but this has the potential to change, particularly in urban conflicts and counter insurgency operations. A modern bullet cartridge can be thought of comprising the following five components:

1. the bullet, as the projectile;
2. the cartridge case, which holds all parts together;
3. the propellant, for example gunpowder or cordite;

J. Breeze (✉)
Academic Department of Military Surgery and Trauma, Royal Centre for Defence Medicine, Birmingham Research Park, Birmingham B15 2SQ, UK
e-mail: johno.breeze@me.com

D.J. Carr, CEng, FIMMM, MCSFS
Impact and Armour Group, Centre for Defence Engineering, Cranfield University at the Defence Academy of the United Kingdom, Shrivenham SN6 8LA, UK
e-mail: d.j.carr@cranfield.ac.uk

A.M.J. Bull et al. (eds.), *Blast Injury Science and Engineering: A Guide for Clinicians and Researchers*,
DOI 10.1007/978-3-319-21867-0_18

Table 18.1 Incidence of battle injury (%) by wounding type in twentieth and twenty-first century conflicts; other causes include interpersonal assault and blunt trauma [2–11]

Conflict	Bullets	Fragmentation	Other
World War 1 (early 20th C)	39–65	35–61	–
World War 2 (middle 20th C)	10–27	73–85	5
Korea (middle 20th C)	7–31	69–92	1
Vietnam (middle 20th C)	35–52	44–65	4
Borneo (middle 20th C)	90	9	1
Northern Ireland (late 20th C)	55	22	20
Falklands (late 20th C)	32	56	12
Iraq (early 21st C)	19	81	–
Afghanistan (early 21st C)	20	74	6

Fig. 18.1 The most common types of bullets utilised on the battlefield (from *left* to *right*); 7.62 NATO BALL and 5.56 × 45 mm rifle bullets compared to 9 × 19 mm handgun bullet

4. the rim, which provides the extractor on the firearm a place to grip the casing to remove it from the chamber once fired; and
5. the primer, which ignites the propellant (Fig. 18.1).

The lethality of bullets has varied with time reflecting developments in technology [2–11] (Table 18.2). There was an initial increase due to the ability of the manufacturers to increase muzzle velocity and therefore both the effective range and the kinetic energy transmitted to the target. Although the introduction of the machine gun was to transform the overall ability of firearms to kill on a new level due to its rate of fire, it actually resulted in the lethality of an individual bullet reducing. Declaration 3 of the Hague Convention of 1899 prohibited the use in international warfare of bullets that easily expand or flatten in the body. Conforming countries changed their bullets to ones with a full metal jacket, consisting of a soft core (usually made of lead; excluding armour piercing (AP) bullets which contain a hardened core) encased in a jacket of harder metal such as gilding metal, usually just around the front and sides with the rear lead part left exposed. The jacket allows for higher muzzle velocities than bare lead and reduces expansion of the lead core on impact with the target (the bullet will mushroom if it impacts a harder structure), thereby causing less energy deposition and a decrease in lethality.

Table 18.2 Probability of lethality from different types of weaponry [2–11]

Weapon	Boer war (UK) Late 19th C	WW1 (UK) Early 20th C	WW2 (US) Middle 20th C	Vietnam (US) Late 20th C
Bullet	0.64	0.38	0.32	0.39
Mortar			0.12	0.13
Grenade		0.08	0.05	0.13
Artillery shell		0.28	0.11	0.25

18.3 Energised Fragments

World War I was the first major conflict to utilise less discriminate methods of ballistic injury, primarily those that employed fragmentation. These ranged from smaller devices, such as the hand grenade, to weapons that could cause widespread fragmentation such as the aerial bombardment produced by shells. Since then, fragmentation wounds have outnumbered those caused by bullets, with the exception of particular smaller

scale conflicts such as the Falklands war or those involving jungle warfare or urban counter insurgency operations (Table 18.1).

A large variety of munitions and devices are designed to produce fragments. Historically the most common types of fragment producing munitions have been grenades, mines, mortars and shells. Such munitions generally either utilise preformed fragments or the explosive force produced within the munition acts to break up the metallic casing. Anti-personnel mines are a form of land mine and can be classified into blast mines or fragmentation mines. While blast mines are designed to cause severe injury to one person, fragmentation mines are designed to project small fragments across a wider area, and thereby causing a greater number of injuries.

Fragmentation grenades can be hand thrown, underslung from a rifle or rocket propelled. The body may be made of hard plastic or steel. Fragments are most commonly produced by notched wire breaking up the plastic or steel outer casing (Fig. 18.2) or by depressions within the actual casing which create fragments by the expanding explosive force (Figs. 18.3 and 18.4). The UK currently uses the L109A1 high explosive grenade as its primary device, with a lethal range of 20 m unprotected, and 5 m wearing body armour and helmet. When the body bursts the manufacturer states that it will produce approximately 1800 fragments weighing about 0.01 g each. The M67 is the primary fragmentation hand grenade utilised by both US forces and Canadian forces and produces fragments that have a lethal radius of 5 m and can produce casualties up to 15 m, dispersing fragments as far away as 230 m.

In addition to fragmenting munitions, the wars in Iraq and Afghanistan have become known for the enemy's reliance on improvised explosive devices (IEDs). An improvised explosive device (IED) is manufactured using easily available materials in order to have a destructive and disruptive effect [12, 13]. IEDs represent the most common threat to soldiers worldwide involved in counter-insurgency operations, and are the leading cause of injury and death for soldiers in modern conflicts [14]. IEDs can be manufactured using conventional weapons, or may be completely homemade; IEDs typically have a fragmentation and blast effect [15]. An IED consists of a casing, an explosive and a fusing mechanism with or without added material to create a fragmentation effect [12]. The casing of a homemade IED can be made out of diverse commonly available objects including metal cans, glass or polymer bottles and pipes [12]. Fragments impacting personnel may be of random or regular shape, originating from a preformed source (e.g. notched casing, ball

Fig. 18.2 Cross section of a fragmentation grenade in which detonation of the explosive core (not present in this demonstration model) causes the scored steel rings within the case to fragment

Fig. 18.3 An early style of fragmentation grenade in which the explosive core causes the outer casing to fragment. Originally the casing was grooved to make it easier to grip and not as an aid to fragmentation, and in practice it has been demonstrated that it does not shatter along the segmented lines (natural fragmentation)

bearings), added material (often referred to as shipyard confetti e.g. nails, ball bearings, screws, washers, bolts etc) or the environment. In addition human body parts can be incorporated in wounds in suicide bombings [16]; (Chap. 6).

Excluding the effects of blast, the lethality of fragmentation weapons is generally far less than bullets, with the exception of artillery shells which produce large fragments at high exit velocities [17]. Hand grenades in particular are designed to produce a high number of small fragments and often incorporate spheres which are more aerodynamic and thereby increase effective range. The result is to produce many survivors with multiple injuries that cause a greater burden on healthcare resources and the logistical chain.

18.4 Classification of Energised Fragments

With such a broad range of weaponry generating energised fragments, the authors favour a method of classification by which not only the method of fragment production, but also fragment characteristics are included (Table 18.3). Fragments can be either random in nature (so called 'natural' fragments) or preformed. Typically the fragments obtained during trials are in the size range of $<$1–5 mm and have a mass of 0.1 to $>$20 g with non-uniform shapes [18]. However, spherical fragments (ball bearings)

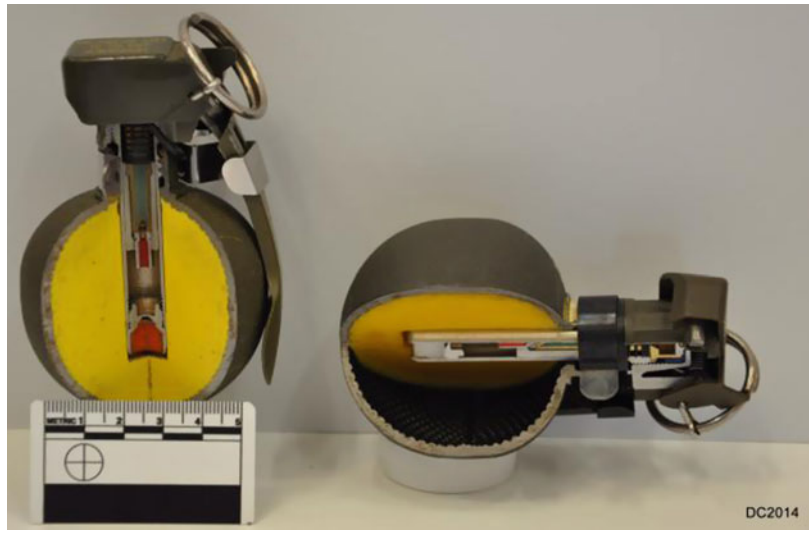

Fig. 18.4 Cross sections of a fragmentation grenade in which the core (*yellow*) contains an explosive which is ignited by the fuse and propels fragments each formed by dimples in the inner surface of the steel casing

Table 18.3 Classification of fragments in terms of deriving appropriate fragment simulating projectile

Type	Method of production	Material	Shape	Mass
Grenade	Preformed	Metallic	Generally spherical or regular	Low (in range of 0.1–0.4 g)
Land mine	Preformed	Metallic	Generally spherical or regular	Low (in range of 0.5–5 g)
Shell	Preformed	Metallic	Random	Medium (in range of 1–10 g)
Shell or grenade casing	Natural	Metallic and non metallic	Random	Low (in range of 0.2–2 g)
Improvised	Improvised	Metallic and non metallic	Random, although often incorporate munitions above	Variable

Fig. 18.5 Range of sizes of energised fragments produced by a typical mortar

are commonly found in traditional munitions and in some IEDs including person-borne IEDs (PBIEDs; 'suicide vests'; 'suicide belts'). Such fragments pack efficiently, are cheap and easy to purchase. Natural fragments are generally produced by larger artillery shells and tend to produce heterogenous range in terms of size and shape. Initial velocities may be very high (>1500 m/s) but because of their irregular shape velocities decline rapidly. Pre-formed fragments are either incorporated into the explosive device itself, or are produced by notching of the metal or plastic casing which break off into predefined shapes (Fig. 18.5). Such pre-formed fragments tend to be relatively light (often 0.1–0.4 g) but numerous [18], increasing the probability of a hit in lightly armoured soldiers but with reduced lethality (Table 18.1).

18.5 Fragment Simulating Projectiles

In experimental studies, fragment simulating projectiles (FSPs) are utilised to be representative of different the different types of energised fragments described previously (Fig. 18.6). Some munitions or devices may produce multiple characteristic fragment types, and therefore a different FSP is required to be representative for each. Those steel FSPs described in the NATO standardising agreement (STANAG) 2920 should ideally be used [19] as this enables greater comparisons between experiments. Standardised FSP shapes described within this document include the cylinder, sphere, cube and flechette, although the latter two shapes

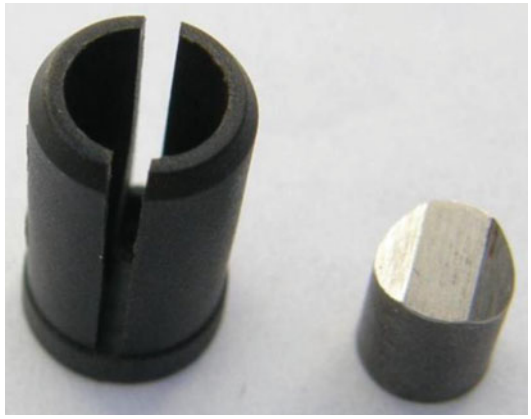

Fig. 18.6 A 1.10 g chisel nosed fragment simulating projectile that can be held within a plastic sabot capable of being fired from a 7.62 barrel

are rarely used in current practice. The 1.1 g chisel nosed cylinder has been the mainstay of body armour ballistic protective material testing since it was first introduced in the 1943 [20]. However, when using such a shape when testing biological tissues it can cause greater variability in testing results by increasing yaw in flight and tumbling. For this reason a sphere is often used in addition, as it reduces the number of experimental shots required, which is particularly important when testing animal tissue with its inherent biological variability due to its varying tissue types.

Currently those FSPs described in the STANAG 2920 are comprised of hardened steel, although there is a desire to agree upon representative shapes and masses of non metallic projectiles [21]. These constituents are thought to be of great importance in accurately representing the heterogenous constituents of IEDs as well as representing plastic casings from some grenades as well as soil ejecta. It should be recognised that such non metallic fragments have in general a far lower mass than their equivalent steel FSP counterparts, such that many don't even breach skin at lower velocities.

18.6 Choice of Fragment Simulating Projectile for Testing

Selecting the most representative FSP for experimental testing continues, is often difficult and clearly relies on an accurate knowledge of the potential threat. Utilising a descriptive classification of fragment characteristics as demonstrated in Table 18.3 will aid in selection. Once the threat has been identified, fragment characteristics can be derived in greater detail from the following sources:

(a) munitions manufacturers' descriptions of preformed fragments;
(b) arena trials to analyse what fragments are produced in controlled explosions of varying munitions and devices;
(c) analysis of fragments retained in armour; and
(d) analysis of fragments retained in the tissues of injured persons.

Manufacturers, as well as the military organisations that use them, are historically reluctant to describe in great detail the shapes and sizes of natural and preformed fragments utilised in their devices. In general, hand held devices utilise preformed fragments with masses less than a NATO standardised 0.51 g sphere or 0.49 cylinder, but shells may be designed to produce fragments greater than 4.0 g. The 1.10 g chisel nosed cylinder remains the most widely used FSP for testing of ballistic protective materials, despite little objective evidence to justify its use (Fig. 18.4). Recent evidence suggests that this FSP was originally identified as the most representative fragment shape and size of a 155 mm artillery shell detonated in early arena trials.

Although the characteristics of fragments removed from injured persons have been described intermittently since World War 1, it has not been until the twenty-first century that a dedicated programme to analyse them was instigated, and now includes those retained in damaged personal protective equipment [22]. Concerns about how representative such samples are have been raised recently, recognising that fragments of low mass and velocity may simply bounce off armour and to a lesser degree skin. Analysing fragments retained in the eye may be more representative as the velocity required to perforate the cornea is far lower than skin. There will also be a number of fragments that fully perforate the body or armour material, or despite careful dissection during post mortem or surgery just cannot be found. Computed Tomography (CT) scans capture all these smaller retained

fragments that cannot be excised and such scans are now routinely performed on all soldiers killed in action or whose wounds generate a trauma call in a deployed field hospital. An analysis of CT scans from injured UK soldiers has recently suggested that the 1.10 g FSP is too large for representing such fragments and that the NATO standardised 0.51 g sphere or 0.49 g cylinder may be more appropriate [22]. The final choice of FSP should ideally take into account all of the aforementioned factors, recognising that an exactly representative FSP will never be found and a compromise will always be sought. For example choosing an FSP of a greater mass than expected will provide greater security in ones injury predictions, but may potentially result in overprotection and thereby increase weight or heat burden.

18.7 Velocity Ranges Utilised for Testing

The requirement for the minimal protective capability of certain pieces of protective equipment will come with a particular type and mass of FSP, in conjunction with an impact velocity. In addition, knowledge of the range of likely impact velocities is essential for accurate experimental ballistic testing and injury model prediction. For example a velocity of 97 m/s was required for a 1.10 g cylindrical FSP to perforate 3 mm of goat skin but when the skin was removed the velocity required for perforation of muscle alone was approximately 60 m/s [23]. Increasing the velocity to 150 m/s results in penetration of 80 mm of muscle, demonstrating the importance of including a skin component in any injury model predicting the penetration of energised fragments. Although the presence of skin is of lesser importance in bullets due to their higher impact velocities and shape effects, wound cavity and tract size are directly correlated to energy deposition, which in turn is highly dependent upon impact velocity amongst other variables. Recent work has indicated that the presence of clothing layers potentially increases wounding severity but making the projectile more unstable [24, 25] and thus possibly also reducing severity in some cases., Whether increased wounding occurs with projectiles that perforate body armour remains unclear [26, 27].

Probable impact velocities for bullets can often be anticipated but such predictions for energised fragments have traditionally been more problematic. Even the most aerodynamic fragments such as spheres lose velocity rapidly, meaning that the impact velocity is highly dependent upon the proximity of the subject to the explosive device at the time of detonation. Exit velocity has been stated as being virtually independent of the fragment mass [28]. In general, the initial velocity of fragments is between 1500 and 2000 m/s and declines rapidly with increasing distance from their origin [29–33]. Typically the fragments obtained during trials are in the size range of $<$1–5 mm and have a mass of 0.1 to $>$20 g with non-uniform shapes [8, 29]. However, experimental evidence to determine fragments produced by smaller devices is rare. Recent experimental evidence recreating the explosions produced by improvised explosive devices such as pipe bombs produced fragment velocities of 332–567 m/s, although some smaller devices produced velocities as low as 51–191 m/s [34, 35]. The availability of CT scans taken from soldiers wounded by energised fragments has provided clinicians with the ability to measure the depth of penetration of any retained fragments. By estimating the retained fragment mass in conjunction with algorithms based on firing of FSPs into animal tissues and ballistic gelatine, it is possible to provide a probable range of impact velocities [22], suggesting that a range of velocities between 300 and 400 m/s would be representative for metallic fragments.

References

1. Ramasamy A, Hill AM, Hepper AE, Bull AM, Clasper JC. Blast mines: physics, injury mechanisms and vehicle protection. J R Army Med Corps. 2009;155(4):258–64.
2. Jackson DS, Batty CG, Ryan JM, McGregor WS. The Falklands war: army field surgical experience. Ann R Coll Surg Engl. 1983;65:281–5.

3. Hardaway RM. Viet Nam wound analysis. J Trauma. 1978;18:635–43.
4. Reister FA. Battle casualties and medical statistics: U.S. Army Experience in the Korean War. Washington, DC: The Surgeon General, Department of the Army; 1973.
5. Beebe GW, DeBakey ME. Location of hits and wounds. In: Battle casualties. Springfield: Charles C. Thomas; 1952. p. 165–205.
6. Garfield RM, Neugut AI. Epidemiologic analysis of warfare. A historical review. JAMA. 1991;266 (5):688–92.
7. Adamson PB. A comparison of ancient and modern weapons in the effectiveness of producing battle casualties. J R Army Med Corps. 1977;123:93–103.
8. Crew FAE. History of the second world war. The army medical services. London: H.M.S.O; 1956.
9. Moffat WC. British forces casualties in Northern Ireland. J R Army Med Corps. 1976;112:3–8.
10. Rees D. Korea the limited war. London: Macmillan; 1964, pA60-1 Appendix C.
11. Carey ME. Analysis of wounds incurred by U.S. Army Seventh Corps personnel treated in Corps hospitals during Operation Desert Storm, February 20 to March 10, 1991. J Trauma. 1996;40(3 Suppl): S165–9.
12. Thurman JT editor. Practical bomb scene investigation. 2nd ed. London: Taylor & Francis; 2011.
13. Kang DG, Lehman Jr RA, Carragee EJ. Wartime spine injuries: understanding the improvised explosive device and biophysics of blast trauma. Spine J. 2012;12(9):849–57.
14. McFate M. Iraq: the social context of IEDs. Milit Rev. 2005;25:37–40.
15. Lucci EB. Chap. 65. Improvised explosive devices. In: Ciottone GR, editor. Disaster medicine. Philadelphia: Elsevier; 2006.
16. Patel HD, Dryden S, Gupta A, Ang SC. Pattern and mechanism of traumatic limb amputations after explosive blast: experience from the 07/07/05 London terrorist bombings. J Trauma Acute Care Surg. 2012;73 (1):276–81.
17. Holmes RH. Wound ballistics and body armor. J Am Med Assoc. 1952;150(2):73–8.
18. Ryan JM, Cooper GJ, Haywood IR, Milner SM. Field surgery on a future conventional battlefield: strategy and wound management. Ann R Coll Surg Engl. 1991;73:13–20.
19. NATO Standardisation Agreement (STANAG 2920): ballistic test method for personal armour materials and combat clothing, 2nd ed. NATO Standardisation Agency; 2003. http://www.nato.int/cps/en/SID-8BF0F167-D3248540/natolive/stanag.htm. Accessed 8 Aug 2014.
20. Sullivan JF. Development of projectiles to be used in testing body armor, to simulate flak and 20 mm H.E. Fragments. Memorandum Report WAL 762/247. Watertown; 1943.
21. Steier V, Carr DJ, Crawford C, Teagle M, Miller D, Holden S, Helliker M. Effect of FSP material on the penetration of a typical body armor fabric. In: Presented at the international symposium on ballistics 22–26 Sept 2014; Atlanta.
22. Breeze J, Leason J, Gibb I, Allanson-Bailey L, Hunt N, Hepper A, Spencer P, Clasper J. Characterisation of explosive fragments injuring the neck. Br J Oral Maxillofac Surg. 2013;51(8): e263–6.
23. Breeze J, James GR, Hepper AE. Perforation of fragment simulating projectiles into goat skin and muscle. J R Army Med Corps. 2013;159:84–9.
24. Kieser DC, Carr DJ, Leclair SC, Horsfall I, Theis JC, Swain MV, Kieser JA. Clothing increases the risk of indirect ballistic fractures. J Orthop Surg Res. 2013;8:42.
25. Carr DJ, Kieser J, Mabbott A, Mott C, Girvan E, Champion S. Damage to apparel layers and underlying tissue due to hand-gun bullets. Int J Legal Med. 2014;128:83–93.
26. Missliwetz J, Denk W, Wieser I. Study on the wound ballistics of fragmentation protective vests following penetration by handgun and assault rifle bullets. J Forensic Sci. 1995;40:582–4.
27. Knudsen PJT, Sørensen OH. The destabilising effect of body armour on military rifle bullets. Int J Legal Med. 1997;110:82–7.
28. Coupland R, Rothschild MA. Thali. In: Kneubuehl B, editor. Wound ballistics: basics and applications, 1st ed. Berlin: Springer Science & Business Media; 2011. ISBN: 9783642203565.
29. Bowyer GW. Management of small fragment wounds in modern warfare: a return to Hunterian principles? Ann R Coll Surg Engl. 1997;79(3):175–82.
30. Champion HR, Holcomb JB, Young LA. Injuries from explosions: physics, biophysics, pathology and required research focus. J Trauma. 2009;66:1468–77.
31. Galbraith KA. Combat casualties in the first decade of the 21st century – new and emerging weapon systems. J R Army Med Corps. 2001;147:7–14.
32. Hill PF, Edwards DP, Bowyer GW. Small fragment wounds: biophysics, pathophysiology and principles of management. J R Army Med Corps. 2001;147 (1):41–51.
33. Gurney RW. The initial velocities of fragments from bombs, shells and grenades. Ballistic Research Lab, Aberdeen Proving Ground Maryland; 1943. Available at: http://www.dtic.mil/dtic/tr/fulltext/u2/a800105.pdf.
34. Bors D, Cummins J, Goodpaster J. The anatomy of a pipe bomb explosion: measuring the mass and velocity distributions of container fragments. J Forensic Sci. 2014;59(1):42–51.
35. Bors D, Cummins J, Goodpaster J. The anatomy of a pipe bomb explosion: the effect of explosive filler, container material and ambient temperature on device fragmentation. Forensic Sci Int. 2014;234:95–102.

Part IV

Applications of Blast Injury Research: Solving Clinical Problems

Coagulopathy and Inflammation: An Overview of Blast Effects

19

Nicholas T. Tarmey and Emrys Kirkman

19.1 Introduction

Blast injury results in a complex pattern of tissue injury, inflammation and coagulopathy, presenting great challenges in clinical management. The pathophysiology of blast-associated inflammation and coagulopathy is only partially understood and there remains a great deal of uncertainty over management strategies.

Although inflammation may be helpful as part of the normal physiological response to injury, the extensive tissue damage of major blast trauma may trigger a profound inflammatory response that is itself life threatening. It may be conceptually appealing to attempt to modify this inflammatory response directly, but there is little evidence to support the use of corticosteroids or other anti-inflammatory drugs.

Haemorrhage is a leading cause of death from blast trauma, and is exacerbated by trauma-associated coagulopathy. Over the past decade important progress has been made in understanding the coagulopathy of trauma, including interactions between tissue injury, inflammation and impaired coagulation. This understanding has been applied to new approaches to treatment, resulting in improved rates of survival following major haemorrhage.

Future developments in the understanding and treatment of blast-associated inflammation and coagulopathy promise to revolutionise clinical management. Improved understanding of biological pathways may open new avenues of treatment, and novel alternatives to refrigerated blood products may drastically alter the balance of risks in managing trauma-induced coagulopathy.

19.2 Pathophysiology of Inflammation and Coagulopathy in Blast

Blast causes injury by a number of different physical mechanisms. Each mechanism generates its own pathophysiological response, which can often interact, leading to clinical consequences that include inflammation and alterations in clotting. Some of these mechanisms may be unique to blast (explosions/primary blast), but others are also seen in other forms of trauma (e.g. blunt tissue injury can also occur in tertiary blast and haemorrhagic shock in major trauma).

To disentangle this complex situation, it is helpful to examine the components of the explosion that cause different types of injury. It is important at the outset to acknowledge that

N.T. Tarmey, FRCA, DICM, DipIMC, RCS(Ed) (✉)
Academic Department of Critical Care, Queen Alexandra Hospital, Portsmouth, UK
e-mail: nicktarmey@doctors.org.uk

E. Kirkman, PhD
CBR Division, Dstl Porton Down, Salisbury, UK
e-mail: ekirkman@dstl.gov.uk

A.M.J. Bull et al. (eds.), *Blast Injury Science and Engineering: A Guide for Clinicians and Researchers*,
DOI 10.1007/978-3-319-21867-0_19

we are only beginning to understand the complex inter-relationships between the different parts of the overall injury. The relative contribution of the different forms of blast injuries depend on a number of factors which include the nature of the explosive device, distance of the casualty from the device, the environment in which the explosion occurred (open space or enclosed) and any protective equipment worn (e.g. ballistic armour) by the casualty. The various categories of blast injury are based upon the component of the explosion that caused them (see Chap. 6, Sect. 6.2).

19.3 Primary Blast Injury and the Inflammatory Response Associated with Blast Lung

Lung injury, discussed in Chap. 12, is one of the most notable forms of blast injury. In the context of this chapter it is the pathophysiological consequences of the widespread haemorrhage into the small airways and lung parenchyma that are of importance and have been investigated in detail by Gorbunov et al. [1–4].

Blast lung is characterised by the influx of blood and extravasation of oedema fluid into lung tissue [3, 5]. This gives rise to haemorrhagic foci, which can be substantial depending on the level of blast loading. The intrapulmonary haemorrhage and oedema contribute to the initial respiratory compromise in blast lung [2]. The problem is exacerbated because free haemoglobin (Hb) and extravasated blood have been shown to induce free radical reactions that cause oxidative damage [2] and initiates/augments a pro-inflammatory response [3]. Free Hb also causes an accumulation of inflammatory mediators and chemotactic attractants [6] thereby amplifying the problem.

Within 3 hours, leucocytes can be demonstrated within the haemorrhagic areas and levels increase for 24 hours or more after exposure [2]. This accumulation of leucocytes is associated with increasing levels of myeloperoxidase (MPO) activity, which in turn is indicative of oxidative events and developing inflammation in the affected areas [2]. Histological and electron microscopic examination reveal prominent perivascular oedema and extensive alveolar haemorrhages without widespread visible damage to endothelial cells during the first 12 hours after exposure [2]. Thereafter, (12–24 hours after exposure) Type 1 epithelial cells show evidence of developing damage, followed later (24–56 hours after exposure) by secondary damage to endothelial cells that become detached from their basement membrane into the capillary lumen [2].

Other groups have shown that exposure of the periphery to blast generates sufficient inflammatory response to impinge on the lungs and cause pulmonary damage [7]. However, this latter finding is perhaps unsurprising since there is substantial literature showing that inflammation originating from peripheral tissue damage can cause secondary inflammatory responses that injure other organs, and can become widespread enough to cause conditions such as Systemic Inflammatory Response Syndrome (SIRS) in animal models and in patients [8].

19.4 Secondary and Tertiary Blast Injuries and Ischaemia/Reperfusion Injuries: Implications for Inflammatory Responses

Blast-injured casualties will often sustain haemorrhage as a consequence of their secondary (penetrating) blast injuries, and substantial tissue damage as a consequence of tertiary (blunt) blast injuries [9]. The casualties will therefore suffer profound haemorrhagic shock and will require resuscitation to sustain life while they are evacuated to hospital. The resultant ischaemia and reperfusion are well established triggers of inflammation [10].

In the multiple injury casualty, the inflammatory response initiated specifically by primary blast injury needs to be placed into the clinical context of the inflammation caused by haemorrhagic shock and blunt tissue injury. An experimental study conducted in the UK may provide some insight.

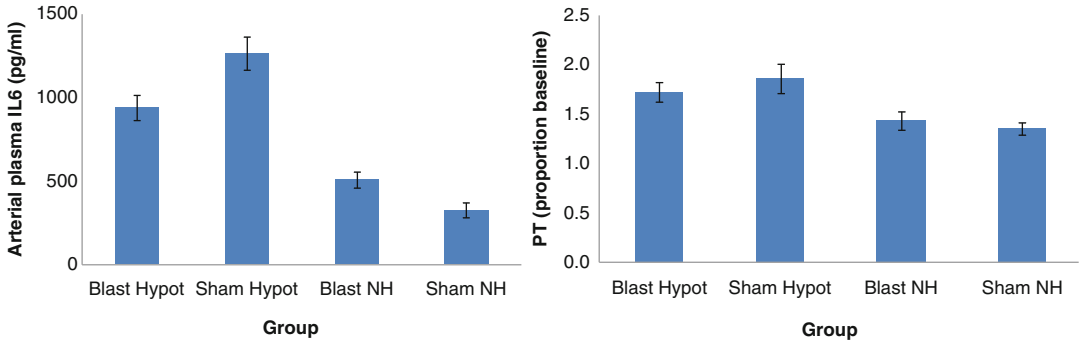

Fig. 19.1 Peak arterial interleukin 6 (IL-6) and prothrombin time (*PT*) in the four groups of terminally anaesthetised animals subjected to haemorrhagic shock and injury following blast exposure (*Blast*) or no blast exposure (*Sham*) and subsequently resuscitated to a hypotensive blood pressure target (*Hypot*) for the reminder of the study or to a hybrid target of 1 h hypotensive resuscitation followed by normotensive resuscitation (*NH*) to improve organ perfusion for the reminder of the study. Maximum duration of resuscitation was 8 h in this study [11] (With permission from Wolters Kluwer Health, Inc.)

This study was designed to investigate potential new resuscitation strategies for extended evacuation of blast and non-blast injured casualties with complex trauma and haemorrhagic shock. It is of note in this study that although the resuscitation strategy had a significant effect on the inflammatory state (seen as levels of Interleukin-6 [11] and HMGB-1 [12]), the difference between blast and non-blast injury strands was not significant (Fig. 19.1). This finding implies that the effects of blast on inflammation may be "lost" on a background of other insults commonly seen in severely injured patients.

19.5 Cerebral Inflammation After Blast Exposure

Blast-induced brain injury is one area where the effects of blast alone have been studied extensively. This is, in part, because evidence exists showing that an episode of cerebral inflammation can lead to long-lasting and significant clinical conditions that range from Post Traumatic Stress Disorder to neurodegenerative disorders [13].

The picture is very complex though. There are several probable pathways of initiating the injury, superimposed on many pathways of biochemical injury within the brain. A number of studies have shown that exposure of the head to a blast wave can initiate an inflammatory response in brain tissue that includes activation of a host of inflammatory genes, release of mediators such as cytokines and chemokines, and activation of inflammatory cells such as leukocytes and microglia [14] leading to blood brain barrier dysfunction and cerebral oedema [15]. These effects can be persistent [16] and are amplified by multiple exposure [17].

A detailed investigation of the mechanism of injury reveals several interesting possibilities. Firstly, direct exposure of the head to blast can result in cerebral inflammation as discussed above. This may be because of endothelial damage, which can be initiated by blast exposure in a dose-dependent manner, since the endothelium orchestrates inflammatory responses. Secondly, in casualties where the whole body has been exposed to blast, a peripheral inflammatory response may also impinge on the brain. Cernak [18] showed that whole body exposure to blast resulted in inflammatory responses in the thorax, abdomen and brain. Protecting the head had little effect on the cerebral inflammation, while torso protection attenuated the cerebral inflammation suggesting a "spill over" of inflammation into the brain from the systemic insult [18]. Other groups have postulated a hydrodynamic pressure wave from the periphery, causing cerebral inflammation [19].

Because of the far-reaching consequences of cerebral inflammation [13] there is intense interest in identifying potential therapeutic strategies. Recent studies have shown that hyperbaric oxygen can attenuate the changes in the blood brain barrier and neuronal apoptosis after blast exposure [20]. Others have focused on pharmacological agents including inhibitors of complement [21] cannabinoid receptor inverse agonists [22] and cholinesterase inhibitors [23] amongst a host of others that might form part of useful therapeutic strategies. In most cases, it is likely to take some time before these pre-clinical studies give rise to a clinical therapy, but clearly this is an important area that is receiving substantial attention.

19.6 Effects of Blast on Clotting

Trauma induced coagulopathy (TIC) is now recognised as a serious secondary consequence of injury and the patient's (patho)physiological response to trauma [24–26]. TIC has an evolving pathology in the patient, often starting with the consequences of tissue hypoperfusion and developing through phases that can include the consequences of shock-driven acidosis, hypothermia, iatrogenic (and autogenic) haemodilution and factor consumption [25, 26].

The immediate effect of blast injury is to cause an enhancement of clotting [27, 28]. When blast injury is quickly followed by hemorrhagic shock there is a reversal of hypercoagulation as a phase of hypocoagulation, characteristic of TIC, develops [11]. Interestingly, Prat et al. [28] have demonstrated for the first time that the hypercoagulation initiated by blast persists for at least 60 minutes after injury when it is not complicated by subsequent hemorrhagic shock, even in the face of mild blast-induced shock. This suggests that tissue injury *per se* causes a relatively persistent enhancement of clotting. However, to put the enhanced clotting into the clinical context of a multiple injury casualty, the effects of tissue perfusion seem to have a greater influence on clotting than the effects of blast.

As was the case with inflammatory responses, resuscitation strategy seemed to have a significant effect on clotting, while the presence of blast injury did not after a period of hypovolaemic shock [11] (Fig. 19.1). However, as new therapies targeting TIC are being developed (see next section) we should be cognizant of the fact that after blast injury there may be a large surface area of damaged endothelium within the pulmonary circulation, with implications for systemic as well as local clotting and thrombus formation.

19.7 Modification of the Inflammatory Response to Blast Trauma

Although inflammation is an important part of the normal response to tissue injury, the exaggerated response seen in blast injury and other forms of critical illness may itself prove life threatening. This concept has led to attempts to modify inflammation with the aim of breaking the cycle of inflammation and organ dysfunction. Most evidence for this approach is in the management of sepsis and acute respiratory distress syndrome where inflammation-modifying corticosteroids remain a controversial therapy. Evidence for steroids in the treatment of blast-associated inflammation is even more limited.

Acute respiratory distress syndrome (ARDS) is defined as a combination of acute hypoxaemia and bilateral pulmonary infiltrates on chest radiograph with no evidence of left atrial hypertension [29]. In practice, this encompasses a wide range of underlying diagnoses from pneumonia to blast lung and transfusion-associated acute lung injury (TRALI). Beyond the primary insult, all causes of ARDS result in sustained systemic and pulmonary inflammation, leading to neutrophil activation, increased pulmonary capillary leak, pulmonary oedema and further lung injury. Some small randomised trials have demonstrated evidence of increased survival with moderate doses of steroids given early in the course of ARDS [30]. However, there are concerns over methodological quality and these findings have not been confirmed in a large, multicentre trial.

Furthermore, there is conflicting evidence over risks of neuropathy, myopathy and infection, and the routine use of steroids in ARDS is not widely accepted [30].

Elsewhere in critical illness, steroids are used in refractory septic shock, where they have been shown to hasten shock reversal, but without an overall improvement in mortality [31]. Here, steroids are thought to play a facilitative role in the action of vasopressors on vascular tone, rather than a direct modification of the underlying inflammatory response [32]. In fact, the immunomodulatory effect of steroids in sepsis may be counterproductive, demonstrated by an increased rate of nosocomial infections in patients receiving steroids [31].

Compared with sepsis and ARDS, blast injury is a rare syndrome and there are few clinical studies examining the role of immunomodulation in trauma. Some preliminary work in animal models has shown a possible role for antioxidants in blast lung, but only to the extent that levels of certain inflammatory markers may be reduced [33]. For now, there is no evidence to support deliberate modification of the inflammatory response to blast injury in clinical practice. Instead, treatment remains focussed on addressing anatomical injuries while correcting coagulopathy and supporting failing organ systems.

19.8 Damage Control Resuscitation and Surgery

Much of the past decade's progress in the management of major trauma has centred around the concept of Damage Control Resuscitation and Surgery (DCRS). This approach sacrifices the completeness of initial anatomical correction during surgery in favour of maintaining tissue oxygenation and correcting physiology. In the UK military, DCRS begins at the point of wounding and continues through to the postoperative phase. At every stage, the priorities are to control bleeding, to correct coagulopathy, and to maintain tissue oxygenation [34].

In the pre-hospital phase, key principles are to minimise further blood loss and expedite transfer to emergency surgery. Compression dressings, splinting, limb tourniquets and topical haemostatic agents help to reduce pre-hospital bleeding. Prioritising evacuation over non-essential interventions in the field reduces time to surgery. Where available, a helicopter-based physician can resolve the conflict between a "stay and play" and a "scoop and run" approach, by delivering essential interventions *en route* to hospital. In Afghanistan, the UK military's Medical Emergency Response Team (MERT), evolved to provide in-flight intubation, ventilation and blood product transfusion using a CH-47 helicopter platform and a 4-person physician-led medical team [35]. This approach has been associated with reduced time to surgery and improved rates of survival following severe military trauma [36].

On arrival in hospital, DCRS should continue seamlessly using a team-based approach with effective leadership and a collective understanding of the key principles [37]. If not begun already, empirical transfusion of blood and clotting factors may be started, along with tranexamic acid and appropriate airway management prior to surgery. In the operating room, the first priority is to gain rapid control of major haemorrhage, while resuscitation is continued by the anaesthetic team. Once bleeding is controlled, all efforts are then directed towards prompt completion of initial surgery, correction of physiology, and seamless transfer to ICU [38].

In blast injury, DCRS may be complicated by an altered physiological response to hypovolaemia and a reduced tolerance for prolonged hypotension. The concept of "hypotensive resuscitation," where pre-hospital fluids are titrated to a sub-normal blood pressure to preserve early clots and limit blood loss, is now widely accepted in major trauma [39]. Evidence for this approach is mainly from a 1994 US study of civilian penetrating trauma (rather than blast injury), where the mean time from injury to surgery was only 75 minutes [40]. The increased survival seen in those randomised to receive no pre-hospital fluids was thought to be due to reduced haemodilution and reduced early clot disruption,

which outweighed the negative effects of hypovolaemia and hypoperfusion.

Recent animal studies of hypotensive resuscitation suggest that this balance may be different following blast injury. In a porcine model of controlled haemorrhage after blast exposure, animals resuscitated with saline to a hypotensive target had lower rates of survival and a more profound metabolic acidosis than those resuscitated to normotension [41]. Additionally, when compared with controls, animals exposed to blast showed a more profound hypotensive response to haemorrhage. These findings suggest that the normal physiological response to hypovolaemia may be altered by blast injury.

A subsequent animal study aimed to assess the utility of a hybrid fluid strategy in uncontrolled bleeding after blast injury [12]. Anaesthetised pigs were exposed to blast before a period of controlled bleeding (30 % blood volume via central line) and then uncontrolled bleeding (from a standardised, uncompressed liver injury). By including a continued source of bleeding in the model, the authors aimed to assess the risk of increased clot disruption with more aggressive fluid therapy. The main finding was that a hybrid fluid strategy, where 1 hour of hypotensive resuscitation was followed by fluids titrated to normotension, with the aim of improving tissue perfusion and hence oxygen delivery, resulted in increased survival compared with prolonged hypotensive resuscitation. This effect was particularly apparent in animals exposed to blast, as was the severity of their coagulopathy, acidosis and systemic inflammation, confirming the impression that prolonged hypotension is particularly harmful after blast injury [11].

Animal studies therefore suggest that, whilst an initial period of hypotensive resuscitation may be beneficial to aid early clot stabilisation, after 1 hour the need to restore tissue perfusion can outweigh any benefit from continued hypotension. This is particularly relevant in blast injury, where prolonged hypotension is poorly tolerated, and where evacuation timelines may be prolonged by military constraints or by an overloaded disaster response system. There is, however, a need to confirm these findings in a human study, where real-life injury patterns and access to early blood and clotting products may alter the balance of risks. For now, clinicians must make a balanced decision on early resuscitation, considering the presence of blast injury, the extent of uncontrolled haemorrhage, access to blood products, and expected time until definitive surgery.

Notwithstanding any controversy over the optimal target blood pressure, it is now widely accepted that fluid resuscitation for major traumatic bleeding should be with blood and blood products, rather than with synthetic crystalloids or colloids. Contrary to previous practice, where resuscitation was initiated with crystalloid and supplemented with red cell concentrate (RCC) and thawed plasma (FFP) according to lab results [42], evidence from major military and civilian trauma now supports RCC and FFP transfusion in a ratio approximating whole blood [43, 44]. The optimal ratio, however, has not yet been determined in a prospective study and there remains some controversy over whether this may be 1:1 or closer to 1:2 (FFP: RCC) [45]. Patients and their injuries are, of course, heterogenous in nature and there may not be any single “ideal” ratio for all patients. While the optimal empirical ratio may theoretically differ for blast injuries, there is not yet any direct evidence to justify deviation from standard guidelines.

Transfusion may be life-saving but it can also cause significant harm. In addition to the risks of over-transfusion, viral infection, and incompatibility errors, transfusion carries the risk of immune-mediated illnesses such as transfusion-related acute lung injury (TRALI) [46]. Although FFP is a relatively high-risk product for causing TRALI (defined as the presence of hypoxia and pulmonary oedema within 6 h of transfusion in the absence of cardiac failure or volume overload), there is no clear evidence of increased TRALI with higher ratios of FFP: RCC in trauma [47, 48].

In blast injury, the true incidence of TRALI is particularly difficult to assess where confounding causes include ARDS from major

trauma and blast lung, both of which may mimic the features of TRALI. In practice, the pragmatic approach to transfusion in blast injury remains the same as for other major trauma: treat uncontrolled haemorrhage initially with a high ratio of FFP: RCC, then individualise according to blood results when bleeding is controlled. Whole blood tests of coagulation (e.g. ROTEM thromboelastometry) at the point of care may prove particularly helpful by guiding platelet transfusion in addition to FFP and cryoprecipitate [49].

There are no specific drug therapies for blast-related haemorrhagic shock, other than those routinely used in major trauma. Following the civilian CRASH-2 and military MATTERS studies, Tranexamic Acid is now given universally in major traumatic bleeding where it has been shown to reduce overall mortality [50, 51]. The role of recombinant human factor VIIa now appears limited after a large randomised trial failed to show benefit [52]. Vasopressors should be avoided where possible and must not be used as a substitute for proper volume resuscitation [53].

Opioid analgesics are commonly used to treat severe pain from the pre-hospital phase onwards. Although conventional wisdom states they may exacerbate hypotension in hypovolaemia, their effect may be more complex than this following blast injury. Animal models differ between species and the results of a human volunteer trial are awaited [54]. In the meantime, opioids remain the standard treatment for severe pain following traumatic injury, especially after initial control of haemorrhage has been achieved.

19.9 Future Directions

There is currently intense interest in both the mechanisms and potential treatment strategies for inflammation after blast, with perhaps the greatest volume of work focusing on cerebral inflammation. Because of the far-reaching implications of cerebral inflammation, a wide range of therapeutic strategies and pharmacological targets are being evaluated. Trauma coagulopathy is another area of intense activity, although much of the effort here is applied to trauma in general, rather than blast in particular. In both fields of inflammation and coagulation we are likely to see significant advances in the relatively near future.

19.10 Summary

- Blast injury causes a complex pattern of tissue injury, inflammation and coagulopathy.
- Blast lung is a classic example of primary blast injury and may lead to early hypoxaemia and systemic inflammation.
- There is little evidence to support attempting to modify the physiological response to blast injury directly with anti-inflammatory drugs.
- Much of the treatment given in blast injury involves addressing the consequences of the inflammatory response, including correction of coagulopathic bleeding with blood and clotting factors.
- The inflammatory response to prolonged shock and delayed resuscitation may be greater than the effects of blast injury itself.

References

1. Elsayed NM, Gorbunov NV, Kagan VE. A proposed biochemical mechanism involving hemoglobin for blast overpressure-induced injury. Toxicology. 1997;121(1):81–90.
2. Gorbunov NV, Asher LV, Ayyagari V, Atkins JL. Inflammatory leukocytes and iron turnover in experimental hemorrhagic lung trauma. Exp Mol Pathol. 2006;80(1):11–25.
3. Gorbunov NV, Elsayed NM, Kisin ER, Kozlov AV, Kagan VE. Air blast-induced pulmonary oxidative stress: interplay among hemoglobin, antioxidants, and lipid peroxidation. Am J Physiol. 1997;272(2 Pt 1):L320–34.
4. Gorbunov NV, McFaul SJ, Van Albert S, Morrissette C, Zaucha GM, Nath J. Assessment of inflammatory response and sequestration of blood iron transferrin complexes in a rat model of lung injury resulting from exposure to low-frequency shock waves. Crit Care Med. 2004;32(4):1028–34.
5. Brown RF, Cooper GJ, Maynard RL. The ultrastructure of rat lung following acute primary blast injury. Int J Exp Pathol. 1993;74(2):151–62.

6. Gorbunov NV, McFaul SJ, Januszkiewicz A, Atkins JL. Pro-inflammatory alterations and status of blood plasma iron in a model of blast-induced lung trauma. Int J Immunopathol Pharmacol. 2005;18(3):547–56.
7. Ning JL, Mo LW, Lu KZ, Lai XN, Wang ZG, Ma D. Lung injury following lower extremity blast trauma in rats. J Trauma Acute Care Surg. 2012;73 (6):1537–44.
8. Volpin G, Cohen M, Assaf M, Meir T, Katz R, Pollack S. Cytokine levels (IL-4, IL-6, IL-8 and TGFbeta) as potential biomarkers of systemic inflammatory response in trauma patients. Int Orthop. 2014;38(6):1303–9.
9. Cooper GJ, Maynard RL, Cross NL, Hill JF. Casualties from terrorist bombings. J Trauma. 1983;23(11):955–67.
10. Keel M, Trentz O. Pathophysiology of polytrauma. Injury. 2005;36(6):691–709.
11. Doran CM, Doran CA, Woolley T, Carter A, Male K, Midwinter MJ, et al. Targeted resuscitation improves coagulation and outcome. J Trauma Acute Care Surg. 2012;72(4):835–43.
12. Kirkman E, Watts S, Cooper G. Blast injury research models. Philos Trans R Soc Lond B Biol Sci. 2011;366(1562):144–59.
13. Prasad KN, Bondy SC. Common biochemical defects linkage between post-traumatic stress disorders, mild traumatic brain injury (TBI) and penetrating TBI. Brain Res. 2015;1599C:103–14.
14. Risdall JE, Carter AJ, Kirkman E, Watts SA, Taylor C, Menon DK. Endothelial activation and chemoattractant expression are early processes in isolated blast brain injury. Neuromolecular Med. 2014;16(3):606–19.
15. Shetty AK, Mishra V, Kodali M, Hattiangady B. Blood brain barrier dysfunction and delayed neurological deficits in mild traumatic brain injury induced by blast shock waves. Front Cell Neurosci. 2014;8:232.
16. Kochanek PM, Dixon CE, Shellington DK, Shin SS, Bayir H, Jackson EK, et al. Screening of biochemical and molecular mechanisms of secondary injury and repair in the brain after experimental blast-induced traumatic brain injury in rats. J Neurotrauma. 2013;30(11):920–37.
17. Ahmed FA, Kamnaksh A, Kovesdi E, Long JB, Agoston DV. Long-term consequences of single and multiple mild blast exposure on select physiological parameters and blood-based biomarkers. Electrophoresis. 2013;34(15):2229–33.
18. Cernak I. The importance of systemic response in the pathobiology of blast-induced neurotrauma. Front Neurol. 2010;1:151.
19. Simard JM, Pampori A, Keledjian K, Tosun C, Schwartzbauer G, Ivanova S, et al. Exposure of the thorax to a sublethal blast wave causes a hydrodynamic pulse that leads to perivenular inflammation in the brain. J Neurotrauma. 2014;31(14):1292–304.
20. Zhang Y, Yang Y, Tang H, Sun W, Xiong X, Smerin D, et al. Hyperbaric oxygen therapy ameliorates local brain metabolism, brain edema and inflammatory response in a blast-induced traumatic brain injury model in rabbits. Neurochem Res. 2014;39(5):950–60.
21. Li Y, Chavko M, Slack JL, Liu B, McCarron RM, Ross JD, et al. Protective effects of decay-accelerating factor on blast-induced neurotrauma in rats. Acta Neuropathol Commun. 2013;1(1):52.
22. Reiner A, Heldt SA, Presley CS, Guley NH, Elberger AJ, Deng Y, et al. Motor, visual and emotional deficits in mice after closed-head mild traumatic brain injury are alleviated by the novel CB2 inverse agonist SMM-189. Int J Mol Sci. 2015;16(1):758–87.
23. Valiyaveettil M, Alamneh YA, Miller SA, Hammamieh R, Arun P, Wang Y, et al. Modulation of cholinergic pathways and inflammatory mediators in blast-induced traumatic brain injury. Chem Biol Interact. 2013;203(1):371–5.
24. Maegele M, Schochl H, Cohen MJ. An update on the coagulopathy of trauma. Shock. 2014;41 Suppl 1:21–5.
25. Asehnoune K, Faraoni D, Brohi K. What's new in management of traumatic coagulopathy? Intensive Care Med. 2014;40(11):1727–30.
26. Cap A, Hunt BJ. The pathogenesis of traumatic coagulopathy. Anaesthesia. 2015;70 Suppl 1:96–101, e32–4.
27. Harrisson S, Watts S, Jacobs N, Granville-Chapman J, Doran C, Anderson S, et al. Clotting is enhanced after blast injury. Br J Surg. 2008;95(S3):3.
28. Prat NJ, Montgomery R, Cap AP, Dubick MA, Sarron JC, Destombe C, et al. Comprehensive evaluation of coagulation in Swine subjected to isolated primary blast injury. Shock. 2015;43:598–603.
29. Force ADT, Ranieri VM, Rubenfeld GD, Thompson BT, Ferguson ND, Caldwell E, et al. Acute respiratory distress syndrome: the Berlin definition. JAMA. 2012;307(23):2526–33.
30. Tang BM, Craig JC, Eslick GD, Seppelt I, McLean AS. Use of corticosteroids in acute lung injury and acute respiratory distress syndrome: a systematic review and meta-analysis. Crit Care Med. 2009;37 (5):1594–603.
31. Sprung CL, Annane D, Keh D, Moreno R, Singer M, Freivogel K, et al. Hydrocortisone therapy for patients with septic shock. N Engl J Med. 2008;358 (2):111–24.
32. Grover V, Handy JM. The role of steroids in treating septic shock. Anaesthesia. 2012;67(2):103–6.
33. Chavko M, Adeeb S, Ahlers ST, McCarron RM. Attenuation of pulmonary inflammation after exposure to blast overpressure by N-acetylcysteine amide. Shock. 2009;32(3):325–31.
34. Hodgetts TJ, Mahoney PF, Kirkman E. Damage control resuscitation. J R Army Med Corps. 2007;153 (4):299–300.
35. Kehoe A, Jones A, Marcus S, Nordmann G, Pope C, Reavley P, et al. Current controversies in military pre-hospital critical care. J R Army Med Corps. 2011;157(3 Suppl 1):S305–9.
36. Morrison JJ, Oh J, DuBose JJ, O'Reilly DJ, Russell RJ, Blackbourne LH, et al. En-route care capability from

point of injury impacts mortality after severe wartime injury. Ann Surg. 2013;257(2):330–4.
37. Mercer SJ, Park CL, Tarmey NT. Human factors in complex trauma. BJA Education 2015;15(5):231–236.
38. Mercer SJ, Tarmey NT, Woolley T, Wood PL, Mahoney PF. Haemorrhage and coagulopathy in the defence medical services. Anaesthesia. 2013;68(Suppl1):49–60.
39. Excellence NIfC. Pre-hospital initiation of fluid replacement in trauma. Technology appraisal guidance. London: NICE; 2004.
40. Bickell WH, Wall Jr MJ, Pepe PE, Martin RR, Ginger VF, Allen MK, et al. Immediate versus delayed fluid resuscitation for hypotensive patients with penetrating torso injuries. N Engl J Med. 1994;331(17):1105–9.
41. Garner J, Watts S, Parry C, Bird J, Cooper G, Kirkman E. Prolonged permissive hypotensive resuscitation is associated with poor outcome in primary blast injury with controlled hemorrhage. Ann Surg. 2010;251 (6):1131–9.
42. Surgeons ACo, editor. Advanced trauma life support for doctors, 2 ed. American College of Surgeons, Chicago; 1997.
43. Borgman MA, Spinella PC, Perkins JG, Grathwohl KW, Repine T, Beekley AC, et al. The ratio of blood products transfused affects mortality in patients receiving massive transfusions at a combat support hospital. J Trauma. 2007;63(4):805–13.
44. Holcomb JB, Wade CE, Michalek JE, Chisholm GB, Zarzabal LA, Schreiber MA, et al. Increased plasma and platelet to red blood cell ratios improves outcome in 466 massively transfused civilian trauma patients. Ann Surg. 2008;248(3):447–58.
45. Kashuk JL, Moore EE, Johnson JL, Haenel J, Wilson M, Moore JB, et al. Postinjury life threatening coagulopathy: is 1:1 fresh frozen plasma: packed red blood cells the answer? J Trauma. 2008;65(2):261–70.
46. Triulzi DJ. Transfusion-related acute lung injury: current concepts for the clinician. Anesth Analg. 2009;108(3):770–6.
47. Chan CM, Shorr AF, Perkins JG. Factors associated with acute lung injury in combat casualties receiving massive blood transfusions: a retrospective analysis. J Crit Care. 2012;27(4):419 e7–14.
48. Starkey K, Keene D, Morrison JJ, Doughty H, Midwinter MJ, Woolley T, et al. Impact of high ratios of plasma-to-red cell concentrate on the incidence of acute respiratory distress syndrome in UK transfused combat casualties. Shock. 2013;40(1):15–20.
49. Woolley T, Midwinter M, Spencer P, Watts S, Doran C, Kirkman E. Utility of interim ROTEM ((R)) values of clot strength, A5 and A10, in predicting final assessment of coagulation status in severely injured battle patients. Injury. 2012;44:593–599.
50. Shakur H, Roberts I, Bautista R, Caballero J, Coats T, Dewan Y, et al. Effects of tranexamic acid on death, vascular occlusive events, and blood transfusion in trauma patients with significant haemorrhage (CRASH-2): a randomised, placebo-controlled trial. Lancet. 2010;376(9734):23–32.
51. Morrison JJ, Dubose JJ, Rasmussen TE, Midwinter MJ. Military application of tranexamic acid in trauma emergency resuscitation (MATTERs) study. Arch Surg. 2012;147(2):113–9.
52. Hauser CJ, Boffard K, Dutton R, Bernard GR, Croce MA, Holcomb JB, et al. Results of the CONTROL trial: efficacy and safety of recombinant activated Factor VII in the management of refractory traumatic hemorrhage. J Trauma Acute Care Surg. 2010;69 (3):489–500.
53. Plurad DS, Talving P, Lam L, Inaba K, Green D, Demetriades D. Early vasopressor use in critical injury is associated with mortality independent from volume status. J Trauma. 2011;71(3):565–70; discussion 70–2.
54. Kirkman E, Watts S. Haemodynamic changes in trauma. Br J Anaesth. 2014;113(2):266–75.

Foot and Ankle Blast Injuries

20

Arul Ramasamy

20.1 Introduction

Since the early twentieth century, the development of motorised transport provided armies with a new-found mobility [1]. To counter this, the anti-vehicle (AV) mine was devised. Since its inception in the Great War (1914–1918), the AV mine has become the main threat to vehicles and their occupants in modern conflicts [2]. It remains a significant cause of injury to combatants and civilians in Iraq and Afghanistan [3–6].

When an explosive detonates beneath a vehicle, the blast wave from the explosion causes the release of a cone of super-heated gas (see Chap. 1, Sect. 1.1.1) and soil which impacts the undersurface of the travelling vehicle. This leads to rapid deflection of the vehicle floor, transmitting a very short duration (less than 10 ms), high amplitude load into anything that is in contact with it. Most frequently it is the lower leg and, in particular, the foot and ankle complex that is injured [7].

Injuries to the foot and ankle complex are of particular interest as it has been demonstrated that patients sustaining foot and ankle injuries have significantly greater disability scores than those without foot and ankle injuries [8, 9]. These effects may be even more pronounced in a young military population, who are likely to place significant functional demands on the foot and ankle complex.

20.2 The Issue

There exist a number of challenges to investigating the mechanism of injury from under vehicle explosions. Despite significant media attention on fatalities from under-vehicle explosions, there remains very little information on the injury profile of the resulting casualties. This has been due to a number of reasons including difficulties in gaining accurate incident data from the battlefield (thus hindering the ability to link particular injury patterns to injury mechanisms), as well as issues of security.

Until recent conflict in the Middle East, clinical information related to under-vehicle mine incidents was limited to a single case series of injuries over a 5-year period in Croatia [10]. Of the 31 survivors described in this study, only limited data was available on the pattern of lower limb injury and there was no data on clinical outcome following injury.

Due to the lack of clinical data on lower limb injuries sustained during under-vehicle explosions, mitigation engineers have extrapolated data from automotive injuries in an attempt to understand the

A. Ramasamy, MA, PhD, FRCS(Tr+Orth)
Department of Bioengineering, Royal British Legion Centre for Blast Injury Studies, Imperial College London, London, UK
e-mail: arul49@doctors.org.uk

A.M.J. Bull et al. (eds.), *Blast Injury Science and Engineering: A Guide for Clinicians and Researchers*,
DOI 10.1007/978-3-319-21867-0_20

injuries they are trying to prevent. In order to address this deficit, there exists an urgent requirement to characterise the injury profile and medium term outcomes of casualties suffering lower limb injuries from under-vehicle explosions. The analysis of contemporary clinical data can give rise to appropriate research questions and hypotheses that drive engineers to develop a greater understanding of areas where the effectiveness of the current protection offered to vehicle occupants may be improved (see Chap. 2, Sect. 2.3).

20.3 Clinical Data Analysis

Using a prospective military trauma registry [11], UK Service Personnel who sustained lower leg injuries following an under-vehicle explosion between Jan 2006 and Dec 2008 were identified and followed up for a mean 33.0 months [12]. This analysis demonstrated that casualties who suffered lower limb injuries from under-vehicle explosives were frequently associated with multi-segmental foot and ankle injuries and resulted in an amputation rate of 30 %. In addition, 75 % of injured limbs were noted to have a poor clinical outcome 3 years following injury. A poor outcome was defined as one of (i) persistent chronic infection either osteomyelitis or persistent wound infection 12 months post injury, (ii) delayed fracture healing greater than 12 months post injury, (iii) symptomatic post-traumatic osteoarthritis or (iv) need for amputation.

Statistical modelling of the injuries demonstrated that open fractures, vascular injuries and hind-foot injuries were associated with an increased risk of amputation [12]. Further sub-group analysis of casualties with hind-foot injuries confirmed that they were associated with significantly higher amputation rates and only 5 % were able to return to pre-injury levels of activity at 3 years post injury [13]. This data showed that attempts to protect the hind-foot from injury may reduce the risk of amputation within this cohort of casualties.

In an attempt to quantify injury and set injury criteria, military researchers have used the Abbreviated Injury Score (AIS) to evaluate lower limb injury. Developed for use in the automotive industry, AIS is based on the likelihood of a particular injury being fatal [14]. As such, its use as a tool to evaluate non-lethal injuries, and in particular, to discern injuries that may result in long-term disability is less certain [15]. Using the clinical data collected, a probit analysis statistical model was created, which compared AIS with the Foot and Ankle Severity Score (FASS) [16] in its ability to predict either amputation or poor clinical outcome. From the results of the statistical modelling, it was demonstrated that FASS was superior in predicting poor clinical outcome compared to AIS [17]. FASS has the advantage of showing greater resolution in differentiating between different foot and ankle injuries, and so it offers a better metric than AIS for setting criteria to evaluate injury and mitigation from under-vehicle explosions. In addition, being an anatomical injury scoring system, it is advantageous over the AIS in evaluating cadaveric specimens or other anatomic lower limb surrogates.

20.4 Future Research Foci

By the nature of military operations, most clinical studies detailing combat injuries are retrospective in nature, and are therefore faced with inherent weaknesses that are present in this type of research. To further understand the association between vehicle design and injury mitigation requires the development of comprehensive trauma registries that combine accurate incident data (the vehicle "casualty") with injured casualties. These provide compelling reasons to ensure that research facilities are embedded into modern combat operations from the outset, to ensure that the lessons from combat casualty care are learned and mistakes are not repeated.

Furthermore, it is necessary to understand the long-term outcomes of such disabling lower limb blast injuries. Although limb salvage could be considered to be advantageous over amputation, early functional outcomes in combat below knee amputees appear to be better than those

undergoing limb salvage [18]. It remains unclear whether those effects will endure longer-term follow up and as combat operations in the Middle East have recently concluded, there remains a requirement to set-up long term longitudinal studies to evaluate the lasting effects of combat injury.

The basis in mitigating the injury burden suffered by the combat casualty lies in a collaborative approach between clinicians and engineers, utilising numerical and physical modelling techniques that are underpinned by accurate contemporary clinical data analysis. These models are discussed in more detail in Chap. 17.

References

1. Guderian HW. "Achtung-Panzer!" Die Entwicklung der panzerwaffe, ihre kampftaktik und ihre operativen maglichkeiten. Stuttgart: Arms and Armor Press; 1937.
2. Tremblay JE, Bergeron DM, Gonzalez R. Key technical activity 1–29: protection of soft-skinned vehicle occupants from landmine effects. Technical Cooperation Program. Defence Research Establishment Valcartier, Val-Belair; 1998.
3. Ramasamy A, Harrisson SE, Clasper JC, Stewart MPM. Injuries from roadside improvised explosive devices. J Trauma. 2008;65(4):910–4.
4. Ramasamy A, Harrisson SE, Stewart MP, Midwinter MJ. Penetrating missile injuries during the Iraqi insurgency. Ann R Coll Surg Engl. 2009;91(7):551–8.
5. Owens BD, Kragh Jr JF, Wenke JC, Macaitis J, Wade CE, Holcomb JB. Combat wounds in operation Iraqi Freedom and operation Enduring Freedom. J Trauma. 2008;64(2):295–9. doi:10.1097/TA.0b013e318163b875. 00005373-200802000-00006 [pii].
6. Ramasamy A, Hill AM, Clasper JC. Improvised explosive devices: pathophysiology, injuries and management. J R Army Med Corps. 2009;155(4):265–74.
7. Ramasamy A, Hill AM, Masouros SD, Gibb I, Bull AMJ, Clasper JC. Blast-related fracture patterns: a forensic biomechanical approach. J R Soc Interface. 2011;8(58):689–98. doi:10.1098/rsif.2010.0476.
8. Tran T, Thordarson D. Functional outcome of multiply injured patients with associated foot injury. Foot Ankle Int. 2002;23(4):340–3.
9. Turchin DC. Do foot injuries significantly affect the functional outcome of multiply injured patients? J Orthop Trauma. 1999;13(1):1–4.
10. Radonic V, Giunio L, Biocic M, Tripkovic A, Lukcic B, Primorac D. Injuries from antitank mines in Southern Croatia. Mil Med. 2004;169(4):320–4.
11. Smith J, Mahoney PF, Russell R. Trauma governance in the UK defence medical services. J R Army Med Corps. 2007;153:239–42.
12. Ramasamy A, Hill AM, Masouros SD, Gibb I, Phillip R, Bull AMJ, Clasper JC. Outcomes of IED foot and ankle blast injuries. J Bone Joint Surg Am. 2013;95(5):e25 21–27.
13. Ramasamy A, Hill AM, Philip R, Gibb I, Bull AMJ, Clasper JC. The modern "deck-slap" injury – calcaneal blast fractures from vehicle explosions. J Trauma. 2011;71(6):1694–8. doi:10.1097/TA.0b013e318227a999.
14. Gennarelli TA, Wodzin E. AIS 2005: a contemporary injury scale. Injury. 2006;37(12):1083–91.
15. Poole GV, Tinsley M, Tsao AK, Thomae KR, Martin RW, Hauser CJ. Abbreviated injury scale does not reflect the added morbidity of multiple lower extremity fractures. J Trauma. 1996;40(6):951–6.
16. Manoli A, Prasad P, Levine RS. Foot and ankle severity score (FASS). Foot Ankle Int. 1997;18(9):598–602.
17. Ramasamy A, Hill AM, Phillip R, Gibb I, Bull AMJ, Clasper JC. FASS is a better predictor of poor outcome in lower limb blast injury than AIS: implications for blast research. J Orthop Trauma. 2013;27(1):49–55.
18. Frisch HM, Andersen RC, Mazurek MT, Ficke JR, Keeling JJ, Pasquina PF, Wain HJ, Carlini AR, MacKenzie EJ. The military extremity trauma amputation/limb salvage (METALS) study outcomes of amputation versus limb salvage following major lower-extremity trauma. J Bone Joint Surg Am. 2013;95(2):138–45.

Traumatic Amputation

21

James A.G. Singleton

21.1 The Issue

Blast-mediated extremity traumatic amputations (TAs) (as shown in Fig. 21.1) became a defining injury pattern in casualties from the combat operations in Iraq and Afghanistan in the late twentieth and early twenty-first century, with the majority due to Improvised Explosive Devices (IEDs) [1]). The driver for improving understanding of the injury biomechanics involved was both powerful and simple:

Traumatic amputations are potentially lethal. IEDs caused over 50 % of all UK combat fatalities in Iraq and Afghanistan. Most of those killed sustained at least one traumatic amputation.

A better understanding of the precise injury mechanism of blast-mediated TA would contribute to informing prevention, mitigation and clinical strategies and research, enabling further improvements in combat casualty care. This could help facilitate improved outcomes following blast-mediated TAs by decreasing injury severity or could even decrease the incidence of such injuries.

J.A.G. Singleton, BSc, MBBS, MRCS(Eng), RAMC
Department of Bioengineering, Royal British Legion Centre for Blast Injury Studies, Imperial College London, London, UK
e-mail: jasingleton@doctors.org.uk

21.2 Limitations of Current Injury Mechanism Theory

Military personnel have risked traumatic amputation from explosive blast since the advent of battlefield explosive munitions in the fourteenth Century. The injurious components of an explosive blast event, such as an IED strike, are categorised as primary to quaternary (Chap. 6, Sect. 6.2) [2, 3].

Initial theories for TA causation centred on simple limb avulsion by the blast wind i.e. pure tertiary blast injury [4]. This was revised by a British Army orthopaedic surgeon, Major (now Lieutenant Colonel, retired) Jonathan Hull, through research published in 1996. He proposed a sequence of initial primary blast injury – the blast wave coupling into the long bones of an extremity and causing diaphyseal fracture through resultant axial stress concentration – followed by tertiary blast injury – limb flail from the blast wind, completing the TA at the level of the fracture [5]. Underpinning this theory were (i) a perceived association between fatal primary blast lung injury (PBLI) and TA in blast casualties, and (ii) a paucity of through-joint TAs identified following blast injury.

Hull's injury mechanism theory of blast-mediated TA, was a summation of literature review, analysis of clinical data – medical reports and photographs of injured extremities from blast casualties, the majority stemming from the troubles in Northern Ireland from the 1970s to

A.M.J. Bull et al. (eds.), *Blast Injury Science and Engineering: A Guide for Clinicians and Researchers*,
DOI 10.1007/978-3-319-21867-0_21

Fig. 21.1 An IED casualty with a left leg traumatic amputation at the level of the knee joint. The tibia is still attached but completely stripped of soft tissue

early 1990s – , live blast tests and computational finite element (FE) modelling [5–7] (see Chap. 17).

TA from pure tertiary blast injury was called into question due to inconsistencies between two datasets previously thought to share a common injury mechanism; blast victims and ejecting fast jet aircrew. Casualty data from Hull et al. showed a diaphyseal skeletal amputation level in the majority of explosive blast victims sustaining TAs and a paucity of through joint TAs (<2 %). This contrasted with the anatomical level of extremity injury (fractures/dislocations, *not amputations*) in ejecting fast jet pilots [8], subject to windblast (i.e. pure tertiary blast injury) at speeds up to 1100 km/h, thought to approximate to blast wind velocities close to the seat of an explosion. These aircrew injuries, due to limb flail, tended to be through or near to joints.

The potential causative role of primary blast (the shockwave) was inferred by an association, again from Northern Ireland casualty data, between fatal primary blast lung injury (PBLI) and TA. Live blast tests conducted by Hull generated long bone fractures in goat hind-limbs. These samples were shielded from secondary and tertiary blast effects, leaving primary blast injury – shockwaves – as the only likely mechanism of fracture causation. Computer modelling confirmed the diaphysis as the area of greatest stress concentration following exposure to primary blast.

Thus the new injury mechanism for TA was put forward and remained unchallenged prior to this work. However, the methodology did not include any radiological imaging analysis and clinical data was, at times, extremely limited.

Analysis of military casualty data from Iraq and Afghanistan called into question some of the supporting elements of the currently accepted TA mechanism theory. Firstly, analysis of 121 combat casualties by Singleton et al. showed no statistical association between PBLI and TA, in either mounted (i.e. in-vehicle) or dismounted (i.e. on foot) blast fatalities [9]. Secondly, the decade of recent conflict in Iraq and Afghanistan generated a large cohort of survivors with TA injuries – some with multiple TAs – who, by definition, had not sustained fatal PBLI [10, 11]. Thirdly, military surgeons with experience of managing IED casualties in Afghanistan reported seeing a number of through joint TAs. This inferred that through joint TAs may not be as rare as previously thought. The final reason for such a review was the adoption in November 2007 of postmortem CT (PM-CT) imaging for UK military combat fatalities. The availability of detailed cross-sectional imaging performed to a standard protocol and, in the vast majority of cases, within a few hours of the fatal injuries and with no confounding surgical intervention, provided a new tool to examine blast injury pathoanatomy at levels of detail never previously available [12].

Cumulatively, these factors highlighted both a need to review understanding of blast-mediated TA mechanism of injury and an opportunity to further our knowledge in this field through new data.

21.3 The Investigation

This work formed the basis of a Bioengineering MD(Res) within the Centre for Blast Injury Studies at Imperial College London. A crucial component of the research was collaboration with both clinicians and academics – including blast

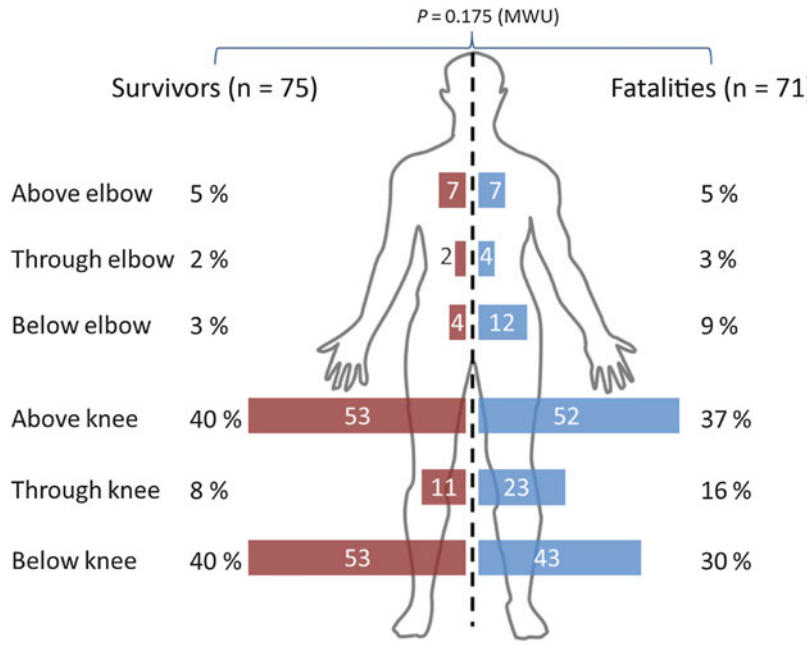

Fig. 21.2 Level of blast-mediated TAs: Survivors vs. Fatalities (Numbers in/by bars represent number of TAs, *MWU* Mann Whitney *U* test)

physicists, biologists and bioengineers – who provided invaluable support, expertise and insight particular to their speciality. Working with such a varied group enabled a far more holistic approach than would have been possible otherwise, which was hugely beneficial in maximising both data exploitation and utility of resultant findings.

The basis of the new research was clinical analysis at a level of detail never previously possible. A national prospectively gathered trauma registry (UK JTTR) and a post mortem CT (PM-CT) database were used to identify casualties (survivors and fatalities) sustaining a blast-mediated major extremity TA (through or proximal to the wrist or ankle joint) between August 2008 and August 2010. Level of TA and associated significant limb, thoracic and other injuries were recorded.

Survivors routinely underwent emergency surgery. The majority were not comprehensively CT scanned pre-operatively, reflecting clinical priorities of lifesaving treatment. The detailed pathoanatomical analysis was possible due to PM-CT imaging; by definition only available for fatality cases. However, as shown in Fig. 21.1, survivor and fatality TA anatomical distributions were not statistically different. Crucially then, fatality TA pathoanatomy data could be considered to be representative for survivor TAs also. Tens of thousands of images were assessed to characterise the bony and soft tissue anatomy of blast-mediated TA injuries.

146 Cases (75 survivors and 71 fatalities) sustaining 271 TAs (130 in survivors and 141 in fatalities) were identified. The lower limb was most commonly affected (117/130 in survivors, 123/141 in fatalities). The overall through-joint TA rate was 47/271 (17.3 %). 34/47 through-joint injuries (72.3 %) were through knee.

More detailed anatomical analysis facilitated by PM-CT imaging of the fatality group (see Fig. 21.2) revealed only 9/34 through joint TAs had a contiguous fracture (i.e. intra-articular involving the joint through which TA occurred) in the proximal remaining long bone/limb girdle. 18/34 had no fracture, and 7/34 had a non-contiguous (i.e. remote from the level of traumatic amputation) fracture. Further analysis revealed that in many cases the amputated limb was grossly intact and had not been fragmented as may have been believed previously (Fig. 21.3).

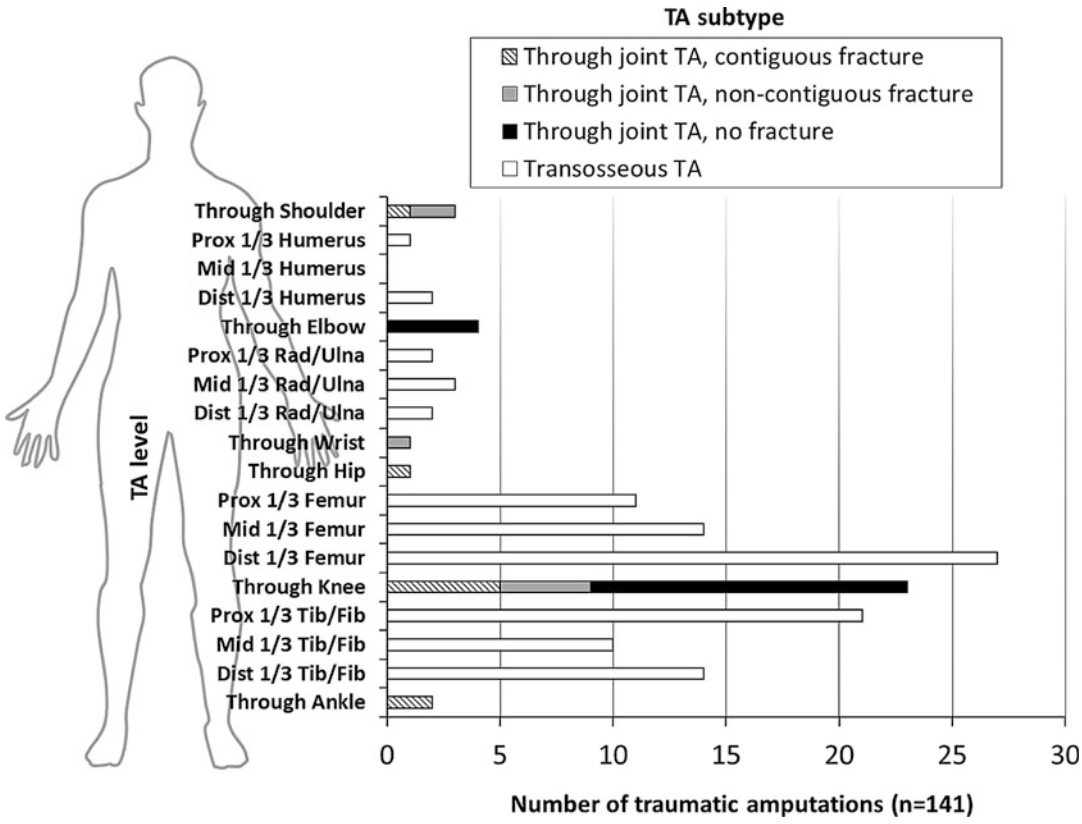

Fig. 21.3 TA incidence by level and TA subtype in fatalities

21.4 The Outcomes

This new data informed a re-evaluation of our understanding of the injury mechanism of blast-mediated TA.

Analysis of the soft tissue injury profiles of through joint and transosseous TAs showed no significant difference. This suggested that there may not be two radically different processes occurring to generate these injuries and thus an injury mechanism theory to explain both types of TA could be valid.

The high rate of through joint TAs (almost 1 in 4 in the fatality group), and the fact that of these, almost 3 in 4 had either no associated fracture or a fracture remote from the level of amputation, strongly inferred a flailing mechanism of injury. This contrasted with accepted theory of shockwave-mediated midshaft fractures of long bones followed by flail. A through joint injury was inconsistent with expected fracture patterns following either primary blast (oblique diaphyseal) or close contact primary and secondary blast injury (brisance – shattering – type fractures) [13].

Furthermore, the relative significance of the shockwave/primary blast is called into question by the lack of any relationship between TA and PBLI, demonstrated in this analysis of modern blast casualties. In contrast to previously held beliefs that proximity to an explosion sufficient to cause TA was lethal due to PBLI, we have shown no such correlation, and the large cohort of survivors with TAs are a clear demonstration that such a link does not hold true with many current blast casualties. Environment of the casualty was minimised as a potential confounder by subgroup analysis of mounted and dismounted cases.

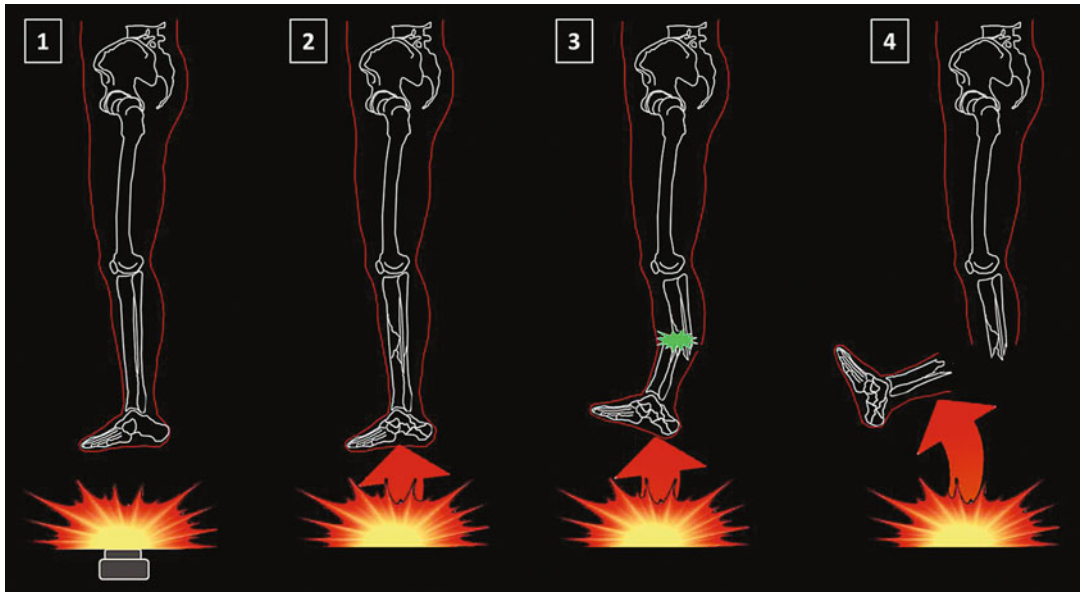

Fig. 21.4 Proposed transosseous TA mechanism from tertiary blast: (*1*) detonation underneath lower limb, (*2*) predominantly axial force transmitted, corresponding hindfoot and long bone fractures, (*3*) flail occurs through long bone fracture site, (*4*) completion of transosseous TA

Combining all the new data analysis, the following blast-mediated TA injury mechanism is proposed:

> Dependent on the position of the extremity and the displacement produced by the explosive blast wind, in some cases the relative stability of the joint and a predominant axial load generate diaphyseal stress concentrations leading to fracture, flail at this point and transosseous TA (see Fig. 21.4). However, in other scenarios with oblique loads caused by less axial, more coronal/sagittal type extremity displacement from the blast wind, the maximal stress concentration is peri- or intra-articular, leading to primary peri-articular soft tissue failure, flail through the joint and a subsequent through joint TA (see Fig. 21.5).

Although modern blast injury data did not support a link between significant primary blast injury and TA, there is insufficient evidence to discount Hull's theory (shockwave-induced diaphyseal fracture followed by flail and TA through the fracture) as a valid injury mechanism. It is possible that there may be multiple blast-mediated TA injury mechanisms, including Hull's theory and isolated flail/tertiary blast injury. Guillotine-type TAs from explosive fragments of sufficient size and energy have also been documented – a type of secondary blast injury. All of these need to be considered in any mitigation/prevention strategy. However, this new work has generated an injury mechanism theory through which tertiary blast injury can account for both transosseous and through joint TAs. Most importantly, this highlights a target to act against to try to prevent these injuries and save both limbs and lives.

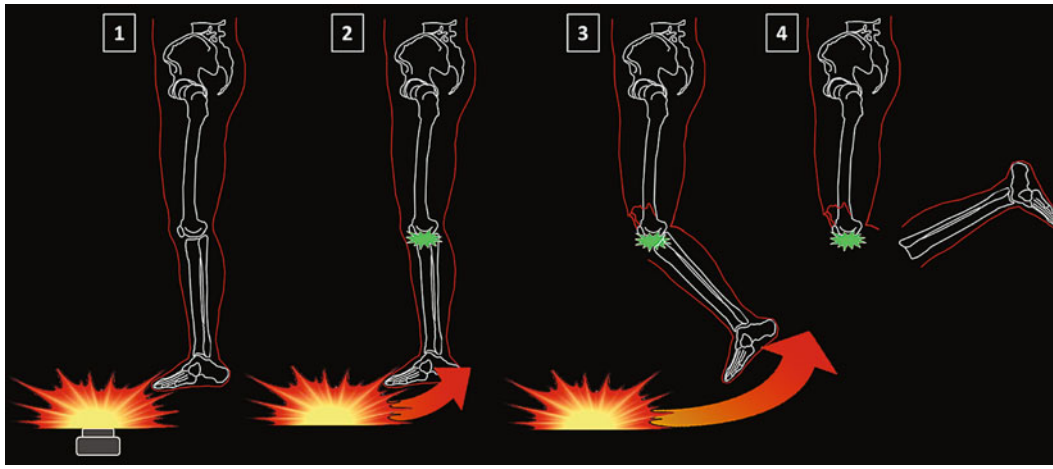

Fig. 21.5 Proposed through joint TA mechanism from tertiary blast. (*1*) IED detonation, biomechanically significant offset from casualty. (*2*) Non-axial force from blast wind, peri-articular soft tissues loaded. (*3*) Peri-articular soft tissue tensile failure, gross displacement of leg. (*4*) Through-joint traumatic amputation

References

1. Ramasamy A, Hill AM, Clasper JC. Improvised explosive devices: pathophysiology, injury profiles and current medical management. J R Army Med Corps. 2009;155(4):265–72.
2. De Candole CA. Blast injury. Can Med Assoc J. 1967;96(4):207–14.
3. US Department of Defense. 6025.21E medical research for prevention, mitigation, and treatment of blast injuries. US Department of Defense Directive [Internet]. 2008 12 Jan 2012. Available from: http://www.dtic.mil/whs/directives/corres/html/602521.htm
4. Mellor SG, Cooper GJ. Analysis of 828 servicemen killed or injured by explosion in Northern Ireland 1970–84: the Hostile Action Casualty System. Br J Surg. 1989;76(10):1006–10.
5. Hull JB. Pattern and mechanism of traumatic amputation by explosive blast. J Trauma. 1996;40 (3S):198S–205.
6. Hull JB. Traumatic amputation by explosive blast: pattern of injury in survivors. Br J Surg. 1992;79 (12):1303–6.
7. Hull JB, Bowyer GW, Cooper GJ, Crane J. Pattern of injury in those dying from traumatic amputation caused by bomb blast. Br J Surg. 1994;81(8):1132–5.
8. Ring WS, Brinkley JW, Noyes FR. USAF non-combat ejection experience 1968-1973: incidence, distribution, significance and mechanism of flail injury. In: Glaister DH, editor. Biodynamic response to windblast. Toronto/London: NATO Advisory Group for Aerospace Research and Development (AGARD); 1975. p. B1–8.
9. Singleton JAG, Gibb IE, Bull AMJ, Clasper JC. Traumatic amputation following explosive blast: evidence for a new injury mechanism. Combined services orthopaedic society (CSOS) annual scientific meeting. Camberley; 2012.
10. Defence Analytical Services and Advice (DASA). Quarterly Afghanistan and Iraq amputation statistics. 7 Oct 2001–31 Mar 2012. http://www.dasa.mod.uk: UK Government; 2012 [cited 16 June 2012]. Available from: http://www.dasa.mod.uk/index.php?pub=AMPUTATION
11. Armed Forces Health Surveillance Center. Amputations of upper and lower extremities, active and reserve components, U.S. Armed Forces, 2000-2011. MSMR. 2012;19(6):2–6.
12. Singleton JAG, Gibb IE, Bull AMJ, Mahoney PF, Clasper JC. Primary blast lung injury prevalence and fatal injuries from explosions: insights from postmortem computed tomographic analysis of 121 improvised explosive device fatalities. J Trauma Injury Infect Crit Care. 2013;75(2):S269–74. doi:10.1097/TA.0b013e318299d93e.
13. Ramasamy A, Hill AM, Masouros S, Gibb I, Bull AMJ, Clasper JC. Blast-related fracture patterns: a forensic biomechanical approach. J R Soc Interface. 2011;8(58):689–98.

Testing and Development of Mitigation Systems for Tertiary Blast

22

Nicolas Newell and Spyros Masouros

22.1 Introduction

Improvised explosive devices that detonate under a vehicle cause dynamic deformation of the floor and therefore transmission of substantial forces axially upwards into the lower extremities of the occupants. These accelerations have the potential to cause the devastating foot and ankle injuries that have been described in more detail in Chap. 20.

Large improvements in the protection offered to occupants during under-vehicle explosions can be made through alterations in vehicle design. Design features such as false floors, V-shaped hulls, increased standoff, increased vehicle mass and seat design have been shown to offer protection to occupants during under-vehicle explosions [1–3]. Many of these features have been incorporated into more recent vehicle designs, however, retrofitting is often not cost effective. Therefore, improvements that can be made through mitigation systems that can be easily retrofitted to existing vehicles are attractive.

N. Newell, MEng, PhD (✉) • S. Masouros, PhD, DIC, CEng, MIMechE
Department of Bioengineering, Royal British Legion Centre for Blast Injury Studies, Imperial College London, London SW7 2AZ, UK
e-mail: n.newell09@imperial.ac.uk; s.masouros04@imperial.ac.uk

22.2 The Issue

Due to the proximity of the foot and ankle to the vehicle floor pan, adjustments to combat boot designs and the introduction of blast mats have the potential to reduce the severity of injury. However, there is currently no clearly defined method or protocol to assess accurately the capability of a mitigation system to reduce the risk of injury to a vehicle occupant. This chapter reviews a number of approaches to assess mitigation systems which have been categorised into: scaled blast experiments, drop rig experiments, traumatic injury simulations, and finally computational models.

22.3 Methods to Assess Mitigation Systems

In order to assess a mitigation system, an experimental method able to reliably replicate the loading seen during an under-vehicle explosion is required. The loading exerted to the lower limb of a vehicle occupant is dependent upon a large number of factors (vehicle design, soil properties, type of explosive and, position of occupant) and therefore it is unlikely that there are clear, consistent floor pan acceleration profiles that experimental devices can aim to replicate. Due to this large range of possible acceleration profiles, a number of different

A.M.J. Bull et al. (eds.), *Blast Injury Science and Engineering: A Guide for Clinicians and Researchers*,
DOI 10.1007/978-3-319-21867-0_22

experimental approaches may be used to assess a mitigation technology. Generally, an experimental technique must accelerate a mass beyond 12 m/s such that it transmits an axial force to the mitigation system over a short duration (<10 ms) [2, 4].

22.3.1 Drop Rig Experiments

A drop rig is an experimental device that allows a mass to be dropped onto a specimen or sample from various heights such that its dynamic response can be assessed. Typically, a transducer is incorporated into the falling mass to capture the force-displacement behaviour. For blast impact research, drop rigs provide a repeatable and reliable means of assessing the dynamic behaviour of mitigation systems. Newell et al. [5] used a drop rig to compare the response of two combat boot designs commonly used by UK troops (Fig. 22.1). The soles of the two designs were impacted with a 7.45 kg mass at ever increasing energies until fracture of the combat boot was seen. The maximum velocity that the combat boot was impacted at was 12 m/s, the same as the estimate of vehicle floor velocity during an under-vehicle explosion made by Wang et al. [2]. The force-displacement response was recorded by a transducer incorporated into the falling mass and the responses of the two combat boots were compared. One of the designs consistently experienced lower peak forces at the lower impact energies and longer time-to-peak forces at higher impact energies in comparison to the other. This method provides a repeatable, reliable way to initially assess the behaviour of a mitigation system. However, the loading environment provided here does not accurately replicate that seen during an under-vehicle explosion since the combat boot is not restrained against a rigid surface in a vehicle; an experimental method that more accurately replicates the behaviour of the floor may provide a more realistic assessment of a mitigation system.

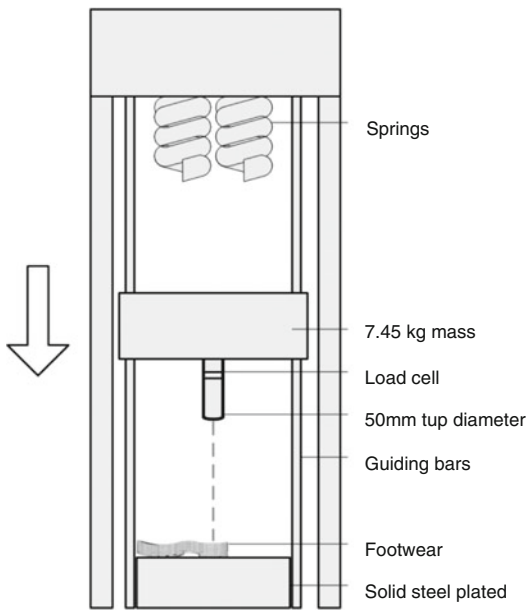

Fig. 22.1 Schematic of the drop rig setup used by Newell et al. [5] to assess the response of two combat boots

22.3.2 Traumatic Injury Simulators

Traumatic injury simulators aim to replicate the loading applied to occupants' lower limbs during under-vehicle explosions in a controlled laboratory environment. Generally, their design incorporates a large mass (6.8-42 kg) that is rapidly accelerated to a target velocity (2.2–12 m/s) before rapidly decelerating to rest. Their target velocities are often based upon data from live blast experiments. However, their mass cannot be as easily justified since the equivalent mass of an accelerating plate is not easily calculated from live blast data. What remains critical however is that the mass is large enough so that upon impact with the mitigation system/lower limb, the behaviour of the accelerating plate is not affected by the mass of the lower limb, and that they do not respond in a coupled manner.

Traumatic injury simulators are often used in conjunction with anthropometric test devices (ATDs) which are designed to approximate human response to high-rate loading. The two most commonly used ATDs are the Hybrid-III and MIL-Lx (see Chap. 16). The biofidelity of these two ATD designs have been discussed in

detail elsewhere [6–9]. Both the Hybrid-III and MIL-Lx measure load in the tibia which can be used in conjunction with risk curves, developed using data obtained from cadaveric tests, to estimate the probability of injury. Using the traumatic injury simulator to mimic the response of the floor of a vehicle during an under-vehicle explosion and the ATD to mimic the response of a human, a mitigation system can be positioned between the simulator and ATD to predict the probability of injury.

Quenneville and Dunning [9] impacted both the Hybrid-III and MIL-Lx ATDs with and without hiking boots using a traumatic injury simulator. At a range of velocities (2.2–7.0 m/s), a 6.8 kg cylindrical projectile (radius 3.3 cm) was accelerated down a tube and impacted the back of a pate upon which the sole of the boot was resting. In these experiments, the addition of the hiking boot reduced the peak forces by approximately 65 % at the highest impact velocities (7 m/s). As well as hiking boots, Quenneville and Dunning [10] have also used their impact rig to compare five commercially available floor mats using a Hybrid-III ATD. Five impact tests were performed on each of the five designs against a control (no floor mat). All of the floor mat designs reduced the force measured in the tibia of the Hybrid-III ATD. This reduction ranged from 35 to 77 %. Interestingly, some of the blast mat designs performed well in response to high velocity impacts but not as well at low velocity impacts, demonstrating the importance of considering the response of the mitigation technologies at a range of impact severities.

A traumatic injury simulator, capable of horizontally accelerating a 36.7 kg plate at velocities up to 12 m/s has been developed at Wayne State University. McKay [11] used this simulator to assess the mitigation capacity of five kinetic energy absorbing materials. These were a collapsible steel plate, aluminium commercial grade (ACG) at three different crush strengths, and an aluminium foam. Floor mat samples were mounted to the impactor footplate which impacted a MIL-Lx. The change in peak force ranged from a 31 % reduction to an 8 % increase. Interestingly, it was a mid strength ACG that performed better than any other design. Since there were two mats with higher crush strengths and one with a lower crush strength, this suggests that there may be an optimal strength under the impact conditions tested; if the mat has a high crush strength it may not compress completely, therefore less force would be absorbed in comparison to if it had compressed completely. Conversely, if it is not stiff enough it may crush very quickly and bottom out, resulting in a large transmitted force.

The Anti-vehicle Under Belly Injury Simulator (AnUBIS) developed at Imperial College London has been developed such that ATDs can rest on a 42 kg mass which is pneumatically accelerated upwards. The acceleration profile of the mass is controlled through careful selection of the material and geometry of a pin which is designed to hold the plate down until a specific pressure is reached, at which point it shears [12]. Tests were performed on three blast mat designs under both the MIL-Lx and Hybrid-III ATDs at a range of severities [6]. The test setup is shown diagrammatically in Fig. 22.2. There was little difference in how the

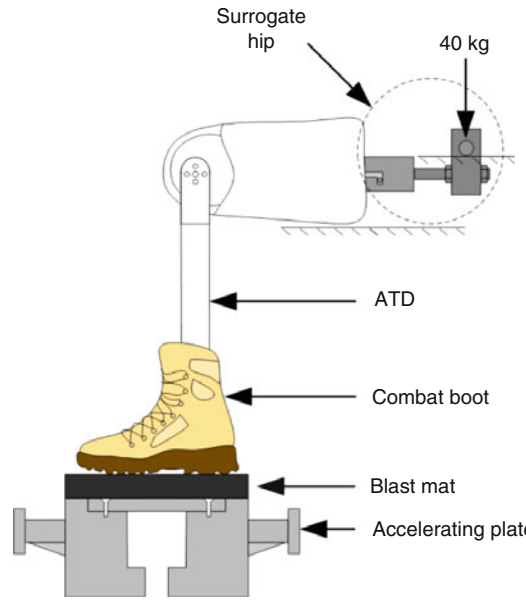

Fig. 22.2 Configuration and mounting for the MiL-Lx ATD on AnUBIS, the traumatic injury simulator used at Imperial College London

two ATDs ranked the mitigation systems but the differences were exaggerated when the Hybrid-III was used rather than the MIL-Lx.

22.3.3 Scaled Blast Experiments

One of the most accurate, but not always repeatable, means of replicating an under-vehicle explosion is simply by detonating an explosive beneath a floor surrogate. The Test Rig for Occupant Safety System (TROSS™) is a vehicle floor simulant, which utilises scaled detonations to provide the same blast parameters to a vehicle occupant as those occurring in an underbelly vehicle blast of 2–10 kg of TNT [13]. Manseau and Keown [14] used this as a test-bed to evaluate the effect of the military boot on the tibia loading response and injury severity using a Hybrid-III ATD. They compared the response of the Hybrid-III to scaled blasts with and without a combat boot. While the impulse transferred to the Hybrid-III was similar, the military boot reduced the peak tibia axial force by approximately 30 % and reduced the loading rate by 43 % in comparison to no military boot.

22.3.4 Computational Models

Finite element models enable engineers to gain an insight into dynamic events which would not be possible experimentally. They also enable sensitivity and optimisation studies to be performed on designs to gain a greater understanding of the parameters that have the greatest effect on certain variables. While they do require a lot of time to acquire accurate geometry and material properties, as well as extensive validation, once developed they provide an invaluable tool to assess mitigation systems since the effect of design changes can be evaluated quickly. One computational model of note is that of Dong et al. [15] who developed an FE model of a lower extremity to predict the minimum axial force required to cause fracture. Their model was used to determine the critical maximum velocity of the floor plate to cause tibia fracture at a range of knee flexion angles finding that, as the angle increased, the critical velocity increased. Aside from the long run time, one limitation of Dong et al.'s model is that it is subject specific. Researchers at Imperial College London have developed a computational model of the MIL-Lx ATD [16], which may allow more powerful predictions of injury since it can be used in conjunction with injury curves that have been developed through analysis of a large number of cadaveric tests.

22.4 The Outcomes

A number of techniques to test and develop mitigation systems have been reviewed in this chapter. All of the approaches are useful for different stages of the development of a mitigation system. Computational models provide a powerful tool for investigating new mitigation system concepts since they allow many alterations of designs to be tested quickly. An experimental assessment is also recommended for complete validation of the mitigation system. Drop rig tests may be considered to be useful for initial assessments of mitigation systems but traumatic injury simulators provide a more realistic test bed to accurately and repeatably simulate an under-vehicle explosion and are therefore more likely to provide results that can be translated to theatre. Furthermore, scaled blast tests may provide the most realistic method of replicating an under-vehicle explosion and should also be considered when evaluating a mitigation system. Both traumatic injury simulators and scaled blast tests are used in conjunction with ATDs. While there is still room to improve the biofidelity of current ATD designs, they provide a useful tool to predict injury risk and therefore assess mitigation design. Ultimately, the collection of clinical data from theatre once a system has been introduced may be the most powerful way of assessing a mitigation design.

References

1. Durocher R. Jowz valley mine strike preliminary technical report: investigation of a mine strike involving Canadian troops in Afghanistan. Valcartier: Defence Research and Development Canada; 2003.
2. Wang J, Bird R, Swinton B, Krstic A. Protection of lower limbs against floor impact in army vehicles experiencing landmine explosion. J Battlef Technol. 2001;4:8–12.
3. Ramasamy A, Hill AM, Masouros SD, Gordon F, Clasper JC, Bull AMJ. Evaluating the effect of vehicle modification in reducing injuries from landmine blasts. An analysis of 2212 incidents and its application for humanitarian purposes. Accid Anal Prev. 2011;43:1878–86. doi:10.1016/j.aap.2011.04.030.
4. Bird R. Protection of vehicles against landmines. J Battlefield Technol. 2001;4:14–7.
5. Newell N, Masouros SD, Pullen AD, Bull AMJ. The comparative behaviour of two combat boots under impact. Inj Prev. 2012;18:109–12.
6. Newell N, Masouros SD, Bull AMJ. A comparison of MiL-Lx and hybrid-III responses in seated and standing postures with blast mats in simulated under-vehicle explosions. In: Proceeding of the IRCOBI conference 2013, Gothenburg; 2013, p. 135–45.
7. Newell N, Masouros SD, Ramasamy M, Bonner TJ, Hill AM, Clasper JC, et al. Use of cadavers and anthropometric test devices (ATDs) for assessing lower limb injury outcome from under-vehicle explosions. In Proceeding of the IRCOBI conference 2012, Dublin; 2012, p. 296–303.
8. Pandelani T. Evaluation of dynamic response characteristics of the MIL-Lx leg compared to the Thor-Lx leg. In: Proceeding of the CSIR Young Researcher Symposium 2011, Pretoria; 2011.
9. Quenneville CE, Dunning CE. Evaluation of the biofidelity of the HIII and MIL-Lx lower leg surrogates under axial impact loading. Traffic Inj Prev. 2011;13:81–5. doi:10.1080/15389588.2011.623251.
10. Quenneville C, Dunning C. Evaluation of energy attenuating floor mats for protection of lower limbs from anti-vehicular landmines. In: Proceeding of the ASME 2011 Summer Bioengineering Conference, Farmington; 2011. p. 1031–2.
11. McKay BJ. Development of lower extremity injury criteria and biomechanical surrogate to evaluate military vehicle occupant injury during an explosive blast event. PhD Thesis. Wayne State University, Detroit; 2010.
12. Masouros SD, Newell N, Ramasamy A, Bonner TJ, West ATH, Hill AM, et al. Design of a traumatic injury simulator for assessing lower limb response to high loading rates. Ann Biomed Eng. 2013;41:1957–67.
13. North Atlantic Treaty Organisation HFM-090 TG 25 2007. Test methodology for protection of vehicle occupants against anti-vehicular landmine and/or IED effects (HFM-090).
14. Manseau J, Keown M. Development of an assessment methodology for lower leg injuries resulting from anti-vehicular blast landmines. In: IUTAM symposium impact biomechanics from fundamental insights to application, vol. 124. Ireland: University College Dublin; 2005, p. 33–40.
15. Dong L, Zhu F, Jin X, Suresh M, Jiang B, Sevagan G, et al. Blast effect on the lower extremities and its mitigation: a computational study. J Mech Behav Biomed Mater. 2013;28:111–24.
16. Newell N, Masouros SD. A finite element model of the military lower extremity surrogate (MIL-Lx) with combat boot validated for high loading-rate inputs. Work. Numer. Anal. Hum. Surrog. Response to Accel. Load., Aberdeen; 2014.

Pelvic Blast Injury

23

Claire Webster and Jon Clasper

23.1 Introduction

Although the majority of wartime trauma concerns the limbs, it is injuries to the head, torso and junctional haemorrhage from the neck, axilla or groin that are the most life threatening. As haemorrhage is the most common cause of preventable death on the battlefield, it is of considerable research interest (see Chap. 19, Sect. 19.1)

In the most recent conflicts, the Improvised Explosive Device (IED) changed the nature of injuries from penetrating wounds from gunshots or fragments, to the extensive tissue loss and heavily contaminated injuries associated with close range explosions. As the majority of the devices are victim operated, lower extremity trauma is almost universal, and those with high injuries and an associated pelvic fracture have the worst clinical outcomes. In addition to junctional haemorrhage, this is often due to non-compressible pelvic bleeding and currently there are few opportunities for control of this in the pre-hospital environment.

The pelvis, consisting of paired iliac, ischial and pubic bones in a ring like structure, forms the inferior margins of the abdomen, and contains small and large bowel, ureters and urethra, and reproductive organs. It also has a rich network of vasculature; paired external iliac and femoral arteries and veins, and multiple branches of the internal iliac leading to the pelvic organs. The pelvic bones are strongly reinforced by a network of ligaments and surrounding musculature requiring a considerable amount of force to cause a fracture. Therefore, when a fracture does occur, there is a high incidence of associated injuries both locally and also to additional body regions such as the head and thoracic structures [1]. It is possible that if fracture could be prevented, or local bleeding controlled, then the mortality from IED and similar pelvic injuries could be reduced. One of the key initial steps is to understand the mechanism of fracture following pelvic blast injury.

23.2 Civilian Pelvic Trauma

It is important to ascertain exactly how the blast loading leads to fracture of the pelvis. This could be a direct effect on the pelvic structures, or indirect, such as axial loading of the pelvis. In addition, flailing of the lower limbs resulting in

C. Webster, MBChB MRCS RAF (✉)
Department of Bioengineering, Royal British Legion Centre for Blast Injury Studies, Imperial College London, London, UK
e-mail: c.webster14@imperial.ac.uk

J. Clasper, CBE DPhil DM FRCSEd Col L/RAMC
Department of Bioengineering, Royal British Legion Centre for Blast Injury Studies, Imperial College London, London, UK

Academic Department of Military Trauma and Surgery, Royal Centre for Defence Medicine, Birmingham, UK
e-mail: jonclasper@aol.co.uk

A.M.J. Bull et al. (eds.), *Blast Injury Science and Engineering: A Guide for Clinicians and Researchers*,
DOI 10.1007/978-3-319-21867-0_23

rotational force being applied to the hemi pelvis may result in injuries such as the 'open book' pattern of injury seen in civilian trauma. This particular fracture pattern is highly likely to cause significant vessel damage and life threatening haemorrhage.

Civilian pelvic classification systems aim to direct patient treatment pathways based on severity. Common systems include the Young and Burgess classification [2], a later modification of the Pennal and Tile classification [3], which describes the fractures based on the direction of the force upon them. They are grouped into anterior posterior compression fractures (APC), lateral compression (LC) and vertical shear (VS) in which one hemi pelvis is displaced superiorly, commonly from a fall from height and landing on the feet. APC and LC injuries are further graded 1–3 depending on severity. In addition, one of the original classifications [4] considers stability of pelvic fracture, dividing fractures into grades A–C depending on the extent of rotational and vertical stability. Type A fractures are considered stable, type B rotationally unstable but vertically stable, and type C unstable both rotationally and vertically.

Although classification systems guide treatment following civilian trauma, military pelvic fractures may not fit into these divisions clearly. As such, the classification is not fit for purpose in this patient group. There is therefore a need to analyse military pelvic fracture patterns to determine if a specific military classification is required. As with civilian fractures this is likely to be based on the mechanism of failure and/or mechanical stability.

23.3 Bleeding Following Pelvic Trauma

Bleeding may result from arterial injury, or from the lower pressure venous system. Venous bleeding has been demonstrated in civilian studies to be responsible for around 90 % of pelvic fracture haemorrhage, commonly to the ileolumbar vein or presacral plexus [5]. However, arterial bleeding, when present, is more likely to lead to haemodynamic instability, and presumably more likely to result in death in the military environment.

There are few civilian studies detailing the exact source of arterial hemorrhage in pelvic fracture. One study of 63 patients demonstrated that superior gluteal, followed by internal pudendal, obturator and lateral sacral arteries respectively were responsible for bleeding [6]. A second study details the frequency of embolisation of arteries, one of the options for treating significant bleeding. The study demonstrated the internal iliac was the most commonly embolised artery, followed by the superior gluteal, internal pudendal, lateral sacral, and obturator and iliacolumbar arteries. However, this study was based on only 87 patients [7].

It is important to know the type and site of bleeding, as venous bleeding can cease by clot formation and tamponade within the retroperitoneal space as the pressure increases [8]. This is less likely to occur following arterial bleeding, and more direct control may be required [9]. In addition, the mechanically unstable pelvic injuries, particularly the APC, or open book fractures result in an increase in pelvic volume, and as a result, retroperitoneal tamponade may not occur and bleeding can continue. Reducing the pelvic volume and stabilisation of the pelvis, by binder or fixation, is paramount in the management of these life-threatening injuries. Previous research at Imperial College London has demonstrated the importance of closure of the pelvic ring, and how improper placement of pelvic binders leads to inadequate closure of open pelvic fractures. This can lead to delays in haemostasis, and ultimately, an increase in mortality from pelvic trauma [10]. This noninvasive technique is taught on all Advanced Trauma Life Support (ATLS) and Military Operational Surgical Training (MOST) courses as a quick and reliable method for pelvic fixation in suspected pelvic fracture in the pre-hospital setting.

Further work is required to investigate the source of bleeding and its relation to the pelvic fracture present. In addition, the published studies are of a civilian cohort, and due to the high energy mechanism of blast, military patients may

sustain a different pattern of vessel injury. It is important to pinpoint the location of injury in order to direct treatment strategies.

23.4 Injury Mitigation

Together with head injury, the IED pelvic injury was responsible for the majority of deaths of UK service personnel injured in Iraq and Afghanistan who initially survive their injuries. Death can occur soon after injury, usually from uncontrollable bleeding as discussed above, or from later multiple organ failure, which is likely to be related to both the initial blood loss as well as significant contamination at the time of injury. The un-paralleled survival rates seen in recent conflicts suggest that mitigation, rather than any additional improvement in treatment, is more likely to improve future outcomes. Currently mitigation is limited to soft tissue protection from the direct effects of the explosion, rather than preventing indirect injury, or an attempt to prevent fracture.

Personnel protective equipment (PPE) to the lower extremity was introduced in response to the frequency of urogenital injuries, with a historical incidence of approximately 5 % [11]. This exists in three tiers, a silk under layer, Kevlar™ shorts, and a further Kevlar genital protection piece [12]. Although it was only possible to compare to a historical control group, this protection has been associated with a significant decrease in injury risk [13].

However, as the protection was aimed at reducing genital injury and not at reducing the incidence of pelvic fracture, further work should be targeted on preventing both the pelvic fracture and significant bleeding following injury.

Prior to determining the research priorities in military pelvic trauma, there is a need to define the extent of the problem.

23.5 UK Military Experience

A search of the Joint Theatre Trauma Registry (JTTR) was performed, and significant pelvic trauma from the conflicts in Iraq and Afghanistan between 2003 and 2014 was identified. From this database pelvic fractures secondary to motor vehicle collisions, gunshot wounds, falls from height and crush injury were subsequently excluded from analysis.

Between 2003 and 2014 there were 364 pelvic fractures associated with a blast mechanism. Of these there were 180 survivors and 184 deaths, giving a mortality rate of 50.5 %. This is significantly higher than that quoted in the civilian literature where published mortality rates are between 8 and 14% [14–16].

As noted above, civilian pelvic fractures are associated with significant trauma to other body regions, which may be the cause of death rather than the pelvic fracture itself. This was consistent with the UK military blast population; in this cohort no casualty sustained a pelvic fracture in isolation. Of the 184 fatalities, 68 (36 %) patients died as a result of the lower extremity injury with pelvic fracture, with the majority (116, 64 %) dying from other injuries, mainly head injury (58), abdominal injury (23) torso (12) spine (7), neck (3) and 13 considered to be 'whole body' injuries such as burns, or multi-region trauma. The majority of those other injuries were considered non-survivable and as such, pelvic trauma mitigation would have little to offer. Further work needs to be directed on the fatalities due solely to blast pelvic trauma, and a comparison made with the survivors in order to identify indicators of mortality to further focus the research effort.

23.6 Research Direction of the Centre for Blast Injuries

The initial requirement is a detailed analysis of the blast pelvic fractures to establish any specific patterns. Computerised tomography (CT) images of the fractures are available, and 3-dimensional CT reconstructions of the pelvic bones can be reviewed and the survivors compared with the deaths, specifically those who died of the pelvic injury. Detailed clinical analysis will allow the specific cause of death to be identified, focusing

on any injured vascular structures associated with the fracture. Mechanistically it may then be possible to determine how the vessel was damaged. Although designed for soft tissue protection, the wearing of PPE may make a difference to the pelvic fracture pattern and this would need to be considered.

Military fracture patterns can be compared with civilian fracture data. This may then determine whether the civilian fracture classifications used in the UK are applicable to these military patients. If not recognised, civilian management pathways may be inappropriate in these instances.

The effect of blast is likely to be different depending on the posture of the patient on impact, in particular, if standing or seated, which will cause different responses, and this needs to be taken into account. Information regarding the incident for example, whether the casualty was mounted or dismounted, surrounding environment, and explosive characteristics should therefore be analysed in order to gain a most complete picture of the forces and direction of force applied. It will also be necessary to determine which aspect of the blast, i.e. primary, secondary or tertiary is responsible (see Chap. 6). Based on this analysis, it may be possible to hypothesise whether the fractures are secondary to lower limb flail or from direct impact, which will be important in terms of mitigation strategies. If a specific blast pelvic fracture pattern can be recognised, the aim would be to recreate the injury in the laboratory using cadaveric specimens, and a previously validated blast rig [17].

Computational modelling of pelvic fracture may be a useful adjunct to the understanding of pelvic fracture. Shape modelling may help define the variability of the blast pelvis, as it has in normal joints [16], and define a point in which the fracture pattern results in an un-survivable injury. Finite element analysis could also be used to create reproducible experiments.

23.7 Conclusion

Blast injury to the pelvis has been a significant cause of death to UK personnel in Iraq and Afghanistan. It is hoped that with a knowledge of the biomechanics of blast injury to the pelvis, mitigation strategies could be developed with the potential to lessen the blast load and maintain the structural integrity of the pelvis, or at least, limit instability or any increase in pelvic volume, to limit vessel injury and/or blood loss.

The ultimate aim is to prevent, mitigate or improve the treatment of severe blast injury, in order to improve survival and morbidity from these injuries.

References

1. Siegel JH, Dalal SA, Burgess AR, Young JWR. Pattern of organ injuries in pelvic fracture: impact force implications for survival and death in motor vehicle injuries. Accid Anal Prev. 1990;22(5):457–66.
2. Burgess AR, Eastridge BJ, Young JW, Ellison TS, Ellison PS, Poka A, Bathon GH, Brumback RJ. Pelvic ring disruptions: effective classification system and treatment protocols. J Trauma. 1990;30(7):848–56.
3. Pennal GF, Tile M, Waddell JP, Garside H. Pelvic disruption: assessment and classification. Clin Orthop Relat Res. 1980;151:12–21.
4. Tile M, Pennal GF. Pelvic disruption: principles of management. Clin Orthop Relat Res. 1980;151:56–64.
5. Gänsslen A, Giannoudis P, Pape H-C. Hemorrhage in pelvic fracture: who needs angiography? Curr Opin Crit Care. 2003;9:515–23.
6. Kam J, Jackson H, Ben-Menachem Y. Vascular injuries in blunt pelvic trauma. Radiol Clin North Am. 1981;19(1):171–86.
7. Velmahos GC, Chahwan S, Falabella A, Hanks SE, Demetriades D. Angiographic embolization for intraperitoneal and retroperitoneal injuries. World J Surg. 2014;24(5):539–45.
8. Grimm MR, Vrahas MS, Thomas KA. Pressure-volume characteristics of the intact and disrupted pelvic retroperitoneum. J Trauma. 1998;44:454–9.
9. Geeraerts T, Chhor V, Cheisson G, Martin L, Bessoud B, Ozanne A, Duranteau J. Clinical review: initial management of blunt pelvic trauma patients with haemodynamic instability. Crit Care. 2007;11(1):204.
10. Bonner TJ, Eardley WGP, Newell N, Masouros S, Matthews JJ, Gibb I, Clasper JC. Accurate placement of a pelvic binder improves reduction of unstable fractures of the pelvic ring. J Bone Joint Surg Br. 2011;93(11):1524–8.
11. Hudak SJ, Morey AF, Rozanski TA, Fox CW. Battlefield urogenital injuries: changing patterns during the past century. Urology. 2005;65(6):1041–6.
12. Lewis EA, Pigott MA, Randall A, Hepper AE. The development and introduction of ballistic protection

of the external genitalia and perineum. J R Army Med Corps. 2013;159 Suppl:i15–7.
13. Oh JS, Do NV, Clouser M, Galarneau M, Philips J, Katschke A, Clasper J, Kuncir EJ. Effectiveness of the combat pelvic protection system in the prevention of genital and urinary tract injuries: an observational study. J Trauma. 2015;79(4 Suppl 2):S193–6.
14. Sathy AK, Starr AJ, Smith WR, Elliott A, Agudelo J, Reinert CM, Minei JP. The effect of pelvic fracture on mortality after trauma: an analysis of 63,000 trauma patients. J Bone Joint Surg Am. 2009;91 (12):2803–10.
15. Chong KH, DeCoster T, Osler T, Robinson B. Pelvic fractures and mortality. Iowa Orthop J. 1997;17:110–4.
16. Giannoudis PV, Grotz MRW, Tzioupis C, Dinopoulos H, Wells GE, Bouamra O, Lecky F. Prevalence of pelvic fractures, associated injuries, and mortality: the United Kingdom perspective. J Trauma. 2007;63(4):875–83.
17. Masouros SD, Newell N, Ramasamy A, Bonner TJ, West ATH, Hill AM, Clasper JC, Bull AMJ. Design of a traumatic injury simulator for assessing lower limb response to high loading rates. Ann Biomed Eng. 2013;41(9):1957–67.

Applications of Blast Injury Research: Solving Clinical Problems and Providing Mitigation

24

Debra J. Carr

24.1 Introduction

Body armour typically comprises a 'soft' fabric waistcoat or tabard style garment covering the torso; in military armour this provides protection from fragments, in police armour it provides protection from sharp-weapons and low velocity handgun bullets. The fabrics used are typically manufactured using para-aramid fibres (e.g. Kevlar®, Twaron®), but may contain ultra-high molecular weight polyethylene fibres (UHMWPE; e.g. Dyneema®, Spectra®). The armour may also contain 'hard' plates which are ceramic faced and composite backed (common combinations include alumina/para-aramid and silicon carbide/UHMWPE), or are 100 % composite (usually UHMWPE). These plates provide protection from high velocity rifle bullets. The level of protection the soft- and hard-armour provides varies according to the threat level that has been conducted [1, 2] as discussed in Chap. 28. Behind armour blunt trauma (BABT) has been defined as "…the non-penetrating injury resulting from the rapid deformation of armours covering the body" [3]. More recently, a definition for injuries occurring when body armour is impacted but not perforated has been suggested. This separates injuries that include skin laceration from those that are restricted to skin contusion and rib damage "Backface injuries are lacerations that occur due to blunt trauma" [4]. There has been an increasing awareness of BABT as an injury mechanism in both the military and civilian worlds [3, 5–9]. Typical injuries include skin contusion, laceration and penetration; rib fracture; and contusions to lungs, kidneys, spleen and (rarely) the heart e.g. [3, 5–13]. BABT also includes pencilling "… a deformation characteristic of body armour, which is *only* associated with the evolution of lightweight and flexible armours." [14] and "…comparable to an entry wound from a ballistic injury." [15]. A narrow, tapered, deep deformation of the soft body armour into the torso occurs, but the armour is not perforated.

24.2 Injury Mechanisms

BABT is considered to be a type of blunt trauma injury. Other injury mechanisms included in the same broad grouping are road traffic accidents and crush injuries [3, 16–18]. However, BABT occurs over a shorter period of time due to an impact event by a faster projectile. During the impact event, the body armour accelerates and deformation occurs on the rear of the armour, resulting in direct transmission of an applied

D.J. Carr, CEng, FIMMM, MCSFS
Impact and Armour Group, Centre for Defence Engineering, Cranfield University at the Defence Academy of the United Kingdom, Shrivenham, SN6 8LA, UK
e-mail: d.j.carr@cranfield.ac.uk

A.M.J. Bull et al. (eds.), *Blast Injury Science and Engineering: A Guide for Clinicians and Researchers*,
DOI 10.1007/978-3-319-21867-0_24

force through the armour and underlying clothing and onto the body. Stress waves are generated; they may be transmitted and/or reflected by the armour (and components) and/or underlying tissues (including those not in direct contact with the armour) depending on the speed of sound in the material [18–21]. Applied shear stresses may result in tearing of tissue [3, 6, 9, 22]. It is generally accepted that (i) the gross deformation of the chest and (ii) the duration and rate at which this deformation occurs affects the injuries observed [3, 9, 21].

24.3 Injury Data

Detailed injury data reported in the open literature is rare, excepting more recent injuries suffered by personal that have been reported in newspapers and via the internet [10–13]. The majority of case studies reported refer to police officers wearing soft armour and impacted with low velocity handgun ammunition (often their own weapon that had been taken off them). These incidents typically resulted in contusions (up to ~50 × 60 mm) and lacerations (up to 30 mm deep) e.g. [4, 8, 23]. A small study comparing female and male US police officer's BABT injuries (n = 4 female; n = 10 male) suggested that female officers suffered a higher risk of injury [24, 25].

Reports of BABT injuries to military personnel impacted with high velocity rifle bullets include incidents in Somalia and Russia [26, 27]. Injuries included a severe flank hematoma that extended to the groin (n = 1), a minor soft-tissue injury to the chest (n = 1), contusion (n = 1), lung rupture (n = 1) and lung abscess (n = 1); the more serious injuries resulted in up to 3 months hospitalisation. All impact sites were on the thorax, some on the back. Such injuries resulting from high-velocity bullet impacts appear similar to those reported in the media for military personnel injured in Iraq and Afghanistan [10–13].

Reports in the open literature of personnel killed due to BABT are limited [5, 28]. In both reports, the body armour being worn was not designed to provide protection from the ammunition that struck it. In a case reported from Vietnam, an M-16 round struck in the area of the third inter-costal space on the left side of the body; the bullet perforated the soldier's body armour, but not the pleural cavity [5]. The soldier died and the post-mortem revealed he had suffered extensive pulmonary contusions to the upper and lower lobes. Details of the body armour worn were not provided, but it is likely to have been a M69 flak jacket containing multiple layers of woven nylon 6,6 fabric (6–12 layers depending on specific location in the garment), which was not designed to provide protection from high-velocity rounds such as those fired from an M-16 [28]. A second fatal BABT case study was reported in the literature in 1982 [29]. A police officer was shot using a .45–70 rifle. The bullet did not perforate the body armour, but the officer died. Injuries included lacerated skin (4.1 × 3.9 cm), fractured rib, contusion to the lung and fractured blood vessels adjacent to the heart. A schematic drawing and photograph of the armour suggests it was a case of pencilling. The body armour worn by the officer was designed to protect from 44 Rem mag ammunition and contained 18 layers of Kevlar®, thus was not designed to protect from the ammunition that killed the officer.

24.4 Body Armour Testing

When body armour is impacted by a projectile, deformation occurs on the rear face. This deformation can be described using physical size (depth, 'diameter', volume) and/or dynamic properties such as velocity and acceleration. A commonly used measure in body armour test methods is to record the depth of the permanent indentation formed in a block of clay-like material (Roma Plastilina no. 1 is typically used) when a non-perforating bullet strikes body armour mounted in front of it. This measurement is known as the back-face signature (BFS). However, the *BFS does not correlate to specific BABT injuries* in humans e.g. "Neither the clay backing material nor the backface signature depth measurement reflects characteristics of the

human torso or its response to ballistic impact" [30]. Some organisations and test methods, particularly those concerned with non-perforating impacts onto plates, use representations of the human thorax to mount the armour on. Acceptable BFS measurements vary from 18 to 44 mm, depending on the test method considered. The origin of this test method lies in work completed in the US in the 1970s when research at Aberdeen Proving Ground (Maryland, USA) used goats to assess the performance of a specific soft body amour with respect to BABT [16, 22, 31]. Previous work had established the goat as a human surrogate with reference to penetrating ballistic injuries [32, 33]. Subsequent work correlated the results of the animal tests, firstly with gelatine blocks, and then Plastilina [23, 34]. However, the validation was only carried out for a specific threat and body armour. Further details are provided in the literature and test methods [2, 35, 36].

24.5 Conclusions

Wilson, writing in 1921 about wound ballistics, stated "Comparatively speaking, it is not the push of the elephant's shoulder with which we are concerned, but rather the kick of the mule" [37]. This quote can equally be applied to BABT. Observations regarding the importance of rate of deformation as well as deformation physical size have been recognised from the earliest 'modern' research into BABT [22, 23, 31, 34]. Difficulties in measuring rate of deformation in the early-1970s resulted in the use of a measured BFS to be adopted. It is important to recognise that the requirement was developed for ***a specified soft body armour*** and ***a specified type of ammunition***. The literature overwhelmingly agrees that a depth measurement in Plastilina (or other clay-like material) does not represent human injury and should not be referred to as a 'trauma measurement'. What is clear is that body armour tested against standards using the 44 mm BFS (or less) requirement saves lives. There is no evidence in the academic literature for fatalities due to BABT when personnel (military or police) are attacked by a threat for which the ***body armour they were wearing was designed***.

Body armour design continues to be optimised resulting in thinner, lighter and more compliant armours; all of which the user desires. However, an enhanced risk due to BABT **might** emerge as this process continues if armour is only designed to provide protection from a specified ballistic threat. In this respect, the inclusion of a BFS measurement provides a further measure of quality assurance to the procurer and user.

References

1. Tobin L, Iremonger M. Modern body armour and helmets: an introduction. Canberra: Argros Press; 2006.
2. Croft J, Longhurst D. HOSDB body armour standards for UK police (2007) part 2: Ballistic resistance Publication No. 39/07/B. Sandridge. St Albans: Home Office Scientific Development Branch; 2007.
3. Cannon L. Behind armour blunt trauma – an emerging problem. J R Army Med Corps. 2001;147(1):87–96.
4. Wilhelm M, Bir C. Injuries to law enforcement officers: the backface signature injury. Forensic Sci Int. 2008;174:6–11.
5. Shephard GH, Ferguson JL, Foster JH. Pulmonary contusion. Ann Thorac Surg. 1969;7:110–9.
6. Carroll AW, Soderstrom CA. A new nonpenetrating ballistic injury. Ann Surg. 1978;188(6):753–7.
7. Galbraith KA. Combat casualties in the first decade of the 21st century – new and emerging weapon systems. J R Army Med Corps. 2001;147:7–14.
8. McBride R. IACP/DuPont Kevlar Survivors' Club®. 2012.
9. Prat N, Rongieras F, Sarron J-C, Miras A, Voiglio E. Contemporary body armor: technical data, injuries, and limits. Eur J Trauma Emerg Surg. 2012. doi:10.1007/s00068-012-0175-0.
10. Firth N. British soldier had sniper's bullet pulled from his back by comrade after being shot by Taliban. Available at: http://www.dailymail.co.uk/news/article-1191872/Soldier-snipers-bullet-pulled-comrade-shot-Taliban.html. Accessed 19 Feb 12: Mail online; 2009.
11. Ministry of Defence. Body armour saves soldier's life in Afghanistan. Available online http://www.mod.uk/DefenceInternet/DefenceNews/MilitaryOperations/BodyArmourSavesSoldiersLifeInAfghanistan.htm. Accessed 19 Feb 12: Ministry of Defence; 2010.
12. Ministry of Defence. Body armour saves UK soldiers in Helmand fire fight. Available online http://www.mod.

uk/DefenceInternet/DefenceNews/MilitaryOperations/BodyArmourSavesUkSoldiersInHelmandFireFight.htm. Accessed 19 Feb 12: Ministry of Defence; 2011.
13. Weaver T. Soldier survives sniper's bullet after stopping to eat. Available online http://www.stripes.com/news/reporter-s-notebook-soldier-survives-sniper-s-bullet-after-stopping-to-eat-1.34885: Stars and Stripes; 2005.
14. Lewis EA, Watson CH, Horsfall I. Behind armour blunt trauma effects after low-velocity ballistic impact. In: Burman N, Anderson J, Katselis G, editors. 21st international symposium on ballistics. Adelaide: Defence Science and Technology Organisation with the cooperation of the International Ballistics Committee; 2004.
15. Lewis EA, Johnson P, Bleetman A, Bir CA, Horsfall I, Watson CH, et al. An investigation to confirm the existence of 'pencilling' as a non-penetrating behind armour injury. In: van Bree JLMJ, editor. Personal armour systems symposium 2004 (PASS2004); TNO Prins Maurits Laboratory. The Hague: TNO Prins Maurits Laboratory; 2004.
16. Soderstrom CA, Carroll AW, Hawkins CE. Technical report EB-TR-77057. The medical assessment of a new soft body armor, Chemical Systems Laboratory. Aberdeen Proving Ground: Department of the Army; 1978.
17. O'Connell KJ, Frazier HA, Clark MA, Christenson PJ, Keyes BT, Iosselson A. The shielding capacity of the standard military flak jacket against ballistic injury to the kidney. J Forensic Sci. 1988;33 (2):410–7.
18. Proud WG, Goldrein HT, Esmail S, Williamson DM. A review of wound ballistics literature: the human body and injury processes. In: Leixeira-Dias F, Dodd B, Torres Marques A, Lach L, Walley S, editors. Security and use of innovative technologies against terrorism LWAG light-weight armour for defence & security; 18–19 May 2009. Aveiro: Universidade de Aveiro; 2009.
19. van Bree JLMJ, van der Heiden N. Behind armour blunt trauma analysis of compression waves. In: Gotts PL, Kelly PM, editors. Personal armour systems symposium 1998 (PASS98). Colchester: Defence Clothing and Textiles Agency, Science and Technology Division, UK MoD; 1998.
20. Cannon L, Tam W. The development of a physical model of non-penetrating ballistic injury. In: Crewther IR, editor. 19th international symposium of ballistics, Interlaken, 7–11 May 2001.
21. Stuhmiller JH, Shen WS, Niu E. Modeling for military operational medicine scientific and technical objectives. San Diego: Jaycor; 2003.
22. Goldfarb MA, Ciure TF, Weinstein MA, Metker L-RW. Technical report EB-TR-74073. A method for soft body armor evaluation: medical assessment. Edgewood Arsenal. Aberdeen Proving Ground: Department of the Army; 1975.
23. Metker L-RW, Prather RN, Johnson EM. Technical report EB-TR-75029. A method for determining backface signatures soft body armor. Edgewood Arsenal. Aberdeen Proving Ground: Department of the Army; 1975.
24. Wilhelm MR. A biomechanical assessment of female body armor. Unpublished PhD thesis. Wayne State University; 2003.
25. Bir CA, Wilhelm M. Female body armor assessment: current methods and future techniques. In: van Bree JLMJ, editor. Personal armour systems symposium 2004 (PASS2004); TNO Prins Maurits Laboratory. The Hague: TNO Prins Maurits Laboratory; 2004.
26. Mabry RL, Holcomb JB, Baker AM, Cloonan CC, Uhorchak JM, Perkins DE, et al. United States Army Rangers in Somalia: an analysis of combat casualties on an urban battlefield. J Trauma Injury Infect Crit Care. 2000;49:515–29.
27. Mirzeabasov TA, Belov DO, Tyurin MV, Klyaus IA. Further investigation of modelling system for bullet-proof vests. In: Gotts PL, Kelly PM, editors. Personal armour systems symposium 2000 (PASS2000). Colchester: Defence Clothing and Textiles Agency, Science and Technology Division, UK MoD; 2000.
28. Dunstan S. Flak jackets 20th century military body armour. London: Osprey Publishing; 1984.
29. Thomas GE. Fatal.45-70 rifle wounding of a policeman wearing a bulletproof vest. J Forensic Sci. 1982;27(2):445–9.
30. U.S Department of Justice. Ballistic resistance of body armor NIJ standard-0101.06. Washington, DC: U.S. Department of Justice; 2008.
31. Montanarelli N, Hawkins CE, Goldfarb MA, Ciure TF. Technical report LWL-TR-30B73. Protective garments for public officials. US Army Land Warefare Laboratory. Aberdeen Proving Ground: Department of the Army; 1973.
32. Krauss M. Studies in wound ballistics: temporary cavity effects in soft tissues. Mil Med. 1957;121 (4):221–31.
33. Mendelson JA, Glover JL. Sphere and shell fragment wounds of soft tissues: experimental study. J Trauma. 1967;7(6):889–914.
34. Prather RN, Swann CL, Hawkins CE. Technical report EB-TR-77055. Backface signatures of soft body armors and the associated trauma effects. Chemical Systems Laboratory. Aberdeen Proving Ground: Department of the Army; 1977.
35. National Institute of Justice. Ballistic resistance of body armour NIJ Standard-0101.06. Washington, DC: U.S. Department of Justice, National Institute of Justice; 2008.
36. Hanlon E, Gillich P. Origin of the 44-mm behind-armour blunt trauma standard. Mil Med. 2012;177:333–9.
37. Wilson LB. Dispersion of bullet energy in relation to wound effects. Milit Surgeon. 1921;XLIX(3):241–51.

Blast Injury to the Spine

25

Edward J. Spurrier

25.1 Introduction

Although spinal injuries in warfare were first reported in the Egyptian era [14, 29], the devastating consequences, with long term pain and sensorimotor disability, have been reported in relatively few papers since then. Publications prior to the Gulf conflict of 2003 made little reference to spinal injuries, but more recently there has been greater interest, possibly related to different wounding mechanisms. It is clear from the recent literature that blast injury causes the bulk of spinal injuries in recent conflicts (Fig. 25.1) and that the patients affected are young (Table 25.1).

Understanding the patterns of injury in blast related spinal fracture is an essential first step in understanding the mechanism of injury. Once the mechanism is understood, mitigation is possible and steps can be taken to change vehicle and equipment design to reduce the risk of injury for future generations. Identifying the most significant injuries might also support targeted treatment to improve overall clinical outcomes for these victims.

E.J. Spurrier, BM, FRCS(Tr+Orth)
Department of Bioengineering, Royal British Legion Centre for Blast Injury Studies, Imperial College London, London, UK
e-mail: edward@edspurrier.co.uk

25.2 Distribution of Injury and Fracture Patterns

Unfortunately, early papers lack details of injury levels and fracture patterns. Barr et al. [1] described the solid blast injury mechanism in 1944, in which victims are injured when an explosion strikes their vehicle, accelerating it upwards and indirectly striking the victim. This is a form of tertiary blast (see Chap. 6, Sect. 6.2.3). In this study, blast victims on ships experienced a significant incidence of spinal fractures. Interest in spinal injury in military patients developed again with progression of the campaign in Afghanistan. Several studies report the general distribution of injuries in these patients, with some detail on spinal injuries.

Studies describing the patterns of injury encountered in warfare do not always detail the mechanism of injury or whether the victim was mounted (in a vehicle) or dismounted. This is critical, as the effect of blast on an exposed victim (primary blast) involves a very different mechanism to the effect of a blast that imparts its force through a vehicle (tertiary blast). Studies that specifically deal with mounted blast victims will be considered separately (see below).

25.3 Military Spinal Injuries

Most of the existing spinal injury literature is based on the JTTR and it's US equivalent.

A.M.J. Bull et al. (eds.), *Blast Injury Science and Engineering: A Guide for Clinicians and Researchers*,
DOI 10.1007/978-3-319-21867-0_25

Table 25.2 summarises the most detailed studies describing military spinal injury patterns.

It can be seen from both Table 25.2 and Fig. 25.2 that the majority of military spinal fractures are in the lumbar region. Figure 25.3 shows the number of fractures in the reviewed literature at each vertebral level in blast related spinal injuries; it is clear that the majority of fractures occur in the junctional regions of the spine.

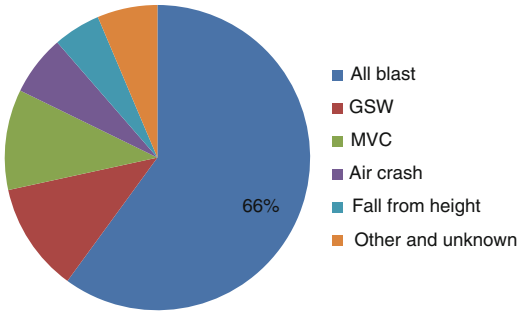

Fig. 25.1 Causes of combat spinal injury in recent literature [2, 3, 6–8, 24, 30–32]

25.4 Mounted Blast

Ragel et al. [26] focussed on survivors of improvised explosive device (IED) strikes on armoured vehicles, therefore describing a solid blast injury (see Chap. 6, Sect. 6.2.3) pattern in 12 patients with 17 thoracolumbar fractures. It was noted that these patients had a high incidence of lumbar flexion-distraction injuries compared to other published series; this injury pattern suggests that the line of force is anterior to the spine and that the spine is flexed at the moment of fracture. Ragel suggested several different mechanisms for these injuries when soldiers are exposed to underbody blast. These include flexion of the spine as a result of the legs being forced upwards by the deforming vehicle floor with the torso held rigid by a seat harness. An alternative mechanism suggested is flexion of the spine around the rigid base of the body armour and seat harness [21]. The frequency of lumbar burst fractures suggests that the lumbar spine is experiencing a significant axial load. These injury patterns and their mechanistic

Table 25.1 Demographics and cause of military spinal injury in recent literature

	Mean age	Male %	Female %	All blast %	Gunshot %	Vehicle collision %	Air crash %	Fall from height %	Other and unknown %
Bell et al. [2]	27	98	2	56	14	7	3		7
Belmont et al. [3]	25.8	98.5	1.5	75	20	3			3
Blair et al. [7]	26.4	98	2	56		27		6	11
Blair et al. [6]	26.5	98	2	56	15	25	5		
Comstock et al. [8]	29.3	99.5	0.5	72	7	9		5	7
Possley et al. [24]	26.5	98.4	1.6	53					
Schoenfeld et al. [30]	27.8	92	8	83	3	3	9		
Schoenfield et al. [32]	26.6	98	2	67	15		11		7
Schoenfield et al. [31]	26.6	99	1	75	14.8	7.8			
Mean from all papers, unweighted	**27**	**98**	**2**	**66**	**13**	**12**	**7**	**6**	**7**

Table 25.2 Overview of military spinal fracture distribution from all causes

Study	Cervical		Thoracic		Lumbar	
Bevevino et al. [4] Spinal injuries in combat amputees	5	(6 %)	15	(18 %)	62	(76 %)
Bilgic et al. [5] Case report of lumbar burst fracture due to anti-personnel mine					1	(100 %)
Blair et al. [6] US Casualties 2000–2009	319	(18 %)	591	(33 %)	857	(49 %)
Comstock et al. [8] Canadian casualties	6	(13 %)	15	(33 %)	25	(54 %)
Davis et al. [9] Injuries on the USS Cole	2	(17 %)	8	(73 %)	1	(8 %)
Eardley et al. [11] Review of British military spinal trauma	2	(5 %)	14	(32 %)	28	(64 %)
Lehman et al. [21] Review of the "Low lumbar burst fracture"					39	(100 %)
Possley et al. [24] Review of spinal injuries in IED strike	279	(17 %)	543	(34 %)	787	(49 %)
Schoenfeld et al. [32] Review of fatal injuries in US troops	704	35 %	731	36 %	579	29 %
Schoenfeld et al. [30] Review of injuries in a single US unit	4	(40 %)	2	(20 %)	4	(40 %)
Schoenfeld et al. [31] Review of US casualties 2005–9	231	(22 %)	300	(28 %)	522	(50 %)
Turegano-Fuentes et al. [33] Review of injuries in the Madrid train bombings	6	(29 %)	15	(71 %)		
Totals	**1558**	**(23 %)**	**2234**	**(33 %)**	**2905**	**(43 %)**

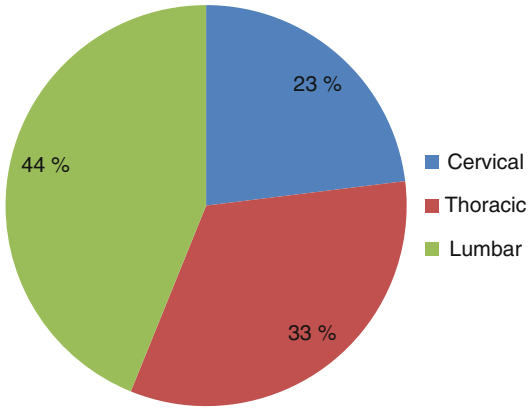

Fig. 25.2 Spinal fracture distribution in all patients

implications have an obvious impact on future seat and harness design (Table 25.3).

25.5 Patterns in Fatal Blast Injury

Most studies do not separate fatal from non-fatal injuries, or do so with insufficient detail to identify any mechanisms which might be associated with fatality. The most detailed studies are summarised in Table 25.4. In this table, it appears that cervical spine fractures may be more common in fatalities than survivors. It is not clear from the published literature whether these fatalities have associated fatal injuries, such as head and skull trauma, or whether the spinal fracture is the cause of death.

25.6 Outcomes and Surgical Management in Wartime Spinal Injury

The Edwin Smith Papyrus [14] records the futility in early medical history of treating spinal injuries associated with paralysis, advising physicians not to attempt to treat such injuries. Little is then published with regard to the outcomes of spinal injury until the recent conflict in Afghanistan except for one series in World War 2.

Fifty-six American soldiers with penetrating spinal wounds were reported at the end of World War 2 [28]. This series followed from explosive fragment or gunshot (secondary blast injuries). Treatment was with laminectomy when there was progressive neurological abnormality or evidence of metallic or bony fragments in the spinal canal on plain radiographs.. At the end of follow up (up to 40 months), 4 of the 19 patients who were paraplegic at the time of injury had made some recovery and 22 % of patients with neurological deficit overall made a complete recovery. However,

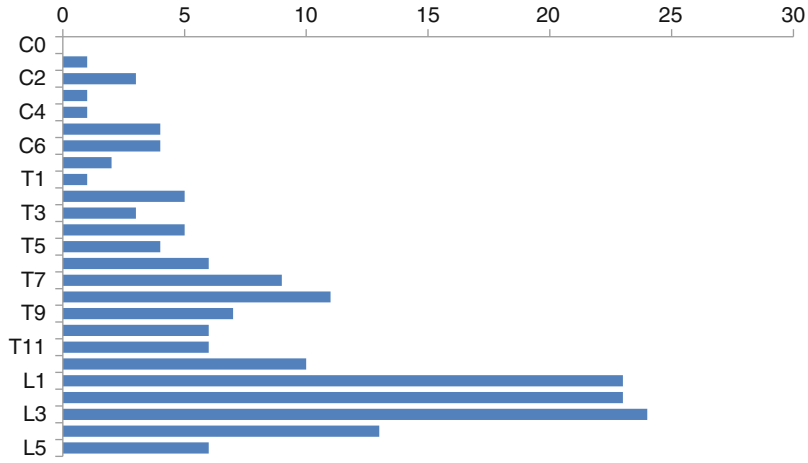

Fig. 25.3 Spinal injury distribution by vertebra, blast injuries, survivors and fatalities using data from the literature [4, 5, 11, 26, 30, 33]

Table 25.3 Published spinal fracture patterns in blast patients according to anatomical location and McAfee mechanistic classification of injury

	Odontoid peg	Facet fracture dislocation	Lamina	Transverse process	Compression	Burst	Flexion-distraction and Chance	All sacral
Bevevino et al. [4]		1		45	18	8		
Comstock et al. [8]			1	14	7			
Eardley et al. [11]					6	19	4	
Helgeson et al. [15]								24
Ragel et al. [26]					7	3	5	
Schoenfeld et al. [30]	1			5	3	1		
Total	**1**	**1**	**1**	**64**	**41**	**31**	**9**	**24**
%	**1 %**	**1 %**	**1 %**	**37 %**	**24 %**	**18 %**	**5 %**	**14 %**

Table 25.4 Spinal injury distribution in fatal casualties – all military mechanisms

	Cervical		Thoracic		Lumbar	
Davis et al. [9]	2	(17 %)	8	(73 %)	1	(8 %)
Schoenfeld et al. [30]	2	(100 %)				
Schoenfeld et al. [32]	1095	(41 %)	924	(35 %)	638	(24 %)
Total	**1099**	**(41 %)**	**932**	**(35 %)**	**639**	**(24 %)**

36 % of patients with a neurological deficit immediately following injury made no recovery.

Specific case reports of individual patient outcomes are rare. Kang et al. [16–19] reported several specific cases. One patient is described with an L5 burst fracture following exposure to blast from an IED associated with bilateral transfemoral amputations and normal neurological function in the residual limbs, but 50 % occlusion of the spinal canal. He was treated with L4 to S1

fusion and achieved a pain-free outcome despite needing steroid injection for radicular pain. In this case, surgery was advocated despite the lack of neurological compromise in order to facilitate rehabilitation.

Complications following treatment of military spinal injuries have been reported in a US series [25]. The overall complication rate following spinal trauma was 9 % with a high rate of multiple complications. Wound infections, venous thrombosis and cerebrospinal fluid leak were the most common complications and patients injured in dismounted mechanisms were at higher risk.

Although the clinical outcome of spinal fractures in blast victims is not known, it is reasonable to assume that fracture patterns which show a poor outcome in civilian injury are likely to also lead to poor outcomes in blast patients. Generally, burst fractures imply a greater risk of neurological complications and pain than compression fractures and flexion-distraction injuries [10, 12, 20]. Given that each of these fracture patterns implies a specific mechanism of injury, if the features of a vehicle, harness or seat design that lead to each mechanism and injury can be elucidated, it might be possible to control the patterns of injury seen in subsequent blast incidents. It might, perhaps, be possible to change devastating burst fractures into minor injuries by altering the seating design and posture.

25.7 Injury Patterns in UK Blast Victims

Injury patterns in UK blast victims have been reviewed by researchers at the Royal British Legion Centre for Blast Injury Studies. The JTTR was interrogated to identify victims of blast with spinal injury between 2008 and 2013 (Fig. 25.4). 134 victims were identified. The mean age was 26 (range 18–55).

Fatalities had a mean of 4.75 fractures each, compared with 2.21 fractures for each survivor ($p = 0.000$). The distribution of fractures in all victims is shown in Table 25.5.

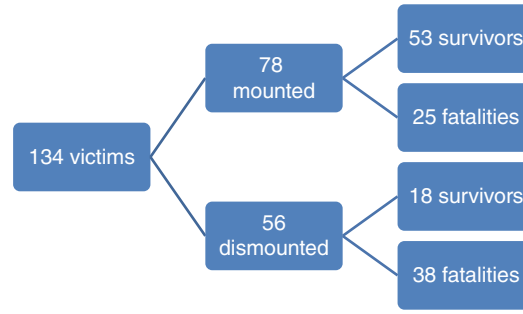

Fig. 25.4 Blast victims in UK data

Table 25.5 UK blast injury victims with spinal fractures in each zone

	Cervical	Thoracic	Lumbar
Survivors (n = 71)	13	33	46
Fatalities (n = 68)	26	30	46
Total			
Significance	***p = 0.004***	***p = 0.516***	***p = 0.263***

Significance by Fisher's Exact test

Of note, there was a significantly higher risk of mortality in the presence of a cervical spine fracture. Similar to the literature presented above, it is unclear at present whether this is because the spinal fractures are lethal, or whether these victims also suffered a fatal head injury.

As noted above, several authors have proposed mechanisms for the patterns of fracture in victims of underbody blast. It has been suggested that there is a combination of axial loading, leading to compression and burst pattern fractures, and flexion of the spine about the harness and body armour leading to wedge and flexion-distraction pattern injuries [13, 26]. The rigidity of the thoracic cage may also protect the thoracic vertebrae, leading to a higher risk of fractures at C7 where the mobile cervical spine meets the rigid thoracic spine, and at the origin of the mobile lumbar spine at L1. This has been observed in sports and motor vehicle crash injuries in the civilian literature [22].

In the series presented here, there is not a statistically significant difference between the risk of fracture at a given level between mounted and dismounted victims except at C1 and L1.

However, Fig. 25.5 shows that there is a trend towards more injuries at the thoracic apex and at the junctions between mobile and supported spine, as suggested in the literature.

The patterns of injury at each level are shown in Table 25.6. The pattern of fracture at each level is of interest as it allows a mechanistic hypothesis to be derived to explain the behaviour of the spine at each level as it failed.

In the cervical spine, most fractures appear to be of a compression pattern, although bilateral arch fractures of C2 and the cervical distraction-extension fractures and compression-extension fractures suggest that the neck was extended at the time of injury. Possible explanations for this include the head of a prone victim being blown upwards, or the head of a mounted victim striking the inside of a vehicle.

In the thoracic and lumbar spine, wedge pattern fractures suggest that the load is anterior to the vertebra and that the spine is flexed at the time of fracture. Burst fractures suggest a significant axial load along the line of the vertebral body, with a higher load leading to unstable burst rather than

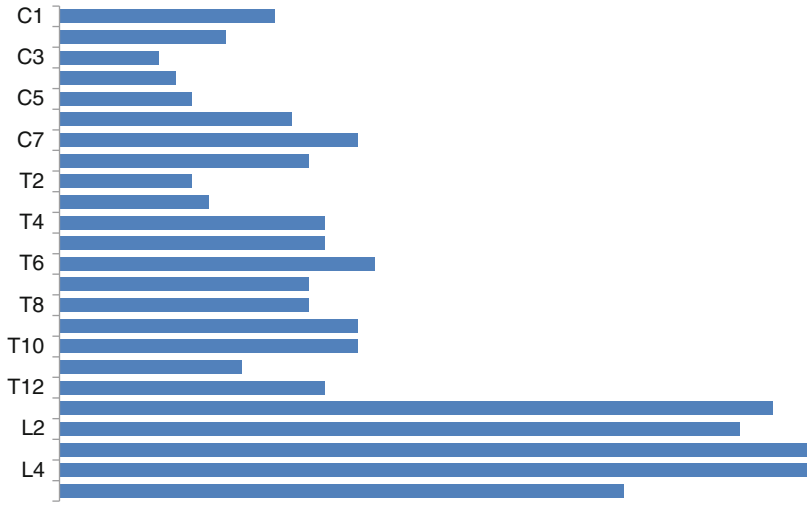

Fig. 25.5 Spinal injury distribution by vertebra in UK military blast victims (Iraq and Afghanistan 2008–2012)

Table 25.6 Most common spinal fracture patterns due to blast at each level

Pattern	Mounted	Dismounted	Significance
C1 Lateral mass	1	3	0.173
C1 Anterior	1	0	0.397
C1 Burst	2	6	0.05
C2 Asymmetric	4	0	0.087
C2 Bilateral arch	2	2	0.736
Cervical compression-flexion	3	4	0.406
Cervical vertical compression	3	3	0.778
Cervical distraction-flexion	3	0	0.139
Cervical compression-extension	4	4	0.682
Cervical distraction-extension	0	3	**0.039**
Cervical lateral flexion	3	0	0.397
Thoracic/lumbar wedge compression	35	7	**0.001**
Thoracic/lumbar stable burst	16	4	**0.047**
Thoracic/lumbar unstable burst	32	11	**0.018**
Thoracic/lumbar flexion-distraction	9	3	0.417
Thoracic/lumbar translation	7	3	0.585

Significance of difference by Mann Whitney *U* test

stable burst patterns. Flexion-distraction fractures occur when a flexion load anterior to the vertebra is combined with a tension load at the posterior side, suggesting a significant load in a flexed spine.

In these victims, the most common thoracic and lumbar pattern changes with location (Fig. 25.6). The preponderance of wedge fractures and the large number of burst fractures at L1 support the published data, which propose flexion about the harness and thoracolumbar junction [13, 26]. Lumbar burst fracture in the civilian literature tend to be high – around L1. In this series there are a significant number of burst fractures in the lower lumbar spine. This has been reported elsewhere in blast and could suggest that the body armour may be supporting the rib cage's role in reducing the flexibility of the thoracic spine [21].

These patterns suggest that the lumbar and thoracolumbar spine are flexed at the time of

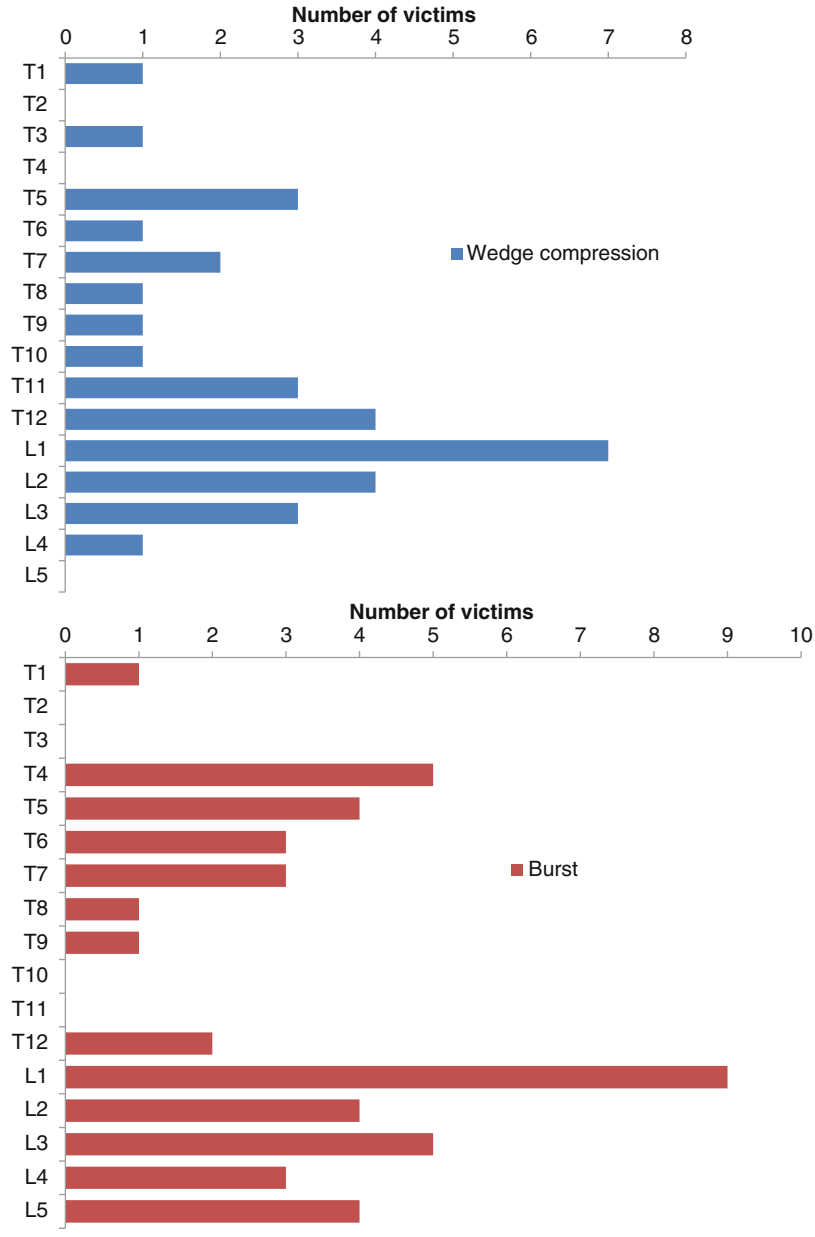

Fig. 25.6 Most common fracture patterns in the thoracic and lumbar spine in mounted UK blast victims

injury. There is a known high incidence of lower limb fractures in mounted blast victims (see Chap. 20, Sect. 20.1) [27]. It seems likely that as the limbs are pushed up by the deforming floor, shattering the feet, the lumbar spine flexes to cause the fracture patterns seen.

It might be possible to use these data to support vehicle design strategies in the future. At present, a standardised injury prediction model for the spine is used to modify vehicle designs, the Dynamic Response Index [23]. This system is extremely simple and might be improved with a new model based on a good mechanistic understanding of the behaviour of the spine under blast loads; which demands knowledge of the injury patterns seen in blast incidents. Similarly, it might be possible to use an understanding of the effect of posture and equipment design to modify the expected patterns of fracture when a vehicle is attacked, potentially turning a devastating burst injury into a less significant pattern of fracture.

25.8 Summary

There is evidence that the incidence of spinal injury in warfare has increased in recent conflicts. While spinal injuries remain less common than limb injuries, they have the potential to cause significant disability and therefore are worthy of attention. There are few publications relating to spinal war injury however until the recent interventions in Iraq and Afghanistan.

The solid blast injury mechanism, in which an explosive attack on a vehicle transmits significant indirect force to the occupants, has received attention in recent literature with regard to lower limb injury. However, case series suggest that there is a significant rate of spinal injury in these patients and the mechanisms and patterns of wounding have not been explored in detail. Published data often do not separate spinal fractures from other spinal column injury and do not always report neurological injury or outcomes. They often do not separate the mechanisms of injury in sufficient detail to enable analysis in depth.

The available data suggest that most spinal injuries in victims of blast are in the thoracolumbar and lower lumbar spine. There appears to be a significant incidence of unstable burst fractures. There may be a different pattern of wounding in dismounted and mounted incidents, but this is not clear. These patterns both appear to be different to that seen in the civilian population with more unstable and low lumbar burst fractures. Several possible mechanisms for this have been proposed but none has been proven. It seems likely that as the seat and legs are accelerated upwards, the pelvis and lumbar spine flex, then the spinal column compresses sequentially with some degree of flexion as it does so, leading to flexion-compression injuries.

Cervical spine fractures appear to be more common in blast fatality. However, many papers do not separate fatalities from survivors, and those that focus on fatalities do not necessarily separate blast from other mechanisms of wounding. It is unclear whether this trend is significant, given the paucity of detail in the published literature. If it is indeed true, then identifying the specific injury patterns might allow changes in vehicle and equipment design to reduce the incidence of such fatal injuries.

In UK victims of blast related spinal fracture, the patterns of injury broadly support the suggestions made in the recent literature. In mounted victims particularly, the apex of the thoracic spine and the thoracolumbar junction appear to be vulnerable, with the patterns of fracture suggesting a combination of axial load and flexion that fits with the proposed mechanism of injury including lumbar spine flexion as a result of the legs being pushed up by the deforming vehicle floor. This hypothesis allows mitigation strategies to be developed for future vehicle design.

References

1. Barr JS, Draeger RH, Sager WW. Solid blast personnel injury: a clinical study. Mil Surg. 1946;98(1):1–12.
2. Bell RS, et al. Military traumatic brain and spinal column injury: a 5-year study of the impact blast and other military grade weaponry on the central nervous system. J Trauma. 2009;66(4 Suppl):S104–11.
3. Belmont Jr PJ, et al. The nature and incidence of musculoskeletal combat wounds in Iraq and Afghanistan (2005–2009). J Orthop Trauma. 2013;27(5):e107–13.

4. Bevevino AJ, et al. Incidence and morbidity of concomitant spine fractures in combat-related amputees. Spine J. 2014;14:646–50.
5. Bilgic S, et al. Burst fracture of the lumbar vertebra due to a landmine injury: a case report. Cases J. 2009;2:6257.
6. Blair JA, et al. Spinal column injuries among Americans in the global war on terrorism. J Bone Joint Surg Am. 2012;94(18):e135(1–9).
7. Blair JA, et al. Military penetrating spine injuries compared with blunt. Spine J. 2012;12(9):762–8.
8. Comstock S, et al. Spinal injuries after improvised explosive device incidents: implications for Tactical Combat Casualty Care. J Trauma. 2011;71(5 Suppl 1):S413–7.
9. Davis TP, et al. Distribution and care of shipboard blast injuries (USS Cole DDG-67). J Trauma. 2003;55 (6):1022–7; discussion 1027–8.
10. Defino HL, Canto FR. Low thoracic and lumbar burst fractures: radiographic and functional outcomes. Eur Spine J. 2007;16(11):1934–43.
11. Eardley W, et al. Spinal fractures in current military deployments. J R Army Med Corps. 2012;158(2):101–5.
12. Folman Y, Gepstein R. Late outcome of nonoperative management of thoracolumbar vertebral wedge fractures. J Orthop Trauma. 2003;17(3):190–2.
13. Freedman B, et al. The combat burst fracture study—results of a cohort analysis of the most prevalent combat specific mechanism of major thoracolumbar spinal injury. Arch Orthop Trauma Surg. 2014;134 (10):1353–9.
14. Goodrich JT. History of spine surgery in the ancient and medieval worlds. Neurosurg Focus. 2004;16:1–13.
15. Helgeson MD, et al. Retrospective review of lumbosacral dissociations in blast injuries. Spine (Phila Pa 1976). 2011;36(7):E469–75.
16. Kang DG, Cody JP, Lehman Jr RA. Open lumbosacral spine fractures with thecal sac ligation after combat blast trauma. Spine J. 2012;12(9):867–8.
17. Kang DG, Cody JP, Lehman Jr RA. Combat-related lumbopelvic dissociation treated with L4 to ilium posterior fusion. Spine J. 2012;12(9):860–1.
18. Kang DG, Dworak TC, Lehman Jr RA. Combat-related L5 burst fracture treated with L4-S1 posterior spinal fusion. Spine J. 2012;12(9):862–3.
19. Kang DG, et al. Large caliber ballistic fragment within the spinal canal. Spine J. 2012;12(9):869–70.
20. Kraemer WJ, et al. Functional outcome of thoracolumbar burst fractures without neurological deficit. J Orthop Trauma. 1996;10(8):541–4.
21. Lehman Jr RA, et al. Low lumbar burst fractures: a unique fracture mechanism sustained in our current overseas conflicts. Spine J. 2012;12(9):784–90.
22. Leucht P, et al. Epidemiology of traumatic spine fractures. Injury. 2009;40(2):166–72.
23. NATO. Test methodology for protection of vehicle occupants against anti-vehicular landmine and/or IED effects, in Nato RTO technical report. 2012; Human Factors and Medicine Group.
24. Possley DR, et al. The effect of vehicle protection on spine injuries in military conflict. Spine J. 2012;12 (9):843–8.
25. Possley DR, et al. Complications associated with military spine injuries. Spine J. 2012;12(9):756–61.
26. Ragel BT, et al. Fractures of the thoracolumbar spine sustained by soldiers in vehicles attacked by improvised explosive devices. Spine (Phila Pa 1976). 2009;34(22):2400–5.
27. Ramasamy A, et al. The modern deck-slap injuries: 3-year outcomes of calcaneal blast fractures. J Bone Joint Surg Br Vol. 2012;94-B(SUPP XXXII):27.
28. Schneider RC, Webster JE, Lofstrom JE. A follow-up report of spinal cord injuries in a group of World War II patients. J Neurosurg. 1949;6(2):118–26.
29. Schoenfeld AJ, Belmont Jr PJ, Weiner BK. A history of military spine surgery. Spine J. 2012;12(9):729–36.
30. Schoenfeld AJ, Goodman GP, Belmont Jr PJ. Characterization of combat-related spinal injuries sustained by a US Army Brigade Combat Team during Operation Iraqi Freedom. Spine J. 2012;12(9):771–6.
31. Schoenfeld AJ, et al. Spinal injuries in United States military personnel deployed to Iraq and Afghanistan. Spine. 2013;38(20):1770–1778.
32. Schoenfeld AJ, et al. Characterization of spinal injuries sustained by American service members killed in Iraq and Afghanistan: a study of 2,089 instances of spine trauma. J Trauma Acute Care Surg. 2013;74(4):1112–8.
33. Turegano-Fuentes F, et al. Injury patterns from major urban terrorist bombings in trains: the Madrid experience. World J Surg. 2008;32(6):1168–75.

Primary Blast Lung Injury

26

Robert A.H. Scott

26.1 Introduction

To facilitate effective gas exchange and act as a blood-gas interface, the adult human lung consists of some 500 million air sacs (alveoli), each only 1/3 mm in diameter but generating a combined surface area of approximately 100 m^2. The alveolar wall measures 0.2–0.3 μm across and is encased in a mesh of very fine and fragile blood vessels, the diameter of which is just sufficient to allow the passage of red blood cells [1]. Whilst elegantly adapted to facilitate rapid diffusion of gas across tissue, the very nature of the lungs' role in gas exchange renders them particularly susceptible to injury following blast exposure. Such injury, due only to exposure to blast wave (primary blast) and not to other consequences of proximity to an explosion (for example penetrating – secondary blast – or burn injuries – quaternary blast) is known as primary blast lung injury (PBLI). As a diagnosis of exclusion, it occurs within 12 hours of blast exposure in the absence of secondary or tertiary lung injury and in the presence of radiological or arterial blood gas evidence of acute lung injury [2].

R.A.H. Scott, FRCS (Ed), FRCOphth, DM, (RAF)
Birmingham and Midland Eye Centre, Dudley Road, Birmingham, UK
e-mail: robertscott3@nhs.net

26.2 Epidemiology

Primary blast lung injury (PBLI) is encountered globally resulting from military conflict, acts of terrorism and industrial accidents. During the most recent Afghan conflict, PBLI was identified in 6–11 % military casualties surviving to reach a field hospital [3, 4]. This figure can rise to almost 80 % in non-survivors [5] in whom it is the only autopsy finding in 17 % [6]. The incidence and severity of PBLI increases significantly with increasing proximity to the explosion and when injuries are sustained within an enclosed space such as a bus or train. In such circumstances in excess of 80 % of survivors may suffer PBLI [7] (see Chap. 7).

26.3 Pathophysiology

The blast wave dissipates its kinetic energy within the lung through the generation of shear and stress waves [8]. Transverse, low velocity shear waves result from deformation of the thoracic wall. They are responsible for the surface haemorrhage seen on lung tissue facing the explosion (Fig. 26.1) and causes random movement of tissues of differing densities around fixed points, resulting in tearing of parenchymal tissue. Supersonic longitudinal stress waves generate more diffuse damage. The speed of transmission through the lung does not allow energised gas to pass along airways and thus

A.M.J. Bull et al. (eds.), *Blast Injury Science and Engineering: A Guide for Clinicians and Researchers*,
DOI 10.1007/978-3-319-21867-0_26

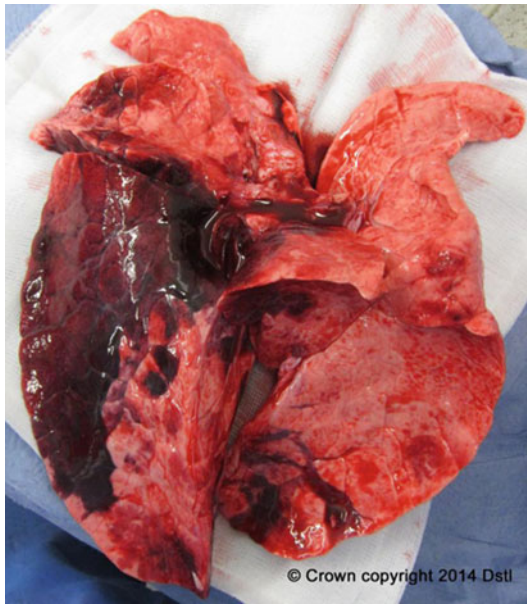

Fig. 26.1 Mammalian lung exposed to a sub-lethal blast overpressure. Extensive parenchymal haemorrhage can be seen on the left hand surface which was facing the explosion (Courtesy of Dr Emrys Kirkman, Defence Science and Technology Laboratories, UK)

"foaming" occurs. As the lung adopts the physical properties of foam, with its much poorer transmission of sound energy, greater kinetic energy is absorbed [9]. Rapid compression and expansion of alveoli leads to alveolar rupture and hence to the hallmark of the disease which is the formation of abnormal air-filled spaces such as pnuematoceles, pneumothoraces and venous air embolism. The stress waves reflect back upon itself as it reaches the denser mediastinum. This causes a "stress concentration" effect in lung tissue around the mediastinum leading to characteristic findings on imaging, discussed later. Microscopically, severe alveolar over-distension is ubiquitous. Concomitantly, alveolar capillaries rupture and, with the formation of alveolovenous fistula, result in localised haemorrhage. This can be significant and cause immediate respiratory compromise. This extravasated blood precipitates a free radical mediated inflammatory process involving leucocyte accumulation and oxidative damage resulting in perivascular oedema. This inflammatory process continues to evolve over the subsequent 24–56 hours. Pulmonary fat embolism contributes significantly to respiratory compromise and to an early risk of death, as does bone marrow embolism in casualties suffering long bone and/or pelvic injury [10]. The extent of this inflammatory process will in part depend on the over-all burden of whole body tissue injury driving a systemic inflammatory response.

Physiologically, the vagal nerve mediates a reflex apnoea, bradycardia and hypotensive episode [11] mediated by stretch of peri-alveolar C-fibres. This lasts up to 15 seconds and is followed by a period of rapid shallow breathing [12]. This mechanism may play a significant role in non-survivors [13].

26.4 Diagnosis

Casualties will most likely be symptomatic by the time they reach a medical facility. They will present with shortness of breath, respiratory distress and haemoptysis. Tachycardia, tachypnoea and cyanosis will reflect the severity of the insult. Severe cases will develop acute respiratory distress syndrome (ARDS) described below.

The classic chest radiograph (CXR) appearance is of bilateral perihilar ("batswing") infiltrates generated as the pressure wave reflects back from the mediastinum (Fig. 26.2). The incidence of this varies considerably between series and may reflect a casualty's proximity to an explosion. Cross sectional imaging also demonstrates increased opacification around the mediastinum, will reveal parenchymal haemorrhage and is more likely to reveal the pneumatoceles and pneumothoraces that are characteristic of the disease (Figs. 26.2 and 26.3).

Alternative diagnosis at this stage include, pulmonary contusion (rib fractures and peripheral lung injury), tension pneumothorax, ARDS due to other causes (inhalation of toxic substances, gastric aspiration) and use of chemical weapons.

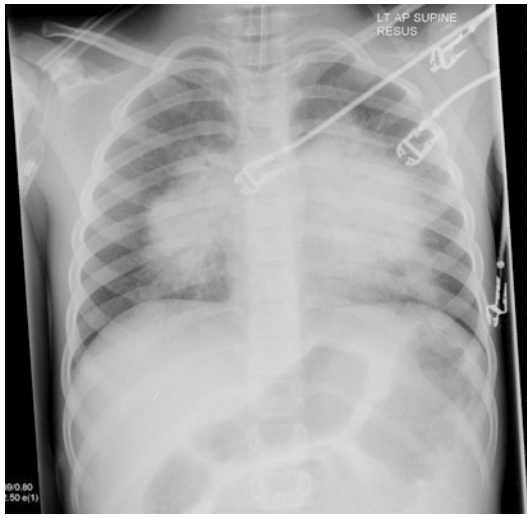

Fig. 26.2 Presenting CXR of an adolescent male exposed to an explosion in an enclosed space. The characteristic "Batswing" distribution of lung injury is seen. The patient made a complete recovery (Courtesy of Lt Col Iain Gibb RAMC, Portsmouth, UK)

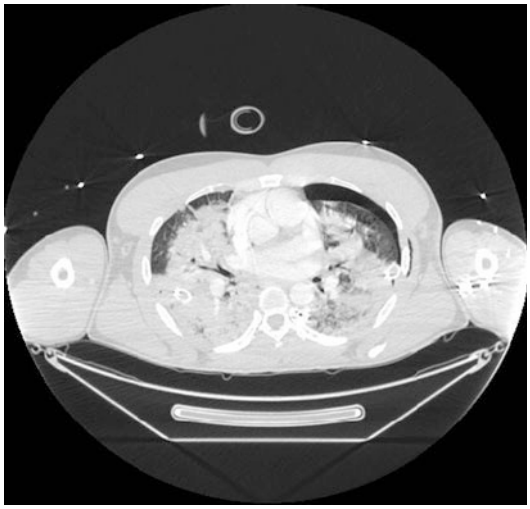

Fig. 26.3 Computed tomography image of a soldier exposed to a significant explosion. The patient required immediate intubation and ventilation requiring a fractional inspired concentration of oxygen of 90 %. Shortly after intubation the patient was referred for ECMO though this was not subsequently required. The patient made a good recovery. Significant consolidation around the mediastinum and a left sided pneumothorax is seen (Courtesy of Lt Col Andy Johnson RAMC, Birmingham, UK)

26.5 Acute Respiratory Distress Syndrome (ARDS)

First described in 1967 and re-defined in 2012 [14], ARDS is the development of non-cardiogenic pulmonary oedema within 7 days of a precipitating insult and demonstrating bilateral opacities on chest imaging. Fluid overload (i.e. renal failure) and heart failure may have to be excluded. This life-threatening syndrome characterised by hypoxia of rapid onset, can result from either direct or indirect injury to the lung (Table 26.1). It is classified as either, mild, moderate or severe depending on the inspired concentration of oxygen to arterial blood oxygen tension ratio (Table 26.2). Affected lungs demonstrate markedly reduced compliance ("stiff lungs") resulting from alveolar flooding with neutrophil rich proteinaceous material and deposition of a hyaline membrane. Histologically, the evolution of the condition is classically described as occurring in three phases, the exudative, proliferative and fibrotic phases. The first exudative and inflammatory phase consists of widespread neutrophil infiltration and alveolar flooding with haemorrhagic oedema. This cumulates in the deposition of a fibrous hyaline

Table 26.1 Causes of ARDS

Direct causes	Indirect causes
Pneumonia	Sepsis
Aspiration	Pancreatitis
Fat emboli	Poly-trauma
Toxic inhalation	Massive blood transfusion
Pulmonary contusion	Cardiopulmonary bypass

Table 26.2 Classification of the severity of ARDS

Oxygenation	PaO_2/FIO_2[a] (mmHg)
Mild	200–300
Moderate	100–200
Severe	<100

PaO_2, partial pressure of arterial oxygen, FIO_2, fraction of inspired concentration of oxygen

[a]In the presence of a positive end expiratory pressure (PEEP) of 5 cmH_2O or greater

membrane. During the proliferative phase, fibrinous exudates become organised with the formation of collagen fibrils as a result of increased fibroblastic activity with concomitant necrosis of the lung's epithelial lining. The final fibrotic phase is characterised by further collagen deposition and intimal thickening of blood vessels.

26.6 Management

Casualties with PBLI require supportive care in a high dependency or intensive care environment. Some 80 % will require mechanical ventilation. Any pneumothoraces should ideally be drained prior to transfer to a CT scanner, though the increasing speed and improving access to cross sectional imaging makes this less vital in patients with relative respiratory stability but who may have other life threatening injuries. It must be borne in mind that large pneumothoraces can be missed on supine CXR's. Ventilatory strategy should adhere to the low-volume "open lung" approach advocated for patients suffering from acute respiratory distress syndrome (Table 26.3) [15]. The fundamental component of this strategy is the recognition that mechanical ventilation can significantly augment pre-existing lung injury due to a combination of barotrauma and volutrauma due to the repeated opening, stretching and collapse of aveoli during the mechanical ventilatory cycle. This is achieved through use of a pressure limited mode of ventilation and "splinting" the lungs open with higher than normal levels of positive end-expiratory pressure (PEEP). The lungs are ventilated at the lower than normal 6–8 ml/kg lean body weight and the inspiratory component of the respiratory cycle is extended as far as an inspiratory to expiratory ratio of 1:1 or greater. This is a compromise ventilator strategy with the clinician accepting relative but not life threatening hypoxia and hypercarbia whilst awaiting resolution of the pulmonary insult.

Alternative forms of ventilation such as High frequency oscillatory ventilation (HFOV) and airway pressure release ventilation (APRV) have been used with success but is dependent on local expertise and availability [16]. All of these ventilator strategies require tolerating hypercapnia within the limits of an acceptable arterial pH. In pyrexial patients, physical cooling or the use of anti-pyretics may ameliorate hypercarbia whilst a bicarbonate infusion can attenuate cardiovascular instability.

Prone positioning of ventilated patients with ARDS can improve oxygenation by reducing ventilation perfusion mismatch. In the prone position, the ventral and normally better-ventilated area of lung now also receives greater proportion of pulmonary perfusion as gravity dictates that dependant tissue is better perfused. When considered, prone positioning should be instigated early and for at least 16 hours a day [17]. Early neuromuscular blockade with Cisatricurium should also be considered [18].

A euvolaemic to hypovolaemic approach to fluid management can attenuate pulmonary

Table 26.3 Recommended ventilatory strategy for severe blast lung/ARDS

Ventilatory settings	Tidal volume of 6–8 ml/kg lean body weight[a]
	Pplat limited to 30 cmH_2O
	PEEP guided by FIO_2 ranging from 5 to 24 cmH_2O
Arterial blood gases	Apply lowest FIO_2 to achieve oxygen saturations of 88–94 %
	Tolerate hypercapnia within limits of cardiovascular stability[b]. As pH drops treat pyrexia and/or consider bicarbonate infusion
Prone positioning	When possible consider early proning
Ventilatory escalation	Consider APRV or HFOV
Treatment failure	Refer to specialist centre for extracorporeal gas exchange

Pplat peak plateau pressure, *APRV* airway pressure release ventilation, *HFOV* high frequency oscillatory ventilation
[a]Predicted body weight for males 50 + 0.91 (height in cm – 152.4) and for females 45.5 + 0.91 (height in cm – 152.4)
[b]Not in head injury

oedema in appropriate patients and reduce mortality [19].

Patients deteriorating despite appropriate ventilator support and management should be referred to a specialist respiratory centre to facilitate extracorporeal membrane oxygenation (ECMO) or extracorporeal carbon dioxide removal. ECMO has proven benefits in ARDS [20] whilst carbon dioxide removal can facilitate ventilation with much lower tidal volumes and thus limit further pulmonary injury due to mechanical ventilation.

Patients who are breathing spontaneously at 2 hours post injury are unlikely to deteriorate further and develop a need for mechanical ventilation due to PBLI alone [21]. Patients who are asymptomatic at 6 hours post exposure can be discharged from close medical observation. Tympanic membrane rupture is poorly correlated with PBLI with a sensitivity of 29 % [22].

In the longer term, patients suffering isolated blast lung injury can expect to make an excellent recovery demonstrated by lack of symptoms, normal exercise tolerance and normal lung function tests [23].

26.7 Future Therapy

Future therapy is likely to involve either pharmacological or genetic manipulation of the inflammatory or immune response to blast injury. The antioxidant N-acetylcysteine has shown early promise by modulating neutrophil mediated pulmonary inflammation in rodent models of blast injury [24]. Systemic administration of multipotent mesenchymal stem cells (MSC) results in significant immunomodulatory activity, which again has shown significant success in reversing lung injury in animal models [25].

References

1. West JB. Respiratory physiology the essentials. 8th ed. Philadelphia: Lippincott Williams & Wilkins; 2003.
2. Mackenzie I, Tunnicliffe B, Clasper J, Mahoney P, Kirkman E. What the intensive care doctor needs to know about blast-related lung injury. J Intensive Care Soc. 2013;14(4):303–12.
3. Smith JE. The epidemiology of blast lung injury during recent military conflicts: a retrospective database review of cases presenting to deployed military hospitals, 2003–2009. Philos Trans R Soc Lond B Biol Sci. 2011;366(1562):291–4.
4. Aboudara M, et al. Primary blast lung injury at a NATO Role 3 hospital. J R Army Med Corps. 2014;160(2):161–6.
5. Singleton JA, et al. Primary blast lung injury prevalence and fatal injuries from explosions: insights from postmortem computed tomographic analysis of 121 improvised explosive device fatalities. J Trauma Acute Care Surg. 2013;75(2 Suppl 2): S269–74.
6. Mellor SG, Cooper GJ. Analysis of 828 servicemen killed or injured by explosion in Northern Ireland 1970–84: the Hostile Action Casualty System. Br J Surg. 1989;76:1006–10.
7. Pizov R, et al. Blast lung injury from an explosion on a civilian bus. Chest. 1999;115(1):165–72.
8. Cooper GJ, Taylor DE. Biophysics of impact injury to the chest and abdomen. J R Army Med Corps. 1989;135:58–67.
9. Rice DA. Sound speed in pulmonary parenchyma. J Appl Physiol. 1983;54:304–8.
10. Tsokos M, et al. Histologic, immunohistochemical, and ultrastructural findings in human blast lung injury. Am J Respir Crit Care Med. 2003;168(5):549–55.
11. Guy RJ, Kirkman PE, Watkins E, Cooper CJ. Physiologic responses to primary blast. J Trauma. 1998;45:983–7.
12. Kirkman E, Watts S. Characterization of the response to primary blast injury. Philos Trans R Soc. 2011;366:286–90.
13. Horrocks CL. Blast injuries: biophysics, pathophysiology and management principles. J R Army Med Corps. 2001;147:28–40.
14. ARDS Definition Task Force, Ranieri VM, Rubenfeld GD, et al. Acute respiratory distress syndrome: the Berlin definition. JAMA. 2012;307:2526–33.
15. The Acute Respiratory Distress Syndrome Network. Ventilation with lower tidal volumes as compared with traditional tidal volumes for acute lung injury and the acute respiratory distress syndrome. N Engl J Med. 2000;342:1301–8.
16. Mackenzie IM, Tunnicliffe B. Blast injuries to the lung: epidemiology and management. Philos Trans R Soc Lond B Biol Sci. 2011;366(1562):295–9.
17. Guerin C, Reignier J, Richard JC, Beuret P, Gacouin A, Boulain T, et al. Prone positioning in severe acute respiratory distress syndrome. N Engl J Med. 2013;368:2159–68.
18. Papazian L, Forel JM, Gacouin A, et al. Neuromuscular blockers in early acute respiratory distress syndrome. N Engl J Med. 2010;363:1107–16.
19. Fanelli V, Vlachou A, Ghannadian S, Simonetti U, Slutsky AS, Zhang H. Acute respiratory distress syndrome: new definition, current and future therapeutic options. J Thorac Dis. 2013;5(3):326–34.

20. Peek GJ, Mugford M, Tiruvoipati R, et al. Efficacy and economic assessment of conventional ventilatory support versus extracorporeal membrane oxygenation for severe adult respiratory failure (CESAR): a multicentre randomised controlled trial. Lancet. 2009;374(9698):1351–63.
21. Avidan V, et al. Blast lung injury: clinical manifestations, treatment, and outcome. Am J Surg. 2005;190(6):927–31.
22. Leibovici D, Gofrit ON, Shapira SC. Eardrum perforation in explosion survivors: is it a marker of pulmonary blast injury? Ann Emerg Med. 1991;34:168–72.
23. Hirshberg B, Oppenheim-Eden A, Pizov R, Sklair-Levi M, Rivkin A, Bardach E, et al. Recovery from blast lung injury. Chest. 1999;116:1683–8.
24. Chavko M, Adeeb S, Ahlers ST, McCarron RM. Attenuation of pulmonary inflammation after exposure to blast overpressure by N-acetylcysteine amide. Shock. 2009;32(3):325–31.
25. Mei SH, Haitsma JJ, Dos Santos CC, et al. Mesenchymal stem cells reduce inflammation while enhancing bacterial clearance and improving survival in sepsis. Am J Respir Crit Care Med. 2010;182:1047–57.

Regional Effects of Explosive Devices: The Neck

27

John Breeze

27.1 The Issue

Neck injury due to secondary blast (explosively propelled fragments) experienced by UK service personnel deployed on current operations has been responsible for significant mortality and long-term morbidity [1, 2]. These injuries reflected that the neck has little inherent anatomical protection to penetrating energised fragments (Fig. 27.1), compounded by the fact that ballistic neck collars to protect against such injuries were rarely worn. The development of a more acceptable neck collar necessitated the manufacture of multiple designs of prototypes, each of which required ergonomics assessments to determine its acceptability for performing representative military tasks. However such trials are costly both financially and in terms of time. The ability to rule out a particular design of personal protective equipment on medical grounds prior to ergonomics assessment would reduce the number of prototypes that have to be tested, with resultant time and financial savings [1]. An ideal model for simulating all aspects of penetrating neck injury should be able to simulate a complex range of interacting variables (Table 27.1). However, such a model does not yet exist and answers are therefore based upon combining answers provided by a variety of individual models.

27.2 Armour and Projectile Design

The ability to compare multiple designs of armour and projectiles without the expense and time constraints of making prototypes for physical all testing is desired [3]. Numerical solutions enable prototypes to be laser scanned into CAD files, which can subsequently be manipulated to reflect different design features (Fig. 27.2).

27.3 Vulnerable Anatomical Structures Representation

Analysis of the injuries sustained in survivors and those who died can provide an accurate knowledge of which anatomical structures require coverage. In the future this may become role specific to provide measures of predicted incapacitation. Numerical injury models utilised by the UK prior to 2012 represented the neck as a homogenous unit with the head and face, despite their fundamental anatomical differences [1, 4].

J. Breeze, PhD, MRCS, MFDS, MBBS, BDS
Academic Department of Military Surgery and Trauma, Royal Centre for Defence Medicine, Birmingham Research Park, Birmingham B15 2SQ, UK
e-mail: johno.breeze@me.com

A.M.J. Bull et al. (eds.), *Blast Injury Science and Engineering: A Guide for Clinicians and Researchers*,
DOI 10.1007/978-3-319-21867-0_27

27.4 Projectile Armour Interaction

A method based on the perforation of body armour material alone potentially represents the most simplistic injury model. For example the testing of ceramic body armour plates is still based upon the concept that if a 1.10 g Fragment Simulating Projectile (FSP) perforates the plate at a certain velocity, the test is a fail irrespective of the interaction between the projectile and any tissue beneath it. It has recently been suggested that the test could be modified to include a block of gelatine beneath it and the distance from skin surface to the closest anatomical structure causing death or morbidity included (Fig. 27.3). Analysis of CT scans of UK soldiers has demonstrated that the minimum mean distance from skin to carotid artery as it travels up the neck is 21 mm (±3.5 mm).

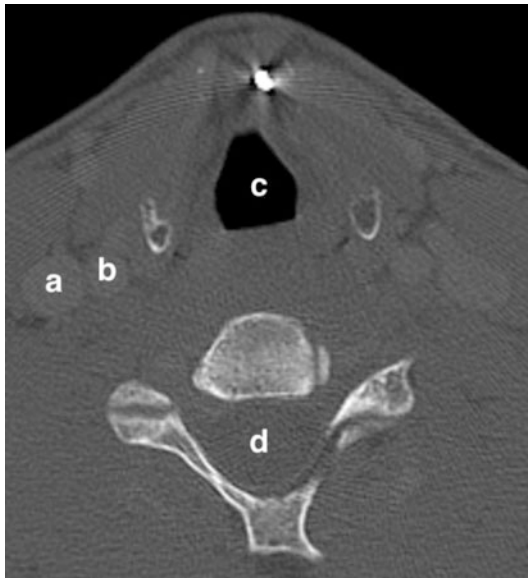

Fig. 27.1 An axial Computed Tomography scan of the neck with energised fragment lodged in neck demonstrating structures with little inherent anatomical protection: *a* jugular vein, *b* carotid artery, *c* trachea, *d* spinal cord

27.5 Physical Models for Neck Injury

Ballistic gelatine, in either a 10 or 20 % concentration, enables the incorporation of projectile factors and is known to be highly representative of homogenous animal muscle (see Chap. 11, Sect. 11.6) [6, 7]. It can accurately represent depth of penetration as well as the magnitude of the temporary cavity. However, it cannot represent the complexities of human anatomical relationships, and its inherent material properties cause a permanent cavity smaller than that seen in animal models [5].

Table 27.1 Interacting variables necessary to generate an injury prediction to enable accurate comparisons between neck protection prototypes

Variable	Description	Potential solutions
Amour and projectile design	Shape, design features, size and thickness	Materials testing ± tissue simulant Finite element model
Projectile armour interaction	Armour and projectile material properties including mass and projectile shape	Materials testing ± tissue simulant Finite element model
Vulnerable anatomical structures representation	Three dimensional representation of structures in correct anatomical relationships to one another	Post mortem human subjects Numerical models based upon geometric anatomical meshes
Projectile tissue interaction	Interaction of the predicted permanent wound tract with individual anatomical structures and additional damage from the temporary cavity	Tissue simulants to derive values for algorithms to underpin a finite element model
Objective injury calculation	Simple scoring system able to predict death, incapacitation and long term morbidity	Outcome based surface wound mapping Analytical boundary models Finite element models

Fig. 27.2 Meshed images of a chisel-nosed cylindrical fragment simulating projectile and the Mark IVa OSPREY half neck collar (http://www.army.mod.uk/documents/general/20120215-Osprey_Mk4_Instruction_Booklet-R.pdf)

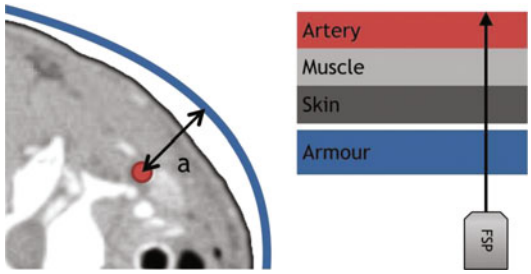

Fig. 27.3 Critical distance to damage (*label a*) for fragment simulating projectile (*FSP*) perforating the ballistic protective material demonstrated on an axial Computed Tomography slice

27.6 Animal Models for Neck Injury

No animal can reproduce the complex cervical anatomy of a human being, and testing generally involves measuring depth of penetration in small groups of tissue types such as skin and muscle alone [6, 7]. Animal testing is also beset with significant difficulties, including expense, a lack of reproducibility (so called 'biological variation') and understandable ethical considerations (see Chap. 8, Sect. 8.3) (Fig. 27.4).

27.7 Use of Post Mortem Human Subjects in Neck Injury

The use of fresh, frozen and refrigerated Post Mortem Human Subjects (PMHS) for ballistic research [8] is currently being undertaken to potentially validate conclusions made from any future neck model, as their anatomy is clearly representative, unlike that of animals (Fig. 27.5). However, little objective evidence exists as to the effect of decomposition, refrigeration and freezing on tissue material properties [9], especially to ballistic impacts, such that this method cannot be used alone.

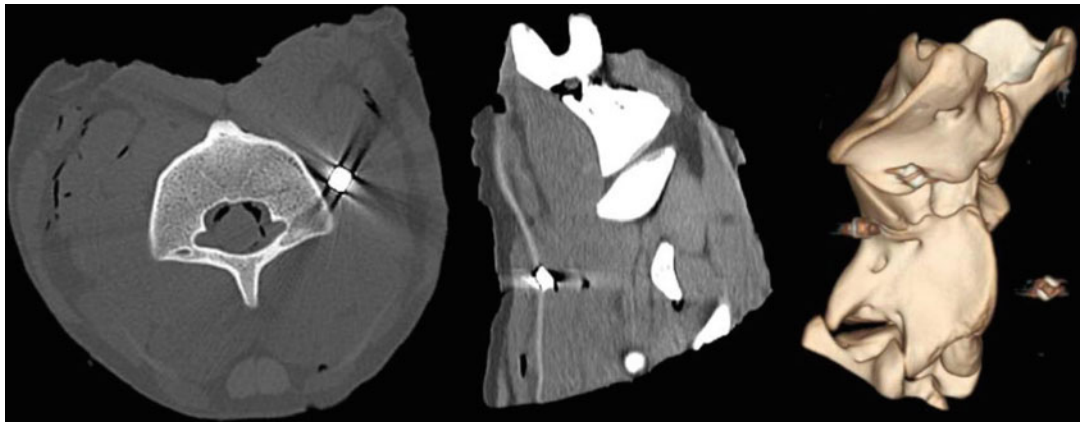

Fig. 27.4 Computed Tomography scans taken after testing of cylindrical FSPs into a goat neck demonstrates anatomy unrepresentative of a human

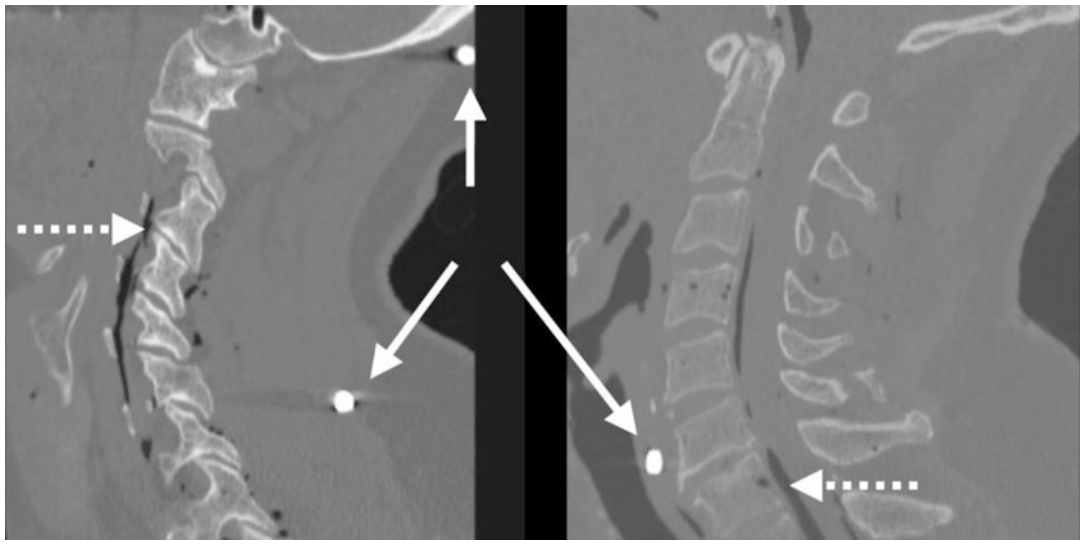

Fig. 27.5 Computed Tomography scans taken after early testing of cylindrical FSPs (*solid arrows*) into the neck of a post mortem human subject demonstrating normal human anatomical relationships. However note inclusion of air (*dashed arrows*) due to post mortem changes that could mistakenly be assumed to be due to the passage of the projectile

27.8 Numerical Models for Neck Injury

The current approach to numerical modelling of penetrating neck injury used in the UK can be thought of as consisting of a number of complimentary models reflecting a spectrum of complexity. The most simplistic is an Analytical Boundary Model (currently the Coverage of Armour Tool, COAT) (see Chap. 28, Sect. 28.7) to the most complex in a Finite Element (FE) model (currently the High Fidelity Neck Model). Each model utilises the same underlying platform, a commercially procured three-dimensional mesh of the surfaces of cervical anatomical structures, accurate to a fidelity of 0.25 mm (Fig. 27.6). This platform is also utilised in computerised surface wound mapping, which although not strictly an injury model, can produce limited comparisons

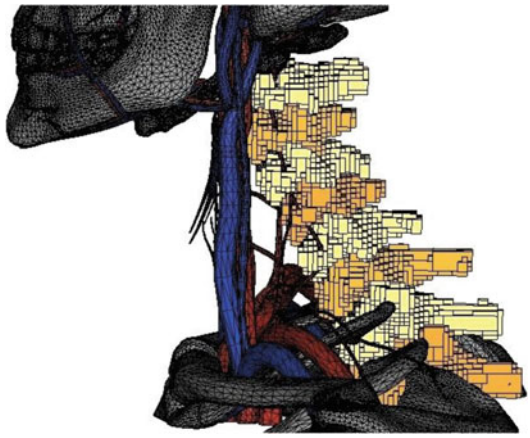

Fig. 27.6 A three dimensional mesh of cervical neurovascular structures in which the spinal cord is undergoing discretisation into elements that can each be assigned a material model for the tissue type it represents

of the medical consequences of wearing different types of armour.

Armour elements can be incorporated by laser scanning of physical specimens or importing manufacturers computer aided design (CAD) files. Although the complex models can produce the most accurate predictions, they require detailed experimental data to underpin their algorithms that is often not available and just a single simulation may take many hours to run and necessitate huge computing power requirements. In contrast the simpler models may still be able to provide objective comparisons between the medical effectiveness of different armour systems and yet be quick, cheap and the information required to provide answers is already available.

27.9 Model Scaling

Models generated from Computed Tomography (CT) and Magnetic Resonance (MR) scans are likely to represent the future of most future numerical models, whether they be commercially procured or derived 'in house' from the source data. It is essential that when they are used for comparing armour coverage, both the armour components and human anatomy are scaled appropriately. The UK programme currently utilises a model that has been scaled to a 50th percentile Caucasian male using external anthropometric measurements derived from a population basis. This required additional scaling of the dimensions of internal anatomical structures and distances from skin surface by analysing CT scans of injured soldiers [10].

27.10 Computerised Surface Wound Mapping

Surface wound mapping is the process by which the entry wound locations demonstrated pictorially [2]. When linked to injury outcome and the protective equipment worn it has the potential to enable limited comparisons in terms of their medical effectiveness. Historically such an approach using paper based systems has been extremely limited but a novel tool using only the skin component of the commercially acquired mesh has been developed (Fig. 27.7). Armour designs are incorporated and injury locations linked to outcome through the use of Abbreviated Injury Scale (AIS) scores, ascertained from injuries to UK soldiers described in the Joint Theatre Trauma Registry (JTTR). Its primary advantage is that information is easy to obtain and such injuries and the threat are relevant. However, any such comparisons are likely to be only relevant for that conflict alone and predictions are most accurate for anatomical areas where no body armour is worn and therefore most injuries occur.

27.11 Shot Line Models

Analytical Boundary Models utilising a shot line approach have been the most commonly used numerical models within the UK for injury prediction in a military setting [1]. A shot line analysis is the concept by which projectiles within the model travel through tissues along a straight line, which is either infinitely thin or the width of the penetrating projectile. Projectiles that

Fig. 27.7 The IMAP Surface Wound Mapping tool demonstrating entry wound locations on the neck of a representative UK male soldier wearing an OSPREY ballistic neck collar

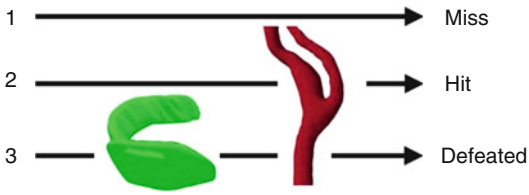

Fig. 27.8 Concept of a shot line model by which underpins the predictions made by the Coverage of Armour Tool (COAT)

intersect a structure or anatomical area are assumed to be hit and those that do not are discarded. In addition, any hits on structures that intersect body armour are also discarded (Fig. 27.8).

The COAT tool is the shot line model currently employed by the UK and has superseded the legacy MAVKILL tool [1]. Only those anatomical structures at risk and thereby requiring protection are included, as identified by extensive analysis of clinical records of survivors and post mortem records in those killed (Fig. 27.9). The percentage coverage of these structures by each armour design can be ascertained from a variety of angles and a pictorial representation of coverage comparisons produced using an azimuth plot (Fig. 27.10).

27.12 Finite Element Models

In a Finite Element (FE) approach, the geometries of anatomical structures, protection mechanisms, as well as any loading entities (in this case an FSP), are represented by a mesh of discrete parallelopoid 'elements'. The anatomical structures requiring protection are identical to those utilised in COAT and comprise the larger neurovascular structures of the neck as well as skin. The elements comprising each cervical anatomical structure are assigned an appropriate 'material model' from which the stresses and strains due to dynamic loading are determined. A 'material model' can be thought of as a set of algorithms that represent the specific biomechanical responses of that individual tissue or material under ballistic impact. Where required, boundary conditions can be assigned to the mesh to constrain the movement of structural components. The numerical analysis can be started via the assignment of an initial condition to a particular entity within the model, such as assigning an initial velocity to a projectile.

The primary challenge to an FE model of energised fragments penetrating the neck is that many of the values required to populate the

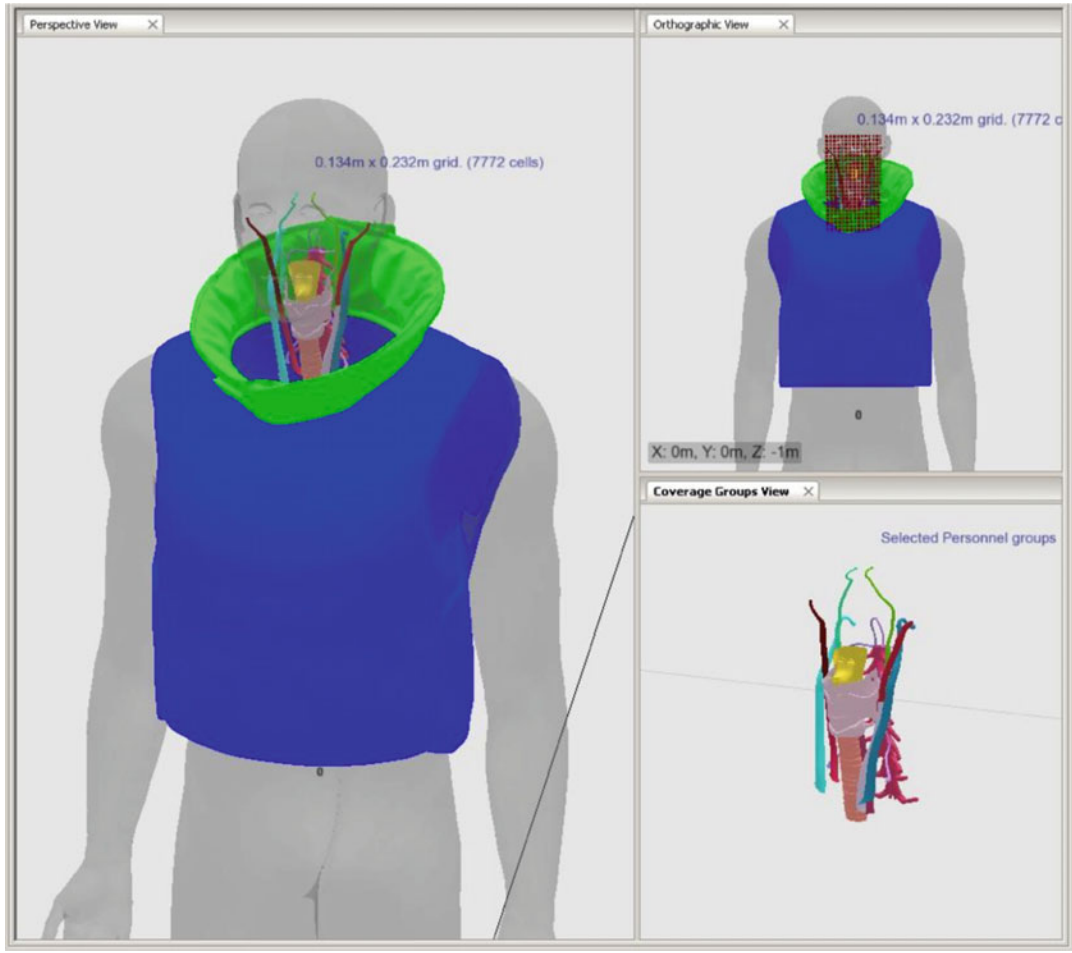

Fig. 27.9 The Coverage of Armour Tool being used to ascertain the coverage of vulnerable cervical anatomical structures by a prototype neck collar

material models are not yet known [11]. Defining the values experimentally is still highly challenging as the high compressive strain rates (100–2500 s^{-1}) and large deformations characteristic of typical impact scenarios require a fresh sample of each tissue type utilising techniques that have only been developed relatively recently [13]. Another challenge is accurately representing the complexities of the Permanent Wound Tract (see Chap. 28, Sect. 28.7), reflecting the irreversible tissue damaged produced by a combination of the cutting and crushing effect of the projectile in conjunction with the rapid radial tissue displacement produced by the temporary cavity [5]. Simplistic methods which utilise either an infinitely thin shot line or irreversible damage the same width of the projectile will inevitably underestimate damage (Fig. 27.11). For the time being the HF neck model utilises FSP penetration variables (permanent and temporary cavities, depth of penetration) upon a 20 % gelatine material model

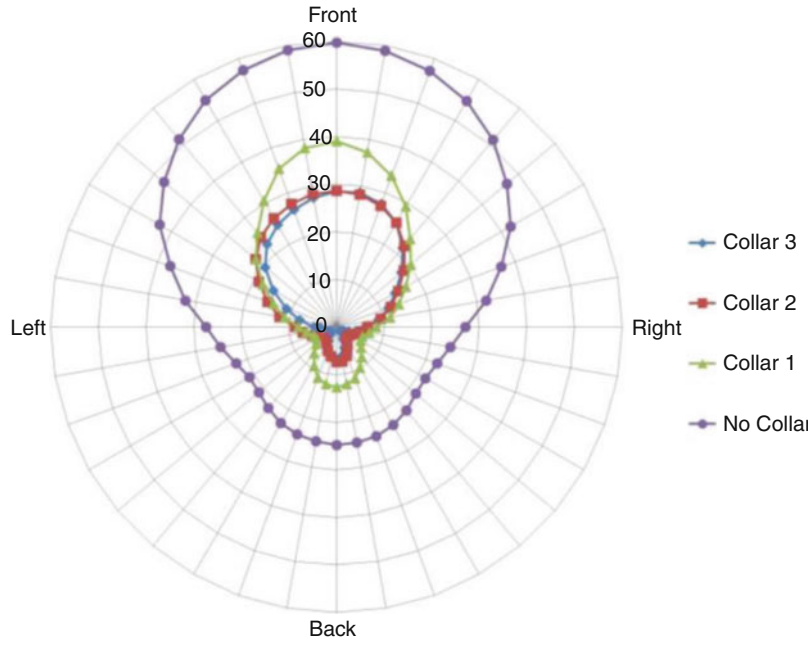

Fig. 27.10 An azimuth plot can demonstrate objectively the coverage provided by different ballistic collar designs from energised fragments fired from a range of angulations

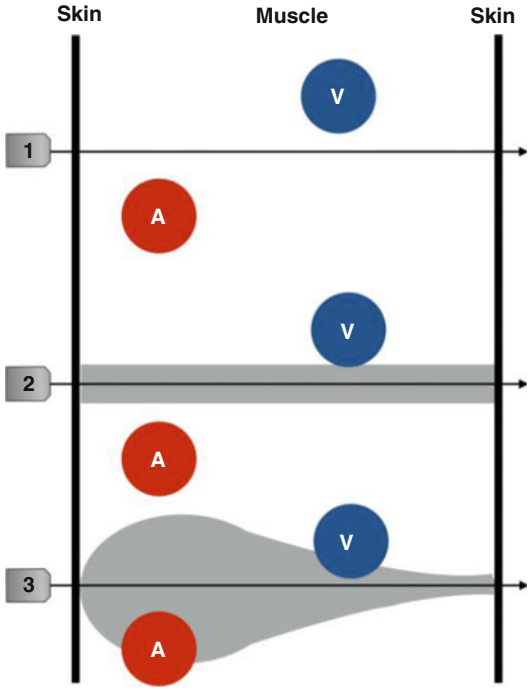

Fig. 27.11 A projectiles passing through tissue using an infinitely thin shot line (*1*) would miss the artery (*A*) and vein (*V*). Damage occurs when the projectile width (*2*) or permanent wound tract (*3*) is utilised

[12], as this simulant is believed to be representative of homogenous animal muscle *in-vivo* (Fig. 27.10).

27.13 Summary

There is a requirement for a model for simulating penetrating neck injury. Existing physical and animal models do not reproduce the complex cervical anatomy of a human being and many of the values required to populate material models are not yet known. Numerical models produce limited comparisons of the medical consequences of neck injury, or indeed the effectiveness of wearing armour which requires detailed experimental data to underpin the algorithms. The use of models generated from CT and MR scans represent the future of numerical models and when linked to injury outcome and the protective equipment worn, has the potential to assess neck protection systems in terms of their medical effectiveness.

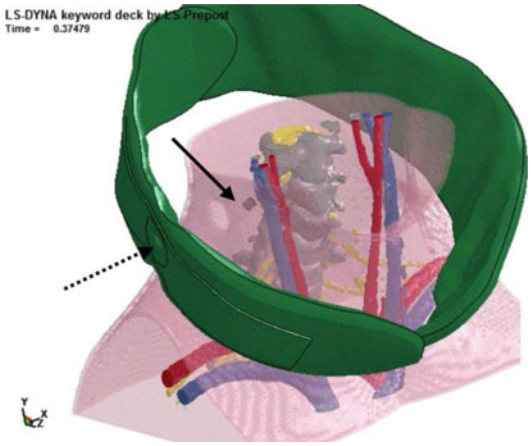

Fig. 27.12 A screenshot of the latest iteration of the High Fidelity neck model demonstrating the temporary cavity produced by a projectile (*solid arrow*) that has penetrated a prototype neck collar (*dashed arrow*)

Acknowledgements The author would like to thank Dr Robert Fryer for kindly providing Figs. 27.9 and 27.10, and Dr Dan Pope for Figs. 27.6 and 27.12.

References

1. Breeze J, Newbery T, Pope D, et al. The challenges in developing a finite element model of the neck to predict penetration of explosively propelled projectiles. J R Army Med Corps. 2014a;160(3): 220–5.
2. Breeze J, Allanson-Bailey LS, Hunt NC, et al. Mortality and morbidity from combat neck injury. J Trauma. 2012;72:969–74.
3. NATO Standardisation Agreement (STANAG) 4512. NATO standardization agency (NZA). Available at: http://www.nato.int/cps/en/SID-8BF0F167-D3248540/natolive/stanag.htm.
4. Flis W. Ballistics 2005: proceedings of the 22nd international symposium on ballistics. DEStech Publications, Inc 2005. ISBN: 9781122093958.
5. Breeze J, Sedman AJ, James GR, et al. Determining the wounding effects of ballistic projectiles to inform future injury models. J R Army Med Corps. 2014b; 160(4):273–8.
6. Breeze J, James G, Mouland M, et al. Perforation of fragment simulating projectiles into goat skin and muscle. J R Army Med Corps. 2013;2013(159):84–9.
7. Breeze J, Hunt NC, Gibb I, et al. Experimental penetration of fragment simulating projectiles into porcine tissues compared with simulants. J Forensic Leg Med. 2013;20:296–9.
8. Bir CA, Stewart SJ, Wilhelm M. Skin penetration assessment of less lethal kinetic energy munitions. J Forensic Sci. 2005;50:1426.
9. Van Ee CA, Chasse AL, Myers BS. Quantifying skeletal muscle properties in cadaveric test specimens: effects of mechanical loading, postmortem time, and freezer storage. J Biomech Eng. 2000;122(1):9–14.
10. Breeze J, West A, Clasper J. Anthropometric assessment of cervical neurovascular structures using CTA to determine zone-specific vulnerability to penetrating fragmentation injuries. Clin Radiol. 2013;68(1):34–8.
11. Van Sligtenhorst C, Cronin DS, Brodland GW. High strain rate compressive properties of bovine muscle tissue found using a split Hopkinson bar apparatus. J Biomech. 2006;39:1852–8.
12. Trexler MM, Lennon AM, Wickwire AC, et al. Verification and implementation of a modified split Hopkinson pressure bar technique for characterizing biological tissue and soft biosimulant materials under dynamic shear loading. J Mech Behav Biomed Mater. 2011;4(8):1920–8.
13. Gojani AB, Ohtani K, Takayama K, et al. Shock Hugoniot and equations of states of water, castor oil, and aqueous solutions of sodium chloride, sucrose and gelatin. Materials Sci For. 2009;566:23–8.

Optimising the Anatomical Coverage Provided by Military Body Armour Systems

28

John Breeze, Eluned A. Lewis, and Robert Fryer

28.1 Introduction

Body armour is a type of protective equipment worn by military personnel that aims to prevent or reduce injury from ballistic projectiles (secondary blast effects) to structures within the thorax and abdomen [1]. Such injuries remain the leading cause of potentially survivable deaths on the modern battlefield [2, 3]. Arresting bleeding from projectiles penetrating the thoracic cavity is difficult as it is not amenable to compression by applying direct pressure [2]. Although modern haemostatic dressings and the early use of blood products can potentially delay time to death or significant complications [4] the only way of definitively stopping ongoing intrathoracic bleeding is surgery [5]. However; not every soldier sustaining a chest wound dies from it, demonstrating the variable vulnerability of the structures within the thorax and abdomen.

J. Breeze, PhD, MRCS, MFDS, MBBS, BDS (✉)
Academic Department of Military Surgery and Trauma, Royal Centre for Defence Medicine, Birmingham Research Park, Birmingham B15 2SQ, UK
e-mail: johno.breeze@me.com

E.A. Lewis
Technical Directorate, Defence Equipment and Support, Ministry of Defence Abbey Wood, Bristol BS34 8JH, UK

R. Fryer
Land Battlespace Systems Department, Defence Science & Technology Laboratory, Portsdown West, Fareham, Hampshire PO17 6 AD, UK

In addition there is also an increasing recognition that prevention of those injuries causing significant long term morbidity is also required, as demonstrated by the recent addition of pelvic and eye protection [6, 7].

28.2 Body Armour Worn by UK Military Personnel

Although body armour has been available in various guises since WW1, the earliest design of body armour comparable to that worn today was issued to US forces in Korea [8]. The vest covered the thorax and abdomen and consisted of a single type of ballistic protective material (originally Nylon) with the requirement to provide protection against fragmenting munitions. This 'soft armour' component remains the primary component of body armour and is made of a flexible fabric, most commonly a para-aramid (Box 28.1). As threats evolved, protection against high velocity rifle bullets was desired, which was achieved through the incorporation of ceramic plates (so called 'hard armour') [9]. The outer material of the vest is termed the carrier which is designed to resist wear.

Box 28.1: The Main Components of Most Modern Types of Body Armour

Hard armour: a rigid ballistic protective material designed to protect against high

(continued)

A.M.J. Bull et al. (eds.), *Blast Injury Science and Engineering: A Guide for Clinicians and Researchers*,
DOI 10.1007/978-3-319-21867-0_28

Fig. 28.1 Enhanced Combat Body Armour (ECBA) system contains a carrier (**a**) soft armour (**b**) worn in conjunction with front and rear ECBA plates (**c**) held in external pockets

Box 28.1 (continued)

velocity bullets. This is currently fulfilled in most systems by one or more ceramic plates.

Soft armour: a flexible ballistic protective material designed to protect against energised fragments. This is currently fulfilled in most systems by a vest comprised of layers of para-aramid but could be made of various types of materials. This is treated by water repellent treatment (WRT) and is encased in a water and UV resistant cover.

Carrier: a flexible waterproof material capable of resisting wear and attaching additional components such as Velcro or straps.

The first examples of this 'modern' body armour utilised by UK forces was the Improved Northern Ireland Body Armour (INIBA) vest and its successor the Enhanced Combat Body Armour (ECBA) system (Fig. 28.1) [10]. Both systems utilised removable front and rear plates held within a front opening vest. The OSPREY body armour system was introduced in 2006 as an urgent operational requirement, and in response to the developing threat in Iraq [9]. The system included new front and rear plates, ('OSPREY plates') with greater coverage and a higher level of protection than 'ECBA plates'. Later versions of OSPREY utilised ECBA plates as side plates to further enhance protection (Fig. 28.2). This carrier has evolved over time as well, from a front-opening waistcoat-style in ECBA to a tabard style in OSPREY for easier access to treat injuries [10]. Grab handles for dragging casualties and straps for tightening round the waist in ECBA have been changed to the MOLLE loops attached to OSPREY for integrated load carriage options.

28.3 Defining Anatomical Coverage

Anatomical coverage can be thought of as 'the identification of those vulnerable anatomical structures requiring protection by a ballistic protective material' [11]. 'Essential coverage' refers to those anatomical structures that should be protected to prevent prior to definitive surgical intervention and long term complications or disability. These are medical judgments and should be independent of the ballistic protective material used. 'Desired coverage' refers to remaining anatomical structures not included in essential

Fig. 28.2 The Mark 4 OSPREY body armour system (**a**), utilises new larger front and rear plates (**b**), original plates now used as side plates (**c**) but a similar soft armour filler (**d**)

coverage but that still require protection. This recognises that damage to these anatomical structures has a lower probability of causing significant mortality and morbidity. Generally, desired coverage is fulfilled by soft armour but other examples include the silk used in pelvic protection. Coverage can then be modified by human factors considerations such as equipment integration and interoperability. It is important to define essential coverage of the anatomical structures and not coverage of the hard and soft armour components.

Box 28.2: Definitions for the Coverage Requirements of Body Armour Subdivided Into 'Essential' and 'desired' Coverage

Essential coverage

The identification of those anatomical structures requiring protection from all threats:

(a) those responsible for death prior to definitive surgical intervention e.g. bleeding from the thorax that cannot be compressed and requires surgery access the thorax and arrest it ie a thoracotomy

(b) those responsible for morbidity necessitating lifelong medical treatment or that result in significant disability. This includes both physical disability as well as psychological disability. E.g. damage to the lower parts of the spinal cord (lumbar or sacral parts) may result in significant loss of function one or both limbs.

Desired coverage

The remaining anatomical structures not included in minimum coverage but that still require protection, e.g. damage to a kidney is unlikely to result in death but may cause long-term complications such as high blood pressure and heart disease.

Definition of the anatomical structures requiring essential coverage has changed over time, reflecting increased medical knowledge and different theatres of operation. Notwithstanding

Table 28.1 Coverage of essential and desired anatomical structures within the thorax and abdomen by different plates when viewed in the horizontal plane

Type of coverage	Anatomical structures requiring essential coverage	Coverage provided by front and rear ECBA plates from horizontal plane	Coverage provided by front and rear OSPREY plates from horizontal plane
Essential	Heart and vena cavae	Complete	Complete
	Liver	Partial	Complete
	Spleen	Partial	Complete
	Spinal cord (thoracic)	Complete	Complete
	Spinal cord (lumbar)	Partial	Partial
	Aorta (thoracic)	Complete	Complete
	Aorta (abdominal)	None	Partial
Desired	Kidneys	None	Partial
	Lungs	None	Partial
	Trachea and main bronchi	Partial	Partial
	Intestines	Partial	Partial

improvements in body armour, reductions in mortality can be attributed to improved tourniquets, haemostatic dressings and early advanced resuscitative capabilities (such as within helicopters). Essential coverage should now be considered within the context of time to medical care, particularly to the time for a definitive surgical procedure as explained previously. For example ECBA was developed for UK soldiers serving in Northern Ireland in the 1980s where an appropriate level of medical attention capable of treating a high velocity bullet wound was approximately 20 minutes away. Essential coverage at this time was defined as heart and great vessels and was achieved by front and rear plates. The larger plates used in OSPREY (Fig. 28.2) were developed during the Iraq conflict when the threat was redefined and essential coverage expanded to encompass the spleen and liver as well in addition to the existing heart and great vessels.

The conflicts in Iraq and Afghanistan have resulted in a further evolution of essential coverage and are based upon structures that, if damaged, are highly likely to lead to either death within 60 minutes or would cause significant long term morbidity [1] (Table 28.1). A time period of 60 minutes from time of injury to arrival at a Role 2 surgical facility was chosen as this is the target that both the UK Ministry of Defence [4] and the US Department of Defence strive to meet [12]. Significant information to determine those essential structures was derived from searches of the Joint Theatre Trauma Registry (JTTR). JTTR is based upon an anatomical injury scoring system, meaning that damage to individual structures can be accurately evaluated in terms of outcome.

The requirement for military body armour (both soft and hard components) is designed to prevent missile injury in the form of fragmentation (secondary blast) or high velocity bullets. There is currently no requirement for it to protect against either primary or tertiary blast. The evidence that Behind Armour Blunt Trauma (BABT) is a real medical threat is equivocal and a recent systematic review [13] demonstrated no objective evidence that the entity BABT leads to adverse medical outcomes (see Chap. 24).

28.4 Computerised Representations of Anatomical Coverage Provided by Body Armour

The ability to compare the potential medical effectiveness of different designs of armour has significantly improved with the development of computerised tools based upon three-dimensional representations of the internal anatomy of the human body. Computed Tomography and Magnetic Resonance scans can be used to

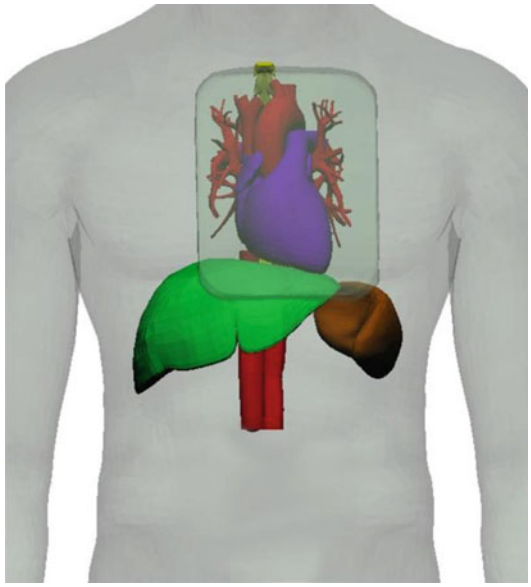

Fig. 28.3 The front plates of the legacy ECBA body armour superimposed over those structures requiring essential coverage: heart (*purple*), great vessels (*red*), liver (*green*), spleen (*brown*) and spinal cord (*yellow*)

provide the three-dimensional coordinates describing the outline and geometry of all anatomical structures down to the fidelity of the smallest named vessels and nerves [14]. Different body armours can then be scanned and superimposed onto those anatomical structures identified as requiring protection. Further conceptual designs can be placed on the body from computer aided drawing files in order to assess different possible designs.

As an example of this current utility, the front and rear plates used in the former ECBA body armour system were superimposed over a geometry representative of a 50th percentile member of the UK armed forces, with those structures within the body identified as requiring essential coverage: heart, great vessels, liver, spleen and spinal cord represented (Fig. 28.3). Good coverage of the heart and great vessels from horizontal shot lines is found, demonstrating how it met the original requirement for Northern Ireland in the 1980s.

28.5 Relating Plate Position to External Anthropometric Landmarks

Three external bone landmarks have been identified to assist with relating the position of the plate on the outer skin surface to those structures currently designated as requiring essential coverage (Fig. 28.4). These landmarks have been purposely chosen as they are easily palpable as well as being recognisable to non- clinicians following essential instruction. The upper boundary is the suprasternal notch (landmark 1), which is believed to equates to a point 2 cm above the aortic arch [15, 16]. The lower boundary of minimum coverage (in blue) is the lower border of the rib cage in the mid clavicular line (landmark 2) and will cover the liver and spleen. The lower border of ideal coverage (in red) is a horizontal line between the uppermost points of the iliac crests (landmark 3); this should cover the aorta down to its bifurcation [17]. Therefore the height of the plate (minimum coverage) should be the distance between points 1 and point A. The height of the vest (ideal coverage) should be the distance between 1 and point B (Fig. 28.4). This conceit recognises that the ceramic plate would not be able to protect against of all of the abdominal aorta and lumbar spinal cord, as ergonomic considerations such as the ability to bend forwards would not allow this. However, haemorrhage is potentially compressible at this point for a limited period without the need for a sternotomy [2], and spinal cord damage from this point downwards may not necessarily result in loss of leg function.

28.6 Scaling of Armour Sizing

Currently OSPREY plates comes in a single size, but there is an increasing recognition that multiple sizes may be more appropriate for future body armour systems, reflecting the increasing anthropometric diversity of those individuals joining the UK armed forces. Different sizes of vests are available but these are fitted to the individual based upon

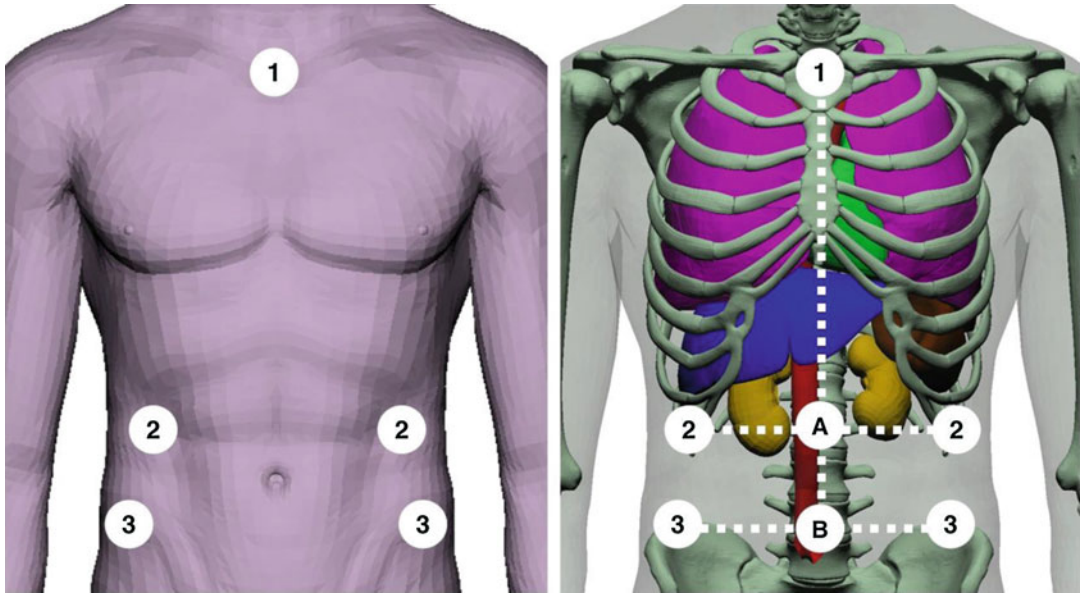

Fig. 28.4 External anthropomorphic landmarks relating to desired coverage; *1* suprasternal notch, *2* costal margin in mid- clavicular plane, *3* superior border of iliac crest, *A* point halfway between points 2, *B* point halfway between points 3

their height and chest circumference. In the shorter term this will mean relating the borders of the plate to these surface bony landmarks, which have in turn been related to the underlying structures requiring essential coverage (Fig. 28.4). The use of bone landmarks will also enable scaling of the computerised representation of humans utilised for body armour coverage assessments; it is however recognised that further investigations will still need to be undertaken to ascertain how anatomical structures within these anatomical representations alter in size in relation to changes in external body dimensions such as height and build.

Limited anthropometric information has been gathered on UK soldiers in the supine position (which is the positioned used in CT scans) and what has been measured is now recognised as insufficient for either scaling the computerised representations or for relating the plate to bone landmarks on the skin surface [18]. Scaling of these external landmarks as well as dimensions of internal anatomical structures is currently being undertaken using CT scans to ascertain how the sizes of the liver and spleen alter in proportion to changes in overall stature. Future anthropometric surveys using these external bony landmarks are required to ascertain if a range of plate sizes for different heights of individual would be more appropriate. In the longer term the use of skin surface scanning technology using these landmarks could enable the most ideal plate shape for that individual to be chosen. This could lead to the ability to produce individually customised armour by three-dimensionally printing plates if such a requirement is desired; the technology required for this is potentially not far off as printing of a simple cortical bone framework (also a ceramic) has been recently achieved [19].

28.7 Future Modelling Capabilities

Superimposition of body armour designs over those anatomical structures deemed to necessitate protection is the premise of the Coverage of Armour Tool (COAT) [20]. COAT enables objective comparisons between armour designs in terms of percentage coverage from different angles under the premise that every armour design stops all projectiles (Fig. 28.5). Limitations to COAT

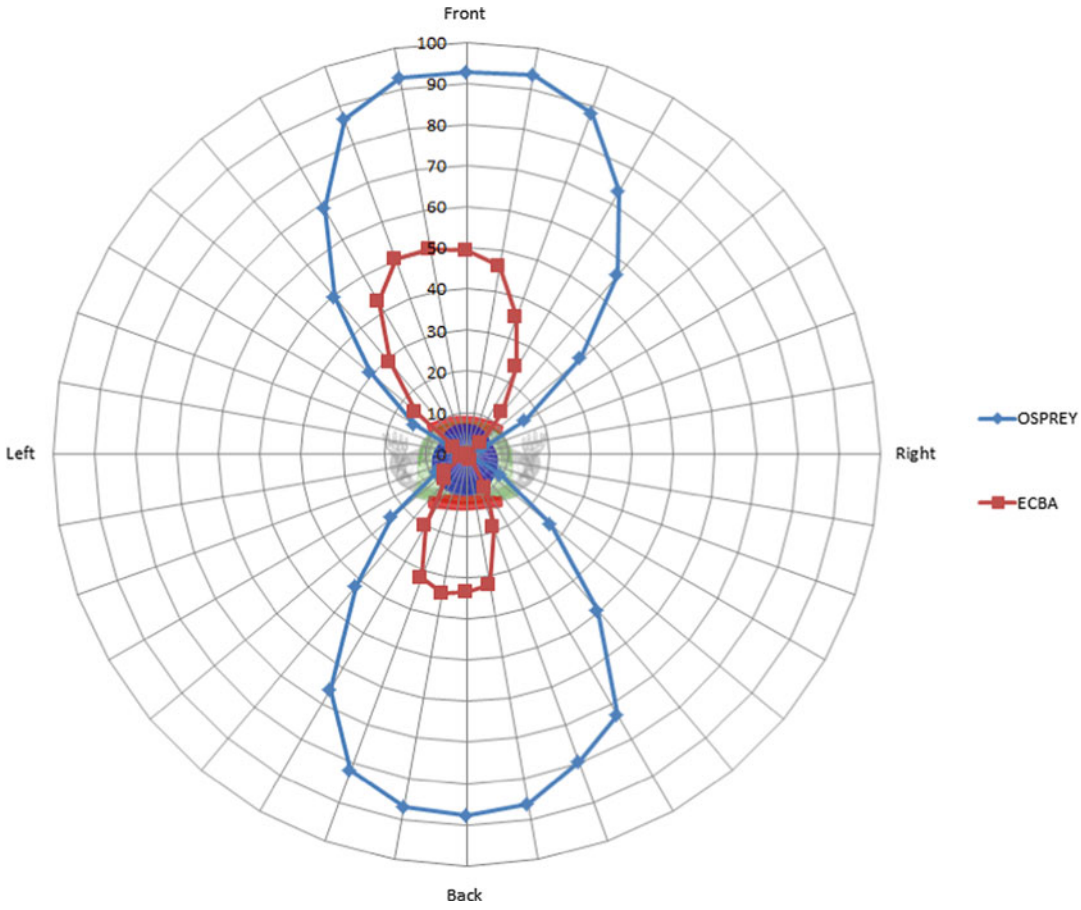

Fig. 28.5 A screenshot of COAT being used to compare essential anatomical structure coverage by the ECBA and OSPREY plates

include an inability to represent the penetrative capability of projectiles with varying masses and velocities. It also does not account for the protective capability of the body armour designs (all armour stops all projectiles in COAT) or dense structures such as bones that may stop a projectile hitting vulnerable structures. However, its success means that it has become the primary method utilised the MoD to predict the relative medical effectiveness of different armour designs in providing essential coverage.

One of the most significant limitations of shotline tools such as COAT is that it cannot model the area of tissue irreversibly damaged by the projectile (the permanent wound tract), which is the result of a highly complex interaction of projectile and tissue factors. High velocity bullets generally result in high-energy transfer, causing irreversible tissue damage at some distance away from the projectile path [21, 22]. Work is currently being undertaken to address these parameters as well as incorporating methods of predicting the resultant injury. The Personal Vulnerability Simulation (PVS) tool calculates the penetration and cavitation caused by a projectile penetration. These algorithms are currently based on gelatine penetration for a variety of projectiles at differing velocities (Fig. 28.6). There is scope to develop and incorporate algorithms for more tissue types in future developments. The importance of this PWT approach can be demonstrated by the analogy of a body armour plate with an upper border level with the suprasternal notch, and thereby approximately 2 cm above the arch of the aorta. Theoretically,

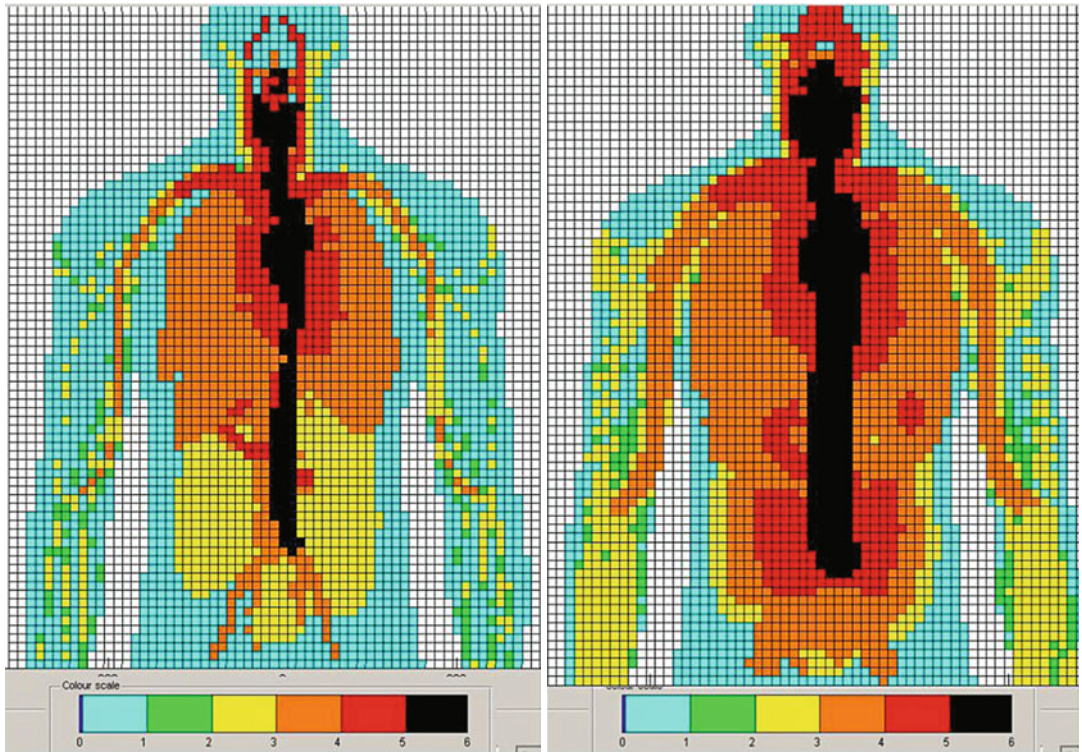

Fig. 28.6 Personal Vulnerability Simulation being used to compare the predicted damage of structures in the thorax using a 8 mm sphere at 400 m/s (*left*) and 12 mm sphere at 800 m/s (*right*). Severity increases from 1 (minor) to 6 (maximal)

assuming a perpendicular approach, this would enable a circular wound tract of up to a 2 cm radius before the aortic arch was damaged. Clearly this is a gross simplification, but does demonstrate the importance of including such a cavity which enables comparisons between projectiles of differing types, masses and velocities.

28.8 Conclusions

Significant recent advances have been made in the process by which coverage of body armour is determined. The definition of those anatomical structures requiring coverage will enable objective comparisons of body armour designs to be made in the future. The identification of external bony landmarks that relate to the approximate margins of essential coverage will enable future anthropometric surveys to be undertaken to ascertain if a range of plate sizes for different heights of individual would be more appropriate. COAT has already been used successfully to compare the essential coverage provided by body armour designs and is expected to underpin determinations of medical effectiveness in future body armour procurement. PVS has the potential to improve the representation of the effects of injury from high velocity projectiles and thereby further optimise the coverage that should be provided by future body armour designs.

References

1. Breeze J, Fryer R, Lewis E, Mahoney P, Clasper J. Defining the medical requirement for body armour plates against high velocity bullets. J R Army Med Corps. 2015. doi:10.1136/jramc-2015-000431.
2. Morrison JJ, Stannard A, Rasmussen TE, Jansen JO, Tai NR, Midwinter MJ. Injury pattern and mortality of

noncompressible torso hemorrhage in UK combat casualties. J Trauma Acute Care Surg. 2013; 75(2 Suppl 2):S263–8.
3. Singleton JA, Gibb IE, Hunt NC, Bull AM, Clasper JC. Identifying future 'unexpected' survivors: a retrospective cohort study of fatal injury patterns in victims of improvised explosive devices. BMJ Open. 2013;3 (8):e003130.
4. Hodgetts TJ, Mahoney PF, Kirkman E. Damage control resuscitation. J R Army Med Corps. 2007;153 (4):299–300.
5. Parker PJ. Damage control surgery and casualty evacuation: techniques for surgeons, lessons for military medical planners. J R Army Med Corps. 2006;152 (4):202–11.
6. Breeze J, Allanson-Bailey L, Hepper A, Midwinter MJ, Lewis EA. Demonstrating the effectiveness of body Armour: a pilot prospective computerised surface wound mapping trial performed at the role 3 hospital in Afghanistan. J R Army Med Corps. 2015;161(1):36–41.
7. Lewis EA, Pigott MA, Randall A, Hepper AE. The development and introduction of ballistic protection of the external genitalia and perineum. J R Army Med Corps. 2013;159 Suppl 1:i15–7.
8. Brayley MJ. Modern body armour. 1st ed. Ramsbury: The Crowood Press Ltd; 2011. ISBN 13: 9781847972484.
9. Lewis EA. Between Iraq and a hard plate. Recent developments in UK military personal armour. Presented at the Personal Armour Systems Symposia conference. Leeds, UK. June 2006.
10. Ryan JM, Bailie R, Diack G, Kierle J, Williams T. Safe removal of combat body armour lightweight following battlefield wounding – a timely reminder. J R Army Med Corps. 1994;140(1):26–8.
11. Breeze J, Baxter D, Carr D, Midwinter MJ. Defining combat helmet coverage for protection against explosively propelled fragments. J R Army Med Corps. 2015;161(1):9–13.
12. Bastian ND, Brown D, Fulton LV, Mitchell R, Pollard W, Robinson M, Wilson R. Analyzing the future of army aeromedical evacuation units and equipment: a mixed methods, requirements-based approach. Mil Med. 2013;178(3):321–9.
13. Carr DJ, Horsfall I, Malbon C. Is behind armour blunt trauma a real threat to users or body armour? A systematic review. J R Amry Med Crops. 2013. doi:10.1136/jramc-2013-000161. [Epub ahead of print].
14. Breeze J, Newbery T, Pope D, Midwinter MJ. The challenges in developing a finite element injury model of the neck to predict the penetration of explosively propelled projectiles. J R Army Med Corps. 2014; 160(3):220–5.
15. Standring S. Gray's anatomy. 40th ed. London, UK: Churchill Livingstone; 2008. ISBN 13: 978-0-443-06684-9.
16. Ellis H, Mahadevan V. Clinical anatomy: applied anatomy for students and junior doctors. 12th ed. Hoboken, New Jersey, USA: Wiley-Blackwell; 2010. ISBN:978–1405186179.
17. Mirjalili SA, McFadden SL, Buckenham T, Stringer MD. A reappraisal of adult abdominal surface anatomy. Clin Anat. 2012;25(7):844–50.
18. Tyrrell A. Anthropometry survey of UK military personnel 2006–7 summary report. QINETIQ/07/02615. 2007 (Unclassified).
19. Vorndran E, Klarner M, Klammert U, Grover LM, Patel S, JBarralet JE, Gbureck U. 3D powder printing of β-Tricalcium phosphate ceramics using different strategies. Adv Eng Mater. 2008;10(12): B67–71.
20. Breeze J, Fryer R, Hare J, Delaney R, Hunt NC, Lewis EA, Clasper J. Clinical and post mortem analysis of combat neck injury used to inform a novel Coverage of Armour Tool. Injury. 2015;46(4):629–33.
21. Berlin R, Gelin LE, Janzon B, Lewis DH, Rybeck B, Sandegård J, Seeman T. Local effects of assault rifle bullets in live tissues. Acta Chir Scand Suppl. 1976; 459:1–76.
22. Holmström A, Larsson J, Lewis DH. Microcirculatory and biochemical studies of skeletal muscle tissue after high energy missile trauma. Acta Chir Scand Suppl. 1982;508:257–9.

Blast Injuries of the Eye

29

Robert A.H. Scott

29.1 Introduction

The eyes occupy 0.1 % of the total, and 0.27 % of the anterior body surface. As vision in the most important sense, the significance of their injury is far more substantial. Loss of vision is likely to lead to loss of career, major lifestyle changes and disfigurement. Eye injuries come at a high cost to society and are largely avoidable. This chapter identifies the range of ocular blast injuries in relation to the anatomical features of the eye (Fig. 29.1).

29.2 Primary Ocular Blast Injuries

The eye consists of several interfacing coats that vary in their elasticity and density that can be damaged by an explosive shock wave to cause a primary blast injury (PBI). It has been postulated that reflection of the shock wave by the bony orbit amplifies this effect [28]. Improved eye protection from secondary injury and improved general survivability from explosive injuries from protective clothing have made pure PBI more common [9]. Factors that influence the severity of a PBI include the size of the explosion, the distance that the eye is from it and the orientation of the eye to the blast wave.

Ocular PBI cases are found among the subgroup of casualties with closed globe injuries and intraocular lesions. The posterior segment of the eye, particularly the retina, is particularly susceptible to PBI and is affected in around 60 % of cases, even though the blast wave traverses the anterior segment to reach it [22]. Ocular PBI cases have a characteristic presentation of a profoundly hypotonic eye without evidence of globe rupture, often with traumatic cataracts. This spontaneously resolves over approximately 7–10 days.

In the anterior segment, conjunctival lacerations and subconjunctival haemorrhages are common after explosions. The iris and ciliary body are damaged causing with hyphaema, iris sphincter rupture, dialysis and spiral tears. This can lead to secondary glaucoma. Ciliary muscle atrophy causes reduced accommodation making reading difficult with associated eyestrain. Traumatic cataracts are common after PBI, these often spontaneously resolve. Occasionally, the lens will swell and extraction is required [4].

In the posterior segment, induced posterior vitreous detachment can lead to vitreous haemorrhage, retinal tears and detachments, or traumatic macular holes [24]. Macula commotio retinae, when photoreceptors are damaged leading to a whitened appearance of the retina is common after PBI. This differs from secondary

R.A.H. Scott, FRCS (Ed), FRCOphth, DM, (RAF)
Birmingham and Midland Eye Centre, Dudley Road, Birmingham, UK
e-mail: robertscott3@nhs.net

A.M.J. Bull et al. (eds.), *Blast Injury Science and Engineering: A Guide for Clinicians and Researchers*,
DOI 10.1007/978-3-319-21867-0_29

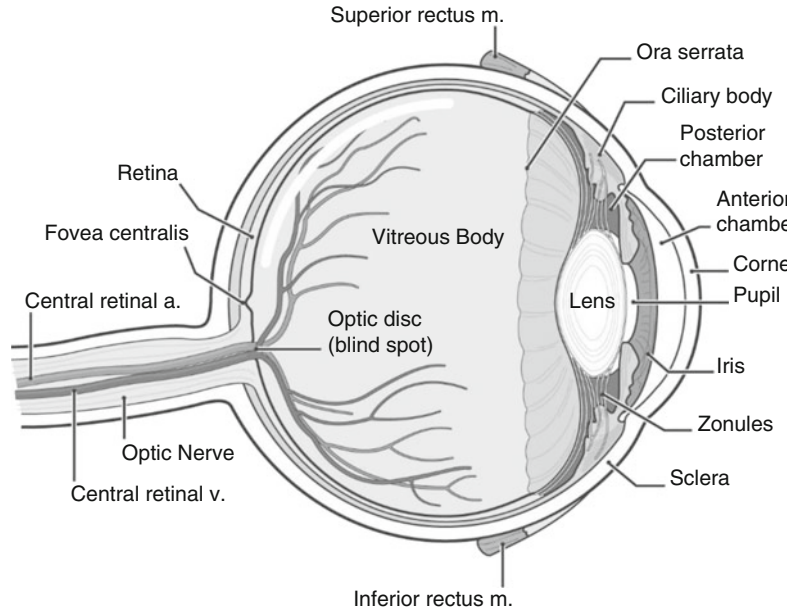

Fig. 29.1 The anatomy of the eye

blast injuries where the commotion retinae is more frequently in a peripheral retinal area. Typically, there is a profound drop in vision that slowly recovers leaving a variable pattern of residual retinal atrophy [6].

Optic neuropathy is a well recorded, if uncommon, PBI associated with large blast forces. Optic atrophy follows massive retinal atrophy, induced vasoconstriction of the optic nerve blood supply, or mechanical disruption of optic nerve axons as they leave the eye through the lamina cribrosa can. A retrobulbar hemorrhage from rupture of the vortex veins as they leave the globe compresses the optic nerve blood supply inducing acute optic nerve ischaemia [25].

The prognosis from ocular blast injuries is generally recorded as poor, with a final visual acuity of 6/12 or better achieved in 16–32 % of cases. Injuries to the optic nerve, choroid, and retina carry a worse prognosis than those to the anterior segment, adnexae, or intraocular haemorrhage [10].

29.3 Secondary Blast Injuries

Secondary blast injuries (SBI) are due to the impact of fragment from the explosive device itself or from exogenous debris propelled by the explosion. They are the most common form of high explosive ocular injuries. The projectiles cause penetrating and perforating injuries to the globe and ocular adnexa. Until recently, it was rare to find a case of PBI without any evidence of contusion or any secondary injury to the eye or adnexae [3].

29.4 Closed Globe Injuries

These are common to both primary and secondary blast injuries, but secondary blast injuries are caused by the impact of an object. When a blunt object strikes the eye, the lens-iris diaphragm is displaced posteriorly centrally while the peripheral structures are expanding outwards. This causes tearing of the ocular tissues, particularly in the iridocorneal angle.

When the compressing object is larger than the orbit, it pushes the globe posteriorly to suddenly increase the orbital pressure, relieved typically by an inferior blow-out fracture of the orbit into the maxillary sinus. This phenomenon often protects the globe from injury though there is up to a 30 % incidence of ruptured globe reported in conjunction with orbital fracture [29].

Corneal and conjunctival abrasions and foreign bodies (FB) are very common after blast injuries. The eyes are very painful, but recover rapidly after FB removal, patching and topical antibiotic ointment. After blast injuries, particularly from improvised explosive device (IED) and mine explosions, there are often multiple deep stromal foreign bodies. After an initial period of inflammation these characteristically become quiescent and the FB lies inert within the stroma, even years after the injury. Apart from problems of glare from light reflecting off the stromal FB, they are usually symptomless [11].

Traumatic iritis is common with perilimbal injection, anterior chamber cells and flare. Hyphaema is caused by bleeding in the anterior chamber and describes the layering of RBC in the inferior anterior chamber. Cyclodialysis clefts are from traumatic separation of the ciliary body from the sclera, this allows aqueous to exit directly to the subchoroidal space and causes ocular hypotony. Iridocorneal angle recession occurs when the ciliary body is torn and displaced posteriorly. It is associated with raised intraocular pressure and secondary glaucoma in 7–9 % of cases [8]. Traumatic cataracts may not appear for years after the injury; causing glare and loss of vision. They can be complicated due to lens zonular dehiscence, with a higher chance of subluxation and surgical complications [20].

Posterior segment contusion injuries are common. Commotio retinae is more likely to be in an extramacular position than with PBI, giving a better visual prognosis. Choroidal ruptures are common; they are typically crescent-shaped and sited at the posterior pole. Visual recovery is the rule, but can be reduced if the rupture involves the fovea, if there is choroidal subretinal neovascularisation or a significant subretinal haemorrhage.

Sclopetaria is a peripeheral traumatic chorioretinal rupture from a high velocity concussion injury. There are often dramatic retinal tears with associated shallow retinal detachment. These characteristically do not require active treatment as scarring from the surrounding tissue seals the retinal break [12].

Optic nerve avulsion occurs when an object intrudes between the globe and orbital wall to disinsert the optic nerve. There is sudden, irreversible. Traumatic optic neuropathy is a common secondary blast injury occurring directly from disruption of the nerve axons, or indirectly from vasoconstriction of the pial vessels that supply the optic nerve causing ischaemic neuropathy. The ensuing neural deficit typically reduces the visual acuity, brightness sense, and colour vision, with partial recovery.

29.5 Traumatic Retinal Tears and Detachments

Retinal dialyses are typical post-traumatic retinal injuries where there is peripheral retinal disinsertion between the edge of the retina and the ora serrata from sudden expansion of the ocular equator from blunt injury. The detachment evolves slowly, often years after the trauma. Eyes sustaining penetrating or open globe trauma have a high risk of retinal detachment, occurring in 10–45 % of cases.

Retinal detachments associated with penetrating and perforating eye trauma are common and frequently associated with a profound retinal scarring response, proliferative vitreoretinopathy (PVR), that causes recurrent detachment and poor visual results. The mean incidence of PVR is 27 % for all open globe trauma [15].

Traumatic macular holes form as a result of acute changes in vitreoretinal traction over the macular area from ocular contusion, they are typically 300–500 microns in diameter but if there is an element of retinal necrosis they can be much larger. There is a good visual prognosis with around half closing spontaneously. Most surgeons will operate to close those that do not close by 3–4 months [27].

Other retinal breaks can form as a result of an induced posterior vitreous detachment from the injury. If there is an area of increased vitreoretinal traction, typically over blood vessels a retinal tear forms often with a vitreous haemorrhage. The tears can cause a rhegmatogenous retinal detachment. Retinal

tears and detachments are managed surgically with retinopexy for retinal tears and vitrectomy and internal tamponade or cryopexy and buckling procedures for retinal detachment.

Penetrating eye injuries are sharp eye injuries that have a single entrance wound from the injury. Perforating eye injuries have an entrance and exit wound. Management is by urgent primary surgical repair, this can be followed by a definitive secondary procedure at during the same procedure or at a later date depending on circumstances. Corneal lamellar lacerations, where the eyewall is not breached can be directly sutured, or if there is a 'flap', a contact lens can be inserted to close the wound [7].

Globe rupture is a full-thickness wound of the eyewall from a blunt injury. The eye is filled with incompressible liquid and the impact causes sufficient pressure to rupture the eye at its weakest point, by an inside-out mechanism. Globe rupture must be excluded by ultrasound scan in all cases of hyphaema or post-traumatic media opacity that prevents indirect ophthalmoscopy of the fundus. Surgical exploration and primary repair is performed if globe rupture is suspected. Secondary procedures for intraocular haemorrhage are delayed for up to 14 days to allow the blood clot to liquefy, when it can be surgically drained as part of a vitrectomy procedure [5].

Intraocular foreign bodies (IOFB) cause 14–17 % of all ocular war injuries; they are a very important subset of eye injuries as they have a modifiable outcome using modern diagnostic, therapeutic, and surgical techniques. In modern warfare a large proportion of IOFBs are from grit and stones thrown up by explosions, they are frequently multiple [26]. Appropriate eye protection significantly reduces the incidence of IOFB injuries. Surgical removal of posterior segment IOFBs is by pars plana vitrectomy. Systemic antibiotic coverage reduces the risk of endophthalmitis until the IOFBs can be removed [30].

Recovery from primary and secondary ocular blast injuries can be divided into 3 main stages. The first stage of active general treatment and healing lasts for 3 weeks. Poor vision at this time does not preclude a satisfactory outcome. The second stage from 4 to 12 weeks is when individual clinical patterns requiring specific treatments appear, an accurate prediction of the final outcome can be made at this stage, largely depending on the state of the macula and other chorioretinal damage. The intraocular pressure recovers at this stage. The third stage, from 3 months to 3 years can see limited further improvement, but the vision rarely deteriorates [19].

29.6 Tertiary Blast Injuries

Tertiary ocular blast injuries are from the effects of being thrown into fixed objects or structural collapse and fragmentation of buildings and vehicles by an explosion. As any body part may be affected, the injury pattern is varied and eye injuries will usually be part of a wider injury pattern, which will often be combined with other facial trauma [21].

Tertiary blast causes direct traumatic injury, as well as indirect ocular injuries. Purtscher's retinopathy is a sudden onset multifocal, vaso-occlusive event, associated with head and chest trauma, causing sudden loss of vision that usually recovers over weeks and months. The appearance is of multiple patches of superficial retinal whitening with retinal haemorrhages surrounding a hyperaemic optic nerve head. Fat embolism syndrome is a potentially fatal variant that causes respiratory and central nervous system failure after long bone fractures [2].

Valsalva retinopathy is a sudden loss of vision from the preretinal hemorrhage that occurs after a sudden increase in intrathoracic pressure and is common after explosions. Spontaeneous recovery is the rule [16].

Terson's syndrome is a vitreous haemorrhage that occurs after an intracranial haemorrhage, thought to be related to an acute rise in intracranial pressure that is transmitted to the retina causing rupture of the papillary and retinal capillaries. It is often diagnosed when a patient recovers from the subarachnoid haemorrhage and is found to be profoundly blind [13].

Water-shed infarcts of the parieto-occipital lobes of the cerebral cortex, are associated with severe blood loss and profound hypotension. The infarct occurs at the borders of cerebral circulation that are sensitive to ischaemic insults. These classically cause bilateral visual pathway damage with cortical blindness [1]. Non-arteritic ischaemic optic neuropathy where there is visual loss in one or both eyes with associated optic atrophy due to optic nerve ischaemia has a similar aetiology following explosive injuries [18].

29.7 Quaternary Blast Injury

Quarternary blast injuries of the eye are explosion related injuries or illnesses not due to primary, secondary, or tertiary injuries. There may be exacerbations of pre-existing conditions, such as glaucoma or cataracts. Chemical and thermal burns are common around the eye and adnexae in association with ballistic injuries. In thermal burns, tissue damage is usually limited to the superficial epithelium, but thermal necrosis and ocular penetration can occur. Chemical burns are blinding emergencies. Alkaline agents such as lye or cement penetrate cell membranes and cause more damage than acidic agents, which precipitate on reaction with ocular proteins [23].

29.8 Quinary Blast Injuries

These are a new entity that describe a hyperinflammatory state, unrelated to the injury complexity and severity of trauma, occurring after an explosion, particularly associated with hypercoaguability. It is postulated that they are caused by unconventional toxic materials used in the manufacture of the explosive [14]. Retinal vascular occlusion occurs in approximately 10 % of ocular explosive blast injuries and has occurred where there has not been any other ocular involvement [17]. Some of these cases may represent quinary ocular blast injuries.

29.9 Summary and Incidence

According to the study of ocular injuries in British Armed Forces in Iraq and Afghanistan between July 2004 and May 2008 [5], a total of 630 British soldiers survived major traumatic injuries. Of these, 63 (10 %) sustained ocular injuries with some 86 % (54) were deemed to be caused by explosive blast. Of these, the most common injury report was open-globe with the mean time to primary repair being 1.9 days with an average of 1.57 operations per eye.

References

1. Adams JH, Brierley JB, et al. The effects of systemic hypotension upon the human brain. Clinical and neuropathological observations in 11 cases. Brain. 1966;89(2):235–68.
2. Agrawal A, McKibbin MA. Purtscher's and Purtscher-like retinopathies: a review. Surv Ophthalmol. 2006;51(2):129–36.
3. Beiran I, Miller B. Pure ocular blast injury. Am J Ophthalmol. 1992;114(4):504–5.
4. Bellows JG. Observations on 300 consecutive cases of ocular war injuries. Am J Ophthalmol. 1947;30 (3):309–23.
5. Blanch RJ, Bindra MS, et al. Ophthalmic injuries in British Armed Forces in Iraq and Afghanistan. Eye (Lond). 2011;25(2):218–23.
6. Blanch RJ, Good PA, et al. Visual outcomes after blunt ocular trauma. Ophthalmology. 2013;120 (8):1588–91.
7. Blanch RJ, Scott RA. Military ocular injury: presentation, assessment and management. J R Army Med Corps. 2009;155(4):279–84.
8. Blanton FM. Anterior chamber angle recession and secondary glaucoma. A study of the aftereffects of traumatic hyphemas. Arch Ophthalmol. 1964;72:39–43.
9. Chalioulias K, Sim KT, et al. Retinal sequelae of primary ocular blast injuries. J R Army Med Corps. 2007;153(2):124–5.
10. Dalinchuk MM, Lalzoi MN. Eye injuries in explosive mine wounds. Voen Med Zh. 1989;(8):28–30.
11. Erdurman FC, Hurmeric V, et al. Ocular injuries from improvised explosive devices. Eye (Lond). 2011;25 (11):1491–8.
12. Fraser EJ, Haug SJ, et al. Clinical presentation of chorioretinitis sclopetaria. Retin Cases Brief Rep. 2014;8(4):257–9.
13. Hassan A, Lanzino G, et al. Terson's syndrome. Neurocrit Care. 2011;15(3):554–8.

14. Kluger Y, Nimrod A, et al. The quinary pattern of blast injury. Am J Disaster Med. 2007;2(1):21–5.
15. Mader TH, Aragones JV, et al. Ocular and ocular adnexal injuries treated by United States military ophthalmologists during Operations Desert Shield and Desert Storm. Ophthalmology. 1993;100(10):1462–7.
16. Michaelides M, Riordan-Eva P, et al. Two unusual cases of visual loss following severe non-surgical blood loss. Eye (Lond). 2002;16(2):185–9.
17. Mouinga Abayi DA, Giraud JM, et al. A rare trauma-associated cause of central retinal vein occlusion in a young subject. J Fr Ophtalmol. 2012;35(6):426–31.
18. Petras JM, Bauman RA, et al. Visual system degeneration induced by blast overpressure. Toxicology. 1997;121(1):41–9.
19. Quere MA, Bouchat J, et al. Ocular blast injuries. Am J Ophthalmol. 1969;67(1):64–9.
20. Ram J, Verma N, et al. Effect of penetrating and blunt ocular trauma on the outcome of traumatic cataract in children in northern India. J Trauma Acute Care Surg. 2012;73(3):726–30.
21. Rezaei A, Salimi Jazi M, et al. A computational study on brain tissue under blast: primary and tertiary blast injuries. Int J Numer Method Biomed Eng. 2014;30 (8):781–95.
22. Scott GI, Michaelson IC. An analysis and follow-up of 301 cases of battle casualty injury to the eyes. Br J Ophthalmol. 1946;30:42–55.
23. Scott R. The injured eye. Philos Trans R Soc Lond B Biol Sci. 2011;366(1562):251–60.
24. Sebag J. Anatomy and pathology of the vitreo-retinal interface. Eye (Lond). 1992;6(Pt 6):541–52.
25. Shek KC, Chung KL, et al. Acute retrobulbar haemorrhage: an ophthalmic emergency. Emerg Med Australas. 2006;18(3):299–301.
26. Thach AB, Ward TP, et al. Intraocular foreign body injuries during Operation Iraqi Freedom. Ophthalmology. 2005;112(10):1829–33.
27. Weichel ED, Colyer MH. Traumatic macular holes secondary to combat ocular trauma. Retina. 2009;29 (3):349–54.
28. Wharton-Young M. Mechanics of blast injuries. War Med. 1945;8(2):73–81.
29. Wilkins RB, Havins WE. Current treatment of blow-out fractures. Ophthalmology. 1982;89(5):464–6.
30. Woodcock MG, Scott RA, et al. Mass and shape as factors in intraocular foreign body injuries. Ophthalmology. 2006;113(12):2262–9.

Hearing Damage Through Blast

30

Tobias Reichenbach

30.1 Introduction

Hearing damage through blast is an escalating problem in the military: it accounted for 25 % of all injuries during Operation Iraqi Freedom in 2004 and was accordingly the most common single injury [1]. Auditory dysfunction in general is now the most prevalent individual service-connected disability, with compensation estimated to exceed $2.2 billion in 2014 in the U.S.A [2]. A recent report on Royal Marines returning from deployment in Afghanistan has found that two-thirds sustained severe and permanent hearing damage [3, 4].

Hearing damage can occur at several key stages of the auditory pathway (Fig. 30.1). The latter consists broadly of the outer ear which collects sound, the middle ear which acts as a lever, the inner ear in which the mechanical sound stimulation is converted into electrical nerve impulses, and the central nervous system that processes and analyzes the auditory signals. Blast can damage all parts of this system [5]. In the following we discuss their impact as well as detection, prevention and treatment strategies.

T. Reichenbach, PhD, MSc
Department of Bioengineering, Imperial College London, RSM Building, South Kensington Campus, London SW6 4RF, UK
e-mail: reichenbach@imperial.ac.uk

30.2 Blast Damage to the Outer Ear

The outer, or external, ear consists of the pinna and the ear canal. The outer ear collects sound and funnels it through the ear canal to the middle ear. It hence plays an important role in the detection of faint sound. The pinna also introduces spectral changes in a sound that are specific for the location of the sound [6, 7]. As the most prominent of these changes, the pinna introduces a spectral notch at an elevation-dependent frequency. This information can then be used by the brain to estimate the location of a sound [8].

Blast exposure can damage the outer ear, namely through burns as well as through damage by flying debris [9–11] As long as the middle and inner ear are not damaged, such impairment of the outer ear leaves the hearing sensitivity largely unchanged. Sound localization, however, will be compromised. Because the outer ear is visible and constitutes a key attribute to a human face, its damage can also have severe psychological implication [12]. Furthermore, burn patients are often treated with antibiotics that can be toxic to the ear, the mechanism of which remains poorly understood [2, 13, 14].

Detection of outer-ear damage is straightforward from visual inspection. Prevention necessitates ear muffs that extend around the outer ear and hence shield it, or helmets. Treatment of outer-ear damage requires surgery, namely amputation of the damaged parts of the outer

A.M.J. Bull et al. (eds.), *Blast Injury Science and Engineering: A Guide for Clinicians and Researchers*,
DOI 10.1007/978-3-319-21867-0_30

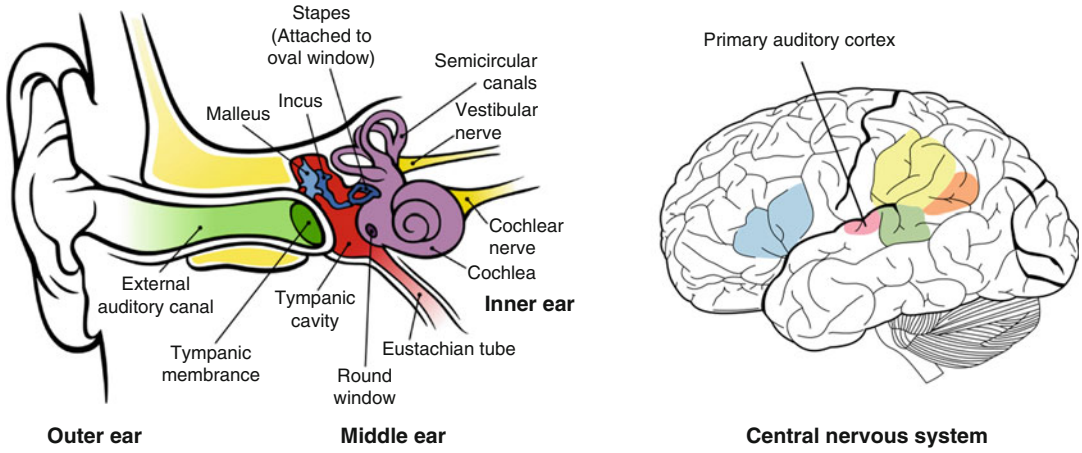

Fig. 30.1 The auditory system consists of the outer, middle, and inner ear. It also encompasses parts of the central nervous system where the evoked neural signals are processed. Exposure to blast can cause damage at all stages

ear. Reconstruction of the amputated parts can then often be successfully achieved, for instance with autologous costal cartilage [12, 15].

30.3 Middle-Ear Damage

The middle ear consists of the ear drum, or tympanic membrane, as well as the ossicles, the three smallest bones in the body: malleus, incus, and stapes. Through these constituents the middle ear forwards the mechanical sound vibration from the ear canal to the inner ear. It thereby acts as a lever, and matches the impedance of the sound wave in air to that of the emerging wave in the inner ear (see below). This impedance-matching by the middle ear is paramount for an effective transmission of sound energy into the inner ear [16, 17].

As for the outer ear, blast trauma is a primary cause of damage to the middle ear [2]. Rupture of the tympanic membrane can occur from peak pressure levels of 130 dB or higher, which are common in a blast wave ([18] – primary blast injury mechanism). Such pressures can also disrupt the ossicles. The resulting damage can cause conductive hearing loss of up to 25 dB SPL [19].

Rupture of the middle ear in a blast wave can have a protective effect on the inner ear. This is because once the ossicle chain has been disrupted, the excess pressure in a blast wave is no longer efficiently forwarded to the inner ear, and hence impairs it less.

Detection of middle-ear damage involves visual inspection through the ear canal as well as tympanometry in which the reaction of the tympanic membrane to sound stimulation is measured.

Passive protection of the middle ear involves either earplugs or earmuffs. Such passive ear protection is most efficient at the high frequencies above 1 kHz where the wavelength of sound is short and where sound can hence be efficiently blocked [20–22]. It also affects speech intelligibility since the latter partly employs these higher frequencies. One problem with wearing this protection is hence that it not only blocks undesired noise but also desired speech signals as well as other environmental sound that is necessary to parse a potentially hostile environment.

Recent development has hence focused on active hearing protection. Such equipment employs a microphone and a small speaker. The microphone records the external sound signal and plays a processed version into the ear. This can achieve noise cancellation as well as protection from overstimulation. Such active hearing protection is now employed in the U.K. armed forces in the form of the Personal Integrated

Hearing Protection system and the Tactical Hearing Protection System [23, 24].

Regarding treatment, about 80 % of ruptures of the tympanic membrane heal spontaneously [25]. In the remaining cases, as well as when the ossicles have been impaired, reconstruction of the middle ear gives often satisfactory results [26].

30.4 Blast-Induced Impairment of the Inner Ear

The inner ear transduces the mechanical sound vibrations into electrical signal in auditory-nerve fibres [27]. This mechanotransduction happens in hair cells, specialized cells that have a hair bundle at their apical end. Mechanosensitive ion channels inside this bundle of parallel stereocilia open and close when the bundle is displaced, and the resulting electrical signal in the hair cell can produce an action potential in the attached auditory-nerve fibers. The displacement of the hair bundles arises from the sound signal.

Due to an intricate hydrodynamics within the inner ear, every hair cells responds particularly well to a certain best frequency [28, 29]. Following a tonotopic map, hair cells from the base of the organ respond best to high frequencies (around 10–20 kHz in humans) and cells further apical respond strongest to progressively lower frequencies (down to 100 Hz, with frequencies down to 20 Hz detectable).

Blast can yield sensorineural hearing loss which is one of the most prominent causes of hearing problems. [30, 31] It refers to damage of the hair cells, typically the hair bundles, which can be disrupted or otherwise damaged by overstimulation. Because each hair cell has a best response at a certain frequency, sensorineural hearing loss is often frequency-dependent. For instance, it may happen that the hair cells in a particular cochlear region are compromised, but remain intact elsewhere. This will then result in a hearing loss in the frequency interval that corresponds to the cochlear region with the damaged hair cells. Because other hair cells will still respond somewhat to frequencies from that interval, the hearing loss there will typically not be total.

The inner ear also contains the vestibular system, in form of the semicircular canals, that is responsible for our sense of balance. The semicircular canals house mechanosensitive hair cells that are similar to those of the inner ear, but detect motion instead of sound. Damage to these hair cells can occur through noise as well. Such damage is indeed often related to sensorineural hearing loss, and causes problems with balance [32, 33].

Diagnosis of sensorineural hearing loss employs pure-tone audiometry in which a subject has to respond to pure tones of different frequencies and intensities. This is, however, not objective as it involves a subject's overt response. An objective diagnostic method employs otoacoustic emissions. These are tones produced by a healthy ear, for example in response to short clicks (transient-evoked otoacoustic emissions) or to two close frequencies (distortion-product otoacoustic emissions) [34, 35]. Lack of these otoacoustic emissions in a certain frequency region signals hearing loss there [36, 37].

Protection against sensorineural hearing loss involves passive or active earplugs as well as ear mugs as described in Sect. 30.4. Another highly promising route for the protection of the inner ear is through drugs that prevent sensorineural hearing loss [38]. Noise exposure induces the generation of reactive oxygen species (ROS) within the inner ear that, over the course of days after noise exposure, damage the mechanosensitive hair cells [39, 40]. Recent research has identified a number of drugs that potentially control the generation of ROS and that can hence serve as otoprotectants. These drugs include single or multiple antioxidants, such as D-methionine [41, 42], ebselen [43, 44], resvaratrol [45], neurotrophic factors [46] and lipoic acid [47, 48], as well as anti-inflammatory drugs such as salicylate [49], steroids [50–52] and TNF-inhibitors [53]. Although some of these drugs are being explored in animal models and

others in clinical trials, none has yet been clinically approved.

There is currently no direct treatment for sensorineural hearing loss. As opposed to the hair cells of birds, for instance, mammalian hair cells do not regenerate and can currently not be replaced [54, 55]. Damage to the hair cells hence accumulates over life, which explains why sensorineural hearing loss is more prevalent in older than in younger people. Current treatments of this type of hearing impairment involve hearing aids that amplify sound as well as, in severe cases, cochlear implants [56, 57]. The latter are devices that bypass the outer, middle, and inner ear to stimulate the auditory-nerve fibers directly. These devices have been developed to provide hearing in deaf people and are a major success of the emerging field of neurotechnology.

30.5 Damage to the Central Nervous System

The central nervous system can be divided into two main parts, the brainstem and the cortex.

The nerve signals emerging from the cochlea within the auditory-nerve fibers are first processed at different stages in the auditory brainstem. The brainstem performs, for instance, sound localization, detects onsets of sounds, and sharpens frequency selectivity [27, 58]. While the neuronal activity in the lowest levels of the brainstem, the cochlear nuclei, is relatively well characterized, the higher levels such as the superior olivary complex and the inferior colliculus remain rather poorly understood.

Importantly, the neural activity in the auditory brainstem can be used to assess the functioning of the ear as well as the brainstem [59, 60]. Indeed, the neural signals of the brainstem can be measured non-invasively with only a few electrodes on the scalp. In response to short clicks, the electrodes detect a characteristic pattern of electrical, neural activity that consists of five peaks at different latencies. These peaks signal activity in different parts of the brainstem, beginning from the auditory nerve fibers to the inferior colliculus. Their height and latencies inform on the integrity of these organs. Current research investigates how these recordings can give more precise information about damage to the ear and to the brainstem, and how more complex responses, such as the frequency-following response to pure tones or the response to speech, arise [61–63].

The auditory cortex receives input from the auditory brainstem and represents the highest level of auditory processing in the brain. It is hence believed to be the site where recognition and processing of complex auditory objects such as speech and music occur. How exactly such processing is achieved remains, however, poorly understood.

Recent research has shown how neural signals from the auditory cortex can give information about sound processing. For example, noninvasive electroencephalographic recordings (EEG) from scalp electrodes have evidenced that the neural activity in the cortex traces the envelope of an attended speech signal as well as the beat of music [64–66]. Measurements from functional magnetic resonance imaging (fMRI), positron emission tomography (PET) and magnetoencephalography (MEG) give more detailed, three-dimensional pictures of brain activity in response to sound [67–69].

The central auditory system can be damaged through traumatic brain injury. This is a particular concern in the military since traumatic brain injury can occur through primary blast exposure or head concussions (a tertiary effect). The resulting injuries of the brain include death of neurons as well as swelling and disconnection of axons due to shearing and stretching, which may particularly affect the central auditory system [70]. Such damage results in auditory processing disorder, the main consequence of which is a deficits with the processing of speech, and in particular with the challenging task of detecting speech in noise [71]. A recent study shows that the majority of war veterans that were exposed to blast during deployment have auditory processing disorder [5].

How to best diagnose auditory processing disorder is still a field of active research. Current diagnosis involves mostly a speech in noise test, and a particularly successful online test has been developed by the U. K. charity *Action on Hearing Loss* [72–74]. Just as pure-tone audiometry, however, such tests are based on a subject's behavioral response and hence require his or her cooperation.

Recent research has shown how noninvasive electroencephalographic recordings (EEG) of brain activity can evidence how a healthy brain processes speech and music [64–66]. This suggests that these recordings can be employed to assess hearing impairment, including central auditory processing disorder. Further research is needed to develop this technology into suitable hearing assessments.

Tinnitus means the perception of a 'phantom' tone for an extended period of time (5 min or longer) [75]. Such perception can presumably arise in different ways in the auditory brainstem and the central auditory system (somatic tinnitus) [76]. Notably, it may also arise from the inner ear itself (otic tinnitus). Tinnitus often accompanies hearing loss, and hearing loss in a certain frequency band typically produces phantom tones at those frequencies. It can severely affect a person's life, and in particular lead to insomnia, fear, withdrawal and depression.

Current assessment of tinnitus is based on a behavioral response from the tested subject, which makes testing slow and potentially inaccurate. Recent research has explored ways of automating such testing [77]. More research is needed to further improve tinnitus testing. It will also be important to investigate how tinnitus can be diagnosed in an objective way. This may involve recordings of neural activity which has been shown to inform on—as well as potentially modulate—tinnitus [78, 79].

Protection and treatment of damage to the central auditory system remain intensely investigated as well. Regarding protection, safety helmets can be efficient in preventing brain injury [80, 81]. A range of pharmacological agents that can potentially protect the central nervous system and help rehabilitating it after injury has been identified in animal models, but confirmation of the effectiveness of these drugs in clinical trials has not yet been achieved [82].

30.6 Conclusion

Hearing loss from blast injury in the armed forces is a highly important emerging medical problem. Major questions remain regarding the prevention, detection and treatment of such hearing loss. Recent progress in a better understanding of the causes of blast-induced hearing loss, in the treatment of sensorineural hearing loss and in a better understanding of the role of the brain processes for hearing suggest that major improvements in all three areas can be achieved. Conquering these issues will have major implications for the wellbeing of military personnel.

References

1. Gondusky JS, Reiter MP. Protecting military convoys in Iraq: an examination of battle injuries sustained by a mechanized battalion during Operation Iraqi Freedom II. Mil Med. 2005;170(6):546–9.
2. Fausti SA, Wilmington DJ, Gallun FJ, Myers PJ, Henry JA. Auditory and vestibular dysfunction associated with blast-related traumatic brain injury. J Rehabil Res Dev. 2009;46(6):797–810.
3. Guardian. Two-thirds of Afghan war veterans are suffering from hearing damage. 2009. http://www.theguardiancom/uk/2009/dec/20/afghan-veterans-hearing-damagez.
4. Pearson C. The extent of operational NIHL. Conference Presentation. Deafness Research, London, UK. 2009.
5. Gallun FJ, Diedesch AC, Kubli LR, Walden TC, Folmer RL, Lewis MS, et al. Performance on tests of central auditory processing by individuals exposed to high-intensity blasts. J Rehabil Res Dev. 2012;49(7):1005.
6. Middlebrooks JC, Green DM. Sound localization by human listeners. Annu Rev Psychol. 1991;42(1):135–59.
7. Walsh WE, Dougherty B, Reisberg DJ, Applebaum EL, Shah C, O'Donnell P, et al. The importance of auricular prostheses for speech recognition. Arch Facial Plast Surg. 2008;10:321–8.
8. Hebrank J, Wright D. Spectral cues used in the localization of sound sources on the median plane. J Acoust Soc Am. 1974;56(6):1829–34.

9. DePalma RG, Burris DG, Champion HR, Hodgson MJ. Blast injuries. N Engl J Med. 2005;352 (13):1335–42.
10. Helling ER. Otologic blast injuries due to the Kenya embassy bombing. Mil Med. 2004;169:872–6.
11. Garth RJN. Blast injury of the auditory system: a review of the mechanisms and pathology. J Laryngol Otol. 1994;108(11):925–9.
12. Gault D. Post traumatic ear reconstruction. J Plast Reconstr Aesthet Surg. 2008;61:S5–12.
13. Dobie RA, Black FO, Pezsnecker SC, Stallings VL. Hearing loss in patients with vestibulotoxic reactions to gentamicin therapy. Arch Otolaryngol. 2006;132(3):253–7.
14. Campbell K. Pharmacology and ototoxicity for audiologists. Clifton Park: Thomson/Delmar Learning; 2007.
15. Pearl RA, Sabbagh W. Reconstruction following traumatic partial amputation of the ear. Plast Reconstr Surg. 2011;127(2):621–9.
16. West PDB, Evans EF. Early detection of hearing damage in young listeners resulting from exposure to amplified music. Br J Audiol. 1990;24(2):89–103.
17. Benesty J, Sondhi MM, Huang Y. Springer handbook of speech processing. Berlin: Springer; 2008.
18. Mayorga MA. The pathology of primary blast overpressure injury. Toxicology. 1997;121(1):17–28.
19. Hirsch FG. Effects of overpressure on the ear – a review. Ann N Y Acad Sci. 1968;152(1):147–62.
20. Dancer A, Buck K, Hamery P, Parmentier G. Hearing protection in the military environment. Noise Health. 1999;2(5):1.
21. Berger EH. The noise manual. Fairfax: Aiha; 2003.
22. Birch RS, Gerges SN, Vergara EF. Design of a pulse generator and shock tube for measuring hearing protector attenuation of high-amplitude impulsive noise. Appl Acoust. 2003;64(3):269–86.
23. Online G. Tactical hearing protection system. http://www.government-onlinenet/tactical-hearing-protection-system/.
24. Loss AoH. Written evidence from action on hearing loss. 2011. http://www.publicationsparliamentuk/pa/cm201012/cmselect/cmdfence/762/762vw06htm.
25. Kerr A, Byrne J. Concussive effects of bomb blast on the ear. J Laryngol Otol. 1975;89(02):131–44.
26. Khan I, Jan AM, Shahzad F. Middle-ear reconstruction: a review of 150 cases. J Laryngol Otol. 2002;116 (06):435–9.
27. Pickles JO. An introduction to the physiology of hearing. London: Academic; 1988.
28. Robles L, Ruggero MA. Mechanics of the mammalian cochlea. Physiol Rev. 2001;81(3):1305–52.
29. Reichenbach T, Hudspeth AJ. The physics of hearing: fluid mechanics and the active process of the inner ear. Rep Prog Phys. 2014;77(7):076601.
30. Rabinowitz PM. Noise-induced hearing loss. Am Fam Physician. 2000;61(9):2759–60.
31. McReynolds MC. Noise-induced hearing loss. Air Med J. 2005;24(2):73–8.
32. Golz A, Westerman ST, Westerman LM, Goldenberg D, Netzer A, Wiedmyer T, et al. The effects of noise on the vestibular system. Am J Otolaryngol. 2001;22(3):190–6.
33. Oosterveld W, Polman A, Schoonheyt J. Vestibular implications of noise-induced hearing loss. Br J Audiol. 1982;16(4):227–32.
34. Hall JW. Handbook of otoacoustic emissions. San Diego: Singular Thomson Learning; 2000. Cengage Learning.
35. Probst R, Lonsbury-Martin BL, Martin GK. A review of otoacoustic emissions. J Acoust Soc Am. 1991;89 (5):2027–67.
36. Kim DO, Paparello J, Jung MD, Smurzynski J, Sun X. Distortion product otoacoustic emission test of sensorineural hearing loss: performance regarding sensitivity, specificity and receiver operating characteristics. Acta Otolaryngol. 1996;116(1):3–11.
37. Probst R, Lonsbury-Martin BL, Martin GK, Coats AC. Otoacoustic emissions in ears with hearing loss. Am J Otolaryngol. 1987;8(2):73–81.
38. Mukherjea D, Rybak LP, Sheehan KE, Kaur T, Ramkumar V, Jajoo S, et al. The design and screening of drugs to prevent acquired sensorineural hearing loss. Expert Opin Drug Discov. 2011;6(5):491–505.
39. Le Prell CG, Yamashita D, Minami SB, Yamasoba T, Miller JM. Mechanisms of noise-induced hearing loss indicate multiple methods of prevention. Hear Res. 2007;226(1):22–43.
40. Yamane H, Nakai Y, Takayama M, Iguchi H, Nakagawa T, Kojima A. Appearance of free radicals in the guinea pig inner ear after noise-induced acoustic trauma. Eur Arch Otorhinolaryngol. 1995;252 (8):504–8.
41. Kopke RD, Coleman JK, Liu J, Campbell K, Riffenburgh RH. Enhancing intrinsic cochlear stress defenses to reduce noise-induced hearing loss. Laryngoscope. 2002;112(9):1515–32.
42. Campbell K, Meech RP, Rybak LP, Hughes LF. The effect of D-methionine on cochlear oxidative state with and without cisplatin administration: mechanisms of otoprotection. J Am Acad Audiol. 2003;14(3):144–56.
43. Lynch ED, Gu R, Pierce C, Kil J. Combined oral delivery of ebselen and allopurinol reduces multiple cisplatin toxicities in rat breast and ovarian cancer models while enhancing anti-tumor activity. Anticancer Drugs. 2005;16(5):569–79.
44. Pourbakht A, Yamasoba T. Ebselen attenuates cochlear damage caused by acoustic trauma. Hear Res. 2003;181(1):100–8.
45. Seidman MD, Khan MJ, Bai U, Shirwany N, Quirk WS. Biologic activity of mitochondrial metabolites on aging and age-related hearing loss. Otol Neurotol. 2000;21(2):161–7.
46. Yamashita D, Shiotani A, Kanzaki S, Nakagawa M, Ogawa K. Neuroprotective effects of T-817MA against noise-induced hearing loss. Neurosci Res. 2008;61(1):38–42.

47. Pouyatos B, Gearhart C, Nelson-Miller A, Fulton S, Fechter LD. Lipoic acid and 6-formylpterin reduce potentiation of noise-induced hearing loss by carbon monoxide: preliminary investigation. J Rehabil Res Dev. 2008;45(7):1053–64.
48. Diao M, Liu H, Zhang Y, Gao W. Changes in antioxidant capacity of the guinea pig exposed to noise and the protective effect of alpha-lipoic acid against acoustic trauma. Acta Physiol Sin. 2003;55(6):672–6.
49. Adelman C, Freeman S, Paz Z, Sohmer H. Salicylic acid injection before noise exposure reduces permanent threshold shift. Audiol Neurootol. 2008;13(4):266–72.
50. Himeno C, Komeda M, Izumikawa M, Takemura K, Yagi M, Weiping Y, et al. Intra-cochlear administration of dexamethasone attenuates aminoglycoside ototoxicity in the guinea pig. Hear Res. 2002;167(1):61–70.
51. Park SK, Choi D, Russell P, John EO, Jung TT. Protective effect of corticosteroid against the cytotoxicity of aminoglycoside otic drops on isolated cochlear outer hair cells. Laryngoscope. 2004;114(4):768–71.
52. Paksoy M, Ayduran E, Şanlı A, Eken M, Aydın S, Oktay ZA. The protective effects of intratympanic dexamethasone and vitamin E on cisplatin-induced ototoxicity are demonstrated in rats. Med Oncol. 2011;28(2):615–21.
53. Van Wijk F, Staecker H, Keithley E, Lefebvre P. Local perfusion of the tumor necrosis factor α blocker infliximab to the inner ear improves autoimmune neurosensory hearing loss. Audiol Neurootol. 2006;11(6):357–65.
54. Stone JS, Rubel EW. Cellular studies of auditory hair cell regeneration in birds. Proc Natl Acad Sci U S A. 2000;97(22):11714–21.
55. Groves AK. The challenge of hair cell regeneration. Exp Biol Med. 2010;235(4):434–46.
56. Knudsen LV, Öberg M, Nielsen C, Naylor G, Kramer SE. Factors influencing help seeking, hearing aid uptake, hearing aid use and satisfaction with hearing aids: a review of the literature. Trends Amplif. 2010;14(3):127–54.
57. Waltzman SB, Roland JT. Cochlear implants. New York: Thieme; 2006.
58. Oertel D, Fay RR, Popper AN. Integrative functions in the mammalian auditory pathway. New York: Springer; 2002.
59. Hall JW. New handbook of auditory evoked responses. Boston: Pearson; 2007. ASHA.
60. Hood LJ. Clinical applications of the auditory brainstem response. San Diego: Singular publishing group; 1998.
61. Skoe E, Kraus N. Auditory brainstem response to complex sounds: a tutorial. Ear Hear. 2010;31(3):302.
62. King C, Warrier CM, Hayes E, Kraus N. Deficits in auditory brainstem pathway encoding of speech sounds in children with learning problems. Neurosci Lett. 2002;319(2):111–5.
63. Galbraith GC. Two-channel brain-stem frequency-following responses to pure tone and missing fundamental stimuli. Electroencephalogr Clin Neurophysiol. 1994;92(4):321–30.
64. Choi I, Rajaram S, Varghese LA, Shinn-Cunningham BG. Quantifying attentional modulation of auditory-evoked cortical responses from single-trial electroencephalography. Front Hum Neurosci. 2013;7:115.
65. Nozaradan S, Peretz I, Mouraux A. Selective neuronal entrainment to the beat and meter embedded in a musical rhythm. J Neurosci. 2012;32(49):17572–81.
66. Horton C, D'Zmura M, Srinivasan R. Suppression of competing speech through entrainment of cortical oscillations. J Neurophysiol. 2013;109(12):3082–93.
67. Ding N, Simon JZ. Emergence of neural encoding of auditory objects while listening to competing speakers. Proc Natl Acad Sci U S A. 2012;109(29):11854–9.
68. Price CJ. The anatomy of language: a review of 100 fMRI studies published in 2009. Ann N Y Acad Sci. 2010;1191(1):62–88.
69. Price CJ. A review and synthesis of the first 20 years of PET and fMRI studies of heard speech, spoken language and reading. Neuroimage. 2012;62(2):816–47.
70. Taber K, Warden D, Hurley R. Blast-related traumatic brain injury: what is known? J Neuropsychiatry Clin Neurosci. 2006;18(2):141–5.
71. Bronkhorst AW. The cocktail party phenomenon: a review of research on speech intelligibility in multiple-talker conditions. Acta Acustica. 2000;86(1):117–28.
72. Nilsson M, Soli SD, Sullivan JA. Development of the hearing in noise test for the measurement of speech reception thresholds in quiet and in noise. J Acoust Soc Am. 1994;95(2):1085–99.
73. Killion MC, Niquette PA, Gudmundsen GI, Revit LJ, Banerjee S. Development of a quick speech-in-noise test for measuring signal-to-noise ratio loss in normal-hearing and hearing-impaired listeners. J Acoust Soc Am. 2004;116(4):2395–405.
74. Loss AoH. http://www.actiononhearingloss.org.uk/your-hearing/look-after-your-hearing/check-your-hearing/about-the-hearing-check.aspx.
75. Jastreboff PJ. Phantom auditory perception (tinnitus): mechanisms of generation and perception. Neurosci Res. 1990;8(4):221–54.
76. Snow JB. Tinnitus: theory and management. Hamilton/Lewiston: Sales and Distribution, U.S./BC Decker; 2004. PMPH-USA.
77. Henry JA, Rheinsburg B, Owens KK, Ellingson RM. New instrumentation for automated tinnitus psychoacoustic assessment. Acta Otolaryngol. 2006;126(S556):34–8.
78. Attias J, Urbach D, Gold S, Shemesh Z. Auditory event related potentials in chronic tinnitus patients with noise induced hearing loss. Hear Res. 1993;71(1):106–13.

79. Dohrmann K, Elbert T, Schlee W, Weisz N. Tuning the tinnitus percept by modification of synchronous brain activity. Restor Neurol Neurosci. 2007;25(3):371–8.
80. Ghajari M, Galvanetto U, Iannucci L, Willinger R. Influence of the body on the response of the helmeted head during impact. Int J Crashw. 2011;16 (3):285–95.
81. Moss WC, King MJ, Blackman EG. Skull flexure from blast waves: a mechanism for brain injury with implications for helmet design. Phys Rev Lett. 2009;103(10):108702.
82. Loane DJ, Faden AI. Neuroprotection for traumatic brain injury: translational challenges and emerging therapeutic strategies. Trends Pharmacol Sci. 2010;31(12):596–604.

Peripheral Nerve Injuries

31

Jon Clasper and Paul R. Wood

Peripheral Nerve Injuries (PNI) have always been a significant problem in war, particularly affecting recovery and rehabilitation after limb injuries; the most common site of wounding in conflict. It can be argued that war has actually been the stimulus, and provided much of the material, for our current understanding of PNI. The first systematic study of PNI was carried out during the American Civil War [1], work continued during the First World War [2], and our current classification was first described in the Second World War [3]. This classification divides the nerve injuries into three types:

1. Neurotmesis is when a nerve that has been completely divided. The injury produces a complete lesion, with surgical repair of the nerve the normal treatment.
2. Axonotmesis is characterised by a nerve that remains in continuity as the nerve sheath and other supporting structures remain intact, however the damage to the nerve cells (neurones) results in distal degeneration of the axon – the long slender projection of the neurone, which is responsible for signal transmission. Distal regrowth, from the site of injury is necessary, with prolonged recovery the rule.
3. Neurapraxia results in short term dysfunction and spontaneous, usually relatively rapid full recovery, without the need for nerve regrowth. Neurapraxic injury involves minimal histological damage to axons, and classically results in short-term conduction block.

Historically it has been reported that most nerve injuries in war are as a result of penetrating fragment injury [4], and following initial surgery. Later, management of these nerve injuries includes surgical repair with resection of scar tissue around the nerve to create a viable bed, excision of the damaged nerve ends creating healthy stumps, and then tension-free suture repair by adequate mobilisation, or by nerve grafting if a gap is present [5].

Given that much of the understanding of PNI at that time was from conflict related wounds, it was appropriate for a further study to be carried out during the recent conflicts in Iraq and Afghanistan. As a result, between 2005 and 2010, all United Kingdom service personnel with PNI from ballistic trauma were examined in the War Nerve Injury Clinic at the Defence Medical Rehabilitation Centre, Headley Court, and data collected

J. Clasper, CBE, DPhil, DM, FRCSEd(Orth)
Department of Bioengineering, Royal British Legion Centre for Blast Injury Studies, Imperial College London, London, UK

Academic Department of Military Trauma and Surgery, Royal Centre for Defence Medicine, Birmingham, UK
e-mail: jonclasper@aol.co.u

P.R. Wood, MB, BCh, FRCA (✉)
Department of Anaesthetics, Queen Elizabeth Hospital Birmingham, Birmingham, UK
e-mail: paul.wood@uhb.nhs.uk

A.M.J. Bull et al. (eds.), *Blast Injury Science and Engineering: A Guide for Clinicians and Researchers*,
DOI 10.1007/978-3-319-21867-0_31

prospectively. Although not anticipated at the time this also allowed a comparison of different wounding mechanisms, as this period corresponded to a change in weapons used against UK troops.

The conflicts in Iraq and Afghanistan were characterised by the use of Improvised Explosive Devices (IED's). In Iraq this was manifest by the use of the Explosively Formed Projectile which resulted in catastrophic injuries, possibly due to a more focused stream of fragments than normally associated with the more discrete fragment wounds seen in previous conflicts [6]. Survivors of a direct impact were few and those that did survive suffered severe injuries. In contrast, the IED's used in Afghanistan were usually buried blast weapons used against dismounted troops or against vehicles [7]. These resulted in tertiary blast injuries sustained within vehicles resulted from significant axial loading from the floor deformation, and causing severe hindfoot injuries [8] (see Chap. 20).

In addition to these types of heel crush injuries, the extensive use of IEDs has also resulted in the most challenging severe limb injuries, commonly traumatic amputations, with associated pelvic trauma. Clearly there is a nerve injury when the distal part of the limb has been removed, but in addition many of these casualties suffered PNI in what was often their only remaining limb.

The UK study identified 100 consecutive patients with 261 PNI seen between April 2005 and April 2010, giving an incidence of 8.1 % of all combat casualties at the time [9]. Explosions caused 164 (63 %) of the nerve lesions, the remainder being the result of gunshot or fragment wounding; 213 nerve lesions (82 %) in 90 patients occurred in open wounds.

Although it could be presumed that the vast majority of the injuries would be associated with division of the nerve, this was not the case. Among the 261 lesions, 116 nerves (in 49 patients) had neuropraxic injuries associated with prolonged conduction block (PCB), and recovery was more delayed than would be normally expected; the mean time to onset of recovery was 4.17 months (0.6–10.2) [5]. Ninety of the 116 nerves (78 %) with PCB showed signs of recovery within 6 months of injury. Penetrating missile wounds accounted for 45 of these nerve injuries, explosion in the other 71. The mean time to recovery in the former was 3.8 months (0.6–6) compared with 4.7 months (2.5–10.2) in the latter ($p = 0.0001$). Also of concern was that 36 patients of the 100 casualties presented with persistent significant or severe neuropathic pain.

Nerve dysfunction despite an intact nerve was noted in the initial studies during the American Civil War [10]; this was believed to be related to the cavitation effect on the missile as energy was transferred to the tissue resulting in traction of the nerve. However, Suneson demonstrated nerve dysfunction experimentally in the contralateral limb of a porcine model shot in the thigh with a high-velocity missile [11]. The nerve appeared macroscopically intact but under light microscopy distortion of the myelin sheath surrounding the axons was evident; the authors felt that the pressure waves moving out radially from the missile were responsible.

The myelin sheath is formed from Schwann cells, and increases the speed of signal transmission along the axon, although not all nerves are myelinated. In addition, Schwann cells help support the nerve cell by providing essential support factors, and aid in nerve cell regeneration. It is felt that disturbance of the Schwann cells and their interaction with the nerve cells may be a factor in the prolonged conduction defect seen after blast injury.

It has been postulated that mechanical forces may be implicated as, in one study, following just 2 hours of shear stress, Schwann cells demonstrated increased proliferation [12]. The exact mechanism is not understood, however Schwann cells can undergo a change from myelinating to growth supportive following initial denervation [13]. Clearly the effect of blast on Schwann cells is of particular research interest.

There may be other factors, particularly in the military environment. Disturbance of the blood supply may also be implicated [14], as tourniquets are almost universally utilised to control the catastrophic haemorrhage that can occur with these injuries; one of the most important causes of death after combat injury. Direct

pressure on the nerve, from dressings, or again from tourniquets, have also been demonstrated to affect nerve conduction [15].

Given the prevalence of PNI following combat wounds, and the confounding factors in the military environment, it can be argued that there is a need to develop appropriate models to study this area.

Another driver for further study is the recognised difficulty in treating neuropathic pain. Although there are different causes of neuropathic pain there is increasing evidence that once established the pathophysiology involves disturbances of both the peripheral and central nervous system. In this respect it can be argued that the term PNI is misleading [16].

Experimental studies implicate possible abnormalities extending from the afferent peripheral nerve through to its synapse at the dorsal root ganglion and consequent spinal cord and cerebral cortical representation.

Following PNI pathological responses involve both injured and unaffected nociceptors and their associated nerves. The net result is abnormal signals arising from 'ectopic' discharges sensitising neurons in the spinal cord creating a 'wind up' of persistent pain, which does not respond to modulating descending cortical – spinal pathways [16].

Magnetic resonance imaging (MRI) has revealed supraspinal changes associated with neuropathic pain [16]. Classically a cortical reorganisation is believed to follow in response to abnormal afferent inputs post amputation [17]. In some patients cortical changes may additionally be influenced by the effects of blast induced traumatic brain injury [18]. At each level the changes may be both structural and biochemical involving various receptor types. Additionally maladaptive peripheral and central immune responses are also implicated [16].

Given these possible multiple aetiologies it is not surprising that neuropathic pain can be extremely resistant to treatment. Pharmacological approaches are limited [19]. Current experience with British military amputees has clearly demonstrated that treatment requires a multi-disciplinary team approach. The essential components of management can be summarised as:

(i) Patient education – current understanding of the mechanism of neuropathic pain and approaches to treatment must be explained and explored with the patient.
(ii) Drug treatment is muti –modal but relies extensively on the use of membrane stabilising drugs. The National Institute for Health and Care Excellence (NICE) clinical guideline 173 is used as a basis [20]. Opiates are not principal agents in neuropathic pain but Tramadol is used because of its additional adrenergic and serotonergic effects. The N- methyl –D-aspartate (NMDA) receptor antagonist Ketamine has also been successful in resistant situations [21].
(iii) While surgical procedures can be curative in selective cases they may also initially exacerbate neuropathic symptoms whether involving the operated limb(s) or anatomy remote from the site of neuropathic injury. When surgery involves a neuropathic limb e.g., excision of a neuroma then UK experience has emphasised regional anaesthesia (epidural or continuous peripheral nerve block) to suppress both surgical pain and neuropathic symptoms [21].
(iv) Free recourse is given to adjuncts where available and appropriate. These include transcutaneous electrical nerve stimulation (TENS), acupuncture and distraction therapy with muti media etc. The most effective form of distraction is continued mobilisation of the patient and here the role of the physiotherapy team is critical in both in the acute and rehabilitation phases [22]

Despite all these interventions the management of neuropathic pain in individual cases often remains disappointing and the prospect of better treatment remains dependent upon advances in basic research.

References

1. Campbell WW. Evaluation and management of peripheral nerve injury. Clin Neurophysiol. 2008;119:1951–65.
2. Delorme E. The treatment of gunshot wounds of the nerves. Br Med J. 1915;1:853–5.
3. Seddon HJ. A classification of nerve injuries. Br Med J. 1942;4260:237–9.
4. Maricevic A, Erceg M. War injuries to the extremities. Mil Med. 1997;162:808–11.
5. Birch R, Misra P, Stewart MP, Eardley WG, Ramasamy A, Brown K, Shenoy R, Anand P, Clasper J, Dunn R, Etherington J. Nerve injuries sustained during warfare: part II: outcomes. J Bone Joint Surg Br. 2012;94:529–35.
6. Ramasamy A, Harrison SE, Clasper JC, Stewart MPM. Injuries from roadside improvised explosive devices. J Trauma. 2008;65:910–4.
7. Ramasamy A, Masouros S, Newell N, Hill A, Proud A, Brown K, Bull A, Clasper JC. In-vehicle extremity injuries from improvised explosive devices: current and future foci. Philos Trans R Soc Lond B Biol Sci. 2011;366:160–70.
8. Ramasamy A, Hill AM, Phillip R, Gibb I, Bull AM, Clasper JC. The modern "deck-slap" injury-calcaneal blast fractures from vehicle explosions. J Trauma. 2011;71:1694–8.
9. Birch R, Misra P, Stewart MP, Eardley WG, Ramasamy A, Brown K, Shenoy R, Anand P, Clasper J, Dunn R, Etherington J. Nerve injuries sustained during warfare: part I – Epidemiology. J Bone Joint Surg Br. 2012;94:523–8.
10. Attributed to Weir Mitchell in: Seddon HJ. Three types of nerve injury. Brain. 1943;66:238–88.
11. Suneson A, Hannson HA, Seeman T. Central and peripheral nerve damage following high-energy missile wounds in the thigh. J Trauma. 1988;28: S197–203.
12. Gupta R, Truong L, Bear D, Chafik D, Modafferi E, Hung CT. Shear stress alters the expression of myelin-associated glycoprotein (MAG) and myelin basic protein (MBP) in Schwann cells. J Orthop Res. 2005;23:1232–9.
13. Mirsky R, Jessen KR. The neurobiology of Schwann cells. Brain Pathol. 1999;9:293–311.
14. Parry PG, Cornblath DR, Brown MJ. Transient conduction block following acute peripheral nerve ischaemia. Nuscle Nerve. 1985;8:409–12.
15. Lundborg G, Myers R, Powell H. Nerve compression injury and increased endoneural fluid pressure: a "miniature compartment syndrome". J Neurol Neurosurg Psychiatry. 1983;46:1119–24.
16. Campbell JN, Meyer RA. Mechanisms of neuropathic pain. Neuron. 2006;52(1):77–92.
17. Flor H, et al. Phantom-limb pain as a perceptual correlate of cortical reorganization following arm amputation. Nature. 1995;375(6531):482.
18. Nampiaparampil DE. Prevalence of chronic pain after traumatic brain injury:a systematic review. JAMA. 2008;300(6):711–9. doi:10.1001/jama.300.6.711.
19. Attal N, et al. EFNS guidelines on pharmacological treatment of neuropathic pain. Eur J Neurol. 2006;13:1153–69.
20. NICE clinical guideline 173. Accessed at http://www.nice.org.uk/guidance/cg173.
21. Blonk MI, et al. Use of oral ketamine in chronic pain management: a review. Eur J Pain. 2009. doi:10.1016/j.ejpain.2009.09.005.
22. Aldington DJ, McQuay HJ, Moore RA. End – to –end military pain management. Philos Trans R Soc Lond B Biol Sci. 2011;366:268–75. doi:10.1098/rstb.2010.0214. Published 13 December.

Glossary

Acoustic impedance A physical property of a material that defines the ease with which stress waves can travel through it.

Actin, f-actin, actin dynamics The most abundant protein in most eukaryotic cells. It is a globular protein that can exist in soluble or polymerised forms. Filamentous, f-actin, is a polymerised form that assembles as microfilaments, which are present in the cytoskeleton. Soluble and polymerised forms play many cellular roles including maintaining cell shape and enabling cell motility. The processes involving transitions between soluble and polymerised forms can be referred to as actin dynamics.

Adenosine triphosphate, ATP A small molecule used by cells in many metabolic processes. Hydrolysis or release of its phosphate groups is the most common chemical reaction associated with its cellular functions that include phosphorylation and signalling.

Adiabatic A process for which there is no heat transfer between a system and its surroundings. An adiabatic process that is reversible is isentropic.

Alginate A polysaccharide that can form gelatinous structures suitable for the encapsulation of cells.

Amorphous Lacking definite form.

Angiogenesis The process involved in the growth of new blood vessels from pre-existing ones.

Anisotropic A material whose microstructure is such that its mechanical behaviour depends on the direction of loading.

Apoptosis A cell-controlled mechanism for causing cell death – sometimes referred to as "programmed cell death". A number of well-known changes occur in cells during apoptosis. These changes can include membrane blebbing (formation of bulges from the plasma membrane), cell shrinkage, chromatin condensation and DNA fragmentation. The remaining cell debris may be engulfed by other cells. A key difference between apoptotic cell death and necrotic cell death is the absence of an inflammatory response.

Aseptic necrosis Cell death arising from a loss of blood flow.

Astrocytes Also known as astroglia. Star-shaped glial cells that interact with and support the function of neural cells.

Atom The smallest component of an element, having the chemical properties of the element.

Bending A loading mode whereby the structure deforms by changing in curvature.

Brisance The shattering behaviour exhibited by a detonating explosive.

Brittle A material that undergoes negligible plastic deformation prior to rupture / failure.

Buckling A failure mode due to instability in the long axis of a slender structure.

Burning The propagation of combustion by a surface process.

Carbide A compound formed of carbon and a less electronegative element.

Cell viability The ability of live cells to survive.

Cerebral vasospasm An intense constriction of arterial vessels in the brain, reducing blood flow to surrounding tissues.

A.M.J. Bull et al. (eds.), *Blast Injury Science and Engineering: A Guide for Clinicians and Researchers*,
DOI 10.1007/978-3-319-21867-0

Chemokines Cytokines that specifically attract cells, usually to sites of inflammation and/or infection.

Coagulopathy (clotting/bleeding disorder) A condition in which the blood's ability to coagulate (clot) is impaired.

Conservation equations Mathematical expressions that state that a property of a physical system (mass, momentum, and energy) are conserved (i.e., do not change) as the system evolves over time. In shock physics they are also known as the jump conditions or the Rankine-Hugoniot relations.

Constitutive relation A relationship between two physical properties (such as temperature, pressure and volume) of a material that describe its behaviour to external loads.

Constructive interference The interference of two or more waves of equal frequency and phase, resulting in their mutual reinforcement thus producing a wave of amplitude equal to the sum of the amplitudes of the individual waves.

Cortical neurons Nerve cells located in the outermost layer of the brain, which is known as the cerebral cortex.

Cytokines A class of small proteins secreted by several cells that interact with other cells and alter cellular behaviour.

Cytoskeleton The complex set of filaments and tubules within a cell that provides mechanical support, maintaining shape and facilitating motility.

Deformable solid A solid that can change shape or volume when external loading is applied; all solids are deformable.

Detonation An extremely fast explosive decomposition in which an exothermic reaction wave follows and also maintains a shock front in the explosive.

Detonation pressure The dynamic pressure in the shock front of a detonation wave.

Discretisation A procedure when setting up a numerical simulation in which the domain is subdivided into cells or elements of finite dimensions.

Ductility The ability of a solid material to sustain plastic deformation prior to rupture / failure.

Eigenvalues A set of scalars associated with a linear system that are invariant under a linear transformation.

Electronegative The tendency of an atom to attract electrons towards itself.

Erk1/2 signalling pathway A cellular pathway triggered by extracellular substances that in turn triggers other cellular pathways to affect cellular functions such as differentiation, proliferation and survival.

Extracellular matrix A mixture of proteins and carbohydrate-containing molecules external to cells that provide structural and biochemical support to surrounding cells.

Extracellular matrix metabolism The processes involved in the production and degradation of the constituents of the extracellular matrix.

Explosion A violent expansion of gas.

Extravasation A passage or escape into the tissues, usually of blood, serum or lymph.

Glycoproteins Proteins containing glycans covalently attached to a polypeptide side chain.

Growth factors Molecules able to interact with cells and cause or "stimulate" them to grow and possibly proliferate. Growth factors can be small molecules such as vitamins or hormones or even large molecules such as proteins.

Haemorrhage (Pathology) bleeding from a ruptured blood vessel.

High (order) explosive An explosive capable of detonation under the normal conditions of use.

Homeostasis The maintenance of cellular parameters (e.g., concentrations of cellular components) within the range for proper functioning of the cell. For example, the cellular processes that maintain the appropriate concentration of cations engage in cation homeostasis.

Hydrophilic Having a tendency to mix with, dissolve in, or be wetted by water.

Hydrodynamic pressure The difference between the pressure of a fluid and the hydrostatic pressure.

Hydrostatic pressure (Fluids) The pressure exerted by a fluid at equilibrium at a given point within the fluid due to gravity.

Hydrostatic stress (Solids) The mean normal stress ($= \frac{1}{3}$ of the sum of the three normal stresses in a three dimensional stress system).

Inflammation; inflammatory responses or pathways Complex biological responses to cell injury that can result in a number of physiological changes such as fever, swelling, and removal of damaged cells and tissues. Inflammation is a protective response and integral part of the healing processes. Poor or dis-regulated inflammation can lead to negative physiological changes such as unwanted tissue destruction or chronic diseases such as arthritis or allergic reactions. Pro-inflammatory responses refer to the induction of biochemical processes that promote inflammation, while anti-inflammatory responses refer to the induction of biochemical processes that reduce inflammation.

Inorganic Not consisting of, or derived from, living matter.

Integrins A class of proteins that transverse cell membranes and that facilitate interactions between different cells or between a cell and the extracellular matrix.

Ischemia A restriction in blood supply to tissues.

Isotropic A material whose microstructure is such that its mechanical behaviour does not depend on the direction of loading.

Lattice A repetitive arrangement of atoms.

Lysis Disruption of a cellular membrane that results in the release of cellular contents.

Machinability The ease with which a material can be cut.

Malleable Capable of being extended or shaped (by hammering or pressure).

Mesemchymal stem cells, MSCs Cells derived from connective-tissue frameworks that have the potential to differentiate into certain cell types. As the source of these cells can vary they are sometimes referred to as multipotent stroma cells.

Microstructure The structure of a material as revealed by a microscope above 25× magnification.

Mitochondria A cellular organelle that primarily functions to enable cellular respiration and energy production.

Mitogen-activated protein kinases, MAPKs see definition of *Erks*.

Necrosis Biochemical processes associated with cell death arising from external factors such as mechanical damage, toxic substances, or infection. Unlike apoptosis, necrotic processes are unregulated and include a loss of membrane integrity and uncontrolled digestion of cell components. Inflammation is often associated with necrosis.

Neurotransmitter A chemical that acts as a messenger for transmitting information between nerve cells.

Oedema, Edema, Dropsy, Hydropsy A condition of abnormally large fluid volume in the circulatory system or in the tissues between cells.

Osteocytes Non-dividing cells, embedded in bone, derived from osteoblasts. The majority of bone cells are osteocytes. Osteocytes are involved in tissue remodelling and biochemical processes such as phosphate metabolism and calcium availability.

Oxidative stress The state a cell is in when there is overabundance of reactive oxidative species, which can cause cellular damage.

Parenchyma The functional parts of an organ in the body. In contrast to the *stroma*, which refers to the structural parts.

Particle velocity The velocity associated with a point of infinitesimal dimensions attached to a material as it flows through space.

Phospholipase C A class of enzymes that cleave phosphate-containing groups from phospholipid molecules. These enzymes are often part of signal transduction pathways.

Phosphorylation The biochemical addition of a phosphate-containing group to a macromolecule such as a protein or a lipid. Phosphorylation is a key biochemical step in many signal transduction pathways.

Polycrystalline Of many crystals of varying size and orientation.

Protein nitration The biochemical modification of proteins, usually at tyrosine residues, involving the addition of a nitro-containing group. Protein nitration is generally associated with stress responses and can involve loss or gain of function.

Proteoglycan Any of a group of polysaccharide-protein conjugates present in connective tissue; they form the ground substance in the extracellular matrix of connective tissue and also have lubricant and support functions.

Quasi static Infinitely slow.

Rarefaction wave A wave that reduces the normal stress (or pressure) inside a material as it propagates; the mechanism by which a material returns to ambient pressure after being shocked (the state behind the wave is at lower stress than the state in front of it). Also known as unloading, expansion, release, relief, or decompression wave.

Reperfusion The act of restoring the flow of blood to an organ or tissue.

Reperfusion Injury The tissue damage caused when blood supply returns to the tissue after a period of ischemia or lack of oxygen.

Shock impedance Defined as $Z = p$ U. Describes the ability of material to generate pressure under given loading conditions. Generally a function of pressure.

Shock velocity The velocity of the shock wave as it passes through the material; the velocity is pressure/stress dependent. In the limit of an infinitesimally small shock wave it is equal to the bulk sound speed of the material.

Shock wave A wave that travels at a velocity higher than the elastic (uncompressed) sound speed of the material.

Signal transduction The transmission of extracellular signals to the interior of a cell. The process can involve a wide range of small molecules and macromolecules.

Spallation The process whereby fragments are ejected from a body due to impact or stress.

Sequelae A pathological condition resulting from disease or injury.

Stem cells Cells that have no specific function other than having the potential to develop into another cell type with a specialised function, or multiple cell types with different functions. In adults, stem cells can be found in bone marrow, blood and fat.

Stem cell differentiation The process of a stem cell changing into a cell type with a specialised function.

Strain energy The energy stored by a system undergoing deformation.

Tetrahedron A polyhedron composed of four triangular faces.

Trabeculae Fine spicules (needle like) forming a network in cancellous (porous) bone.

Trace evidence Fragments of physical evidence such as hairs, fibres and glass, transferred when two objects touch or when small particles are disbursed by an action of movement.

Tropocollagen The basic structural unit of all forms of collagen; a helical structure of three polypeptides wound around each other.

Velocity of detonation This is the speed at which a detonation wave progresses through an explosive. When, in a given system, it attains such a value that it will continue without change, it is called the stable velocity of detonation for that system.

Viscoelasticity The property of materials that exhibit both viscous and elastic characteristics when undergoing deformation.

Viscosity A measure of a fluid's resistance to flow.

Vulcanise To treat with sulphur and heat thereby imparting strength, greater elasticity and durability.

Index

A.M.J. Bull et al. (eds.), *Blast Injury Science and Engineering: A Guide for Clinicians and Researchers*,
DOI 10.1007/978-3-319-21867-0